

# **Vybrané aspekty dynamické elektrokardiografie**

Habilitační práce

MUDr. Irena Andršová, Ph.D.

Interní kardiologická klinika

Lékařská fakulta Masarykovy univerzity

Brno 2024

## **Struktura textu práce**

Tuto habilitační práci tvoří 17 publikovaných prací, jejichž je uchazečka autorem či spoluautorem. Publikované práce jsou vloženy v PDF formátu, tedy v grafické podobě a jazyku odpovídajícím příslušnému časopisu. Jednotlivé články jsou uvedeny krátkými shrnujícími komentáři (je zmíněna případná hodnota impakt faktoru a počet citací ve Web of Science). Komentáře jsou také propojeny doplňujícím textem, který je uvádí do kontextu se současným stavem znalostí.

## Obsah

Struktura textu práce.....	2
Obsah.....	3
Abstract.....	6
Poděkování.....	7
1 Úvod.....	8
2. Hereditární arytmiické syndromy jako model arytmogeneze .....	11
2.1 Klinické projevy hereditárních arytmiických syndromů a jejich genetické poklady .....	11
<i>Andrsova I, Valaskova I, Kubus P, Vit P, Gaillyova R, Kadlecova J, Manouskova L, Novotny T. Clinical characteristics and mutational analysis of the RyR2 gene in seven Czech families with catecholaminergic polymorphic ventricular tachycardia. Pacing Clin Electrophysiol 2012; 35:798-803.....</i>	12
<i>Andrsova I, Novotny T, Kadlecova J, Bittnerova A, Vit P, Florianova A, Sisakova M, Gaillyova R, Manouskova L, Spinar J. Clinical characteristics of 30 Czech families with long QT syndrome and KCNQ1 and KCNH2 gene mutations: Importance of exercise testing. J Electrocardiol 2012; 45:746-751.....</i>	19
<i>Mazzanti A, Guz D, Trancuccio A, Pagan E, Kukavica D, Chargeishvili T, Olivetti N, Biernacka EK, Sacilotto L, Sarquella-Brugada G, Campuzano O, Nof E, Anastasakis A, Sansone VA, Jimenez-Jaimez J, Cruz F, Sánchez-Quiñones J, Hernandez-Afonso J, Fuentes ME, Średniawa B, Garoufi A, <b>Andršová I</b>, Izquierdo M, Marinov R, Danon A, Expósito-García V, Garcia-Fernandez A, Muñoz-Esparza C, Ortíz M, Zienciuk-Krajka A, Tavazzani E, Monteforte N, Bloise R, Marino M, Memmi M, Napolitano C, Zorio E, Monserrat L, Bagnardi V, Priori SG. Natural History and Risk Stratification in Andersen-Tawil Syndrome Type 1. J Am Coll Cardiol. 2020; 75:1772-1784. ....</i>	26
2.2. Mutace s efektem zakladatele (founder mutation) varianty genu KCNQ1 u českých rodin s LQTS .....	39
<i>Synková I, Bébarová M, <b>Andršová I</b>, Chmelikova L, Švecová O, Hošek J, Pásek M, Vít P, Valášková I, Gaillyová R, Navrátil R, Novotný T. Long-QT founder variant T309I-Kv7.1 with dominant negative pattern may predispose delayed afterdepolarizations under <math>\beta</math>-adrenergic stimulation. Scientific Reports 2021; 11:3573. doi: 10.1038/s41598-021-81670-1.....</i>	40

2.3. Genetické aspekty komorových arytmií u běžných chorob srdce .....	82
<i>Novotny T, Kadlecova J, Raudenska M, Bittnerova A, <b>Andrsova I</b>, Florianova A, Vasku A, Neugebauer P, Kozak M, Sepsi M, Krivan L, Gaillyova R, Spinar J. Mutation analysis ion channel genes ventricular fibrillation survivors with coronary artery disease. Pacing Clin Electrophysiol 2011;34:742-749. ....</i>	
	83
<i><b>Andršová I</b>, Novotný T, Valášková I, Kadlecová J, Kuderová D, Sepši M, Kozák M, Křivan L, Gaillyová R, Špinar J. Mutation analysis of RyR2 gene in patients after arrhythmic storm. Cor Vasa 2012;54:e84-e87.....</i>	
	92
<i>Novotný T, Raudenská M, Kadlecová J, <b>Andršová I</b>, Floriánová A, Vašků A, Kozák M, Sepši M, Křivan L, Gaillyová R, Špinar J. Mutační analýza promotorů genů pro iontové kanály u pacientů s ischemickou chorobou srdeční, kteří přežili fibrilaci komor (Mutation analysis of ion channel genes promoters in ventricular fibrillation survivors with coronary artery disease). Cor Vasa (2013) doi: 10.1016/j.crvasa.2013.06.009.....</i>	
	97
<b>3. Návrat k elektrokardiogramu a elektrofyzilogii repolarizace myokardu .....</b>	<b>103</b>
3.1. Analýza chování QT intervalu.....	103
3.2. Vztah QT a RR intervalu – nepřesnosti korekčních vzorců .....	103
<i><b>Andršová I</b>, Hnatkova K, Šišáková M, Toman O, Smetana P, Huster KM, Barthel P, Novotný T, Schmidt G, Malik M. Influence of heart rate correction formulas on QTc interval stability. Scientific Reports 2021; 11:14269. doi: 10.1038/s41598-021-93774-9.....</i>	
	106
3.3. QT/RR v dětské populaci.....	127
<i><b>Andršová I</b>, Hnatkova K, Helánová K, Šišáková M, Novotný T, Kala P, Malik M. Individually rate corrected QTc intervals in children and adolescents. Front Physiol 2019;10:994. doi: 10.3389/fphys.2019.00994.....</i>	
	129
3.4. Korekční vzorce v dětské populaci .....	144
<i><b>Andršová I</b>, Hnatkova K, Helánová K, Šišáková M, Novotný T, Kala P, Malik M. Problems with Bazett QTc correction in paediatric screening of prolonged QTc interval. BMC Pediatrics 2020; 20:558. doi: 10.1186/s12887-020-02460-8 .....</i>	
	145
3.5. Hystereze QT intervalu .....	155
<i><b>Andršová I</b>, Hnatkova K, Šišáková M, Toman O, Smetana P, Huster KM, Barthel P, Novotný T, Schmidt G, Malik M. Sex and rate change differences in QT/RR hysteresis in healthy subjects. Front Physiol 2022; 12:814542. doi: 10.3389/fphys.2021.814542. ....</i>	
	157

3.6. Prostorový úhel QRS-T .....	182
<i>Andršová I, Hnatkova K, Toman O, Šišáková M, Smetana P, Huster KM, Barthel P, Novotný T, Schmidt G and Malik M. Intra-subject stability of different expressions of spatial QRS-T angle and their relationship to heart rate. Front. Physiol 2022; 13:939633. doi: 10.3389/fphys.2022.939633.....</i>	
	184
3.7. Tpeak – Tend interval .....	212
<i>Andršová I, Hnatkova K, Šišáková M, Toman O, Smetana P, Huster KM, Barthel P, Novotny T, Schmidt G, Malik M. Heart rate dependency and interlead variability of the T peak - T end intervals. Front Physiol 2020; 11:595815. doi: 10.3389/fphys.2020.595815.....</i>	
	214
3.8. QT variabilita .....	233
<i>Andršová I, Hnatkova K, Šišáková M, Toman O, Smetana P, Huster KM, Barthel P, Novotný T, Schmidt G, Malik M. Heart rate influence on the QT variability risk factors. Diagnostics 2020; 10:1096; doi:10.3390/diagnostics10121096. ....</i>	
	235
<i>Toman O, Hnatkova K, Šišáková M, Smetana P, Huster KM, Barthel P, Novotný T, Andršová I, Schmidt G, Malik M. Short-term beat-to-beat QT variability appears influenced more strongly by recording quality than by beat-to-beat RR variability. Front Physiol 2022; 12: 863873. doi: 10.3389/fphys.2022.863873.....</i>	
	252
<b>4. Prostorové komponenty a fragmentace QRS komplexu .....</b>	<b>277</b>
4.1. Prostorové komponenty QRS komplexu .....	277
<i>Hnatkova K, Andršová I, Toman O, Smetana P, Huster KM, Šišáková, Barthel P, Novotný T, Schmidt G, Malik M. Spatial distribution of physiologic 12-lead QRS complex. Scientific Reports 2021; 11:4289. doi: 10.1038/s41598-021-83378-8.....</i>	
	279
4.2. Fragmentace QRS komplexu .....	301
<i>Hnatkova K, Andršová I, Novotný T, Britton A, Shipley M, Vandenberg B, Sprenkeler DJ, Junttila J, Reichlin T, Schlögl S, Vos MA, Friede T, Bauer A, Huikuri HV, Willems R, Schmidt G, Franz MR, Sticherling C, Zabel M, Malik M. QRS micro-fragmentation as a mortality predictor. Eur Heart J 2022; 43:4177–4191.....</i>	
	302
<b>5. Závěr.....</b>	<b>337</b>
<b>6. Seznam literatury doprovodného komentáře.....</b>	<b>339</b>

## **Abstract**

Despite substantial scientific progress over the past decades, sudden cardiac death (SCD) remains a high-priority public health problem with multifaceted treatment and prevention requirements. As SCD occurs in all population strata, a risk stratification strategy is needed that would be universally appropriate, and therefore not only effective but also inexpensive and broadly applicable. At present, however, no such risk stratification technique is available.

The most easily applicable cardiac investigations are based on electrocardiography (ECG). Thus, the analysis of ECG signals appears to be a primary candidate of examinations to consider when developing SCD screening tools. Contemporary technological advances permit collecting ECG signals digitally which allows the development of novel aspects of dynamic electrocardiography. These include both spatial- and time-domain signal evaluations. Although some of these dynamic techniques have already been, with some success, applied to recordings obtained in well-defined clinical populations, substantial unresolved uncertainties exist in terms of their normal physiologic levels and regulation processes.

The original articles included in and commented on in this thesis are devoted to several such uncertainties in dynamic electrocardiography. All studies described in these articles have been conducted with the aim of contributing to the development of strategies for effective SCD risk screening. The thesis encompasses 17 contributions to this field, broadly classified into three areas covered in separate thesis sections.

Initially, our interest concentrated on hereditary arrhythmic syndromes, their genetic classification, and electrocardiographic manifestations. Subsequently, we turned our attention to the principles of non-invasive electrophysiology. Because of the obvious link between ventricular arrhythmias and cardiac repolarisation abnormalities, a number of our studies were devoted to the dynamics of electrocardiographic repolarisation parameters. We investigated a series of ECG characteristics potentially promising in terms of their SCD predictive power. Finally, we also investigated spatial dynamics of ventricular depolarisation and were able to propose a novel risk stratification marker that could be derived from standard 10-second ECGs. This makes it applicable in a broad variety of clinical settings.

## **Poděkování**

Ráda bych poděkovala nejenom spoluautorům vložených publikací, ale i vedení a kolegům z IKK i dalších spolupracujících pracovišť, zejména prof. MUDr. Jindřichu Špinarovi, CSc., který umožnil moje postgraduální studium, a obzvláště pak prof. MUDr. Petru Kalovi, Ph.D., bez jehož soustavné podpory a pomoci by realizace výzkumných projektů nebyla možná.

Zvláštní poděkování patří prof. MUDr. Tomáši Novotnému, Ph.D., který mě jako můj školitel provedl postgraduálními vědeckými začátky a který mi dále trpělivě pomáhá v oblasti vědy a výzkumu. Obrovský dík patří prof. RNDr. MUDr. Marku Malíkovi, DrSc., DSc., jehož přínos nejen v této práci, ale i ve formování mého odborného zaměření je díky jeho trpělivosti a zároveň důslednosti zásadní. Jsem vděčná za jeho pomoc při získání uznání a pozice v mezinárodních týmech. Věřím, že moje další spolupráce s prof. Novotným a prof. Malíkem povede k důležitým výsledkům.

Zároveň děkuji své rodině za podporu, obětavý přístup a nemalou dávku tolerance.

## 1 Úvod

Náhlá srdeční smrt (NSS)<sup>1</sup> zůstává i přes pokrok v lékařském výzkumu a v klinické medicíně stále velmi aktuálním tématem. Podle definice NSS zahrnuje přirozené úmrtí z kardiálních příčin uvozené ztrátou vědomí do jedné hodiny (nebo do 24 hodin, pokud dojde ke smrti beze svědků) od počátku akutních příznaků; může být známo preexistující srdeční onemocnění, avšak čas a způsob smrti jsou neočekávané. Kardiální etiologii náhlé smrti je nutno zvažovat i v případech, kdy není nalezena jiná orgánová nebo systémová patologie. Je známo, že pravděpodobnost úspěšné resuscitace NSS s časem rapidně klesá.<sup>2</sup> Všeobecně je také známo, že tento pokles je až o 7-10% každou minutu. Prevalence NSS je v populaci vyspělého světa přibližně dvakrát vyšší u mužů (kolem 0,06% ročně) ve srovnání s ženami (kolem 0,03% ročně)<sup>3</sup>, což jistě souvisí s rozdílným výskytem kardiovaskulárních onemocnění mezi pohlavími.

Zásadním problémem, i přes veškerý pokrok, zůstává identifikace rizikových jedinců. Odhaduje se, že zhruba 80% všech NSS je způsobeno maligní arytmií (komorová tachykardie, flutter nebo fibrilace komor), 15% tvoří bradykardie a 5% zbývající příčiny.<sup>1,4</sup> Vysoce rizikové pacienty, kteří maligní arytmií přežili, jsme schopni ve valné většině případů velmi dobře identifikovat a zajistit implantabilním kardioverterem defibrilátorem (ICD).<sup>5</sup> Většina náhlých smrtí (80%) nastává doma a pouze asi 15% na veřejných místech.<sup>6</sup> Zhruba 40% úmrtí proběhne beze svědků,<sup>1,7</sup> ačkoli některé práce popisují NSS beze svědků u více než poloviny případů.<sup>8</sup>

Důležitost identifikace těchto rizikových jedinců je určena nepoměrem mezi celkovou prevalencí NSS a jejím výskytem v jednotlivých subpopulacích. Tato rozdílnost je dobře známá jako takzvaný Myerburgův paradox.<sup>9,10</sup> Například, zatímco incidence NSS mezi pacienty s pokročilý srdečním selháním dosahuje až 20 %, tyto případy představují pouze asi 40 % všech případů NSS. Podobně výskyt NSS u pacientů v období rekonvalescence po infarktu myokardu, kteří prodělali arytmiickou příhodu, může být až 35 %. Tito jedinci však nepředstavují více než 10 % všech případů NSS.

Největší skupinu pacientů zmrávajících NSS tedy tvoří nemocní, kteří doposud maligní arytmií neprodělali nebo u nichž není předchozí arytmie známa. U přibližně 25% až 35% případů bývá NSS prvním projevem srdečního onemocnění a je tedy nepředvídatelná.<sup>3</sup> U 75% procent zemřelých NSS je anamnéza předchozího srdečního onemocnění známa a nejčastějším patologicko-anatomickým podkladem je aterosklerotické onemocnění věnčitých tepen (ICHS).<sup>2,4,7</sup> Dilatační kardiomyopatie (DKMP) je odpovědná za zhruba 15%. V dospělé populaci tak dramaticky roste závislost výskytu NSS na věku, a to paralelně s rostoucí incidencí těchto dvou diagnóz. Zbýlých 10% NSS pak tvoří jiné příčiny, které jsou velmi podstatné, protože postihují pacienty převážně v prvních 3 dekádách života.<sup>11</sup> U těchto pacientů je pak třeba



myslet na vrozené anomálie věnčitých tepen, myokarditidu, skryté hypertrofické kardiomyopatie, arytmogenní kardiomyopatie a v neposlední řadě na hereditární arytmiické syndromy, jako jsou např. syndrom dlouhého QT intervalu (LQTS), syndrom krátkého QT intervalu, katecholaminergně vázaná polymorfni komorová tachykardie (CPVT), Brugada syndrom a další. Rozlišení jednotlivých příčin musí být zohledněno v identifikaci a stratifikaci pacientů se zvýšeným rizikem NSS. Důležité je, jak již bylo popsáno, že NSS trpí jen malá část pacientů, u kterých je diagnostikována některá ze základních kardiovaskulárních patologií, ačkoli je výskyt těchto onemocnění, zejména ICHS, poměrně vysoký. Právě nepoměr mezi prevalencí kardiovaskulárních chorob a incidencí NSS brání plošnému využití podrobnějších, ale více komplikovaných, a proto finančně náročných vyšetřovacích metod, které by ulehčilo identifikaci těchto vysoce rizikových pacientů (např. zátěžová magnetická rezonance srdce, či invazivní elektrofyziologické vyšetření). Z tohoto důvodu je zapotřebí strategie postupných kroků, při níž by se na všechny pacienty (ideálně včetně pacientů s nekardiální diagnózou) uplatnil jednoduchý, nenákladný a široce dostupný diagnostický algoritmus, který by selektoval potenciálně rizikové pacienty, kteří by pak dále podstoupili právě tyto složitější a nákladnější vyšetření.

Nejjednodušší a nejrozšířenější vyšetření v kardiologii jsou založena na elektrokardiografii. Elektrokardiografické vyšetření (EKG) je proto zřejmým kandidátem testu první linie screeningového vyhledávání jedinců se zvýšeným rizikem NSS. Přestože je EKG vyšetření známo více než jedno století, klinická využitelnost je dosud omezena, protože v běžné klinické praxi se především využívá vizuální popis a jednoduchá elementární měření parametrů zobrazené EKG křivky. Toto není překvapivé, jelikož papírový záznam EKG křivky nabízí jen malý prostor pro pokročilejší analýzy. Díky současnému technologickému pokroku a možnosti digitalizace EKG můžeme v EKG signálu nalézt a hodnotit i parametry, které nejsou dosažitelné vizuálním hodnocením. Jednou takovou možností je kupříkladu rozklad signálu na jednotlivé singularity, které jsou následně kombinovány v různých algebraických dimenzích, čímž se dostáváme k doposud skrytým prostorovým a časovým charakteristikám EKG signálu. Tyto pouhým okem nezachytitelné vlastnosti EKG signálu tvoří jeden z konceptů moderní dynamické elektrokardiografie.<sup>12,13</sup>

Ačkoli některé z metod tohoto vysoce specifického odvětví kardiologie již byly úspěšně použity v dobře definovaných klinických populacích (a jsou tak připraveny hrát roli v klinickém managementu jednotlivých pacientů),<sup>14,15,16</sup> stále existují podstatné nevyřešené otázky v oblasti stanovení fyziologických hodnot a jejich nastavení v neinvazivní srdeční elektrofyziologii. Tyto normy je třeba stanovit pomocí analýzy velkého množství elektrokardiografických záznamů zdravých jedinců.

Články zahrnuté a komentované v této práci jsou věnovány právě problematice dynamické elektrokardiografie. Všechny studie popsané v těchto člancích byly provedeny s cílem přispět

k řešení problémů s vývojem testů a strategií, které by zajistily účinné vyhledávání rizika NSS ve všeobecné populaci.

Naše příspěvky v oboru lze obecně rozdělit do tří oblastí, kterým se věnují samostatné části práce. Zpočátku se náš zájem soustředil na dědičné arytmiické syndromy a na elektrokardiografickou manifestaci u pacientů trpících těmito syndromy, včetně klasifikace důsledků základních genetických abnormalit.

Následně jsme rozvíjením klasifikačních algoritmů provedli řadu studií na zdravých jedincích a vytvořili schéma pro budoucí vyšetřování v klinicky dobře definovaných populacích. Vzhledem k zřejmé souvislosti mezi komorovými arytmiemi a abnormalitami srdeční repolarizace se tyto studie soustředily především na dynamiku parametrů elektrokardiografické repolarizace. Popsali jsme řadu elektrokardiografických charakteristik, které se jeví jako potenciálně slibné z hlediska jejich prediktivních schopností. V další oblasti jsme zkoumali prostorovou dynamiku komorové depolarizace, díky čemuž jsme byli schopni navrhnout nový a zároveň velmi slibný marker rizikové stratifikace. Tento marker je možno odvodit ze standardních 10-ti sekundových digitálních 12-svodých EKG záznamů, což umožňuje jeho široké využití. V jednom z našich nejnovějších příspěvků jsme prokázali prediktivní sílu tohoto nového markeru ve velkých a nezávislých klinických populacích.

EKG veličiny je třeba porovnávat s dostupnějšími a metodologicky méně náročnými ukazateli NSS. Takovým je například dnes rutinně využívaná hodnota ejekční frakce levé komory srdeční (EFLK), která je nezávislým rizikovým faktorem. Dle literárních dat však dysfunkce levé komory srdeční, ať už u pacientů s ICHS či DKMP, spíše predikuje celkovou mortalitu než způsob smrti.<sup>17,18,19</sup> S tíží systolického srdečního selhání roste mortalita i z jiných příčin než NSS.

Naším cílem je tedy stratifikace rizikových jedinců pomocí jednoduchých neinvazivních metod založených na rozboru dynamických elektrokardiografických parametrů. Během desítek let byla sice vyvinuta celá řada tzv. „solistikovaných“ rizikově stratifikačních metod (např.: analýza variability tepové frekvence, senzitivity baroreflexů, mikrovolt alternance T vlny nebo detekce pozdních komorových potenciálů, QT dynamicita),<sup>20,21,22,23,24,25,26,27</sup> žádná z nich však není schopna identifikovat jedince s vysokým rizikem NSS. Proto se stále snažíme přispívat k této problematice.

## 2. Hereditární arytmiické syndromy jako model arytmogeneze

### 2.1 Klinické projevy hereditárních arytmiických syndromů a jejich genetické poklady

Následující publikace systematicky popisují rodiny vyšetřené ve FN Brno s LQT syndromem, s CPVT a dále správně diagnostikovanou a léčenou rodinu s velmi vzácným Andersen Tawil syndromem, dříve označovaným též jako LQTS 7.

**Andrsova I**, Valaskova I, Kubus P, Vit P, Gaillyova R, Kadlecova J, Manouskova L, Novotny T. Clinical characteristics and mutational analysis of the *RyR2* gene in seven Czech families with catecholaminergic polymorphic ventricular tachycardia. *Pacing Clin Electrophysiol* 2012; 35:798-803.

IF 1,746. Počet citací ve Web of Science 2

Publikovaná původní práce – kvantitativní podíl uchazečky 30 % - koncept, identifikace vhodných pacientů, analýza dat, text publikace.

# Clinical Characteristics and Mutational Analysis of the RyR2 Gene in Seven Czech Families with Catecholaminergic Polymorphic Ventricular Tachycardia

IRENA ANDRISOVA, M.D.,\* IVETA VALASKOVA, Dr.S.,† PETER KUBUS, M.D.,‡  
PAVEL VIT, M.D., Ph.D.,§ RENATA GAILLYOVA, M.D., Ph.D.,†  
JITKA KADLECOVA, Dr.S., Ph.D.,† LENKA MANOUSKOVA, R.N.,\*  
and TOMAS NOVOTNY, M.D., Ph.D.\*

From the \*Department of Internal Medicine and Cardiology; †Department of Medical Genetics, University Hospital and Faculty of Medicine of Masaryk University, Brno, Czech Republic; ‡Children's Heart Centre, University Hospital Motol, Prague, Czech Republic; and §Department of Pediatrics, University Hospital and Faculty of Medicine of Masaryk University, Brno, Czech Republic

**Background:** Catecholaminergic polymorphic ventricular tachycardia (CPVT) is a rare hereditary arrhythmia. The onset of clinical symptoms usually occurs during childhood, and is typically related to exercise. The aim of our study was to describe the clinical characteristics of seven Czech families with CPVT and the results of mutational analysis of the RyR2 gene in these families.

**Methods:** The subjects and their relatives were investigated at the participating departments. They underwent basic clinical investigation, and history was focused on possible CPVT symptoms, that is, syncope during exercise. Bicycle ergometry was performed to obtain electrocardiogram recording during adrenergic stimulation. In all the investigated individuals, blood samples were taken for mutation analysis of the RyR2 gene.

**Results:** To date, seven families have been investigated, comprising 11 adults and 13 children. In seven CPVT patients, the indication for examination was syncope during exercise. Diagnosis was confirmed by bicycle ergometry-induced polymorphic ventricular tachycardia. In one relative, polymorphic ventricular tachycardia was also induced. All eight affected individuals were treated with  $\beta$ -blockers and in two, a cardioverter-defibrillator was implanted due to recurrent syncope. Coding variants of the RyR2 gene were found in four probands.

**Conclusions:** This is a systematic description of CPVT families in the Czech Republic. Our data support the importance of exercise testing for the diagnosis of CPVT. In addition, RyR2 gene coding variants were found in 50% of affected individuals. (PACE 2012; 35:798–803)

## exercise testing, polymorphic ventricular tachycardia, RyR2

### Background

Catecholaminergic polymorphic ventricular tachycardia (CPVT) occurring in the structurally intact heart is an inherited cardiac arrhythmic disorder showing a highly malignant clinical course. CPVT can be inherited in an autosomal dominant<sup>1–5</sup> or recessive<sup>6</sup> manner; in some cases, the exact mode of inheritance could not be entirely

assessed.<sup>7</sup> The onset of clinical symptoms usually occurs during childhood, and is typically related to exercise. Sudden cardiac death is the first symptom in almost 30% of patients with CPVT.<sup>8</sup> In affected patients, stress-induced ventricular arrhythmias arise from multiple foci and can lead to typical ventricular tachyarrhythmia (VT), the so-called bidirectional VT. These arrhythmias are not sufficiently rapid to disrupt hemodynamics suggesting that the lethal arrhythmia, when it occurs, is ventricular fibrillation. In about 60% of patients with clinical diagnosis of CPVT, mutation of the ryanodine receptor (RyR2) gene is present in cases of autosomally dominantly inherited CPVT. The ryanodine receptor is an intracellular calcium channel in the sarcoplasmic reticulum of cardiomyocytes, with important roles in intracellular calcium metabolism. Patients with autosomally recessive inherited CPVT carry mutations of the calsequestrin 2 (CASQ2) gene,

---

Address for reprints: Tomas Novotny, M.D., Ph.D., Department of Internal Medicine and Cardiology, University Hospital Brno, Jihlavská 20, Brno, 625 00, Czech Republic. Fax: 420 53223 2611; e-mail: novotny-t@seznam.cz

The research was supported by grant 2B08061 of the Ministry of Education, Youth and Sports of the Czech Republic.

The authors have no relationship to industry to disclose.

Received December 27, 2011; revised February 21, 2012; accepted February 23, 2012.

doi: 10.1111/j.1540-8159.2012.03399.x

which encodes a Ca<sup>2+</sup> buffering protein in the lumen of the sarcoplasmic reticulum.<sup>9</sup>

The aim of our study was to describe the clinical characteristics of seven Czech families with CPVT and the results of mutational analysis of the *RyR2* gene.

**Methods**

**Clinical Examination**

Proband was identified among syncope cases investigated at the participating departments. All their first-degree living relatives were then investigated according to their age at either pediatric or adult cardiology departments. Basic cardiological investigation was performed in all individuals. History was focused on possible CPVT symptoms (stress syncope). All individuals were evaluated by bicycle ergometry (off therapy) to obtain electrocardiograms (ECGs) during adrenergic stimulation. Twelve-lead ECG was recorded in modification by Mason-Likar and electronically stored (CardioSys version 2.5, Marquette-Hellige, Freiburg, Germany). Initial stress was 0.5 W/kg, elevated by 0.5 W/kg every 3 minutes. The aim of the stress test was to obtain the maximum heart rate for each age category and gender. All recorded ECGs were printed with a paper speed of 50 mm/s and voltage of 20 mm/mV. Besides common ECG intervals, the QT intervals corrected for heart rate using Bazett's formula and possible Brugada signs were also assessed.<sup>10</sup>

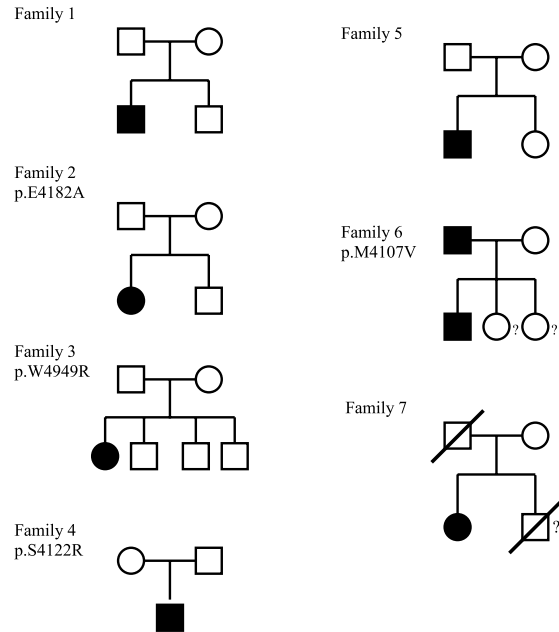
**Mutation Analysis**

All the clinically investigated individuals gave their informed consent, and peripheral blood samples were taken. Mutation analysis of the *RyR2* gene was performed in all individuals with clinical diagnosis of CPVT confirmed by ergometry. Genomic DNA samples were isolated from peripheral blood lymphocytes. Exons 2–4, 6–15, 17–20, 37, 39–49, 83, 84, 87–105 were amplified by polymerase chain reaction and analyzed by direct sequencing on an ABI PRISM 3130 (Life Technologies, Carlsbad, CA, USA). For mapping of the deletions and duplication in exons 3, 97, and 105, multiplex ligation-dependent probe amplification analysis was used. The detailed methodology has been described elsewhere.<sup>11–14</sup>

**Results**

**Clinical Results**

The investigated group consists of 24 members from seven families, 11 adults and 13 children (Fig. 1). Clinical characteristics are summarized in Table I. In the seven probands, the diagnosis was confirmed by ergometry-induced polymorphic ventricular tachycardias (Figs. 2



**Figure 1.** Pedigrees of families with CPVT diagnosis. Mutations of *RyR2* gene are indicated if found. Females are indicated by circles and males by squares. The noninvestigated individuals are denoted by a question mark. Affected individuals are shown as filled symbols and healthy individuals as empty symbols. Deceased individuals are denoted by a slash.

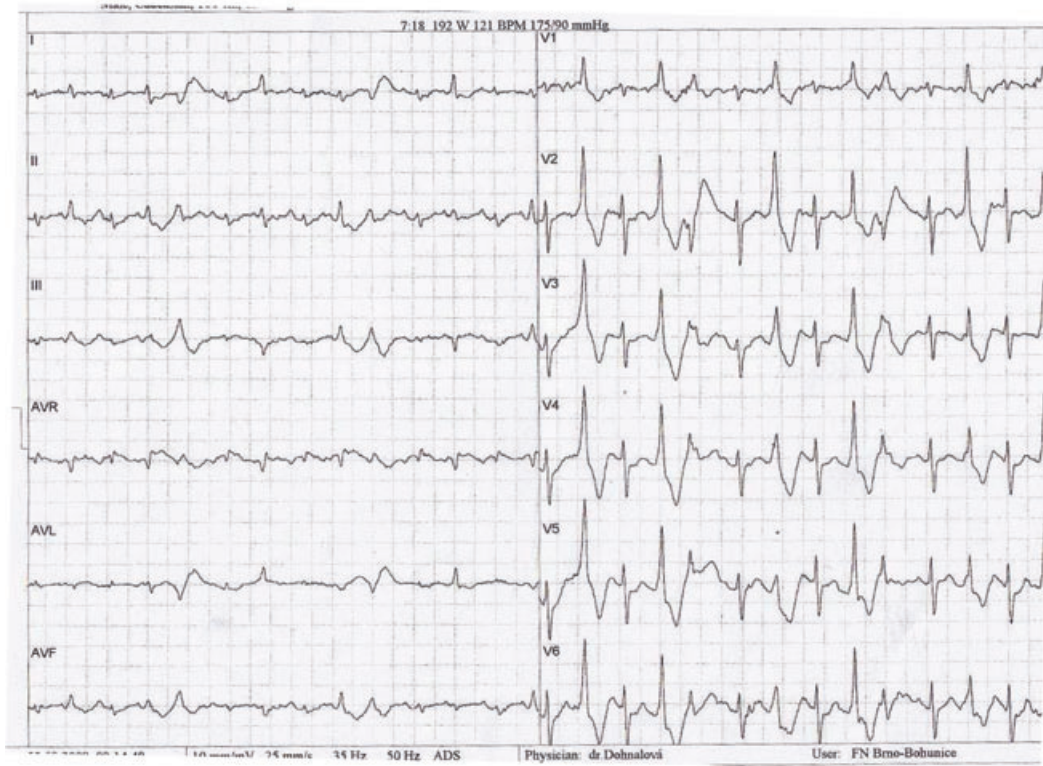
**Table I.**

Clinical Characteristics of Investigated Individuals

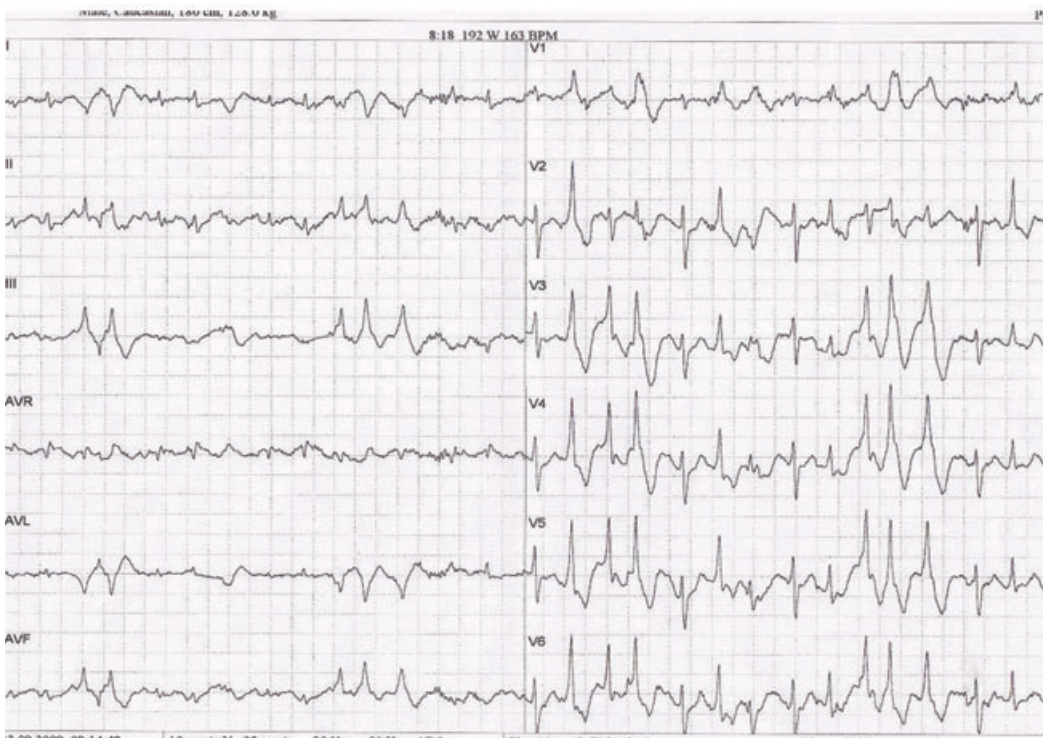
	Children (n = 13)	Adults (n = 11)
Age	12.82 ± 3.57	42.92 ± 8.50
Age of the first symptoms	7 ± 0.71 (n = 6)	18 (n = 1)
Age of the confirmation of CPVT diagnosis	9.4 ± 2.3 (n = 6)	37.5 ± 0.71 (n = 2)
Syncope	7	1
Native polymorphic VT	7	0
Polymorphic VT induced by ergometry	6	2
Native bidirectional VT	1	0
Bidirectional VT induced by ergometry	4	1
Supraventricular arrhythmias	2	0
β-blockers	7	1
β-blockers and verapamil	1	0
ICD	1	1

VT = ventricular tachycardia; ICD = implantable cardioverter-defibrillator.

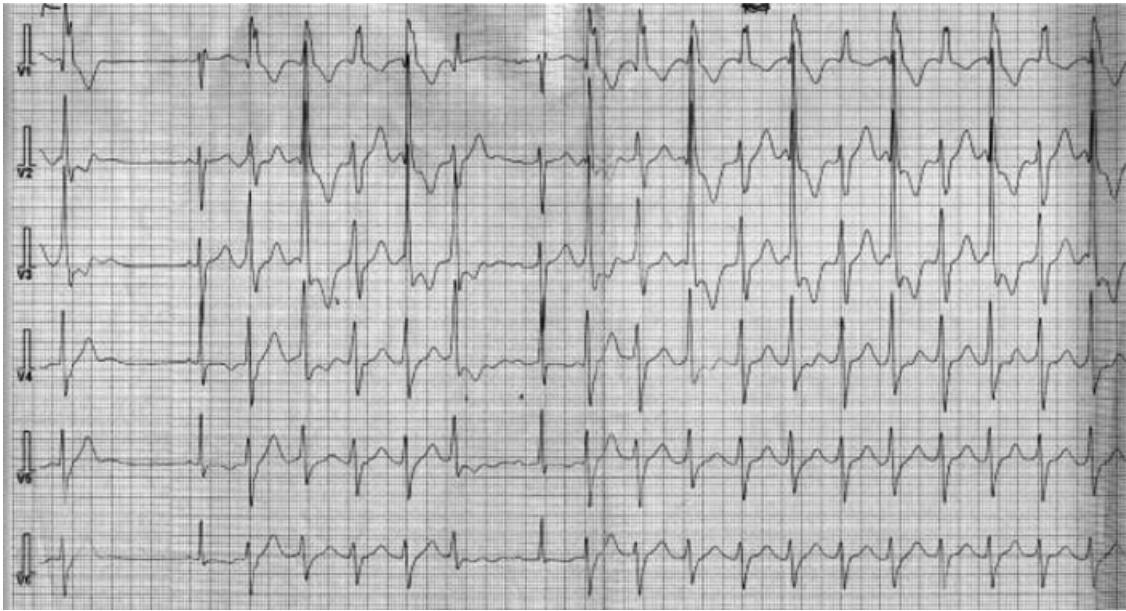
A



B



**Figure 2.** Examples of exercise-induced polymorphic ventricular arrhythmias in affected individuals. Sweep 25 mm/s, voltage 10 mm/mV.



**Figure 3.** Exercise-induced bidirectional ventricular arrhythmia in one proband.

and 3). The test was considered positive if polymorphic ventricular ectopic beats were induced (at least four consecutive beats). In one asymptomatic family member, arrhythmia was also detected during the stress test. None of the investigated individuals exhibited prolonged QTc interval or Brugada ECG and also other ECG features were unremarkable. All eight clinically affected patients were treated with  $\beta$ -blockers: atenolol 25–150 mg per day in four pediatric patients, metoprolol 50 mg per day in other two pediatric patients. In two adult patients, either betaxolol 20 mg per day or metoprolol 200 mg per day were used. In one case, atrial ectopic tachycardia was present and it was effectively suppressed by verapamil. Two patients received implantable cardioverter-defibrillators (ICDs) due to syncope recurrence despite  $\beta$ -blocker therapy.

### Mutation Analysis Results

In four of seven probands (57%), coding variants of the *RyR2* gene not previously described were detected (Table II). These four variants were not found in 141 control individuals. The exons containing rare coding variants found in CPVT probands were sequenced in all clinically investigated family members. In none of them, these variants were present. None of the patients with previously implanted ICD was a mutation carrier.

**Table II.**

List of Mutations of *RyR2* Gene

Nucleotide Change	Amino Acid Change	Exon	Domain
c.[12643A>G]+[=]	p.[M4107V]+[=]	90	III
c.[12545A>C]+[=]	p.[E4182A]+[=]	90	III
c.[12364A>C]+[=]	p.[S4122R]+[=]	90	III
c.[15162T>C]+[=]	p.[W4949R]+[=]	105	IV

### Discussion

This study is a systematic description of CPVT families in the Czech Republic. In the majority of cases, exercise-related syncope in childhood was the indication for investigation. In our study, in one patient the CPVT manifested in adulthood, and in another, in the father of a proband who was otherwise asymptomatic, the diagnosis was established only with ergometry. In pediatric patients, diagnosis was established after an average delay of 2 years from the first syncope, since these events were often attributed to vasovagal etiology or to neurological factors.<sup>6</sup> The characteristics of our group are in concordance with data reported previously.<sup>12,13</sup>

Since the resting ECG in CPVT is normal, exercise testing is of great importance. In more than 80% of CPVT patients, complex ventricular

arrhythmias are present during the stress test.<sup>15</sup> This can lead to typical polymorphic ventricular tachycardia-bidirectional ventricular tachycardia. In all our patients, complex forms of ventricular arrhythmias were induced during exercise, emphasizing the role of ergometry in arrhythmologic investigation.

It is important to note that supraventricular arrhythmias and tachycardias are also part of the CPVT phenotype.<sup>2</sup> Indeed, in two of our patients supraventricular arrhythmias occurred.

The molecular pathogenesis of *RyR2*-mediated CPVT underlines the role of increased adrenergic activity as a factor in triggering attacks. In fact, administration of  $\beta$ -adrenergic-blocking drugs is the standard treatment for CPVT, although they are less effective compared to long QT syndrome. In almost 30% of CPVT patients, incomplete protection from exercise-induced arrhythmias or recurrence of stress syncope are observed, and in these cases the implantation of an ICD is indicated.<sup>16</sup> In  $\beta$ -blocker nonresponsive patients, flecainide or left cardiac sympathetic denervation is the treatment of choice.<sup>17</sup> In two of our affected patients, implantation of an ICD was performed, and in the other, treatment with  $\beta$ -blockers was sufficient.

In almost 60% of patients with a clinical diagnosis of CPVT, mutations of the *RyR2* gene are found.<sup>18</sup> The *RyR2* gene is one of the largest

genes in the human genome. The majority of mutations appear to cluster in four regions of the predicted *RyR2* protein topology, and about 65% of published mutations of the *RyR2* gene are located in these regions.<sup>12,19</sup> Using a tiered targeting strategy suggested by groups in the Mayo Clinic and the Netherlands,<sup>12</sup> we detected different coding variants of the *RyR2* gene in four (57%) of seven probands. Mutations were undetectable in any of the parents, which can be explained either by gonadal mosaicism in one of the parents or by *de novo* mutation. Even the one affected father was not a carrier of his son's mutation. A possibility would be that the proband is a compound or double heterozygote and the father's mutation may be on a nonanalyzed exon.

The most important limitation of our study is a rather small group of investigated individuals. None of the novel mutations identified in our group of Czech CPVT families have been investigated in functional studies and pathogenicity has been suspected based on their absence in control subjects. Tiered targeting strategy can have an impact on the robustness of the estimate of the prevalence of *RyR2* mutations among the cohort. No other CPVT-related genes were analyzed.

In conclusion, in a small group of Czech CPVT patients, the clinical characteristics and percentage of *RyR2* mutations did not differ from internationally published data.

## References

- Leenhardt A, Lucet V, Denjoy I, Grau F, Ngoc DD, Coumel P. Catecholaminergic polymorphic ventricular tachycardia in children. A 7-year follow-up of 21 patients. *Circulation* 1995; 91:1512–1519.
- Fisher JD, Krikler D, Hallidie-Smith KA. Familial polymorphic ventricular arrhythmias. A quarter century of successful medical treatment based on serial exercise-pharmacologic testing. *J Am Coll Cardiol* 1999; 43:2015–2022.
- Swan H, Piippo K, Viitasalo M, Heikkilä P, Paavonen K, Kainulainen K, Kere J, et al. Arrhythmic disorder mapped to chromosome 1q42–q43 causes malignant polymorphic ventricular tachycardia in structurally normal hearts. *J Am Coll Cardiol* 1999; 34:2035–2042.
- Laitinen PJ, Brown KM, Piippo K, Swan H, Devaney JM, Brahmabhatt B, Donarum EA, et al. Mutations of the cardiac ryanodine receptor (*RyR2*) gene in familial polymorphic ventricular tachycardia. *Circulation* 2001; 103:485–490.
- Priori SG, Napolitano C, Tiso N, Memmi M, Vignati G, Bloise R, Sorrentino V, et al. Mutations in the cardiac ryanodine receptor gene (*hRyR2*) underlie catecholaminergic polymorphic ventricular tachycardia. *Circulation* 2001; 103:196–200.
- Lahat H, Eldar M, Levy-Nissenbaum E, Bahan T, Friedman E, Khoury A, Lorber A, et al. Autosomal recessive catecholamine- or exercise-induced polymorphic ventricular tachycardia. Clinical features and assignment of the disease gene to chromosome 1p13–21. *Circulation* 2001; 103:2822–2827.
- Postma AV, Denjoy I, Hoortje TM, Lupoglazoff J-M, Da Costa A, Sebillon P, Mannens MM, et al. Absence of calsequestrin 2 causes severe forms of catecholaminergic polymorphic ventricular tachycardia. *Circ Res* 2002; 91:21–26.
- Bauce B, Rampazzo A, Basso C, Bagattin A, Daliento L, Tiso N, Turrini P, et al. Screening for ryanodine receptor type 2 mutations in families with effort-induced polymorphic ventricular arrhythmias and sudden death. *J Am Coll Cardiol* 2002; 40:341–349.
- Viatchenko-Karpinski S, Terentyev D, Györke I, Terentyeva R, Volpe P, Priori SG, Napolitano C, et al. Abnormal calcium signaling and sudden cardiac death associated with mutation of calsequestrin. *Circ Res* 2004; 94:471–477.
- Antzelevich C, Brugada P, Borggrefe M, Brugada J, Brugada R, Corrado D, Gussak I, et al. Brugada syndrome: Report of the Second Consensus Conference endorsed by the Heart Rhythm Society and the European Heart Rhythm Association. *Circulation* 2005; 111:659–670.
- Bagattin A, Veronese C, Bauce B, Wuyts W, Settimo L, Nava A, Rampazzo A, et al. Denaturing HPLC-based approach for detecting *RyR2* mutations involved in malignant arrhythmias. *Clin Chem* 2004; 50:1148–1155.
- Medeiros-Domingo A, Bhuiyan ZA, Tester DJ, Hofman N, Bikker H, vanTintelen P, Mannens M, et al. The *RyR2*-encoded ryanodine receptor/calcium channel in patients diagnosed previously with either catecholaminergic polymorphic ventricular tachycardia or genotype negative, exercise-induced long QT syndrome. *J Am Coll Cardiol* 2009; 54:2065–2074.
- Postma AV, Denjoy I, Kamblock J, Alders M, Lupoglazoff JM, Vaksman G, Dubosq-Bidot L, et al. Catecholaminergic polymorphic ventricular tachycardia: *RyR2* mutations, bradycardia, and follow up of the patients. *J Med Genet* 2005; 42:863–870.
- Bhuiyan ZA, van den Berg MP, van Tintelen JP, Alders M, Postma VA, van Langen I, Mannens MMAM, et al. Expanding spectrum of human *RyR2*-related disease: New electrocardiographic, structural, and genetic features. *Circulation* 2007; 116:1569–1576.
- Mohamed U, Napolitano C, Priori GS. Molecular and electrophysiological bases of catecholaminergic polymorphic ventricular tachycardia. *J Cardiovasc Electrophysiol* 2007; 18:791–797.
- Zipes DP, Camm AJ, Borggrefe M, Buxton AE, Chaitman B, Fromer M, Gregoratos G, et al. ACC/AHA/ESC 2006 guidelines for management of patients with ventricular arrhythmias and the prevention of sudden cardiac death: A report of the



## CPVT IN CZECH FAMILIES

- American College of Cardiology/American Heart Association Task Force and the European Society of Cardiology Committee for Practice Guidelines (Writing Committee to Develop Guidelines for Management of Patients with Ventricular Arrhythmias and the Prevention of Sudden Cardiac Death) developed in collaboration with the European Heart Rhythm Association and the Heart Rhythm Society. *Europace* 2006; 8:746–837.
17. Watanabe H, Chopra N, Laver D, Hwang HS, Davies SS, Roach DE, Duff HJ, et al. Flecainide prevents catecholaminergic polymorphic ventricular tachycardia in mice and humans. *Nat Med* 2009; 15:380–383.
  18. Priori SG, Chen W. Inherited dysfunction of sarcoplasmic reticulum  $Ca^{2+}$  handling and arrhythmogenesis. *Circ Res* 2011; 108:871–883.
  19. George GH, Jundi H, Thomas NL, Scoote M, Walters N, Williams AJ, Lai FA. Ryanodine receptor regulation by intramolecular interaction between cytoplasmic and transmembrane domains. *Mol Biol Cell* 2004; 15:2627–2638.

**Andrsova I**, Novotny T, Kadlecova J, Bittnerova A, Vit P, Florianova A, Sisakova M, Gaillyova R, Manouskova L, Spinar J. Clinical characteristics of 30 Czech families with long QT syndrome and *KCNQ1* and *KCNH2* gene mutations: Importance of exercise testing. *J Electrocardiol* 2012; 45:746-751.

IF 1,290. Počet citací ve Web of Science 7

Publikovaná původní práce – kvantitativní podíl uchazečky 30 % - koncept, identifikace vhodných pacientů, analýza dat, text publikace.

# Clinical characteristics of 30 Czech families with long QT syndrome and *KCNQ1* and *KCNH2* gene mutations: importance of exercise testing<sup>☆,☆☆</sup>

Irena Andrsova, MD,<sup>a</sup> Tomas Novotny, MD, PhD,<sup>a,\*</sup> Jitka Kadlecova, DrS, PhD,<sup>b</sup>  
Alexandra Bittnerova, MA,<sup>b</sup> Pavel Vit, MD, PhD,<sup>c</sup> Alena Florianova, MD,<sup>a</sup>  
Martina Sisakova, MD,<sup>a</sup> Renata Gaillyova, MD, PhD,<sup>b</sup> Lenka Manouskova, RN,<sup>a</sup>  
Jindrich Spinar, MD, PhD<sup>a</sup>

<sup>a</sup>Department of Internal Medicine and Cardiology, University Hospital and Faculty of Medicine of Masaryk University, Brno, Czech Republic

<sup>b</sup>Department of Medical Genetics, University Hospital and Faculty of Medicine of Masaryk University, Brno, Czech Republic

<sup>c</sup>Department of Pediatrics, University Hospital and Faculty of Medicine of Masaryk University, Brno, Czech Republic

Received 13 January 2012

## Abstract

**Background:** Classic symptoms of long QT syndrome (LQTS) include prolongation of QT interval on electrocardiograph, syncope, and cardiac arrest due to a distinctive form of polymorphic ventricular tachycardia, known as Torsade de Pointes. We assessed occurrence of LQTS signs in individuals from 30 Czech families with mutations in *KCNQ1* and *KCNH2* genes.

**Methods and Results:** One hundred five individuals from 30 Czech families with LQTS were genotyped for *KCNQ1* and *KCNH2*. The occurrence of typical LQTS signs (pathologic prolongation of QT interval; syncope; cardiac arrest; Torsade de Pointes) was clinically assessed by exercise test with QT interval analysis. Family history of sudden cardiac death was taken. Statistical analysis was performed to determine correlation of clinical results and mutation status. *KCNQ1* gene mutations were found in 23 families, and *KCNH2* gene mutations in eight families. Only 46 (70%) of the 66 mutation carriers had at least two of the typical LQTS signs. The others were minimally or asymptomatic. From 39 noncarrier individuals, only 1 fulfilled the clinical criteria of LQTS diagnosis, another 4 had an intermediate probability of diagnosis. The exercise test had 92% sensitivity and 93% specificity for LQTS diagnosis.

**Conclusions:** Incidence of classical signs of LQTS was not high in Czech carriers of *KCNQ1* and *KCNH2* mutations. Therefore, proper diagnosis relies on detection of symptoms at presentation. The exercise test may be beneficial owing to its high sensitivity and specificity for LQTS diagnosis.

© 2012 Elsevier Inc. All rights reserved.

## Keywords:

Exercise test; LQT syndrome; Mutation; Sudden cardiac death; Torsades de Pointes

## Introduction

Long QT syndrome (LQTS) is characterized by an abnormality in myocardial repolarization that leads to typical changes on surface electrocardiogram (ECG), including prolongation of the QT interval, morphological changes of T waves, and appearance of the Torsades de Pointes (TdP).<sup>1</sup> The global prevalence of LQTS has been estimated at 1:2500 but is believed to be higher due to missed diagnosis.<sup>2</sup>

Recent advances in genotyping technologies have led to the recognition of several genes associated with LQTS. Not surprisingly, genes encoding myocardial ion channels have been implicated in LQTS family linkage analysis studies.<sup>3</sup> The *KCNQ1* and *KCNH2* genes, encoding subunits of potassium channels, are among the most frequently associated with LQTS. The aim of this study was to assess genotype–phenotype correlation in 30 Czech families with history of LQTS and mutations in *KCNQ1* and *KCNH2* genes and to evaluate exercise test contribution for the diagnosis of LQTS.

## Methods

### Study participants

A total of 105 members from 30 families with occurrence of LQTS were included consecutively into the study. All

<sup>☆</sup> The research was supported by grant No. NS/10429-3 of the Internal Grant Agency of the Ministry of Health of the Czech Republic.

<sup>☆☆</sup> The authors have no relationship to industry to disclose.

\* Corresponding author. Department of Internal Medicine and Cardiology, University Hospital Brno, Jihlavská 20, Brno, 625 00, Czech Republic.

E-mail address: [novotny-t@seznam.cz](mailto:novotny-t@seznam.cz)

individuals underwent physical examination, ECG, and exercise test. The probability of LQTS diagnosis was established using the revised criteria suggested by Schwartz et al.<sup>4</sup> Informed consent was obtained from all participants and blood samples were taken for DNA isolation.

#### Exercise test

All the individuals were examined by bicycle ergometry to obtain ECG recordings at different adrenergic states. A 12-lead ECG with Mason-Likar modification was used (Marquette-Hellige, CardioSys version 2.5). The initial stress was set to 0.5 W/kg and increased by 0.5 W/kg every 3 minutes.

All ECGs were recorded as paper printings at the speed of 50 mm/s and voltage of 20 mm/mV. QT and R-R intervals were manually measured by 2 blinded investigators for the periods of rest and for each of the first 6 minutes of the recovery period. In most cases the QT interval was measured in lead V<sub>5</sub>, the other leads were used only when the end of T wave could not be discriminate in this lead. The QT intervals were corrected for heart rate using Bazett's formula: QTc = (QT/RR)<sup>1/2</sup> measured in seconds.<sup>5</sup>

#### Mutation analysis

Genomic DNA was isolated from the venous blood samples of each study participant. The purified DNA was applied as template to polymerase chain reaction with exon-specific primers targeting the *KCNQ1* and *KCNH2* genes. The polymerase chain reaction products were screened for the presence of mutation by the single-strand conformational polymorphism method and temperature gradient gel electrophoresis.<sup>6</sup> Exons

were sequenced on an ABI PRISM 310 (Applied Biosystems, Foster City, CA, USA). The detailed methodology for this procedure, including exon-specific primer sequences, has been described elsewhere.<sup>7</sup>

#### Statistical analysis

Parametric data were analyzed by the *F* test for variance and Student *t* test. Nonparametric data were analyzed by the Mann-Whitney *U* and Fisher exact tests.

## Results

### *KCNQ1* gene mutations

*KCNQ1* gene mutations (LQTS1) were identified in 22 families (Table 1). Forty-nine individuals were mutation carriers (30 women; 19 men; mean age: 36,6 ± 16,1 years), and 30 had no mutation (21 women; 9 men; mean age: 40,4 ± 11,9 years). Homozygous mutations of the *KCNQ1* gene were found in 2 families, one of which was consanguineous. Both of these familial cases had been described in detail previously.<sup>19,20</sup> Six novel mutations were detected, and none of these was present in the group of healthy individuals (n = 90) with no previous or current symptoms of LQTS. In 1 case yet undescribed, DNA mutation (c.1772G>C) resulted in amino acid change published previously (pR591C).<sup>21</sup>

The previously established LQTS mutation, T309I (C926T), of the *KCNQ1* gene was present in 5 families. It is located in the pore region and its estimated predictive value to be a pathologic mutation is 96% according to Kapa et al.<sup>22</sup>

Table 1  
List of mutations.

Gene	Exon	Region	Nucleotide change	Amino acid change	References
<i>KCNQ1</i>	1	N-term	c.453_454insCC	p.P151fsX14	-
	3	S2-S3	c.569G>T	p.R190L <sup>†</sup>	[8]
	4	S4	c.674C>T	p.S225L	[9]
	6	S5	c.805_819del	p.269_273del	-
	6	Pore	c.916G>C	p.G306R	[8,10]
	7	Pore	c.926C>T	p.T309I <sup>*,‡</sup>	[8,11]
	7	Pore	c.935C>T	p.T312I	[8,10]
	7	Pore	c.940G>A	p.G314S	[8,12]
	7	S6	c.973G>A	p.G325R	[8,13]
	7	S6	c.1048G>C	p.G350R	[14]
	13	C-term	c.1645_1665del	p.M549_H555del	-
	14	C-term	c.1686G>C	p.R562S	-
	15	C-term	c.1760C>T	p.T587M	[8,15]
	15	C-term	c.1772G>A	p.R591H	[8,7]
	15	C-term	c.1772G>C	p.R591C	-
	16	C-term	c.1831G>A	p.D611N	[8]
16	C-term	c.1893insC	p.P631fsX650 <sup>†</sup>	[7]	
<i>KCNH2</i>	4	N-term	c.815C>T	p.A228V	-
	6	S1-S2	c.1342G>A	p.A448T	-
	7	S4	c.1600C>T	p.R534C	[15]
	7	S5	c.1714G>A	p.G572S	[16]
	7	Pore	c.1894C>T	p.P632S	[17]
	7	S6	c.1919_1921delTCT	p.P640del	-
	13	C-term	c.3131G>T	p.R1047L <sup>‡</sup>	[18]
	14	C-term	c.3161delG	p.T1054TfsX2	-

\* Mutation found in 5 unrelated families.

<sup>†</sup> Homozygous mutations (2 families).

<sup>‡</sup> Compound heterozygosity mutations (1 family).

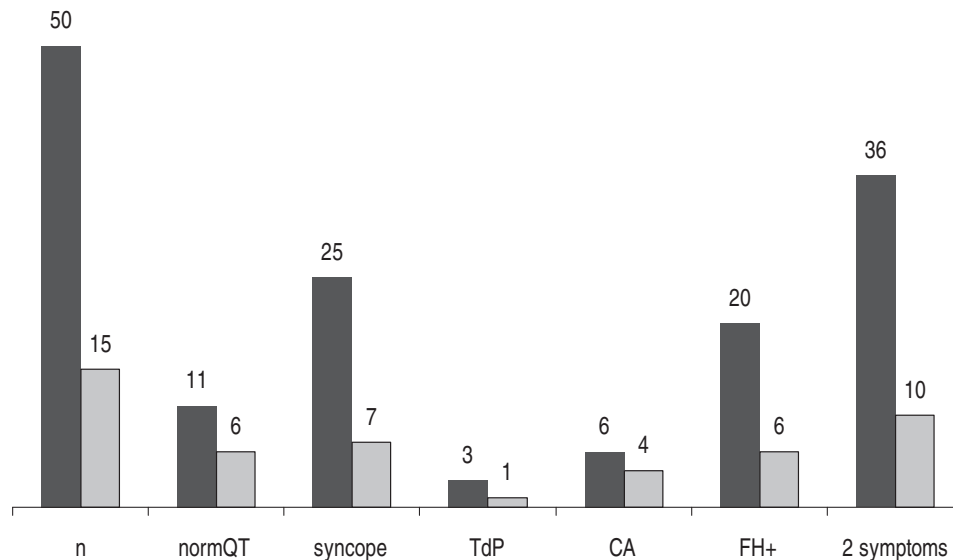


Fig. 1. Incidence of symptoms at initial examination in *KCNQ1* and *KCNH2* mutation carriers. Total num: number of investigated patients; norm QT: number of patients with normal Qtc; TdP: Torsade de Pointes; FH+: number of patients with sudden cardiac death in family history; CA: number of patients who had cardiac arrest; 2 symptoms: patients with two or more LQTS symptoms at initial examination. The dark gray color represents the LQT1 patients and light gray the LQT2 patients.

#### *KCNH2* gene mutation

The mutations of *KCNH2* gene (LQTS2) were found in 7 families (Table 1). We detected 15 mutation carriers (12 women, 3 men, mean age  $38,9 \pm 15,7$ ). In 8 family members, the mutation of *KCNH2* gene was not found (6 women, 2 men; mean age,  $48,7 \pm 17,9$  years). One of the *KCNH2* gene mutations was novel.

#### Compound heterozygosity

In one family of 4 members, the compound heterozygosity of *KCNQ1* and *KCNH2* mutations was present (*KCNQ1*: p.[Thr309Ile], *KCNH2*: p.[Arg1047Leu]). We detected 2 mutation carriers—proband and his father, mother and older brother were healthy.

#### Baseline clinical findings in families with *KCNQ1* gene mutations

The mean QTc at rest was longer in the mutation carriers than in the non-mutation carrier family members ( $479 \pm 57$  vs  $413 \pm 31$  milliseconds,  $P < .001$ ). Nevertheless, 11 pathologic mutation carriers (22%) had physiological QTc at baseline assessment, and only 36 patients (73%) had at least 2 typical signs of LQTS. Fig. 1 summarizes the incidence of symptoms in mutation carriers. Moreover, the mean QTc at rest was also longer in symptomatic carriers than in asymptomatic carriers ( $510 \pm 72$  vs  $459 \pm 32$  milliseconds,  $P < .001$ ).

According to Schwartz scores, only 32 mutation carriers (65%) had a high probability of diagnosis, while the other mutation carriers were minimally symptomatic or asymptomatic (Fig. 2A). According to clinical symptoms (QTc 480 milliseconds and sudden cardiac death in family history), only 1 woman among the non-mutation-carrier family members had an intermediate probability of LQTS diagnosis, while another 2 were minimally symptomatic (Fig. 2B).

#### Baseline clinical findings in families with *KCNH2* gene mutations

The mean QTc at rest was longer in the mutation carriers than in the non-mutation carrier family members ( $454 \pm 47$  vs  $414 \pm 33$  milliseconds,  $P < .001$ ). Difference in QTc value between symptomatic and asymptomatic mutation carriers was not statistically significant ( $482 \pm 56$  vs  $440 \pm 36$  milliseconds). Six mutation carriers (40%) had normal QTc value at start. Incidence of symptoms in mutation carriers is summarized in Fig. 1. The probability of LQTS diagnosis according to Schwartz score in mutation carriers is summarized in Fig. 2A and in mutation noncarriers in Fig. 2B.

#### Baseline clinical findings in families with compound heterozygosity

Both of the mutation carriers were asymptomatic. The proband was investigated due to palpitation and detection of QTc prolongation during the 24 hours ECG monitoring. The rest QTc value was 440 milliseconds, the longest QTc from 24 hours ECG monitoring was 507 milliseconds. The other mutation carrier, the father, had QTc of 480 milliseconds initially.

#### Bicycle ergometry findings in families with *KCNQ1* gene mutations

The patients completed the bicycle ergometer test. It was possible to assess 95% of the resultant ECG prints, but 5% were excluded due to obvious artifactual data.

Forty-eight (96%) mutation carriers were found to have further pathologic prolongation of QTc during exercise test, which increased the numerical values of their Schwartz scores. Two non-carrier family members had pathologic prolongation of QTc, as well. The detected changes in QT

-interval are summarized in Tables 2 and 3.

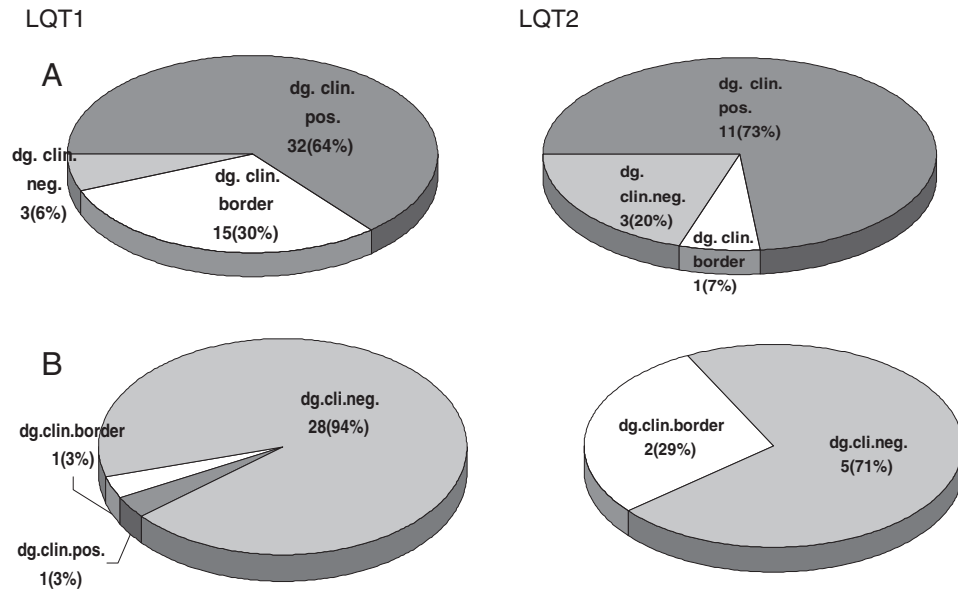


Fig. 2. A. LQTS diagnosis probability according to clinical symptoms at initial examination in pathologic mutation carriers, B. LQTS diagnosis probability according to clinical symptoms at initial examination in non-mutation carriers. (dg clin +: high probability of diagnosis according to clinical signs – Schwartz score  $\geq 3.5$ ; dg clin neg: low probability of diagnosis according to clinical signs Schwartz score  $\leq 1$ ; dg clin border: intermediate probability of diagnosis according to clinical signs - Schwartz score 1.5-3).

*Bicycle ergometry findings in families with KCNH2 gene mutations*

The pathologic prolongation of QTc interval during the stress test was detected in 12 (80%) mutation carriers. In one non carrier family member pathologic prolongation was observed too. The detected changes in QT interval are summarized in Tables 2 and 3.

*Bicycle ergometry findings in families with compound heterozygosity*

The proband did not undergo ergometry because of low age and low body height. The pathologic prolongation of QTc interval was observed only in the father (510 milliseconds). The non carrier members—the mother and the older brother—had physiologic QTc values.

**Discussion**

This study was designed to determine the genotype-phenotype correlation in a small group of Czech patients with LQTS that was confirmed by mutational analysis. It

represents the first systematic description of LQTS individuals in the central European region.

Our data supported the previously published findings that indicate a large proportion of LQTS mutation carriers are minimally symptomatic or asymptomatic.<sup>23,24</sup> Therefore, careful clinical investigations and physician awareness are important to identify LQTS patients and reduced missed diagnosis.<sup>25-27</sup> The bicycle ergometer test is a convenient, noninvasive method used to evaluate the QT interval; because it induces the adrenergic condition naturally and modern ergometers can produce high quality ECG recordings, it is considered acceptable by both patients and treating physicians/institutions.<sup>28</sup> Another exercise equipment-based method that is available is the treadmill; however, this test produces more ECG artifacts due to upper body movements.

Fifty-nine (89%) mutation carriers produced further pathologic prolongation of QTc during the exercise test in this study. This stress test induced symptoms that increased the numerical value of the individual’s Schwartz score. Therefore, despite the known technical limitations of the stress test, including determination of the T wave end and

Table 2  
QTc values in mutation carriers vs. non-mutation family members.

LQT1	Mutation carriers n = 49	Non-mutation family members n = 39	P
QTc rest	0.479 ± 0.057	0.413 ± 0.031	<.001
QTc exercise	0.534 ± 0.057	0.426 ± 0.020	<.001
LQT2	n = 5	n = 10	
QTc rest	0.454 ± 0.047	0.414 ± 0.033	<.001
QTc exercise	0.484 ± 0.045	0.427 ± 0.028	<.001

Data are presented as average ± SD.

Table 3  
QTc values in symptomatic vs. asymptomatic mutation carriers.

LQT1	Symptomatic mutation carriers n = 20	Asymptomatic mutation carriers n = 30	P
QTc rest	0.504 ± 0.069	0.455 ± 0.34	<.001
QTc exercise	0.549 ± 0.062	0.504 ± 0.047	<.005
LQT2	n = 5	n = 10	
QTc rest	0.510 ± 0.072	0.459 ± 0.032	.08
QTc exercise	0.557 ± 0.066	0.516 ± 0.044	.04

- 22 - Data are presented as average ± SD.

methodology of QT interval correction, it was considered to significantly contribute to establishment of clinical diagnosis of LQTS. Moreover, in our study the stress test helped to identify individuals with increased risk of life-threatening arrhythmias.

In Czech patients mutations of *KCNQ1* gene were 3 times more frequent than mutations of *KCNH2* gene. On the contrary the Danish registry has the opposite distribution.<sup>29</sup> Other groups report balanced proportion of both genes mutations.<sup>22</sup> If these are truly regional differences or they are rather caused by low numbers of investigated patients remains to be established.

Original mutations were found in almost all families evaluated in our study. The exception was the T309I mutation of the *KCNQ1* gene, which has been previously identified in other LQTS populations. This variant was present in 5 unrelated families in our study and it segregated with the LQTS phenotype. While no functional studies have yet been published for this particular variant, it is known to be located in the pore region, where it is very likely to affect pore function and LQTS. Moreover, the estimated predictive value of this mutation was previously reported as 96%.<sup>22</sup> Further investigations should be conducted, however, to determine whether T309I is a founder mutation in ethnic-specific population.

There are several limitations to be considered. The technical problems were cited above for the ergometry test. QTc measurements were made using Bazett's formula. This formula has wide acceptance and use, but it can overcorrect and undercorrect for heart rates greater than 100 and 60 bpm, respectively.<sup>30</sup> Other limitations of our study exist and should be considered when interpreting our results. For example, small group of patients especially in the LQT2 families which affected the statistical results. Also, none of the novel mutations identified in our set of Czech LQTS families have been investigated in functional studies. Nevertheless, the phenotype-genotype correlations were clear in most families, and we believe future functional studies of mutated channels will provide insights into their functional effects in LQTS.

## Conclusion

The incidence of classical signs of LQTS was not high in the Czech *KCNQ1* and *KCNH2* mutation carriers. The exercise test, using a bicycle ergometer, has high sensitivity and specificity and may be a feasible and effective method of diagnosis. Mutation analysis may still prove useful as an additional means of risk stratification.

## Author contributions

*Concept:* Irena Andrsova, Tomas Novotny.

*Data analysis:* Irena Andrsova, Tomas Novotny, Pavel Vit, Jitka Kadlecova, Alexandra Bittnerova, Alena Florianova, Martina Sisakova, Renata Gaillyova, Lenka Manouskova.

*Drafting article:* Irena Andrsova.

*Approval of article:* Jindrich Spinar, Tomas Novotny.

*Critical version of article:* Tomas Novotny, Alena Florianova. - 23 -

*Data collection:* Alena Florianova, Lenka Manouskova, Irena Andrsova, Pavel Vit.

## References

- Schwartz PJ, Periti M, Malliani A. The long QT syndrome. *Am Heart J* 1975;89:378.
- Schwartz PJ, Stramba-Badiale M, Crotti L, et al. Prevalence of the congenital long-QT syndrome. *Circulation* 2009;120:1761.
- Schwartz PJ, Priori SG. Long QT syndrome: genotype-phenotype correlations. In: Zipes DP, Jalife J, editors. *Cardiac electrophysiology: from cell to bedside*. 4th ed. Philadelphia: Saunders; 2004. p. 651.
- Schwartz PJ, Crotti L. QTc behavior during exercise and genetic testing for the long-QT syndrome. *Circulation* 2011;124:2181.
- Hodges M. Rate correction of the QT interval. *Card Electrophysiol Rev* 1997;1:360.
- Larsen LA, Andersen PS, Kanters JK, Jacobsen JR, Vuust J, Christiansen M. A single strand conformation polymorphism/heteroduplex (SSCP/HD) method for detection of mutations in 15 exons of the KVLQT1 gene, associated with the long QT syndrome. *Clin Chim Acta* 1999;280:113.
- Neyroud N, Richard P, Vignier N, et al. Genomic organization of the *KCNQ1* K<sup>+</sup> channel gene and identification of C-terminal mutations in the long QT syndrome. *Circ Res* 1999;84:290.
- Leiden Open Variation Database, [http://www.lovd.nl/2.0/index\\_list.php](http://www.lovd.nl/2.0/index_list.php).
- Priori SG, Napolitano C, Schwartz PJ. Low penetrance in the long-QT syndrome: clinical impact. *Circulation* 1999;99:529.
- Wang Q, Curran ME, Splawski I, et al. Positional cloning of a novel potassium channel gene: KVLQT1 mutations cause cardiac arrhythmias. *Nat Genet* 1996;12:17.
- Ko YL, Tai DY, Chen SA, Lee-Chen GJ, Chu CH, Lin MW. Linkage and mutation analysis in two Taiwanese families with long QT syndrome. *J Formos Med Assoc* 2001;100:767.
- Russell MW, Dick II M, Collins FS, Brody LC. KVLQT1 mutations in three families with familial or sporadic long QT syndrome. *Hum Mol Genet* 1996;5:1319.
- Tanaka T, Nagai R, Tomoike H, et al. Four novel KVLQT1 and four novel HERG mutations in familial long-QT syndrome. *Circulation* 1997;95:565.
- Napolitano C, Priori SG, Schwartz PJ, et al. Genetic testing in long QT syndrome: development and validation of an efficient approach to genotyping in clinical practice. *JAMA* 2005;294:2975.
- Itoh T, Tanaka T, Nagai R, et al. Genomic organization and mutational analysis of KVLQT1, a gene responsible for familial long QT syndrome. *Hum Genet* 1998;103:290.
- Fodstad H, Swan H, Laitinen P, et al. Four potassium channel mutations account for 73% of the genetic spectrum underlying long-QT syndrome (LQTS) and provide evidence for a strong founder effect in Finland. *Ann Med* 2004;36(Suppl 1):53.
- Splawski I, Shen J, Timothy KW, et al. Spectrum of mutations in long-QT syndrome genes. KVLQT1, HERG, SCN5A, KCNE1, and KCNE2. *Circulation* 2000;102:1178.
- Sun Z, Milos PM, Thompson JF, et al. Role of a *KCNH2* polymorphism (R1047L) in dofetilide-induced Torsades de Pointes. *J Mol Cell Cardiol* 2004;37:1031.
- Novotny T, Kadlecova J, Janousek J, et al. The homozygous *KCNQ1* gene mutation associated with recessive Romano-Ward syndrome. *Pacing Clin Electrophysiol* 2006;29:1013.
- Kanovsky J, Novotny T, Kadlecova J, Gaillyova R. A new homozygous mutation of the *KCNQ1* gene associated with both Romano-Ward and incomplete Jervell-Lange-Nielsen syndromes in two sisters. *Heart Rhythm* 2010;7:531.
- Moss AJ, Shimizu W, Wilde AA, et al. Clinical aspects of type 1 long QT syndrome by location, coding type, and biophysical function of mutations involving the *KCNQ1* gene. *Circulation* 2007;115(19):2481.
- Kapa S, Tester DJ, Salisbury BA, et al. Genetic testing for long-QT syndrome. Distinguishing pathogenic mutations from benign variants. *Circulation* 2009;120:1752.

23. Priori GS, Schwartz PJ, Napolitano C, et al. Risk stratification in the long QT syndrome. *N Engl J Med* 2003;348:1866.
24. Schwartz PJ, Priori SG, Spazzolini C, et al. Genotype-phenotype correlations in the long QT syndrome: gene-specific triggers for life-threatening arrhythmias. *Circulation* 2001;103:89.
25. Shimizu W, Noda T, Takaki H, et al. Epinephrine unmasks latent mutation carriers with LQT1 form of a congenital long-QT syndrome. *J Am Coll Cardiol* 2003;41:633.
26. Takenaka K, Ai T, Shimizu W, et al. Exercise stress test amplifies genotype-phenotype correlation in the LQT1 and LQT2 forms of the long-QT syndrome. *Circulation* 2003;107:838.
27. Wong JA, Gula LJ, Klein GJ, Yee R, Skanes AC, Krahn AD. Utility of treadmill testing in identification and genotype prediction in long-QT syndrome. *Circ Arrhythm Electrophysiol* 2010;3:120.
28. Horner JM, Horner MM, Ackerman MJ. The diagnostic utility of recovery phase QTc during treadmill exercise stress testing in the evaluation of long QT syndrome. *Heart Rhythm* 2011;8:1698.
29. Kanters JK, Haarmark C, Vedel-Larsen E, et al. TpeakTend interval in long QT syndrome. *J Electrocardiol* 2008;41:603.
30. Hodges M. Rate correction of the QT interval. *Cardiac Electrophysiol Rev* 1997;1:360.



Mazzanti A, Guz D, Trancuccio A, Pagan E, Kukavica D, Chargeishvili T, Olivetti N, Biernacka EK, Sacilotto L, Sarquella-Brugada G, Campuzano O, Nof E, Anastasakis A, Sansone VA, Jimenez-Jaimez J, Cruz F, Sánchez-Quiñones J, Hernandez-Afonso J, Fuentes ME, Średniawa B, Garoufi A, **Andršová I**, Izquierdo M, Marinov R, Danon A, Expósito-García V, Garcia-Fernandez A, Muñoz-Esparza C, Ortíz M, Zienciuk-Krajka A, Tavazzani E, Monteforte N, Bloise R, Marino M, Memmi M, Napolitano C, Zorio E, Monserrat L, Bagnardi V, Priori SG. Natural History and Risk Stratification in Andersen-Tawil Syndrome Type 1. *J Am Coll Cardiol.* 2020; 75:1772-1784.

IF 3,706. Počet citací ve Web of Science 30

Publikovaná původní práce – kvantitativní podíl uchazečky 10 % - identifikace vhodných pacientů, analýza dat, revize textu publikace.

# Natural History and Risk Stratification in Andersen-Tawil Syndrome Type 1



Andrea Mazzanti, MD, PhD,<sup>a,b,c</sup> Dmitri Guz, MD,<sup>a</sup> Alessandro Trancuccio, BS,<sup>b</sup> Eleonora Pagan, MSc,<sup>d</sup> Deni Kukavica, MD,<sup>a,b</sup> Tekla Chargeishvili, MD,<sup>a,b</sup> Natalia Olivetti, MD,<sup>a</sup> Elżbieta Katarzyna Biernacka, MD, PhD,<sup>e</sup> Luciana Sacilotto, MD,<sup>f</sup> Georgia Sarquella-Brugada, MD, PhD,<sup>g</sup> Oscar Campuzano, PhD,<sup>h</sup> Eyal Nof, MD,<sup>i</sup> Aristides Anastasakis, MD,<sup>j</sup> Valeria A. Sansone, MD, PhD,<sup>k</sup> Juan Jimenez-Jaimez, MD,<sup>l</sup> Fernando Cruz, MD,<sup>m</sup> Jessica Sánchez-Quiñones, MD,<sup>n</sup> Julio Hernandez-Afonso, MD,<sup>o</sup> Maria Eugenia Fuentes, MD,<sup>p</sup> Beata Średniawa, MD,<sup>q</sup> Anastasia Garoufi, MD, PhD,<sup>r</sup> Irena Andršová, MD, PhD,<sup>s</sup> Maite Izquierdo, MD, PhD,<sup>t</sup> Rumen Marinov, MD, PhD,<sup>u</sup> Asaf Danon, MD,<sup>v</sup> Victor Expósito-García, MD,<sup>w</sup> Amaya Garcia-Fernandez, MD,<sup>x</sup> Carmen Muñoz-Esparza, MD,<sup>y</sup> Martín Ortíz, MD,<sup>z</sup> Agnieszka Zienciuk-Krajka, MD,<sup>aa</sup> Elisa Tavazzani, PhD,<sup>b</sup> Nicola Monteforte, MD,<sup>a</sup> Raffaella Bloise, MD,<sup>a</sup> Maira Marino, RN,<sup>a</sup> Mirella Memmi, BSc,<sup>a</sup> Carlo Napolitano, MD, PhD,<sup>a,b,c</sup> Esther Zorio, MD, PhD,<sup>bb</sup> Lorenzo Monserrat, MD, PhD,<sup>z</sup> Vincenzo Bagnardi, PhD,<sup>d</sup> Silvia G. Priori, MD, PhD<sup>a,b,c,cc</sup>

## ABSTRACT

**BACKGROUND** Andersen-Tawil Syndrome type 1 (ATS1) is a rare arrhythmogenic disorder, caused by loss-of-function mutations in the *KCNJ2* gene. We present here the largest cohort of patients with ATS1 with outcome data reported.

**OBJECTIVES** This study sought to define the risk of life-threatening arrhythmic events (LAE), identify predictors of such events, and define the efficacy of antiarrhythmic therapy in patients with ATS1.

**METHODS** Clinical and genetic data from consecutive patients with ATS1 from 23 centers were entered in a database implemented at ICS Maugeri in Pavia, Italy, and pooled for analysis.

**RESULTS** We enrolled 118 patients with ATS1 from 57 families (age  $23 \pm 17$  years at enrollment). Over a median follow-up of 6.2 years (interquartile range: 2.7 to 16.5 years), 17 patients experienced a first LAE, with a cumulative probability of 7.9% at 5 years. An increased risk of LAE was associated with a history of syncope (hazard ratio [HR]: 4.54;  $p = 0.02$ ), with the documentation of sustained ventricular tachycardia (HR 9.34;  $p = 0.001$ ) and with the administration of amiodarone (HR: 268;  $p < 0.001$ ). The rate of LAE without therapy (1.24 per 100 person-years [py]) was not reduced by beta-blockers alone (1.37 per 100 py;  $p = 1.00$ ), or in combination with Class Ic antiarrhythmic drugs (1.46 per 100 py,  $p = 1.00$ ).

**CONCLUSIONS** Our data demonstrate that the clinical course of patients with ATS1 is characterized by a high rate of LAE. A history of unexplained syncope or of documented sustained ventricular tachycardia is associated with a higher risk of LAE. Amiodarone is proarrhythmic and should be avoided in patients with ATS1. (J Am Coll Cardiol 2020;75:1772-84)  
© 2020 Published by Elsevier on behalf of the American College of Cardiology Foundation.



Listen to this manuscript's audio summary by Editor-in-Chief Dr. Valentin Fuster on JACC.org.

From the <sup>a</sup>Molecular Cardiology, IRCCS ICS Maugeri, Pavia, Italy; <sup>b</sup>Department of Molecular Medicine, University of Pavia, Pavia, Italy; <sup>c</sup>European Reference Network for Rare and Low Prevalence Complex Diseases of the Heart; <sup>d</sup>Department of Statistics and Quantitative Methods, University of Milan-Bicocca, Milan, Italy; <sup>e</sup>Department of Congenital Heart Diseases, National Institute of Cardiology, Warsaw, Poland; <sup>f</sup>Department of Cardiology, Hospital das Clinicas Faculdade de Medicina Universidade de São Paulo (HCFMUSP), São Paulo, Brazil; <sup>g</sup>Arrhythmia Inherited Cardiac Diseases and Sudden Death Unit, Hospital Sant Joan de Déu, Barcelona, Spain; <sup>h</sup>Cardiovascular Genetics Center-Gencardio, IDIBGI Medical Sciences Department, Medical School, University of Girona, Girona, Spain; <sup>i</sup>Leviv Heart Center, Chaim Sheba Medical Center Affiliated to Sackler Medical School, Tel-Aviv University, Tel Hashomer, Israel; <sup>j</sup>Department of Cardiology, Onassis Cardiac Surgery Center, Athens, Greece; <sup>k</sup>NEMO Center, Neuro-rehabilitation Unit, University of Milan, ASST Niguarda Hospital, Milan, Italy; <sup>l</sup>Department of Cardiology, Virgen de las Nieves University Hospital, Granada, Spain; <sup>m</sup>Arrhythmia and Electrophysiology Unit, Instituto Nacional de Cardiologia, Rio de Janeiro, Brazil; <sup>n</sup>Department of Cardiology, Hospital de Vinalopó, Elche, Spain; <sup>o</sup>Department of Cardiology, Hospital Universitario Nuestra Señora de Candelaria, Santa Cruz de Tenerife, Canary Islands, Spain; <sup>p</sup>Department of Cardiology, Hospital Infanta Cristina, Badajoz, Spain; <sup>q</sup>Department of Cardiology, Medical University of Silesia, Katowice, Poland; <sup>r</sup>Second Department of Pediatrics, National and Kapodistrian University of Athens, "P&A Kyriakou" Children's Hospital, Athens, Greece; <sup>s</sup>Department of Internal Medicine and Cardiology, University Hospital Brno and Faculty of Medicine of Masaryk University, Brno, Czech Republic; <sup>t</sup>Department of Cardiology, Hospital Clinico Universitario, Valencia, Spain; <sup>u</sup>Department of Pediatrics, University of Medicine Hospital,

**A**ndersen-Tawil Syndrome type 1 (ATS1) (1,2) is a rare (3) autosomal dominant disorder, characterized by dysmorphic features, periodic muscular weakness, and frequent ventricular arrhythmias (VA). The disease is caused by *loss-of-function* mutations in the *KCNJ2* gene (4), encoding for the potassium channel Kir2.1 that conducts the inward rectifier current  $I_{K1}$ , exerting a pivotal role in the late phase of ventricular repolarization (5).

Although patients with ATS1 often manifest a remarkable arrhythmic burden (1,2), their prognosis is generally considered “relatively good” (6). However, the disease has a low prevalence, estimated at a minimum of 1 case per million (3), and consequently information on the clinical course derive from case series that are either small (7) or devoid of outcome data (8).

The present study, based on the largest cohort of patients with ATS1 with outcome data reported in the literature, allows a robust assessment of long-term prognosis and identifies for the first time risk factors for the occurrence of life-threatening arrhythmic events (LAE) at follow-up. Furthermore, we demonstrate that beta-blockers and Class Ic antiarrhythmic drugs fail to reduce LAE, whereas amiodarone increases the rate of LAE and should be avoided. Overall, our data provide new information that will influence the management of patients with ATS1.

SEE PAGE 1785

## METHODS

**DATA COLLECTION AND DATA SHARING.** The study population included 118 individuals (57 probands and their 61 affected relatives) with a diagnosis of ATS1 (9) and bearing a pathogenic or a likely pathogenic *KCNJ2* mutation (10). Anonymous clinical data were acquired since the first visit by investigators from 23 centers in 9 countries and filed in a registry developed at the coordinating center in Pavia. Data in the registry included demographic information, personal and

family history of symptoms, arrhythmic events, electrocardiographic (ECG) parameters, therapies at enrollment and during follow-up, and data related to extracardiac manifestations of ATS1 (muscular weakness and dysmorphic traits).

Because no guidelines for the management of ATS1 exist, referring physicians prescribed therapy according to clinical judgment. Treatment options included beta-blockers, alone or in combination with Class Ic antiarrhythmic drugs (flecainide and propafenone), and amiodarone.

The study was approved by the ethics committee of ICS Maugeri, Pavia, Italy, and enrolling centers obtained project approval by local ethical committees. All patients provided informed consent for genetic and clinical studies.

The goals of the study were to:

1. characterize the molecular profile and the impact of the genetic substrate on the phenotype of patients with ATS1;
2. quantify the risk of LAEs (sudden cardiac death [SCD], aborted cardiac arrest, or hemodynamically nontolerated ventricular tachycardia [VT] [11]) at follow-up;
3. identify risk factors for the occurrence of a first LAE at follow-up; and
4. assess the response to conventional antiarrhythmic therapy.

A list of the definitions used is presented in [Supplemental Table 1](#).

**GENETIC ANALYSIS AND INTERPRETATION OF DNA VARIANTS.** Genetic analysis was performed by national competent bodies and genetic variants identified were independently evaluated by 2 expert laboratories (ICS Maugeri, IRCCS Pavia, Italy, and Health in Code, La Coruña, Spain) according to current criteria (10). Only carriers of variants adjudicated

## ABBREVIATIONS AND ACRONYMS

<b>ATS1</b>	= Andersen-Tawil Syndrome type 1 with <i>KCNJ2</i> mutation
<b>BidVT</b>	= bidirectional VT
<b>CI</b>	= confidence interval
<b>CPVT</b>	= catecholaminergic polymorphic ventricular tachycardia
<b>ECG</b>	= electrocardiogram
<b>HR</b>	= hazard ratio
<b>ICD</b>	= implantable cardioverter defibrillator
<b>IQR</b>	= interquartile range
<b>LAE</b>	= life-threatening arrhythmic event
<b>LQTS</b>	= long QT syndrome
<b>py</b>	= person-years
<b>SCD</b>	= sudden cardiac death
<b>VA</b>	= ventricular arrhythmia
<b>VT</b>	= ventricular tachycardia
<b>VTs</b>	= sustained ventricular tachycardia

Stara Zagora, Bulgaria; <sup>v</sup>Department of Cardiology, Hillel Yaffe Medical Center, Hadera, Israel; <sup>w</sup>Department of Cardiology, Marqués de Valdecilla University Hospital, Santander, Spain; <sup>x</sup>Department of Cardiology, Hospital General Universitario de Alicante, Alicante, Spain; <sup>y</sup>Department of Cardiology, Hospital Clínico Universitario Virgen de La Arrixaca, Murcia, Spain; <sup>z</sup>Health in Code, La Coruña, Spain; <sup>aa</sup>Department of Cardiology and Electrotherapy, Medical University of Gdansk, Gdansk, Poland; <sup>bb</sup>Department of Cardiology, Hospital Universitario y Politécnico La Fe, Valencia, Spain and Center for Biomedical Network Research on Cardiovascular Diseases (CIBERCV), Madrid, Spain; and the <sup>cc</sup>Molecular Cardiology, Fundación Centro Nacional de Investigaciones Cardiovasculares, Madrid, Spain. Dr. Andrišová has been supported by the Ministry of Health, Czech Republic, Conceptual Development of Research Organization (Grant FNBr/65269705). Dr. Priori has been supported by the Ricerca Corrente Funding scheme of the Italian Ministry of Health and the Italian Ministry of Research and University Dipartimenti di Eccellenza 2018–2022 grant to the Molecular Medicine Department (University of Pavia). Dr. Ortiz has received personal fees and has been a consultant to Health in Code. Dr. Monserrat is a stockholder in Health in Code. All other authors have reported that they have no relationships relevant to the contents of this paper to disclose. P.K. Shah, M.D., served as Guest Associate Editor for this paper.

**TABLE 1 Characteristics of the Study Population (N = 118) at Diagnosis**

	Overall Population (N = 118)		Probands (n = 57)		Family Members (n = 61)	
	Evaluated	Finding	Evaluated	Finding	Evaluated	Finding
<b>Demographics</b>						
Female	118 (100)	80 (68)	57 (100)	47 (82)	61 (100)	33 (54)
Age, yrs	118 (100)	23 ± 18	57 (100)	20 ± 15	61 (100)	24 ± 21
Follow-up time, yrs	118 (100)	11 ± 12	57 (100)	11 ± 10	61 (100)	10 ± 14
Syncope	118 (100)	19 (16)	57 (100)	12 (21)	61 (100)	7 (11)
<b>Extracardiac features</b>						
Dysmorphic features	118 (100)	89 (75)	57 (100)	45 (79)	61 (100)	44 (72)
Muscular weakness	118 (100)	41 (35)	57 (100)	25 (44)	61 (100)	16 (26)
<b>ECG parameters</b>						
Heart rate, bpm	108 (92)	76 ± 20	53 (93)	76 ± 21	55 (90)	76 ± 20
PR interval, ms	108 (92)	141 ± 28	53 (93)	141 ± 27	55 (90)	142 ± 29
QRS interval, ms	108 (92)	89 ± 16	53 (93)	91 ± 14	55 (90)	87 ± 17
QTc interval, ms	86 (73)	424 ± 42	40 (70)	422 ± 39	46 (75)	425 ± 44
QUc interval, ms	76 (64)	647 ± 61	34 (60)	662 ± 53	42 (69)	635 ± 64
U wave amplitude, mV	76 (64)	1.21 ± 0.6	34 (60)	1.16 ± 0.5	42 (69)	1.25 ± 0.68
U wave duration, ms	76 (64)	199 ± 49	34 (60)	205 ± 47	42 (69)	194 ± 50
<b>Cardiac arrhythmias</b>						
PVCs/24 h	84 (71)	14,399 ± 17,408	45 (79)	19,690 ± 19,824	39 (64)	8,293 ± 11,638
VTns	109 (92)	69 (63)	50 (88)	40 (80)	59 (97)	29 (49)
VTs	109 (92)	13 (12)	50 (88)	9 (18)	59 (97)	4 (7)

Values are n (%) or mean ± SD.  
bpm = beats per minute; ECG = electrocardiogram; PVCs = premature ventricular contractions; QTc = corrected QT interval; QUc = corrected QU interval; VTns = nonsustained ventricular tachycardia; VTs = sustained VT.

as pathogenic or likely pathogenic by both teams were included in the study.

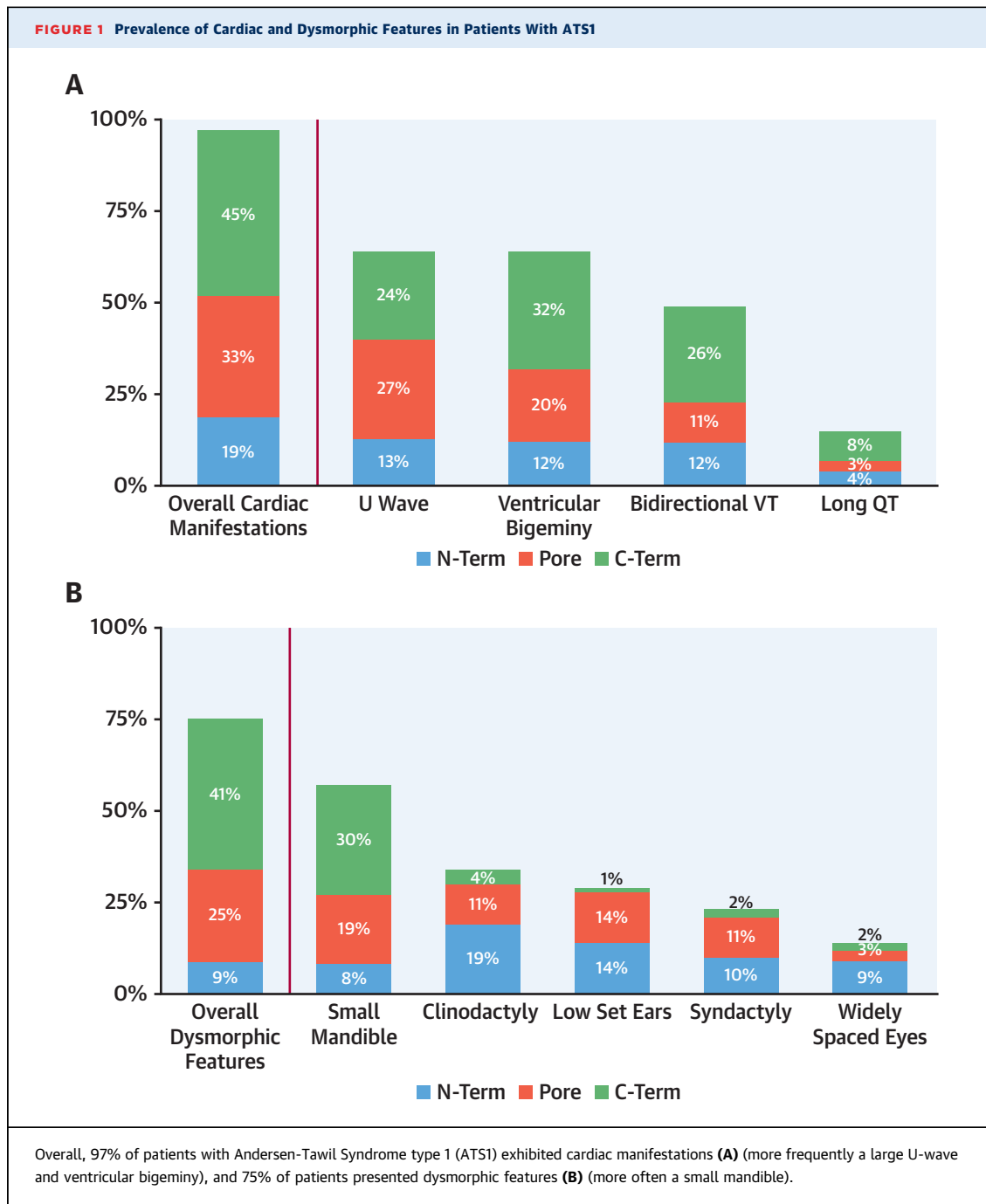
Following the identification of a causative variant in each proband, cascade genetic screening identified a total of 61 genetically affected relatives in 30 (57%) of the 53 kindreds accepting the screening.

The amino acid sequence of the protein was obtained from “Uniprot” to define the location of mutations within the Kir2.1 channel. For the topological characterization of mutations, we included residues 1 to 80 in the “N-terminal” cytoplasmic segment, residues 81 to 182 in the “pore region,” and residues 183 to 428 in the “C-terminal” cytoplasmic domain (12). Furthermore, because phosphatidylinositol bisphosphate binding sites are frequent targets of mutations causing ATS1 (13), we explored whether mutations affecting these residues (H53, R67, R82, K182, K185, K187, K188, R189, T192, L217, R218, K219, R228, H271, R312, W322 [14–16]) were associated with specific phenotypical aspects.

**STATISTICAL ANALYSIS.** Categorical data were reported with frequencies and percentages; continuous data were reported with mean ± SD or median (interquartile range [IQR]). Chi-square test and Student’s *t*-test were used to compare categorical and continuous data, respectively.

To depict the natural history of our patients, we considered 96 (81%) of 118 patients in our registry who had a valid observation time free from antiarrhythmic therapies (beta-blockers alone and in combination with Class Ic antiarrhythmic drugs, and amiodarone). Because our cohort was assembled at the time of diagnosis of ATS1, patients diagnosed at older ages, by virtue of having survived to the time of diagnosis, could not have had an event between birth and the time of diagnosis. To avoid this survivorship bias, we excluded patients from the risk set between birth and diagnosis of ATS1 and considered only the time during which patients were followed prospectively. Time to first LAE was defined from the first medical contact to the occurrence of the first LAE. Patients were censored at initiation of antiarrhythmic therapy, at last visit, or at the occurrence of death for nonarrhythmic causes. We adapted the Kaplan-Meier estimator of the LAE-free survival function, with age as the time scale, to the presence of left truncated observations (17).

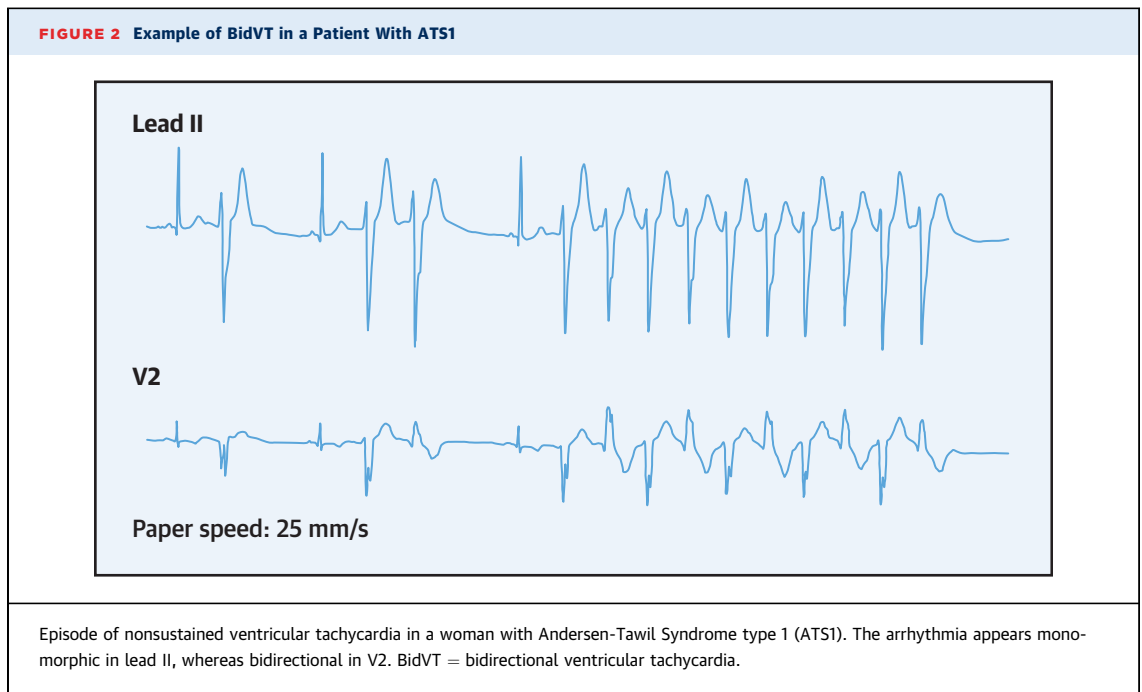
Furthermore, because no antiarrhythmic treatment has demonstrated to influence the outcome of patients with ATS1, we repeated the survival analysis including all the 118 patients in the



database, without interrupting the observation at initiation of antiarrhythmic treatment. On this second analysis we applied univariable Cox proportional hazards models to identifying risk factors for a first LAE. In cases of zero events among strata, the exact Poisson regression model was used. Multivariable Cox model was then used to estimate the independent effects of syncope, hemodynamically tolerated sustained VT (VTs) and

antiarrhythmic therapy on the risk of experiencing a first LAE.

To investigate the effect of antiarrhythmic treatment on the risk of LAE, we used a modified Kaplan-Meier method (18) that estimates the cumulative hazard rates of events according to the presence or absence of treatment over time. We fitted an univariable Cox regression model in which a patient's status (off- or on-therapy) was updated, and the



results expressed as hazard ratio (HR) with 95% confidence interval (CI), expressing the rate of LAE during the off-therapy time to the rate of LAE during the on-therapy time. Because some patients experienced multiple LAEs during observation, a robust sandwich estimator for the covariance matrix of the Cox regression coefficients was used to account for within-patient correlation. For the comparison between rates of LAE observed off-therapy and on-therapy with specific classes of drugs (beta-blockers, beta-blockers combined with Class Ic antiarrhythmic drugs, amiodarone), the exact Poisson regression model was used.

Statistical analysis was performed using SAS version 9.4 (SAS Institute, Cary, North Carolina). Two-tailed p values were calculated with the statistical significance threshold set at  $p < 0.05$ .

## RESULTS

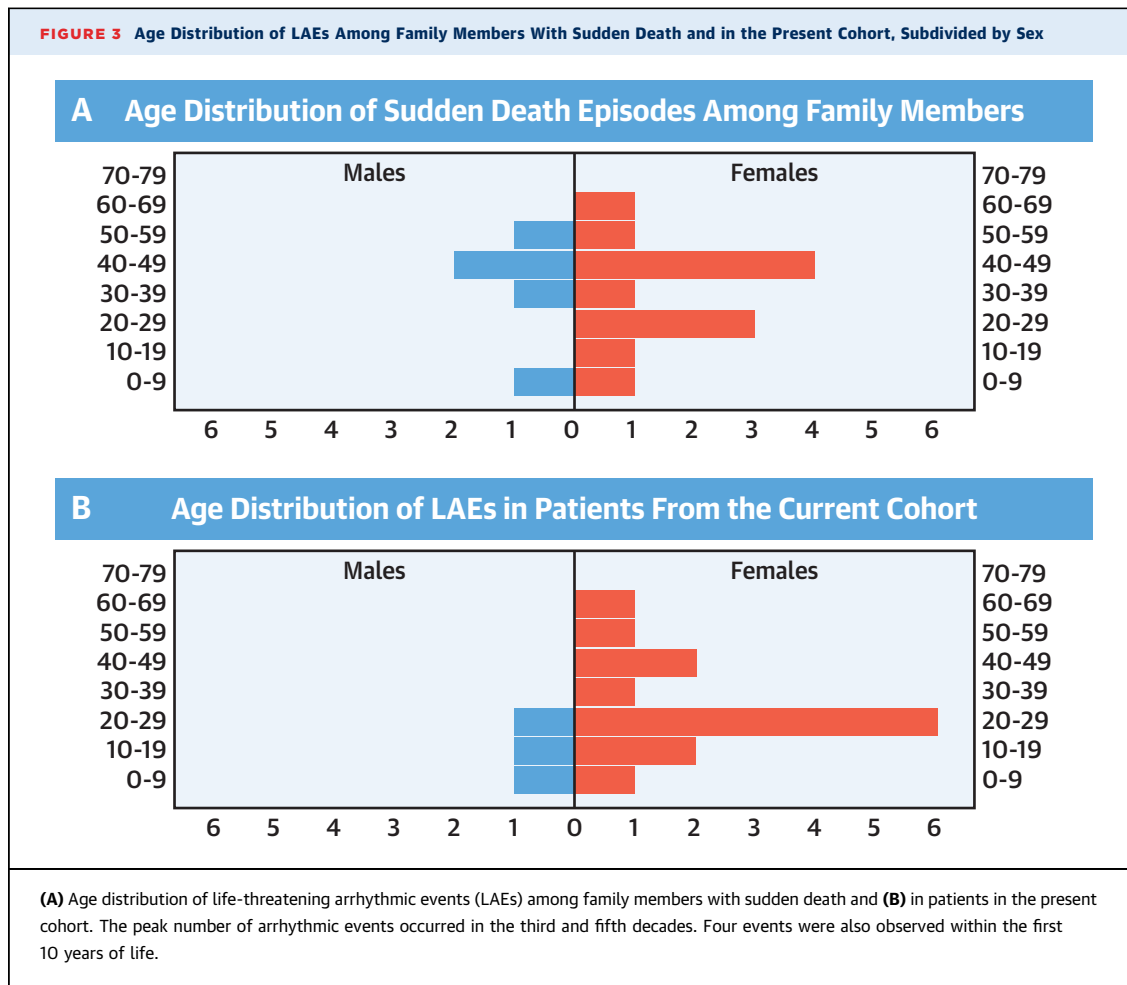
**STUDY POPULATION.** The population included 57 probands (82% female; age at first visit  $20 \pm 15$  years, range 1.5 years to 51 years) and their 61 affected relatives (54% female; age  $24 \pm 21$  years, range 1 month to 69 years). Characteristics of the population are presented in [Table 1](#). The reasons that brought the probands to medical attention included the documentation of frequent VA ( $n = 38$  of 57, 66%), recurrent muscular weakness ( $n = 9$  of 57, 16%), unexplained syncopal spells ( $n = 9$  of 57, 16%), or a suspicion of long QT syndrome (LQTS,  $n = 1$  of 57, 2%).

Overall, 114 (97%) of 118 patients presented 1 or more of the cardiac manifestations typical of ATS ([Figure 1A](#)); in addition, 89 (75%) of 118 patients showed dysmorphic features described in ATS ([Figure 1B](#)), and 41 (35%) of 118 had recurrent episodes of muscular weakness. The ECG features are presented in the [Supplemental Appendix](#).

A total of 77 patients with ATS1 had the documentation of VTs and/or nonsustained VT during their clinical evaluation, and in 58 (75%) of 77 of them we recorded episodes of bidirectional VT (BidVT). In most cases, the episodes of BidVT were observed as brief “interludes” that interrupted prolonged episodes of polymorphic VT ([Figure 2](#)).

A family history of sudden death was present in 11 (19%) of 57 kindreds, with a total of 19 individuals (68% female), who died suddenly at  $29 \pm 18$  years of age ([Figure 3A](#)). All sudden death cases occurred in families in which the *KCNJ2* mutation segregated with the ATS1 phenotype. As illustrated in [Figure 3B](#), the highest incidence of LAEs in our population occurred between the third and the fifth decades. Remarkably, in 4 cases, the arrhythmic events occurred within the first decade of life, suggesting that the disease may manifest with LAE during childhood.

**RESULTS OF GENETIC SCREENING AND GENOTYPE TO PHENOTYPE CORRELATIONS.** Genetic screening identified 35 pathogenic or likely pathogenic *KCNJ2* mutations in the 57 probands ([Figure 4](#), [Supplemental Table 2](#)). In 14 (35%) of 40 families in which both



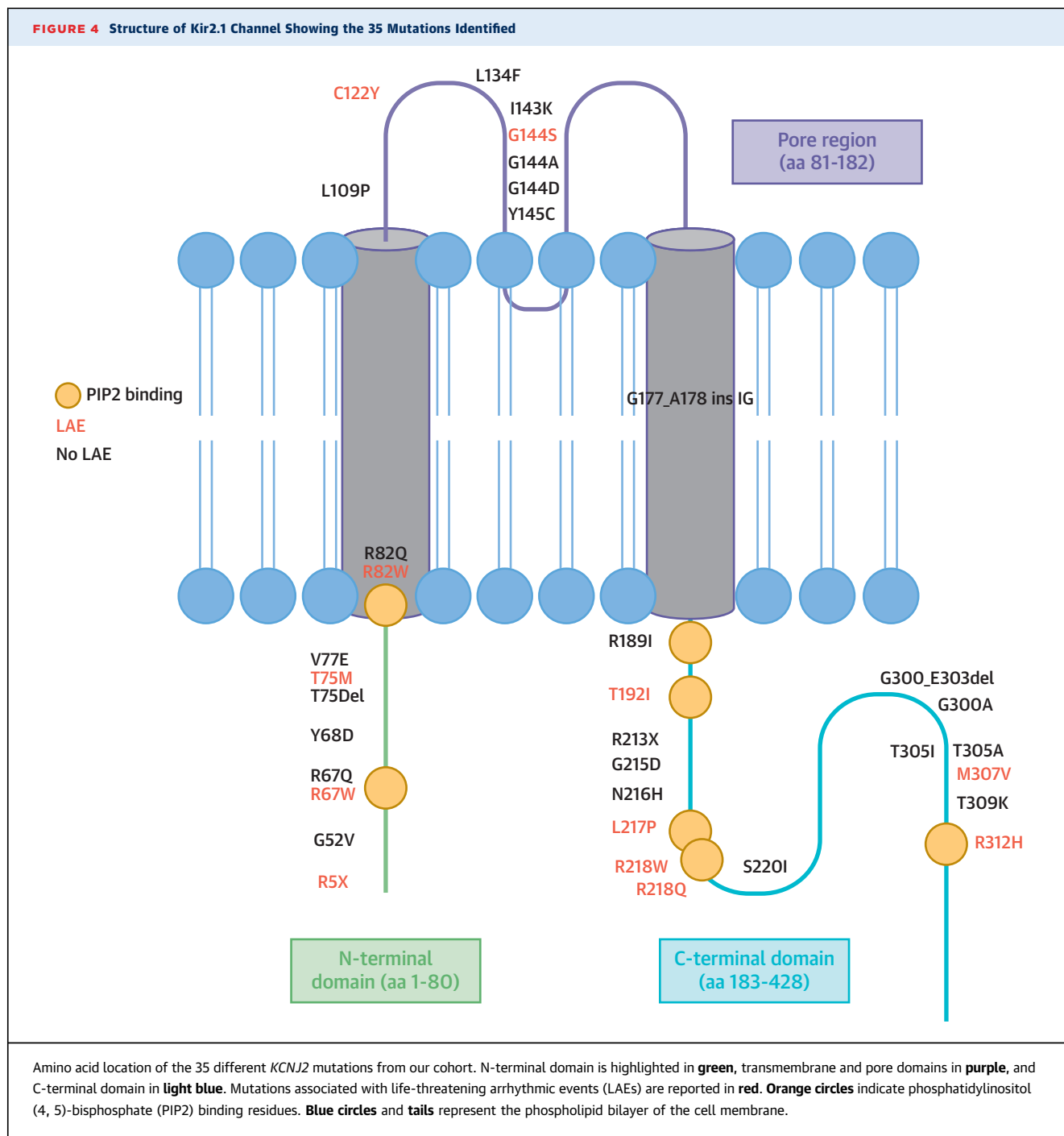
parents of the proband were available for genetic screening, the causative *KCNJ2* mutation was “likely de novo” (10). Overall, 28 (80%) of 35 variants have been reported as pathogenic or likely pathogenic in the literature, whereas 7 (20%) of 35 mutations are newly described here (Supplemental Table 2). We retrieved from the literature studies characterizing the electrophysiological properties of 22 (79%) of 28 previously described mutations (details about their effect on the  $I_{K1}$  current are provided in Supplemental Table 2).

The mutations identified in our cohort spanned all regions of the Kir2.1 channel: 8 (23%) of 35 mutations were in the N-terminal, 11 (31%) of 35 in the pore domain, and 16 (46%) of 35 in the C-terminal (Figure 4). The mutations clustered in 2 regions: the phosphatidylinositol bisphosphate binding residues (14-16), where 10 mutations were found in 25 probands, and the filter area of the pore domain (residues 141 to 156), where we found 4 mutations in 5 probands in position 144 to 145.

Interestingly, patients with mutations in the C-terminal manifested a higher prevalence of skeletal dysmorphisms (48 of 54 patients, 89%), as compared with pore domain (30 of 41 patients, 73%) and N-terminal mutation carriers (11 of 23 patients, 48%;  $p = 0.001$ ).

**OUTCOME OF PATIENTS WITH ATs1.** To obtain information on the occurrence of LAE before therapy, we pooled treatment-free intervals from 96 of 118 patients observed over a median time of 1.4 years (IQR: 0.2 to 6.5 years). Overall, 7 (7.3%) of 96 patients experienced a first LAE, with a LAE rate of 1.1% per year (7 LAEs over 652 person-years [py] of observation). The cumulative probability of experiencing a first LAE since birth was 9.5% (95% CI: 0% to 25.6%) and 20.2% (95% CI: 0% to 38.6%) at 20 and 40 years, respectively (Figure 5A).

We then aimed to understand the rate of occurrence of a first LAE during the entire observation

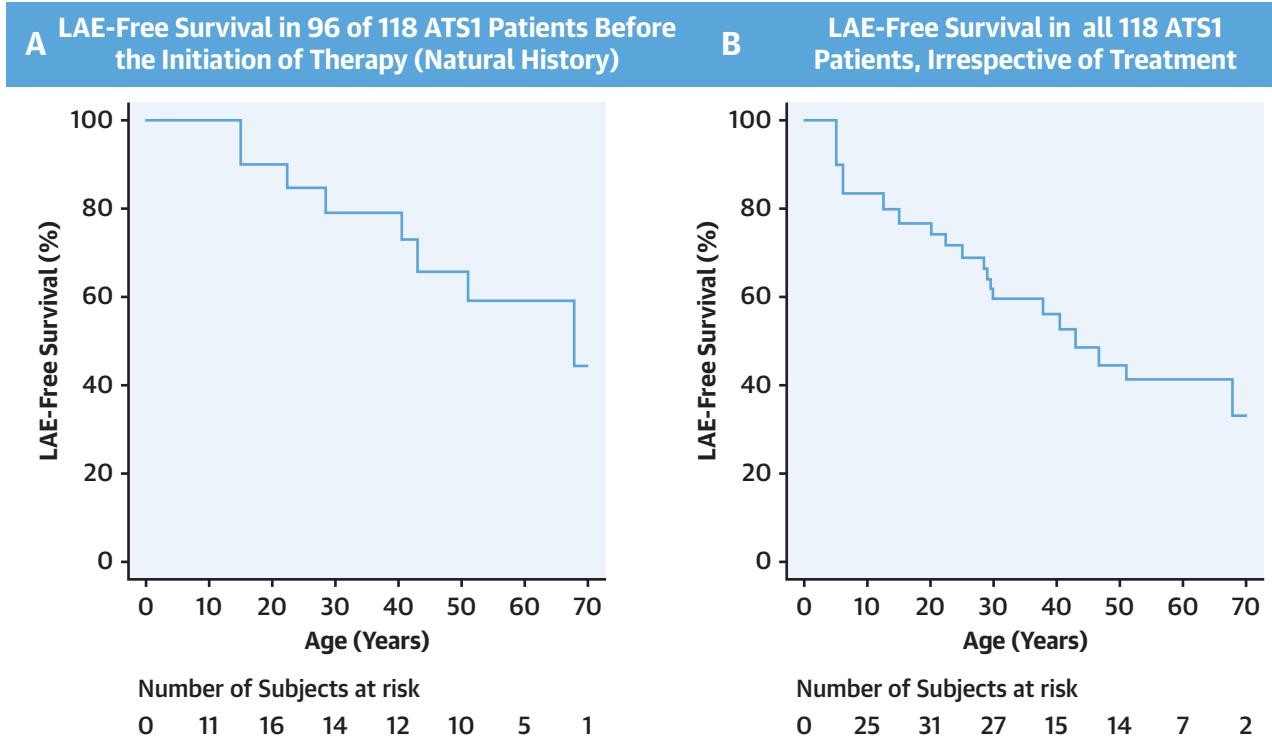


time of the cohort, irrespective of treatment. The analysis included all 118 patients, observed over a median of 6.2 years (IQR: 2.7 to 16.5 years; mean follow-up  $10.5 \pm 11.8$  years). Overall, 17 (14%) of 118 patients (14 of 17 females, 82%) experienced a first LAE, with a rate of LAE of 1.5% per year (17 first

events in 118 patients over 1,139 py; age at first LAE  $30 \pm 17$  years, age range: 5 to 68 years). The cumulative probability of experiencing a first LAE was 7.9% (95% CI: 4% to 15.3%) at 5 years of follow-up (Figure 5B). Of the 17 patients who experienced a first LAE, 2 (12%) died suddenly at age 28 and 43



**FIGURE 5 LAEs at Follow-Up**



Kaplan-Meier estimate of cumulative survival free from the first life-threatening arrhythmic event (LAE). **(A)** Data from 96 patients followed up in the absence of antiarrhythmic therapy (natural history). **(B)** Data from all the 118 patients included in the study, irrespective of treatment. The number of patients at risk are reported under the curves.

years, 9 (53%) were rescued by external defibrillation, and 6 (35%) experienced a syncopal episode presented with fast VTs, which reverted spontaneously to sinus rhythm. In 8 patients, the LAE occurred at rest, in 5 patients during mild exertion, and in 1 subject the event was prompted by sudden emotional stress. LAE circumstances are unknown for 3 patients. Four (27%) of the 15 patients surviving a first LAE experienced multiple LAEs during their life (median 3, IQR: 2.3 to 3.8).

**IDENTIFICATION OF RISK FACTORS FOR A FIRST LAE.** The univariable analysis (Table 2) showed that a history of syncope, the documentation of hemodynamically tolerated sustained VT, and therapy with amiodarone were associated with an increased risk of experiencing a first LAE. Although the percentage of women who experienced 1 or more episodes of LAE was higher than that of male patients, female sex was not found as a risk factor for the occurrence of LAEs in univariable analysis (Supplemental Results, Supplemental Table 3). Interestingly, neither beta-

blockers alone nor in combination with Class Ic antiarrhythmics modified the risk of experiencing a first LAE.

Cox multivariable analysis confirmed a significant increase in the risk of LAE associated with a previous history of syncope (HR: 4.5; 95% CI: 1.3 to 15.9;  $p = 0.02$ ), with the documentation of sustained VTs (HR: 9.3; 95% CI: 2.5 to 35.1;  $p = 0.001$ ) and with the administration of amiodarone (HR: 268; 95% CI: 20.5 to 3,507;  $p < 0.001$ ) (Table 3).

**IMPACT OF PHARMACOLOGIC TREATMENT ON THE CLINICAL COURSE.** We analyzed the annual rate of all LAEs that occurred while patients received antiarrhythmic therapies: in this analysis, we included not only the first LAE, but all LAEs occurring throughout the observation period. Overall, the analysis included 1,290 py of observation, during which 26 LAEs were recorded, with an overall event rate of 2.0 per 100 py.

During this period, 76 patients had treatment periods of only beta-blockers (the most used

**TABLE 2 Univariable Cox Regression Analysis for the Occurrence of First LAE**

	n	Events/py	Rate × 100 py	HR	95% CI	p Value
<b>Sex</b>						
Female	80	14/809	1.73	Ref.		
Male	38	3/330	0.91	0.56	0.16-1.97	0.37
<b>Syncope (time dependent)*</b>						
No		8/871	0.92	Ref.		
Yes		9/268	3.36	4.05	1.48-11.1	0.006
<b>Basal QTc†</b>						
<460 ms	69	8/539	1.48	Ref.		
≥460 ms	17	3/248	1.21	0.71	0.15-3.38	0.67
<b>U duration‡</b>						
≤200 ms	51	5/400	1.25	Ref.		
>200 ms	32	5/353	1.42	1.50	0.40-5.65	0.55
<b>VTs/VTns§</b>						
No VT	38	0/345	0	Ref.		
VTns	58	9/613	1.47	n.e.	—	0.04
VTs	13	6/82	7.32	n.e.	—	<0.001
<b>Gene region</b>						
Pore	41	4/324	1.23	Ref.		
N-terminal	23	4/181	2.21	2.44	0.55-10.9	0.24
C-terminal	54	9/633	1.42	1.63	0.44-6.12	0.47
<b>Mutations in PIP2 binding residues #</b>						
No	65	7/701	1.00	Ref.		
Yes	45	9/413	2.18	2.54	0.90-7.18	0.08
<b>Therapy (time dependent)</b>						
No therapy		7/681	1.03	Ref.		
BB		2/293	0.68	0.66	0.13-3.30	0.61
BB + AA Class I		1/135	0.74	0.77	0.09-6.5	0.81
Amiodarone		5/12	41.7	39.7	8.97-175	<0.001

\*19 patients (16.1%) had syncope before/at first visit, 14 patients (11.9%) had syncope during follow-up. †Data from 86 patients. ‡Data from 83 patients. §Data from 109 patients. ||Exact Poisson p value. #8 patients with non-missense mutations were excluded.

AA = antiarrhythmic drugs; BB = beta-blockers; CI = confidential interval; HR = hazard ratio; LAE = life-threatening arrhythmic event; PIP2 = phosphatidylinositol (4,5)-bisphosphate; Ref. = reference; n.e. = not estimated; py = person years; VTns = nonsustained ventricular tachycardia; VTs = sustained ventricular tachycardia.

drugs were propranolol, metoprolol, nadolol, and bisoprolol, at a daily dosage of  $2.2 \pm 1.6$  mg/kg,  $1.7 \pm 1.2$  mg/kg,  $1.3 \pm 0.8$  mg/kg, and  $0.3 \pm 0.7$  mg/kg, respectively); 34 patients had at least 1 period of treatment with beta-blockers associated with Class Ic antiarrhythmic drugs (propafenone and flecainide, at a daily dosage of  $6.5 \pm 3.1$  mg/kg and  $2.5 \pm 1.3$  mg/kg, respectively); and 10 patients received amiodarone (at a daily dosage of  $5.6 \pm 2.9$  mg/kg).

Ninety-nine patients had at least 1 period without therapy, for a total observation time of 723 py (Table 4). As compared with the overall rate of LAE occurring in the absence of therapy (1.24 per 100 py), the rate of LAEs remained almost unchanged during treatment with beta-blockers alone (1.37 per 100 py;  $p = 1.00$ ) or in combination with Class Ic antiarrhythmic drugs (1.46 per 100 py;  $p = 1.00$ ). Interestingly, when we analyzed the effect of beta-blocker and Class I antiarrhythmic drugs in 12 patients with a

Holter ECG recorded before and after the initiation of therapy, we obtained a signal of the efficacy of treatment in reducing the burden of ventricular extrasystoles ( $15,940 \pm 17,106$  before treatment to  $3,459 \pm 8,849$  after treatment,  $p = 0.018$ ); nonetheless, 2 of these patients who showed a reduction of extrasystole count experienced a cardiac arrest while on treatment.

Finally, the use of amiodarone was associated with a higher rate of LAEs (24 per 100 py of treatment,  $p < 0.001$ ) (Supplemental Table 4).

#### IMPLANTABLE CARIOVERTER DEFIBRILLATORS.

Twenty-four patients received an implantable cardioverter defibrillator (ICD) (18 female patients, 75%); 7 (29%) of them were implanted after surviving an LAE, and 17 (71%) received the device in primary prevention of SCD. During a median follow-up of 7.3 years (IQR: 3.1 to 12.6 years), 4 (17%) of 24 patients experienced 1 or more appropriate ICD shocks on LAE (incidence rate of 2.2 per 100 py): 3 of them were implanted in secondary prevention, and 1 in primary prevention of SCD. In this latter case, 2 ICD shocks were ineffective in interrupting ventricular fibrillation, and the patient was rescued by external defibrillation. During the same period, 3 (13%) of 24 patients experienced 1 inappropriate shock each. Two (8%) patients experienced major complications, requiring surgical intervention.

#### DISCUSSION

ATS1 is a rare hereditary arrhythmic disease characterized by extracardiac manifestations, including periodic paralysis and a variety of skeletal and facial dysmorphisms (1). The disease is caused by *loss-of-function* mutations in the *KCNJ2* gene (4), encoding for the Kir2.1 channel that conducts the cardiac inward rectifier current  $I_{K1}$  and contributes to the duration of action potential and to the maintenance of resting membrane potentials in cardiac myocytes (5). Although it may seem complicated to attribute such a heterogeneous set of clinical manifestations to the reduction of a single ionic current, it has emerged that the loss of  $I_{K1}$  current and the attendant depolarization of the resting membrane potential of cardiac cells, skeletal muscle fibers, and ectodermal tissue that generate craniofacial structures may be the connecting element of the syndromic manifestations of ATS1 (4,19-21).

In cardiac cells, the reduction of  $I_{K1}$  depolarizes cardiac cells, facilitating the development of triggered activity mediated by delayed afterdepolarizations secondary to altered  $[Ca^{2+}]_i$  cycling (20). From a different standpoint, in 2001, Plaster

et al. (4), when discovering the role of *KCNJ2* loss-of-function mutations in ATS1, hypothesized that depolarization of the fibers of skeletal muscle causes reduced availability of sodium channels, thus preventing the ability of the muscle to contract and generating periodic paralysis. Finally, with regard to craniofacial abnormalities, it was only in 2016 that Adams et al. (21) demonstrated that expression of ATS1 *KCNJ2* mutations with the loss of  $I_{K1}$  current in *Xenopus laevis* embryos causes craniofacial abnormalities, by altering the physiological distribution of membrane voltage.

**DIAGNOSTIC HALLMARKS OF ATS1.** Despite that ATS1 was initially considered a variant of LQTS, it is clear that the presence of a prolonged QT interval is not mandatory to establish the diagnosis. Rather, other ECG aspects may help to identify patients with ATS1 (Central Illustration). The presence of prominent U waves, possibly related to the reduction of  $I_{K1}$  current (22), is a pivotal hallmark of the disease, albeit it may also be present in patients with catecholaminergic polymorphic ventricular tachycardia (CPVT). When looking at arrhythmias, once more, the presence of BidVT mandates consideration of CPVT as an alternative possibility (23). The concomitant presence of polymorphic and BidVT is an established feature of ATS1 that may be missed in the absence of 12-lead recordings, because the BidVT morphology usually is evident in only a few leads (Figure 2). Remarkably, although in patients with CPVT, VA are usually elicited by adrenergic activation, in ATS1 they frequently initiate and persist in resting conditions.

Among facial dysmorphisms and bone abnormalities, the presence of a small jaw is probably the most distinguishing hallmark of ATS1 and it may contribute to the diagnosis (Central Illustration). Unfortunately, this feature is less prominent during infancy, and pediatricians should mainly rely on the ECG to identify ATS1. Considering that in our cohort the causative mutation was de novo in one-third of the probands, family history is unlikely to be of a major help in early-onset forms of the disease. Finally, episodes of skeletal muscle weakness were

**TABLE 3 Multivariable Cox Model With Follow-Up Time as Time Scale**

	HR	95% CI	p Value
Syncope (time dependent)			
No	Ref.		
Yes	4.54	1.30-15.9	0.02
sVT			
No*	Ref.		
Yes	9.34	2.48-35.1	0.001
Therapy (time dependent)			
Off-therapy	Ref.		
On-therapy with amiodarone	268	20.5-3507	<0.001
On-therapy with other drugs†	0.89	0.22-3.61	0.87

\*No VT + VTns. †This category includes beta-blockers alone or in combination with Class I antiarrhythmic drugs.  
 Abbreviations as in Table 2.

present in 35% of our patients; interestingly, however, they accounted only for 16% of the reasons for the first medical referral, suggesting that symptoms may be elusive and they may be difficult to spot in the pediatric population.

**CORRELATIONS BETWEEN GENOTYPE AND PHENOTYPE.**

We found a higher prevalence of bone dysmorphisms in patients carrying mutations in the C-terminal segment of the Kir2.1 protein. As far as we are concerned, this is the first time that specific *KCNJ2* mutations are associated with peculiar skeletal manifestations. At variance with what occurs in LQTS in which arrhythmic triggers are correlated with the genetic substrate, we were unable to identify a specific condition associated with the development of ventricular tachycardias in ATS1. Similarly, we were also unable to identify links between the topology of the mutations on the *KCNJ2* gene and the severity of clinical manifestation: a link that has been reported to occur both for LQT1 and LQT2. This aspect further confirms that ATS1 should not be regarded as a form of LQTS.

**CLINICAL MANIFESTATIONS AND PROGNOSIS OF PATIENTS WITH ATS1.**

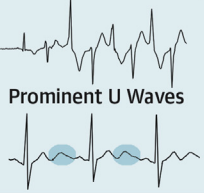
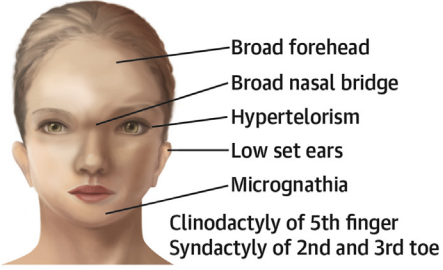

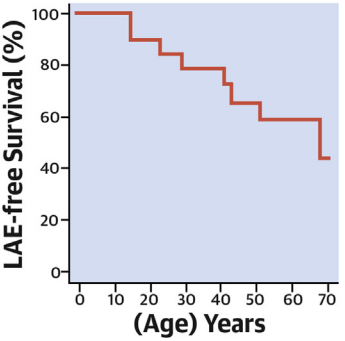
As it happens for rare diseases, information on the clinical outcome of ATS1 is scant and it has been proposed that ATS1 is a “benign” condition (6). Our outcome data challenge the current perception, demonstrating that ATS1 is associated with a high incidence of potentially life-threatening arrhythmias. The combination of a large number of patients and of a mean follow-up that exceeds 10 years allowed us to disclose an unexpectedly high risk of LAE. Accordingly, our data showed a 5-year cumulative probability of 7.9% of experiencing a life-threatening arrhythmia, which is comparable to the odds of patients with LQTS with a remarkably long QT interval (11), for whom clinical guidelines

**TABLE 4 Event Rate of LAE According to Type of Therapy**

	Patients at Risk	Events/py	Rate × 100 py	p Value
No therapy	99	9/723	1.24	Ref.
Only BB	76	5/366	1.37	1.00
BB + AA Class Ic	34	2/137	1.46	1.00
Amiodarone	10	6/25	24.00	<0.001

AA = anti-arrhythmic drugs; BB = beta-blockers; LAE = life-threatening arrhythmic event; py = person-years.

**CENTRAL ILLUSTRATION** Main Features of Andersen-Tawil Syndrome Type 1

Diagnostic Features	Prognostic Factors	Outcomes
<p><b>1. Electrocardiogram</b></p> <p>Bidirectional Ventricular Tachycardia</p>  <p>Prominent U Waves</p> <p><b>2. Dysmorphic Features</b></p>  <p><b>3. Muscular Weakness</b></p>	<p><b>Syncope</b> HR 4.54, P=0.02</p> <p><b>Sustained VT</b> HR 9.34, P=0.001</p>  <p><b>Amiodarone Contraindicated</b></p>	 <p><b>Rate of Life-Threatening Arrhythmic Events</b> 1.1% per year</p> <p><b>Beta-blockers, alone or with Class Ic antiarrhythmics, did not reduce the incidence of LAEs.</b></p>

**Mazzanti, A. et al. J Am Coll Cardiol. 2020;75(15):1772-84.**

The diagnostic hallmarks of Andersen-Tawil Syndrome type 1 (ATS1) (**left column**), the predictors of arrhythmic risk (**middle column**), and the outcome (**right column**).  
HR = hazard ratio; LAE = life-threatening arrhythmic event; VT = ventricular tachycardia.

advise to consider treatment with the combination of beta-blockers and an ICD (24).

The challenge when managing patients with ATS1 is therefore to recognize in advance patients at high risk of experiencing an LAE, in a setting in which no risk stratifier for LAE has been identified. When we performed a multivariable analysis in our cohort, we found that both a history of unexplained syncope and the documentation of hemodynamically tolerated VTs should be considered as risk factors for LAE.

**RESPONSE TO THERAPY.** Antiarrhythmic treatment for patients with ATS1 is empirical and no data exist concerning whether currently used drugs confer protection from SCD. The use of beta-blockers has

been derived from the early view that considered ATS1 as a variant of LQTS (25) and from the assumption that patients would respond to antiadrenergic interventions, despite the lack of robust mechanistic underpinnings.

The use of Class Ic antiarrhythmic drugs originated from the report that flecainide and propafenone could be used to reduce frequent VA in patients with ATS1 (26). An elegant mechanistic interpretation for the antiarrhythmic efficacy of these drugs was proposed by Caballero et al. (27) and from Gómez et al. (28), who demonstrated that flecainide and propafenone interact with the Cysteine 311 of the Kir2.1 subunit and reduce polyamine-induced rectification of the current.

Finally, amiodarone has been suggested as effective in a patient with ATS1 who had survived VF and at follow-up experienced several ICD shocks in whom the drug was combined with acetazolamide (29) and abolished arrhythmic recurrences over 6 months of observation. In addition, Delannoy et al. (7) reported 2 cases of patients with ATS1 who had a reduction of arrhythmias with amiodarone. Our data challenge the previous reports, highlighting that in our cohort, amiodarone was associated with an increase in the risk of LAE. From a mechanistic standpoint, it is known that amiodarone blocks  $I_{K1}$  (30) and that it might therefore predispose to the onset of LAE. Overall, our data call for avoiding the use of amiodarone in ATS1 (Central Illustration), whereas they do not question the view that the sodium channel blockers flecainide and propafenone might be useful to reduce the arrhythmic burden, as we have also observed in our cohort. Nonetheless, in our population, we documented the fact that these drugs were not useful to prevent life-threatening arrhythmias. In this respect, also beta-blockers should not be used when the objective of therapy is to prevent SCD.

This observation is similar to the finding that, in patients with arrhythmogenic right ventricular cardiomyopathy, antiarrhythmic drugs are useful for the treatment of arrhythmic symptoms, but not for the prevention of SCD (31,32). We believe that the threshold for the use of the ICD should be lowered in patients presenting the risk factors that we have identified, that is, unexplained syncope and who have documentation of prolonged episodes of VT.

**STUDY LIMITATIONS.** Our study presents limitations inherent to registries. Specifically, because patients are followed for many years, it is difficult to ensure a standardization of treatment regimens. Furthermore, considering the rarity of the condition, although our

data provide evidence for the management of patients with ATS1, they should not be regarded as definitive.

The small number of patients treated with amiodarone made it difficult to estimate precisely the HR associated with its use, yielding wide CIs. Nonetheless, in our patients with ATS1, the association between starting amiodarone and developing life-threatening arrhythmias is worth reporting to avoid further amiodarone use.

## CONCLUSIONS

Our data demonstrate that the clinical course of patients with ATS1 is characterized by a high rate of LAE. A history of unexplained syncope or of documented sustained ventricular tachycardia is associated with a higher risk of LAE. Amiodarone is proarrhythmic and should be avoided in patients with ATS1.

**ADDRESS FOR CORRESPONDENCE:** Prof. Silvia G. Priori, Molecular Cardiology - IRCCS ICS Maugeri, Via Maugeri, 10 - 27100 Pavia, Italy. E-mail: [silvia.priori@icsmaugeri.it](mailto:silvia.priori@icsmaugeri.it). Twitter: @SilviaPriori.

## PERSPECTIVES

**COMPETENCY IN MEDICAL KNOWLEDGE:** Andersen-Tawil Syndrome type 1 is caused by loss-of-function mutations in the *KCNJ2* gene and associated with facial dysmorphism and a high risk of life-threatening ventricular arrhythmias.

**TRANSLATIONAL OUTLOOK:** Further studies are needed to find effective antiarrhythmic treatment strategies in addition to implanted automatic defibrillators.

## REFERENCES

1. Andersen ED, Krasilnikoff PA, Overvad H. Intermittent muscular weakness, extrasystoles, and multiple developmental anomalies. A new syndrome? *Acta Paediatr Scand* 1971;60:559-64.
2. Tawil R, Ptacek LJ, Pavlakis SG, et al. Andersen's syndrome: potassium-sensitive periodic paralysis, ventricular ectopy, and dysmorphic features. *Ann Neurol* 1994;35:326-30.
3. Stunnenberg BC, Raaphorst J, Deenen JCW, et al. Prevalence and mutation spectrum of skeletal muscle channelopathies in the Netherlands. *Neuromuscul Disord* 2018;28:402-7.
4. Plaster NM, Tawil R, Tristani-Firouzi M, et al. Mutations in *Kir2.1* cause the developmental and episodic electrical phenotypes of Andersen's syndrome. *Cell* 2001;105:511-9.
5. Sakmann B, Trube G. Conductance properties of single inwardly rectifying potassium channels in ventricular cells from guinea-pig heart. *J Physiol* 1984;347:641-57.
6. Wilde AAM. Andersen-Tawil syndrome, scarier for the doctor than for the patient? Who, when, and how to treat. *Europace* 2013;15:1690-2.
7. Delannoy E, Sacher F, Maury P, et al. Cardiac characteristics and long-term outcome in Andersen-Tawil syndrome patients related to *KCNJ2* mutation. *Europace* 2013;15:1805-11.
8. Zhang L, Benson DW, Tristani-Firouzi M, et al. Electrocardiographic features in Andersen-Tawil syndrome patients with *KCNJ2* mutations: characteristic T-U-wave patterns predict the *KCNJ2* genotype. *Circulation* 2005;111:2720-6.
9. Veerapandian A, Statland JM, Tawil R. Andersen-Tawil syndrome. November 22, 2004 [Updated June 7, 2018]. In: Adam MP, Ardinger HH, Pagon RA, et al., editors. *Gene Reviews*® [Internet]. Seattle, WA: University of Washington, 1993-2019.
10. Richards S, Aziz N, Bale S, et al. Standards and guidelines for the interpretation of sequence variants: a joint consensus recommendation of the American College of Medical Genetics and Genomics and the Association for Molecular Pathology. *Genet Med* 2015;17:405-24.

11. Mazzanti A, Maragna R, Vacanti G, et al. Interplay between genetic substrate, QTc duration, and arrhythmia risk in patients with long QT syndrome. *J Am Coll Cardiol* 2018;71:1663-71.
12. Hibino H, Inanobe A, Furutani K, Murakami S, Findlay I, Kurachi Y. Inwardly rectifying potassium channels: their structure, function, and physiological roles. *Physiol Rev* 2010;90:291-366.
13. Donaldson MR, Jensen JL, Tristani-Firouzi M, et al. PIP2 binding residues of Kir2.1 are common targets of mutations causing Andersen syndrome. *Neurology* 2003;60:1811-6.
14. Lopes CM, Zhang H, Rohacs T, Jin T, Yang J, Logothetis DE. Alterations in conserved Kir channel-PIP2 interactions underlie channelopathies. *Neuron* 2002;34:933-44.
15. Ai T, Fujiwara Y, Tsuji K, et al. Novel KCNJ2 mutation in familial periodic paralysis with ventricular dysrhythmia. *Circulation* 2002;105:2592-4.
16. Davies NP, Imbrici P, Fialho D, et al. Andersen-Tawil syndrome: new potassium channel mutations and possible phenotypic variation. *Neurology* 2005;65:1083-9.
17. Tsai W-Y, Jewell NP, Wang M-C. A note on the product-limit estimator under right censoring and left truncation. *Biometrika* 1987;74:883-6.
18. Snapinn SM, Jiang Q, Iglewicz B. Illustrating the impact of a time-varying covariate with an extended Kaplan-Meier estimator. *Am Stat* 2012;59:301-7.
19. Sacconi S, Simkin D, Arrighi N, et al. Mechanisms underlying Andersen's syndrome pathology in skeletal muscle are revealed in human myotubes. *Am J Physiol Cell Physiol* 2009;297:C876-85.
20. Radwański PB, Veeraghavan R, Poelzing S. Cytosolic calcium accumulation and delayed repolarization associated with ventricular arrhythmias in a guinea pig model of Andersen-Tawil syndrome. *Heart Rhythm* 2010;7:1428-14235.e1.
21. Adams DS, Uzel SGM, Akagi J, et al. Bioelectric signalling via potassium channels: a mechanism for craniofacial dysmorphogenesis in KCNJ2-associated Andersen-Tawil Syndrome. *J Physiol* 2016;594:3245-70.
22. Morita H, Zipes DP, Morita ST, Wu J. Mechanism of U wave and polymorphic ventricular tachycardia in a canine tissue model of Andersen-Tawil syndrome. *Cardiovasc Res* 2007;75:510-8.
23. Priori SG, Napolitano C, Memmi M, et al. Clinical and molecular characterization of patients with catecholaminergic polymorphic ventricular tachycardia. *Circulation* 2002;106:69-74.
24. Priori SG, Blomström-Lundqvist C, Mazzanti A, et al. 2015 European Society of Cardiology Guidelines for the management of patients with ventricular arrhythmias and the prevention of sudden cardiac death summarized by co-chairs. *Eur Heart J* 2015;36:2757-9.
25. Tristani-Firouzi M, Jensen JL, Donaldson MR, et al. Functional and clinical characterization of KCNJ2 mutations associated with LQT7 (Andersen syndrome). *J Clin Invest* 2002;110:381-8.
26. Miyamoto K, Aiba T, Kimura H, et al. Efficacy and safety of flecainide for ventricular arrhythmias in patients with Andersen-Tawil syndrome with KCNJ2 mutations. *Heart Rhythm* 2015;12:596-603.
27. Caballero R, Dolz-Gaitón P, Gómez R, et al. Flecainide increases Kir2.1 currents by interacting with cysteine 311, decreasing the polyamine-induced rectification. *Proc Natl Acad Sci U S A* 2010;107:15631-6.
28. Gómez R, Caballero R, Barana A, et al. Structural basis of drugs that increase cardiac inward rectifier Kir2.1 currents. *Cardiovasc Res* 2014;104:337-46.
29. Junker J, Haverkamp W, Schulze-Bahr E, Eckardt L, Paulus W, Kiefer R. Amiodarone and acetazolamide for the treatment of genetically confirmed severe Andersen syndrome. *Neurology* 2002;59:466.
30. Riera AR, Uchida AH, Ferreira C, et al. Relationship among amiodarone, new class III antiarrhythmics, miscellaneous agents and acquired long QT syndrome. *Cardiol J* 2008;15:209-19.
31. Priori SG, Blomström-Lundqvist C, Mazzanti A, et al. 2015 ESC Guidelines for the management of patients with ventricular arrhythmias and the prevention of sudden cardiac death. *Eur Heart J* 2015;36:2793-867.
32. Mazzanti A, Ng K, Faragli A, et al. Arrhythmogenic right ventricular cardiomyopathy: clinical course and predictors of arrhythmic risk. *J Am Coll Cardiol* 2016;68:2540-50.

---

**KEY WORDS** genetics, inherited arrhythmias, *KCNJ2*, life-threatening arrhythmic events, sudden cardiac death

---

**APPENDIX** For supplemental tables, results, and bibliography, please see the online version of this paper.

## 2.2. Mutace s efektem zakladatele (founder mutation) varianty genu *KCNQ1* u českých rodin s LQTS

Ve spolupráci s Ústavem lékařské genetiky a genomiky FN Brno a LFMU a Fyziologickým ústavem LFMU jsme identifikovali a funkčně charakterizovali tzv. founder variantu genu *KCNQ1* asociovanou s klinicky jasnou diagnózou LQTS. Podrobnosti jsou uvedeny v následující vložené publikaci.

Synková I, Bébarová M, **Andršová I**, Chmelikova L, Švecová O, Hošek J, Pásek M, Vít P, Valášková I, Gaillyová R, Navrátil R, Novotný T. Long-QT founder variant T309I-Kv7.1 with dominant negative pattern may predispose delayed afterdepolarizations under  $\beta$ -adrenergic stimulation. *Scientific Reports* 2021; 11:3573. doi: 10.1038/s41598-021-81670-1.

IF 4,997. Počet citací ve Web of Science 2

Publikovaná původní práce – kvantitativní podíl uchazečky 20 % - identifikace vhodných pacientů, analýza dat, revize textu publikace.



OPEN

## Long-QT founder variant T309I-Kv7.1 with dominant negative pattern may predispose delayed afterdepolarizations under $\beta$ -adrenergic stimulation

Iva Synková<sup>1,2</sup>, Markéta Bébarová<sup>3</sup>✉, Irena Andršová<sup>4</sup>, Larisa Chmelikova<sup>5</sup>, Olga Švecová<sup>3</sup>, Jan Hošek<sup>6</sup>, Michal Pásek<sup>3,7</sup>, Pavel Vít<sup>8</sup>, Iveta Valášková<sup>1</sup>, Renata Gaillyová<sup>1</sup>, Rostislav Navrátil<sup>9</sup> & Tomáš Novotný<sup>4</sup>

The variant c.926C>T (p.T309I) in *KCNQ1* gene was identified in 10 putatively unrelated Czech families with long QT syndrome (LQTS). Mutation carriers (24 heterozygous individuals) were more symptomatic compared to their non-affected relatives (17 individuals). The carriers showed a mild LQTS phenotype including a longer QTc interval at rest ( $466 \pm 24$  ms vs.  $418 \pm 20$  ms) and after exercise ( $508 \pm 32$  ms vs.  $417 \pm 24$  ms), 4 syncope and 2 aborted cardiac arrests. The same haplotype associated with the c.926C>T variant was identified in all probands. Using the whole cell patch clamp technique and confocal microscopy, a complete loss of channel function was revealed in the homozygous setting, caused by an impaired channel trafficking. Dominant negativity with preserved reactivity to  $\beta$ -adrenergic stimulation was apparent in the heterozygous setting. In simulations on a human ventricular cell model, the dysfunction resulted in delayed afterdepolarizations (DADs) and premature action potentials under  $\beta$ -adrenergic stimulation that could be prevented by a slight inhibition of calcium current. We conclude that the *KCNQ1* variant c.926C>T is the first identified LQTS-related founder mutation in Central Europe. The dominant negative channel dysfunction may lead to DADs under  $\beta$ -adrenergic stimulation. Inhibition of calcium current could be possible therapeutic strategy in LQTS1 patients refractory to  $\beta$ -blocker therapy.

Long QT syndrome (LQTS), the most often diagnosed familial electrical disease of the heart<sup>1</sup>, is characterised by a prolonged QTc interval and occurrence of polymorphic ventricular tachycardias of the *torsades de pointes* (TdP) type, degenerating into ventricular fibrillation in extreme cases. It results in syncope or sudden cardiac deaths. Seventeen genes have been associated with LQTS so far<sup>2,3</sup>, while three "major" genes (*KCNQ1*, *KCNH2*, *SCN5A*) contribute to 75% of clinically diagnosed LQTS<sup>4,5</sup>. As confirmed recently, a substantial number of the other "minor" genes show only limited or disputed association with LQTS<sup>6</sup>.

<sup>1</sup>Department of Medical Genetics, University Hospital Brno and Faculty of Medicine, Masaryk University, Jihlavská 20, 625 00 Brno, Czech Republic. <sup>2</sup>Department of Experimental Biology, Faculty of Science, Masaryk University, Kotlářská 267/2, 611 37 Brno, Czech Republic. <sup>3</sup>Department of Physiology, Faculty of Medicine, Masaryk University, Kamenice 5, 625 00 Brno, Czech Republic. <sup>4</sup>Department of Internal Medicine and Cardiology, University Hospital Brno and Faculty of Medicine, Masaryk University, Jihlavská 20, 625 00 Brno, Czech Republic. <sup>5</sup>Department of Biomedical Engineering, Faculty of Electrical Engineering and Communication, Brno University of Technology, Technická 10, 616 00 Brno, Czech Republic. <sup>6</sup>Division of Biologically Active Complexes and Molecular Magnets, Regional Centre of Advanced Technologies and Materials, Faculty of Science, Palacký University in Olomouc, Šlechtitelů 27, 783 71 Olomouc, Czech Republic. <sup>7</sup>Institute of Thermomechanics, Czech Academy of Sciences, Dolejškova 5, 182 00 Prague, Czech Republic. <sup>8</sup>Department of Paediatrics, University Hospital Brno and Faculty of Medicine, Masaryk University, Černoplní 9, 613 00 Brno, Czech Republic. <sup>9</sup>Repromeda, Clinic for Reproductive Medicine and Preimplantation Genetic Diagnosis, Biology Park, Studentská 812/6, 625 00 Brno, Czech Republic. ✉email: mbebar@med.muni.cz



Identification of the same mutation in apparently unrelated LQTS patients in a particular geographic region suggests derivation of the mutation from a common ancestor (a so-called “founder”). Several founder mutations in the *KCNQ1* gene associated with LQTS have been reported<sup>7–19</sup>. Founder populations have proven to be useful for studying genotype–phenotype correlations, which are important for patients’ management as prevalence of the disease can be increased in some geographical regions<sup>20</sup>.

This study is a complex analysis of the c.926C>T variant (p.Thr309Ile or T309I), the first founder mutation in the *KCNQ1* gene in Central Europe. Based on the acquired functional data, the underlying arrhythmogenic mechanism and possible alternative therapeutic way of its prevention were predicted by in silico modelling in a human ventricular cell model.

## Methods

**Clinical diagnostics.** The study conformed to the principles outlined in the Declaration of Helsinki and was approved by the Multicenter Ethical Committee, University Hospital Brno (Brno, Czech Republic). All participants signed a written informed consent form. In the case of participants under the age of 18 years, the written informed consent was obtained from a parent and/or legal guardian.

LQTS diagnosis was established according to ESC Guidelines<sup>21</sup>. All individuals underwent clinical examination and bicycle ergometry. The initial stress was set to 0.5 W/kg, and increased by 0.5 W/kg every three minutes to achieve a heart rate higher than the submaximal value with respect to age and sex. A 12-lead ECG with Mason-Likar modification was employed. QT and RR intervals were measured manually (the end of QT interval was established using the threshold method); the Bazett’s correction formula was used. Detailed description is provided in the Supplementary Methods.

**Genetic analysis.** Molecular analysis of LQTS-associated genes was performed according to current practices for molecular genetics diagnostics: multiplex PCR/SSCP analysis of 3 LQTS major genes (*KCNQ1*, *KCNH2* and *SCN5A*), Sanger sequencing on ABI 3100 Genetic Analyser (*Applied Biosystems*, Foster City, CA, USA; genes *KCNQ1*, *KCNH2* and *SCN5A*), and massive parallel sequencing MPS on GS Junior (*Roche*, Basel, Switzerland; genes *KCNQ1*, *KCNH2*, *SCN5A*, *KCNE1*, *KCNE2*) and, since 2016, on MiSeq (*Illumina*, San Diego, CA, USA; genes *KCNQ1*, *KCNH2*, *SCN5A*, *AKAP9*, *CACNA1C*, *CALM1*, *CALM2*, *CAV3*, *KCNE1*, *KCNE2*, *KCNJ5*, *SCN4B*, *SNTA1*). Genetic counselling and testing of first-degree relatives were offered to patients at risk.

The functional impact of the T309I variant was predicted with various in silico tools (SIFT, Provean<sup>22</sup>, MutationTaster, FATHMM<sup>23</sup>, and PMUT; Suppl. Tab. S1)<sup>24</sup>. Its conservation was measured with LRT and Mutation-Assessor. Allele frequency was determined from online databases ExAC<sup>25</sup> and GnomAD.

For the haplotype analysis, 9 STR (short tandem repeats) markers spanning the ~11.9-Mb region of chromosome 11 (including the *KCNQ1* gene) were chosen from the UCSC Genome Browser (Suppl. Tab. S2). Multiplex PCR with fluorescently labelled primers and fragment analysis with capillary electrophoresis were performed on SeqStudio Genetic Analyzer (*Applied Biosystems*, Foster City, CA, USA). The haplotype linked to the mutation was identified by studying segregation in families. In the probands, SNP (single nucleotide polymorphism) marker analysis followed; 6219 SNPs on the p-arm of chromosome 11 were analysed. Population allele frequency analysis was performed after identifying a common STR allele in the marker D11S4088 in all mutation carriers. The control group was formed by 52 unrelated patients examined at the Department of Clinical Genetics, Faculty Hospital Brno, with a signed written informed consent from each patient agreeing that their DNA samples could be used for clinical research. STR alleles (104) were analysed with capillary electrophoresis. Detailed description is provided in the Supplementary Methods.

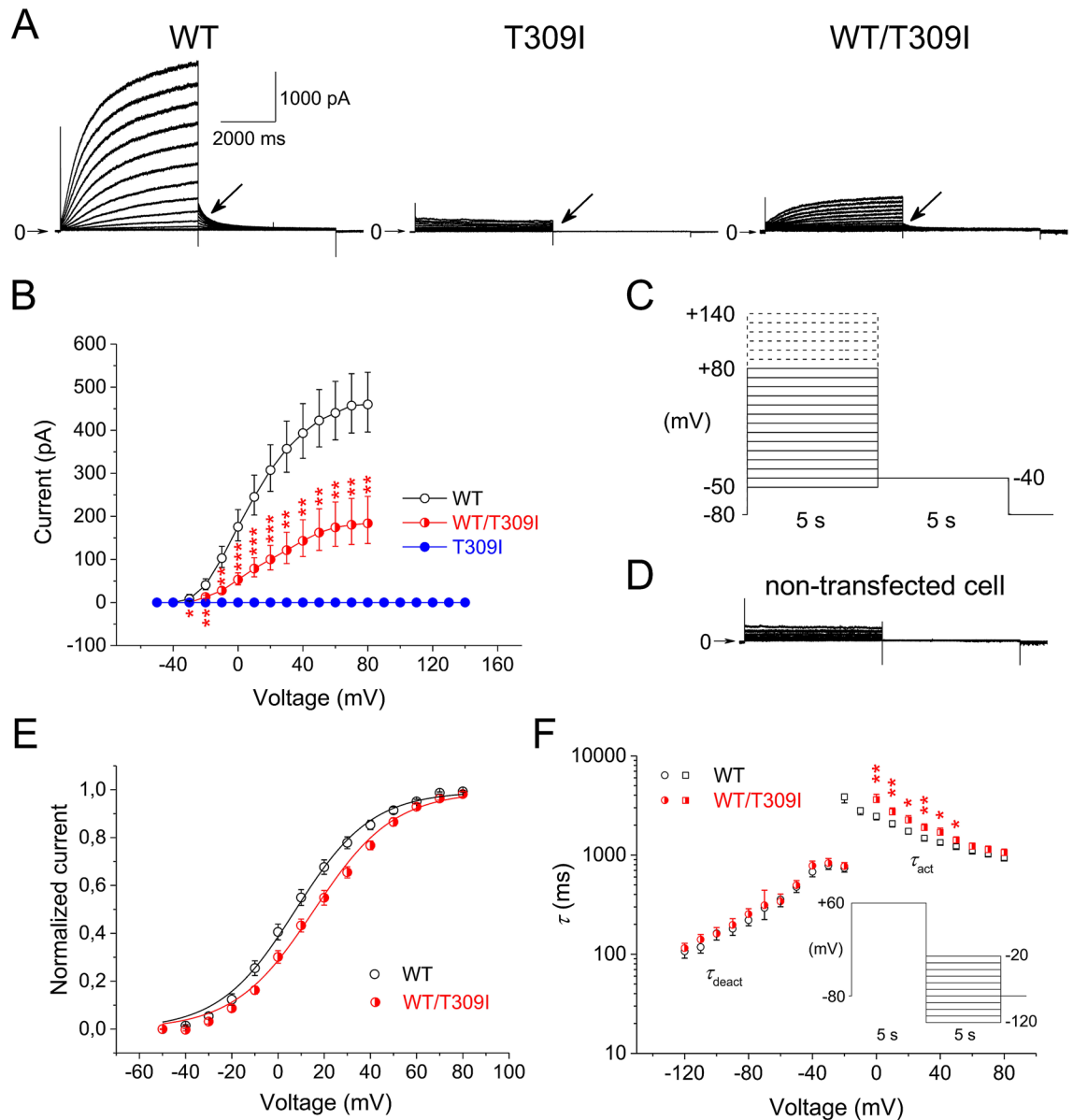
**Functional analysis.** Plasmids containing wild-type (WT) human *KCNQ1* in a pIRES2-eGFP vector, *KCNE1* in a pKB-CMV vector, and *Yotiao* in a pGW1 vector were isolated from *Escherichia coli* using the endotoxin-free QIAprep Spin Miniprep Kit (*Qiagen*, Hilden, Germany). The mutation c.926C>T in the human *KCNQ1* (p.T309I) was generated by site-directed mutagenesis using QuikChange II XL Site-Directed Mutagenesis Kit (*Agilent Technologies*, Cedar Creek, TX, USA). Detailed description is provided in the Supplementary Methods.

TransFast Transfection Reagent (*Promega*, Madison, WI, USA) was used for transfection of the plasmids *KCNQ1*, *KCNE1* and *Yotiao* (the molar ratio 1:2:4, total amount of *KCNQ1* DNA 1 µg, ratio of DNA to transfection agent 1:1.5) into Chinese hamster ovary (CHO) cells cultured at 37 °C / 5% CO<sub>2</sub> in the Ham’s F-12 medium supplemented with 10% foetal calf serum and 0.005% gentamycin. *KCNQ1* was transfected in one of three ways: 1) WT variant alone (1 µg; WT); 2) T309I variant alone (1 µg; T309I); 3) both the WT and T309I variants cotransfected in the ratio 1:1 (0.5 µg of WT *KCNQ1* and 0.5 µg of the T309I variant; WT/T309I) to mimic the heterozygous state in the mutation carriers.

Biophysical analysis was performed ~24 h after the transfection by the whole cell patch clamp technique at 37 °C. The resistance of filled glass electrodes was < 2.5 MΩ the series resistance was compensated up to 60%. Tyrode solution of the following composition was used (in mmol/L): NaCl 132, KCl 4.8, CaCl<sub>2</sub> 2.0, MgCl<sub>2</sub> 1.2, HEPES 10, glucose 5 (pH 7.4, NaOH). The patch electrode filling solution contained (in mmol/L): K-aspartate 110, K<sub>2</sub>ATP 5, CaCl<sub>2</sub> 1, MgCl<sub>2</sub> 1, EGTA 11, HEPES 10 (pH 7.3, KOH). To simulate β-adrenergic stimulation, the pipette solution was supplemented with cyclic adenosine monophosphate (cAMP, 200 µmol/L) and okadaic acid (OA, 0.2 µmol/L). The junction potential was +15 mV.

Considering missing proportionality between the measured current and estimated cell membrane capacitance, conversion of the magnitude of the current to the current density was avoided in this study, as recently recommended by Kula et al.<sup>26</sup>. The average cell membrane capacitance was comparable in cells expressing the wild type (WT), T309I, and WT/T309I *I<sub>Ks</sub>* channels (13.8 ± 1.7, 13.3 ± 2.0, and 13.5 ± 1.8 pF, respectively; *P* > 0.05).

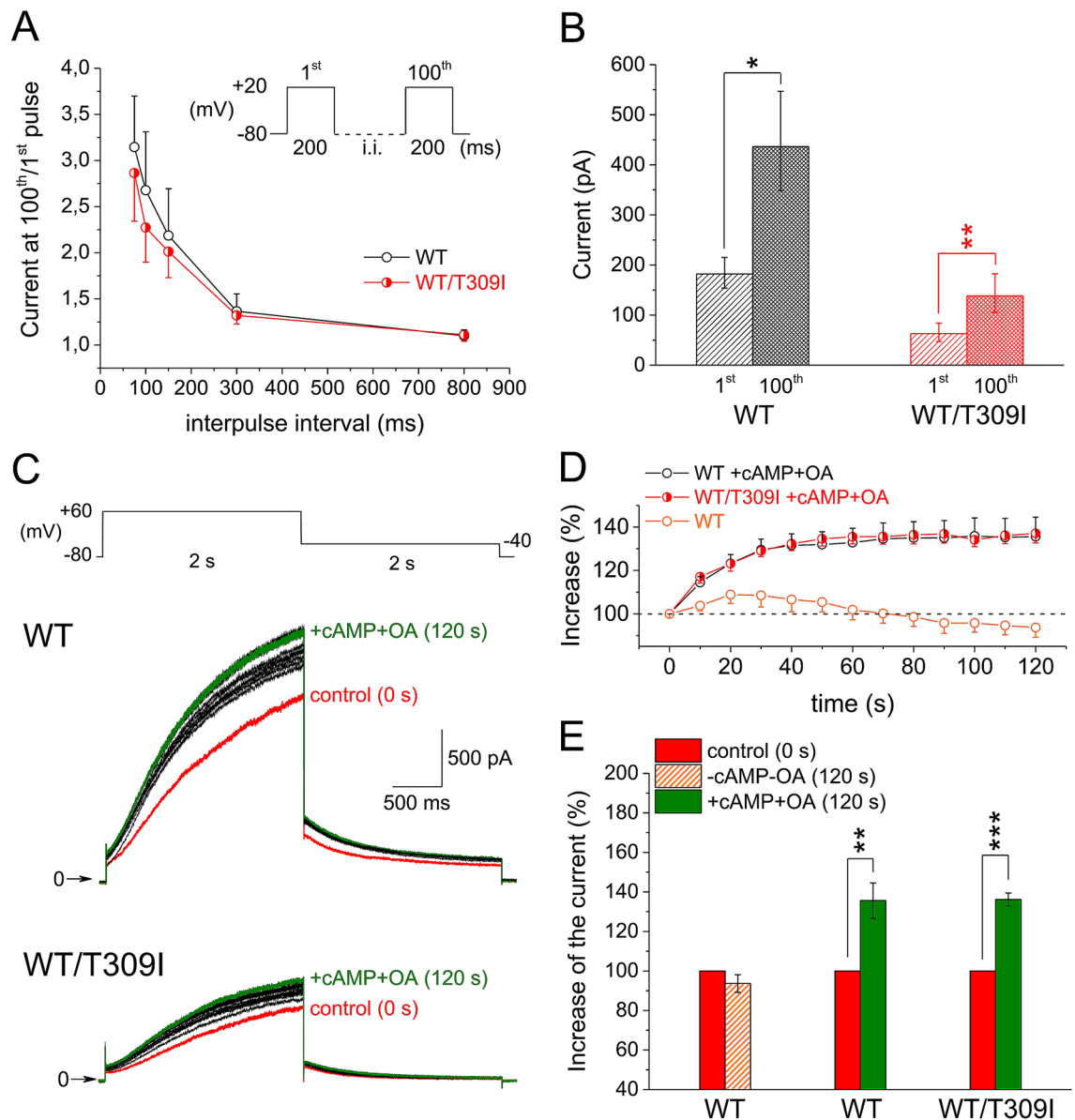




**Figure 2.** Biophysical impact of T309I mutation. (A) Representative records in wild type (WT), T309I, and WT/T309I channels (KCNE1 subunit cotransfected); arrows point to the tail current. (B) Average voltage dependence of tail current activation ( $n=20, 9$ , and  $16$  in WT, T309I, and WT/T309I channels, respectively); the half-maximal activation voltage  $V_{1/2}=8.3 \pm 2.2$  mV in WT channels and  $15.6 \pm 2.1$  mV in WT/T309I channels;  $P < 0.05$ . (C) Activation experimental protocol; the dashed lines—steps used for stimulation only in T309I channels. (D) Representative trace from a non-transfected CHO cell. (E) Average voltage dependence of steady-state activation. (F) Average voltage dependence of the time constant of activation ( $\tau_{act}$ ) and time constant of deactivation ( $\tau_{deact}$ ;  $n=11$  and  $9$  in WT and WT/T309I channels, respectively); inset: deactivation experimental protocol; \*, \*\* and \*\*\* statistical significance between WT and WT/T309I channels at  $P < 0.05, 0.01$  and  $0.001$ , respectively. The stimulation frequency was  $0.08$  Hz. All graphs were prepared using the software Origin, version 8.5.1.

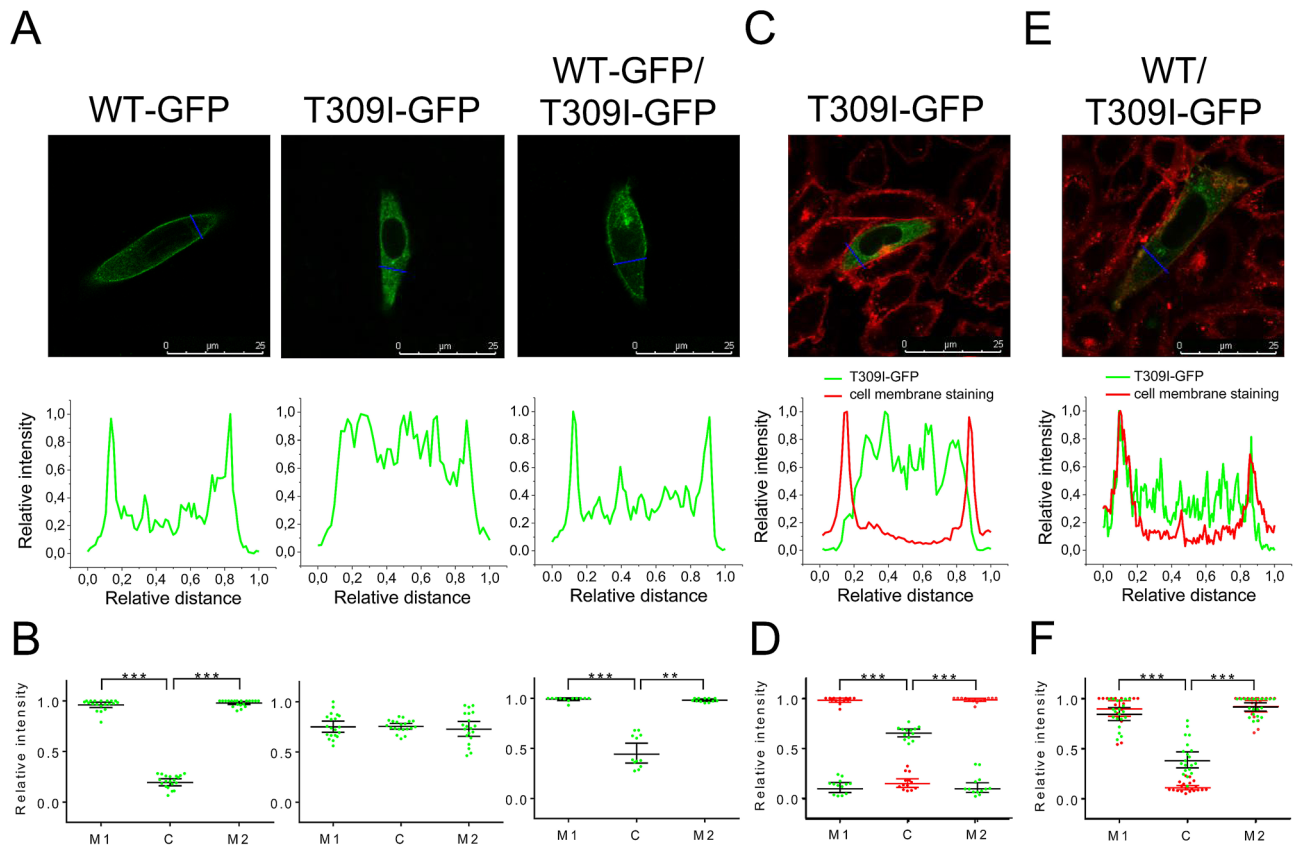
For the fluorescence image acquisition, a confocal laser scanning microscope Leica TCS SP8 X (Leica microsystems, Wetzlar, Germany) was used. WT and T309I human *KCNQ1* tagged with GFP at the 3'-terminus, or WT-*KCNQ1* without GFP in a pBK-CMV vector, as well as WT human *KCNE1* in a pBK-CMV vector were transfected into CHO cells seeded on glass bottom dishes (Cellvis, Mountain View, CA, USA) coated with fibronectin  $\sim 48$  h before the evaluation (*KCNQ1* and *KCNE1* in the molar ratio 1:2). In some experiments, WT with no GFP was cotransfected with the GFP-tagged T309I-*KCNQ1* and *KCNE1*, and the cell membrane was stained (CellMask Orange Plasma Membrane Stain; Invitrogen, Carlsbad, CA, USA).

Detailed description is provided in the Supplementary Methods. The chemicals were purchased from Sigma-Aldrich (Prague, Czech Republic) unless otherwise indicated.



**Figure 3.** Accumulation of WT and WT/T309I currents (KCNE1 subunit cotransfected). (A) Average relative rate-dependent accumulation of the currents at interpulse intervals between 75 and 800 ms ( $n = 10$  and  $8$  in WT and WT/T309I channels, respectively); inset: experimental protocol applied after a 30-s pause; i.i.—interpulse interval. (B) Average absolute currents at the 1st and 100th pulse of the accumulation protocol with the interpulse interval of 100 ms. (C) Experimental protocol (the stimulation frequency 0.1 Hz), and representative traces of WT and WT/T309I currents under simulated  $\beta$ -adrenergic stimulation (cAMP and OA in the pipette solution); red trace—time 0, control (no cAMP/OA stimulation); green trace—time 120 s, steady-state  $\beta$ -adrenergic stimulation; black traces—time 10 to 110 s in 10-s intervals, development of  $\beta$ -adrenergic response. (D) Time course of the relative increase of the current in presence of cAMP and OA (+cAMP+OA) in WT and WT/T309I channels ( $n = 14$  and  $8$ ;  $n = 9$  in WT without cAMP and OA). (E) Relative steady-state increase of the current in +cAMP+OA; \*, \*\* and \*\*\*statistical significance at  $P < 0.05$ ,  $0.01$  and  $0.001$ , respectively. All graphs were prepared using the software Origin, version 8.5.1.

**Mathematical modelling.** A previously published model of human ventricular subepicardial myocyte<sup>27</sup> was modified and adapted to changes accompanying  $\beta$ -adrenergic stimulation induced by  $1 \mu\text{M}$  isoproterenol (Suppl. Fig. S1, Suppl. Tab. S3; for validation of the new model, see Suppl. Fig. S3–S5). The measured gating properties of WT and WT/T309I  $I_{Ks}$  channels were incorporated into the model (Suppl. Fig. S6). Detailed description is provided in the Supplementary Methods. The Matlab code of the control model can be downloaded at <https://www.it.cas.cz/en/d3/l033/>.



**Figure 4.** Subcellular localization of WT- and T309I-Kv7.1 subunits expressed in CHO cells (KCNE1 subunit cotransfected). **(A)** Confocal microscopic images of representative cells expressing WT-GFP (*i.e.* tagged with GFP at the C-terminal end), T309I-GFP, or both WT-GFP and T309I-GFP subunits (upper panels), and respective relative fluorescence intensity profiles (lower panels) under the blue lines in the upper panels; scale bar 25  $\mu\text{m}$ . **(B)** The resulting maximal relative fluorescence intensity at the cell membrane (M1 and M2) and its mean value in the cytosol (C) in all investigated cells ( $n = 20$ , 20 and 12 in WT-GFP, T309I-GFP and WT-GFP/T309I-GFP subunits, respectively; cells from 4 to 7 transfections used in each variant); \*\* and \*\*\* statistical significance of the difference in fluorescence intensity among M1, M2 and C in the respective group of cells at  $P < 0.01$  and  $0.001$ , respectively. **(C,E)** Subcellular localization of the T309I-GFP subunits, either expressed alone (C) or co-expressed with non-tagged WT (no GFP; E); the cell membrane was stained with red fluorescent dye. Representative cells (upper panels) and respective relative fluorescence intensity profiles (lower panels) under the blue lines in the upper panels of the GFP signal (green lines) and of the membrane staining signal (red lines; both at the cell cross-sections indicated by the blue lines in the upper panels). **(D, F)** The resulting maximal relative fluorescence intensities of both GFP and membrane staining fluorescence (green and red dots, respectively) at the cell membrane (M1 and M2) and their mean values in the cytosol (C) in all investigated cells ( $n = 13$  and 20 in D and F, respectively; cells from 3 and 7 transfections used); \*\*\* statistical significance of the difference in fluorescence intensity among M1, M2 and C at  $P < 0.001$ . Figure 4A,C, E were prepared using the software LAS X, version 3.5.2.18963 (upper panels) and Origin, version 8.5.1 (lower panels), Fig. 4B,D,F using the software GraphPad Prism, version 6.05.

**Statistical analysis.** The data are mostly presented by the arithmetic mean ( $\pm$  SD from  $n$  patients, or  $\pm$  SEM from  $n$  cells; Origin, version 8.5.1; *OriginLab Corporation*). To determine the statistical significance of the differences, paired/unpaired *t*-tests and one-way/repeated measures ANOVA with the Bonferroni post-test were performed using the software GraphPad Prism, version 6.05 (*GraphPad Software, Inc.*). The same software was used for curve fitting. If the difference between the arithmetic and geometric means was  $> 10\%$  (considering a recent study by Kula et al.<sup>28</sup>), the geometric mean  $x/\text{geometric SE}$  and the non-parametric Mann–Whitney test were used (Figs. 2B, 3B).  $P < 0.05$  was considered statistically significant.

To compare the statistical significance of differences in relative fluorescence intensity in Fig. 4 (where several data samples did not show the normal distribution according to the Shapiro–Wilk test; the mean values are represented by the geometric mean  $\pm$  95% confidence interval), either the Friedman test or the Kruskal–Wallis test (both with the Dunn’s multiple comparison) were used, the first one in the case of paired data (comparison within individual groups), the latter in the case of unpaired data (comparison among various groups).

Following software was used to prepare the figures: Figs. 1A and 4B,D,F—GraphPad Prism, version 6.05 (*GraphPad Software, Inc.*); Fig. 1B,C,D—Inkscape, version 0.92.2 (*Inkscape Project*; <https://inkscape.org/cs/about/branding/>); the map in Fig. 1B, lower panel, was generated using the software QGIS, version 3.10, with data

All individuals (n = 54)		
	T309I+ (n = 30)	T309I- (n = 24)
Age (years)	30.0 ± 20.2	32.2 ± 20.1
Females	25 (83.3%)	13 (54.2%)
Individuals with completed clinical investigation (n = 41)		
	T309I+ (n = 24)	T309I- (n = 17)
Age (years)	26.3 ± 18.4	30.1 ± 15.6
Females	20 (83.3%)	9 (52.9%)
Children under 16 years	10	3
Syncope/ACA	4/2	0/0
QTc, rest (ms)	466 ± 24 <sup>†††</sup>	418 ± 20
QTc, rest—children (ms)	465 ± 27 <sup>††</sup>	410 ± 10
QTc, rest—adults (ms)	466 ± 22 <sup>†††</sup>	420 ± 21
QTc, recovery (ms)	508 ± 32 <sup>***†††</sup>	417 ± 24
QTc, recovery—children (ms)	510 ± 40 <sup>**†</sup>	425 ± 7
QTc, recovery—adults (ms)	508 ± 27 <sup>***†††</sup>	416 ± 25

**Table 1.** Clinical characteristics of investigated individuals, members of 10 unrelated families. T309I+, T309I carriers; T309I-, T309I non-carriers; mean ± SD, n—number of individuals; QTc, QT interval corrected to the heart rate (Bazett's formula); QTc, recovery, QTc, 4th minute of the recovery phase after ergometry; ACA, aborted cardiac arrest; statistics in the respective groups of patients (all/children/adults): \*\* and \*\*\*—statistical significance of QTc difference at rest and during recovery at  $P < 0.01$  and  $0.001$ , respectively, †, †† and †††—statistical significance of the respective QTc difference between T309I+ and T309I- at  $P < 0.05$ ,  $0.01$  and  $0.001$ , respectively.

downloaded from <https://www.arcdata.cz/produkty/geograficka-data/arccr-500>); Figs. 2, 3 and 4A,C,E (lower panels, and 5—Origin, version 8.5.1; OriginLab Corporation); Fig. 4A,C,E (upper panels)—LAS X, version 3.5.2.18963 (Leica Microsystems CMS GmbH).

## Results

**Clinical characteristics of T309I carriers.** Members of 10 putatively unrelated families with occurrence of the T309I variant were investigated (Table 1). All of the 4 syncopes and 2 aborted cardiac arrests (ACA) which were reported in the investigated T309I carriers appeared during physical exertion (ice hockey, swimming, exercise at school). QTc intervals were significantly longer in T309I carriers compared to their healthy relatives, both at rest ( $466 \pm 24$  ms vs.  $418 \pm 20$  ms,  $P < 0.001$ ) and in the fourth minute of exercise test recovery ( $508 \pm 32$  ms vs.  $417 \pm 24$  ms,  $P < 0.001$ ; Fig. 1A). The QTc prolongation after exercise was significant in T309I carriers ( $P < 0.001$ ). Representative ECG traces at rest and during recovery in symptomatic and asymptomatic T309I carriers are shown in Suppl. Fig. S7. In children under 16 years, the available QTc values were similar to the values in the adult population of the respective patient group (Table 1). No significant changes were apparent in PQ interval and QRS complex (Suppl. Fig. S8). Cardioverter defibrillators were implanted in the 2 ACA cases. In the other T309I carriers,  $\beta$ -blocker therapy (preferably with nadolol) has been administered and no syncope recurrences have been observed since.

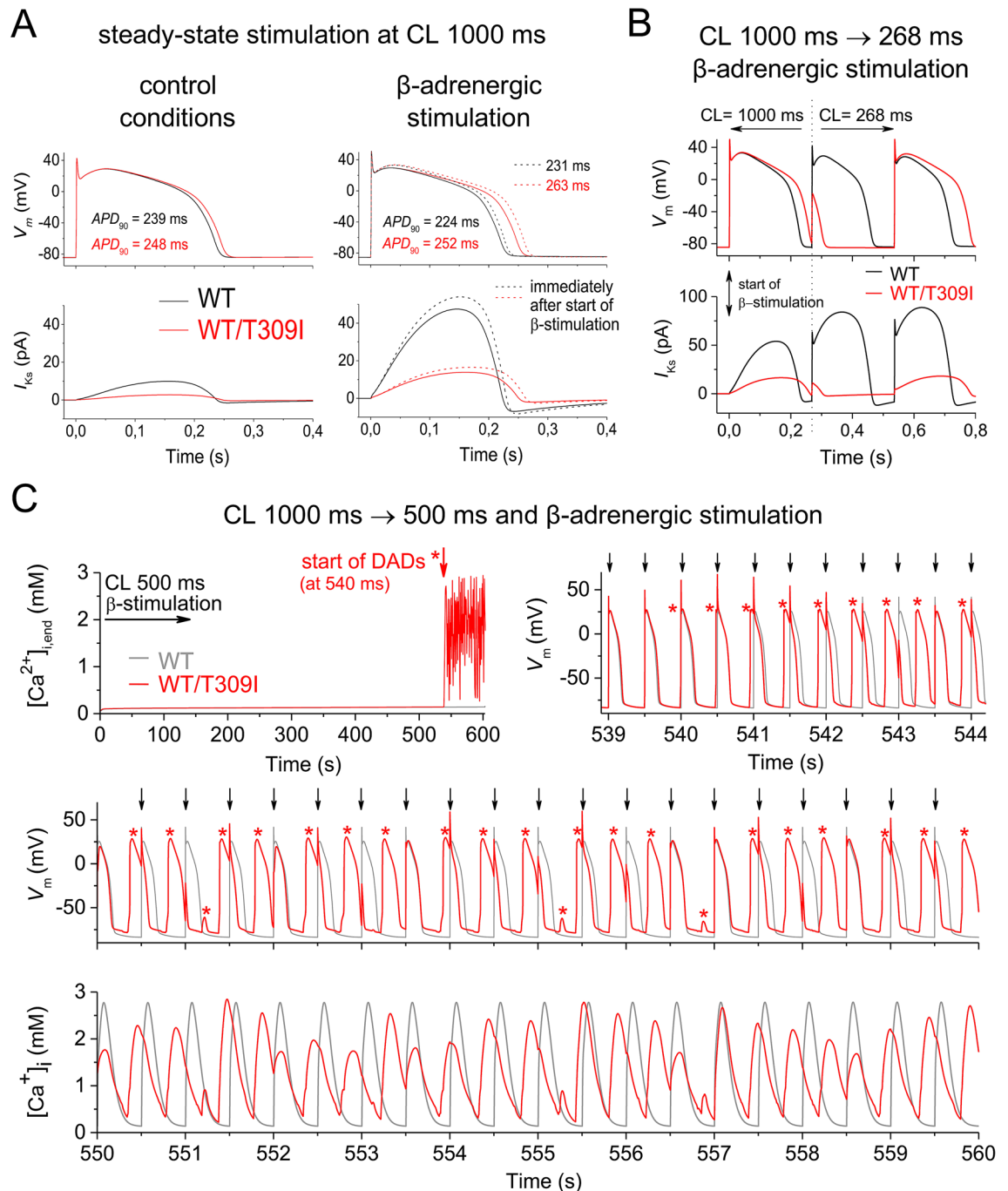
**Genetic characteristics of families with T309I variant.** The same substitution c.926C>T (NM\_000218.2) in the *KCNQ1* gene (Suppl. Fig. S9) resulting in T309I amino acid change in the P-loop of Kv7.1 protein (Fig. 1B, upper panel) was identified in 10 unrelated probands, and in 30 carriers in total (Fig. 1C; heterozygous carriers in all cases). The birthplaces of the oldest known T309I carrier in every family are shown in Fig. 1B, lower panel.

The in silico predictive tools which were used suggested a damaging or disease-causing effect of T309I variant and evolutionary analysis showed high conservation of threonine at this position across species (Suppl. Fig. S9). The T309I variant was found neither in the ExAC nor in the GnomAD online databases.

The same haplotype was identified by STR analysis in the region nearest to the mutation spot in all T309I carriers (Fig. 1D). The same allele was detected in 100 SNPs surrounding the variant in all probands with SNP analysis, which also delimited the maximal size of the area shared by all affected individuals to 658,407 bp. This area contained the whole *KCNQ1* gene.

STR and SNP analysis of markers lying more distant from the *KCNQ1* gene identified 3 subgroups of families sharing the same haplotype spanning longer chromosome regions (Fig. 1D). SNP analysis also identified possible crossing-over spots (crosses in Fig. 1D). The maximum size of the area shared by two families (8 and 10) was delimited with 1847 SNPs and measured 12,633,501 bp. Genealogical analysis also revealed that the oldest carriers of T309I variant in these two families came from two neighbouring villages.

In the marker D11S4088 (the closest one to the *KCNQ1* gene), the same fragment with a length of 211 bp segregating with T309I variant was detected in all families. This marker was highly polymorphic in a control population; the fragment lengths varied between 203 and 253 bp. The 211-bp fragment was detected in 13 out



**Figure 5.** Impact of WT/T309I dysfunctional channels on action potential (AP) configuration in a human ventricular cell model. **(A)** APs (upper panels) and  $I_{Ks}$  (lower panels) at steady-state stimulation at the cycle length (CL) 1000 ms in control conditions and during  $\beta$ -adrenergic stimulation;  $APD_{90}$ —AP duration at 90%-re-polarization. **(B)** APs (upper panels) and  $I_{Ks}$  (lower panels) at extrastimulation within the vulnerable period of AP in the WT/T309I model during  $\beta$ -adrenergic stimulation—CL suddenly shortened from 1000 to 268 ms. **(C)** Intracellular  $Ca^{2+}$  concentration at the end of stimulation cycle ( $[Ca^{2+}]_{i, end}$ ; left upper panel), APs (right upper and middle panels) and intracellular  $Ca^{2+}$  transients ( $[Ca^{2+}]_i$ ; lower panel) after change of CL from 1000 to 500 ms and contemporary start of  $\beta$ -adrenergic stimulation (for sequence of changes, note the time axes in all graphs); arrows—stimuli at CL 500 ms, \*delayed afterdepolarization (DAD) or AP activated by DAD. All graphs were prepared using the software Origin, version 8.5.1.

of 104 chromosomes, resulting in allele frequency of 0.125. The probability that 10 unrelated people would have this allele is negligible ( $9.5 \times 10^{-7}$ ).

**Impact of T309I variant on  $I_{Ks}$  channel function.** All functional data were measured in the presence of KCNE1 subunits. If not otherwise stated, the stimulation frequency was 0.08 Hz. Considering the study by Kula et al.<sup>26</sup>, conversion of the magnitude of the measured current to the current density was avoided (for details, see Methods).

The homozygous T309I channels resulted in a complete absence of  $I_{Ks}$  (Fig. 2A,B), even if stimulated up to +140 mV (for the experimental protocol, see Fig. 2C). The membrane current responses in non-transfected CHO cells did not differ from those in homozygous T309I channels (Fig. 2D).

In the heterozygous WT/T309I channels,  $I_{Ks}$  amplitude was significantly decreased compared to WT channels (Fig. 2A,B). The dysfunction showed characteristics of dominant negativity—WT/T309I current was suppressed by 82 to 55% at voltages between -30 and +20 mV (*i.e.* at voltages relevant for the cardiac action potential). The voltage dependence of steady-state activation was significantly shifted to the right in WT/T309I channels (Fig. 2E; the half-maximal activation voltage  $V_{1/2} = 8.3 \pm 2.2$  mV in WT channels and  $15.6 \pm 2.1$  mV in WT/T309I channels,  $P < 0.05$ ); the slope factors  $k$  remained unaltered ( $15.7 \pm 0.7$  and  $17.3 \pm 0.8$ ). The time course of activation was significantly decelerated in WT/T309I channels at voltages between 0 and +50 mV (Fig. 2F; the time constant of activation  $\tau_{act}$  at +20 mV:  $1740 \pm 110$  ms in WT channels and  $2254 \pm 240$  ms in WT/T309I channels,  $P < 0.05$ ). No significant changes of the time constant of deactivation ( $\tau_{deact}$ ) were observed (Fig. 2F;  $220.5 \pm 26.9$  ms in WT channels and  $253.6 \pm 33.8$  ms in WT/T309I channels at -80 mV; the experimental protocol shown in the inset of Fig. 2F).

Subsequently, sets of hundred 200-ms pulses from -80 to +20 mV were applied after a 30-s pause (inset in Fig. 3A).  $I_{Ks}$  amplitude was not significantly different during the 1st and 100th pulse during stimulation with the interpulse interval of 800 ms (Fig. 3A). At shorter interpulse intervals,  $I_{Ks}$  accumulated in both WT and WT/T309I channels, up to a similar extent in the relative scale (Fig. 3A; for data in absolute values at the interpulse interval of 100 ms, see Fig. 3B). Accumulation of  $I_{Ks}$  during simulated  $\beta$ -adrenergic stimulation (cAMP and OA in the pipette solution) was preserved in WT/T309I channels, being similar in WT and WT/T309I channels in the relative scale (reaching relative steady-state increase of the tail current by 36.2% in WT/T309I channels on average, vs. 35.6% in WT channels; Fig. 3C–E). As demonstrated in Fig. 3B,C, the preserved reactivity of WT/T309I channels to both the high-rate and  $\beta$ -adrenergic stimulations was not sufficient to reach adequate  $I_{Ks}$  magnitude (not reaching even the level of the WT current before start of the stimulations).

**Subcellular localization of  $I_{Ks}$  channels with T309I variant.** Since  $I_{Ks}$  was absent in the homozygous T309I channels (Fig. 2A,B), the subcellular localization of WT and T309I subunits (in the presence of KCNE1) was studied. WT-GFP channels showed clear fluorescence preferentially localized at the cell membrane (Fig. 4A,B, left panels;  $P < 0.001$ ). In contrast, T309I-GFP channels seemed to be retained inside of the cell (Fig. 4A,B, middle panels). To prove this hypothesis, experiments with cells expressing T309I-GFP channels were repeated in a new set of cells, with the cell membrane marked by a red fluorescent dye. GFP fluorescence tagged with T309I subunits (green line/dots) was detected only inside of the cells, *i.e.* not in the cell membrane (red line/dots; Fig. 4C,D).

When WT-GFP and T309I-GFP subunits were co-transfected, the GFP fluorescence signal was present both on the cell membrane and inside the cells (Fig. 4A,B, right panels). It was significantly more intense on the cell membrane ( $P < 0.001$ ). The relative intensity of the fluorescence signal at cytosol was significantly different in all tested transfection variants (Fig. 4B;  $P < 0.001$  in WT vs. T309I,  $P < 0.01$  in WT/T309I vs. T309I, and  $P < 0.05$  in WT vs. WT/T309I). This suggests that trafficking is impaired in the WT/T309I channels; however, contribution of T309I subunits to formation of the cell membrane channels is likely. To prove this hypothesis, channels composed of WT subunits without GFP and T309I subunits tagged with GFP (WT/T309I-GFP) were prepared, and the cell membrane was marked by red fluorescent dye. The fluorescence intensity profile peaks of the cell membrane staining (red line/dots) and of the GFP fluorescence tagged with T309I subunits (green line/dots) overlapped (Fig. 4E,F). This implies that T309I subunits contributed to the formation of  $I_{Ks}$  channels localized in the cell membrane when co-expressed with the WT subunits.

**Functional impact of T309I variant in human cardiac cell model.** At slow steady-state stimulation (cycle length, CL, 1000 ms), the action potential duration at 90%-repolarization ( $APD_{90}$ ) was only slightly prolonged in the model with WT/T309I channels in control conditions (by 3.8% vs. the WT model; Fig. 5A, left panel). This agrees with the well-known limited impact of  $I_{Ks}$  on action potential configuration at low stimulation rates<sup>29–31</sup>. Under  $\beta$ -adrenergic stimulation (Fig. 5A, right panel),  $APD_{90}$  decreased by 6.3% in the WT model (as usual<sup>32</sup>) but increased by 1.6% in the WT/T309I model. This resulted in substantially longer  $APD_{90}$  in the WT/T309I vs. WT model at  $\beta$ -adrenergic stimulation (by 12.5%, or, during the first action potential after start of  $\beta$ -adrenergic stimulation, even by 13.9%).

If extrastimulation was applied within the vulnerable period of the first WT/T309I action potential after the start of  $\beta$ -adrenergic stimulation, the first action potential was suppressed and the following one was extremely prolonged in the WT/T309I model (it was longer by 31% in comparison with WT model; Fig. 5B). Irregular suppression of action potentials and action potential alternans followed (not illustrated). To provoke this, CL had to be decreased below 269 ms in the WT/T309I model, and below 238 ms in the WT model.

If CL was shortened to 500 ms and  $\beta$ -adrenergic stimulation was started at the same time (*i.e.* conditions comparable to the start of physical activity), the prolonged action potential in the WT/T309I model under



$\beta$ -adrenergic stimulation resulted in  $\text{Ca}^{2+}$  overload and development of delayed afterdepolarizations (DADs), often eliciting a premature action potential, within 540 s (Fig. 5C).

## Discussion

In this study, we performed a detailed description of the c.926C>T-*KCNQ1* (p.T309I-Kv7.1) variant, the first identified founder LQTS mutation in Central Europe. The dominant negative dysfunction of T309I  $I_{Ks}$  channels was observed in the heterozygous setting. Mathematical modelling demonstrated formation of DADs and action potential alternans at short CLs during  $\beta$ -adrenergic stimulation.

**Founder effect of T309I variant.** The T309I variant was identified almost simultaneously in a Taiwanese family<sup>33</sup> and in our earlier report<sup>34</sup>. No functional data has been available so far.

As the T309I variant was detected in 10 probands in our cohort of 44 LQTS1 families, its prevalence is unusually high in our region<sup>25</sup>. Majority of these 10 carrier families is geographically clustered (Fig. 1B, lower panel). Such characteristics are typical for mutations derived from the founder effect. Using detailed haplotype analysis of both STR and SNP markers, we confirmed that all affected individuals shared the same haplotype spanning ~658 kbp including the complete coding region of the *KCNQ1* gene (Fig. 1D). Allelic variability at a greater distance from the mutation spot can be explained by crossing overs in T309I ancestors. We identified three subgroups of haplotypes among the 10 investigated families, which are shared also in distant markers. The maximum length of the shared haplotype between two families (8 and 10) was ~12.63 Mb, and was represented by the same allele in the 1847 SNPs analysed (Fig. 1D). Hence, these two families are more closely related, which also correlates with their geographical origin. A close common ancestor could be also predicted in two other subgroups of families with shared haplotypes.

**Functional defect in T309I  $I_{Ks}$  channels.** Considering the position of the T309I-Kv7.1 variant in a highly conserved pore helix<sup>35</sup> and the replacement of the small polar residue by the bigger non-polar one, serious functional defect may be expected.

$I_{Ks}$  was completely missing in the homozygous T309I channels (Fig. 2A,B) due to impaired channel trafficking (Fig. 4A,B), similarly as in the near variant A302V<sup>36</sup> and in some other pore-region LQTS1 variants<sup>37,38</sup>. However, other  $I_{Ks}$  pore region variants showed unaffected trafficking<sup>39,40</sup>. This implies that only specific residues within the  $I_{Ks}$  pore play a role in the process.

In the heterozygous WT/T309I channels, dominant negativity was observed (Fig. 2A,B), as is often found in the pore-region LQTS1 variants<sup>36–42</sup>. A rightward shift of the voltage dependence of channel activation (Fig. 2E), which was also detected in some other pore-region LQTS1 variants<sup>37,38,40–42</sup>, suggests that even pore residues can modify the voltage sensitivity of the  $I_{Ks}$  channel. It has to be noted that variable expression ratio of *KCNQ1* and *KCNE1* in WT and WT/T309I channel complexes might contribute to the rightward activation shift. In WT/T309I channels, we also observed significantly decelerated activation kinetics (Fig. 2F). No other study analysing functional defects in the pore-region LQTS1 variants that we have found reported data on the activation kinetics; thus, we cannot assume that these variants generally exert an analogical effect. Response to  $\beta$ -adrenergic stimulation was preserved in WT/T309I channels (Fig. 3C–E), comparable to that reported by Spätjens et al.<sup>31</sup> under similar conditions. Since the P-loop mutations studied so far showed unaltered  $\beta$ -adrenergic  $I_{Ks}$  accumulation<sup>43</sup>, P-loop is not likely involved in this essential regulation of  $I_{Ks}$  channel function.

Considering the data presented in Fig. 4E,F, a reverse way of cotransfection of WT and T309I subunits (WT tagged with GFP and T309I without GFP) might help to elucidate if a trafficking defect of WT subunits contributes to the observed  $I_{Ks}$  channel dysfunction described in Fig. 2. Comparing the intracellular GFP signals in Fig. 4B (right panel) and 4F (being not significantly different,  $P > 0.05$ ), it seems that most of the subunits retained inside the cell are T309I subunits if both WT and T309I subunits are coexpressed. However,  $I_{Ks}$  channel is a heterotetrameric channel that is indeed formed by various combinations of WT and T309I subunits if both are transfected (and if even the mutated T309I subunit is present on the cell membrane, Fig. 4E,F). Taking all this into account, we speculate that a slight intracellular retention of WT subunits might happen if WT and T309I subunits are coexpressed.

**Genotype—phenotype correlation in the T309I variant.** A mild LQTS phenotype was observed in the heterozygous T309I carriers, similarly to many other founder variants<sup>14,44</sup> and also to some other pore region LQTS1 variants<sup>36,40,42</sup>. Surprisingly, a dominant negative dysfunction was revealed in the heterozygous T309I channels (Figs. 2 and 3). A similar contradiction between the channel dysfunction and clinical phenotype was described in the near A302V variant<sup>36</sup>. The mild T309I phenotype likely results from the preserved reactivity of the heterozygous mutated channels to high-rate and  $\beta$ -adrenergic stimulations (Fig. 3). This may partially compensate the dominant negative dysfunction at situations when  $I_{Ks}$  is essential for proper cardiac cell repolarization, namely during exercise or stress.

As predicted by in silico modelling on a human ventricular cell model, stimulation with shortened CL during  $\beta$ -adrenergic stimulation may trigger proarrhythmic activity in patients with WT/T309I  $I_{Ks}$  channels (Fig. 5B,C). DADs were observed, which even promoted premature action potentials. This observation may seem unexpected considering previously published studies which typically demonstrated occurrence of EADs in LQTS1 under  $\beta$ -adrenergic stimulation, including studies performed on patient-specific derived cardiomyocytes<sup>45–47</sup> and on animal models<sup>48–50</sup>. According to other studies, EADs as an arrhythmogenic mechanism seem to be preferentially connected to LQTS type 2 which is based on mutations in the *KCNH2* gene (the rapid delayed rectifier current  $I_{Kr}$  is affected) and in which the TdP arrhythmia is usually pause-dependent<sup>51,52</sup>. In contrast, pause-independent TdP has been observed in LQTS1<sup>52</sup>. The fast heart rate preceding TdP (absence of pause) in LQTS1 is compatible with

the mechanism of genesis of DADs<sup>53</sup>. Genesis of DADs at fast rates during  $\beta$ -adrenergic stimulation accompanied by  $I_{Ks}$  dysfunction (both pharmacologically-induced) was demonstrated in canine cardiac cells and tissue<sup>54,55</sup>, similarly as we have seen it in our human ventricular cell model with WT/T309I channels (Fig. 5C). The above listed contradictory data on LQTS1 arrhythmogenic mechanism suggest necessity of a further detailed study within this field.

In our model, the development of DADs was caused by an increase of sodium-calcium exchange current and calcium-activated non-specific current, due to a premature release of  $Ca^{2+}$  from the sarcoplasmic reticulum at intracellular  $Ca^{2+}$  overload, which in turn was caused by prolonged action potentials at the fast heart rate (for details, see Suppl. Fig. S10). This proarrhythmic events predicted by in silico modelling may explain the occurrence of arrhythmias during physical exertion in T309I carriers (see “Clinical characteristics of T309 I carriers”).

The essential proarrhythmogenic role of  $Ca^{2+}$  overload suggested by in silico modelling should be considered in clinical practise in the future. It implies that, beside the standard treatment with  $\beta$ -blocking agents, additional or modified treatment may be beneficial in some LQTS1 patients, namely those who insufficiently respond to the standard  $\beta$ -blocking therapy. As demonstrated in Suppl. Fig. S11, a slight (5%) inhibition of the cardiac calcium current  $I_{Ca}$  is able to prevent development of DADs in our WT/T309I model during the tested period of 600 ms with a negligible effect on the magnitude of the intracellular  $Ca^{2+}$  transient (thus, likely not significantly impairing cardiac contractility). It implies that possible new treatment strategy of low doses of verapamil might be relevant in some LQTS1 patients, similarly as in patients with refractory catecholaminergic polymorphic ventricular tachycardia<sup>56</sup>. In patients with compromised cardiac contractility (in whom even a mild  $I_{Ca}$  inhibition would be contraindicated), a decrease of the late sodium current ( $I_{Na,late}$ ) might be beneficial<sup>57,58</sup>.

**Limitations of the study.** Use of the human ionic channels heterogeneously expressed in a cell line limits possibilities of direct experimental investigation of impact of a particular mutation on complex cardiac cell electrophysiology. Therefore, it might be beneficial to prove the data in another model, for example in isolated cardiomyocytes of the affected patient/s (which is however very problematic, if not impossible, from ethical reasons), or in patient-specific cardiomyocytes derived from the induced pluripotent stem cells. Likewise, such more complex in vitro models might be helpful to better validate the human ventricular cell in silico model. In addition, introduction of the experimental data presented here into a mathematical model of electromechanical activity of the left ventricle or even of the whole heart might reveal the effects of  $I_{Ks}$  suppression on propensity of the heart to development of reentry-based arrhythmias and on ECG under control conditions and at adrenergic stimulation. In coexpression of WT and T309I subunits, a slight trafficking defect of WT subunits might contribute to the observed  $I_{Ks}$  channel dysfunction. Unfortunately, a direct proof of this suspicion is missing in the study.

**Conclusions.** The c.926C>T-KCNQ1 pore variant (p.T309I-Kv7.1) is the first LQTS-related founder mutation in Central Europe. Its dominant negative effect on  $I_{Ks}$  channel function is in contrast with the mild phenotype. As predicted by in silico modelling, the dysfunction may result in genesis of proarrhythmic DADs and action potential alternans at fast rates during  $\beta$ -adrenergic stimulation. Elimination of DADs by  $I_{Ca}$  modulation might be a possible new treatment strategy in some LQTS1 patients.

## Data availability

The relevant data are available from the authors upon reasonable request.

Received: 4 September 2020; Accepted: 30 December 2020

Published online: 11 February 2021

## References

- Schwartz, P. J. *et al.* Prevalence of the congenital long QT syndrome. *Circulation* **120**, 1761–1767 (2009).
- Schwartz, P. J., Crotti, L. & Insolia, R. Long-QT syndrome: from genetics to management. *Circ. Arrhythm. Electrophysiol.* **5**, 868–877 (2012).
- Crotti, L. *et al.* Calmodulin mutations associated with recurrent cardiac arrest in infants. *Circulation* **127**, 1009–1017 (2013).
- Tester, D. J., Will, M. L., Haglund, C. M. & Ackerman, M. J. Compendium of cardiac channel mutations in 541 consecutive unrelated patients referred for long QT syndrome genetic testing. *Heart Rhythm*. **2**, 507–517 (2005).
- Kapplinger, J. D. *et al.* Spectrum and prevalence of mutations from the first 2,500 consecutive unrelated patients referred for the FAMILION® long QT syndrome genetic test. *Heart Rhythm*. **6**, 1297–1303 (2009).
- Adler, A. *et al.* An international, multicentered, evidence-based reappraisal of genes reported to cause congenital long QT syndrome. *Circulation* **141**, 412–428 (2020).
- Russell, M. W., Dick, M., Collins, F. S. & Brody, L. C. KVLQT1 mutations in three families with familial or sporadic long QT syndrome. *Hum. Mol. Genet.* **5**, 1319–1324 (1996).
- Piippo, K. *et al.* A founder mutation of the potassium channel KCNQ1 in long QT syndrome: Implications for estimation of disease prevalence and molecular diagnostics. *J. Am. Coll. Cardiol.* **37**, 562–568 (2001).
- Brink, P. A. *et al.* Phenotypic variability and unusual clinical severity of congenital long-QT syndrome in a founder population. *Circulation* **112**, 2602–2610 (2005).
- Fodstad, H. *et al.* Molecular characterization of two founder mutations causing long QT syndrome and identification of compound heterozygous patients. *Ann. Med.* **38**, 294–304 (2006).
- Arbour, L. *et al.* A KCNQ1 V205M missense mutation causes a high rate of long QT syndrome in a First Nations community of northern British Columbia: a community-based approach to understanding the impact. *Genet. Med.* **10**, 545–550 (2008).
- Bhuiyan, Z. A. *et al.* Clinical and genetic analysis of long QT syndrome in children from six families in Saudi Arabia: Are they different?. *Pediatr. Cardiol.* **30**, 490–501 (2009).
- Marjamaa, A. *et al.* High prevalence of four long QT syndrome founder mutations in the Finnish population. *Ann. Med.* **41**, 234–240 (2009).
- Winbo, A., Diamant, U.-B., Stattin, E.-L., Jensen, S. M. & Rydberg, A. Low incidence of sudden cardiac death in a Swedish Y111C type 1 long-QT syndrome population. *Circ. Cardiovasc. Genet.* **2**, 558–564 (2009).

15. Eldstrom, J. *et al.* Mechanistic basis for LQT1 caused by S3 mutations in the KCNQ1 subunit of  $I_{Ks}$ . *J. Gen. Physiol.* **135**, 433–448 (2010).
16. Gray, C. *et al.* Expression of a common LQT1 mutation in five apparently unrelated families in a regional inherited arrhythmia clinic. *J. Cardiovasc. Electrophysiol.* **21**, 296–300 (2010).
17. Hofman, N. *et al.* Recurrent and founder mutations in the Netherlands: the long-QT syndrome. *Neth. Heart J.* **19**, 10–16 (2011).
18. Stattin, E.-L. *et al.* Founder mutations characterise the mutation panorama in 200 Swedish index cases referred for Long QT syndrome genetic testing. *BMC Cardiovasc. Disord.* **12**, 95. <https://doi.org/10.1186/1471-2261-12-95> (2012).
19. Zafari, Z. *et al.* Identification and characterization of a novel recessive KCNQ1 mutation associated with Romano-Ward Long-QT syndrome in two Iranian families. *J. Electrocardiol.* **50**, 912–918 (2017).
20. Offerhaus, J. A., Bezzina, C. R. & Wilde, A. A. M. Epidemiology of inherited arrhythmias. *Nat. Rev. Cardiol.* **17**, 205–215 (2020).
21. Priori, S. G. *et al.* ESC Guidelines for the management of patients with ventricular arrhythmias and the prevention of sudden cardiac death: The Task Force for the Management of Patients with Ventricular Arrhythmias and the Prevention of Sudden Cardiac Death of the European Society of Cardiology (ESC). Endorsed by: Association for European Paediatric and Congenital Cardiology (AEPCC). *Eur. Heart J.* **36**, 2793–2867 (2015).
22. Choi, Y. & Chan, A. P. PROVEAN web server: a tool to predict the functional effect of amino acid substitutions and indels. *Bioinformatics* **31**, 2745–2747 (2015).
23. Shihab, H. A. *et al.* Ranking non-synonymous single nucleotide polymorphisms based on disease concepts. *Hum. Genomics*. **8**, 11. <https://doi.org/10.1186/1479-7364-8-11> (2014).
24. López-Ferrando, V., Gazzo, A., de la Cruz, X., Orozco, M. & Gelpí, J. L. PMut: a web-based tool for the annotation of pathological variants on proteins, 2017 update. *Nucleic Acids Res.* **45**, W222–W228 (2017).
25. Lek, M. *et al.* Analysis of protein-coding genetic variation in 60,706 humans. *Nature* **536**, 285–291 (2016).
26. Kula, R., Běbarová, M., Matejovič, P., Šimurda, J. & Pásek, M. Current density as routine parameter for description of ionic membrane current: is it always the best option? *Prog. Biophys. Mol. Biol.* **157**, 24–32 (2020).
27. Hrabcová, D., Pásek, M., Šimurda, J. & Christé, G. Effect of ion concentration changes in the limited extracellular spaces on sarcolemmal ion transport and  $Ca^{2+}$  turnover in a model of human ventricular cardiomyocyte. *Int. J. Mol. Sci.* **14**, 24271–24292 (2013).
28. Kula, R., Běbarová, M., Matejovič, P., Šimurda, J. & Pásek, M. Distribution of data in cellular electrophysiology: Is it always normal? *Prog. Biophys. Mol. Biol.* **157**, 11–17 (2020).
29. Jost, N. *et al.* Restricting excessive cardiac action potential and QT prolongation: a vital role for IKs in human ventricular muscle. *Circulation* **112**, 1392–1399 (2005).
30. Roden, D. M. & Yang, T. Protecting the Heart Against Arrhythmias: Potassium Current Physiology and Repolarization Reserve. *Circulation* **112**, 1376–1378 (2005).
31. Spätjens, R. L. H. M. G. *et al.* Long-QT mutation p.K557E-Kv7.1: dominant-negative suppression of IKs, but preserved cAMP-dependent up-regulation. *Cardiovasc. Res.* **104**, 216–225 (2014).
32. Szentandrassy, N. *et al.* Role of action potential configuration and the contribution of  $Ca^{2+}$  and  $K^{+}$  currents to isoprenaline-induced changes in canine ventricular cells: Isoprenaline in canine heart. *Br. J. Pharmacol.* **167**, 599–611 (2012).
33. Ko, Y. L. *et al.* Linkage and mutation analysis in two Taiwanese families with long QT syndrome. *J. Formos. Med. Assoc. Taiwan Yi. Zhi.* **100**, 767–771 (2001).
34. Andrsova, I. *et al.* Clinical characteristics of 30 Czech families with long QT syndrome and KCNQ1 and KCNH2 gene mutations: importance of exercise testing. *J. Electrocardiol.* **45**, 746–751 (2012).
35. Bohnen, M. S. *et al.* Molecular pathophysiology of congenital long QT syndrome. *Physiol. Rev.* **97**, 89–134 (2017).
36. Steffensen, A. B. *et al.* IKs gain- and loss-of-function in early-onset lone atrial fibrillation. *J. Cardiovasc. Electrophysiol.* **26**, 715–723 (2015).
37. Mousavi, N. A., Gharaie, S. & Jeong, K. H. Cellular mechanisms of mutations in Kv7.1: auditory functions in Jervell and Lange-Nielsen syndrome vs Romano-Ward syndrome. *Front. Cell. Neurosci.* **9**, 32. <https://doi.org/10.3389/fncel.2015.00032> (2015).
38. Burgess, D. E. *et al.* High-risk long QT syndrome mutations in the Kv71 (KCNQ1) pore disrupt the molecular basis for rapid  $K^{+}$  permeation. *Biochemistry (Mosc)*. **51**, 9076–9085 (2012).
39. Ikrar, T. *et al.* A double-point mutation in the selectivity filter site of the KCNQ1 potassium channel results in a severe phenotype, LQT1, of long QT syndrome. *J. Cardiovasc. Electrophysiol.* **19**, 541–549 (2008).
40. Bianchi, L. *et al.* Mechanisms of IKs suppression in LQT1 mutants. *Am. J. Physiol. Heart Circ. Physiol.* **279**, H3003–H3011 (2000).
41. Li, W. *et al.* The G314S KCNQ1 mutation exerts a dominant-negative effect on expression of KCNQ1 channels in oocytes. *Biochem. Biophys. Res. Commun.* **383**, 206–209 (2009).
42. Aidery, P. *et al.* Impaired ion channel function related to a common KCNQ1 mutation: implications for risk stratification in long QT syndrome 1. *Gene* **511**, 26–33 (2012).
43. Policarová, M., Novotný, T. & Běbarová, M. Impaired Adrenergic/Protein Kinase A Response of Slow Delayed Rectifier Potassium Channels as a Long QT Syndrome Motif: Importance and Unknowns. *Can. J. Cardiol.* **35**, 511–522 (2019).
44. Winbo, A. *et al.* Phenotype, origin and estimated prevalence of a common long QT syndrome mutation: a clinical, genealogical and molecular genetics study including Swedish R518X/KCNQ1 families. *BMC Cardiovasc. Disord.* **14**, 22. <https://doi.org/10.1186/1471-2261-14-22> (2014).
45. Moretti, A. *et al.* Patient-specific induced pluripotent stem cell models for long-QT syndrome. *N. Engl. J. Med.* **363**, 1397–1409 (2010).
46. Sogo, T. *et al.* Electrophysiological properties of iPSC cell-derived cardiomyocytes from a patient with long QT syndrome type 1 harboring the novel mutation M437V of KCNQ1. *Regen. Ther.* **4**, 9–17 (2016).
47. Wang, Z. *et al.* Pathogenic mechanism and gene correction for LQTS-causing double mutations in KCNQ1 using a pluripotent cell model. *Stem Cell Res.* **38**, 101483. <https://doi.org/10.1016/j.scr.2019.101483> (2019).
48. Liu, G. X. *et al.* Differential conditions for early after-depolarizations and triggered activity in cardiomyocytes derived from transgenic LQT1 and LQT2 rabbits. *J. Physiol.* **590**, 1171–1180 (2012).
49. Kim, T. Y. *et al.* Complex excitation dynamics underlie polymorphic ventricular tachycardia in a transgenic rabbit model of long QT syndrome type 1. *Heart Rhythm.* **12**, 220–228 (2015).
50. ter Bekke, R. M. A. *et al.* Proarrhythmic proclivity of left-stellate ganglion stimulation in a canine model of drug-induced long-QT syndrome type 1. *Int. J. Cardiol.* **286**, 66–72 (2019).
51. Liu, J. & Laurita, K. R. The mechanism of pause-induced torsades de pointes in long QT syndrome. *J. Cardiovasc. Electrophysiol.* **16**, 981–987 (2005).
52. Tan, H. L. *et al.* Genotype-specific onset of arrhythmias in congenital long-QT syndrome: possible therapy implications. *Circulation* **114**, 2096–2103 (2006).
53. Marban, E., Robinson, S. W. & Wier, W. G. Mechanisms of arrhythmogenic delayed and early afterdepolarizations in ferret ventricular muscle. *J. Clin. Invest.* **78**, 1185–1192 (1986).
54. Burashnikov, A. & Antzelevitch, C. Block of IKs does not induce early afterdepolarization activity but promotes beta-adrenergic agonist-induced delayed afterdepolarization activity. *J. Cardiovasc. Electrophysiol.* **11**, 458–465 (2000).
55. Johnson, D. M. *et al.* Diastolic spontaneous calcium release from the sarcoplasmic reticulum increases beat-to-beat variability of repolarization in canine ventricular myocytes after  $\beta$ -adrenergic stimulation. *Circ. Res.* **112**, 246–256 (2013).

56. Swan, H., Laitinen, P., Kontula, K. & Toivonen, L. Calcium channel antagonism reduces exercise-induced ventricular arrhythmias in catecholaminergic polymorphic ventricular tachycardia patients with RyR2 mutations. *J. Cardiovasc. Electrophysiol.* **16**, 162–166 (2005).
57. Shryock, J. C., Song, Y., Rajamani, S., Antzelevitch, C. & Belardinelli, L. The arrhythmogenic consequences of increasing late INa in the cardiomyocytes. *Cardiovasc. Res.* **99**, 600–611 (2013).
58. Belardinelli, L. *et al.* A novel, potent, and selective inhibitor of cardiac late sodium current suppresses experimental arrhythmias. *J. Pharmacol. Exp. Ther.* **344**, 23–32 (2013).

## Acknowledgements

This work was supported by the Ministry of Health of the Czech Republic, Grant No. 16-30571A. The authors thank prof. Paul G.A. Volders (Maastricht University, Netherlands) and prof. Robert S. Kass (Columbia University, USA) for kindly providing the plasmids, to Mrs. B. Vyoralová for technical assistance, and to Joseph Lennon, BA, PhD for English proofreading.

## Author contributions

I.S.—data acquisition and evaluation (genetic analysis including the haplotype analysis), preparation of Fig. 1, Suppl. Fig. S9, and of Suppl. Tabs. S1 and S2, writing of the manuscript; M.B.—study design, data acquisition and evaluation (whole cell patch clamp), preparation of Figs. 1, 2, 3, 4 and 5, Suppl. Fig. S8, and of Table 1, writing of the manuscript; I.A.—data acquisition and evaluation (clinical analysis in adults), preparation of Table 1; L.C.—data acquisition and evaluation (confocal microscopy), writing of the manuscript; O.Š.—data acquisition and evaluation (whole cell patch clamp, confocal microscopy), preparation of Fig. 4; J.H.—data acquisition and evaluation (site direction mutagenesis and amplification of plasmids), writing of the manuscript; M.P.—data acquisition and evaluation (mathematical modelling), preparation of Fig. 5, Suppl. Figs. S1–S6 and S10–S11, and of Suppl. Tab. S3, writing of the manuscript; P.V.—data acquisition and evaluation (clinical analysis in children); I.V.—data acquisition (genetic analysis); R.G.—data acquisition (genetic analysis); R.N.—data acquisition (haplotype analysis); T.N.—study design, data acquisition and evaluation (clinical analysis in adults), preparation of Suppl. Fig. S7, writing of the manuscript. All authors reviewed the manuscript.

## Competing interests

The authors declare no competing interests.

## Additional information

**Supplementary Information** The online version contains supplementary material available at <https://doi.org/10.1038/s41598-021-81670-1>.

**Correspondence** and requests for materials should be addressed to M.B.

**Reprints and permissions information** is available at [www.nature.com/reprints](http://www.nature.com/reprints).

**Publisher's note** Springer Nature remains neutral with regard to jurisdictional claims in published maps and institutional affiliations.



**Open Access** This article is licensed under a Creative Commons Attribution 4.0 International License, which permits use, sharing, adaptation, distribution and reproduction in any medium or format, as long as you give appropriate credit to the original author(s) and the source, provide a link to the Creative Commons licence, and indicate if changes were made. The images or other third party material in this article are included in the article's Creative Commons licence, unless indicated otherwise in a credit line to the material. If material is not included in the article's Creative Commons licence and your intended use is not permitted by statutory regulation or exceeds the permitted use, you will need to obtain permission directly from the copyright holder. To view a copy of this licence, visit <http://creativecommons.org/licenses/by/4.0/>.

© The Author(s) 2021



OPEN

# Author Correction: Long-QT founder variant T309I-Kv7.1 with dominant negative pattern may predispose delayed afterdepolarizations under $\beta$ -adrenergic stimulation

Iva Synková, Markéta Bébarová, Irena Andršová, Larisa Chmelikova, Olga Švecová, Jan Hošek, Michal Pásek, Pavel Vít, Iveta Valášková, Renata Gaillyová, Rostislav Navrátil & Tomáš Novotný

Correction to: *Scientific Reports* <https://doi.org/10.1038/s41598-021-81670-1>, published online 11 February 2021

This Article contains an error in concentration unit in Fig. 5c and Supplementary Figure S11 where,

“milimole (mM)”

should read:

“micromole ( $\mu$ M)”

The correct Figure 5c and S11 appear below as Figures 1 and 2 respectively.

Published online: 29 April 2021

CL 1000 ms → 500 ms and β-adrenergic stimulation

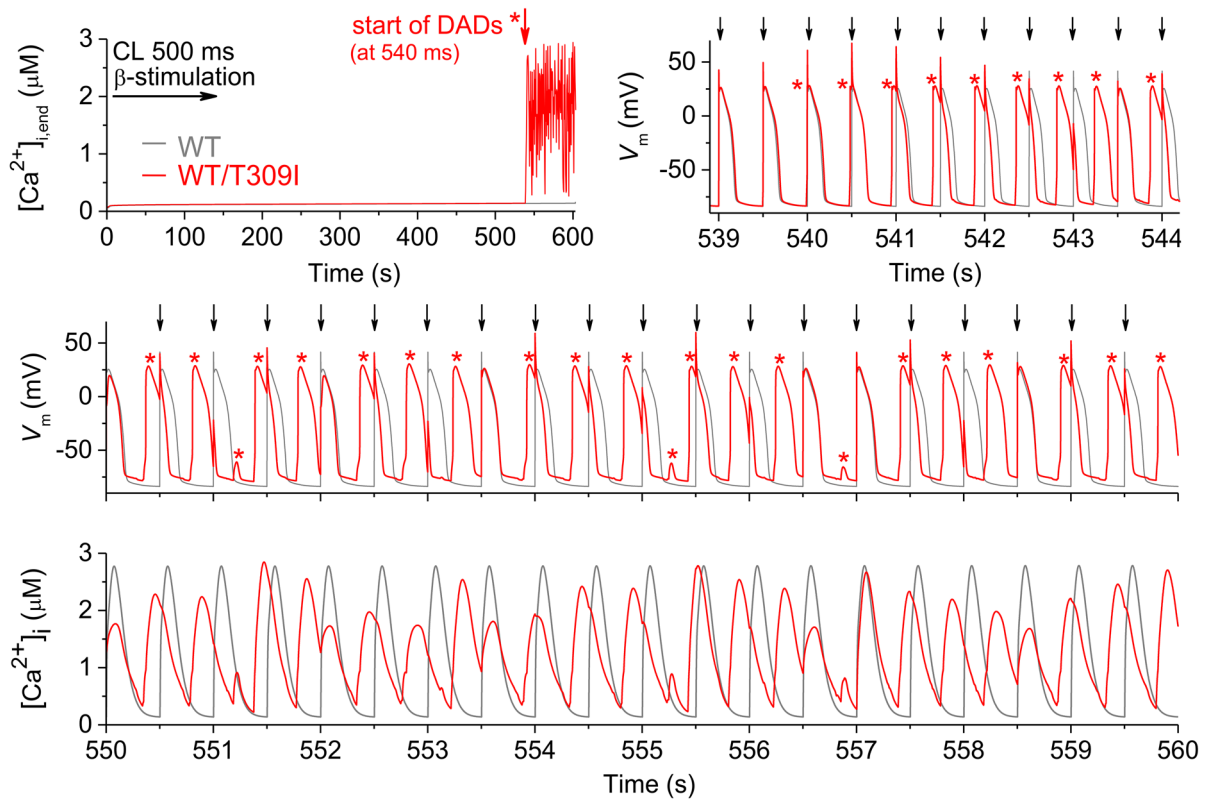


Figure 1. A correct version of the original Figure 5c.

CL 1000 ms → 500 ms and β-adrenergic stimulation

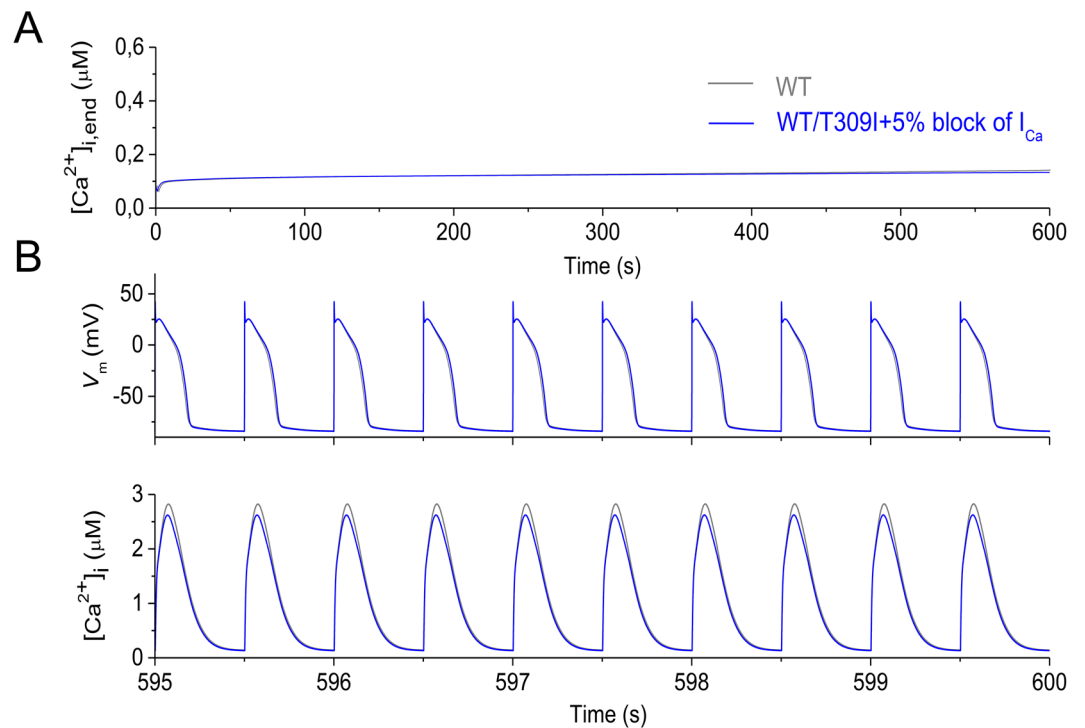


Figure 2. A correct version of the original Figure S11.



**Open Access** This article is licensed under a Creative Commons Attribution 4.0 International License, which permits use, sharing, adaptation, distribution and reproduction in any medium or format, as long as you give appropriate credit to the original author(s) and the source, provide a link to the Creative Commons licence, and indicate if changes were made. The images or other third party material in this article are included in the article's Creative Commons licence, unless indicated otherwise in a credit line to the material. If material is not included in the article's Creative Commons licence and your intended use is not permitted by statutory regulation or exceeds the permitted use, you will need to obtain permission directly from the copyright holder. To view a copy of this licence, visit <http://creativecommons.org/licenses/by/4.0/>.

© The Author(s) 2021

**Long-QT founder variant T309I-Kv7.1 with dominant negative pattern  
may predispose delayed afterdepolarizations  
under  $\beta$ -adrenergic stimulation**

SUPPLEMENTARY MATERIAL

Iva Synková, Markéta Bébarová, Irena Andršová, Larisa Chmelikova, Olga Švecová, Jan  
Hošek, Michal Pásek, Pavel Vít, Iveta Valášková, Renata Gaillyová, Rostislav Navrátil,  
Tomáš Novotný

Correspondence to:

Assoc. Prof. MUDr. Markéta Bébarová, Ph.D.

Department of Physiology  
Faculty of Medicine  
Masaryk University  
Kamenice 5  
625 00 Brno  
Czech Republic

tel. +420-549493147, [mbebar@med.muni.cz](mailto:mbebar@med.muni.cz)



## **Supplemental Methods**

### *Clinical diagnostics*

Patients with suspected LQTS are regularly investigated at the Department of Internal Medicine and Cardiology, and at the Department of Paediatrics (both at the University Hospital Brno and Faculty of Medicine, Masaryk University, Brno, Czech Republic). The diagnosis is established according to ESC Guidelines.<sup>1</sup> The study conformed to the principles outlined in the Declaration of Helsinki. All participants signed a written consent form prior to their inclusion in the study. In the case of participants under the age of 18 years, the written informed consent was obtained from a parent and/or legal guardian. The study was approved by the Multicenter Ethical Committee, University Hospital Brno (Brno, Czech Republic).

All individuals included in this study underwent clinical examination and bicycle ergometry to obtain ECG traces at different adrenergic states. A 12-lead ECG with Mason-Likar modification was used. The initial stress was set to 0.5 W/kg, and increased by 0.5 W/kg every three minutes to achieve a heart rate higher than the submaximal value with respect to age and sex.

All ECGs were recorded as paper printings at the speed of 50 mm/s and voltage of 20 mm/mV, and QT and RR intervals were measured manually for the periods of rest and in the fourth minute of the recovery period of the exercise test. In the majority of cases, the QT interval was measured in the lead V5; the other leads were used only when the end of the T wave could not be discriminated in this lead. In cases when the end of T wave was not clearly visible, the threshold method was used. The QT intervals were corrected for the respective heart rate using Bazett's formula:  $QTc = QT/\sqrt{RR}$  (both intervals were measured in seconds).

### *Genetic testing*

Between 2000 and 2018, 132 unrelated index cases with susceptibility to LQTS were

examined at the Department of Medical Genetics (University Hospital Brno and Faculty of Medicine, Masaryk University, Brno, Czech Republic). Informed consents and peripheral blood samples were collected from patients. DNA was extracted by standard molecular techniques. Molecular analysis of LQTS-associated genes including the *KCNQ1* gene was performed according to current practises for molecular genetics diagnostics. The classical method (multiplex PCR/SSCP analysis of 3 LQTS major genes) was followed by Sanger sequencing on ABI 3100 Genetic Analyser (*Applied Biosystems*<sup>™</sup>, Foster City, CA, USA). Primers for the screening of entire coding regions of genes *KCNQ1*, *KCNH2* and *SCN5A* were designed with Primer-BLAST tool.<sup>2</sup> Direct Sanger sequencing was then replaced with massive parallel sequencing (MPS) of 5 LQTS-related genes (*KCNQ1*, *KCNH2*, *SCN5A*, *KCNE1*, *KCNE2*) on GS Junior (*Roche*, Basel, Switzerland). The sequencing library in this case was prepared with a hybridization capture-based target enrichment method using NimbleGen SeqCap EZ Choice Library Kit (*Roche*, Basel, Switzerland). Since 2016, MPS of 13 LQTS-associated genes (*KCNQ1*, *KCNH2*, *SCN5A*, *AKAP9*, *CACNA1C*, *CALM1*, *CALM2*, *CAV3*, *KCNE1*, *KCNE2*, *KCNJ5*, *SCN4B*, *SNTA1*) has been performed on MiSeq (*Illumina*, San Diego, CA, USA). Two types of sequencing library have been used: 1) Amplicon library prepared with commercial kit TruSeq Custom Amplicon Kit (*Illumina*, San Diego, CA, USA); and 2) Target enriched library prepared with hybridization capture-based method using KAPA HyperPlus Kit with SeqCap EZ Choice Library Kit (*Roche*, Basel, Switzerland). The procedure has been performed as recommended by the manufacturer. Genetic counselling and testing of first-degree relatives have been offered to patients at risk.

### *In silico analysis*

Various *in silico* tools were used to predict the possible clinical impact of the identified sequence variant (Suppl. Tab. S1). The functional impact of the amino acid substitution was

predicted with SIFT, Provean,<sup>3</sup> MutationTaster, FATHMM,<sup>4</sup> and PMUT.<sup>5</sup> The conservation of the impacted amino acid position was measured with LRT and MutationAssessor. The visualization of protein conservation across species was performed in MEGA7 software.<sup>6</sup> Protein sequences of included species were obtained from Ensembl Genome Browser ([www.ensembl.org/index.html](http://www.ensembl.org/index.html)). Sequences were aligned with ClustalW with preset parameters. Allele frequency of the substitution was determined from online databases ExAC<sup>7</sup> and GnomAD.

Suppl. Tab. S1: *In silico* prediction of the *KCNQ1* substitution c.926C>T

Tool	Score	Result
SIFT	0	Damaging
Provean	-5.8	Damaging
MutationTaster	1	Disease-Causing
FATHMM	-5.03	Damaging
Pmut	0.94	Disease-Causing
LRT	0.00000199	Deleterious
MutationAssessor	4.1149	High

SIFT - The Sorting Intolerant From Tolerant algorithm, Provean - Protein variation effect analyzer, FATHMM - Functional Analysis through Hidden Markov Models (v2.3), LRT - Likelihood Ratio Test

### *Haplotype analysis*

For the haplotype analysis, 9 STR (short tandem repeats) markers spanning the ~11.9-Mb region of chromosome 11 (including the *KCNQ1* gene) were chosen from UCSC Genome Browser: D11S1363, D11S922, D11S4046, D11S4088, D11S4146, D11S1760, D11S1338, D11S4149, D11S4116 (Suppl. Tab. S2). Multiplex PCR with fluorescently labelled primers and fragment analysis with capillary electrophoresis were performed on SeqStudio Genetic Analyzer (*Applied Biosystems*<sup>TM</sup>, Foster City, CA, USA). The haplotype linked to the mutation was identified by studying segregation in families.

To obtain results with higher resolution and to identify possible crossing over spots, a SNP (single nucleotide polymorphism) marker analysis using HumanKaryomap-12 DNA

Analysis Kit (*Illumina*, San Diego, CA, USA) was also performed in the probands; 6219 SNPs on the p-arm of chromosome 11 were analysed.

Population allele frequency analysis was performed after identifying a common STR allele in the marker D11S4088 in all of the affected individuals. The control group was formed by 52 unrelated patients examined at the Department of Clinical Genetics, Faculty Hospital Brno, with a signed informed consent from each patient agreeing that their DNA samples could be used for clinical research. STR alleles (104) were amplified with fluorescently labelled primers and analysed with capillary electrophoresis.

Suppl. Tab. S2: Analysed STR markers and their distance to the mutation

marker	distance (bp)
D11S1363	-1542365
D11S922	-999468
D11S4046	-641034
c.926C>T	0
D11S4088	150263
D11S1923	633093
D11S4146	1137420
D11S1760	2779668
D11S1338	3383243
D11S4149	6525241
D11S4116	10345930
D11S902	14883773

(UCSC Genome Browser; [www.genome.ucsc.edu/](http://www.genome.ucsc.edu/))

### *Biophysical analysis*

Wild-type (WT) human *KCNQ1* in a pIRES2-eGFP vector and WT human *KCNE1* in a pKB-CMV vector were kindly provided by Prof. Paul G.A. Volders, MD, PhD (Maastricht University, Maastricht, Netherlands). *Yotiao* in a pGW1 vector was the kind gift of Prof. Robert R. Kass (Columbia University, New York, USA).

Plasmid DNA was cloned into chemically competent *Escherichia coli* cells from

NovaBlue Singles™ Competent Cells (*Novagen*, Madison, WI, USA) by the heat-shock technique according to the manufacturer's manual. After cultivation, plasmids were isolated from bacterial cells using endotoxin-free QIAprep Spin Miniprep Kit (*Qiagen*, Hilden, Germany). The quantity and purity of isolated plasmids were measured spectrophotometrically by BioPhotometer (*Eppendorf*, Hamburg, Germany).

The mutation c.926C>T in the human *KCNQ1* (p.T309I) was generated by site-directed mutagenesis using QuikChange II XL Site-Directed Mutagenesis Kit (*Agilent Technologies*, Cedar Creek, TX, USA) with the following primers:

5'-TGGTGGTGACTATGACCACCCCCCACC-3'

5'-GGTGGGGGGTGGTCATAGTCACCACCA-3'

The presence of the mutation in *KCNQ1* was verified by sequencing performed by the *Generi Biotech* company (Hradec Králové, Czech Republic).

TransFast Transfection Reagent (*Promega*, Madison, WI, USA) was used for transfection of the plasmids (*KCNQ1*, *KCNE1* and *Yotiao* in the molar ratio 1:2:4, total amount of DNA was 1 µg and the ratio of DNA to transfection agent was 1:1.5) into Chinese hamster ovary (CHO) cells that were cultured at 37°C / 5% CO<sub>2</sub> in Ham's F-12 medium supplemented with 10% foetal calf serum and 0.005% gentamycin (*Sigma-Aldrich*, St. Louis, MO, USA). *KCNQ1* was transfected in one of three ways: 1) WT variant alone (WT); 2) T309I variant alone (T309I); 3) both the WT and T309I variants cotransfected in the ratio 1:1 (WT/T309I) to mimic the heterozygous state in the mutation carriers.

Measurements were performed ~24 h after the transfection by the whole cell patch clamp technique in the voltage clamp mode at 37°C. The patch pipettes were pulled from borosilicate glass capillary tubes and heat-polished on a programmable horizontal puller (*Zeitz-Instruments Vertriebs GmbH*, Martinsried, Germany). The resistance of the filled glass electrodes was below 2.5 MΩ to keep the access resistance as low as possible. For the

generation of experimental protocols and data acquisition, the Axopatch 200A equipment and pCLAMP 9.2 software (*Molecular Devices*, San José, CA, USA) were used. The series resistance was compensated up to 60%. The measured ionic currents were digitally sampled at 2 kHz (after low-pass filtering at 5 kHz) and stored on the hard disc. For the experimental protocols, please see Results; if not mentioned, the stimulation frequency was 0.08 Hz. The average cell membrane capacitance was comparable in WT, T309I, and WT/T309I  $I_{Ks}$  channels ( $13.8 \pm 1.7$ ,  $13.3 \pm 2.0$ , and  $13.5 \pm 1.8$  pF, respectively;  $P > 0.05$ ).

Tyrode solution of the following composition was used to perfuse the measured cells (in mmol/L): NaCl 132, KCl 4.8, CaCl<sub>2</sub> 2.0, MgCl<sub>2</sub> 1.2, HEPES 10, glucose 5 (pH was adjusted to 7.4 with NaOH). The patch electrode filling solution contained (in mmol/L): K-aspartate 110, K<sub>2</sub>ATP 5, CaCl<sub>2</sub> 1, MgCl<sub>2</sub> 1, EGTA 11, HEPES 10 (pH 7.3 adjusted with KOH). The junction potential was +15 mV. To simulate  $\beta$ -adrenergic stimulation, the pipette solution was supplemented with cyclic adenosine monophosphate (cAMP, 200  $\mu$ mol/L) and inhibitor of serine/threonine phosphatases okadaic acid (OA, 0.2  $\mu$ mol/L) in some experiments. The stock solutions were kept frozen and the chemicals were added to the pipette solution before the measurements were started. The pipette solution was subsequently kept in the fridge, lying on ice, before being filled to the measuring micropipette. The chemicals were purchased from *Sigma-Aldrich* (Prague, Czech Republic) unless otherwise indicated.

The voltage dependence of steady-state activation was fitted using the Boltzmann equation:  $y = I_{\max} / (1 + \exp((V_{1/2} - V) / k))$  to determine the half-maximal activation voltage  $V_{1/2}$  and the slope factor  $k$ . Time courses of activation and deactivation were fitted with a single exponential function:  $y = A \cdot (1 - \exp(-t/\tau))$ , where  $A$  is amplitude and  $\tau$  is the time constant.

### *Confocal microscopy*

WT human *KCNQ1* tagged with GFP at the 3'-terminus or without GFP in a pBK-CMV vector (vector without GFP marker), as well as WT human *KCNE1* in a pBK-CMV vector were kindly provided by Prof. Paul G.A. Volders, MD, PhD (Maastricht University, Maastricht, Netherlands). The mutation c.926C>T (p.T309I) in the human *KCNQ1* with tagged GFP was generated by site-directed mutagenesis technique, as described above.

TransFast Transfection Reagent (*Promega*, Madison, WI, USA) was used for transfection of the plasmids (*KCNQ1* and *KCNE1* in the molar ratio 1:2, the total amount of DNA was 1 µg and the ratio of DNA to transfection agent was 1:1.5) into CHO cells. The cells were cultured at 37°C / 5% CO<sub>2</sub> in Ham's F-12 medium supplemented with 10% foetal calf serum and 0.005% gentamycin (*Sigma-Aldrich*, St. Louis, MO, USA) in glass bottom dishes (*Cellvis*, Mountain View, CA, USA) coated with fibronectin (*Sigma-Aldrich*, St. Louis, MO, USA) to enhance cell adhesion. After ~24 h, the CHO cells were transiently transfected in one of three ways: 1) WT variant alone (WT-GFP); 2) T309I variant alone (T309I-GFP); 3) both the WT and T309I variants cotransfected in the ratio 1:1 (WT-GFP/T309I-GFP). Additional experiments with cotransfected T309I-GFP and WT with no GFP were also performed to analyse cell membrane expression of the mutated subunits if cotransfected with WT. In these experiments, the cell membrane staining with CellMask™ Orange Plasma Membrane Stain (*Thermo Fisher Scientific*, Waltham, MA, USA) was used to identify distribution of GFP signal at the cell membrane.

Measurements were performed ~48 h after the transfection. A confocal laser scanning microscope Leica TCS SP8 X (*Leica microsystems*, Wetzlar, Germany) was used to analyse the subcellular localization of WT, T309I, and WT/T309I *I<sub>Ks</sub>* channels. Excitation wavelength was set to 488 nm and emission range to 500-544 nm, corresponding to the GFP spectral properties. When the cells were labelled with CellMask™ Orange Plasma Membrane Stain,

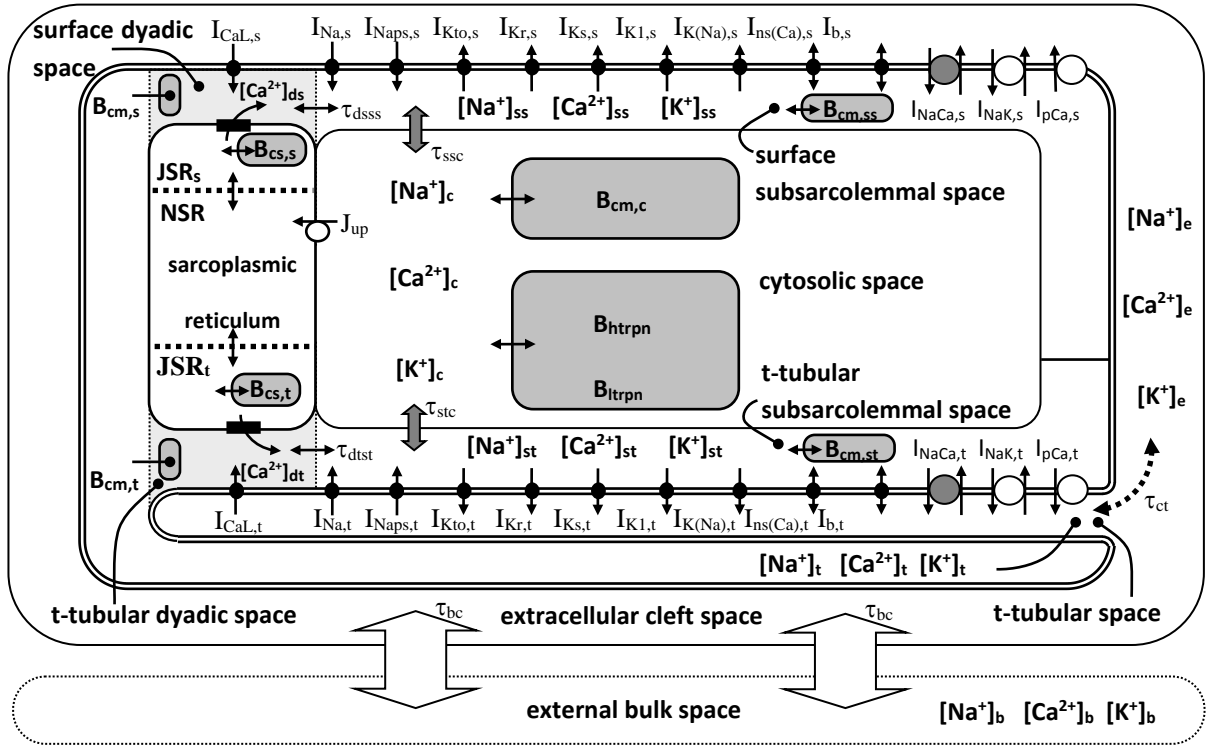
the excitation wavelength was set to 554 nm and the detection range was set between 565 and 610 nm. The samples were observed using an oil lens 63X objective. The acquired images (at a spatial resolution of  $1024 \times 1024$  pixels, physical length of  $184.52 \times 184.52 \mu\text{m}$ , and bit depth of 8 bit) were averaged three times and exported in the TIFF image format. GFP localization was analysed by relative intensity of line plot profiles.

### *Mathematical modelling*

A previously published model of human ventricular myocyte<sup>8</sup> was modified and used for mathematical simulations. The principal modification includes: (i) incorporation of separate dyadic spaces adjacent to the tubular and surface membranes; (ii) incorporation of separate junctional sarcoplasmic reticulum (JSR) compartments adjacent to the t-tubular and surface dyadic spaces ( $\text{JSR}_t$  and  $\text{JSR}_s$ ); (iii) incorporation of separate sub-sarcolemmal spaces adjacent to the t-tubular and surface membrane; and (iv) reformulation of description of  $I_{Ks}$  and  $I_{K1}$  to be more consistent with our new experimental data and data from literature.

The schematic diagram of the model is illustrated in Suppl. Fig. S1. The volume of the model cell ( $V_{\text{tot}}$ ) and total volumes of myoplasm, network sarcoplasmic reticulum (NSR), junctional sarcoplasmic reticulum (JSR), and dyadic space (20.9, 14.2, 1.15, 0.088, and 0.00067 pL, respectively) were left the same as in our previous model.<sup>8</sup> The total volume of subsarcolemmal space (0.412 pL) was set to represent 2% of  $V_{\text{tot}}$ ;<sup>9</sup> the fractional volumes of surface and t-tubular subsarcolemmal spaces ( $f_{v,s} = 0.49$  and  $f_{v,t} = 0.51$ , respectively) were set to be proportional to the non-junctional area of each membrane in the model cell (95.4% of the surface membrane and 79.4% of the t-tubular membrane).<sup>10</sup> The fractional volumes of t-tubular and surface dyadic spaces and of corresponding JSR compartments (0.8 and 0.2, respectively) were set to be proportional to the junctional area of each membrane in the model





Suppl. Fig. S1: Schematic diagram of the modified model of human ventricular cell. Description of electrical activity of the surface (s) and t-tubular (t) membranes comprises formulations of the following ion currents: fast sodium current ( $I_{Na}$ ), persistent sodium current ( $I_{Naps}$ ), L-type calcium current ( $I_{CaL}$ ), transient outward potassium current ( $I_{Kto}$ ), rapid and slow components of delayed rectifier potassium current ( $I_{Kr}$  and  $I_{Ks}$ ), inward rectifier potassium current ( $I_{K1}$ ), background currents ( $I_b$ ), sodium-activated potassium current ( $I_{K(Na)}$ ), calcium-activated non-specific current ( $I_{ns(Ca)}$ ), sodium-calcium exchange current ( $I_{NaCa}$ ), sodium-potassium pump current ( $I_{NaK}$ ), and calcium pump current ( $I_{pCa}$ ). The intracellular space contains the cytosolic space (c), surface and t-tubular subsarcolemmal subspaces (ss, st), surface and t-tubular dyadic spaces (dt, ds), and network and junctional compartments of sarcoplasmic reticulum (NSR, JSR<sub>s</sub>, JSR<sub>t</sub>; for explanations of the abbreviations, see the text).  $J_{up}$  represents  $Ca^{2+}$  flow via SERCA and the small filled rectangles in JSR membrane ryanodine receptors. The small black and grey bi-directional arrows denote intracellular ion diffusion; the related ion fluxes between dyadic spaces, subsarcolemmal spaces and cytosol are controlled by the time constants  $\tau_{dsss}$ ,  $\tau_{dtst}$ ,  $\tau_{ssc}$ , and  $\tau_{stc}$ . Ion diffusion between the t-tubular and cleft spaces (controlled by  $\tau_{ct}$ ) is represented by the dashed arrow, and between the cleft and external bulk spaces (controlled by  $\tau_{bc}$ ) by the thick white arrows.

cell. This implicates that the fraction of L-type  $Ca^{2+}$  channels in the t-tubular membrane  $f_{CaL,t}$  and related  $f_{KL,t}$  should be around 0.8.

The time constants related to the rate of ion diffusion from the dyadic spaces to the subsarcolemmal spaces ( $\tau_{dsss} = 0.819$  ms,  $\tau_{dtst} = 0.214$  ms) were set to be consistent with the rate of ion diffusion from dyads in our previous model.<sup>8</sup> The time constants of ion diffusion

from the subsarcolemmal spaces to the cytosol ( $\tau_{ssc} = 2.8$  ms,  $\tau_{stc} = 2.7$  ms) were adjusted to reflect the ratio of diffusional areas between both spaces and cytosol and to ensure the physiological magnitude of  $\text{Ca}^{2+}$  transients under the sarcolemma and in the bulk cytosol.<sup>9</sup>

To meet the experimental data showing that non-NCX  $\text{Ca}^{2+}$  transport (predominately mediated by the sarcolemmal  $\text{Ca}^{2+}$  pump, PMCA) is responsible for about 23% of total sarcolemmal  $\text{Ca}^{2+}$  extrusion in human induced pluripotent stem cells,<sup>11</sup> that mean AP duration at 90% repolarisation ( $\text{APD}_{90}$ ) at the 15<sup>th</sup> stimulation pulse applied at 1 Hz lies within  $271 \pm 13$  ms,<sup>12</sup> and that inhibition of  $I_{K1}$  and  $I_{Ks}$  causes only a minor change of the human AP (prolongation of  $\text{APD}_{90}$  by 3 to 5%)<sup>13</sup>, a partial modification of the parameters describing membrane transport system in ref.<sup>8</sup> was necessary. This included: (i) reduction of  $P_{\text{Ca}}$  and  $I_{\text{pCa,max}}$  to 0.00173 cm/s and 0.5  $\mu\text{A}/\text{cm}^2$ ; (ii) substitution of the original description of  $I_{K1}$ <sup>8</sup> by the formulation proposed in ref.<sup>14</sup>; and (iii) change of conductivities related to  $I_{K1}$  ( $g_{K1}$ ),  $I_{Kr}$  ( $g_{Kr}$ ), and  $I_{Ks}$  ( $g_{Ks}$ ) to 0.682, 0.276, and 0.014 mS/cm<sup>2</sup>, respectively. Following these changes a readjustment of  $I_{\text{NaK,max}}$ ,  $g_{\text{Nab}}$ , and  $g_{\text{Cab}}$  to 1.17  $\mu\text{A}/\text{cm}^2$ , 0.564  $\mu\text{S}/\text{cm}^2$ , and 1.1  $\mu\text{S}/\text{cm}^2$ , respectively, was also needed to preserve the physiological levels of cytosolic ion concentrations of the model cell at rest ( $[\text{Ca}^{2+}]_{\text{c,rest}} = 34$  nM,  $[\text{Na}^+]_{\text{c,rest}} = 7.4$  mM, and  $[\text{K}^+]_{\text{c,rest}} = 140$  mM). The conductivities ( $g_x$ ), permeabilities ( $P_x$ ), or maximum current densities ( $I_{x,\text{max}}$ ) of all ion transporters and their t-tubular fractions ( $f_{x,t}$ ) are specified in Suppl. Tab. S3.

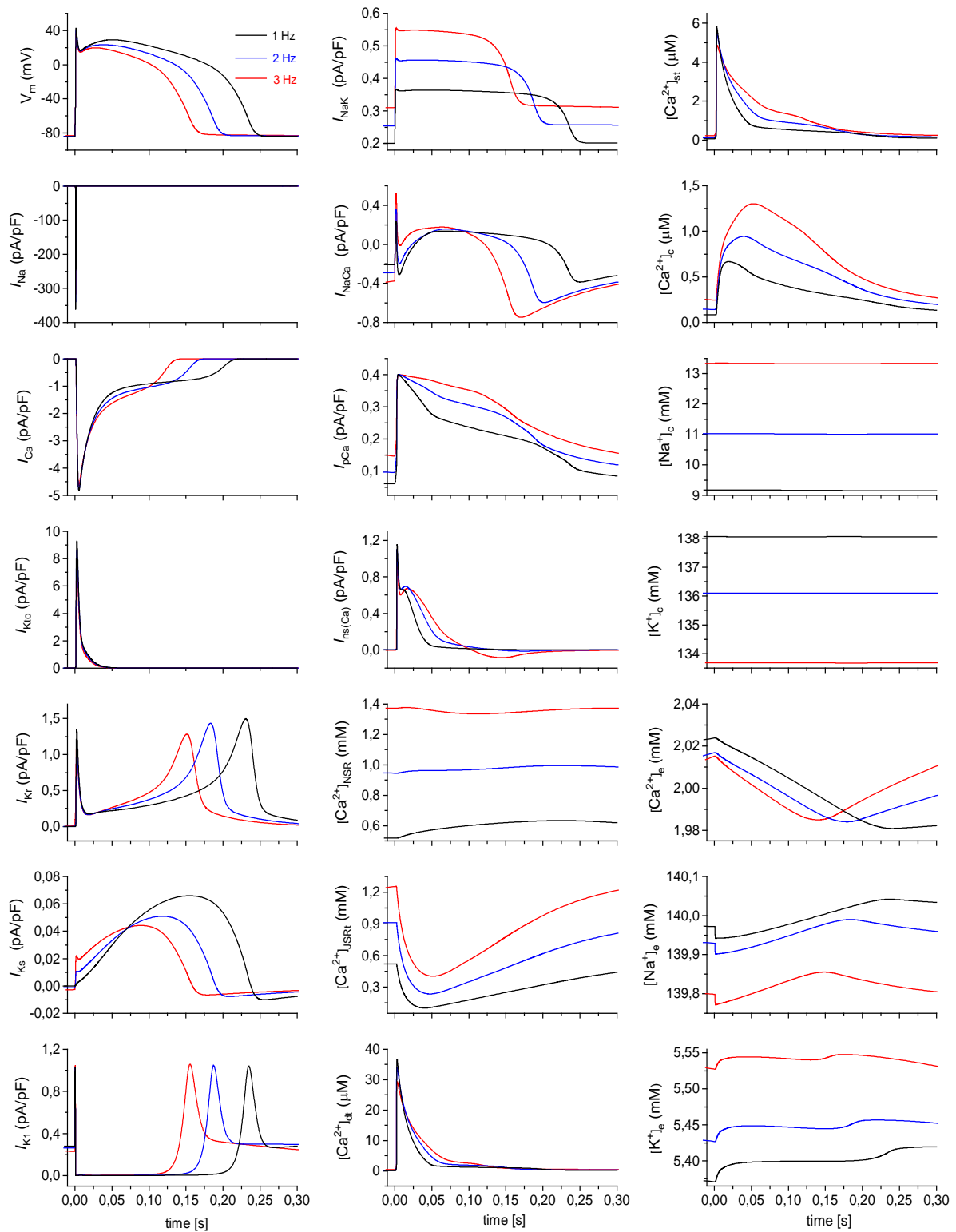
Suppl. Tab. S3: Electrical properties of ion transporters in the modified model of human ventricular cardiomyocyte.

$g_{\text{Na}}$	25 mS/cm <sup>2</sup>	$f_{\text{Na,t}}$	0.57	$g_{\text{K(Na)}}$	0.129 mS/cm <sup>2</sup>	$f_{\text{K(Na),t}}$	0.56
$g_{\text{Naps}}$	0.01 mS/cm <sup>2</sup>	$f_{\text{Naps,t}}$	0.56	$g_{\text{Nab}}$	0.564 $\mu\text{S}/\text{cm}^2$ *	$f_{\text{Nab,t}}$	0.56
$P_{\text{CaL}}$	0.00173 cm/s*	$f_{\text{CaL,t}}$	0.80*	$g_{\text{Cab}}$	1.1 $\mu\text{S}/\text{cm}^2$ *	$f_{\text{Cab,t}}$	0.56
$P_{\text{KL}}$	0.0000032 cm/s	$f_{\text{KL,t}}$	0.80*	$P_{\text{ns(Ca)}}$	1.75 nm/s	$f_{\text{ns(Ca),t}}$	0.56
$g_{\text{Kto}}$	0.132 mS/cm <sup>2</sup>	$f_{\text{Kto,t}}$	0.56	$k_{\text{NaCa}}$	0.15 nA/cm <sup>2</sup> · mM <sup>4</sup>	$f_{\text{NaCa,t}}$	0.56
$g_{\text{Kr}}$	0.276 mS/cm <sup>2</sup> *	$f_{\text{Kr,t}}$	0.56	$I_{\text{NaK,max}}$	1.17 $\mu\text{A}/\text{cm}^2$ *	$f_{\text{NaK,t}}$	0.56
$g_{\text{Ks}}$	0.014 mS/cm <sup>2</sup> *	$f_{\text{Ks,t}}$	0.56	$I_{\text{pCa,max}}$	0.5 $\mu\text{A}/\text{cm}^2$ *	$f_{\text{pCa,t}}$	0.56*
$g_{\text{K1}}$	0.682 mS/cm <sup>2</sup> *	$f_{\text{K1,t}}$	0.80				

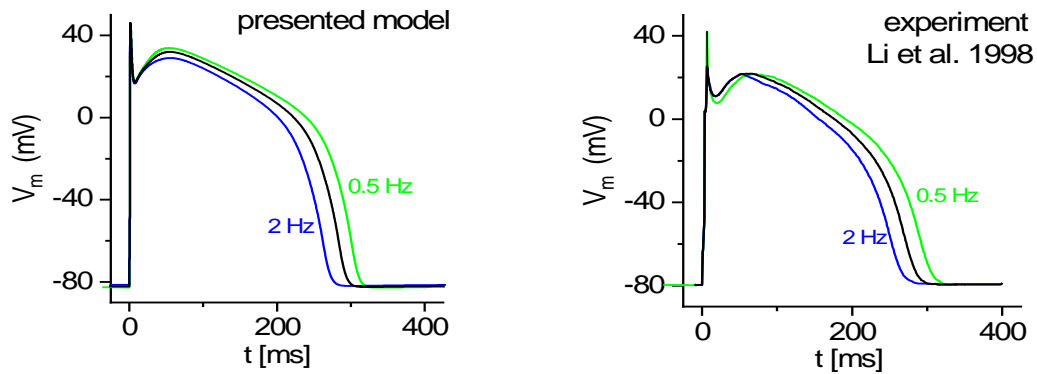
The t-tubular fractions of ion transporters ( $f_{x,t}$ ) were adopted from <sup>8</sup> except for  $f_{\text{Ca,t}}$ ,  $f_{\text{KL,t}}$ , and  $f_{\text{pCa,t}}$ . \*Modified values.

The basic behaviour of the model is illustrated in Suppl. Fig. S2 which shows the superimposed action potentials (APs), principal membrane currents, and ion concentrations in intracellular and extracellular compartments as recorded during 1, 2 and 3 Hz steady-state stimulation. Similarly, as our previous model<sup>8</sup> the modified model reproduces well the frequency-dependent shortening of AP and increase of cytosolic  $\text{Ca}^{2+}$  and  $\text{Na}^+$  concentrations observed in human ventricular myocytes<sup>15,16</sup>; the model reconstruction of rate dependent changes of AP configuration published by Li et al.<sup>12</sup> is illustrated in Suppl. Fig. S3. A critical point of the present simulations is a proper formulation of  $g_{\text{Ks}}$ . As demonstrated by Suppl. Fig. S4, the effect of total suppression of  $I_{\text{Ks}}$  on AP in the presented model (increase of  $\text{APD}_{90}$  by 5.4%) is fully consistent with that observed in the previously published and validated model by O'Hara et al.<sup>17</sup> that is freely available in Matlab or CellML codes.

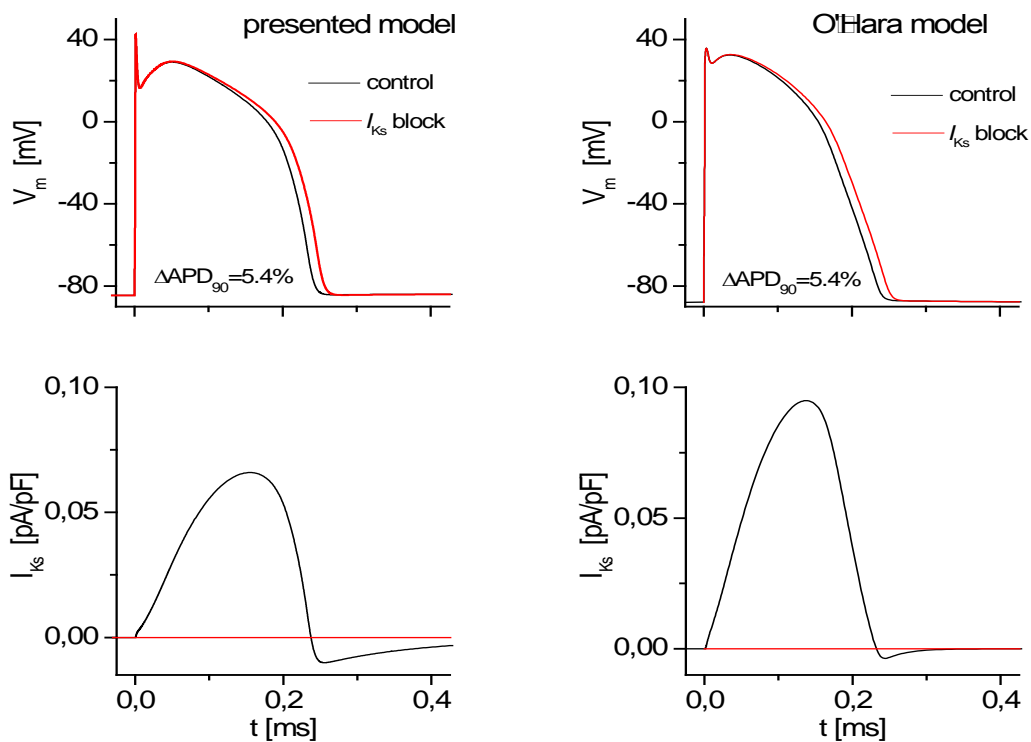
To simulate changes of the model behaviour under  $\beta$ -adrenergic stimulation, some transport and  $\text{Ca}^{2+}$  buffering mechanisms of the model cell were reformulated to reflect cellular effects of 1  $\mu\text{M}$  isoproterenol described in the Supplement to ref.<sup>18</sup> The reformulation includes: (i) increase of  $g_{\text{Na}}$  to 32.5  $\text{mS}/\text{cm}^2$ ; (ii) increase of  $P_{\text{Ca}}$  to 0.00433  $\text{cm}/\text{s}$ ; (iii) increase of  $g_{\text{Ks}}$  to 0.0717  $\text{mS}/\text{cm}^2$ ; (iv) incorporation of description of  $I_{\text{Kb}}$  based on the Ohm law with conductivity of 0.0075  $\text{mS}/\text{cm}^2$  (density of  $I_{\text{Kb}}$  in the t-tubular and surface membranes is assumed to be the same); (v) increase of  $\text{Ca}^{2+}$  release rate from  $\text{JSR}_i$  and  $\text{JSR}_s$  to corresponding dyadic spaces 1.75 times; (vi) decrease of NSR  $\text{Ca}^{2+}$ -ATPase forward half-saturation constant to 90.7 nM; (vii) decrease of  $[\text{Na}^+]_c$  half saturation constant of  $I_{\text{NaK}}$  to 7 mM; and (viii) decrease of  $\text{Ca}^{2+}$  on rate constants for high and low affinity sites of troponin to 12500 and 25000  $\text{mM}^{-1} \text{s}^{-1}$ , respectively. A reconstruction of the effects of  $\beta$ -adrenergic stimulation on AP (increased amplitude and decreased AP duration) and on cytosolic  $\text{Ca}^{2+}$  transient (increased amplitude) at 3.3 Hz stimulation published in the Supplement to ref.<sup>18</sup> is illustrated in Suppl. Fig. S5.



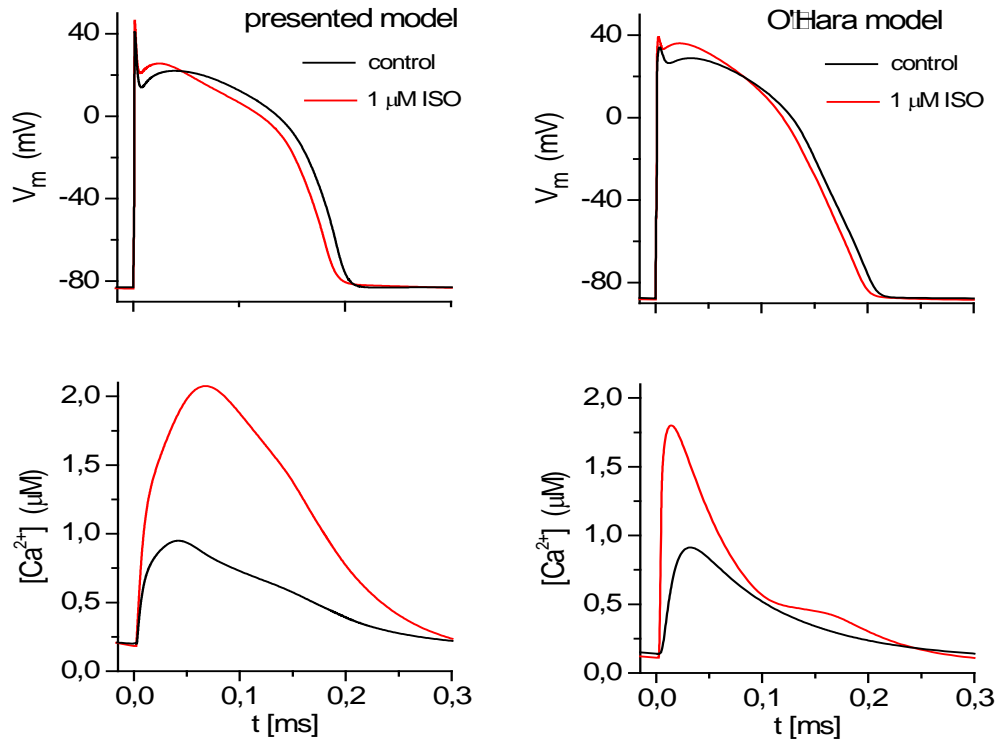
Suppl. Fig. S2: Membrane voltage ( $V_m$ ), currents ( $I_{Na}$ ,  $I_{Ca}$ ,  $I_{Kto}$ ,  $I_{Kr}$ ,  $I_{Ks}$ ,  $I_{K1}$ ,  $I_{NaK}$ ,  $I_{NaCa}$ ,  $I_{pCa}$ ,  $I_{ns(Ca)}$ ),  $Ca^{2+}$  concentration changes in NSR ( $[Ca^{2+}]_{NSR}$ ), JSR<sub>t</sub> ( $[Ca^{2+}]_{JSRt}$ ), t-tubular dyadic space ( $[Ca^{2+}]_{dt}$ ), t-tubular subsarcolemmal space ( $[Ca^{2+}]_{st}$ ) and ion concentration changes in cytosolic space ( $[Ca^{2+}]_c$ ,  $[K^+]_c$ ,  $[Na^+]_c$ ) and extracellular cleft space ( $[Ca^{2+}]_e$ ,  $[K^+]_e$ ,  $[Na^+]_e$ ) during 1, 2 and 3 Hz steady-state stimulation in the model of human epicardial myocyte. All traces represent steady states after 600 s of real time stimulation under body temperature and external bulk ion concentrations:  $[Na^+]_b = 140$  mM,  $[K^+]_b = 5.4$  mM,  $[Ca^{2+}]_b = 2$  mM.



Suppl. Fig. S3: Comparison of model reconstruction of APs recorded at 0.5, 1 and 2 Hz with representative human subepicardial AP waveforms digitized from Li et al.<sup>12</sup>. To meet the experimental conditions reported by Li et al.<sup>12</sup>, the extracellular cleft ion concentrations  $[Na^+]_e$ ,  $[K^+]_e$ , and  $[Ca^{2+}]_e$  were fixed at 136, 5.4 and 2 mM, respectively, and  $[K^+]_i$  was fixed at 130 mM. Individual traces represent 15<sup>th</sup> AP from resting state.



Suppl. Fig. S4: Comparison of the effect of total suppression of  $I_{Ks}$  on AP in the presented model and in the validated model of human epicardial myocyte published by O'Hara et al.<sup>17</sup>. The red traces represent the first AP elicited from 1 Hz steady state after  $I_{Ks}$  suppression.

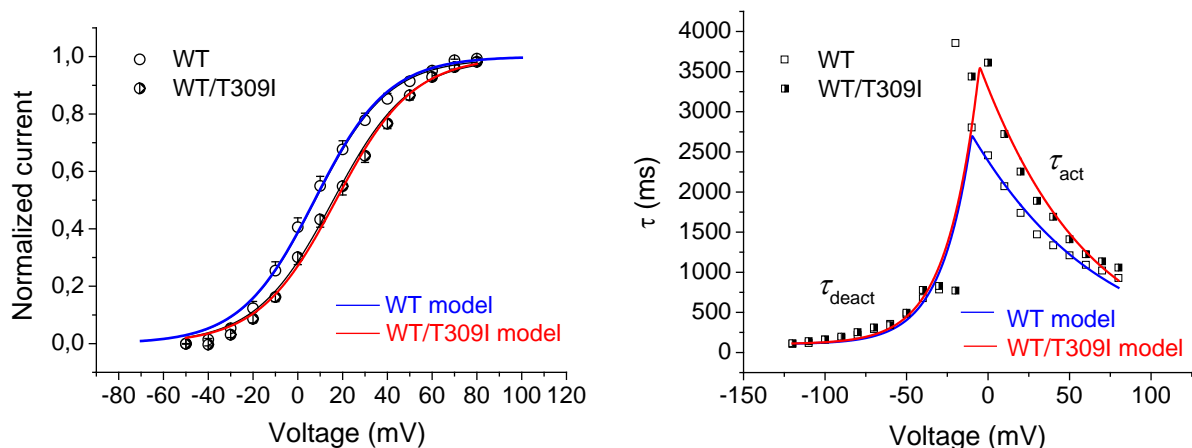


Suppl. Fig. S5: Model reconstruction of the effect of  $\beta$ -adrenergic stimulation on AP configuration and cytosolic  $Ca^{2+}$  transient  $[Ca^{2+}]_c$  presented in the supplement to O'Hara et al.<sup>17</sup>. The traces represent simulated responses of both models after 30 s pacing at 3.3 Hz in control conditions (black lines) and under the effect of 1  $\mu M$  isoproterenol (red lines). To meet the conditions used in O'Hara et al.<sup>17</sup> model, the extracellular cleft ion concentrations  $[Na^+]_e$ ,  $[K^+]_e$ , and  $[Ca^{2+}]_e$  were fixed at 140, 5.4 and 1.8 mM, respectively, in the presented model.

The gating properties of WT and WT/T309I  $I_{Ks}$  channels were incorporated into the model to comply with our experimental data (Suppl. Fig. S6). Beside this, an additional reduction of  $g_{Ks}$  to 40% of the control value was necessary to simulate the experimentally observed reduction of  $I_{Ks}$  caused by the WT/T309I mutation (Fig. 2B in the main text). To attain a dynamic steady state at all stimulation frequencies, the model was paced for 600 s of equivalent cell lifetime at external  $Na^+$ ,  $K^+$ , and  $Ca^{2+}$  concentrations set to 140, 5.4, and 2 mmol/L, respectively. The numerical solution of the system of equations describing the model cell function was performed using the computational software MATLAB v. 7.2 (MathWorks, Inc.).

### Statistical analysis

The data are mostly presented by the arithmetic mean ( $\pm$  SD from  $n$  patients, or  $\pm$  SEM from  $n$  cells; Origin, version 8.5.1; *OriginLab Corporation*). To determine statistical significance of differences, paired/unpaired  $t$ -tests, and one-way/repeated measures ANOVA with the Bonferroni post-test were used;  $P < 0.05$  was considered statistically significant. If the difference between the arithmetic and geometric means was  $>10\%$ , the geometric mean  $\times$  geometric SE (geometric SE = geometric SD $^{1/n}$ ) and the non-parametric Mann-Whitney test were used (Figs. 2B and 3B in the main text file). To compare the statistical significance of differences in relative fluorescence intensity in Fig. 4 in the main text file (where several data samples did not show the normal distribution according to the Shapiro-Wilk test; the mean values are represented by the geometric mean  $\pm$  95% confidence interval), either the Friedman test or the Kruskal-Wallis test (both with the Dunn's multiple comparison) were used, the first one in the case of paired data (comparison within individual groups), the latter in the case of unpaired data (comparison among various groups). The curve fitting and the statistical tests were performed using the GraphPad Prism, version 6.05 (*GraphPad Software, Inc.*).



Suppl. Fig. S6: Voltage dependence of steady-state activation (A) and time constants of activation and deactivation ( $\tau_{act}$  and  $\tau_{deact}$ , respectively; B) in the model of human ventricular cell<sup>8</sup> after incorporation of the gating properties of WT (blue lines) and WT/T309I (red lines)  $I_{Ks}$  channels (experimental data are represented by empty and half-filled symbols, respectively). Lines in the part A were fitted using the Boltzmann equations Eq. 1 and Eq. 2 and lines in the part B were fitted using the Eq. 3 and Eq. 4 (below).

$$I_{WT} = \frac{1}{1 + e^{(7.5-V)/16.5}} \quad (1)$$

$$I_{WT/T309I} = \frac{1}{1 + e^{(17.08-V)/17.26}} \quad (2)$$

$$\tau_{WT} = 0.105 + \frac{40}{\left(1 + e^{(-(V+10)/0.2)^{0.01333}}\right) \cdot \left(1 + e^{((V+90)/129)^{2.6}}\right)} \quad (3)$$

$$\tau_{WT/T309I} = 0.105 + \frac{40}{\left(1 + e^{(-(V+5.6)/0.2)^{0.01333}}\right) \cdot \left(1 + e^{((V-90)/140)^6}\right)} \quad (4)$$

## Supplemental Results

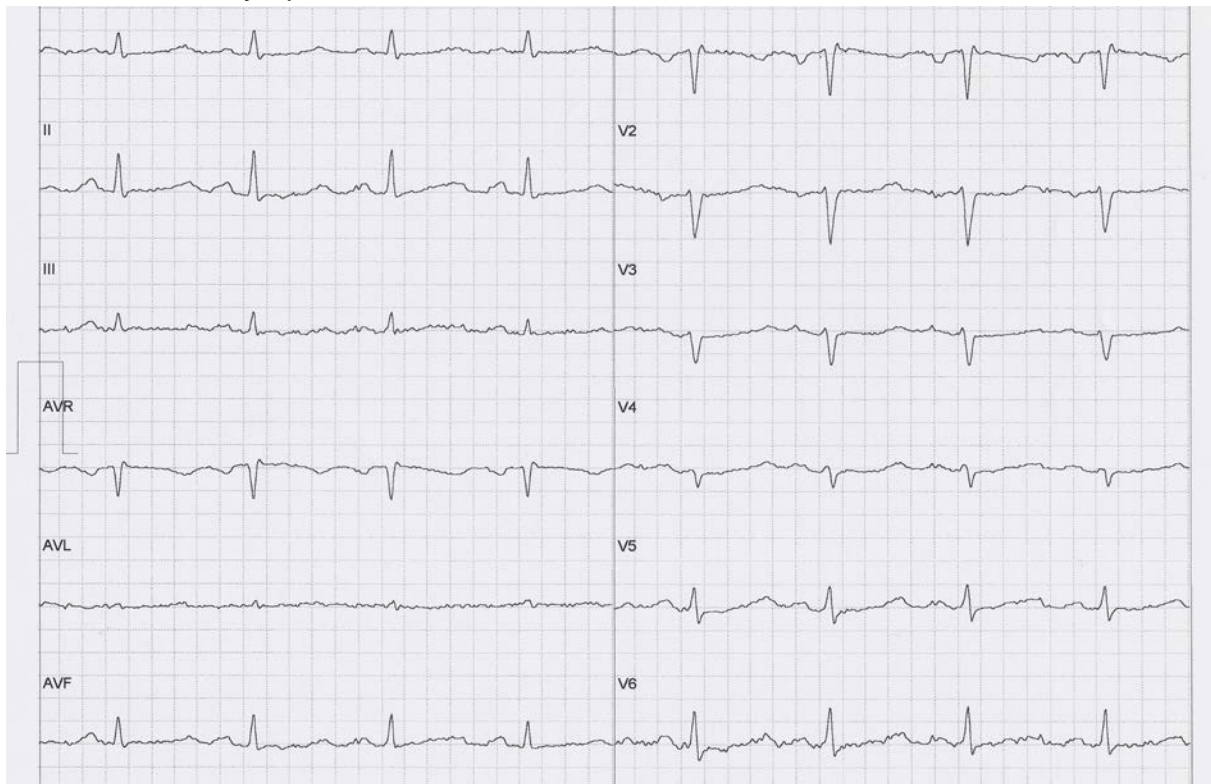
### *Clinical diagnostics*

Representative examples of electrocardiograms (EGCs) of two T309I carriers, recorded at rest and in the 4<sup>th</sup> minute of recovery after the exercise, are shown in Suppl. Fig. S7, the first one recorded in a female who suffered cardiac arrest and was successfully resuscitated (parts A and B), the second one from an asymptomatic female (parts C and D). For results characterizing differences in QTc lengths in T309I carriers and their unaffected relatives, see Fig. 1A in the main text.

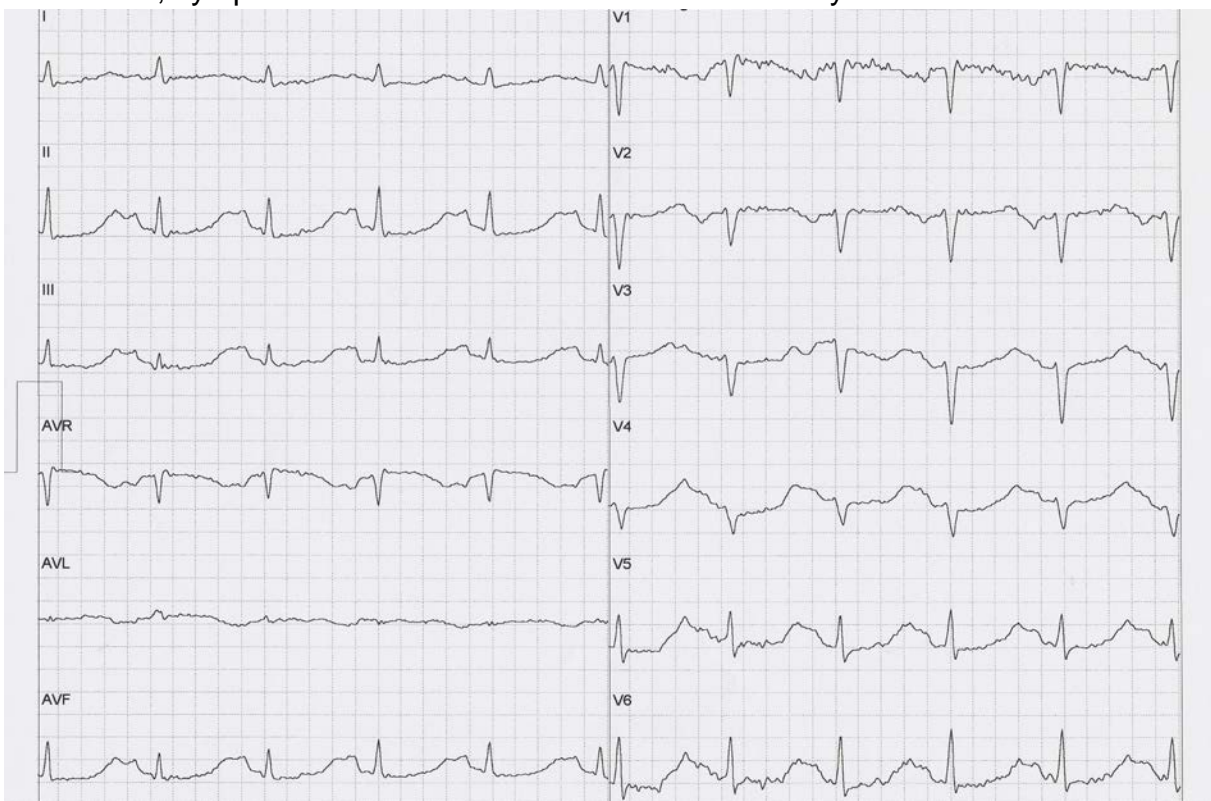
No significant changes were apparent in PQ interval and QRS complex (Suppl. Fig. S8). In the population over 16 years old, a non-significant tendency to a prolonged PQ interval ( $P = 0.07$ ) and a shortened QRS complex ( $P = 0.11$ ) was apparent in T309I carriers.



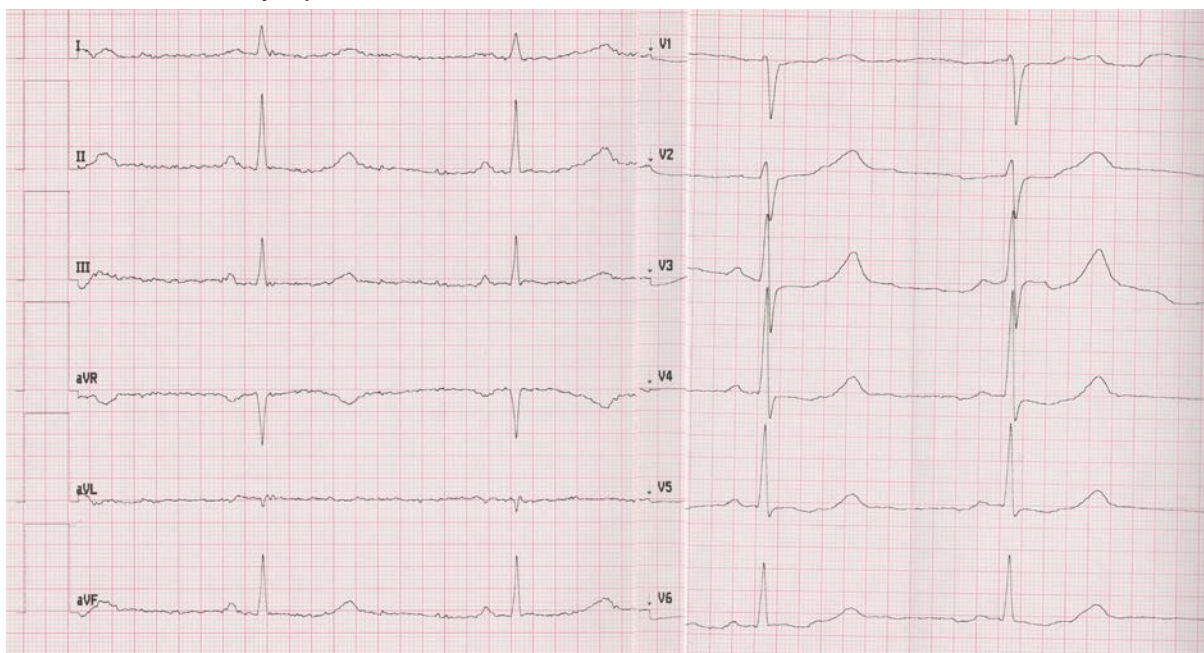
**A** T309I, symptomatic female – at rest before start of the exercise test



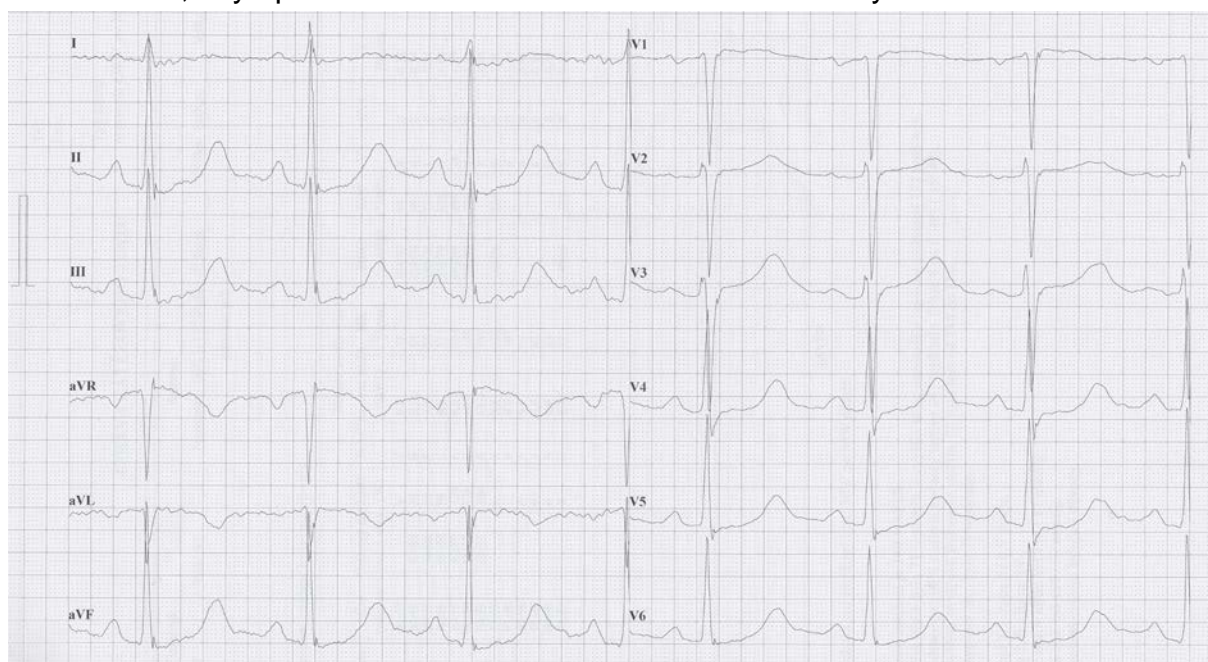
**B** T309I, symptomatic female – in the 4<sup>th</sup> min of recovery after the exercise



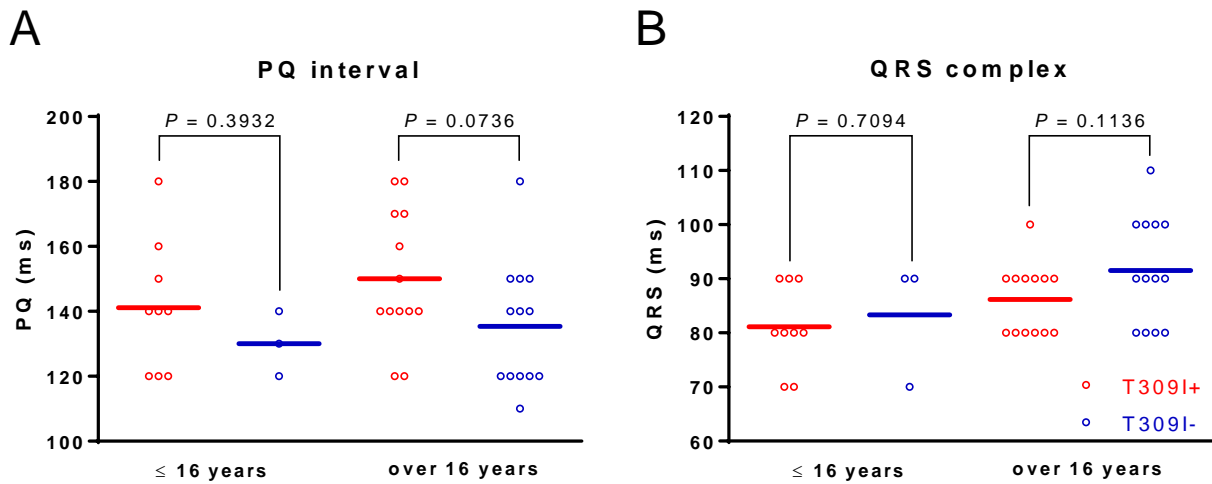
**C** T309I, asymptomatic female – at rest before start of the exercise test



**D** T309I, asymptomatic female – in the 4<sup>th</sup> min of recovery after the exercise



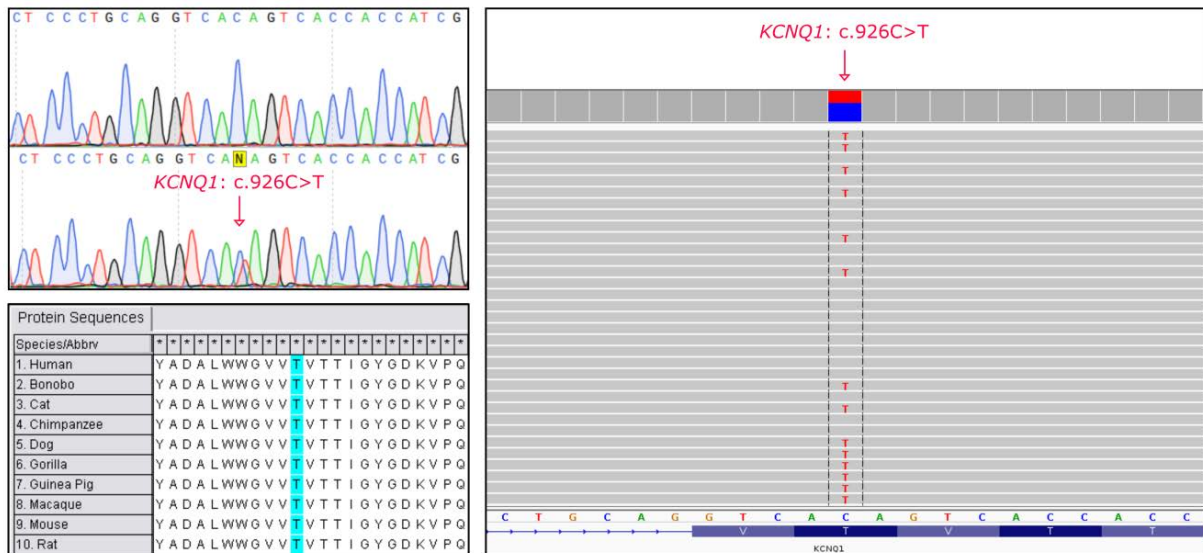
Suppl. Fig. S7: ECG examples of T309I carriers. A and B: ECG recordings (50 mm/s, 20 mm/mV) of an adult female with T309I variant who suffered cardiac arrest and was successfully resuscitated. The recordings were taken 6 months after the event during bicycle ergometry, before the exercise (sitting on the ergometer, A – QTc = 500 ms) and in the 4<sup>th</sup> minute of recovery after the exercise (B – QTc = 530 ms). C and D: ECG recordings (50 mm/s, 20 mm/mV) of an asymptomatic adult female with T309I variant at rest (C – QTc = 480 ms) and in the 4<sup>th</sup> minute of recovery after the exercise (D – QTc = 500 ms).



Suppl. Fig. S8: PQ interval and QRS complex durations in T309I carriers (T309I+, red circles) and in their unaffected relatives (T309I-, blue circles) as observed in persons up to 16 years old and in persons over 16 years old. No significant changes were observed between T309I+ and T309I-.

#### Genetic testing

In our cohort of 132 patients, pathogenic or probably pathogenic variants in any of LQTS-related genes were identified in 74 probands, mostly in the *KCNQ1* gene (in 44 probands, ~59%). The same substitution c.926C>T (NM\_000218.2) in the *KCNQ1* gene (Suppl. Fig. S9) resulting in T309I amino acid change in the P-loop of Kv7.1 protein was identified in 10 unrelated probands out of all the 44 probands (~23%). Presence of other pathogenic variants (including other LQTS-related genes) was negated in all index cases.

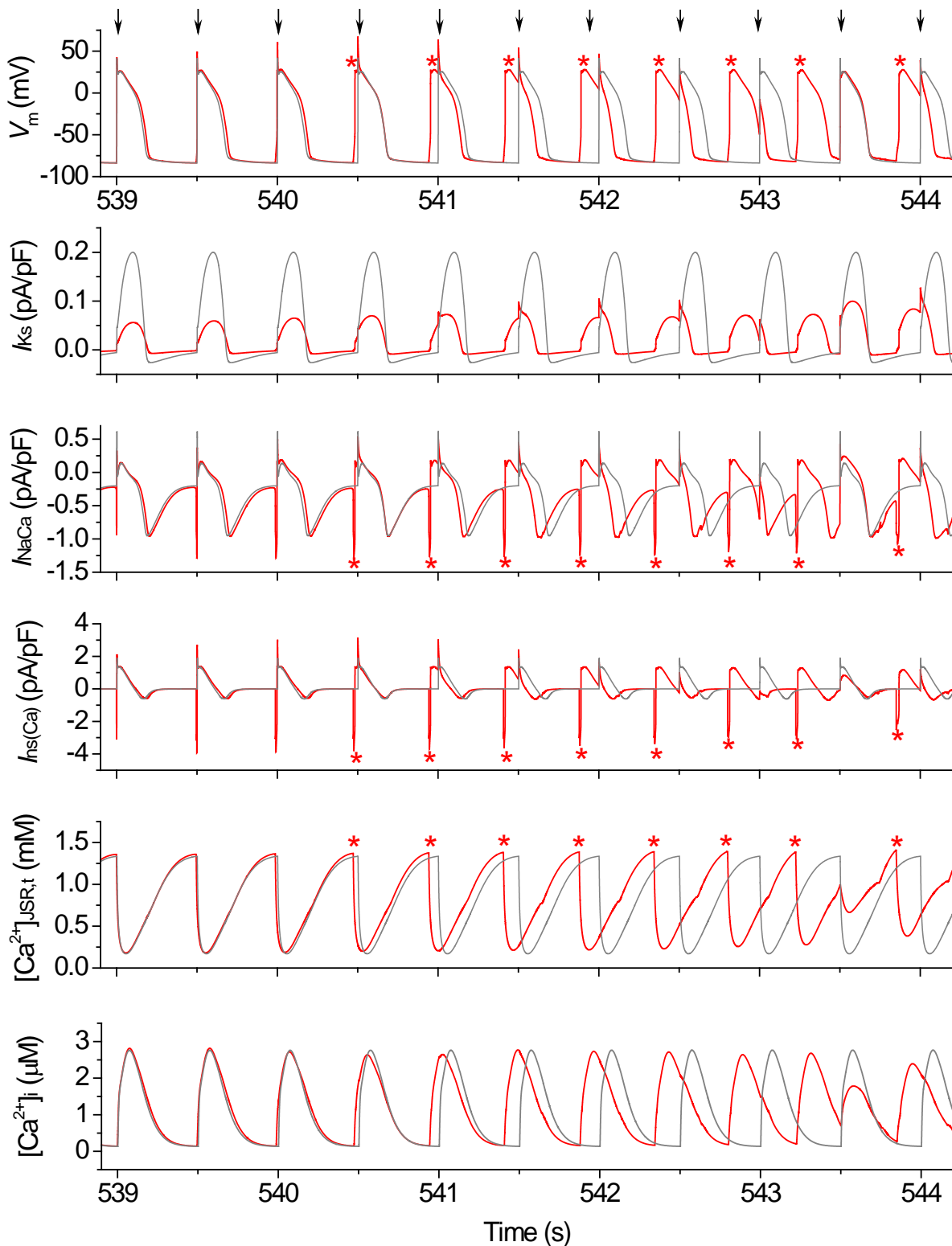


Suppl. Fig. S9: Genetic characterization of c.926C>T-KCNQ1 variant. Results of sequencing analysis and evolutionary conservation analysis; left upper panel: variant c.926C>T detected by the Sanger sequencing, right panel: result of massive parallel sequencing, left lower panel: analysis of region 291-327 of the Kv7.1 human protein - threonine at the position 309 (where the T309I variant is located - highlighted in blue) is highly conserved in the analysed species.

### Mathematical modelling

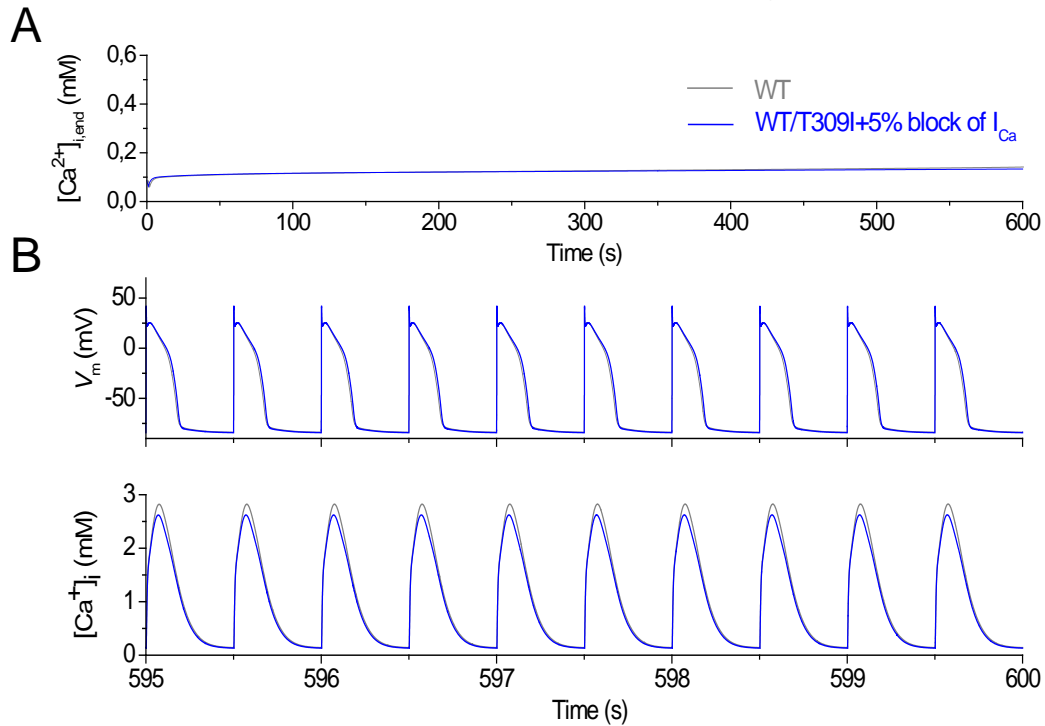
A detailed view on the mechanisms of development of delayed afterdepolarisations (DADs) observed in the model with WT/T309I mutation under  $\beta$ -adrenergic stimulation provides Suppl. Fig. S10. As indicated by asterisks in the figure, DADs were initiated by premature release of  $\text{Ca}^{2+}$  from JSR (due to the SR  $\text{Ca}^{2+}$  overload at the time of 540 s) and consequent step increase of inward components of  $I_{\text{NaCa}}$  and  $I_{\text{ns(Ca)}}$ .

The proarrhythmic action of WT/T309I channels was prevented by 5%-inhibition of cardiac calcium current ( $I_{\text{Ca}}$ ); contemporary change in the peak value of  $\text{Ca}^{2+}$  transient was negligible (Suppl. Fig. 11).



Suppl. Fig. S10: Onset of DADs in the model with WT/T309I dysfunctional channels under cycle length (CL) 500 ms and  $\beta$ -adrenergic stimulation. The individual graphs from up to down represent action potentials, membrane currents  $I_{Ks}$ ,  $I_{NaCa}$  and  $I_{ns(Ca)}$ , changes of  $Ca^{2+}$  concentration in JSR<sub>t</sub>, and cytosolic  $Ca^{2+}$  transients in the control model (grey line) and in the model with WT/T309I mutation (red line) 539 s after  $\beta$ -adrenergic stimulation and 2 Hz stimulation. The asterisks show the premature release of  $Ca^{2+}$  from JSR<sub>t</sub> due to SR  $Ca^{2+}$  overload and subsequent activation of  $Ca^{2+}$  dependent currents ( $I_{NaCa}$  and  $I_{ns(Ca)}$ ) responsible for DAD.

CL 1000 ms → 500 ms and  $\beta$ -adrenergic stimulation



Suppl. Fig. S11: Proarrhythmic action of WT/T309I channels under  $\beta$ -adrenergic stimulation at the cycle length (CL) of 500 ms may be prevented by a slight inhibition of cardiac calcium current ( $I_{Ca}$ ). If  $I_{Ca}$  was inhibited by 5% in WT/T309I model, the intracellular  $Ca^{2+}$  load (reflected by the level of  $[Ca^{2+}]_{i, end}$ ) was comparable to that in WT model without  $I_{Ca}$  inhibition (A) and DADs were not generated (B; compare with Fig. 5C in the main text file). The action potential prolongation in WT/T309I model was negligible under these conditions (APD<sub>90</sub> longer by 3% in WT/T309I model than in WT model; B, upper panel). The peak value of  $Ca^{2+}$  transient was diminished by 7% (B, lower panel).

## References:

1. Priori SG, Blomström-Lundqvist C, Mazzanti A, et al. 2015 ESC Guidelines for the management of patients with ventricular arrhythmias and the prevention of sudden cardiac death: The Task Force for the Management of Patients with Ventricular Arrhythmias and the Prevention of Sudden Cardiac Death of the European Society of Cardiology (ESC). Endorsed by: Association for European Paediatric and Congenital Cardiology (AEPC). *Eur Heart J.* 2015;36(41):2793-2867.
2. Ye J, Coulouris G, Zaretskaya I, Cutcutache I, Rozen S, Madden TL. Primer-BLAST: a tool to design target-specific primers for polymerase chain reaction. *BMC Bioinformatics.* 2012;13:134.
3. Choi Y, Chan AP. PROVEAN web server: a tool to predict the functional effect of amino acid substitutions and indels. *Bioinformatics.* 2015;31(16):2745-2747.
4. Shihab HA, Gough J, Mort M, Cooper DN, Day INM, Gaunt TR. Ranking non-synonymous single nucleotide polymorphisms based on disease concepts. *Hum Genomics.* 2014;8:11.
5. López-Ferrando V, Gazzo A, de la Cruz X, Orozco M, Gelpí JL. PMut: a web-based tool for the annotation of pathological variants on proteins, 2017 update. *Nucleic Acids Res.* 2017;45(Web Server issue):W222-W228.
6. Kumar S, Stecher G, Tamura K. MEGA7: Molecular Evolutionary Genetics Analysis Version 7.0 for Bigger Datasets. *Mol Biol Evol.* 2016;33(7):1870-1874.
7. Lek M, Karczewski KJ, Minikel EV, et al. Analysis of protein-coding genetic variation in 60,706 humans. *Nature.* 2016;536(7616):285-291.

8. Hrabcová D, Pásek M, Šimurda J, Christé G. Effect of ion concentration changes in the limited extracellular spaces on sarcolemmal ion transport and  $\text{Ca}^{2+}$  turnover in a model of human ventricular cardiomyocyte. *Int J Mol Sci.* 2013;14(12):24271-24292.
9. Shannon TR, Wang F, Puglisi J, Weber C, Bers DM. A Mathematical Treatment of Integrated Ca Dynamics within the Ventricular Myocyte. *Biophys J.* 2004;87(5):3351-3371.
10. Page E, Surdyk-Droske M. Distribution, surface density, and membrane area of diadic junctional contacts between plasma membrane and terminal cisterns in mammalian ventricle. *Circ Res.* 1979;45(2):260-267.
11. Hwang HS, Kryshtal DO, Feaster TK, et al. Comparable calcium handling of human iPSC-derived cardiomyocytes generated by multiple laboratories. *J Mol Cell Cardiol.* 2015;85:79-88.
12. Li G-R, Feng J, Yue L, Carrier M. Transmural heterogeneity of action potentials and  $I_{\text{to1}}$  in myocytes isolated from the human right ventricle. *Am J Physiol-Heart Circ Physiol.* 1998;275(2):H369-H377.
13. Jost N, Virág L, Comtois P, et al. Ionic mechanisms limiting cardiac repolarization reserve in humans compared to dogs: Weak  $I_{\text{K1}}$ ,  $I_{\text{Ks}}$  limit human repolarization reserve. *J Physiol.* 2013;591(17):4189-4206.
14. Fink M, Noble D, Virag L, Varro A, Giles WR. Contributions of HERG  $\text{K}^+$  current to repolarization of the human ventricular action potential. *Prog Biophys Mol Biol.* 2008;96(1-3):357-376.
15. Schmidt U, Hajjar RJ, Helm PA, Kim CS, Doye AA, Gwathmey JK. Contribution of



Abnormal Sarcoplasmic Reticulum ATPase Activity to Systolic and Diastolic Dysfunction in Human Heart Failure. *J Mol Cell Cardiol.* 1998;30(10):1929-1937.

16. Pieske B, Maier LS, Piacentino V, Weisser J, Hasenfuss G, Houser S. Rate Dependence of  $[Na^+]_i$  and Contractility in Nonfailing and Failing Human Myocardium. *Circulation.* 2002;106(4):447-453.
17. O'Hara T, Virág L, Varró A, Rudy Y. Simulation of the Undiseased Human Cardiac Ventricular Action Potential: Model Formulation and Experimental Validation. McCulloch AD, ed. *PLoS Comput Biol.* 2011;7(5):e1002061.
18. O'Hara T, Rudy Y. Arrhythmia formation in subclinical ("silent") long QT syndrome requires multiple insults: Quantitative mechanistic study using the KCNQ1 mutation Q357R as example. *Heart Rhythm.* 2012;9(2):275-282.

### 2.3. Genetické aspekty komorových arytmií u běžných chorob srdce

Hereditární arytmiické syndromy, tzv. kanalopatie, patří do skupiny monogenně podmíněných chorob, jsou v poslední době označovány spíše jako familiární elektrické choroby srdce. Představují užitečný molekulární model pro studium procesů arytmogeneze. Navíc genetický podklad NSS je nepopiratelný, a to díky výsledkům řady populačních studií, které prokázaly familiární agregaci výskytu NSS.<sup>13,28,29,30,31</sup>

Dále je známo, že u pacientů se strukturálním onemocněním srdce se na rozvoji arytmiické formy NSS podílí mnoho faktorů, včetně mechanických, elektrofyziologických i autonomních. Typickými příklady jsou jizva po proběhlém IM, kde prolínání zdravé a vazivové tkáně vytváří „optimální“ prostředí pro vznik reentry arytmií, či chronicky snížená perfuze myokardu, která umožňuje tak zvané náhodné reentry okruhy. Jako jedna z možností genetického podkladu NSS u strukturálního onemocnění srdce může být i skrytá mutace iontových kanálů projevujících se až v zátěžových situacích, jakými jsou ICHS či DKMP. Touto hypotézou se zabývalo již několik autorů, kteří porovnávali souvislost mezi NSS u pacientů se strukturálním postižením srdce a výskytem vzácných sekvenčních variant v genech asociovaných s Brugada syndromem a LQTS.<sup>32,33</sup> Výsledky těchto studií pak naznačovaly mírně vyšší výskyt mutací těchto genů u pacientů s NSS. I naše studie prokázala u pacientů s ICHS s dokumentovanou fibrilací komor (FK) statisticky vyšší výskyt vzácných sekvenčních variant v genech *KCNQ1*, *KCNH2*, *SCN5A*, *KCNE1* a *KCNE2* oproti kontrolní skupině. Detailnější popis přináší následující publikace.

Novotny T, Kadlecova J, Raudenska M, Bittnerova A, **Andrsova I**, Florianova A, Vasku A, Neugebauer P, Kozak M, Sepsi M, Krivan L, Gaillyova R, Spinar J. Mutation analysis ion channel genes ventricular fibrillation survivors with coronary artery disease. *Pacing Clin Electrophysiol* 2011;34:742-749.

IF 1,351. Počet citací ve Web of Science 9

Publikovaná původní práce – kvantitativní podíl uchazečky 10 % identifikace vhodných pacientů, analýza dat, revize text publikace.

# Mutation Analysis Ion Channel Genes Ventricular Fibrillation Survivors with Coronary Artery Disease

TOMAS NOVOTNY, M.D., PH.D.,\* JITKA KADLECOVA, DR.S., PH.D.,†  
MARTINA RAUDENSKA,‡ ALEXANDRA BITTNEROVA,†  
IRENA ANDRISOVA, M.D.,\* ALENA FLORIANOVA, M.D.,\* ANNA VASKU, M.D., PH.D.,‡  
PETR NEUGEBAUER, M.D., PH.D.,\* MILAN KOZAK, M.D., PH.D.,\* MILAN SEPSI, M.D.,\*  
LUBOMIR KRIVAN, M.D., PH.D.,\* RENATA GAILLYOVA, M.D., PH.D.,†  
and JINDRICH SPINAR, M.D., PH.D.\*

From the\*Department of Internal Medicine and Cardiology, †Department of Medical Genetics, University Hospital Brno and Faculty of Medicine of Masaryk University, Brno, Czech Republic; and ‡Department of Pathological Physiology, Faculty of Medicine, Masaryk University, Brno, Czech Republic

**Background:** Observations from population-based studies demonstrated a strong genetic component of sudden cardiac death. The aim of this study was to test the hypothesis that ion channel genes mutations are more common in ventricular fibrillation (VF) survivors with coronary artery disease (CAD) compared to controls.

**Methods:** The entire coding sequence of *KCNQ1*, *KCNH2*, *SCN5A*, *KCNE1*, and *KCNE2* genes was analyzed in 45 (five females) CAD individuals—survivors of documented VF and in 90 matched healthy controls. In another control group of 141 matched patients with CAD without malignant arrhythmias, the exons containing rare coding variants found in the VF survivors were sequenced.

**Results:** The carrier frequency of all the rare sequence variants was significantly higher in the VF survivors (8/45, 17.8%) than in CAD controls (3/141, 2.2%,  $P = 0.001$ ). In VF survivors, four coding variants in eight individuals were found. Three in *KCNH2* gene: R148W and GAG186del are novel; P347S was previously related to long QT syndrome. In *SCN5A* gene, P2006A variant was found in five unrelated males. This variant has been demonstrated previously to have small effect on sodium channel kinetics. No rare coding variants were found in the healthy controls. The P2006A variant was found in three CAD controls.

**Conclusion:** The prevalence of selected, rare coding variants in five long QT genes was significantly higher in cases versus controls, confirming a mechanistic role for these genes among a subgroup of patients with coronary disease and VF. (*PACE* 2011; 34:742–749)

**sudden death, ventricular fibrillation, ion channel, mutation**

## Introduction

Approximately 50% of all coronary heart disease deaths are sudden. Each year, several hundred thousand individuals die due to sudden cardiac death (SCD) in both the United States and the European Union.<sup>1</sup> Observations from population-based studies demonstrate a strong genetic component of SCD.<sup>2,3,4,5</sup> It is clear that

there must be genetically determined variations of physiological processes that increase the risk of SCD. One of the pathways by which genetic variation in pathophysiological mechanisms may contribute to increased risk of SCD is electrogenesis and conduction in myocardium. It is well known that myocardial ion channel gene mutations lead to increased SCD risk in patients with relatively rare diseases, such as long QT syndrome (LQTS) and Brugada syndrome. In some LQTS families, up to 75% of carriers of pathologic mutations remain completely asymptomatic, that is, they did not even present with prolonged QT interval.<sup>6</sup> Therefore, a normal QT interval value does not automatically exclude that particular individual as a carrier of potentially dangerous mutation. Recently, it has been shown that the prevalence of LQTS is at least 1:2500. Similarly, in the general population the prevalence of ion-channel gene polymorphisms may be much higher than previously thought.<sup>7</sup> Such variants could predispose individuals in the general population

The authors have no relationship to disclose.

The research was supported by grant No. NR9340-3 of the Internal Grant Agency of the Ministry of Health of the Czech Republic and grant No. 2B08061 of the Ministry of Education, Youth and Sports of the Czech Republic.

Address for reprints: Tomas Novotny, M.D., Ph.D., Department of Internal Medicine and Cardiology, University Hospital, Brno Jihlavska 20, Brno 625 00, Czech Republic. Fax: +420 53223 2611; e-mail: novotny-t@seznam.cz

Received September 19, 2010; revised November 24, 2010; accepted December 21, 2010.

doi: 10.1111/j.1540-8159.2011.03045.x

to SCD. In the present study, we performed mutational analysis of five LQTS-related myocardial ion-channel genes in patients with coronary artery disease (CAD) and ventricular fibrillation (VF) documented at the time of SCD event and in a control population.

## Methods

### Investigated Subjects

The group of patients consisted of 45 Caucasian patients (five females) from the region of south Moravia in the Czech Republic (population approximately 1.5 million individuals). The primary inclusion criterion was VF documented at the time of circulatory arrest not related to acute phase of myocardial infarction (i.e., more than 48 hours after index event). Such individuals were identified from the implantable cardioverter defibrillator (ICD) registry of our department, partially retrospectively (years 1998–2006); from 2007 new consecutive patients were included prospectively. Two patients suffered VF while staying in a hospital for more than 72 hours after acute myocardial infarction. All other individuals suffered circulatory arrest in the out-of-hospital setting; VF was recorded by emergency car staff. Patients were successfully resuscitated and then transferred to our department, either directly or via regional hospitals. After circulatory stabilization and improvement in mental status, all patients underwent comprehensive cardiological examination. None of the patients had an acute myocardial infarction at the time of arrhythmia according to electrocardiogram (ECG) and serum troponin level analysis. In all patients, CAD was confirmed by coronary angiography findings of significant stenoses (>70%) or chronic occlusions. The left ventricle ejection fraction (LVEF) was calculated from echocardiography analysis. In three patients, QT interval assessment was not possible due to left bundle branch block or atrial fibrillation. None of the other 42 patients showed substantial QT interval prolongation or Brugada-like ECG.

A total of 231 geographically, sex-, and age-matched control individuals were divided into two groups. The first control group consisted of 90 individuals who underwent basic medical investigation and were assessed as healthy; detailed ECG information was not available for this cohort. The second group consisted of 141 patients with CAD who were hospitalized at our department owing to an acute coronary event. For all patients, the diagnosis was confirmed by coronary angiography. All patients had depressed LVEF and they were alive at least 3 years after the index event. Thus, they could be considered

**Table I.**

Clinical Characteristics of Investigated Individuals

	<b>SCD Survivors (n = 45)</b>	<b>Healthy Controls (n = 90)</b>	<b>CAD Controls (n = 141)</b>
Male/female	40/5	80/10	129/12
Age	63.2 ± 7.9	66.6 ± 6.2	66.7 ± 10.7
Left ventricle ejection fraction	40 ± 12%	–	42 ± 9%
History of myocardial infarction	32 (71%)	0	127 (90%)

SCD = sudden cardiac death; CAD = coronary artery disease.

as a CAD group with a low risk of SCD. Clinical characteristics of both groups are summarized in Table I

Informed consent was obtained from all the individuals and peripheral blood samples were taken for genomic DNA preparation. The study protocol was approved by the Ethical Committee of the University Hospital Brno and conforms to the ethical guidelines of the 1975 Declaration of Helsinki.

### Genomic DNA Samples and Polymerase Chain Reaction Amplification

The coding sequences of *KCNQ1*, *KCNH2*, *SCN5A*, *KCNE1*, and *KCNE2* genes were analyzed (GenBank accession nos. AF000571, NM000238, NT022517, NM000219, NM005136). Genomic DNA was extracted from peripheral blood samples according to a standard protocol using DNA BloodSpin Kit (MO BIO Laboratories, Inc., Carlsbad, CA, USA), and the classical method of ethanol precipitation. Exons of *KCNQ1*, *KCNH2*, and *KCNE1* genes were amplified by multiplex polymerase chain reaction (PCR); previously reported intronic oligonucleotide primers were used.<sup>8,9</sup> A total of 34 intronic oligonucleotide primer pairs were used to amplify the coding area of *SCN5A* (modified according to reference 10) The PCR amplifications were performed using *Taq* DNA polymerase (Fermentas, Inc., Glen Burnie, MD, USA) and HotStarTaq Master Mix (Qiagen, Inc., Valencia, CA, USA). Each PCR was performed in 200- $\mu$ L thin-walled PCR tubes in a total reaction volume of 25  $\mu$ L. Each PCR amplification was performed using a SensoQuest Labcycler (Progen Scientific, Ltd., Mexborough, UK) and a Perkin Elmer 2400 machine (Applied Biosystem, Foster City, CA, USA).

### Mutation Analysis

Single-strand conformation polymorphism (SSCP) and DNA sequence analyses were used to screen for *KCNQ1*, *KCNH2*, *SCN5A*, and *KCNE1* gene mutations. In the case of exons 15, 17-1, and 23 of *SCN5A* and exon 3 of *KCNE1*, the high-resolution melting (HRM) method was used.

### SSCP Analysis

For the analysis of all genes, 2- $\mu$ L aliquots of the amplified samples were mixed with 4  $\mu$ L of bromphenol blue loading dye (95% formamide; 10 mmol/L ethylenediaminetetraacetic acid (EDTA); 0.1% bromphenol blue; 0.1% xylene cyanol) and were denatured at 94°C for 5 minutes, then cooled rapidly on ice and held for 5 minutes. Denatured multiplex PCR samples of *KCNQ1* were analyzed in multiplex SSCP in 10% and 12% polyacrylamide gels (crosslinking 40:1) at 10°C and 15°C/12 h/120 V. The fragments shown to have single-strand mobility in multiplex SSCP were reanalyzed by separate exon SSCP analysis under the same electrophoretic conditions. Analysis of multiplex PCR of *KCNH2* gene was performed using 8% polyacrylamide gel (crosslinking 50:1) at 8.5°C/3 h/40 W followed by separate exon SSCP analysis under the same electrophoretic conditions.

Denatured samples of the *SCN5A* gene were loaded into nondenaturing polyacrylamide gels with two layers (5% and 9%) and run at 210 V and 10°C for 6–8 hours according to the length of each fragment (Multigel-Long, Whatman Biome-tral, GmbH, Göttingen, Germany).

The bands were visualized by silver staining.

### HRM Analysis

HRM analysis was performed using a LightCycler 480 real-time PCR system and high-resolution Melting Master Kit (Roche Diagnostics, GmbH, Mannheim, Germany). PCR products were used as loaded samples. Primers were the same as those used for SSCP.

### DNA Sequencing

In cases of different band patterns, sequencing was performed with forward and reverse primers. To reduce the risk of polymerase-induced errors and false-positive results, the PCR products suspected of sequence change were reamplified before sequencing.

For purification of the amplified samples, MinElute PCR Purification Kit (Qiagen, Inc.) was used. Cycle sequencing was performed using the Big Dye Terminator Kit (Applied Biosystems), and the DyeEx2.0 Spin Kit (Qiagen, Inc.) was used for purification of samples after cycle sequencing.

Exons were sequenced using the ABI PRISM 310 instrument (Applied Biosystems).

The resulting sequences of the screened *KCNQ1*, *KCNH2*, *SCN5A*, and *KCNE1* genes were aligned with the wild-type sequences deposited in NCBI (GenBank accession nos AF000571, NM000238, NT022517, NM000219).

### Statistics

The distributions of allelic frequencies and their differences were calculated using  $\chi^2$  tests. Odds ratio (OR) and 95% confidence interval (CI) were calculated to estimate the risks associated with the detected polymorphisms. To calculate the significance of OR, Fisher's exact test was used. The program package Statistica v. 8.0 (Statsoft Inc., Tulsa, OK, USA) was used for all statistical analyses.

## Results

### Coding Variants in VF Survivors

The full coding sequences of *KCNQ1*, *KCNH2*, *SCN5A*, *KCNE1*, and *KCNE2* genes of all the VF survivors were analyzed. Nonsynonymous single nucleotide polymorphisms (SNP) were present in eight male patients. None of these individuals showed QT interval prolongation or Brugada-like ECG.

In the *KCNQ1* gene, nonsynonymous changes were not identified. In the *KCNH2* gene, three nonsynonymous changes in three individuals were found: R148W and the in-frame deletion GAG186del are novel, whereas P347S has previously been reported as related to LQTS.<sup>11</sup>

In the *SCN5A* gene, we identified the known common polymorphism H558R with an allelic frequency of 20.46%. A nonsynonymous variant P2006A was found in five unrelated male patients, yielding an allelic frequency of 5.68%. This variant had been described previously as rarely reported in only two of 829 healthy individuals<sup>12</sup> and also in one individual who died due to sudden infant death syndrome.<sup>13</sup> Previously, the P2006A variant has been shown to have a small, yet statistically significant, effect on sodium channel kinetics.

In the *KCNE1* gene, two known common polymorphisms were found: G38S with an allelic frequency of 42.2%, and D85N found in one patient (1.11%). In the *KCNE2* gene, no DNA changes were found.

### Coding Variants in Healthy Controls

The full coding sequences of *KCNQ1*, *KCNH2*, *SCN5A*, *KCNE1*, and *KCNE2* genes were analyzed in 90 healthy control individuals. In the *SCN5A* gene, the known common polymorphism H558R

**Table II.**  
Coding Variants in SCD Survivors and CAD Controls

Gene	Exon	Nucleotide Change	Amino Acid Change	Region	Minor Allele Frequency (%) SCD Survivors (N = 45)	Number of Genotypes	Minor Allele Frequency (%) CAD Controls (N = 141)	Number of Genotypes	P
<i>KCNH2</i>	3	C442T	R148W	N-term	1.11	CC = 44, CT = 1, TT = 0	0	CC = 141, CT = 0, TT = 0	–
	4	560_568del9	GAG186del	N-term	1.11	non = 44, non/del = 1, del = 0	0	non = 141, non/del = 0, del = 0	–
	5	C1039T	P347S	N-term	1.11	CC = 44, CT = 1, TT = 0	0	CC = 141, CT = 0, TT = 0	–
<i>SCN5A</i>	28	C6016G	P2006A	C-term	5.6	CC = 40, CG = 5, GG = 0	1.1	CC = 138, CG = 3, GG = 0	0.01

SCD = sudden cardiac death; N-term = N-terminus of the gene; C-term = C-terminus of the gene; CAD = coronary artery disease; P = P-value of probability of case-control difference in allelic frequencies.

was found with an allelic frequency of 27.01%. In the *KCNE1* gene, two common polymorphisms were found: G38S with an allelic frequency of 29.3% and D85N with an allelic frequency of 1.67%. No rare coding variants were found in this group.

### Coding Variants in CAD Controls

The exons containing rare coding variants found in VF survivors were sequenced in the control group of 141 patients with CAD without arrhythmias. The *KCNH2* gene variants R148W, GAG186del, and P347S were not present in any of these control samples. The *SCN5A* gene variant P2006A was found in three CAD control individuals, giving an allelic frequency of 1.1%.

### Statistics

The allelic frequency of the common polymorphism H558R of the *SCN5A* gene did not differ between the VF survivors (20.46%) and the healthy controls (26.67%,  $P = 0.319$ ). The same was true for the two previously described common SNPs of the *KCNE1* gene: G38S, which had an allelic frequency of 42.2% in the patients and 29.4% in the healthy controls ( $P = 0.04$ ), and D85N, which was found in one patient and three controls ( $P = 0.721$ ).

The carrier frequency of all the rare sequence variants (R148W, GAG186del, P347S in *KCNH2*, P2006A in *SCN5A*) was significantly higher in the VF survivors (8/45, 17.8%) than in the CAD controls (3/141, 2.2%,  $P = 0.001$ ). Evaluated according to OR, the risk of this genotype in the VF survivors is 8.36 (95% CI 2.13–32.84,  $P = 0.001$ ).

The allelic frequency of the rare variant P2006A of the *SCN5A* gene was significantly higher among the VF survivors (5.6%) compared with the healthy control subjects (0%, OR 11.13, 95% CI 1.26–98.34,  $P = 0.003$ ). The same was true for allelic frequencies of this polymorphism in the VF survivors (5.6%) and the CAD control subjects (1.1%,  $P = 0.01$ , OR 5.75, 95% CI = 1.32–25.11,  $P = 0.02$ ). There were no differences in the frequency of this variant between the healthy controls (0%) and the CAD control subjects (1.1%,  $P = 0.226$ ).

The results are summarized in Tables II–IV.

### Discussion

In the present study, we performed a mutation analysis of five cardiac ion-channel genes in VF survivors with CAD to test the hypothesis that ion-channel gene polymorphisms are more common in SCD cases compared with a control population. Our hypothesis was based on findings from previous population studies that demonstrated

**Table III.**  
Coding Variants in SCD Survivors and Healthy Controls

Gene	Exon	Nucleotide Change	Amino Acid Change	Region	Minor Allele Frequency (%) SCD survivors (N = 90)	Number of Genotypes	Minor Allele Frequency (%) Healthy Controls (N = 90)	Number of Genotypes	P
<i>KCNH2</i>	3	C442T	R148W	N-term	1.11	CC = 44, CT = 1, TT = 0	0	CC = 90, CT = 0, TT = 0	0.333
	4	560_568del9	GAG186del	N-term	1.11	non = 44, non/del = 1, del = 0	0	non = 90, non/del = 0, del = 0	–
	5	C1039T*	P347S	N-term	1.11	CC = 44, CT = 1, TT = 0	0	CC = 90, CT = 0, TT = 0	0.333
<i>KCNE1</i>	3	G112A	G38S	Extracellular	42.2	GG = 14, GA = 24, AA = 7	29.4	GG = 41, GA = 41, AA = 5	0.04*
	3	G253A	D85N	Cytoplasmatic	1.11	GG = 44, GA = 1, AA = 0	2	GG = 87, GA = 3, AA = 0	0.721
<i>SCN5A</i>	12	A1673G	H558R	DI-DII	21.11	AA = 26, AG = 19, GG = 0	26.67	AA = 47, AG = 38, GG = 5	0.319
	28	C6016G	P2006A	C-term	5.6	CC = 40, CG = 5, GG = 0	0	CC = 90, CG = 0, GG = 0	0.003

SCD = sudden cardiac death; N-term = N-terminus of the gene; DI-DII = linker of the DI and DII domains of the gene; CAD = coronary artery disease; P = P-value of probability of case-control difference in allelic frequencies. \*Not significant after correction on double polymorphism.

a strong genetic component of SCD. One of the pathways by which genetic variation in pathophysiological mechanisms may contribute to increased risk of SCD is electrogenesis and conduction in the myocardium. In our study, the carrier frequency of all the rare sequence variants was significantly higher in the VF survivors (8/45, 17.8%) than in CAD controls (3/141, 2.2%,  $P = 0.001$ ). In the healthy controls no rare coding variants were found.

Recently, several studies have investigated this issue. The first was conducted as part of the Oregon Sudden Unexpected Death Study.<sup>14</sup> In 67 (18% female) SCD cases and 91 control individuals, mutation analysis of the *SCN5A* gene was performed. Nonsynonymous nucleotide changes were found in 4% of the cases and 1% of the controls ( $P = 0.31$ ). Other genes were not analyzed. In the most recent study, the authors

performed mutation analysis of five cardiac ion-channel genes, *SCN5A*, *KCNQ1*, *KCNH2*, *KCNE1*, and *KCNE2*, in 113 SCD cases included in two large prospective cohorts of women (Nurses' Health Study) and men (Health Professional Follow-Up Study).<sup>15</sup> No mutations or rare variants were identified in any of the 53 male subjects, whereas five rare missense variants were identified in *SCN5A* in six of 60 women (10%). Exons containing these variants were sequenced in 733 control samples from the same population; the overall frequency of these rare variants in *SCN5A* was significantly higher in the SCD cases (6/60, 10.0%) than in controls (12/733, 1.6%,  $P = 0.001$ ). The other exons were not analyzed in the control individuals included in this study. The conclusion from these studies was that rare variants in ion-channel genes were not common causes of SCD. However, the results might have been influenced

**Table IV.**  
Coding Variants in the Investigated Individuals—Statistic Summary

Gene	Exon	Nucleotide Change	Amino Acid Change	Region	Minor Allele Frequency (%)				P	
					SCD Survivors (N = 45)	CAD Controls (N = 141)	Healthy Controls (N = 90)	SCD vs Healthy	SCD vs CAD	CAD vs Healthy
KCNH2	3	C442T	R148W	N-term	1.11	0	0	NS	NS	—
	4	560_568del	GAG186del	N-term	1.11	0	0	NS	NS	—
	5	C1039T	P347S	N-term	1.11	0	0	NS	NS	—
SCN5A	28	C6016G	P2006A	C-term	5.6	1.1	0	0,003	0,01	NS

SCD = sudden cardiac death; CAD = coronary artery disease; N-term = N-terminus of the gene; C-term = C-terminus of the gene; P = P-value of probability of case-control difference in allelic frequencies; NS = not significant.

by the fact that in both reports, the initial ECG was not available in a substantial proportion of the investigated individuals. Thus, the cause of death was not necessarily arrhythmic; previous studies have reported that the first recorded rhythm in patients with sudden cardiac arrest is not VF in at least 20%–25% of patients of either sex.<sup>16</sup>

In contrast to the previous two studies, we included only individuals with documented VF. In all patients, CAD was confirmed by coronary angiography. Although we excluded individuals in whom VF was related to acute myocardial infarction, the majority of these VF survivors had suffered a previous myocardial infarction in the past and consequently they had depressed LVEF. In this purely arrhythmic SCD group, the frequency of nonsynonymous DNA changes was significantly higher in the VF survivors compared with the control subjects.

Nonsynonymous DNA change does not necessarily indicate a change in protein function. The presence or absence of such rare variants in control populations does not always predict whether the variant will be associated with a functional alteration in channel properties. In the *SCN5A* gene, the C-terminal P2006A polymorphism was found in five unrelated patients in our study. This variant has been described previously as being rare, reported in only two of 829 healthy individuals<sup>12</sup> and in one infant who died due to sudden infant death syndrome.<sup>13</sup> In that study, the P2006A variant was associated with a small, yet statistically significant, level of increased persistent current combined with depolarizing shifts in voltage dependence of inactivation and more rapid recovery from inactivation. The authors speculated that the level of increased persistent current is not sufficient to evoke arrhythmia and that other factors are probably needed for full pathological expression. This fits well with the concept of repolarization reserve proposed by Roden in 1998: normal hearts include multiple, redundant mechanisms to accomplish normal repolarization. Deterioration of one of these mechanisms will not lead to failure of repolarization and no QT interval changes will be present, but under stress conditions such as CAD and hypokalemia, latent ion-channel mutations can increase the risk of malignant arrhythmias.<sup>17</sup>

Due to technical reasons, it was not possible to perform functional studies of mutated variants of the *KCNH2* channel and a literature search was performed to assess the putative functional effects of the SNPs found in the present study. In the *KCNH2* gene, all three polymorphisms were located in the N-terminal part of the protein. N-terminal residues are instrumental in rapid inactivation and sensor-effector coupling



for channel opening.<sup>18</sup> Nevertheless, in one study deletion of cca 220 amino acids, preserving a cluster of mainly positively charged residues upstream to S1 segment ( $\Delta 143-361$ ), induced activation properties that closely resembled the wild-type channel. These results indicate that a large part of the proximal domain is not essential for a wild-type channel activation phenotype.<sup>19</sup> All three changes found in this study were located within that region. On the other hand, N-terminal mutations (including P347S found in our study) have previously been shown to be related to LQTS.<sup>11</sup> Thus, further functional studies are necessary.

To date, in LQTS patients, hundreds of mutations have been reported within the five most common genes, more than half of which are unique, novel mutations. We had anticipated a similar situation in SCD survivors. However, in contrast, in five unrelated patients, the same *SCN5A* variant P2006A was found. A larger study is needed to determine if this variant is a, probably region-specific, risk stratification marker.

The prevalence of ion-channel variants remains largely unknown. Recently, Ackerman et al. published two studies determining the frequency and spectrum of ion-channel variants in approximately 800 apparently healthy individuals.<sup>12,20</sup> Excluding the common polymorphisms, 14%–25% of subjects (according to ethnicity) had at least one nonsynonymous potassium-channel variant and 3%–5.6% of subjects had at least one nonsynonymous sodium-channel variant. The authors commented that these analyses do not represent a population-based genetic epidemiologic study. Another study in Germany included 94 individuals from monozygotic twin pairs and 47 pairs of dizygotic twins,<sup>21</sup> all of whom were healthy. Excluding the common polymorphisms, only two rare nonsynonymous polymorphisms

were found in this group. In our group of 90 healthy individuals, no rare coding variants were found. Comparison of these data sets is difficult, also due to probable regional differences.

There are several limitations to our study, the most important of which is the small number of investigated individuals. Sufficient numbers could only be provided by a multicenter study owing to the incidence of SCD events and the capacity of individual centers to perform routine genetic methods. The sensitivity of SSCP is about 90%, thus, some variants might be missed. Due to the small number of women included in the present study, it was not possible to perform any sex-related associations. Missing information on SCD in family history prevents an analysis of familial segregation of the event.

In conclusion, the prevalence of selected, rare coding variants in five long QT genes was significantly higher in cases versus controls, confirming a mechanistic role for these genes among a subgroup of patients with CAD and VF.

Despite the great hopes that were expressed after sequencing of the human genome a decade ago, our understanding of the genetic background of pathophysiological processes remains poor. Recent observations have indicated that genomic architecture is not collinear and that the same sequences are used for multiple independently regulated transcripts and as regulatory regions.<sup>22</sup> The possible SCD susceptibility alleles are likely to be as prevalent in noncoding regions of the genome as in coding sequences.<sup>23</sup> Identification of such alleles will be a task for genome-wide association studies and the new emerging technologies developed for mass DNA sequencing. Any future genetic screening for SCD risk stratification should involve evaluation of large numbers of genomic variants in many pathways, each of which may be relevant to the risk of arrhythmias.

## References

- Myerburg RJ, Wellens HJJ. Epidemiology of cardiac arrest. In: Priori SG, Zipes DP (eds.): Sudden Cardiac Death. A Handbook for Clinical Practice. Malden, MA, Blackwell Publishing, 2006, pp. 3–20.
- Friedlander Y, Siscovick DS, Weinmann S, Austin MA, Psaty BM, Lemaitre RN, Arbogast P, et al. Family history as a risk factor for primary cardiac arrest. *Circulation* 1998; 97:155–160.
- Jouvan X, Desnos M, Guerot C, Ducimetière P. Predicting sudden death in the population: The Paris Prospective Study I. *Circulation* 1999; 99:1978–1983.
- Kaikkonen KS, Kortelainen ML, Linna E, Huikuri HV. Family history and the risk of sudden cardiac death as a manifestation of an acute coronary event. *Circulation* 2006; 114:1462–1467.
- Dekker LR, Bezzina CR, Henriques JP, Tanck MW, Koch KT, Alings MW, Arnold AER, et al. Familial sudden death is an important risk factor for primary ventricular fibrillation: A case-control study in acute myocardial infarction patients. *Circulation* 2006; 114:1140–1145.
- Priori SG, Napolitano C, Schwarz PJ. Low penetrance in the long-QT syndrome: Clinical impact. *Circulation* 1999; 99:529–533.
- Schwartz PJ, Stramba-Badiale M, Crotti L, Pedrazzini M, Besana A, Bosi G, Gabbarini F, et al. Prevalence of the congenital long-QT syndrome. *Circulation* 2009; 120:1761–1767.
- Larsen LA, Andersen PS, Kanters JK, Jacobsen JR, Vuust J, Christiansen M. A single strand conformation polymorphism/heteroduplex (SSCP/HD) method for detection of mutations in 15 exons of the KVLQT1 gene, associated with long QT syndrome. *Clin Chim Acta* 1999; 280:113–125.
- Splawski I, Shen J, Timothy KW, Vincent GM, Lehman MH, Keating MT. Genomic structure of three long QT syndrome genes: KVLQT1, HERG and KCNE1. *Genomics* 1998; 51:86–97.
- Syrris P, Murray A, Carter ND, McKenna WM, Jeffery S. Mutation detection in long QT syndrome: A comprehensive set of primers and PCR conditions. *J Med Genet* 2001; 38:705–710.
- Splawski I, Shen J, Timothy KW, Lehmann MH, Priori SG, Robinson JL, Moss AJ, et al. Spectrum of mutations in long-QT syndrome genes: KVLQT1, HERG, SCN5A, KCNE1, and KCNE2. *Circulation* 2000; 102:1178–1185.
- Ackerman MJ, Splawski I, Makielski JC, Tester DJ, Will ML, Timothy KW, Keating MT, et al. Spectrum and prevalence of cardiac sodium channel variants among black, white, Asian, and Hispanic

- individuals: Implications for arrhythmogenic susceptibility and Brugada/long QT syndrome genetic testing. *Heart Rhythm* 2004; 1:600–607.
13. Wang DW, Desai RR, Crotti L, Rognum TO, Insolia R, Pedrazzini M, Ferrandi C, et al. Cardiac sodium channel dysfunction in sudden infant death syndrome. *Circulation* 2007; 115:368–376.
  14. Stecker EC, Sono M, Wallace E, Gunson K, Jui J, Chugh SS. Allelic variants of SCN5A and risk of sudden cardiac arrest in patients with coronary artery disease. *Heart Rhythm* 2006; 3:697–700.
  15. Albert CM, Nam EG, Rimm EB, Jin HW, Hajjar RJ, Hunter DJ, MacRae CA, et al. Cardiac sodium channel gene variants and sudden cardiac death in women. *Circulation* 2008; 117:16–23.
  16. Albert MA, Cobbe SM. Clinical characteristics of sudden cardiac death victims and precipitating events. In: Priori SG, Zipes DP (eds.): *Sudden Cardiac Death. A Handbook for Clinical Practice*. Malden, MA, Blackwell Publishing, 2006, pp. 74–87.
  17. Roden DM. Taking the idio out of idiosyncratic – predicting torsades de pointes. *Pacing Clin Electrophysiol* 1998; 21:1029–1034.
  18. Varshney A, Mathew MK. A tale of two tails: Cytosolic termini and K<sup>+</sup> channel function. *Prog Biophys Mol Biol* 2003; 83:153–170.
  19. Saenen JB, Labro AJ, Raes A, Snyders DJ. Modulation of HERG gating by a charge cluster in the N-terminal proximal domain. *Biophys J* 2006; 91:4381–4391.
  20. Ackerman MJ, Tester DJ, Jones G, Will MK, Burrow CR, Curran M. Ethnic differences in cardiac potassium channel variants: Implications for genetic susceptibility to sudden cardiac death and genetic testing for congenital long QT syndrome. *Mayo Clin Proc* 2003; 78:1479–1487.
  21. Aydin A, Bähring S, Dahm S, Guenther UP, Uhlmann R, Busjahn A, Luft FC. Single nucleotide polymorphism map of five long-QT genes. *J Mol Med* 2005; 83:159–165.
  22. Kapranov P, Willingham AT, Gingeras TR. Genome-wide transcription and the implications for genomic organization. *Nat Rev Genet* 2007; 8:413–423.
  23. Spooner PM. Sudden cardiac death: The larger problem...the larger genome. *J Cardiovasc Electrophysiol* 2009; 20:585–596.

Uvedené studie se zabývaly pouze geny souvisejícími s LQTS. Data ze studie Testera et al.<sup>34</sup> poukazují na nezanedbatelný podíl variant *RyR2* genu, kauzálního genu CPVT, v případech NSS. V této studii byla provedena post mortem analýza tohoto genu u 49 jedinců zemřelých nevysvětlitelnou náhlou smrtí a z výsledků analýzy vyplývá, že jednu ze sedmi NSS způsobuje právě patogenní mutace v genu *RyR2*. Jedná se však o pacienty bez předešlého dokumentovaného strukturálního postižení srdce. S ohledem na tyto skutečnosti jsme se rozhodli porovnat výskyt variant genu *RyR2* u pacientů po prodělané arytmiické bouři, která nebyla vysvětlitelná jinou příčinou, se skupinou pacientů s ICHS a dysfunkční levou komorou bez záchytu arytmií. Mutační analýzou jsme detekovali několik sekvenčních variant charakteru polymorfismů, avšak výskyt byl v obou skupinách praktický stejný. Role variant genu *RyR2* tak bude mít v patofyziologii NSS spíše omezenou roli.

**Andršová I**, Novotný T, Valášková I, Kadlecová J, Kuderová D, Sepši M, Kozák M, Křivan L, Gaillyová R, Špinar J. Mutation analysis of *RyR2* gene in patients after arrhythmic storm. *Cor Vasa* 2012;54:e84-e87.

Uvedeno ve Web of Science bez IF. Počet citací ve Web of Science 0

Publikovaná původní práce – kvantitativní podíl uchazeče 30 % - koncept, koordinace práce zúčastněných pracovišť, identifikace vhodných pacientů, analýza dat, text publikace.



ELSEVIER



## Původní sdělení | Original article/research

# Mutation analysis of *RyR2* gene in patients after arrhythmic storm

Irena Andršová<sup>a</sup>, Tomáš Novotný<sup>a</sup>, Iveta Valášková<sup>b</sup>, Jitka Kadlecová<sup>b</sup>, Dana Kuderová<sup>a</sup>, Milan Sepšič<sup>a</sup>, Milan Kozák<sup>a</sup>, Lubomír Křivan<sup>a</sup>, Renata Gaillyová<sup>b</sup>, Jindřich Špinar<sup>a</sup>

<sup>a</sup> Interní kardiologická klinika, Fakultní nemocnice Brno, Brno, Česká republika

<sup>b</sup> Oddělení lékařské genetiky, Fakultní nemocnice Brno, Brno, Česká republika

## INFORMACE O ČLÁNKU

## Historie článku:

Došel do redakce: 11. 2. 2012

Přepřacován: 7. 3. 2012

Přiját: 7. 3. 2012

## Key words:

Arrhythmic storm

Mutation analysis

*RyR2* gene

Sudden cardiac death

## ABSTRACT

**Introduction:** Mutations of *RyR2* gene encoding calcium channel of sarcoplasmic reticulum are the cause of congenital catecholaminergic polymorphic ventricular tachycardia. The aim of this study was to test the hypothesis that *RyR2* variants can increase occurrence of malignant arrhythmias in patients with structural heart diseases.

**Methods:** The investigated group consisted of 36 patients with structural heart diseases with ICD implanted who suffered arrhythmic storm. In the control group there were 141 patients with coronary artery disease who were hospitalized at our department owing to an acute coronary event and they were alive at least 3 years after the index event. Thus, they could be considered as a group with a low risk of sudden cardiac death. In all of them mutation analysis of *RyR2* gene was performed.

**Results:** We detected 16 different sequence changes of *RyR2* gene in both groups. None of found nucleotide polymorphisms led to amino acid changes, were located close to splice sites or had any similarity to known splicing enhancer motifs. The occurrence of these variants was not different in both groups.

**Conclusions:** The prevalence of *RyR2* gene variants was not different in cases versus controls suggesting a limited role of this gene in the arrhythmogenesis in structural heart disease patients.

## SOUHRN

## Klíčová slova:

Arytmická bouře

Gen *RyR2*

Mutační analýza

Náhlá srdeční smrt

**Úvod:** Mutace genu *RyR2* kódujícího vápníkový kanál sarkoplazmatického retikula jsou příčinou kongenitální arytmie katecholaminergní polymorfni komorové tachykardie. Cílem práce je ověřit hypotézu, zda varianty genu *RyR2* nemohou zvyšovat výskyt maligních arytmií u pacientů se strukturálním onemocněním srdce.

**Metody:** Soubor vyšetřených tvořilo 36 pacientů se strukturálním onemocněním srdce zajištěných implantačním kardioverterem-defibrilátorem (ICD), kteří prodělali arytmiickou bouři. Kontrolní skupinu tvořilo 141 jedinců s ischemickou chorobou srdeční hospitalizovaných na našem pracovišti z důvodu akutního koronárního syndromu a dobou přežití delší než tři roky od příhody, tedy pacienti s relativně nízkým rizikem náhlé srdeční smrti. U všech zařazených byla provedena mutační analýza genu *RyR2*.

**Výsledky:** V obou skupinách jsme detekovali celkem 16 sekvenčních změn DNA genu *RyR2*. Odhalené nukleotidové polymorfismy nezahrnují žádnou změnu, která by vedla k zařazení odlišné aminokyseliny.

**Závěr:** Výskyt sekvenčních změn byl stejný v obou skupinách vyšetřených pacientů.

## Introduction

The leading cause of cardiovascular mortality is sudden cardiac death (SCD). Estimated incidence of SCD is more than 3 million people in the world per year. It means about 200–400 thousand in the U.S. population per year and in Europe it accounts for about 2,500 deaths per day. Nevertheless, the SCD incidence in the general population is low (0.1–0.2% per year, i.e. 1–2 patients/1,000 population). Approximately 50% of all coronary heart disease deaths are sudden [1]. In most cases, the underlying cause of death is the rapid onset of lethal ventricular arrhythmias in the setting of acquired heart disease. In our study we considered the common knowledge, that the risk of sudden cardiac death is higher in patients with structural heart disease (it means chronic ischemic heart disease or dilated cardiomyopathy) and with systolic dysfunction of left ventricle. Data from MADIT-II study showed that during 3 years only one third of patients with primary preventive implantation of ICD needed the therapy from the device due to malignant arrhythmias. The remaining two thirds of patients were only ICD carriers [2]. Observations from population-based studies

demonstrate a strong genetic component of SCD [3–6]. It is clear that there must be genetically determined variations of physiological processes that increase the risk of SCD. It is well known that myocardial ion channel gene mutations lead to increased SCD risk in patients with relatively rare diseases, such as long QT syndrome (LQTS), Brugada syndrome and catecholaminergic polymorphic ventricular tachycardia (CPVT).

Ventricular premature complexes (VPCs) could initiate malignant arrhythmias. High occurrence of VPCs is typical for rare hereditary disease called CPVT. For this disorder stress syncope or sudden cardiac death are typical, manifested in young patients most often before 40 years of age. The mortality is high, almost 50%. Mutations of *RyR2* gene are found in about 60% of patients with clinical diagnosis of CPVT [7]. An important fact is that the resting ECG is completely normal. But during stress VPCs are becoming more frequent and can progress in typical bidirectional ventricular tachycardia. In our study we tried to test the hypothesis, that mutation of *RyR2* receptor could increase the risk of malignant arrhythmias in patients with structural heart disease.

**Table 1 – Clinical characteristics of investigated individuals.**

	Arrhythmic storm (n = 36)	CAD controls (n = 141)	<i>p</i>
Male/Female	33/3	129/12	0,4676
Age (years)	69,4 ± 11,4	66,7 ± 10,7	0,4610
Left ventricle ejection fraction	32 ± 9 %	42 ± 9 %	< 0,0001
CAD	69%	100%	< 0,0001
History of myocardial infarction	21 (58%)	129 (90%)	< 0,0001
DCM	11 (31%)	0	< 0,0001

CAD – coronary artery disease; DCM – dilated cardiomyopathy.

**Table 2 – *RyR2* gene variants in investigated individuals.**

Nucleotide change	Exon/intron	Allelic frequency %		<i>p</i>	References
		Arrhythmic storm n = 36	Control group n = 141		
c.[268-100G>T]	intron 3-4	4,0	6,2	0,5414	–
c.[458-8A>C]	intron 7-8	16,2	12,1	0,2991	12
c.[671-11T>A]	intron 9-10	43,2	53,8	0,1003	12
c.[1000-31T>A]	intron 12-13	1,3	2,7	0,4860	–
c.[1353C>T]	exon 15	33,8	40,5	0,2708	12
c.[6682+72T>G]	intron 43-44	36,5	47,0	0,0924	12
c.[6682+93C>A]	intron 43-44	27,0	16,2	0,0487	–
c.[6900T>C]	exon 45	94,5	87,8	0,1117	13
c.[11320-23C>T]	intron 82-83	35,1	29,7	0,4182	12
c.[12957T>C]	intron 89-90	58,1	68,9	0,0928	–
c.[13470+16A>G]	intron 92-93	33,8	28,3	0,4091	12
c.[13470+47G>A]	intron 92-93	36,5	43,2	0,2722	12
c.[13777-21G>A]	intron 94-95	55,4	42,5	0,0479	12
c.[13777-6A>G]	intron 94-95	50,0	36,2	0,0318	12
c.[13907+12A>C]	intron 95-96	59,5	46,0	0,0390	12
c.[14085-(11-22delT)]	intron 97-98	47,3	40,8	0,3231	–

## Methods

### Investigated subjects

The investigated group consisted of 36 Caucasian patients from the region of south Moravia in the Czech Republic. These individuals were identified from the ICD registry of our department, partially retrospectively (years 1998–2006) and from 2007 new consecutive patients were included prospectively. The inclusion criteria were: 1. history of arrhythmic storm defined as 3 or more sustained ventricular tachyarrhythmias within 24 hours detected and treated from ICD; 2. structural heart disease such as dilated cardiomyopathy (DCM) or CAD verified by echocardiography and coronary angiography.

The control group consisted of 141 patients with CAD who were hospitalized at our department owing to an acute coronary event. For all patients the diagnosis was confirmed by coronary angiography. All patients had depressed left ventricle ejection fraction (LVEF) and they were alive at least 3 years after the index event. Thus, they could be considered as a CAD group with a low risk of SCD. Clinical characteristics of both groups are summarized in Table 1.

Informed consent was obtained from all patients and peripheral blood samples were taken for genomic DNA preparation. The study protocol was approved by Ethical Committee of the University Hospital Brno and conforms to the ethical guidelines of the 1975 Declaration of Helsinki.

### Mutation analysis

Mutation analysis of the *RyR2* gene was performed in all members of the arrhythmic storm group. Genomic DNA samples were isolated from peripheral blood lymphocytes and PCR amplified fragments covering hot spot areas of *RyR2* exons 2-4, 6-15, 17-20, 39-49, 83, 84, 87-97-105 were analyzed by direct sequencing on the instrument ABI PRISM 3130 (Life Technologies, USA). For mapping of exons 3, 97 and 105 deletions multiplex ligation-dependent probe amplification analysis (MLPA) was used. Detailed methodology has been described elsewhere [8–10]. The regions containing sequence variants found in the arrhythmic storm group were sequenced in the control group of 141 patients with CAD without arrhythmias.

### Statistics

Values are given as mean  $\pm$  SD. Demographic data were analyzed by the F test for variance and Student's *t*-test. The distributions of allelic frequencies and their differences were calculated using  $\chi^2$  tests. The program package Statistica v. 8.0 (Statsoft Inc., Tulsa, OK, USA) was used for all statistical analyses.

## Results

We detected 16 different sequence changes in both groups. Twelve of these DNA changes were already described in the study of Bagattin et al. [11] or in the database Ensembl [12]. The other have not been described yet. None of the found nucleotide polymorphisms led to amino acid changes and were located close to splice sites

or had any similarity to known splicing enhancer motifs. The occurrence of these variants was not different in both groups. The results are summarized in Table 2.

## Discussion

In the present study, we performed a mutation analysis of a cardiac ion channel gene important in arrhythmogenesis. We test the hypothesis that mutation of *RyR2* gene could increase risk of malignant arrhythmias in patients with structural heart diseases. Our hypothesis was based on findings of previous population studies that demonstrated a strong genetic component of SCD.

Recently, several studies have investigated the issue of the influence of genetic variants on the risk of arrhythmias in patients with structural heart diseases. In these studies the prevalence of rare coding variants in so called long QT genes was significantly higher in patients suffering from ventricular fibrillation as compared to control group [13–15].

The *RyR2* gene was chosen because of its well known role in the arrhythmogenesis in CPVT. This disease is characterized by high occurrence of VPCs. We hypothesized that such *RyR2* mutations can exist which remain usually latent, but under stress conditions, such as structural heart disease, they can increase the risk of ventricular arrhythmias also in normal population.

The *RyR2* gene is one of the largest genes in the human genome and its analysis is time consuming. The majority of mutations appear to cluster in three regions of the predicted *RyR2* protein topology, and about 65% of published mutations of the *RyR2* gene are located in these regions [9,16]. Therefore we used a tiered targeting strategy suggested by groups in the Mayo Clinic and the Netherlands [9]. Although we expected only rare finding of sequence changes of *RyR2* gene, the opposite was true. The occurrence of sequence variants was common in both groups. This suggests that these regions are probably rather polymorphic in population. In our study 16 sequence changes of *RyR2* gene were detected in both groups. None of the found nucleotide polymorphisms led to amino acid changes, were located close to splice sites or had any similarity to known splicing enhancer motifs. Nevertheless, there is emerging evidence that even synonymous DNA variants can play important role in protein structure changes. On the other side there were no statistical differences in their allelic frequencies, thus the probability of any functional effect of these variants is low.

The most important limitation of our study is the small number of investigated individuals. Although the control group was age and sex matched and all the control individuals have depressed left ventricular systolic function and coronary artery disease confirmed by angiography, there were differences in ejection fraction and the etiology of heart failure. This could have possible impact on the results. Nevertheless, the prevalence of DNA variants was high also in the control group. Using the tiered targeting strategy of *RyR2* gene mutation analysis can have an impact on the robustness of the estimate of the prevalence of *RyR2* mutations among the cohort. Due to the

small number of women included in the present study, it was not possible to perform any sex-related associations.

## Conclusions

The prevalence of *RyR2* gene variants was not different in cases versus controls suggesting a limited role of this gene in the arrhythmogenesis in structural heart disease patients.

## Acknowledgements

The research was supported by grant 2B08061 of the Ministry of Education, Youth and Sports of the Czech Republic and Specific research project of the Masaryk University SVMUNI/A/0811/2011.

The authors have no relationship to industry to disclose.

## References

- [1] Myerburg RJ, Wellens HJJ. Epidemiology of Cardiac Arrest. In: Priori SG, Zipes DP (Eds.). Sudden Cardiac Death: A handbook for clinical practice. Oxford: Blackwell Publishing Ltd., 2006:3–17.
- [2] Moss AJ, Zareba W, Hall WJ, et al; for the Multicenter Automatic Defibrillator Implantation Trial II investigators. Prophylactic implantation of a defibrillator in patients with myocardial infarction and reduced ejection fraction. *N Engl J Med* 2002;346:877–83.
- [3] Friedlander Y, Siscovick DS, Weinmann S, Austin MA, Psaty BM, Lemaitre RN, et al. Family history as a risk factor for primary cardiac arrest. *Circulation* 1998;97:155–60.
- [4] Jouvan X, Desnos M, Guerot C, Ducimetière P. Predicting sudden death in the population: The Paris Prospective Study I. *Circulation* 1999;99:1978–83.
- [5] Kaikkonen KS, Kortelainen ML, Linna E, Huikuri HV. Family history and the risk of sudden cardiac death as a manifestation of an acute coronary event. *Circulation* 2006;114:1462–7.
- [6] Dekker LR, Bezzina CR, Henriques JP, Tanck MW, Koch KT, Alings MW, et al. Familial sudden death is an important risk factor for primary ventricular fibrillation: A casecontrol study in acute myocardial infarction patients. *Circulation* 2006;114:1140–5.
- [7] Priori SG, Chen W. Inherited dysfunction of sarcoplasmic reticulum Ca<sup>2+</sup> handling and arrhythmogenesis. *Circ Res* 2011;108:871–83.
- [8] Bagattin A, Veronese C, Baucé B, Wuys W, Settimo L, Nava A, et al. Denaturing HPLC-based approach for detecting RYR2 mutations involved in malignant arrhythmias. *Clinical Chemistry* 2004;50:1148–55.
- [9] Medeiros-DA, Bhuiyan ZA, Tester DJ, Hofman N, Bikker H, vanTintelen P, et al. The RYR2-encoded ryanodine receptor/calcium channel in patients diagnosed previously with either catecholaminergic polymorphic ventricular tachycardia or genotype negative, exercise-induced long QT syndrome. *J Am Coll Cardiol* 2009;54:2065–74.
- [10] Postma AV, Denjoy I, Kamblock J, Alders M, Lupoglazoff JM, Vaksman G, et al. Catecholaminergic polymorphic ventricular tachycardia: RYR2 mutations, bradycardia, and follow up of the patients. *J Med Genet* 2005;42:863–70.
- [11] Bagattin A, Veronese C, Rampazzo A, Danieli GA. Gene symbol: RYR2. Disease: Effort-induced polymorphic ventricular arrhythmias. *Hum Genet* 2004;114:404–5.
- [12] Ensembl release 65 – Dec 2011. [http://www.ensembl.org/Homo\\_sapiens/Info/Index](http://www.ensembl.org/Homo_sapiens/Info/Index)
- [13] Stecker EC, Sono M, Wallace E, Gunson K, Jui J, Chugh SS. Allelic variants of SCN5A and risk of sudden cardiac arrest in patients with coronary artery disease. *Heart Rhythm* 2006;3:697–700.
- [14] Albert CM, Nam EG, Rimm EB, Jin HW, Hajjar RJ, Hunter DJ, et al. Cardiac sodium channel gene variants and sudden cardiac death in women. *Circulation* 2008;117:16–23.
- [15] Novotný T, Kadlecová J, Raudenská M, Bittnerová A, Andršová I, Floriánová A, et al. Mutation Analysis Ion Channel Genes Ventricular Fibrillation Survivors with Coronary Artery Disease. *PACE* 2011,34:742–9.
- [16] George GH, Jundi H, Thomas NL, Scoote M, Walters N, Williams AJ, et al. Ryanodine receptor regulation by intramolecular interaction between cytoplasmic and transmembrane domains. *Mol Biol Cell* 2004;15:2627–38.

S ohledem na záchyt signifikantně vyššího výskytu kódujících variant genů pro iontové kanály myokardu, vyjma *RyR2* genu, jsme u stejné skupiny pacientů s ICHS po FK provedli i analýzu variant promotorů těchto genů a porovnali s kontrolním souborem. Výskyt byl opět stejný v obou skupinách. Výskyt variant naznačuje s ohledem na porovnání s mezinárodními databázi významné geografické odlišnosti.

Novotný T, Raudenská M, Kadlecová J, **Andršová I**, Floriánová A, Vašků A, Kozák M, Sepši M, Křivan L, Gaillyová R, Špinar J. Mutační analýza promotorů genů pro iontové kanály u pacientů s ischemickou chorobou srdeční, kteří přežili fibrilaci komor (Mutation analysis of ion channel genes promoters in ventricular fibrillation survivors with coronary artery disease). *Cor Vasa* (2013) doi: 10.1016/j.crvasa.2013.06.009

Uvedeno ve Web of Science bez IF. Počet citací ve Web of Science 0

Publikovaná původní práce – kvantitativní podíl uchazečky 20 % - identifikace vhodných pacientů, analýza dat, revize textu publikace.





## Původní sdělení | Original research article

## Mutační analýza promotorů genů pro iontové kanály u pacientů s ischemickou chorobou srdeční, kteří přežili fibrilaci komor

(Mutation analysis of ion channel genes promoters in ventricular fibrillation survivors with coronary artery disease)

Tomáš Novotný<sup>a</sup>, Martina Raudenská<sup>b</sup>, Jitka Kadlecová<sup>c</sup>, Irena Andršová<sup>a</sup>, Alena Floriánová<sup>a</sup>, Anna Vašků<sup>b</sup>, Milan Kozák<sup>a</sup>, Milan Sepši<sup>a</sup>, Lubomír Křivan<sup>a</sup>, Renata Gaillyová<sup>c</sup>, Jindřich Špinar<sup>a</sup>

<sup>a</sup> Interní kardiologická klinika, Lékařská fakulta Masarykovy univerzity a Fakultní nemocnice Brno, Brno, Česká republika

<sup>b</sup> Ústav patologické fyziologie, Lékařská fakulta Masarykovy univerzity, Brno, Česká republika

<sup>c</sup> Oddělení lékařské genetiky, Lékařská fakulta Masarykovy univerzity a Fakultní nemocnice Brno, Brno, Česká republika

## INFORMACE O ČLÁNKU

## Historie článku:

Došel do redakce: 19. 3. 2013

Přepřevzat: 19. 6. 2013

Přiját: 24. 6. 2013

Dostupný online: 1. 7. 2013

## SOUHRN

**Úvod:** Existují pádné důkazy pro to, že náhlá srdeční smrt (NSS) je geneticky podmíněna. V naší předchozí studii jsme zjistili, že prevalence vybraných vzácných kódujících variant v pěti genech se vztahem k syndromu dlouhého intervalu QT (LQTS) byla signifikantně vyšší u pacientů s ischemickou chorobou srdeční (ICHS), kteří přežili fibrilaci komor (FK), ve srovnání s kontrolami. V nynější studii jsme provedli mutační analýzu promotorů pěti LQTS genů ve stejné skupině pacientů a v kontrolních populacích.

**Metody:** Promotory genů *KCNQ1*, *KCNH2*, *SCN5A*, *KCNE1* a *KCNE2* byly analyzovány u 45 jedinců s ICHS, kteří přežili FK. Alelické frekvence byly srovnávány s daty z projektu 1000 Genomes Project nebo z lokální DNA banky pacientů s ICHS bez maligních arytmií (141 jedinců).

**Výsledky:** U 34 (75,5 %) ze 45 jedinců přeživších FK bylo nalezeno devět různých variant promotorů: dvě v promotoru genu *KCNQ1*, jedna v promotoru genu *KCNE1* a šest v promotoru genu *SCN5A*. Statisticky signifikantně se lišily alelické frekvence obou variant promotoru genu *KCNQ1*: 1-182C>T ( $p = 0,008$ ), 1-119G>A ( $p = 0,007$ ). Tyto varianty však v předchozí studii nesegregovaly s LQTS fenotypem. Alelická frekvence varianty 225-1072T>C promotoru genu *SCN5A* u pacientů přeživších FK se signifikantně lišila ve srovnání s daty z 1000 Genomes Project ( $p = 0,001$ ), nikoliv však oproti skupině lokálních kontrol s ICHS.

**Závěry:** Naše výsledky ukazují, že varianty promotorů genů pro iontové kanály jsou časté jak u pacientů přeživších FK, tak v kontrolních skupinách. Naznačují, že varianty promotorů jsou geograficky specifické a nejsou běžnou příčinou NSS.

## Klíčová slova:

Iontový kanál

Ischemická choroba srdeční

Náhlá srdeční smrt

Promotor

© 2013, ČKS. Published by Elsevier Urban and Partner Sp. z o.o. All rights reserved.

**Adresa:** MUDr. Tomáš Novotný, Ph.D., Interní kardiologická klinika, Lékařská fakulta Masarykovy univerzity a Fakultní nemocnice Brno, Jihlavská 20, 625 00 Brno-Bohunice, e-mail: [novotny-t@seznam.cz](mailto:novotny-t@seznam.cz)

DOI: 10.1016/j.crvasa.2013.06.009

## ABSTRACT

**Introduction:** Strong evidence suggests that sudden cardiac death (SCD) is genetically determined. In our previous study we found that the prevalence of selected, rare coding variants in 5 long QT genes was significantly higher in ventricular fibrillation (VF) survivors with coronary artery disease (CAD) than in controls. In the present study we performed mutational analysis of the promoters of 5 LQTS-related myocardial ion channel genes in the same group of patients and in control populations.

**Methods:** The promoters of *KCNQ1*, *KCNH2*, *SCN5A*, *KCNE1* and *KCNE2* genes were analyzed in 45 CAD individuals – survivors of documented VF. The allelic frequencies were compared either to data from the 1000 Genomes Project or from a local DNA bank of patients with coronary artery disease and no malignant arrhythmia (141 individuals).

**Results:** In 34 (75.5%) of 45 VF survivors 9 different promoter variants were found: 2 in *KCNQ1* gene promoter, 1 in *KCNE1* promoter, and 6 in *SCN5A* promoter. Statistically significant differences were found in the allelic frequencies of both *KCNQ1* gene promoter variants: 1-182C>T ( $p=0.008$ ), 1-119G>A ( $p=0.007$ ). Nevertheless, these variants did not segregate with long QT phenotype in a previous study. While the allelic frequency of the *SCN5A* gene promoter variant 225-1072T>C significantly differed in VF survivors compared to the 1000 Genomes Project ( $p=0.001$ ), this allelic frequency was not different when compared to the group of local CAD controls.

**Conclusions:** Our findings demonstrated that variants of ion channel gene promoters are common, both in VF survivors and control groups. These results suggest that promoter variants are geographically-specific and are not a common cause of SCD.

**Keywords:**

Coronary artery disease

Ion channel

Promoter

Sudden cardiac death

**Úvod**

Existují pádné důkazy pro to, že náhlá srdeční smrt (NSS) je geneticky podmíněná [1–4]. V naší předchozí studii jsme zjistili, že prevalence vybraných vzácných kódujících variant v pěti genech se vztahem k syndromu dlouhého intervalu QT (LQTS) byla signifikantně vyšší u pacientů s ischemickou chorobou srdeční (ICHS), kteří přežili fibrilaci komor (FK), ve srovnání s kontrolami, což potvrzuje mechanistickou roli těchto genů v takto definované podskupině pacientů [5].

Deset let po publikaci výsledků sekvenace lidského genomu je jasné, že kódující sekvence představují jen asi 1,5 % lidského genomu [6]. Zbývající část je buď „DNA junk“ – „odpad“, nebo mnohem pravděpodobněji obsahuje důležité regulační sekvence.

V nynější studii jsme provedli mutační analýzu nekódujících částí genů – promotorů – pět LQTS genů ve stejné skupině pacientů s ICHS s dokumentovanou FK v okamžiku NSS a v kontrolních populacích.

**Metody****Vyšetřované subjekty**

Skupina pacientů byla identická jako v předchozí studii [5] a byla tvořena 45 bělošskými pacienty (5 žen, 40 mužů) z oblasti jižní Moravy (cca 1,5 milionu obyvatel). Primárním zařazovacím kritériem byla FK dokumentovaná v době oběhové zástavy, která nebyla v souvislosti s akutní fází infarktu myokardu (tj. více než 48 h po příhodě). Takoví jedinci byli identifikováni v registru ICD našeho pracoviště, částečně retrospektivně (1998–2006), od roku 2007 byli noví pacienti zařazováni prospektivně. U dvou pacientů došlo k FK za hospitalizace více než 72 h po akutním infarktu myokardu. Všichni ostatní prodělali oběhovou zástavu mimo nemocnici, FK byla dokumentována posádkou vozu rychlé záchranné pomoci. Pacienti byli úspěšně resuscitováni a poté odesláni na naše pra-

covišťe buď přímo, nebo přes regionální nemocnice. Po oběhové stabilizaci a úpravě mentálního stavu všichni pacienti podstoupili podrobné kardiologické vyšetření. U žádného z pacientů nebyly zjištěny známky akutního infarktu myokardu ani podle EKG, ani hodnot troponinu. Ischemická choroba srdeční byla u všech pacientů potvrzena koronarografickým nálezem signifikantních stenóz (> 70 %) nebo chronických uzávěrů. Ejekční frakce levé komory (EFLK) byla hodnocena echokardiograficky. U tří pacientů nebylo možno interval QT hodnotit kvůli přítomnosti blokády levého Tawarova raménka nebo fibrilace síní. Žádný ze zbývajících 42 pacientů nevykazoval významné prodloužení intervalu QT či EKG známky syndromu Brugadových.

Jako kontrolní soubor byla využita data z 1000 Genomes Project, v rámci kterého jsou sekvenovány genomy velkého počtu osob a jehož účelem je vytvoření zevrubného zdroje informací o lidských genetických variacích. V současné době databáze obsahuje data o genetických variacích v 1 092 lidských genomech z různých populací [7].

V případech, kdy data z 1000 Genomes Project nebyla k dispozici, byla použita kontrolní skupina 141 pacientů s ICHS, kteří byli hospitalizováni na našem pracovišti pro akutní koronární syndrom. U všech pacientů byla diagnóza ICHS potvrzena koronarografií. Všichni pacienti měli sníženou EFLK a přeživali minimálně čtyři roky po příhodě. Je tedy možno je považovat za jedince s nízkým rizikem NSS. Klinickou charakteristiku obou skupin shrnuje tabulka 1.

Po získání informovaného souhlasu byl u všech jedinců proveden odběr periferní krve k izolaci DNA. Protokol studie byl schválen etickou komisí FN Brno a je v souladu s etickými doporučeními Helsinské deklarace z roku 1975.

**Genomické DNA vzorky a polymerázová řetězová reakce**

Genomická DNA všech pacientů přeživších FK byla analyzována na přítomnost mutací v promotorových oblastech genů *KCNQ1*, *KCNH2*, *SCN5A*, *KCNE1* a *KCNE2*. Genomická DNA byla extrahována ze vzorků periferní krve podle

standardního protokolu s využitím DNA BloodSpin kitu a klasické metody ethanolové progresse.

Promotorové sekvence genů *KCNQ1*, *KCNH2* a *KCNE1* (GenBank přístupová čísla NG008935.1, NG008916.1, NG009091.1) byly amplifikovány multiplexní polymerázovou řetězovou reakcí (PCR). Byly navrženy a použity následující páry primerů: sedm párů primerů pro *KCNQ1* promotor, šest párů primerů pro *KCNH2* promotor a jeden pár primerů pro *KCNE1* promotor. Při PCR amplifikacích byl použit HotStarTaq Master Mix (Qiagen, Inc., Valencia, CA, USA). Každá PCR byla prováděna ve 200 μl tenkostěnných PCR zkumavkách v celkovém reakčním objemu 25 μl za využití Verity Thermal Cycler (Applied Biosystem, Foster City, CA, USA).

K amplifikaci promotorové oblasti genu *SCN5A* (GenBank přístupové číslo AY313163) bylo navrženo celkem 12 párů primerů. Pomocí programu Web Promoter Scan Service (verze 1.7) byl promotor genu *KCNE2* predikován do oblasti párů bází 7481–7746 sekvence DQ784804. Tato oblast byla amplifikována pomocí jednoho páru primerů s využitím Taq DNA polymerázy (Fermentas, Inc., Glen Burnie, MD, USA) a HotStarTaq Master Mix (Qiagen, Inc., Valencia, CA, USA). Každá PCR byla prováděna ve 200 μl tenkostěnných PCR zkumavkách v celkovém reakčním objemu 25 μl za využití Verity Thermal Cycler (Applied Biosystem, Foster City, CA, USA), SensoQuest Labcycler (Progen Scientific, Ltd., Mexborough, Spojené království) a Perkin Elmer 2400 (Applied Biosystem, Foster City, CA, USA).

### DNA sekvenace

DNA sekvenace byla prováděna na přístroji ABI 3130 (Applied Biosystem, Foster City, CA, USA) s cílem nalézt varianty promotorů genů *KCNQ1*, *KCNH2*, *SCN5A*, *KCNE2* a *KCNE1*, a to za použití forward i reverse primerů.

Amplifikované vzorky byly přečištěny pomocí MinElute PCR Purification Kit (Qiagen, Inc., Valencia, CA, USA). Sekvenace byla prováděna za využití Big Dye Terminator Kit (Applied Biosystems, Foster City, CA, USA). DyeEx2.0 Spin Kit (Qiagen, Inc., Valencia, CA, USA) byl použit pro přečištění po sekvenaci.

Výsledné sekvence analyzovaných promotorů genů *KCNQ1*, *KCNH2*, *SCN5A*, *KCNE2* a *KCNE1* byly srovnávány s „wild-type“ sekvencemi uloženými v NCBI (GenBank přístupová čísla NG008935.1, NG008916.1, NG009091.1, AY313163, DQ784804). Číslování bylo odvozeno podle Yanga a spol. [8] a alelické frekvence byly srovnávány s daty z 1 000 Genomes Project [7]. V případě, že nalezená varianta nebyla v tomto projektu popsána, sekvenovaly se oblasti obsahující sekvenční varianty v kontrolní skupině 141 pacientů s ICHS bez arytmií (popsáno výše).

### Statistika

Distribuce alelických frekvencí a jejich rozdíly byly kalkulovány pomocí  $\chi^2$  testu. Odds ratio (OR) a 95% interval spolehlivosti (confidence interval – CI) byl kalkulován k odhadu rizika spojeného s nalezeným polymorfismem. K hodnocení významnosti nebo OR byl použit Fisherův přesný test. Všechny statistické analýzy byly prováděny v programu Statistica v. 8.0 (Statsoft Inc., Tulsa, OK, USA).

### Výsledky

U 34 (75.5%) ze 45 pacientů přeživších FK bylo nalezeno devět různých variant DNA sekvence: dvě v promotoru genu *KCNQ1*, jedna v promotoru genu *KCNE1* a šest v promotoru genu *SCN5A*. V promotorech genů *KCNH2* a *KCNE2* nebyly detekovány žádné varianty. U šesti pacientů byly přítomny varianty v promotorech více než jednoho genu, vícečetné varianty v promotoru stejného genu byly nalezeny u 16 pacientů.

#### Varianty promotoru genu *KCNQ1*

V promotoru genu *KCNQ1* byly nalezeny varianty c. 1-182C>T u 15 pacientů a c. 1-119G>A u tří pacientů. Ve všech třech případech segregoval polymorfismus c. 1-119G>A společně s c. 1-182C>T. Data o těchto variantách byla k dispozici z 1000 Genomes Project.

#### Varianty promotoru genu *KCNE1*

Varianta c. 1-107insG byla nalezena v promotoru genu *KCNE1* u tří pacientů. Data o této variantě nebyla k dispozici z 1000 Genomes Project a její alelická frekvence byla testována ve skupině kontrol s ICHS.

#### Varianty promotoru genu *SCN5A*

V promotoru genu *SCN5A* bylo nalezeno šest variant u 22 pacientů. Více než jedna varianta promotoru genu *SCN5A* byla přítomna u 13 pacientů. Z nalezených variant byly v rámci 1000 Genomes Project popsány následující: c. -225-2038G>T, c. -225-1823C>T, c. -225-834T>C, c. -225-1744G>C, c. -225-1072T>C. Data o variantě c. -225-775T>A nebyla k dispozici z 1000 Genomes Project a její alelická frekvence byla testována ve skupině kontrol s ICHS.

### Statistické výsledky

Alelické frekvence všech promotorových variant u pacientů přeživších FK a u kontrolních skupin shrnuje tabulka 2. Statisticky signifikantní rozdíly byly nalezeny u obou variant v promotoru genu *KCNQ1*: c. 1-182C>T (OR = 2,57,

Tabulka 1 – Klinická charakteristika vyšetřovaných jedinců

	Pacienti přeživší FK (n = 45)	Kontroly s ICHS (n = 141)	p
Muži/ženy	40/5	129/12	0,8181
Věk	68,6 ± 9,5	66,7 ± 10,7	0,2885
Ejekční frakce levé komory	40 ± 12 %	42 ± 9 %	0,35238
Anamnéza infarktu myokardu	32 (71 %)	127 (90 %)	0,2718

FK – fibrilace komor; ICHS – ischemická choroba srdeční.

CI = 1,18–5,57 pro C alelu u pacientů přeživších FK ve srovnání s kontrolami s ICHS,  $p = 0,008$ ) a c. 1-119G>A (OR = 7,76, 95% CI = 1,06–56,77 pro G alelu u pacientů přeživších FK ve srovnání s kontrolní skupinou,  $p = 0,007$ ). Alelická frekvence variant c. 225-1072T>C promotoru genu *SCN5A* se signifikantně lišila u pacientů přeživších FK ve srovnání s daty z 1000 Genomes Project (OR = 7,28, 95% CI = 1,00–53,28 pro T alelu u pacientů přeživších FK ve srovnání s kontrolní skupinou,  $p = 0,001$ ), mezi pacienty přeživšími FK a kontrolami s ICHS však nebyl zjištěn signifikantní rozdíl.

## Diskuse

V předkládané studii jsme provedli mutační analýzu promotorů pěti genů pro srdeční iontové kanály u pacientů s ICHS, kteří přežili FK. Cílem bylo testovat hypotézu, že polymorfismy v těchto oblastech jsou častější u jedinců přeživších FK než v kontrolních populacích. Šlo o rozšíření naší předchozí studie, ve které jsme zjistili, že frekvence výskytu vzácných kódujících variant těchto genů byla signifikantně vyšší u pacientů přeživších FK (8/45, 17,8 %) než u kontrol s ICHS (3/141, 2,2 %,  $p = 0,001$ ). V promotorových oblastech stejných genů jsme našli devět různých variant DNA sekvence. Alelické frekvence tří z těchto variant se signifikantně lišily oproti datům z 1000 Genomes Project, který byl použit jako primární kontrolní soubor pro jeho statistickou sílu umožňující detekovat většinu genetických variant s frekvencí nejméně 1 %. Hlavním cílem 1000 Genomes Project je identifikace více než 95 % jednonukleotidových polymorfismů s 1% frekvencí v širokém souboru populací a do dnešního dne zahrnuje data o genetických variacích v 1 092 lidských ge-

nomech ze 14 populací z Evropy, východní Asie, subsaharské Afriky a obou Amerik [7].

Data o prevalenci polymorfismů promotorů genů pro iontové kanály u arytmiických pacientů jsou velmi omezená [9]. Varianty, které jsme našli v promotoru genu *KCNQ1*, byly popsány i v rámci 1000 Genomes Project a výskyt obou polymorfismů nalezených v promotoru tohoto genu se signifikantně lišil u pacientů přeživších FK ve srovnání s 1000 Genomes Project. Informace o možném funkčním vlivu těchto polymorfismů chybí: v naší předchozí práci jsme tyto konkrétní varianty našli i u pacientů s klinickou diagnózou LQTS, kdy však v žádné z rodin neseletovaly s LQTS fenotypem [10]. Z toho vyplývá, že jejich možný funkční efekt je málo pravděpodobný.

Varianta námi nalezená v promotoru genu *KCNE1* dosud nebyla v literatuře popsána [11] a její alelická frekvence se nelišila v souborech pacientů přeživších FK a ICHS pacientů bez maligních arytmií.

Promotor genu *SCN5A* je velmi polymorfní, čemuž odpovídá i fakt, že v naší studii bylo v tomto promotoru identifikováno šest různých polymorfismů. S výjimkou c. -225-1072T>C byly všechny další varianty předmětem studie Yanga a spol. [8], kteří zjistili, že pouze varianta c. -225-775 T>A signifikantně snižovala promotorovou aktivitu v srdečních myocytech. Taková varianta může modulovat fyziologické chování sodíkového kanálu v zátěžové situaci, kterou může být například právě ischemie myokardu. Nicméně alelické frekvence této varianty se nelišily v souborech pacientů přeživších FK a kontrol s ICHS, což naznačuje, že možnost jejího významného funkčního efektu je limitována.

Pro variantu c. -225-1072T>C nejsou k dispozici žádná funkční data. Zatímco alelické frekvence této varianty se významně lišily u pacientů přeživších FK ve srovnání s daty

Tabulka 2 – Alelické frekvence variant promotorů

Gen	Varianta	Pacienti přeživší FK (n = 45)	1000 Genomes Project	ICHS kontroly (n = 141)	p
<i>KCNQ1</i>	c. 1-182C>T	C = 0,823 T = 0,177	C = 0,643 T = 0,357	–	0,008
	c. 1-119G>A	G = 0,967 A = 0,033	G = 0,850 A = 0,150	–	0,007
<i>SCN5A</i>	c. -225-2038G>T	G = 0,86 T = 0,14	G = 0,864 T = 0,136	–	NS
	c. -225-1823C>T	C = 0,87 T = 0,13	C = 0,859 T = 0,141	–	NS
	c. -225-1744G>C	G = 0,97 C = 0,03	G = 0,993 C = 0,007	–	NS
	c. -225-1072T>C	C = 0 T = 1	C = 0,142* T = 0,86	C = 0,003+ T = 0,997	*0,001 +NS
	c. -225-834T>C	T = 0,87 C = 0,13	T = 0,883 C = 0,117	–	NS
	c. -225-775T>A	T = 0,98 A = 0,02	–	T = 1 A = 0	NS
<i>KCNE1</i>	c. 1-107insG	Alela – = 0,956 insG = 0,044	–	Alela – = 0,933 insG = 0,067	NS

FK – fibrilace komor; ICHS – ischemická choroba srdeční; \* – pacienti přeživší FK ve srovnání s 1000 Genomes Project; + – pacienti přeživší FK ve srovnání s ICHS kontrolami; NS – není signifikantní.

z 1000 Genomes Project, rozdíl nebyl významný při srovnání se souborem lokálních kontrol s ICHS. Tyto výsledky naznačují, že tato varianta může být regionálně specifická a pravděpodobně nepředstavuje funkční polymorfismus.

### Limitace

Naše studie má několik limitací, z nichž nejdůležitější je malý počet vyšetřených jedinců. Důvodem je incidence NSS a kapacita individuálních center provádějících rutinní genetické metody. Větší soubor by mohl vzniknout jen v rámci multicentrické studie. Vzhledem k malému počtu žen nebylo možné hodnotit žádné pohlavně podmíněné asociace. Alelické frekvence variant nalezených u pacientů přeživších FK byly srovnávány s daty z 1000 Genomes Project, tedy s nespécifickou populací. V případě *KCNQ1* variant byly chybějící funkční studie nahrazeny analýzou korelací genotypu s fenotypem u LQTS subjektů.

### Závěr

I když varianty promotorů genů pro iontové kanály jsou časté jak u pacientů přeživších FK, tak v kontrolních skupinách, naše výsledky naznačují, že varianty promotorů nejsou běžnou příčinou NSS.

*Výzkum byl podpořen granty NSI10429-3 a NT13767 Interní grantové agentury Ministerstva zdravotnictví České republiky a projektem specifického výzkumu Masarykovy univerzity SVMUNIIA/0811/2011.*

### Literatura

- [1] Y. Friedlander, D.S. Siscovick, S. Weinmann, et al., Family history as a risk factor for primary cardiac arrest, *Circulation* 97 (1998) 155–160.
- [2] X. Jouvan, M. Desnos, C. Guerot, P. Ducimetière, Predicting sudden death in the population: the Paris Prospective Study I, *Circulation* 99 (1999) 1978–1983.
- [3] K.S. Kaikkonen, M.L. Kortelainen, E. Linna, H.V. Huikuri, Family history and the risk of sudden cardiac death as a manifestation of an acute coronary event, *Circulation* 114 (2006) 1462–1467.
- [4] L.R. Dekker, C.R. Bezzina, J.P. Henriques, et al., Familial sudden death is an important risk factor for primary ventricular fibrillation: a case-control study in acute myocardial infarction patients, *Circulation* 114 (2006) 1140–1145.
- [5] T. Novotny, J. Kadlecova, M. Raudenska, et al., Mutation analysis of ion channel genes in ventricular fibrillation survivors with coronary artery disease, *Pacing and Clinical Electrophysiology* 34 (2011) 742–749.
- [6] E.S. Lander, Initial impact of the sequencing of the human genome, *Nature* 470 (2011) 187–197.
- [7] The 1000 Genomes Consortium. An integrated map of genetic variation from 1092 human genomes, *Nature* 491 (2012) 56–65.
- [8] P. Yang, T.T. Koopmann, A. Pfeufer, et al., Polymorphisms in the cardiac sodium channel promoter displaying, *European Journal of Human Genetics* 16 (2008) 350–357.
- [9] X. Luo, J. Xiao, H. Lin, et al., Genomic structure, transcriptional control, and tissue distribution of *HERG1* and *KCNQ1* genes, *American Journal of Physiology. Heart and Circulatory Physiology* 294 (2008) H1371–H1380.
- [10] T. Novotny, J. Kadlecova, M. Raudenska, et al., Mutation analysis of ion channel genes promoters in patients with malignant arrhythmias – pilot study, *Journal of Cardiovascular Electrophysiology* 22 (Suppl 1) (2011) S9.
- [11] Z. Mustapha, L. Pang, S. Nattel, Characterization of the cardiac *KCNE1* gene promoter, *Cardiovascular Research* 73 (2007) 82–91.

*Z anglického originálu přeložil autor.*

Není tedy pochyb o tom, že v patofyziologii NSS hrají hereditární faktory významnou roli.<sup>28,35</sup> Ovšem nejčastějším patologickým substrátem NSS v běžné populaci je ICHS. Je tedy třeba brát v úvahu její celou širokou etiopatogenezi. V této souvislosti se genetická variabilita rizika náhlé smrti může uplatňovat nejen v procesech tvorby a propagace elektrického impulsu, ale také v centrálním i místním řízení excitability myokardu a v neposlední řadě v procesech a faktorech tvorby a stability aterosklerotického plátu, trombózy a ischémie v koronárním řečišti. Musíme si tedy klást otázku, zda je riziko u běžných chorob výsledkem spolupůsobení celé řady běžných variant DNA (hypotéza „*common disease – common variant*“) nebo naopak menšího počtu vzácných variant DNA („*common disease – rare variant*“). Vzhledem k tomu, že tzv. kódující sekvence, tedy geny, tvoří necelé 2 % lidského genomu, bude potřeba hledat odpovědi i ve zbylých oblastech tzv. nekódujících sekvencích, které zjevně tvoří důležité regulační části DNA. Funkce těchto částí DNA není v současné době objasněna, což lze demonstrovat na výsledcích celogenomových asociačních studií (*genome-wide association studies – GWAS*). V dosud největší studii zabývající se genomikou NSS<sup>36</sup> se autoři pokusili replikovat výsledky předchozích GWAS, avšak nové studie (NSS versus zdraví jedinci) nepotvrdily souvislost rizika NSS s 26 dříve popsanými běžnými jednonukleotidovými polymorfizmy (*single nucleotide polymorphism – SNP*) a ani s běžnými variantami v 54 genech se známou asociací s arytmiemi. Navzdory obrovskému pokroku v poznání lidského genomu tedy zatím chybí dostatečně účinné nástroje k rozpoznání možných minimálních účinků jednotlivých variant, které až v komplexním působení vedou ke změně míry rizika.

Odhalení univerzálních genetických variant a jejich využití v rámci stratifikace NSS je tedy mimo současné možnosti. To potvrdil i Schwartz v editoriale v *European Heart Journal* k výše uvedené GWAS práci, kdy napsal: „Hledání svatého grálu pokračuje.“<sup>37</sup>

Je proto potřeba zkoumat jiné metody, které usnadní identifikaci rizikových pacientů. Právě těmto metodám je věnována následující část.

### 3. Návrat k elektrokardiogramu a elektrofyziologii repolarizace myokardu

Elektrokardiografické vyšetření je metoda používaná v kardiologii již přes 100 let. Nedávné pokroky v digitální elektrokardiografii umožnily zaznamenávání dlouhodobých elektrokardiogramů (EKG) a jejich měření s vysokou přesností. Přesto stále nejsme schopni plně využít potenciál této neinvazivní a provozně nenáročné metody při vyhledávání rizikových pacientů. Abychom mohli identifikovat patologii, musíme znát fyziologické chování a limity. Vztahy mezi různými charakteristikami EKG záznamu jsou převážně neznámé a dosud není zřejmé, zda různé charakteristiky odrážejí rozdílné fyziologické procesy nebo zda se vztahují k různým aspektům stejného fyziologického základu. K vysvětlení těchto nejasností se snažily přispět naše cílené fyziologické studie nejrůznějších elektrokardiografických charakteristik za různých podmínek.

Vzhledem ke známému vztahu srdeční repolarizace k arytmogenezi<sup>38</sup> zkoumala řada našich studií fyziologické vlastnosti repolarizace myokardu.

#### 3.1. Analýza chování QT intervalu

Důkazy o vztahu trvání mechanické systoly k srdeční frekvenci se datují do doby ještě před érou EKG. Autoři používali k zaznamenání srdeční systoly sfygmografický záznam z radiální tepny a mechanický apexogram.<sup>39</sup> I když z počátku existovaly domněnky, že délka trvání systoly je neměnná a nezávislá na srdeční frekvenci,<sup>40</sup> opak se ukázal být pravdou. Už roku 1870 Garrod publikoval pozorování, že trvání systoly se mění s třetí odmocninou délky srdečního cyklu.<sup>41</sup> S užitím mechanického kardiografu pak týž autor popsal tento vztah pomocí druhé odmocniny.<sup>42</sup> S rozvojem EKG přístroje se dostalo do popředí mimo jiné i zkoumání vztahu mechanické srdeční systoly a QT intervalu. Ačkoliv Garrod předpovídal, že přesný vztah mechanické a elektrofyziologické systoly ke změnám srdeční frekvence (SF) bude objasněn před rokem 1900, tento vztah je předmětem debat a studií dosud.

#### 3.2. Vztah QT a RR intervalu – nepřesnosti korekčních vzorců

Obecně je dobře známo, že QT interval se postupně zkracuje v závislosti na zvyšující se SF. V zásadě je úkolem korekčních vzorců eliminovat vliv SF. Díky přepočtu naměřeného (nekorigovaného) intervalu QT k aktuální SF (obvykle vyjádřené odpovídajícím intervalem RR) na hodnotu korigovaného intervalu QTc pak můžeme porovnat jednotlivá měření QT intervalu při různých SF. Podstata korekce je jednoduchá a odpovídá například filozofii korekce naměřeného atmosférického tlaku pro danou nadmořskou výšku. Výsledkem převodu atmosférického tlaku pro jednotlivé nadmořské výšky je hodnota, která by (teoreticky) byla naměřena u hladiny moře. Naprosto stejným způsobem fungují i korekční vzorce QT intervalu pro danou SF. Cílem je tedy získat hodnotu QT intervalu, která by byla měřena, kdyby SF byla

60/min. Hodnota 60/min není zcela fyziologicky optimální, ale vychází z původních prací, které tuto hodnotu používaly, neboť odpovídá srdečnímu cyklu jedné sekundy (což zjednodušuje matematické vzorce původně navržených korekcí).

K popisu tohoto vztahu bylo vytvořeno mnoho korekčních vzorců. V roce 1920 popsal Bazett prakticky stejnou závislost QT intervalu na SF, kterou několik let předtím navrhnul Garrod při zkoumání změn mechanické srdeční systoly (tedy lineární závislost na druhé odmocnině délky srdečního cyklu).<sup>43</sup> Ve stejném roce publikoval svou práci Fridericia, který se v popisu vztahu QT/RR shodoval opět s prvotním Garrodovým návrhem a odvodil třetí odmocninu délky srdečního cyklu.<sup>44</sup> V průběhu dalších let se objevilo několik desítek korekčních vzorců QT intervalu vzhledem k SF.<sup>45</sup> Ačkoli některé z nich v klinické praxi „zlidověly“, žádný z nich však při podrobnějším zkoumání neprokázal možnost univerzálního použití převážně v situacích, kdy je potřeba získat poměrně přesné hodnoty (např. ve farmaceutických studiích zkoumajících vliv léku na QT interval, či u jedinců s hraničními hodnotami QTc intervalu).<sup>46,47,48,49,50,51,52,53</sup> Bylo opakovaně dokázáno, že nemalý vliv na (ne)přesnost těchto korekčních vzorců mají i extrakardiální příčiny, převážně regulace autonomního nervového systému,<sup>54,55,56</sup> jehož změny vedou k nestabilitě SF. Při pátrání po dalších důvodech nepřesnosti jednotlivých „univerzálních“ korekčních vzorců byla pozornost věnována zkoumání individuálního QT/RR vztahu. Následně byla potvrzena výrazná interindividuální variabilita QT/RR při jasné i několik měsíců trvající intraindividuální stabilitě.<sup>57,58</sup> Jinými slovy: každý jedinec má v sobě „zakódovanou“ svoji závislost QT intervalu na SF. Tuto charakteristiku lze zjistit analýzou dlouhodobých EKG záznamů s dostatečným rozsahem SF.<sup>58</sup>

Bylo kupříkladu ukázáno, že u jednotlivců se při hodnotách ustálené SF 60 a 100/min může QT interval lišit v různém rozmezí, třeba o méně než 30 ms u jednoho jedince a naopak i o více než 50 ms u jiného jedince.<sup>59</sup> V zásadě tedy nemůže existovat jednoduchý univerzální vzorec, který by byl použitelný pro všechny jedince. Pouze v případě, kdy odchylky SF od „standardu“ 60/min jsou poměrně malé (např. mezi 55 a 70/min), mohou být chyby některých korekčních vzorců pro klinickou praxi považovány za přijatelné. Toto však neplatí v případě nutnosti přesnějšího měření, jako při hodnocení účinku nových léčiv na repolarizaci myokardu.

Následující práce se věnuje porovnání deseti nejčastěji užívaných korekčních vzorců s individuální korekcí QT (QTcI).



**Andršová I**, Hnatkova K, Šišáková M, Toman O, Smetana P, Huster KM, Barthel P, Novotný T, Schmidt G, Malik M. Influence of heart rate correction formulas on QTc interval stability. Scientific Reports 2021; 11:14269. doi: 10.1038/s41598-021-93774-9.

IF 4,997. Počet citací ve Web of Science 20

Původní práce – kvantitativní podíl uchazečky 45%: Návrh struktury práce, elektrokardiologická měření, interpretace statistických výsledků, text publikace.



OPEN

# Influence of heart rate correction formulas on QTc interval stability

Irena Andršová<sup>1</sup>, Katerina Hnatkova<sup>2</sup>, Martina Šišáková<sup>1</sup>, Ondřej Toman<sup>1</sup>, Peter Smetana<sup>3</sup>, Katharina M. Huster<sup>4</sup>, Petra Barthel<sup>4</sup>, Tomáš Novotný<sup>1</sup>, Georg Schmidt<sup>4</sup> & Marek Malik<sup>2,5</sup>✉

Monitoring of QTc interval is mandated in different clinical conditions. Nevertheless, intra-subject variability of QTc intervals reduces the clinical utility of QTc monitoring strategies. Since this variability is partly related to QT heart rate correction, 10 different heart rate corrections (Bazett, Fridericia, Dmitrienko, Framingham, Schlamowitz, Hodges, Ashman, Rautaharju, Sarma, and Rabkin) were applied to 452,440 ECG measurements made in 539 healthy volunteers (259 females, mean age  $33.3 \pm 8.4$  years). For each correction formula, the short term (5-min time-points) and long-term (day-time hours) variability of rate corrected QT values (QTc) was investigated together with the comparisons of the QTc values with individually corrected QTcI values obtained by subject-specific modelling of the QT/RR relationship and hysteresis. The results showed that (a) both in terms of short-term and long-term QTc variability, Bazett correction led to QTc values that were more variable than the results of other corrections ( $p < 0.00001$  for all), (b) the QTc variability by Fridericia and Framingham corrections were not systematically different from each other but were lower than the results of other corrections ( $p$ -value between 0.033 and  $< 0.00001$ ), and (c) on average, Bazett QTc values departed from QTcI intervals more than the QTc values of other corrections. The study concludes that (a) previous suggestions that Bazett correction should no longer be used in clinical practice are fully justified, (b) replacing Bazett correction with Fridericia and/or Framingham corrections would improve clinical QTc monitoring, (c) heart rate stability is needed for valid QTc assessment, and (d) development of further QTc corrections for day-to-day use is not warranted.

Good clinical practice requires the assessment of heart rate corrected QTc interval in a variety of situations<sup>1</sup>. As well known, QTc assessment and/or monitoring is mandated when administering drugs recognised to affect myocardial repolarisation and to potentially induce torsade de pointes tachycardia<sup>2</sup>; when diagnosing the sources of syncopal and/or pre-syncopal episodes<sup>3</sup>; when considering the proarrhythmic consequences of treatment-induced electrolyte abnormalities<sup>4,5</sup>; when screening relatives of patients with recognised repolarisation channelopathy<sup>6</sup> or of unexplained sudden death victims<sup>7</sup>; and in a further spectrum of other circumstances and conditions. To support this practice, some healthcare providers stipulate corresponding guidelines. QTc prolongation assessment has also been the topic of proposed scoring systems<sup>8</sup>.

Reports have also been published evaluating the effectiveness of the suggested good clinical practice<sup>9–11</sup>. Regrettably, it has been reported that while the introduction of guidelines and monitoring schemes increases the awareness of the proarrhythmic potentials, therapeutic implications of prolonged QTc interval, such as therapy changes and/or more intensive monitoring, are not necessarily systematically implemented<sup>12,13</sup>.

Speculations of the reasons for these discrepancies between healthcare guidelines and day-to-day practice include, among others, the intra-subject variability of QTc intervals that does not allow monitoring QTc changes and/or detecting QTc abnormalities with sufficiently robust accuracy<sup>14</sup>. It is surely true that QTc interval changes may reflect not only treatment-related and channelopathy-based repolarisation abnormalities<sup>2</sup> but also electrolyte differences<sup>15</sup>, fever<sup>16</sup>, hormonal changes<sup>17</sup>, and alteration in autonomic and central nervous status<sup>18</sup>. Nevertheless, it is also apparent that imprecisions of QT interval measurement and inaccuracies of its heart rate correction may substantially contribute to an increased variability of measured QTc values<sup>19</sup>.

Electrocardiographic experience from clinical pharmacology studies suggests that intra-subject QTc variability is substantially reduced not only by systematic QT interval measurements but also, and largely, by using

<sup>1</sup>Department of Internal Medicine and Cardiology, Faculty of Medicine, University Hospital Brno, Masaryk University, Jihlavská 20, 625 00 Brno, Czech Republic. <sup>2</sup>National Heart and Lung Institute, Imperial College, ICTEM, Hammersmith Campus, 72 Du Cane Rd, Shepherd's Bush, London W12 0NN, England, UK. <sup>3</sup>Wilhelminenspital der Stadt Wien, Montleartstraße 37, 1160 Vienna, Austria. <sup>4</sup>Klinikum rechts der Isar, Technische Universität München, Ismaninger Straße 22, 81675 Munich, Germany. <sup>5</sup>Department of Internal Medicine and Cardiology, Faculty of Medicine, Masaryk University, Jihlavská 20, 625 00 Brno, Czech Republic. ✉email: marek.malik@imperial.ac.uk

subject-specific heart rate corrections<sup>20</sup>. These observations are of little help in clinical practice when baseline subject-specific QT/RR profiles are not and cannot be available. Nevertheless, scores of different heart rate corrections have previously been proposed<sup>21,22</sup>. Although it has repeatedly been shown that some of these corrections are superior to others at eliminating the heart rate dependency of QTc intervals<sup>22</sup>, the differences between corrections in terms of intra-subject QTc variability have not been systematically investigated.

With this in mind, we conducted a study that utilised data in healthy volunteers and investigated whether and how different heart rate corrections influence the intra-subject QTc variability and whether and how this variability might be reduced by recordings strategies and conditions.

## Methods

**Investigated population and long-term electrocardiographic recordings.** Clinical pharmacology studies conducted at 4 different locations enrolled 539 healthy volunteers (259 females) aged, on average,  $33.3 \pm 8.4$  years (no statistical age differences between females and males). Before study enrolment, all the volunteers had a normal standard electrocardiogram (ECG) and all had normal clinical investigation. Standard inclusion and exclusion criteria mandated for Phase I pharmacology studies<sup>23</sup> were used including negative tests for recreational substances and negative pregnancy tests for females. All the source studies were ethically approved by the institutional ethics bodies (Parexel in Baltimore; California Clinical Trials in Glendale; PPD in Austin; and Spaulding in Milwaukee). Consistent with Helsinki declaration, all subjects gave informed written consent to study participation and to research use of data collected during the studies. As only drug-free data were analysed in the present investigation and as there were no differences in clinical handling of study subjects at the investigation sites during the drug-free days, further details of the source clinical studies are of no relevance.

Demographic descriptors were available for all study subjects. Body mass index (BMI) was defined as body weight in kilograms divided by the squared body height in metres; lean body mass (LBM) was calculated as  $LBM = 0.29569 \times (\text{body weight}[\text{kg}]) + 41.813 \times (\text{body height}[\text{m}]) - 43.2933$  for females, and  $LBM = 0.3281 \times (\text{body weight}[\text{kg}]) + 33.929 \times (\text{body height}[\text{m}]) - 29.5336$  for males<sup>24</sup>.

In all volunteers, repeated long-term 12-lead Holter ECG recordings were obtained covering the full day-time periods. These recordings included ECG collected during days when the subjects were on no medication. The subjects were also not allowed to smoke and/or consume alcohol or caffeinated drinks. The principal analysis of the investigation reported here concerned only the first day of the source clinical pharmacology studies which made the data fully consistent across the clinical centres. The protocols of the source studies were also fully consistent with each other as far as handling of the volunteers during the drug-free baseline days was concerned. Among others, all the volunteers were fasting during the morning hours of the baseline days and their first meal of the day consisted of a standardised lunch, as mandated during the Phase I clinical studies. No high fat diet loading was used. During the day-time hours of the baseline days, the study subjects were also not permitted to sleep.

Using previously described technology<sup>25,26</sup>, multiple 10-s ECG segments were extracted from the long-term ECGs (see also further details in this text) and in each of these segments, QT interval was measured including repeated visual controls of all the measurements and assurance that corresponding ECG morphologies were interpreted in a consistent way<sup>27</sup>. The interval measurements were performed using representative median waveforms of the 10-s segments (sampled at 1000 Hz) with the superimposition of all 12 leads on the same isoelectric axis<sup>28,29</sup>. Exactly the same measurement organisation was applied to all source ECG data. This included, among others, the same algorithms for 10-s ECG segment extraction and for creation of the representative waveforms, the same system for initial QT measurement and consistency checks, and identical organisation of visual control and manual correction of the QT measurements.

Also using previously described techniques and procedures, individual curvatures of QT/RR patterns (i.e. how much the QT interval changes in response to underlying heart rate changes) including the individual profiles of QT/RR hysteresis (i.e. how quickly the QT interval changes following a heart rate change) were constructed for each study subject<sup>30,31</sup>. In more detail, multiple measurements of QT intervals with the preceding history of RR intervals were available in each subject. This allowed, in each subject separately, to construct a curvilinear regression  $QT_i = \chi + \phi \left(1 - \left(\widetilde{RR}_i\right)^\gamma\right) + \varepsilon_i$  where  $QT_i$  are individual QT interval measurements in seconds,  $\widetilde{RR}_i$  are RR interval durations (in seconds) representing the hysteresis corrected<sup>31</sup> heart rate underlying the  $QT_i$  measurement,  $\chi$  and  $\phi$  are intercept and slope of linear regression,  $\varepsilon_i$  are normally distributed zero centred errors, and the parameter  $\gamma$  is individually optimised so that it leads to the lowest regression residual. These were converted into individual heart rate correction of the measured QT intervals,  $QTc_i = QT + \phi \left(1 - \widetilde{RR}^\gamma\right)$ . Individually corrected QTcI values for each of the measured ECG segments were obtained in this way. In further investigation, the QTcI values were used as the “gold standard” control data for the comparison of different heart rate correction formulas.

**Heart rate correction formulas.** To investigate the influence of different generic heart rate corrections on the character and variability of QTc data, 10 previously proposed correction formulas were considered. In order to model standard clinical situations, the average of all RR intervals found in the measured 10-s ECG sample (or the corresponding heart rate) was used in all the corrections. The following corrections were used:

- Bazett (BAZ)<sup>32</sup>  $QTc = QT/RR^{1/2}$
- Fridericia (FRI)<sup>33</sup>  $QTc = QT/RR^{1/3}$
- Dmitrienko (DMI)<sup>34</sup>  $QTc = QT/RR^{0.413}$
- Framingham (FRA)<sup>35</sup>  $QTc = QT + 0.154 \times (1 - RR)$
- Schlamowitz (SCH)<sup>36</sup>  $QTc = QT + 0.205 \times (1 - RR)$

- Hodges (HOD)<sup>37</sup>  $QT_c = QT + 0.00175 \times (HR - 60)$
- Ashman (ASH)<sup>38</sup>  $QT_c = QT / \log_{10}(10 \times (RR + 0.07)) \times \log_{10}(10.7)$
- Rautaharju (RAU)<sup>39</sup>  $QT_c = QT + 0.24251 - 0.434 \times e^{-0.0097 \times HR}$
- Sarma (SAR)<sup>40</sup>  $QT_c = QT - 0.04462 + 0.664 \times e^{-2.7 \times RR}$
- Rabkin (RAB)<sup>41</sup>  $QT_c = [\widehat{QT}(60, 0, 50.3) + 1000 \times QT - \widehat{QT}(HR, sex, age)] / 1000$

In these formulas, QT and averaged RR intervals are measured in seconds, HR is the heart rate in beats per minute (bpm) corresponding to the measured averaged RR interval, *sex* is the numerical sex indicator of the sex of the subject, and *age* is the age of the subject in years. In the formula by Rabkin et al.<sup>41</sup>,  $\widehat{QT}$  is a published spline function<sup>42</sup> dependent on the HR value with additional sex and age components. Specifically, the formula by Rabkin et al. denotes  $\widehat{QT}(HR, sex, age) = \vartheta_0 - \sum_{i=1}^7 \vartheta_i \mathcal{B}_i(HR) + 9.35 \times sex + 0.18 \times age$  (in milliseconds), where  $\mathcal{B}_i$  are composed of polynomial fractions that depend only on heart rate,  $\vartheta_i$  are numerical coefficients, *age* is the age of the subject in years, and *sex* is an indicator 1 and 0 for females and males, respectively<sup>42</sup>. Contrary to other formulas that aim at correcting the QT intervals to the heart rate of 60 bpm (and thus, at the heart rate of 60 bpm, lead to  $QT_c = QT$ ) the formula by Rabkin et al. normalizes the measured QT intervals to a distribution in a 50.3-year male at 60 bpm (derived from the data analysed by Rabkin et al.<sup>41,42</sup>). Intentionally, this formula aims at eliminating the difference between females and males by reporting the  $QT_c$  values in females reduced by 9.35 ms and also aims at eliminating  $QT_c$  prolongation with advanced age.

The measured QT and RR intervals as well as the  $QT_c$  intervals provided by the formulas that we listed are expressed in seconds. Note that some of the original publications showed the formulas for QT and  $QT_c$  in milliseconds rather than in seconds, this is also the reason why we used the 1000 coefficient in the Rabkin et al. formula implementation since the spline function  $\widehat{QT}$  provides  $QT_c$  estimates in milliseconds—in the implementation of other formulas, the coefficients shown above have been adopted for the millisecond-second conversion where necessary.

We selected these formulas from the large spectrum of previously made proposals to investigate different mathematical forms as well as to include both older and more recent suggestions.

In the comparisons of the correction possibilities, we applied all these formulas as well as the individual-specific  $QT_c$  formula to the same set of the ECGs. That is, for each measured 10-s ECG segment, we obtained altogether 11  $QT_c$  values. Note also that while the generic formulas (BAZ through RAB) used averages of RR intervals in 10-s ECG recordings, the  $QT_c$  formula used hysteresis corrected RR intervals. We used this approach to increase the accuracy of  $QT_c$  values.

**Electrocardiographic data.** *Time-points.* The protocol of all source studies included 27 time-points during which the subjects were kept motionless in undisturbed stable positions without any external interference. Each of the time-points lasted for 10 min and during the last 5 min, QT interval measurements were made in 5 different 10-s ECG segments that were separated by at least 20 s of each other. As described subsequently,  $QT_c$  variability and accuracy was investigated among these QT (and corresponding RR) interval measurements.

*Exclusion of post-prandial changes.* Since meal intake is known to influence QT (and  $QT_c$ ) interval duration<sup>43,44</sup>, separate  $QT_c$  analysis was performed using only segments of study time-points that occurred during the morning hours while the subjects were fasting.

*Stable time-points.* The QT/RR hysteresis is a known problem affecting the  $QT_c$  assessment if the simultaneous RR interval measurement does not correspond to the underlying heart rate that influences the QT interval duration<sup>31,45</sup>. While keeping the study subjects in undisturbed stable positions eliminates all physical activity that might cause heart rate changes, other heart rate variations (e.g. due to mental processes) cannot be removed<sup>46</sup>. Heart rate variations might therefore occur even during the stable undisturbed positions. During such episodes, substantial QT/RR hysteresis problems might occur (example in Fig. 1).

Separate analyses of  $QT_c$  variability and accuracy were therefore conducted considering only data from time-point windows during which the heart rate span (defined as the difference between the fastest and slowest heart rate of the measured 10-s ECG segments) was below 5 bpm. The same restriction was also additionally applied to fasting time-points.

*Additional ECG measurements.* In addition to the 10-s ECG segments extracted from the per-protocol study time-points, further extractions of additional 10-s segments (all preceded by stable heart rates) were made with the aim of covering different stable heart rates encountered during each recording. As described further, these additional QT and RR measurements were combined with the extractions from all time-points and used in the analysis of whether the heart rate correction formulas eliminated the influence of heart rate on the  $QT_c$  intervals.

**Data investigations.** *Population characteristics.* Since the variability and accuracy of  $QT_c$  values by different formulas is likely influenced by the ECG-related characteristics of the investigated population, we have investigated these properties independently of any of the generic correction formulas.

In each subject, the mean  $QT_c$  interval and the standard deviation (SD) of the  $QT_c$  intervals measured in all the measured 10-s ECG segments as described in the previous section, and the slope of the log-linear QT/RR relationship (for hysteresis corrected RR intervals) were related to age, BMI, and LBM. (Note that the log-linear

**Figure 1.** Example of three 10-s ECGs recorded in a 30-year old male in a short succession while the subject was kept in a strict motionless position. On the baseline drug-free day, the recordings A, B, and C were recorded at 13:34:38, 13:34:58, and 13:35:28, respectively. Their 10-s heart rates were 52.7, 52.6, and 85.9 bpm, and their uncorrected QT intervals were 405, 405, and 395 ms, respectively. When individual QT/RR hysteresis profile was incorporated into the assessment, the heart rates underlying the QT interval duration were 53.6, 53.4, 58.3 bpm which led to individually corrected QTcI intervals of 391.0, 390.7, and 391.5 ms, respectively. However, when the 10-s heart rates were used to correct the QT intervals, Bazett correction led to QTc values of 379.4, 379.2, and 472.7 ms, respectively (92 ms QTc increase). Fridericia correction led to QTc values of 387.7, 387.6, 445.2 ms, respectively (58 ms QTc increase). These QTc increases were erroneous since they resulted from the disassociation of the QT interval duration from the underlying heart rate. Similar erroneous QTc increases were found with all the investigated correction formulas (QTc increase of 74, 58, 81, 48, 74, 62, 60, and 61 ms for the Dmitrienko, Framingham, Schlamowitz, Hodges, Ashman, Rautaharju, Sarma, and Rabkin corrections, respectively).

model of the QT/RR relationship is not an individually optimal expression of the QT/RR relationship<sup>47</sup> but we used it since it corresponds to the mathematics of the first 3 of the evaluated formulas.)

**Short-term QTc variability.** Short-term variability of the QTc values reported by the different formulas was investigated in the windows of individual time-points of the original studies. That is, each separate time-point defined a 5-min window during which five repeated QT and 10-s heart rate measurements were made. From these data, SD of the QTc values were obtained and related to the range of the measured heart rates, i.e. to the difference between the fastest and the slowest of the five 10-s heart rate measurements. The intra-subject dependencies of the SD of the QTc values on the heart rate ranges were compared between different correction formulas.

**Day-time QTc variability.** In each subject, SD of all QTc values were compared between the correction formulas when considering ECG measurements in (a) all ECG extractions from the Holter recordings (i.e. including those that were made outside the per-protocol study time-points), (b) all ECG extractions from per-protocol study time-points, (c) ECG extractions from per-protocol study time-points while the subjects were fasting during the morning of the baseline day, (d) all ECG extractions from study time-points that showed heart rate range below 5 bpm, and (e) ECG extractions from fasting study time-points that showed heart rate range below 5 bpm.

**Difference between general and individual QTc corrections.** By definitions, the individual corrections create QTcI values that are, over the entire recording of the given subject, independent of the underlying heart rates. To investigate how much the generic correction formulas differed from this ideal situation, the slopes of linear regressions between the QTc values by the different corrections and the corresponding 10-s RR intervals were calculated in each subject. For this purpose, all ECG extractions from the Holter recordings were used. While in some previous studies, the slopes and correlations between QTc values and the RR intervals of the underlying heart rates were investigated over complete population of different subjects or patients<sup>48</sup>, we have evaluated the linear QTc/RR regressions in each subject separately. This was because the optimisation of a correction formula over a population of different subjects may (and frequently does) lead to corrections that are systematically biased in all or a majority of subjects of the population if applied to each of them separately<sup>49,50</sup>.

The differences between QTc values by the different corrections and the corresponding QTcI intervals were evaluated, in each subject, considering the (a) ECG extractions from all per-protocol study time-points, (b) ECG extractions from fasting per-protocol study time-points, (c) ECG extractions from study time-points with heart rate range below 5 bpm, and (d) ECG extractions from fasting study time-points with heart rate range below 5 bpm.

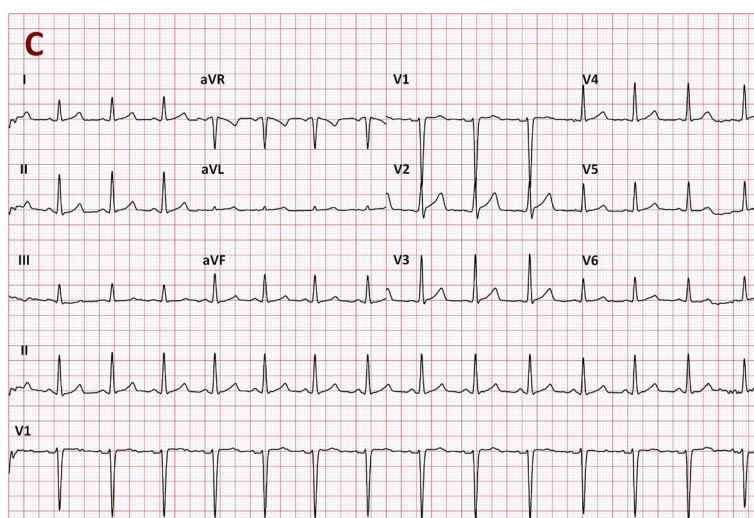
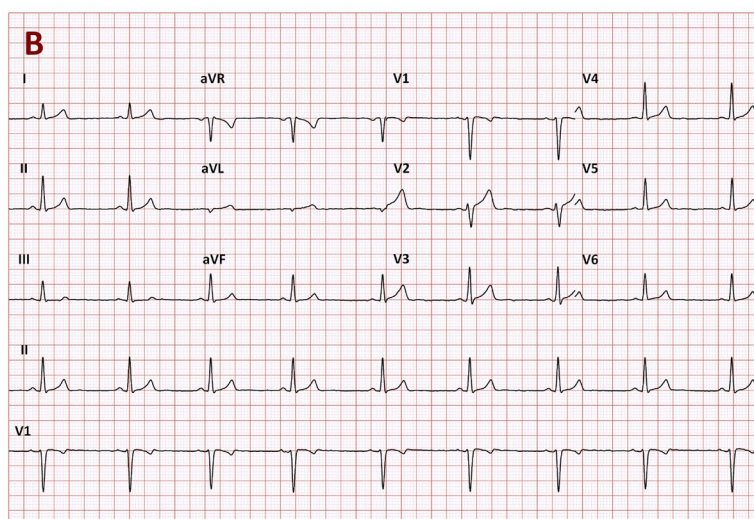
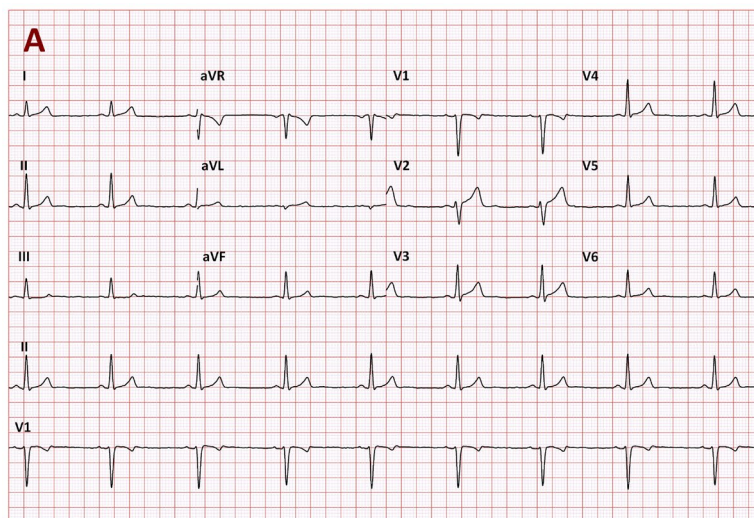
**Statistics and data presentation.** Descriptive data are presented as means  $\pm$  SD. The QTc variability and QTc—QTcI differences are presented as population medians, inter-quartile ranges, and 90 percent ranges, that is the intervals between the 5th and 95th population percentile. Where appropriate, linear regressions were calculated together with the 95% bands of the regression lines. Comparisons between female and male subjects were based on two-sample two-tail t-tests assuming different variances of the compared samples. Within subject comparisons were based on paired two-sample t-tests. *P* value below 0.05 was considered statistically significant. Because of the inter-dependence of the data, no adjustment for multiplicity of testing was performed.

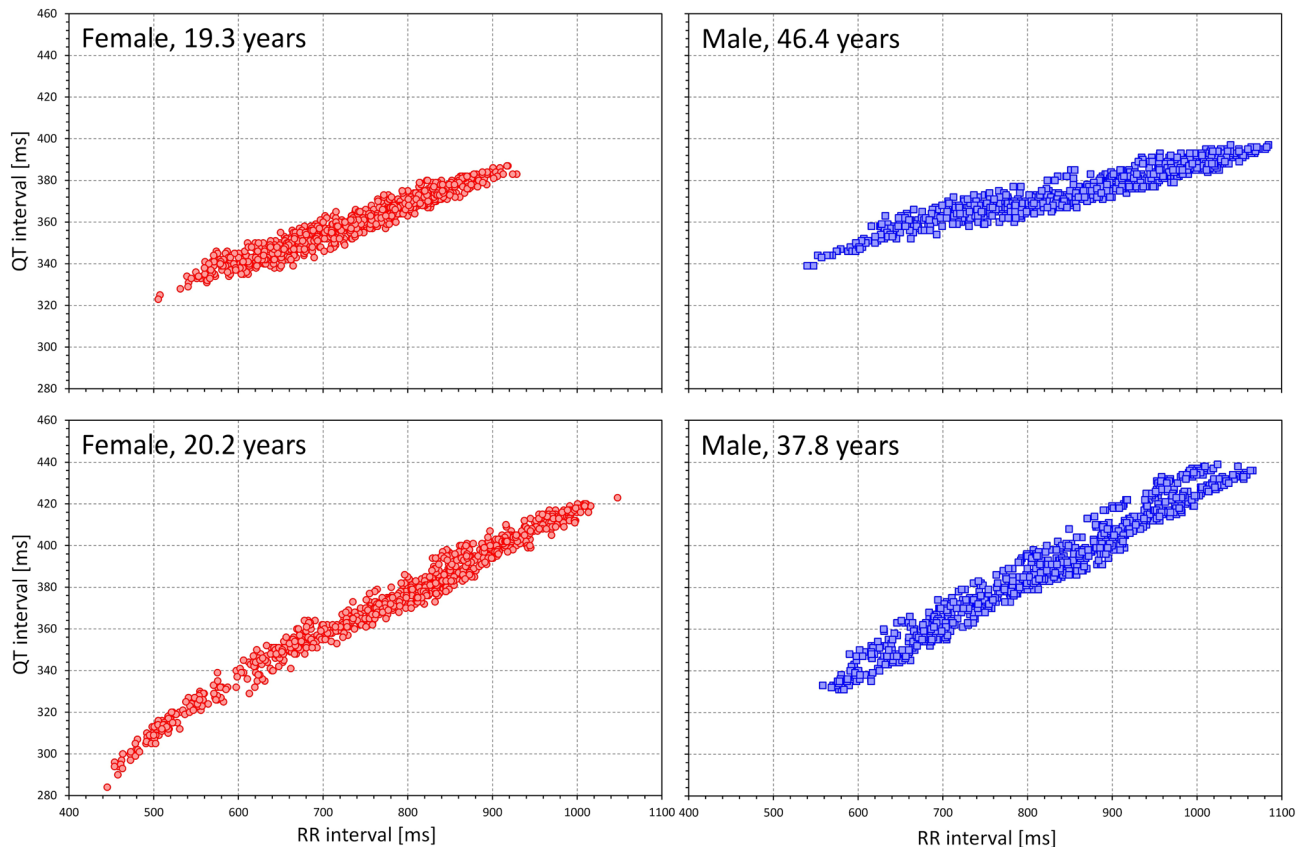
## Results

The data of the 539 healthy volunteers involved altogether 452,440 measurements of individual 10-s ECG samples.

**Population QTcI characteristics.** As expected<sup>51</sup>, the individual QT/RR patterns differed substantially between study subjects (examples in Fig. 2). To characterise them we have considered intra-subject QTcI averages over (a) all time-points, (b) stable time-points, and (c) fasting time-points.

Also as expected, intra-subject averages of QTcI durations were longer in females compared to males<sup>52</sup>. When considering the data of all study time-points, the averaged QTcI values in females and males were  $419.6 \pm 13.3$  and  $399.6 \pm 12.5$  ms, respectively ( $p < 0.00001$  for the comparison between sexes). The averaged intra-subject QTcI values of stable time-points (averages in females and males of  $419.6 \pm 13.3$  and  $399.6 \pm 12.6$ , respectively) were not statistically different from the intra-subject averages of all time-points. Nevertheless, considering only fasting





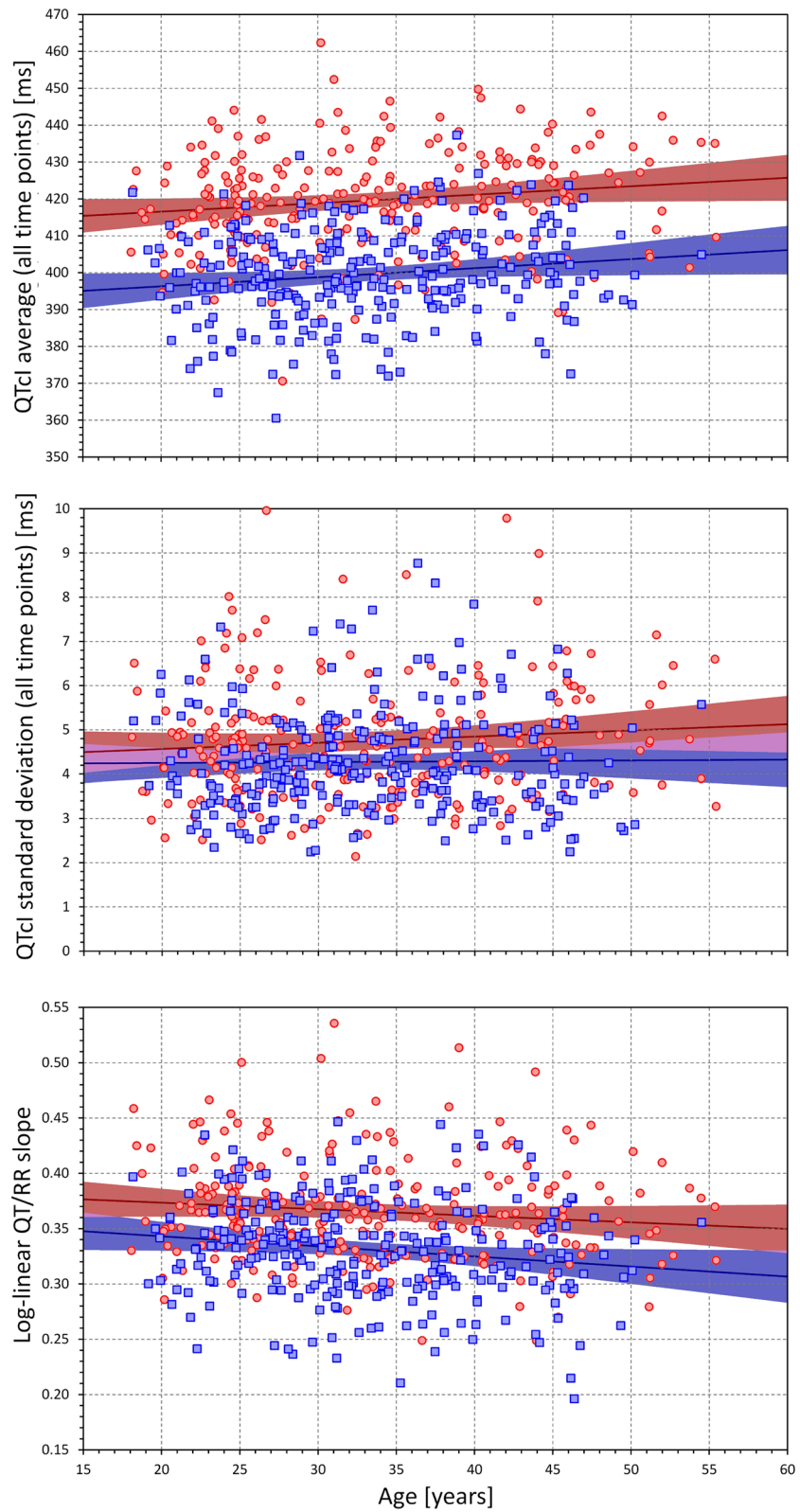
**Figure 2.** Examples of repeated intra-subject drug-free QT measurements related to the underlying (hysteresis corrected) RR intervals. The examples in females and males are shown with red and blue symbols, respectively, ages of the subjects are shown in the individual panels. Note the substantial differences of the slopes of the patterns.

time-points, the intra-subject QTcI averages (averages in females and males of  $421.5 \pm 13.5$  and  $400.9 \pm 12.7$  ms, respectively) were marginally but statistically significantly prolonged compared to the intra-subject averages of all time-points ( $p < 0.00001$  for pair-wise comparisons in both sexes). This was consistent with previous reports of post-prandial QTc shortening<sup>43,44</sup>. The intra-subject SD of QTcI values taken from all the time-points was also larger in females compared to males ( $4.75 \pm 1.36$  vs.  $4.27 \pm 1.16$ ,  $p < 0.00001$ ). In both sexes, these SD values were reduced by eliminating the post-prandial effects, and the statistical sex difference was reduced although it remained statistically significant ( $3.30 \pm 1.40$  vs.  $3.05 \pm 1.35$  ms,  $p = 0.035$ ). The full profile QT/RR patterns were also steeper in females compared to males<sup>30,52,53</sup>, with log-linear slopes of  $0.366 \pm 0.047$  vs.  $0.331 \pm 0.045$ ,  $p < 0.00001$ .

Figures 3, 4 and 5 show the relationship between the individual QT/RR characteristics derived from ECG measurements in all study time-points and age, BMI, and LBM. While different trends can be detected in these scatter diagrams, the only significant relationships were the QTcI prolongation with advancing age ( $p = 0.01$  in both sexes), decrease with QT/RR slope with age in males ( $p = 0.009$ , NS in females), and decrease in QT/RR slope with increased BMI ( $p = 0.011$  and  $p = 0.016$  in females and males, respectively). Despite expectations, we have not found any significant influence of age, BMI, or LBM on the intra-subject SD of QTcI.

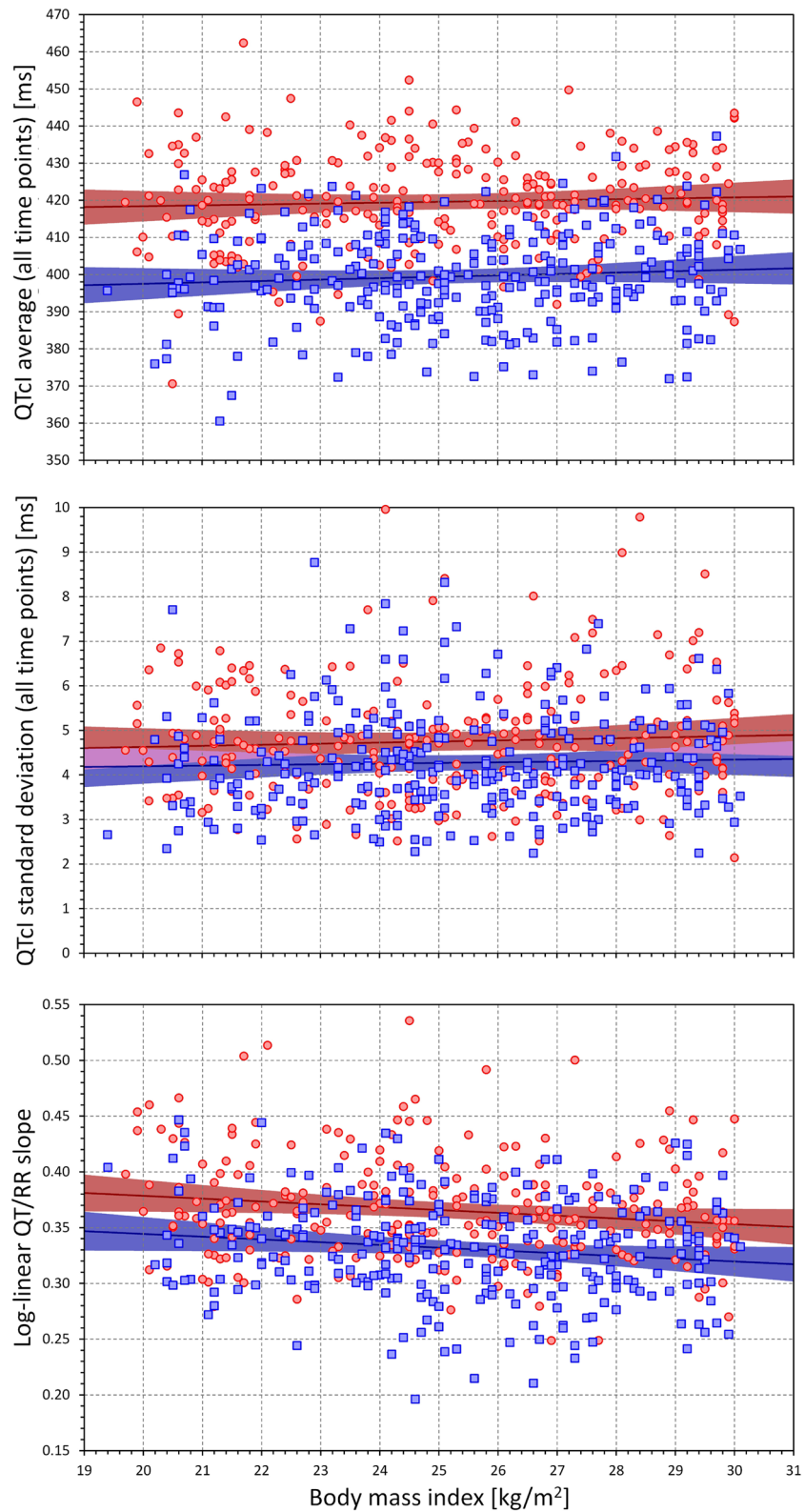
**Short-term QTc variability.** Figures 6 and 7 show scatter diagrams that relate 5-min SDs of QTc values measured within the same study time-point to the range (max–min) of heart rates among the same 10-s ECG samples in which the QTc values were measured. This relationship is shown for the QTcI values (top left panel of Fig. 6) and for 7 of the investigated correction formulas. The figures show that while the short-term variability of the QTcI values is little influenced by the heart rate ranges, the short-term variability of heart rates of the measured ECG samples influenced the short-term variability of all the QTc formulas with the strongest relationship visible for the Bazett formula.

The data summarised in the images of Figs. 6 and 7 are not suitable for statistical analysis since for each subject, the scatter diagrams contain data of multiple study time-points. Data suitable for statistical analysis are shown in the left panel of Fig. 8. This panel of Fig. 8 shows, for each heart rate correction, the spread of linear regression slopes between the 5-min SDs of QTc values and the corresponding 5-min heart rate ranges. In each subject, the regression was calculated over all study time-points. While for QTcI, the displayed slopes were not significantly different between females and males, the slopes were significantly lower in females compared to males for all correction formulas ( $p = 0.0347$  for Fridericia formula,  $p = 0.0079$  for Framingham formula,

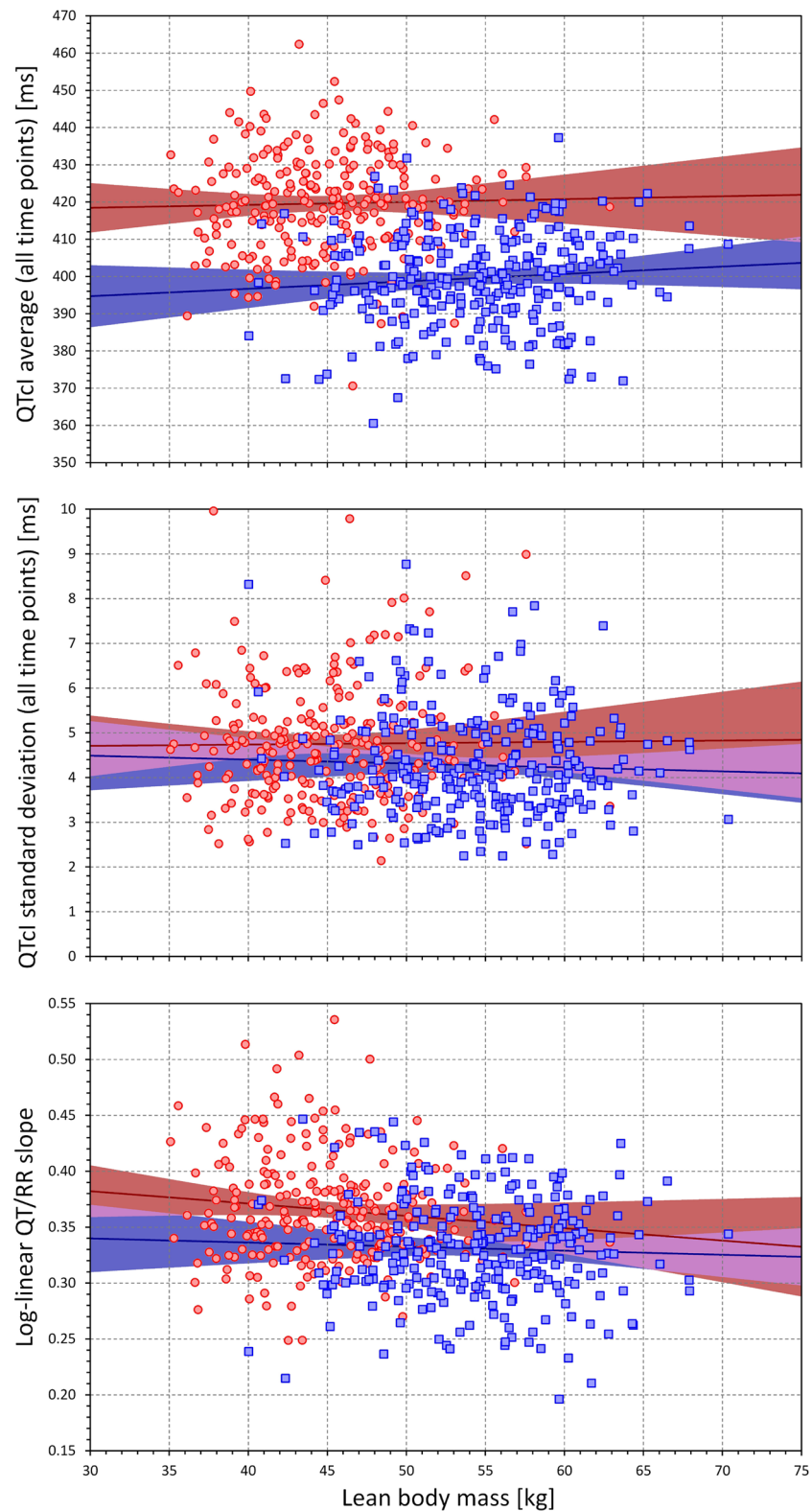


**Figure 3.** Scatter diagrams between age and mean QTcl values of all ECG measurements in all study time-points (top panel), standard deviation of QTcl values of all ECG measurements in all study time-points (middle panel), and subject-specific log-linear QT/RR slope (bottom panel). In each panel, the red circles and blue squares correspond to female and male subjects, respectively. The solid red and solid blue lines show the linear regressions between the age and the measured QT characteristics in females and males, respectively. The red shaded and blue shaded areas are the 95% confidence intervals of the regression lines; the violet areas are the overlaps between the confidence intervals of the sex-specific regressions. *ms* milliseconds.

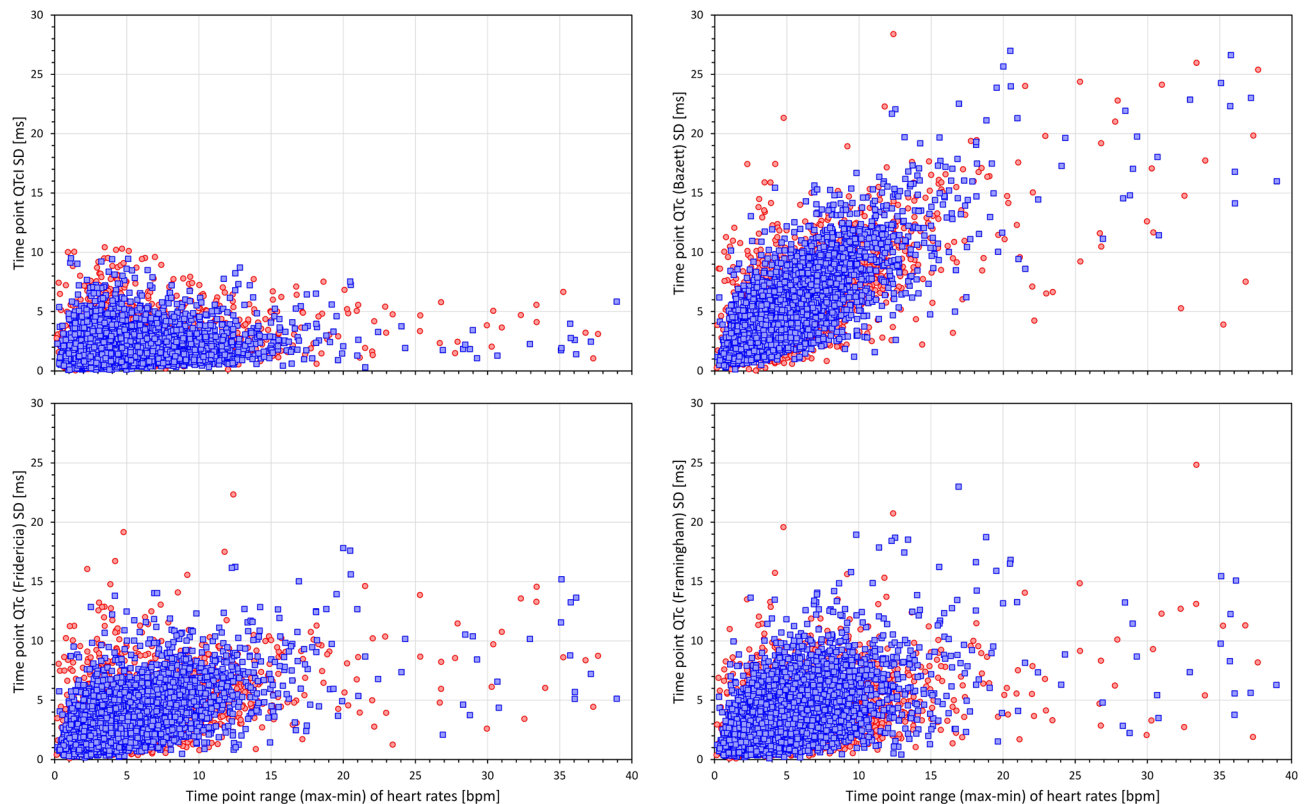




**Figure 4.** Scatter diagrams between the body mass index and mean QTcI values of all ECG measurements in all study time-points (top panel), standard deviation of QTcI values of all ECG measurements in all study time-points (middle panel), and subject-specific log-linear QT/RR slope (bottom panel). The meaning of symbols and Figure layout is the same as in Fig. 3. *kg* kilograms, *m* metre, *ms* milliseconds.



**Figure 5.** Scatter diagrams between the lean body mass and mean QTcI values of all ECG measurements in all study time-points (top panel), standard deviation of QTcI values of all ECG measurements in all study time-points (middle panel), and subject-specific log-linear QT/RR slope (bottom panel). The meaning of symbols and Figure layout is the same as in Fig. 3. *kg* kilograms, *ms* milliseconds.



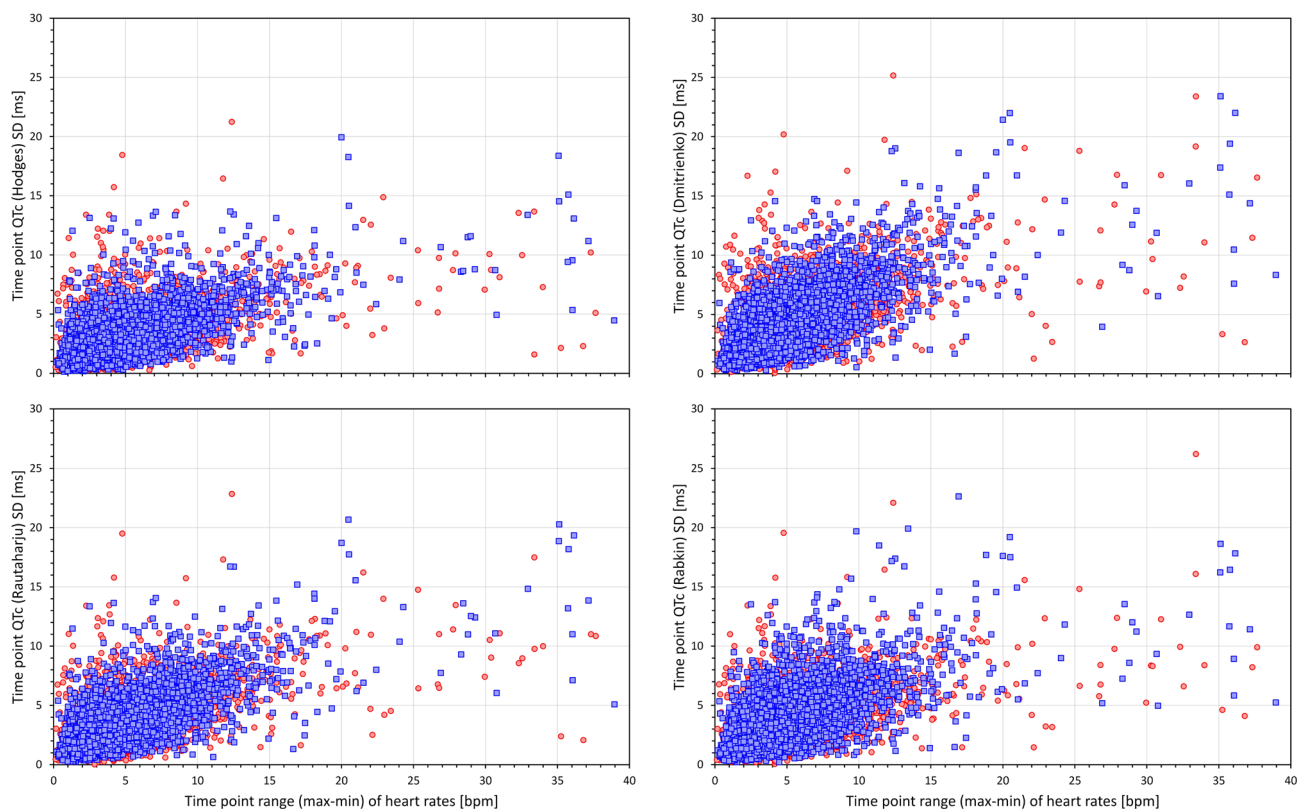
**Figure 6.** Scatter diagrams between heart rate ranges (maximum–minimum) and standard deviations of QTc values of individual study time-points. The left top panel shows the relationship for QTcI intervals, the top right, bottom left, and bottom right panels show the relationship for Bazett, Fridericia, and Framingham corrected QTc intervals, respectively. In all panels, all time-points of all study subjects are pooled together, red and blue marks show the data of female and male subjects, respectively. Outliers beyond the ranges of the axes were also present in the data. Note that pooling all time-points of all subjects together is not suitable for statistical analysis but serves visual interpretation—the stronger the relationship between the variability of the underlying heart rate and the variability of the QTc intervals within the same time-point, the greater the failure of the correction formula in eliminating the effects of heart rate on QTc values. Compare the panels with panels of Fig. 7. *bpm* beats per minute, *max* maximum, *min* minimum, *SD* standard deviation.

$p < 0.00001$  for all other formulas). Paired comparison between the formulas showed that (a) the QTcI slopes were smaller than for any other correction formula ( $p < 0.00001$  for all comparisons), (b) the slopes of Bazett formula were larger than for any other formula ( $p < 0.00001$  for all comparisons), (c) the slopes of Fridericia and Framingham formula were only little different of each other, and (d) the slopes of all other formulas were larger compared to the slopes and Fridericia and Framingham formulas ( $p < 0.00001$  for all comparisons).

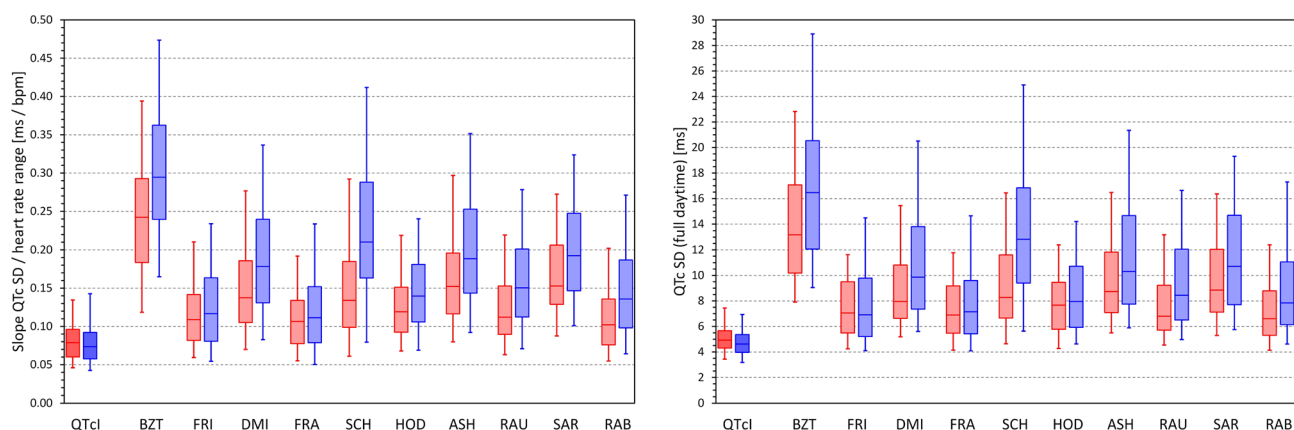
**Day-time QTc variability.** For comparisons of results discussed in the previous section, the right panel of Fig. 8 shows the distribution of SDs of QTc values over all the ECG readings available during the baseline day. It is well visible that the patterns of the two panels of Fig. 8 closely replicate each other. Indeed, the data led to the very same statistical comparisons: For all formulas, the SDs of QTcI were significantly smaller ( $p < 0.00001$  for all), SDs of Bazett QTc were larger than any other formula ( $p < 0.00001$  for all), SDs of Fridericia and Framingham QTc were not significantly different, and SDs of Fridericia and Framingham were significantly smaller than those of any other formula ( $p < 0.00001$  for all comparisons).

Figure 9 shows the distributions of SDs of QTc values obtained from all study time-points, stable time-points, fasting time-points, and fasting stable time-points. The QTc variability values decreased in this order of time-point selection. For instance, for SDs of QTcI values, the corresponding population means of the SDs (females and males combined) were 4.50, 4.38, 3.17, and 3.06 ms, respectively ( $p < 0.002$  for statistical comparisons at all individual steps). For Bazett correction, the corresponding values were 12.14, 10.37, 6.90, and 5.85 ms ( $p < 0.00001$  at all steps) while for Fridericia correction, the corresponding values were 6.42, 5.87, 4.20, and 3.86 ms ( $p < 0.00001$  at all steps). Systematically, the SDs of the Bazett QTc values were significantly larger than those of any other formula ( $p < 0.00001$  for all comparisons) and those of Fridericia correction were smaller than those of any other formula ( $p$  values ranged between 0.033 and  $< 0.00001$  for all comparisons).

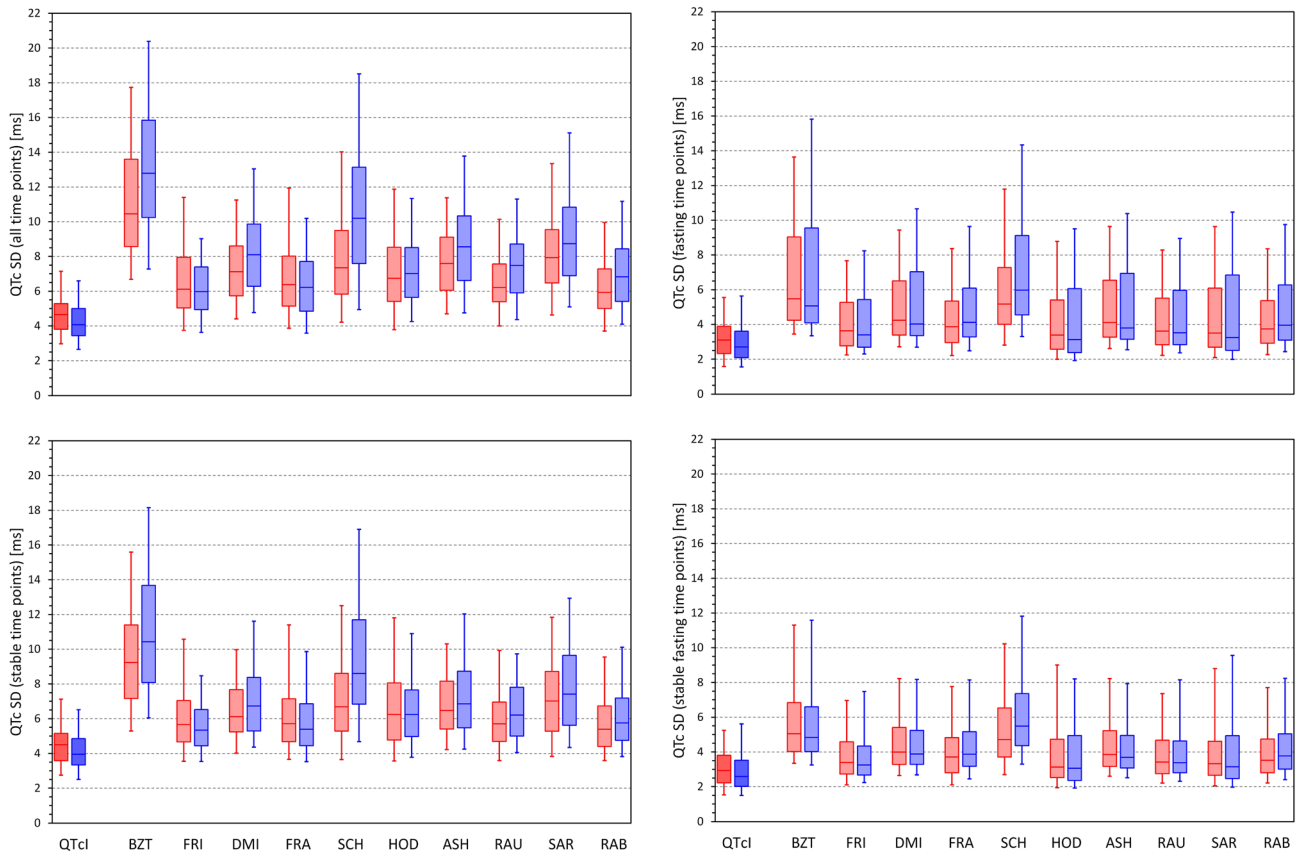
**Difference between general and individual QTc corrections.** Figure 10 shows the distribution of slopes of intra-subject linear regressions between QTc values and corresponding 10-s averages of RR intervals. Very clearly, Bazett correction led to QTc values that were least independent of the underlying RR intervals (i.e.



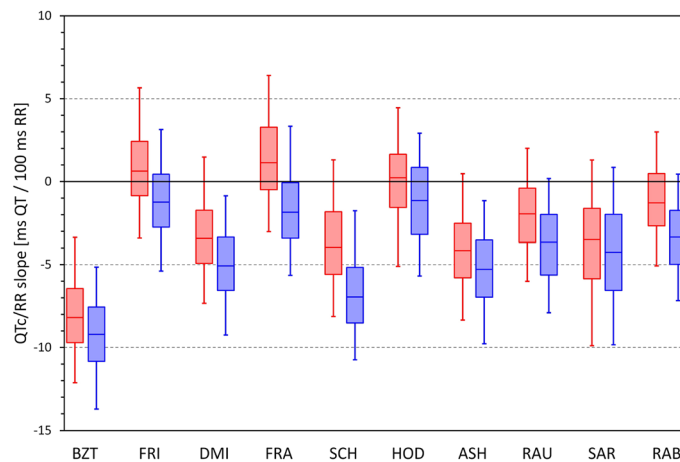
**Figure 7.** Scatter diagrams between heart rate ranges (max–min) and standard deviations of QTc values of individual study time-points. The left top, top right, bottom left, and bottom right panels show the relationship for Hodges, Dmitrienko, Rautaharju, and Rabkin corrected QTc intervals, respectively. In all panels, all time-points of all study subjects are pooled together, red and blue marks show the data of female and male subjects, respectively. Outliers beyond the ranges of the axes were also present in the data. The abbreviations and meaning of panels are the same as in Fig. 6. The note in the caption of Fig. 6 also applies—compare the panels with panels of Fig. 6.



**Figure 8.** The left panel shows the distribution of the intra-subject linear slopes between heart rate ranges (max–min) and standard deviations of QTc intervals calculated over the different study time-points. The right panel shows the distribution of the intra-subject standard deviations of the QTc intervals calculated over all the ECG readings within the drug-free baseline day. For each correction formula (see the abbreviations at the horizontal axes) red and blue box and whisker entries are shown corresponding to the distribution of the data in female and male subjects, respectively. Each of the box and whisker entries shows the population median (horizontal line within the box), inter-quartile range (the top and bottom of the box) and the range between the 5th and 95th percentile (the bottom and top whiskers). *bmp* beats per minute, *ms* milliseconds, *SD* standard deviation.

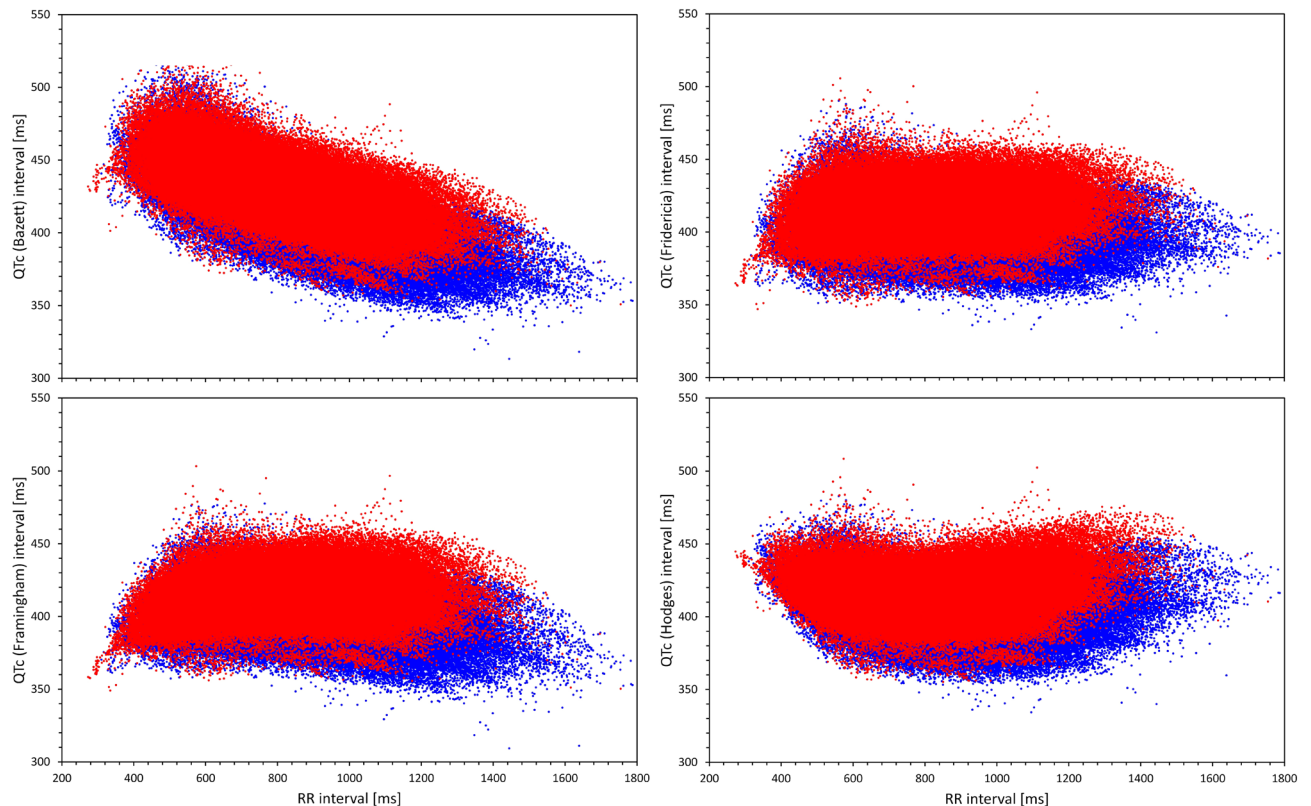


**Figure 9.** Distribution of the intra-subject standard deviations of QTc values calculated over all study time-points (top left panel), time-points with stable heart rate (bottom left panel), morning fasting time-points (top right panel), and morning fasting time-points with stable heart rate (bottom right panel). The layout of the panels and the meaning of the box and whisker graphs is the same as in Fig. 8. *ms* milliseconds, *SD* standard deviation.



**Figure 10.** Distribution of intra-subject linear slopes between QTc values and corresponding 10-s averages of RR intervals calculated over all ECG reading during the baseline drug-free day. The layout of the panel and the meaning of the box and whisker graphs is the same as in Fig. 8. *ms* milliseconds.

led to the poorest elimination of the QTc dependency on the underlying heart rate) while Fridericia and Hodges corrections led to slopes that were, on average, closest to zero. (Understandably, the figure does not show the results for QTcI since the individual corrections are designed to produce 0 slopes.) The fact that, compared to other correction, Bazett formula leads to QTc values that are not independent of the underlying heart rate is also visible when pooling individual ECG data of all subjects together (Fig. 11).



**Figure 11.** For Bazett (top left panel), Fridericia (top right panel), Framingham (bottom left panel) and Hodges (bottom right panel) correction, the Figure shows scatter diagrams of QTc values versus underlying heart rate (10-s measurement) in all study data pooled together. The data in females (in red) are shown superimposed on top of the data in males (in blue).

Figure 12 shows the distribution of the differences between QTcI values and the QTc values by different correction formulas for all study time-points, stable time-points, fasting time-points, and fasting stable time-points. For each Formula, there is an appreciable spread of the differences but the largest is seen for Bazett and Schlamowitz corrections. The figure also shows the attempt of eliminating QTc differences between females and males and eliminating the age difference by Rabkin et al. leads to systematic bias of the formula, especially in females.

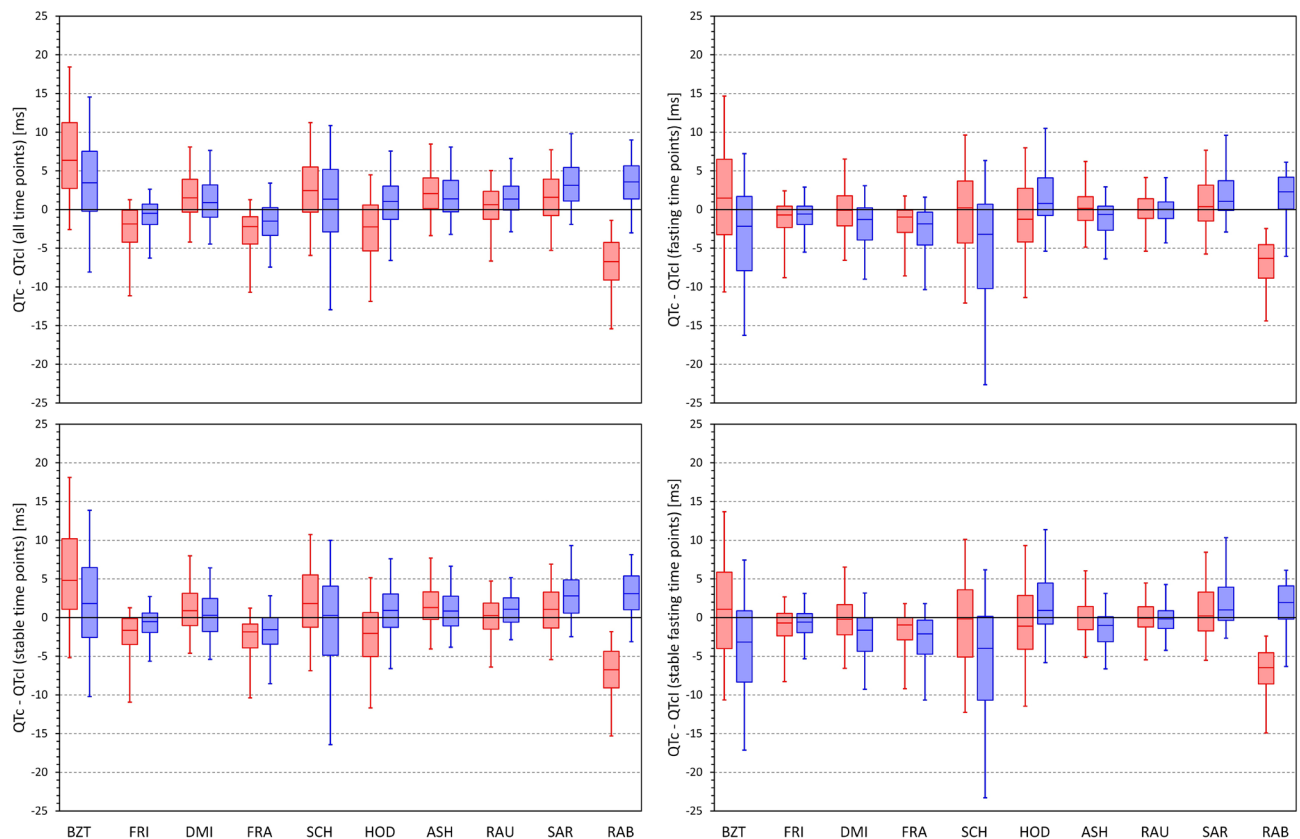
Importantly, Fig. 13 shows that when considering data of all study time-points, there was a systematic trend between the QTcI values and the QTc (Bazett)—QTcI differences. This trend was persistent also when considering only stable time-points but it was reduced when analysing only fasting time-points and further reduced when considering the stable fasting time-points. Figures 14, 15 and 16 show that this observation was also present for other formulas (the Figures show the details for Fridericia, Framingham, and Hodges corrections).

## Discussion

**Principal observations.** Four principal observations may be derived from the study; all with potentially important implications for clinical electrocardiography.

Whilst this is not the first study to document substantial problems with Bazett correction<sup>34,35,37,39,41,54–56</sup>, we show that this correction not only fails to remove the relationship between QTc intervals and the underlying heart rate, it also leads to QTc data that are much more variable compared to all the other corrections that we investigated. We recognise that Bazett correction became somewhat entrenched in clinical reporting, possibly because historically it was very easy to implement and calculate. With the widespread advances of technical possibilities, this superficial advantage has been lost. We are therefore of the strong opinion that all the previous criticism of Bazett formula should finally be heard. The clinical practice needs to be changed and Bazett correction should stop being used. This would not only improve the assessment of QTc interval in clinical cases but would also correspond to the regulatory evaluation of QTc interval in clinical drug studies in which Bazett correction has now been abandoned<sup>20</sup>.

Obviously, a generic correction formula is needed in clinical practice since, as already stated, individual-specific baseline QT/RR profile cannot possibly be obtained for clinical purposes (investigations over full drug-free day or days are needed for this purpose in clinical pharmacology studies<sup>25,26,57</sup>). The overall comparison of the 10 formulas that we investigated give a clear preference to Fridericia or Framingham corrections that not only lead to lesser variable results compared to the other formulas but, in our data, appeared not very far from the QTcI values. The argument that the presently available clinical experience based on Bazett correction cannot be easily applied to these corrections needs to be refuted. For heart rates close to 60 bpm, the results of all

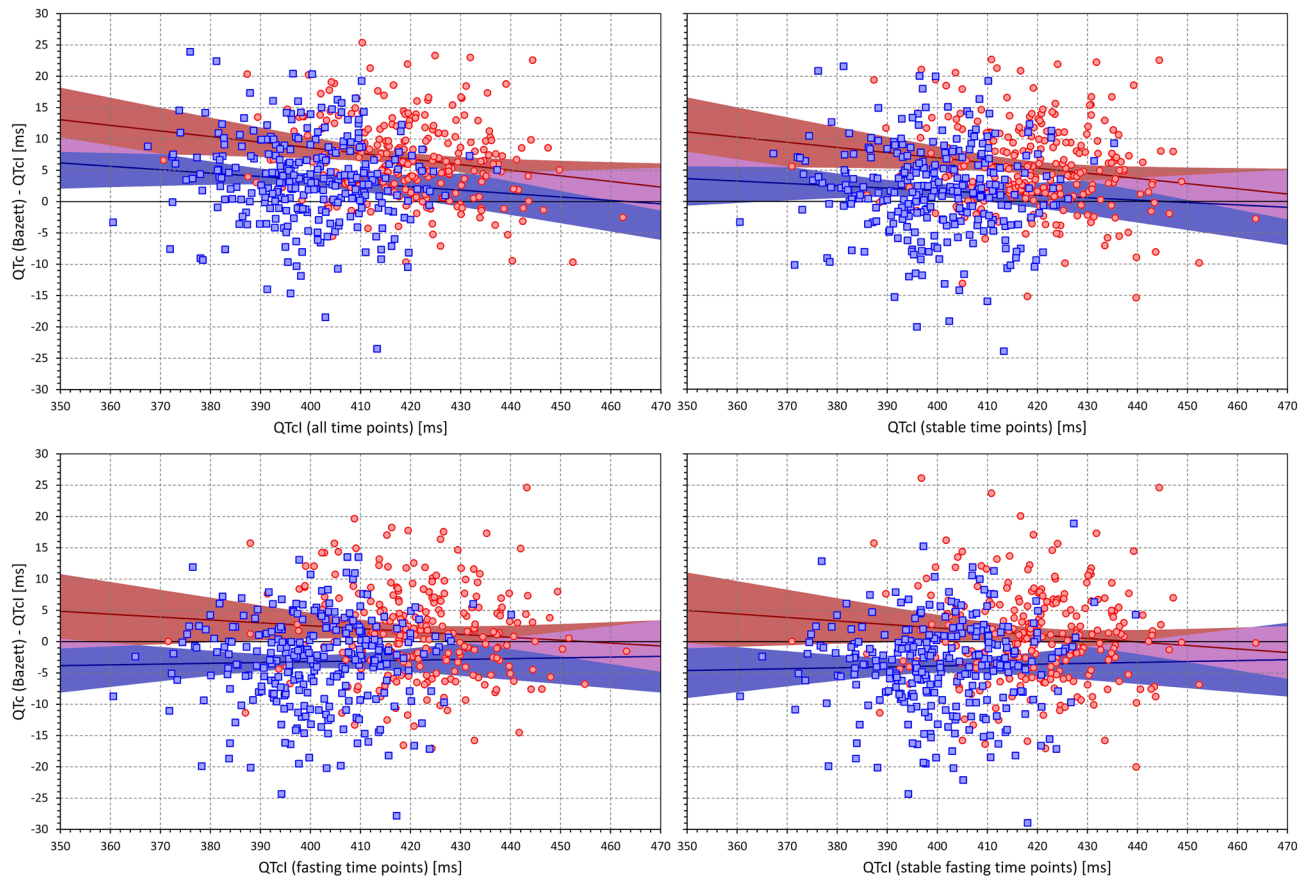


**Figure 12.** Distribution of the mean intra-subject differences between QTc intervals by different correction formulas and the corresponding QTcI values. The distribution of the differences is shown for calculations over all study time-points (top left panel), time-points with stable heart rate (bottom left panel), morning fasting time-points (top right panel), and morning fasting time-points with stable heart rate (bottom right panel). The layout of the panels and the meaning of the box and whisker graphs is the same as in Fig. 8. *ms* milliseconds.

the corrections are the same and heart rate departures from 60 bpm make Bazett QTc values polluted by larger errors compared to the other corrections. Contrary to Framingham formula, Fridericia formula suffers from non-linearity<sup>58</sup> (also present with Bazett formula) which makes it much less accurate with other ECG intervals (e.g. the JT interval). Nevertheless, when applied to the physiologically plausible QT durations, the effects of this problem are not large. Recently, we have also found preference for Fridericia and Framingham formulas when assessing QTc duration in school-aged children<sup>59</sup>.

While “normalisation” attempts by the Rabkin formula may lead to homogeneity of QTc values across a population of both sexes, the bias of the formula seen in Fig. 11 makes its usefulness very limited for any practical purposes. The artificial reduction of QTc in females as well as in subjects of advanced age means that in clinical use, the formula would compromise detection of susceptibility to drug-induced QTc prolongation (known to be increased in females<sup>60</sup>) and of reduced repolarisation reserve (known to be more frequent with advanced age<sup>61,62</sup>). Thus, while the reproducibility of the QTc by Rabkin formula was comparable to that of Fridericia and Framingham formulas (see Fig. 9), the comparison with the QTcI values showed that for practical use, this formula would be reproducibly “off target”.

The situations of heart rate instability effects demonstrated in Figs. 1, 6 and 7 need to be considered carefully. It has already been discussed that positioning subjects in motionless position might reduce heart rate changes due to physical demands but cannot eliminate heart rate instability due to other (e.g., psychological) factors<sup>46</sup>. For clinical practice, we would like to suggest that repeated ECG recordings are obtained within an interval of some (e.g., 3 to 5) minutes and that QTc interval is only derived from these recordings if they all show similar heart rate (e.g., within a 5 bpm range). To be properly understood: we are not advocating that multiple QTc interval measurements are averaged to reduce the QTc variability. Such an approach would not eliminate the potentially large errors due to the effects of QT/RR hysteresis. We suggest that multiple ECG recordings should be used to assure that the ECG in which the QT interval is measured (e.g. the last of the repeated recordings) is preceded by stable heart rate. As shown in the example of Fig. 1, variable heart rate preceding the QT measurement can invalidate QTc assessment well above the inaccuracy of generic correction formulas. The fact that the duration of the profile of QT/RR hysteresis, i.e. the time needed for QT interval to adapt to changing heart rate, is longer in cardiac patients compared to healthy subjects<sup>63</sup> makes the considerations of QT/RR hysteresis even more important for clinical practice. Seeking heart rate stability over the interval of some minutes is bound to suppress gross errors of QTc assessment.



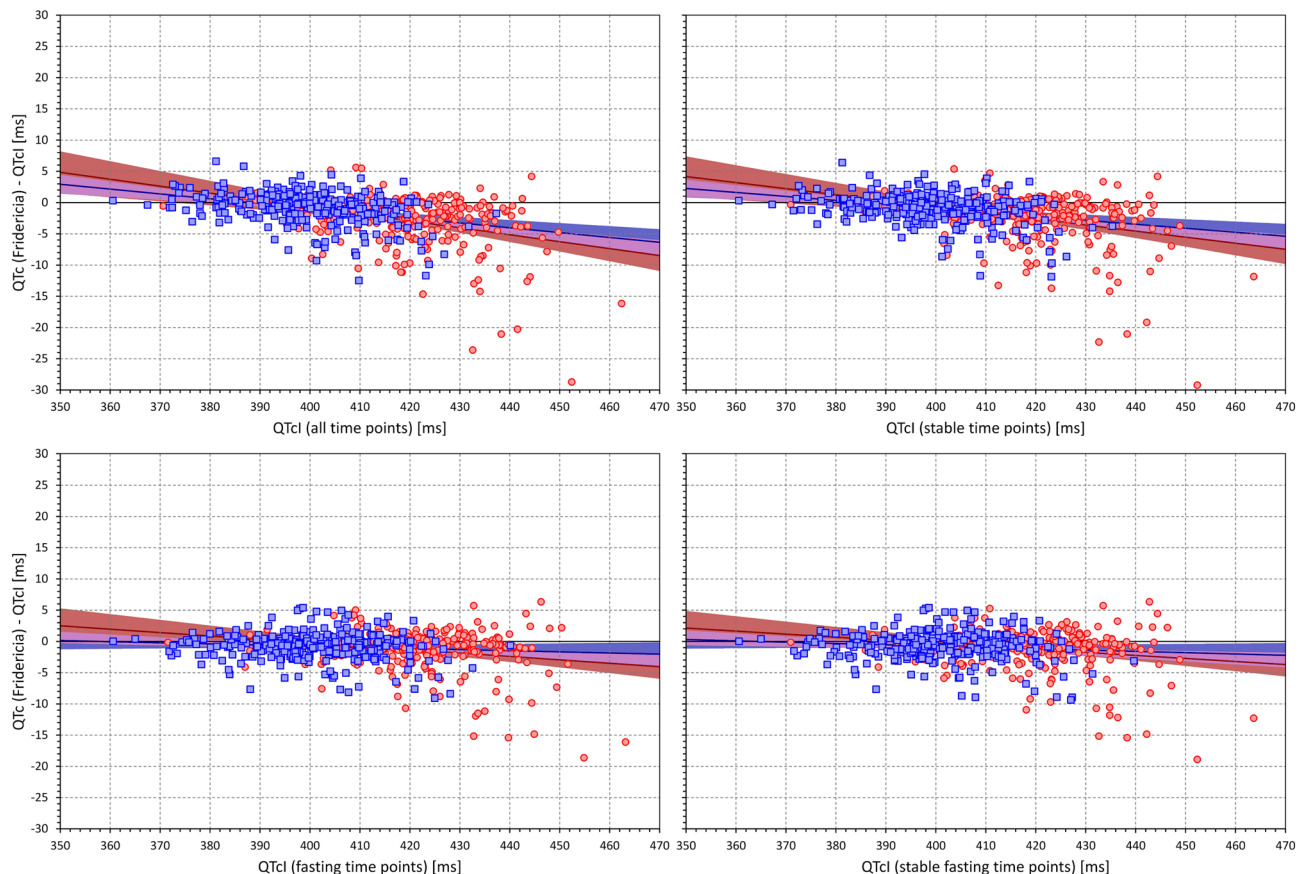
**Figure 13.** Scatter diagrams of the mean intra-subject differences between Bazett corrected QTc intervals and corresponding QTcI intervals plotted against the intra-subject means of QTcI intervals. The diagrams are shown for data of all study time-points (top left panel), time-points with stable heart rate (top right panel), morning fasting time-points (bottom left panel), and morning fasting time-points with stable heart rate (bottom right panel). In each panel, the red circles and blue squares correspond to female and male subjects, respectively. The solid red and solid blue lines show the linear regressions between the intra-subject QTcI means and the mean intra-subject QTc – QTcI differences in females and males, respectively. The red shaded and blue shaded areas are the 95% confidence intervals of the regression lines; the violet areas are the overlaps between the confidence intervals of the sex-specific regressions. *ms* milliseconds.

Finally, although we included several correction formulas that have been proposed more recently and utilise fairly complex mathematical forms (e.g. the definition of the spline formula used in the correction by Rabkin et al. occupies 27 lines of complex mathematical text<sup>42</sup>), we have not found these advantageous in comparison to the older and also much simpler Fridericia and Framingham corrections. We therefore believe that efforts to design yet another correction formula for general use are fruitless and will not lead to anything substantially more accurate and/or more stable than Fridericia and/or Framingham corrections.

**Physiologic comments.** It is not surprising that none of the investigated general correction produces data very close to subject-specific corrections. This is because, in principle, no correction can exist that would faithfully reproduce the QT/RR relationship in all subjects and patients<sup>51,64</sup>. This is well documented in the images in Fig. 2. If we consider RR interval changes between 600 and 900 ms, it can be seen in this Figure that some subjects change their physiologic QT interval durations by as little as 15 ms while in other subjects, the corresponding QT interval change exceeds 30 ms. Therefore, there cannot be a mathematical form (regardless of how complicated) that would correctly model all these cases. The best of what can be achieved is to find a mathematical form that is reasonably close to the physiologic “middle” of different QT/RR patterns and that will, correspondingly, be overestimating and underestimating the true QTc values with equal or similar frequencies. Since the individual QT/RR patterns differ not only in their slopes but also in their curvatures<sup>30</sup>, even substantial complexity of mathematical forms would not be too helpful. For the reasons of substantial individuality of QT/RR adaptation, proposals of different formulas for females and males are also of little value (despite the statistical sex differences in QTc duration and QT/RR slope<sup>52</sup>). There is a very substantial overlap in the subject-specific QT/RR patterns and slopes between both sexes<sup>46</sup>.

Because of the substantial spread of intra-individual QT/RR patterns, it seems problematic to diagnose QTc abnormality based on ECG recordings with heart rate very remote from the 60 bpm “centre”. This is particularly





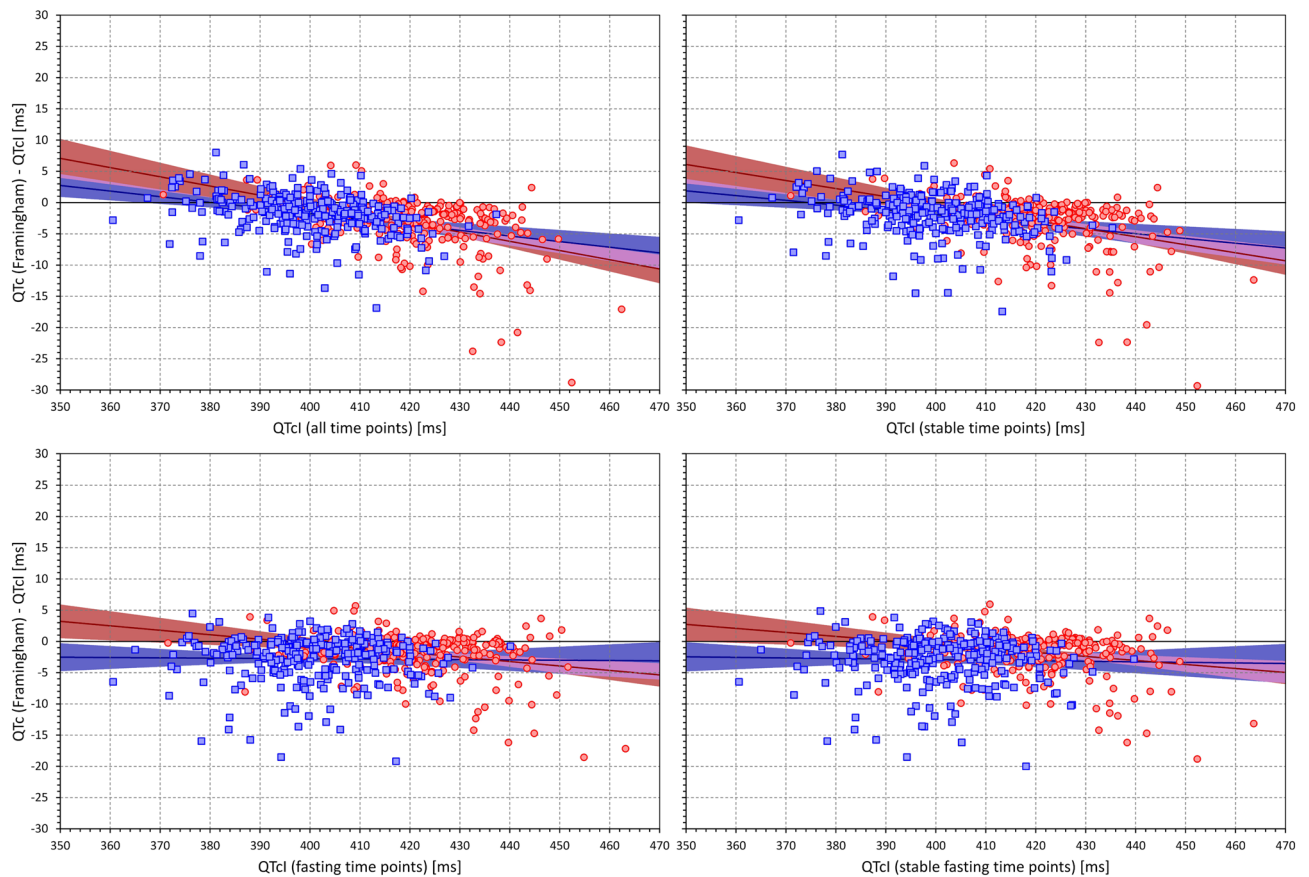
**Figure 14.** The figure meaning and layout correspond to those of Fig. 12 but instead Bazett QTc data, Fridericia QTc data were used.

true for the Bazett formula while Fridericia and Framingham formulas are somewhat more robust when used to assess QTc duration at heart rates between, say, 55 and 75 bpm<sup>65</sup>. Within such heart rate ranges, the “standard” abnormal prolongation cut-offs (e.g. 470 and 450 ms for females and males, respectively) might be used also with these formulas since the population spread of their QTc values is not very far from that at 60 bpm<sup>65</sup>.

It might also be speculated that in addition to heart rate and QT/RR hysteresis effects, QT interval might also be corrected for other factors such as autonomic status and/or plasma electrolyte and glucose levels<sup>43,66,67</sup>. In this sense, our “gold standard” individual correction might be further improved. Nevertheless, as previously shown and as also demonstrated in our present results, the intra-subject variability of QTcI values is fairly low<sup>64,68</sup> and considerations of rate-independent QT covariates might only lead to minimal advances.

Contrary to individuality of QT/RR adaptation patterns (i.e. how much does the QT interval change in response to different heart rate) the QT/RR hysteresis profiles (i.e. how quickly the QT interval reacts to heart rate changes) are similar in different healthy subjects. Hence, while in different healthy subjects, even Fridericia and Framingham formulas may lead to noticeable differences between QTc and QTcI (see, Figs. 13 and 14) the use of universal hysteresis correction leads only to minimal departures from individually optimised QT/RR hysteresis models of healthy subjects<sup>46</sup>. As already mentioned, QT/RR hysteresis is slower in cardiac patients<sup>63</sup>, but it is not known whether the previously proposed universal model of QT/RR hysteresis correction would lead to substantial discrepancies in the QTc assessment in such patients. Nevertheless, for clinical practice, these considerations are rather academic since the application of hysteresis correction requires the data of a prolonged history of QT measurement, well exceeding the standard 10-s ECG duration. Therefore, elimination of the need to correct for QT/RR hysteresis needs to be the method of choice. This leads to the assurance of heart rate stability as we have already proposed. It remains to be investigated whether the rate stability limit of 5 bpm that we have used might be proposed for clinical electrocardiography or whether different criteria should be applied, especially when recordings patients with cardiac abnormalities.

Comment should also be made on the fact that we observed both short-term and long-term variations not only of QTc values by the different correction formulas but also, albeit to a much lesser degree, of the individually corrected QTcI values. While direct heart rate influence on the QTcI duration is removed, ventricular repolarisation interval is also under the influence of autonomic nervous system<sup>67</sup> as well as of other regulatory mechanisms, e.g. those responsible for post-prandial effects<sup>43</sup>. This means that even at the same underlying heart rate, differences in the QT interval duration still exist (note the “width” of the QT/RR patterns shown in Fig. 2). The dual influence of autonomic reflexes on both heart rate and QT interval duration is not necessarily in synchrony and thus, short-term QTcI variability might be more pronounced during episodes of increased autonomic



**Figure 15.** The figure meaning and layout correspond to those of Fig. 12 but instead Bazett QTc data, Framingham QTc data were used.

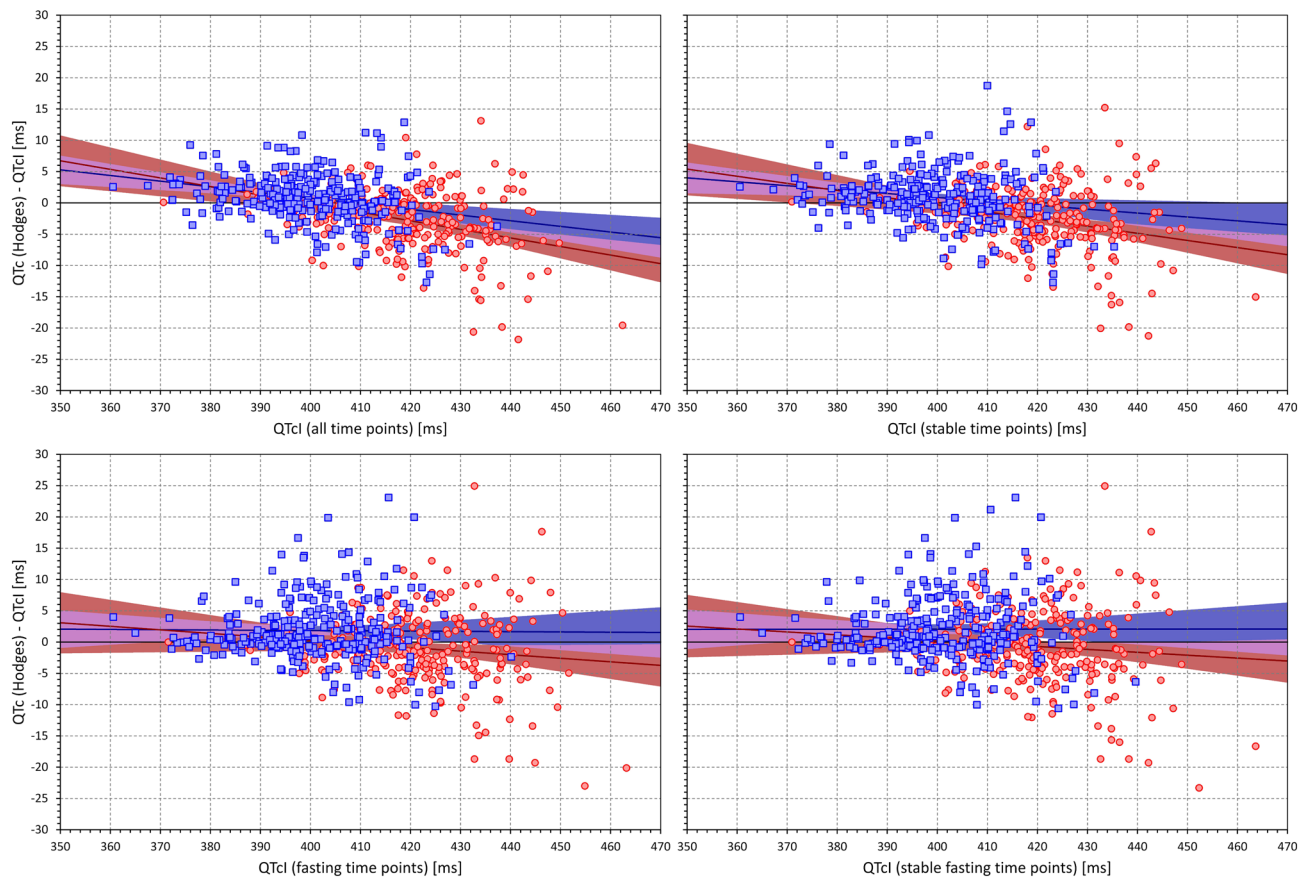
and thus also heart rate fluctuations. Indeed, we have recently reported that increased heart rate and increased short-term RR interval variability are significant contributors to the beat-to-beat QT interval variations<sup>69</sup>. The autonomic influence of QTcI intervals also contributes to the observed increased mean QTcI with advancing age. Similarly, the decline of the QT/RR slope with advancing age and with increased BMI and LBM might be attributed to the decline of autonomic responsiveness which is known not only with an increased age but also with changes in body habitus.

**Limitations.** The study used data of healthy volunteers rather than of patients in whom QTc monitoring is needed for clinical reasons. Nevertheless, while the inter-subject spread of QT/RR patterns might be wider among patients with different diagnoses compared to healthy subjects, it can hardly be narrower. Hence, a correction formula that performs poorly in healthy subjects is very unlikely to operate more reasonably in a patient population.

Some of the previous reports tried to select an optimum formula not only for accurate rate correction of the QT interval (that is, for obtaining QTc values independent of heart rate) but also for other purposes, such as the prediction of poor survival and/or arrhythmic risk<sup>22</sup>. We have not addressed such approaches since they are, in principle, methodologically flawed. Increased heart rate is a known risk factor in its own right<sup>70,71</sup> and trying to incorporate its risk predictive influence into a QT correction formula is both physiologically and clinically problematic. If risk prediction is needed involving both QTc interval duration and heart rate, multivariable stratification models are required.

The 10 correction formulas that we have investigated have been selected from a very broad spectrum of other proposals. We believe that the formulas that we selected cover the spectrum of previously published correction methods reasonably and that it would be fruitless to include also other possibilities. When we experimented with several other formulas not included in this study, the results (not shown here) were fully consistent with the observations that we described.

In the setup of “gold standard” QTcI values, we used the subject-specific QT/RR curvature modelling combined with the exponential decay QT/RR hysteresis model<sup>30,31</sup>. The variability of the QTcI might have been further reduced not only by employing more complex hysteresis corrections<sup>72–74</sup> but also by differentiating the speed of QT adaptation to heart rate acceleration and deceleration. As far as we are aware, such a distinction of different QT/RR hysteresis components has never been attempted before. Likewise, it might be possible to correct QT interval not only for underlying heart rate but also for the spectral components of heart rate variability that approximate the sympatho-vagal balance of heart rate modulations. Again, we are not aware of any technology



**Figure 16.** The figure meaning and layout correspond to those of Fig. 12 but instead Bazett QTc data, Hodges QTc data were used.

available for such a purpose although the different levels of sympatho-vagal modulations are likely to influence QT interval differently even at the same level of the underlying heart rate. In any case, however, only miniscule increases of QTcI stability might be achieved by all these approaches since the variability that we reported was already very low.

**Conclusion.** The principal conclusions of the study might be summarised as follows:

Our observations fully support the previous criticism of Bazett correction. In all investigated aspects, this correction performed more poorly compared to all other possibilities. A repeated strong call to the clinical community is needed so that this correction is finally eliminated from everyday use.

Among the broad spectrum of correction formulas that we investigated, most stable and (on average) reasonably accurate QTc corrections were obtained with Fridericia and Framingham corrections. While for research and investigative use, these corrections are less suitable than the subject-specific optimisation approaches, clinical practice would substantially benefit from using either of these corrections instead of the Bazett formula.

To eliminate potentially large QTc inaccuracies due to preceding variable heart rate, repeated ECG recordings within a short interval and some minutes should be obtained and the heart rate stability objectively verified.

Further attempts of finding a universally applicable correction formula that would accurately correct QT intervals in different conditions appear unproductive and clearly impossible to succeed because of the large physiological spread of individual QT/RR profiles.

### Data availability

The raw data supporting the conclusions of this article will be made available by the authors, without undue reservation but pending the approval by the sponsors of the source clinical studies.

Received: 12 April 2021; Accepted: 30 June 2021

Published online: 12 July 2021

### References

1. Vandael, E., Vandenberg, B., Vandenberghe, J., Willems, R. & Foulon, V. Risk factors for QTc-prolongation: Systematic review of the evidence. *Int. J. Clin. Pharm.* **39**, 16–25 (2017).
2. Drew, B. J. *et al.* Prevention of torsade de pointes in hospital settings: A scientific statement from the American Heart Association and the American College of Cardiology Foundation. *Circulation* **121**, 1047–1060 (2010).

3. Buttà, C. *et al.* Use of QT intervals for a more accurate diagnose of syncope and evaluation of syncope severity. *Int. J. Clin. Pract.* **68**, 864–870 (2014).
4. Rometo, A. B., Beerman, L. & Arora, G. Electrolyte screening in the evaluation of prolonged QTc interval. *Cardiol. Young* **25**, 398–399 (2015).
5. Genovesi, S. *et al.* Electrolyte concentration during haemodialysis and QT interval prolongation in uraemic patients. *Europace* **10**, 771–777 (2008).
6. Quenin, P. *et al.* Clinical yield of familial screening after sudden death in young subjects: The French experience. *Circ. Arrhythm. Electrophysiol.* **10**, e005236. <https://doi.org/10.1161/CIRCEP.117.005236> (2017).
7. Marcus, F. I. Electrocardiographic features of inherited diseases that predispose to the development of cardiac arrhythmias, long QT syndrome, arrhythmogenic right ventricular cardiomyopathy/dysplasia, and Brugada syndrome. *J. Electrocardiol.* **33**(Suppl), 1–10 (2000).
8. Tisdale, J. E. *et al.* Development and validation of a risk score to predict QT interval prolongation in hospitalized patients. *Circ. Cardiovasc. Qual. Outcomes* **6**, 479–487 (2013).
9. Warnier, M. J. *et al.* Are ECG monitoring recommendations before prescription of QT-prolonging drugs applied in daily practice? The example of haloperidol. *Pharmacoepidemiol. Drug Saf.* **24**, 701–708 (2015).
10. Sharma, S. *et al.* Providers' response to clinical decision support for QT prolonging drugs. *J. Med. Syst.* **41**, 161 (2017).
11. Pezo, R. C., Yan, A. T., Earle, C. & Chan, K. K. Underuse of ECG monitoring in oncology patients receiving QT-interval prolonging drugs. *Heart* **105**, 1649–1655 (2019).
12. Good, M. M., Riad, F. S., Good, C. B. & Shalaby, A. A. Provider response to QTc prolongation on standard 12-Lead EKG: Do we notice or do we care?. *Pacing Clin. Electrophysiol.* **39**, 1174–1180 (2016).
13. Benjamin, L. N. *et al.* Recommendations for QTc monitoring: Rational or arbitrary?. *Prim. Care Comp. CNS Disord.* **20**, 18f02327. <https://doi.org/10.4088/PCC.18f02327> (2018).
14. Gueta, I. *et al.* Clinically significant incidental QTc prolongation is subject to within-individual variability. *Ann. Noninvasive Electrocardiol.* **25**, e12699. <https://doi.org/10.1111/anec.12699> (2020).
15. Genovesi, S. *et al.* Acute effect of a peritoneal dialysis exchange on electrolyte concentration and QT interval in uraemic patients. *Clin. Exp. Nephrol.* **23**, 1315–1322 (2019).
16. Drew, D., Baranchuk, A., Hopman, W. & Brison, R. J. The impact of fever on corrected QT interval. *J. Electrocardiol.* **50**, 570–575 (2017).
17. Albert, B. B., Eckersley, L. G., Skinner, J. R. & Jefferies, C. QT prolongation in a child with thyroid storm. *BMJ Case Rep.* **2014**, bcr2013202595. <https://doi.org/10.1136/bcr-2013-202595> (2014).
18. Capparelli, F. J. *et al.* QTc prolongation after brain surgery. *Neurol. Res.* **35**, 159–162 (2013).
19. Hnatkova, K. & Malik, M. Sources of QTc variability: Implications for effective ECG monitoring in clinical practice. *Ann. Noninvasive Electrocardiol.* **25**, e12730. <https://doi.org/10.1111/anec.12730> (2020).
20. Garnett, C. E. *et al.* Methodologies to characterize the QT/corrected QT interval in the presence of drug-induced heart rate changes or other autonomic effects. *Am. Heart J.* **163**, 912–930 (2012).
21. Malik, M. The imprecision in heart rate correction may lead to artificial observations of drug induced QT interval changes. *Pacing Clin. Electrophysiol.* **25**, 209–216 (2002).
22. Rabkin, S. W. & Cheng, X. B. Nomenclature, categorization and usage of formulae to adjust QT interval for heart rate. *World J. Cardiol.* **7**, 315–325 (2015).
23. Guideline, I. C. H. Safety pharmacology studies for human pharmaceuticals S7A. *Fed. Regist.* **66**, 36791–36792 (2001).
24. Hume, R. Prediction of lean body mass from height and weight. *J. Clin. Path.* **19**, 389–391 (1966).
25. Malik, M. *et al.* Thorough QT/QTc Study in patients with advanced Parkinson's disease: Cardiac safety of rotigotine. *Clin. Pharmacol. Therap.* **84**, 595–603 (2008).
26. Malik, M. *et al.* Proarrhythmic safety of repeat doses of mirabegron in healthy subjects: A randomized, double-blind, placebo-, and active-controlled thorough QT study. *Clin. Pharm. Therap.* **92**, 696–706 (2012).
27. Hnatkova, K. *et al.* Systematic comparisons of electrocardiographic morphology increase the precision of QT interval measurement. *Pacing Clin. Electrophysiol.* **32**, 119–130 (2009).
28. Malik, M. Errors and misconceptions in ECG measurement used for the detection of drug induced QT interval prolongation. *J. Electrocardiol.* **37**(Suppl), 25–33 (2004).
29. Xue, J. Q. Robust QT interval estimation: From algorithm to validation. *Ann. Noninvasive Electrocardiol.* **14**(Suppl 1), S35–S41 (2009).
30. Malik, M., Hnatkova, K., Kowalski, D., Keirns, J. J. & van Gelderen, E. M. QT/RR curvatures in healthy subjects: Sex differences and covariates. *Am. J. Physiol. Heart Circ. Physiol.* **305**, H1798–H1806 (2013).
31. Malik, M., Hnatkova, K., Novotny, T. & Schmidt, G. Subject-specific profiles of QT/RR hysteresis. *Am. J. Physiol. Heart Circ. Physiol.* **295**, H2356–H2363 (2008).
32. Bazett, J. C. An analysis of time relations of electrocardiograms. *Heart* **7**, 353–367 (1920).
33. Fridericia, L. S. Die Systolendauer im Elektrokardiogramm bei normalen Menschen und bei Herzkranken. *Acta Med. Scand.* **53**, 469–486 (1920).
34. Dmitrienko, A. A. *et al.* Electrocardiogram reference ranges derived from a standardized clinical trial population. *Drug Inf. J.* **39**, 395–405 (2005).
35. Sagie, A., Larson, M. G., Goldberg, R. J., Bengtson, J. R. & Levy, D. An improved method for adjusting the QT interval for heart rate (the Framingham study). *Am. J. Cardiol.* **70**, 797–801 (1992).
36. Schlamowitz, I. An analysis of time relationship within cardiac cycle in electrocardiogram in normal men: The duration of the QT interval and its relationship to the cycle length (RR interval). *Am. Heart J.* **31**, 329–342 (1946).
37. Hodges, M., Salerno, D. & Erlien, D. Bazett's QT correction reviewed: Evidence that a linear QT correction for heart rate is better. *J Am Coll Cardiol* **1**, 694 (1983).
38. Ashman, R. The normal duration of the Q-T interval. *Am. Heart J.* **28**, 522–534 (1942).
39. Rautaharju, P. M., Warren, J. W. & Calhoun, H. P. Estimation of QT prolongation: A persistent, avoidable error in computer electrocardiography. *J. Electrocardiol.* **23**(Suppl), 111–117 (1990).
40. Sarma, J. S. M., Sarma, R. J., Bilitch, M., Katz, D. & Song, S. L. An exponential formula for heart rate dependence of QT interval during exercise and pacing in humans: Reevaluation of Bazett's formula. *Am. J. Cardiol.* **54**, 103–108 (1984).
41. Rabkin, S. W., Szefer, E. & Thompson, D. J. S. A new QT interval correction formulae to adjust for increases in heart rate. *JACC Clin. Electrophysiol.* **3**, 756–766 (2017).
42. <https://ars.els-cdn.com/content/image/1-s2.0-S2405500X16305199-mm1.pdf>
43. Täubel, J. *et al.* Single doses up to 800 mg of E-52862 do not prolong the QTc interval: A retrospective validation by pharmacokinetic-pharmacodynamic modelling of electrocardiography data utilising the effects of a meal on QTc to demonstrate ECG assay sensitivity. *PLoS ONE* **10**, e0136369. <https://doi.org/10.1371/journal.pone.0136369> (2015).
44. Hnatkova, K., Kowalski, D., Keirns, J. J., van Gelderen, E. M. & Malik, M. Reproducibility of QTc interval changes after meal intake. *J. Electrocardiol.* **48**, 194–202 (2015).
45. Gravel, H., Jacquemet, V., Dahdah, N. & Curnier, D. Clinical applications of QT/RR hysteresis assessment: A systematic review. *Ann. Noninvasive Electrocardiol.* **23**, e12514. <https://doi.org/10.1111/anec.12514> (2018).

46. Malik, M., Johannesen, L., Hnatkova, K. & Stockbridge, N. Universal correction for QT/RR hysteresis. *Drug Saf.* **39**, 577–588 (2016).
47. Malik, M., Hnatkova, K., Kowalski, D., Keirns, J. J. & van Gelderen, E. M. Importance of subject-specific QT/RR curvatures in the design of individual heart rate corrections of the QT interval. *J. Electrocardiol.* **45**, 571–581 (2012).
48. Vandenberk, B. *et al.* Which QT correction formulae to use for QT monitoring?. *J. Am. Heart Assoc.* **5**, e003264. <https://doi.org/10.1161/JAHA.116.003264> (2016).
49. Malik, M., Hnatkova, K. & Batchvarov, V. Differences between study-specific and subject-specific heart rate corrections of the QT interval in investigations of drug induced QTc prolongation. *Pacing Clin. Electrophysiol.* **27**, 791–800 (2004).
50. Malik, M. *et al.* Implications of individual QT/RR profiles-part 1: Inaccuracies and problems of population-specific QT/heart rate corrections. *Drug Saf.* **42**, 401–414 (2019).
51. Malik, M., Färbon, P., Batchvarov, V., Hnatkova, K. & Camm, A. J. Relation between QT and RR intervals is highly individual among healthy subjects: Implications for heart rate correction of the QT interval. *Heart* **87**, 220–228 (2002).
52. Linde, C. *et al.* Sex differences in cardiac arrhythmia: A consensus document of the European Heart Rhythm Association, endorsed by the Heart Rhythm Society and Asia Pacific Heart Rhythm Society. *Europace* **20**, 1565ao–151565 (2018).
53. Fujiki, A., Yoshioka, R. & Sakabe, M. Evaluation of repolarization dynamics using the QT-RR regression line slope and intercept relationship during 24-h Holter ECG. *Heart Vessels* **30**, 235–240 (2015).
54. Hnatkova, K. & Malik, M. “Optimum” formulae for heart rate correction of the QT interval. *Pacing Clin. Electrophysiol.* **22**, 1683–1687 (1999).
55. Malik, M. *et al.* Sample size, power calculations, and their implications for the cost of thorough studies of drug induced QT interval prolongation. *Pacing Clin. Electrophysiol.* **27**, 1659–1669 (2004).
56. Indik, J. H., Pearson, E. C., Fried, K. & Bazett, W. R. L. Fridericia QT correction formulas interfere with measurement of drug-induced changes in QT interval. *Heart Rhythm* **3**, 1003–1007 (2006).
57. Malik, M. Methods of subject-specific heart rate corrections. *J. Clin. Pharmacol.* **58**, 1020–1024 (2018).
58. Hnatkova, K., Johannesen, L., Vicente, J. & Malik, M. Heart rate dependency of JT interval sections. *J. Electrocardiol.* **50**, 814–824 (2017).
59. Andršová, I. *et al.* Problems with Bazett QTc correction in paediatric screening of prolonged QTc interval. *BMC Pediatr.* **20**, 558. <https://doi.org/10.1186/s12887-020-02460-8> (2020).
60. Johannesen, L. *et al.* Quantitative understanding of QTc prolongation and gender as risk factors for torsade de pointes. *Clin. Pharmacol. Therap.* **103**, 304–309 (2018).
61. Wolbrette, D. Antiarrhythmic drugs: Age, race, and gender effects. *Card Electrophysiol. Clin.* **2**, 369–378 (2010).
62. Gonzalez, R. *et al.* Sex and age related differences in drug induced QT prolongation by dofetilide under reduced repolarization reserve in simulated ventricular cells. *Annu. Int. Conf. IEEE Eng. Med. Biol. Soc.* **2010**, 3245–3248 (2010).
63. Pueyo, E. *et al.* Characterization of QT interval adaptation to RR interval changes and its use as a risk-stratifier of arrhythmic mortality in amiodarone-treated survivors of acute myocardial infarction. *IEEE Trans. Biomed. Eng.* **51**, 1511–1520 (2004).
64. Batchvarov, V. N. *et al.* QT-RR relationship in healthy subjects exhibits substantial intersubject variability and high intrasubject stability. *Am. J. Physiol. Heart Circ. Physiol.* **282**, H2356–H2363 (2002).
65. Hnatkova, K. *et al.* Errors of fixed QT heart rate corrections used in the assessment of drug-induced QTc changes. *Front Physiol.* **10**, 635. <https://doi.org/10.3389/fphys.2019.00635> (2019).
66. Cirincione, B., Sager, P. T. & Mager, D. E. Influence of meals and glycemic changes on QT interval dynamics. *J. Clin. Pharmacol.* **57**, 966–976 (2017).
67. Sampedro-Puente, D. A. *et al.* Time course of low-frequency oscillatory behavior in human ventricular repolarization following enhanced sympathetic activity and relation to arrhythmogenesis. *Front Physiol.* **10**, 1547. <https://doi.org/10.3389/fphys.2019.01547> (2020).
68. Malik, M., Hnatkova, K., Schmidt, A. & Smetana, P. Accurately measured and properly heart-rate corrected QTc intervals show little daytime variability. *Heart Rhythm* **5**, 1424–1431 (2008).
69. Andršová, I. *et al.* Heart rate influence on the QT variability risk factors. *Diagnostics* **10**, 1096. <https://doi.org/10.3390/diagnostic10121096> (2020).
70. Copie, X. *et al.* Predictive power of increased heart rate versus depressed left ventricular ejection fraction and heart rate variability for risk stratification after myocardial infarction: Results of a two-year follow-up study. *J. Am. Coll. Cardiol.* **27**, 270–276 (1996).
71. Seravalle, G. & Grassi, G. Heart rate as cardiovascular risk factor. *Postgrad. Med.* **132**, 358–367 (2020).
72. Pueyo, E., Smetana, P., Laguna, P. & Malik, M. Estimation of the QT/RR hysteresis lag. *J. Electrocardiol.* **36**(Suppl), 187–190 (2003).
73. Halámek, J. *et al.* Use of a novel transfer function to reduce repolarization interval hysteresis. *J. Interv. Card Electrophysiol.* **29**, 23–32 (2010).
74. Gravel, H., Curnier, D., Dahdah, N. & Jacquemet, V. Categorization and theoretical comparison of quantitative methods for assessing QT/RR hysteresis. *Ann. Noninvasive Electrocardiol.* **22**, e12463. <https://doi.org/10.1111/anec.12463> (2017).

## Author contributions

Study design I.A., K.H., M.M., Software development K.H., M.M., ECG interpretation G.S., I.A., K.M.H., M.Š., O.T., P.B., P.S., T.N., ECG measurement G.S., I.A., K.M.H., M.Š., O.T., P.B., P.S., T.N., Supervision of the measurements G.S., T.N., O.T., P.S., Quality control of the measurements G.S., M.M., T.N., Statistics and figures K.H., M.M., Initial manuscript draft I.A., K.H., M.M., Final manuscript G.S., I.A., K.H., K.M.H., M.M., M.Š., O.T., P.B., P.S., T.N., Approval of the submission G.S., I.A., K.H., K.M.H., M.M., M.Š., O.T., P.B., P.S., T.N.

## Funding

Supported in part by the British Heart Foundation New Horizons Grant NH/16/2/32499, by Ministry of Health, Czech Republic, conceptual development of research organization (Grant FNBr/65269705), and by the Specific Research of Masaryk University MUNI/A/1446/2019.

## Competing interests

The authors declare no competing interests.

## Additional information

**Correspondence** and requests for materials should be addressed to M.M.

**Reprints and permissions information** is available at [www.nature.com/reprints](http://www.nature.com/reprints).

**Publisher's note** Springer Nature remains neutral with regard to jurisdictional claims in published maps and institutional affiliations.



**Open Access** This article is licensed under a Creative Commons Attribution 4.0 International License, which permits use, sharing, adaptation, distribution and reproduction in any medium or format, as long as you give appropriate credit to the original author(s) and the source, provide a link to the Creative Commons licence, and indicate if changes were made. The images or other third party material in this article are included in the article's Creative Commons licence, unless indicated otherwise in a credit line to the material. If material is not included in the article's Creative Commons licence and your intended use is not permitted by statutory regulation or exceeds the permitted use, you will need to obtain permission directly from the copyright holder. To view a copy of this licence, visit <http://creativecommons.org/licenses/by/4.0/>.

© The Author(s) 2021

Práce jednoznačně potvrzuje, že Bazettova korekce jeví největší nadhodnocování QTc intervalu při vyšších SF a podobně podhodnocuje QTc při nižších SF. Tento korekční vzorec může tedy vést k falešně patologickým hodnotám i u zcela zdravých jedinců, a podobně k falešně normálním hodnotám u pacientů, u kterých je prodloužený QT interval kombinován s pomalou SF. V klinické praxi by proto neměl být používán a měl by být nahrazen méně chybovým vzorcem dle Fridericii či Framinghamskou korekcí. Zajímavostí jistě je, že pokud původně publikovaná data EKG měření Bazettovy práce zpracujeme pomocí jednoduché regresní analýzy, výsledná korekční rovnice se více blíží korekci dle Fridericii, než druhé odmocnině RR.<sup>60</sup>

### **3.3. QT/RR v dětské populaci**

Výše popsané práce se věnovaly převážně chování QT intervalu v dospělé populaci, ve které jsou k dispozici již stanovené fyziologické hodnoty korigovaného QT intervalu. Patologické prodloužení QT intervalu je patognomické pro LQTS, který je zmíněn výše jako jeden z možných modelových příkladů arytmogeneze. Délka QT intervalu se liší u dospělých žen a mužů, za fyziologické jsou považovány hodnoty QTc do 460 ms u žen a do 440 ms u mužů. Tyto hodnoty jsou ale závislé na měřené SF neboť rozdíly mezi ženami a muži se snižují s rostoucí SF.<sup>61</sup> Proto lze u zejména starších mužů, kteří mají vyšší klidovou SF, považovat hodnoty do 450 ms za fyziologické.

U malých dětí není tento pohlavně vázaný rozdíl QT intervalu vyjádřen a překvapivě více než 100 let od zavedení EKG nebylo zcela známo, v jakém věku dochází k rozvoji pohlavních rozdílů ani jaký je jejich charakter. Při běžných krátkých EKG záznamech (10 sekund) nelze hodnotit vliv změn SF na QT interval, což neumožní detailní zhodnocení diskrétních změn QT intervalu. Teprve nedávno se nám podařilo provést u více než 1000 dětí a adolescentů (věk 4-19 let) dlouhodobé záznamy 12-svodového EKG v průběhu jednoduchých autonomních provokačních manévrů a tak získat unikátní data, která naznačují, že v průběhu puberty dochází u chlapců ke zkrácení QTc o cca 15-20 ms, naproti tomu se u dívek QTc interval prodlouží o poněkud nižší hodnotu. Mechanismus však zatím není zcela jasný. Zatímco u chlapců k maximálním změnám hodnot QTc intervalu dochází v návaznosti na rozvoj sekundárních pohlavních znaků, u dívek k nejvýraznějšímu prodloužení QTc intervalu dojde až mezi 15. – 18. rokem života, ačkoli se u nich sekundární pohlavní znaky objevují již před 10. rokem věku. Detailnější informace pak přináší následující publikace.

**Andršová I**, Hnatkova K, Helánová K, Šišáková M, Novotný T, Kala P, Malik M. Individually rate corrected QTc intervals in children and adolescents. *Front Physiol* 2019;10:994. doi: 10.3389/fphys.2019.00994.

IF 3,367. Počet citací ve Web of Science 9

Původní práce - kvantitativní podíl uchazečky 60%: Návrh projektu, návrh struktury publikace, sběr EKG signálů, elektrokardiologická měření, interpretace statistických výsledků, text publikace.





# Individually Rate Corrected QTc Intervals in Children and Adolescents

Irena Andršová<sup>1</sup>, Katerina Hnatkova<sup>2</sup>, Kateřina Helánová<sup>1</sup>, Martina Šišáková<sup>1</sup>, Tomáš Novotný<sup>1</sup>, Petr Kala<sup>1</sup> and Marek Malik<sup>2\*</sup>

<sup>1</sup> Department of Internal Medicine and Cardiology, University Hospital Brno, Faculty of Medicine, Masaryk University, Brno, Czechia, <sup>2</sup> National Heart and Lung Institute, Imperial College London, London, United Kingdom

## OPEN ACCESS

### Edited by:

Marcel van der Heyden,  
University Medical Center Utrecht,  
Netherlands

### Reviewed by:

Wojciech Zareba,  
University of Rochester, United States  
Elise Laura Kessler,  
University Medical Center Utrecht,  
Netherlands

### \*Correspondence:

Marek Malik  
marek.malik@imperial.ac.uk

### Specialty section:

This article was submitted to  
Cardiac Electrophysiology,  
a section of the journal  
Frontiers in Physiology

**Received:** 27 May 2019

**Accepted:** 18 July 2019

**Published:** 02 August 2019

### Citation:

Andršová I, Hnatkova K,  
Helánová K, Šišáková M, Novotný T,  
Kala P and Malik M (2019) Individually  
Rate Corrected QTc Intervals  
in Children and Adolescents.  
*Front. Physiol.* 10:994.  
doi: 10.3389/fphys.2019.00994

Accurate evaluation of the appearance of QTc sex differences during childhood and adolescence is intricate. Inter-subject differences of individual QT/RR patterns make generic heart rate corrections inaccurate because of fast resting heart rates in children. The study investigated 527 healthy children and adolescents aged 4–19 years (268 females, 50.9%). All underwent continuous ECG 12-lead monitoring while performing postural changes during a 70-min investigative protocol to obtain QT interval measurements at different heart rates. On average, more than 1200 ECG measurements (QT interval and its 5-min history of preceding RR intervals) were made in each subject. Curvilinear QT/RR regression involving intra-individual correction for QT/RR hysteresis were calculated in each subject. The projection of the QT/RR regressions to the heart rate of 60 beats per minute defined individually corrected QTc intervals. In males, gradual QTc shortening by about 15 ms appeared during the ages of 13–19 years synchronously with the incidence of secondary sex signs ( $p = 0.016$ ). On the contrary, whilst gradual QTc prolongation by about 10 ms appeared in females, it occurred only during ages 16–19 years and was not related to the incidence of secondary sex signs ( $p = 0.18$ ). The study also showed that in children and adolescents, linear QT/RR models fit the intra-subject data significantly more closely than the log-linear models ( $p < 0.001$ ). The study speculates that hormonal shifts during puberty might be directly responsible for the QTc shortening in males but that QTc prolongation in females is likely more complex since it was noted to follow the appearance of secondary sex signs only after a considerable delay.

**Keywords:** age, sex differences, individual QT/RR patterns, QT/RR hysteresis, QTc interval, QT/RR slope

## INTRODUCTION

As recently reviewed in detail (Linde et al., 2018), there are substantial sex differences in many electrophysiology processes and characteristics. While many of the sex differences have important clinical implications, their physiologic origin is frequently insufficiently understood. Among others, as repeatedly observed (Linde et al., 2018), adult pre-menopausal females have higher resting heart rate and longer QTc interval compared to males of the same age. Based on large ECG collections, it was previously suggested that these changes occur during puberty which lead to the conclusion that sex hormones trigger these differences (Rautaharju et al., 1992;

Kurokawa et al., 2016). Indeed, the role of hormones was supported by other studies, e.g., by the observation that the sex of the recipient rather than that of the donor influences QTc sex differences after heart transplant (Novotný et al., 2014).

Nevertheless, the previous studies of the development of QTc interval during childhood and adolescence suffered from the problem of inaccurate heart rate correction. It is well known that in adults, the relationship between QT duration and the underlying heart rate is subject-specific with substantial differences between different individuals (Batchvarov et al., 2002) and that generic heart rate corrections (e.g., Bazett, Fridericia, or Framingham formulae) may lead to noticeable QTc inaccuracy if applied to QT intervals measured at heart rate considerably remote from 60 beats per minute (bpm) (Malik et al., 2002; Garnett et al., 2012). While it is not known whether similar inter-subject differences exist in children, fast resting heart rates are well recognized in young children (Sarganas et al., 2017). Generic QT heart rate corrections may therefore be highly imprecise in individual children (Hnatkova et al., 2019) while normative data obtained from population-based regressions between QT intervals and simultaneously measured heart rates (Rautaharju et al., 2014) might be influenced by substantial correction errors (Malik et al., 2019).

These methodological shortcomings impact not only on the physiologic understanding of the QTc development during childhood but may also lead to difficult judgment of QTc interval in borderline clinical cases. Having these problems in mind, we have designed a physiologic study of healthy school-age children and adolescents and recorded their continuous 12-lead electrocardiograms (ECG) during provocative maneuvers. This allowed us to study individual QT/RR profiles and to investigate their development and sex differences during childhood and adolescence.

## MATERIALS AND METHODS

### Investigated Population

Per protocol, the study investigated healthy children of school age with the aim of obtaining, in both sexes, uniform age distribution between the ages of 6–19 years. The recruitment was organized at six primary (including preparatory years) and secondary schools in northern and southern Moravia offering ECG-based health check. While every child or adolescent who agreed to participate was investigated, the data used in the analysis presented here excluded those who were on repolarization affecting drugs<sup>1</sup> or on hormonal contraceptives, and those with cardiac abnormality. The study protocol was approved by the Ethics Committee of the University Hospital Brno. All participants (if legally allowed to do so) or their parents or legal guardians gave informed written consent according to the Helsinki declaration.

Standard demographic data were collected in all participants; body mass index was calculated according to the formula  $W/H^2$

where  $W$  is the body weight in kilograms and  $H$  is body height in meters. Presence of secondary sex characteristics corresponding to recognized standards (Harlan et al., 1979, 1980; Mickey and Brooke, 2019) was detected by a combination of visual inspection and a questionnaire submitted by parents/guardians of the investigated subjects.

### Investigative Protocol

Continuous 12-lead ECG (SEER MC version 2, sampled at 1000 Hz) with electrodes in the Mason-Likar position was recorded in each participant during 70-min provocative postural maneuvering that consisted of supine, sitting, standing, supine, standing, sitting, and supine positions (in this order) each of 10-min duration. The sitting and standing positions were maintained without external support and the position changes were accomplished within less than 20 s.

Participants were investigated in the mid-morning hours in groups of up to 20 subjects of similar ages performing the positional changes at the same time. During the investigation, younger children listened to non-exciting age-appropriate stories, others were investigated in quiet noise-free environment.

To make the study practical, the ECG recordings were started before the provocative maneuvering and terminated afterward. Consequently, the duration of the ECG recordings before and after the provocative maneuvering differed in different subjects. During these times, the subjects were engaged in standard school activities excluding physical education. None of the participants smoked before or during the ECG recording.

### Electrocardiographic Measurements

For the purposes of the present investigation, all ECGs were divided into 10-s segments with 5-s overlap between adjacent segments. In each segment, QRS complexes were identified, and in each lead, representative P-QRS-T beatform was constructed by calculating sample-by-sample medians of superimposed beats. An algebraic composite of threshold, tangent, wavelet, and polynomial interpolation algorithms that provided pre-review QT assessment in previous studies (Malik et al., 2008a, 2012b) was used to obtain automatic QT interval measurements. The same algorithm of this composite method was used in all recordings of this study; i.e., there were no measurement differences between different study subjects and/or between different ECGs of the same subject. Consistency of QT interval measurements between neighboring (non-adjacent) segments was used to eliminate noise-influenced and other problematic QT values. In each subject, all non-eliminated QT measurements were subsequently adjusted by pattern-matching algorithms (Malik et al., 2004; Hnatkova et al., 2009) to ensure that QRS onset and T wave offset patterns of similar morphology were measured consistently.

For each QT interval measurement, individual RR intervals within the measured 10-s segment and in the preceding 5 min were identified and the sequence of their durations obtained. The accurate QRS detection needed for this purpose was based on a combination of automatic QRS detectors (Kohler et al., 2002;

<sup>1</sup><https://www.crediblemeds.org>

Pahlm and Sornmo, 1984; Kors et al., 1986) with visual control and manual corrections where appropriate.

## Heart Rate and QT/RR Hysteresis Correction

Using previously published technology (Malik et al., 2008a, 2012b), individual QT/RR patterns were investigated in each study participant including the curvilinear regression of the relationship. Since the QT interval duration depends on the underlying heart rate rather than on the rate of the immediately preceding heartbeat cycle (Franz et al., 1988), QT/RR hysteresis was taken into account. Hence, as previously published (Malik et al., 2012b), the assessment of QT/RR patterns was combined with subject-specific assessment of the QT/RR hysteresis profiles which were modeled using the exponential decay forms (Malik et al., 2008b).

Curvilinear models of the hysteresis-corrected QT/RR patterns were used to estimate the QT interval duration at RR interval of 1 s (i.e., at heart rate of 60 bpm). This was based on averaging individually corrected QT values of all measurements available in the given subject. The result of this averaging is further called the QTcI interval.

To estimate the importance of QT/RR hysteresis correction, QT/RR patterns were also investigated relating the QT interval measurements to the average of 3 RR intervals in the middle of the 10-s ECG segment in which the QT measurement was made as well as to the average of all RR intervals in this segment. The range of heart rates available in each subject (i.e., the “width” of heart-rate data allowing to study the subject-specific QT/RR pattern) was defined as the difference between the maximum and minimum hysteresis corrected heart rates for which the QT measurements were available.

To compare the hysteresis corrected QT/RR patterns between different study subjects, linear and log-linear regression models were further used in the forms  $QT_i = \beta_0 + \beta RR_i + \varepsilon_i$  and  $\log QT_i = \alpha_0 + \alpha \log RR_i + \varepsilon_i$ , respectively. Here  $QT_i$  and  $RR_i$  are mutually corresponding QT and RR interval measurements (expressed in seconds) in the given subject and in both formulae,  $\varepsilon_i$  are zero-centered normally distributed errors. The standard deviations or the  $\varepsilon_i$  errors (i.e., the individual-specific regression residuals) were used to compare the accuracy of both regression models. These models were used since, as well known, they lead to the QT correction formulae  $QTc = QT + \beta(1 - RR)$  and  $QTc = QT/RR^\alpha$ .

## Statistics and Data Presentation

Numerical data are presented as mean  $\pm$  standard deviation. Dependency of ECG measurements on age was investigated using linear regression models that were displayed together with the 95% confidence intervals (CI) of the regression lines. When the age dependency appeared non-linear, averages and standard deviations were calculated and compared in separate age bands <8 years, 7–9 years, 8–10 years, etc. up to 16–18 years, and >17 years (the overlaps were used to obtain sufficient case numbers in each band). Intra-subject differences of the QT/RR regression residuals were assessed by the non-parametric

Wilcoxon matched-pair test. Differences between females and males, differences between subjects showing and not showing secondary sex signs, and differences between males or females younger and older than a dichotomy age limit were investigated using non-parametric Kolmogorov–Smirnov test. Dichotomy age limits of 10, 11, . . . , 16 years were used. Statistical calculations were made in the SPSS Statistics 64-bit version 25 package (IBM, Armonk, NY, United States). *P*-values < 0.05 were considered statistically significant.

## RESULTS

### Population

After the call for participation, 555 subjects (295 females) were enrolled and underwent the investigative protocol. Of these, 27 (4.9%) had to be excluded because of potentially interfering drug therapy, cardiac structural congenital abnormalities (including those with a history of cardiac surgery), cardiac conduction abnormality, and (in one case) sex-transversal procedures. Of the remaining 528 subjects, further one (0.2%) was excluded because of technical failure.

The analysis reported here is thus based on 527 subjects. Of these, 268 were females and 259 were males. Secondary sex signs were observed in 182 (67.9%) and 145 (56.0%) of females and males, respectively. **Table 1** shows the characteristics of the investigated population in individual age groups. **Supplementary Figure 1** shows that, as expected, the body weight and height was similar between sexes of young age. With increasing age, males became taller and heavier compared to females. Body mass index (**Supplementary Figure 2**) was also increasing with advancing age but no significant difference between sexes was observed.

Altogether 19 subjects (3.6% of the investigated populations; 13 females and 6 males) have not completed the investigation protocol because of pre-syncopal episodes, nausea, or vomiting. Nevertheless, in all these subjects, sufficient ECG data were collected before such side-effects occurred. No ECG data potentially influenced by the side-effects were included in the analysis.

The ECG data reported are based on 642,003 measurements of the QT interval and of its 5-min RR interval history. On average, 1218 measurements were made per subject (**Table 1**).

**Supplementary Tables 1, 2** summarize electrocardiographic measurements (as presented in subsequent sections in more detail) in individual age groups.

### QT/RR Hysteresis

**Figure 1** shows examples documenting that the inclusion of QT/RR hysteresis led to substantially more tight relationship between the measured QT intervals and the underlying heart rate. This was verified by the regression residuals. With the incorporation of QT/RR hysteresis, the curvilinear QT/RR regression residuals (i.e., the spread of the QT data around the curvature of the relationship) were  $4.59 \pm 2.60$  ms and  $3.87 \pm 1.16$  ms in females and males, respectively ( $p < 0.001$ ). With the RR intervals averaged from the 10-s ECG segments, these residuals were  $7.05 \pm 2.40$  ms and  $6.73 \pm 1.64$  ms, whilst

TABLE 1 | Investigated population.

Age [years]	Females					Males				
	N	Sign	Height [cm]	Weight [kg]	ECG	N	Sign	Height [cm]	Weight [kg]	ECG
≤7	17	0	115.7 ± 5.2	20.5 ± 2.8	868 ± 353	15	0	119.1 ± 6.9	24.7 ± 7.4	1019 ± 348
7–8	14	1	128.1 ± 9.8	26.1 ± 3.9	1113 ± 501	14	0	128.5 ± 6.0	25.9 ± 3.5	1017 ± 389
8–9	23	1	132.5 ± 5.4	28.4 ± 4.1	1012 ± 455	18	0	135.4 ± 5.7	31.9 ± 5.6	1113 ± 301
9–10	15	5	139.2 ± 7.0	33.7 ± 6.3	1459 ± 501	11	0	141.9 ± 7.8	36.1 ± 8.6	1075 ± 442
10–11	23	7	144.2 ± 5.6	36.5 ± 5.6	1548 ± 501	24	1	145.0 ± 7.1	38.0 ± 8.1	1200 ± 489
11–12	15	12	149.9 ± 7.8	38.4 ± 7.5	1365 ± 493	24	9	150.3 ± 6.9	44.6 ± 9.7	1235 ± 431
12–13	22	18	159.1 ± 5.6	48.3 ± 10.3	1181 ± 419	29	20	160.6 ± 10	52.9 ± 12.5	1449 ± 430
13–14	23	22	160.8 ± 8.0	48.2 ± 6.1	1146 ± 401	20	16	163.5 ± 6.6	49.6 ± 9.2	1295 ± 602
14–15	22	22	166.2 ± 5.2	58.3 ± 12.7	1122 ± 435	16	13	173.7 ± 7.3	59.9 ± 10.7	1514 ± 388
15–16	34	34	165.8 ± 5.3	56.7 ± 7.5	1011 ± 448	33	31	177.8 ± 6.9	68.1 ± 9.7	1346 ± 501
16–17	28	28	167.6 ± 5.4	58.3 ± 6.7	1087 ± 340	20	20	180.0 ± 7.7	72.7 ± 8.6	1359 ± 478
17–18	11	11	173.5 ± 4.6	64.3 ± 12.6	1298 ± 672	16	16	182.2 ± 6.4	70.6 ± 9.2	1234 ± 378
>18	21	21	165.9 ± 7.3	57.0 ± 8.3	1054 ± 292	19	19	178.5 ± 6.5	70.4 ± 11.9	1519 ± 511

For each age bin, the table shows the number (N) of investigated females and males, the number of those showing secondary sex signs (Sign), their heights and weights in centimeters and kilograms, respectively, the number of ECG measurement per subject (ECG). Data are shown as mean ± standard deviation.

with the averages of three RR intervals, the residuals increased to  $9.34 \pm 2.56$  ms and  $9.04 \pm 1.97$  ms. All comparisons of these data were highly statistically significant ( $p < 0.001$  for all). **Figure 2** shows that the increase of the QT/RR regression residuals from the hysteresis corrected relationship to either RR interval averages over 10 s or RR interval averages over three heart cycles occurred in every study participant.

The top panel of **Figure 3** shows that in both females and males, the QT/RR regression residuals (hysteresis corrected) increased with increasing age. In both sexes, the increase was modest with an increase of 0.11 ms per year in females and 0.06 ms in males (both statistically significant,  $p < 0.01$ ). The bottom panel of **Figure 3** shows cumulative distributions of the QT/RR regression residuals in both sexes and demonstrates that both in females and males, the curvilinear relationship between the QT interval duration and the underlying heart rate was very tight (note that in both sexes, the median QT/RR residual was below 4 ms).

The extent of the QT/RR hysteresis is standardly expressed by its time constant defined as the time interval required for 95% of the adaptation of QT interval to occur after a heart rate change. The dependence of this hysteresis time constant on the age of study subjects is shown in **Figure 4**. The extent of the QT/RR hysteresis was independent of age and, on average, very close to the constant of 2 min.

Since in every subject, QT intervals were more closely related to the hysteresis corrected RR interval values compared to the other possible RR interval expressions, the measurements involving QT/RR hysteresis correction were used in the subsequent parts of the study.

## Heart Rate Changes

**Figure 5** shows the age-dependency of slowest and fastest heart rates at which the QT intervals were measured as well as of the intra-subject heart rate ranges over which the individual QT/RR patterns were assessed.

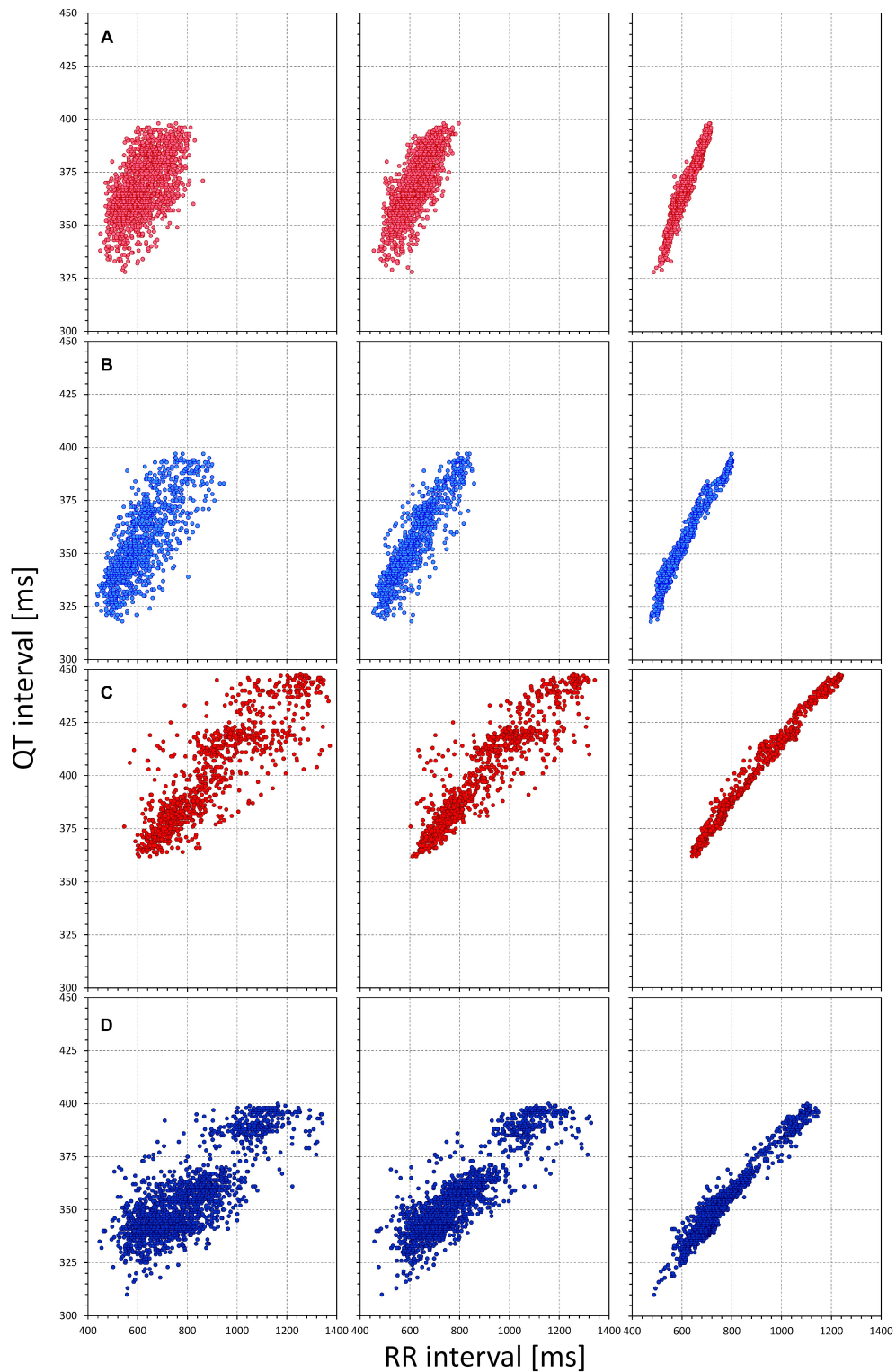
As expected, both the slowest and fastest heart rates were higher in younger children compared to adolescents (in both sexes, the minimum heart rates were decreasing by 1.9 bpm per year of age,  $p < 0.001$ ; the decrease of maximum heart rate was approximately 50% shallower but still highly statistically significant,  $p < 0.001$ ). Nevertheless, the bottom panel of **Figure 5** shows that in all study subjects, the heart rate spreads of QT/RR patterns were substantial. The individual QT/RR patterns were thus accurately defined.

## QTcI Interval

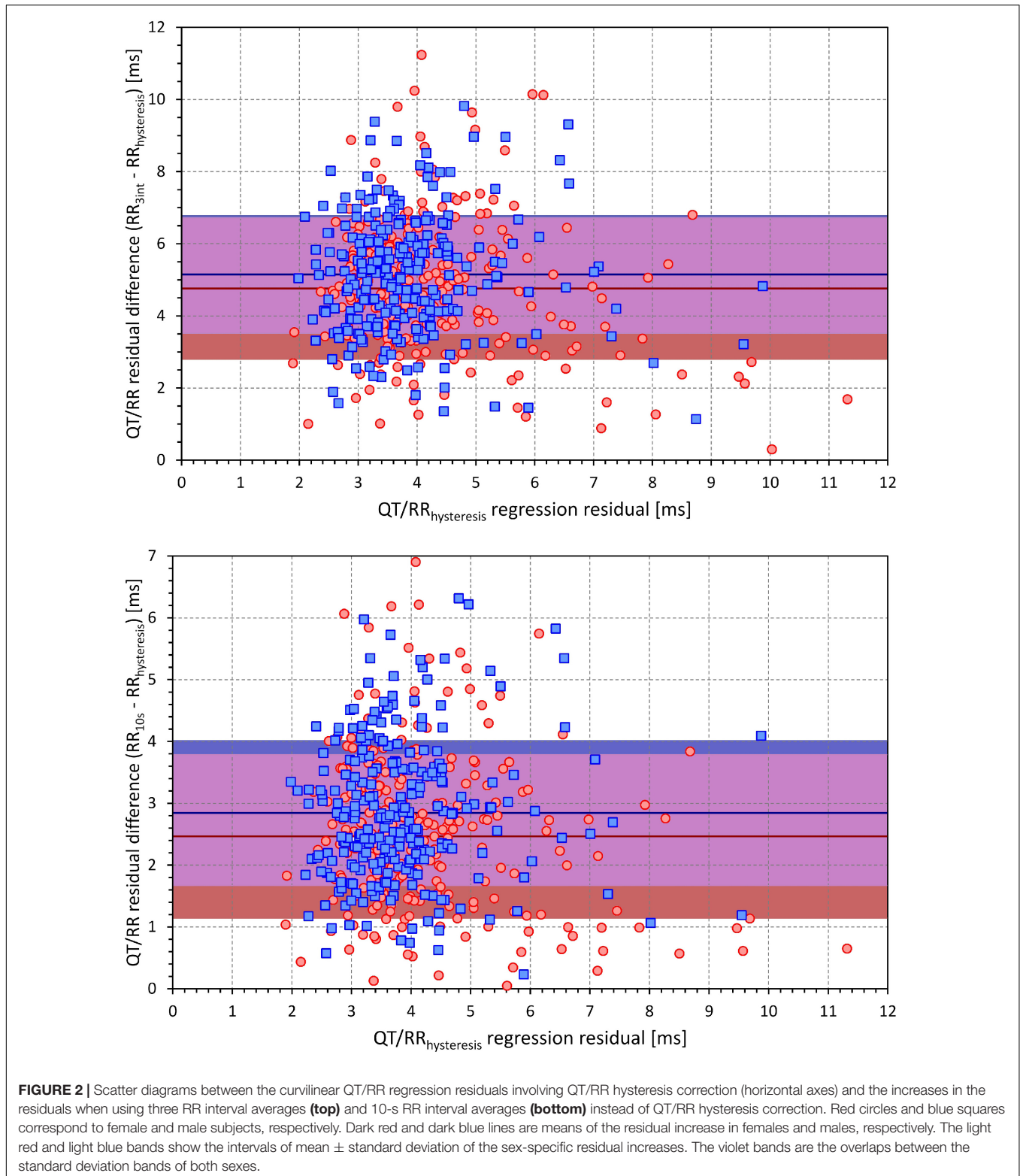
**Figure 6** shows the relationship of QTcI intervals to age which was one of the principal results of the study. In the linear regression analysis (top panel of **Figure 6**), there was significant of QTcI prolongation with advancing age in females (0.70 ms per year,  $p = 0.02$ ) and significant QTcI shortening with advancing age in males (0.64 ms per year,  $p = 0.03$ ).

Nevertheless, as shown in the middle panel of **Figure 6**, the change with age was highly non-linear. No clear differences between the sexes were found up till the age of approximately 12–13 years. From that age on, QTcI interval was gradually decreasing in males. In females, no obvious QTcI change was seen up till the age of approximately 16 years following which, the QTcI interval increased substantially. In the highest age bin of >17 years, the average QTcI differences between the sexes was 24.1 ms.

The surprising late onset of the QTcI change in females was confirmed by the comparison of QTcI distributions in subjects showing and not showing secondary sex signs, as demonstrated in the bottom panel of **Figure 6**. There was no difference between the distributions in females and males without secondary sex signs. The comparison between those with and without secondary sex signs led to only a non-significant trend in females ( $p = 0.181$ ) whilst in males, the same comparison resulted in a clear statistical significance ( $p = 0.016$ ). The sex difference



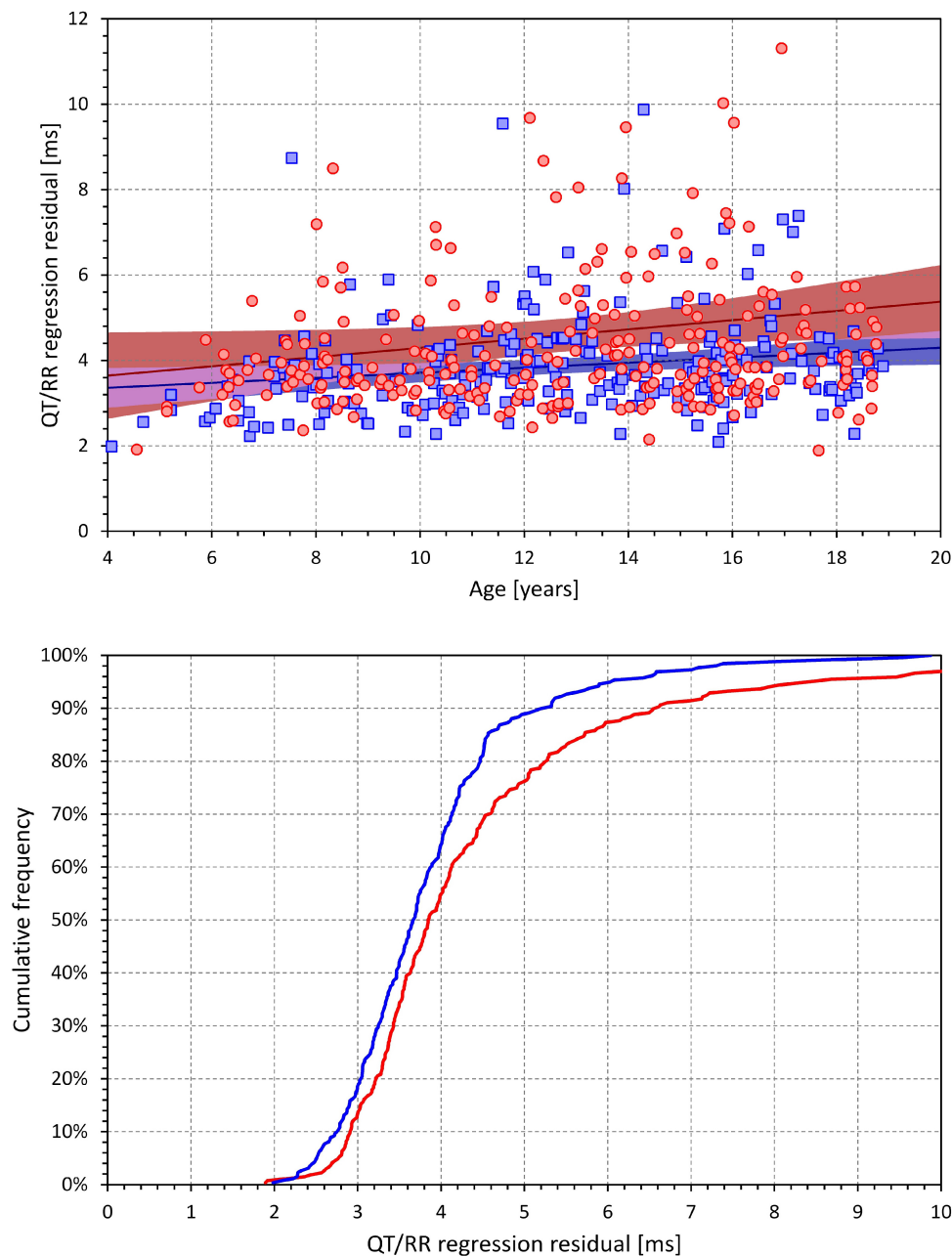
**FIGURE 1 |** The figure shows examples of comparisons of QT/RR relationship using different RR interval expressions. Each row of panels corresponds to one subject. In each subject, the QT interval measurements are the same but the panels on the left relate the QT intervals to the averages of three RR intervals, the panels in the middle to 10-s RR interval averages, and the panels of the right to the RR interval values obtained from the 5-min histories of the QT interval measurements by individual QT/RR hysteresis profiles. Note the increase of the regression fit from the left panels to the right panels. Cases (A–D) correspond to a female aged 7.4 years, a male aged 7.7 years, a female aged 18.7 years, and a male aged 18.7 years, respectively.



between females and males showing the secondary sex signs was highly significant ( $p < 0.001$ ).

When dichotomizing the population (females and males separately) into those younger and older than 10, 11, 12,

..., 16 years, the QTcI difference between older and younger males appeared at the dichotomy of 13 years ( $p = 0.001$ ) and was maintained in subsequent dichotomies ( $p < 0.001$  for all dichotomies of 14, 15, and 16 years). On the contrary, the QTcI



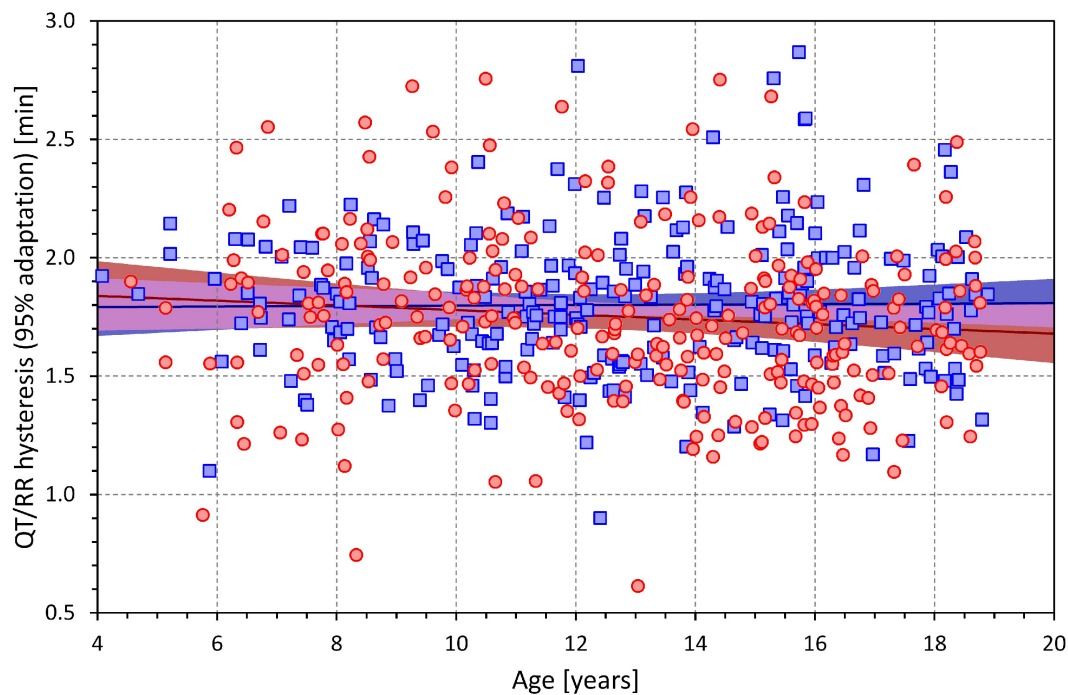
**FIGURE 3 |** The (top) panel show the age dependency of the curvilinear QT/RR regression residuals. The red circles and blue squares correspond to the female and male subjects, respectively. The dark red and dark blue lines are linear regressions in females and males, respectively; the light red and light blue areas are the 95% confidence bands of the sex-specific linear regression lines. The violet areas are the overlaps between the confidence bands of the regression lines of both sexes. The (bottom) panel shows the cumulative distributions of QT/RR regression residuals in female (bold red line) and male (bold blue line) subjects.

difference between younger and older females was not significant for all dichotomies 10–15 years and became only significant at the dichotomy of 16 years ( $p = 0.014$ ).

### QT/RR Dependency

By definition, both linear and log-linear regressions are bound to lead to larger QT/RR residuals compared to the curvilinear regressions (that is, the linear and log-linear QT/RR regression

models cannot fit the data as closely as the curvilinear regressions). Nevertheless, in both sexes, the increases of QT/RR residuals from curvilinear to linear models ( $0.16 \pm 0.30$  ms and  $0.12 \pm 0.24$  ms in females and males, respectively) were significantly smaller compared to the residual increases from curvilinear to log-linear models ( $0.89 \pm 0.63$  ms and  $0.65 \pm 0.30$  ms in females and males, respectively;  $p < 0.001$  for comparisons in both sexes). The increases of the residuals from



**FIGURE 4** | Age dependency of the intra-subject QT/RR hysteresis time constants (i.e., time intervals needed for 95% adaptation of QT interval duration after heart rate change). The layout and symbol definition are the same as in **Figure 3**.

the curvilinear models were also significantly smaller in males compared to females ( $p = 0.02$  for linear models,  $p < 0.001$  for log-linear models).

Consequently, the linear models described the individual QT/RR relationships better compared to log-linear models and were used in the analysis of age dependency. The corresponding results are shown in **Figure 7**. In both sex groups, the QT/RR patterns became gradually shallower with advancing age (for both sexes  $p < 0.005$ ; linear regression of QT/RR slopes vs. age). The middle panel of **Figure 7** shows that this age effect was again non-linear with the age effect visible in both sexes from approximately 13 years onward. The bottom panel of **Figure 7** shows sex-specific trends to shallower QT/RR slopes in subjects with secondary sex signs (compared to those without the signs) as well as trends to shallower QT/RR slopes in males compared to females (irrespective of the secondary sex signs) but none of these trends was statistically significant.

Corresponding analysis of the log-linear slopes is shown in **Figure 8**. This shows that the log-linear slopes led to erratic results, probably caused by the significantly lesser precision of the log-linear analysis.

## DISCUSSION

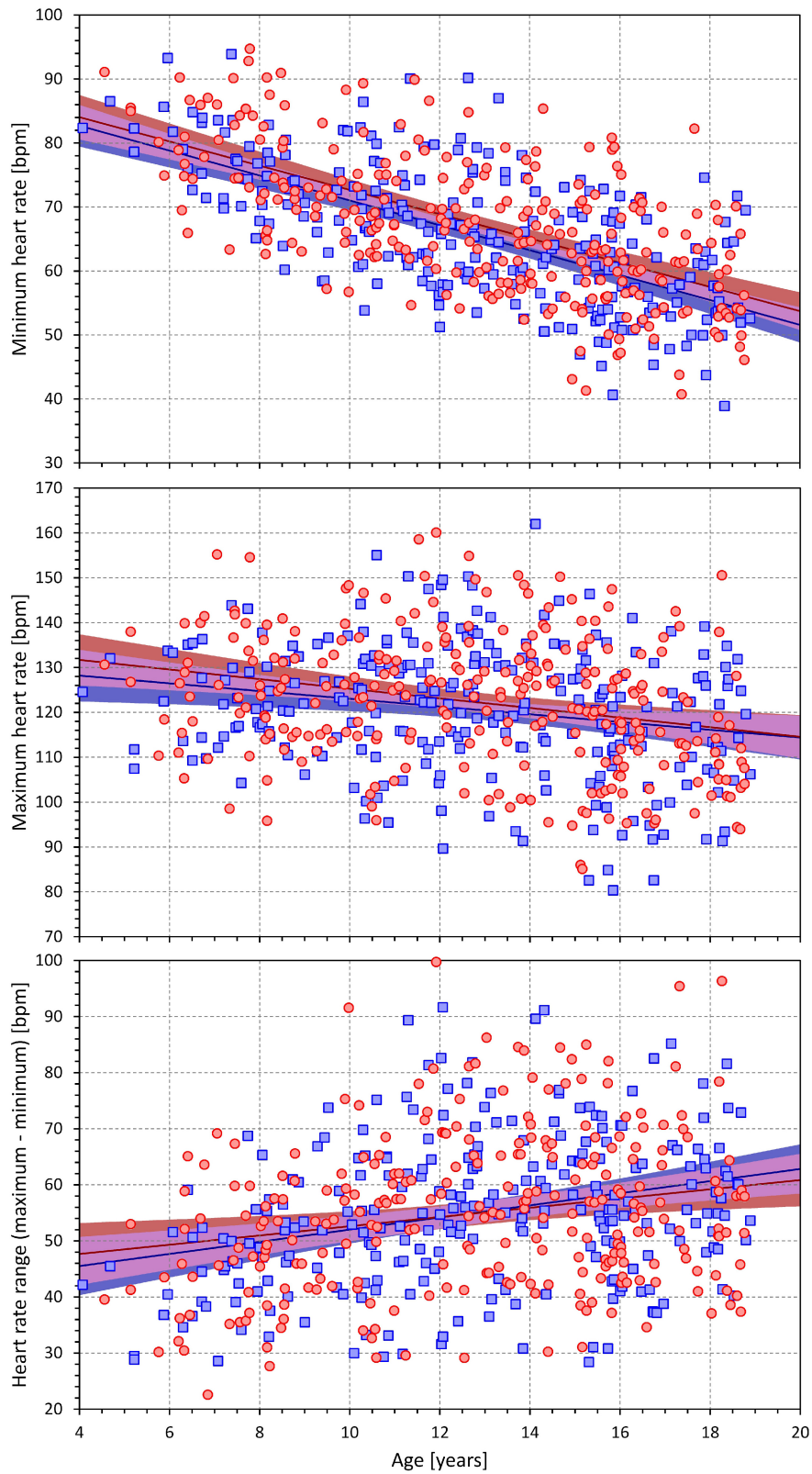
The results of the study show that during puberty, the known sex difference in QTc interval does not appear at the same time as secondary sex signs. Whilst, as expected, we observed earlier onset of secondary sex signs in females

compared to males (Mickey and Brooke, 2019), statistically significant QTc changes in females occurred some 3 years later compared to males (in addition to the statistical tests presented, compare also the middle panel of **Figure 6** with **Figure 9** that shows the development of incidence of secondary sex signs). Purely speculatively, this may suggest that simple hormonal shifts during puberty might be responsible for the QTc shortening in males but are unlikely the principal direct cause of QTc prolongation in females. If our observation is independently confirmed, other mechanisms need to be considered and researched, including the long-term pubertal conditioning, prolonged adaptation to perioding menstruation blood loss, or central and autonomic regulation changes. Indeed, the stability of menstrual cycle appears also after a considerable delay, perhaps similar to the delay that we observed with QTc prolongation, after the appearance of menarche (Lenton et al., 1984; Apter et al., 1987). Thus, while hormonal shifts might still contribute to the QTc prolongation in females, the mechanisms responsible for these repolarization changes are likely more intricate compared to the QTc shortening in males.

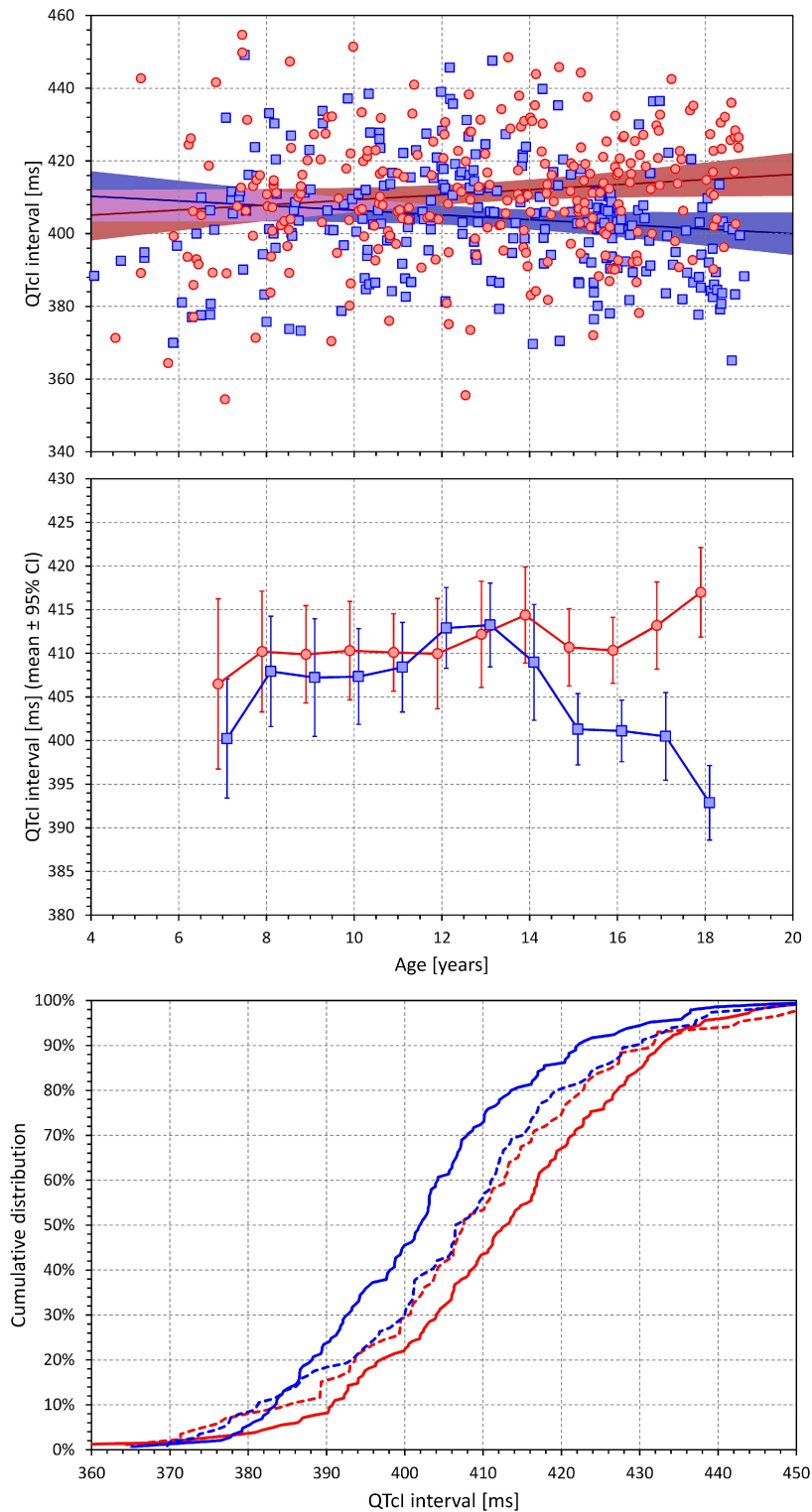
The study also shows that with simple postural maneuvering, wide heart rate spans known from clinical studies in adults (Malik et al., 2012b) may also be achieved in relatively young children. This has implications for studying the subject-specific QT/RR profiles that might be helpful when judging borderline cases of QTc interval abnormalities.

While the QT interval and heart rate data of this study might theoretically be also analyzed using previously proposed

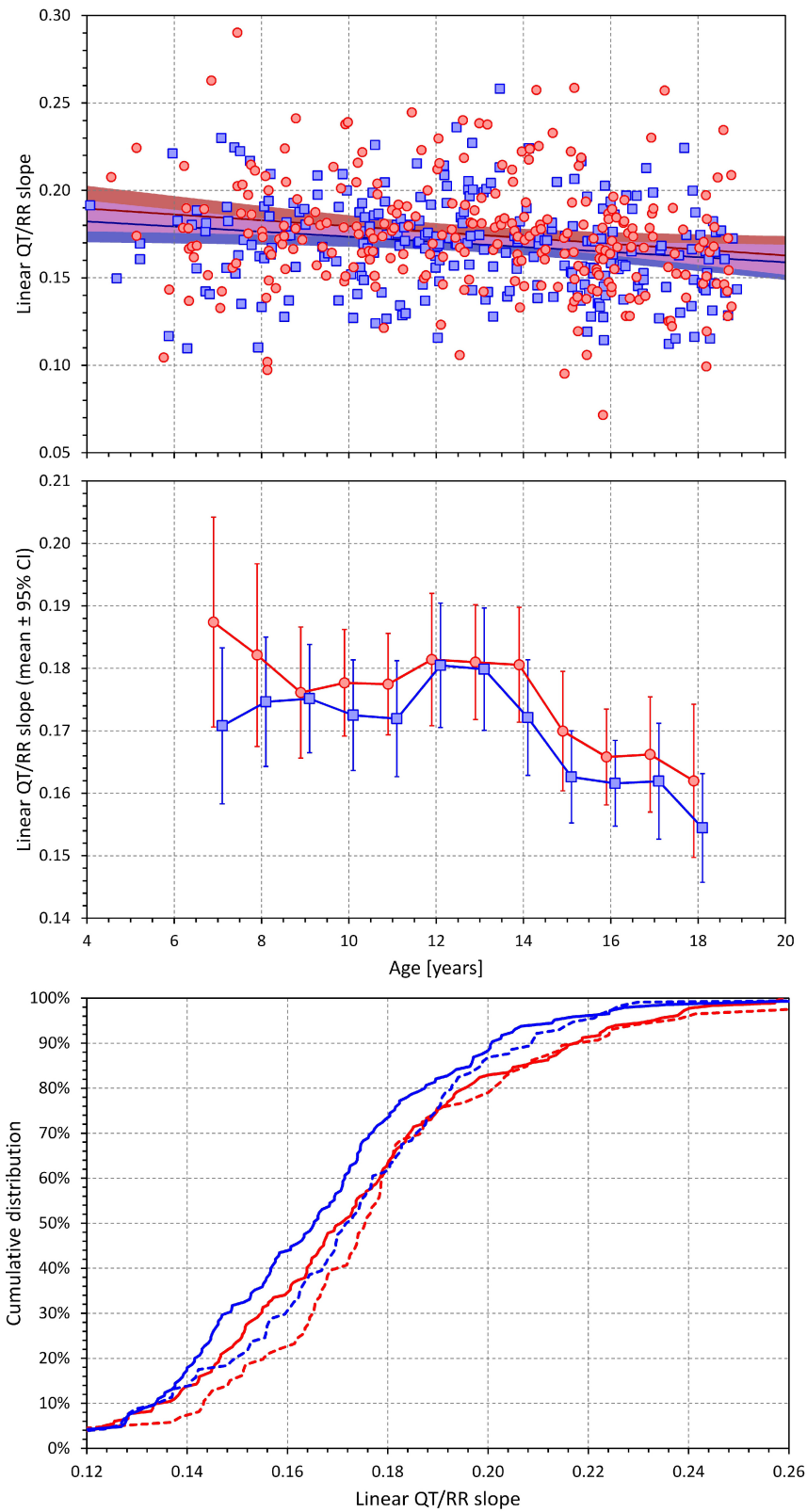




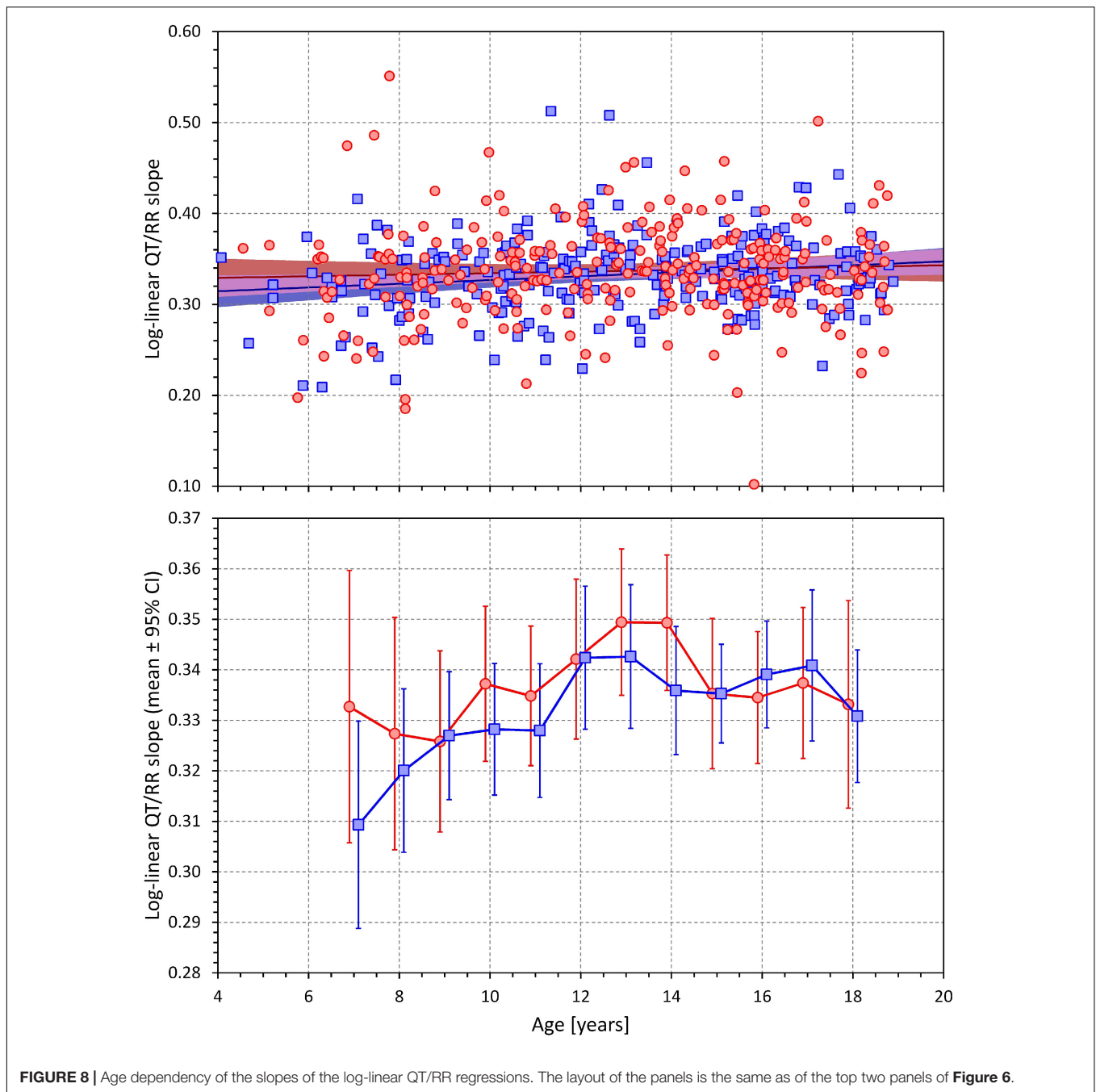
**FIGURE 5 |** Scatter diagrams between the age and minimum heart rate (**top**) maximum heart rate (**middle**) and the range between the minimum and maximum heart rate (**bottom**). The layout and symbol definition in each panel are the same as in **Figure 3**.



**FIGURE 6 |** The **(top)** panel shows the scatter diagram between age and QTcI interval (see the legend of **Figure 2** for symbol explanations). The **(middle)** panel shows the averages of QTcI intervals in age bands <8 years, 7–9 years, 8–10 years, etc. up to 16–18 years, and > 17 years (each shown approximately at the middle age of the band). The error bars are the corresponding standard deviations. The red and blue marks correspond to the females and males, respectively. The **(bottom)** panel shows the cumulative distributions of QTcI intervals in subjects without (dashed lines) and with (full lines) secondary sex signs. The red and blue lines again correspond to females and males, respectively.

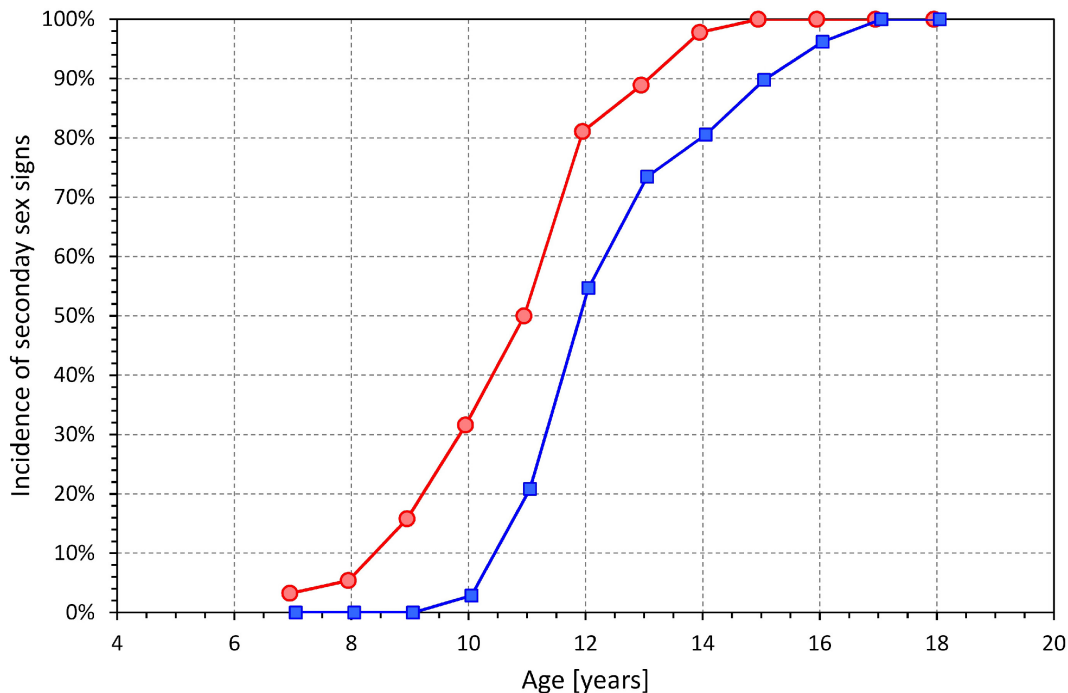


**FIGURE 7 |** Development of the age dependency of linear QT/RR slopes in both sexes. The layout and meaning of the three panels are the same as the layout and meaning of the three panels of **Figure 6**.



general correction formulae (e.g., Bazett, Fridericia, Hodges, or Framingham corrections), we have intentionally omitted such analyses since they would not only be inaccurate but potentially also highly misleading. It has recently been demonstrated (Hnatkova et al., 2019) that in the presence of heart rate changes exceeding 10 bpm, the use of fixed heart rate corrections might be substantially erroneous. The individually corrected QTc values that we obtained in this population were derived from averages over heart rate spans that well exceeded this “safety” limit (see **Figure 5**). In addition, the age-related changes in slopes of the QT/RR profiles further suggest that the experience with

QTc heart rate correction formulae obtained in adult patients cannot be directly translated to accurate studies and/or clinical evaluations in children. In particular, the significantly worse log-linear regression fits of QT/RR profiles show that formulae based on this type of regression (e.g., Bazett or Fridericia corrections) are potentially highly misleading in individual clinical cases of school-aged children. Also, at fast rates as observed in younger children, the log-linear QT/RR relationship breaks down because the short uncorrected QT interval measurements (Hnatkova et al., 2017) making the use of formulae based on this relationship even more problematic.



**FIGURE 9** | Incidence of secondary sex signs in age bands <8 years, 7–9 years, 8–10 years, etc. up to 16–18 years, and >17 years (each shown approximately at the middle age of the band). Compare with the development of QTcI changes shown in the middle panel of **Figure 6**.

The observation that taking QT/RR hysteresis (Malik et al., 2008b; Gravel et al., 2018) into account decreases the QT/RR residuals and thus increases accuracy of the QTcI assessment is consistent with previous observations in adults. It was previously shown that considerations of QT/RR hysteresis are not only essential during episodes of heart rate changes (Malik et al., 2016; Hnatkova et al., 2019) but also valuable during episodes without any physical activity since psychologically driven fluctuations of heart rate can hardly ever be eliminated (Malik et al., 2016, 2018). In the present study, short-term variability of heart rate, likely influenced by mental reactions, was also present during the individual episodes of the investigative protocol. The observations shown in **Figure 1** were therefore not driven solely by the implications of the postural changes.

In agreement with previously published adult data (Malik et al., 2004, 2012b, 2013), we found only miniscule curvilinear QT/RR residuals (see the bottom panel of **Figure 3**). This means, among others, that in separate study individuals, the individually corrected QTc interval was practically constant during the postural provocations (detailed comparison not shown) and that the minimal variability along the curvilinear QT/RR regressions was only caused by the measurement jitter due to recordings noise. The QTcI values shown in **Figure 6** and **Supplementary Table 2** are thus applicable to different parts of the investigation experiments. Thus, similar to adult data (Malik et al., 2008c, 2013), we found the QT interval duration to be practically exclusively determined by the underlying heart rate (including

the considerations of the QT/RR hysteresis) during these experiments in children and adolescents. Note also that the intra-individual QTcI stability was achieved by the sufficiently large intra-individual heart rate ranges over which the QT measurements were made and over which the QT/RR regressions were calculated.

We are not aware of other studies of individual-specific QT/RR profiles in children and adolescents with which we could compare the results of this study. Nevertheless, number of comparisons with adult data are possible. The averaged hysteresis constant close to 2 min is the same as previously reported based on adult investigations (Franz et al., 1988; Malik et al., 2008b). Clinical investigations in young to middle-aged adults found similar spans of minimal to maximal heart rates in response to similar postural maneuvering (Malik et al., 2012b). Like the adult studies, the investigated children and adolescents showed remarkable inter-subject variability of QT/RR profiles (Batchvarov et al., 2002; Malik et al., 2002). The comparison between the linear and log-linear QT/RR regressions is also known to have led to similar conclusions in adult data (Malik et al., 2012a).

Although we do not have detailed measurements of heart sizes available, it is reasonable to expect that as the body enlarges with advancing age (see **Supplementary Figures 1, 2**) so does the heart and ventricular mass. Nevertheless, this obviously cannot explain the QTc discrepancy between the sexes since with advancing age, the QTc interval changes differently in females and males. Also, while simple heart size might have some physiologic implications

for heart rate, the influence on QTc interval, if it exists, is bound to be more complex and likely multifaceted.

While we observed a slightly higher heart rates in females compared to males (see the top panel of **Figure 5**), the differences were much smaller than the sex distinction known in adult resting heart rates (Linde et al., 2018). The reasons are possibly similar to those for the discrepancy between the secondary sex-sign maturity in females and their QTc prolongation. Prolonged autonomic conditioning in menstruating females might be needed for the autonomic regulatory equilibrium (Smetana and Malik, 2013) responsible for increased heart rates in adult pre-menopausal females.

The QTcI calculation was based on the projection of intra-subject curvilinear QT/RR regressions to predict the QT interval duration at a stable heart rate of 60 bpm. While this projection corresponded to the standard practice of heart rate correction, it required extrapolation of available data in younger children in whom the minimum heart rate was much higher (see the top panel in **Figure 5**). The low regression residuals (obtained when considering QT/RR hysteresis) suggest that this process did not lead to any substantial imprecision but in future studies in pediatric populations, corrections of QT interval to a different heart rate (e.g., 80 bpm) might prove somewhat more reliable.

## Limitations

Limitations of the investigation also need to be considered. While we collected demographic data and made sure that only normal subjects without clinically apparent abnormalities were included in the analysis, we were unable (for funding reasons) to subject the participants to further testing such as echocardiography, biochemistry, or detailed anthropometric measurements. For the same reasons, we were unable to collect continuous blood pressure data. Single instance blood pressure measurements were not collected since in children, the “white coat” effects are highly noticeable. This prevents us from considering renin-angiotensin regulation. For ethical reasons, we were also unable to collect any data on mental comprehension that might potentially be important for the development of autonomic conditioning. Nevertheless, as far as we can tell, it was unlikely that cognitions skills among the participants would have shown any sex-related or age-related bias outside the standard expectations of human development. For practicality reasons, it was also impossible to synchronize the investigations with a particular phase of menstrual cycle in menstruating females. Nevertheless, data on the last menstruation were also collected and when it was attempted to analyze the data considering the menstruation cycle, no meaningful influence was found (data not shown). Our observations of a very tight relationship between the QT interval duration and the underlying (hysteresis corrected) heart rate were made during awake state. We cannot comment on the QT/RR relationship in children during sleep which is known to influence QTc duration in adults (Stramba-Badiale et al., 2000; Lanfranchi et al., 2002). Finally, while the accuracy of RR interval histories of QT interval measurements was visually validated and manually corrected where necessary, the measurements of QT intervals relied on automatic computerized processing with exclusion of noise polluted ECG episodes. Nevertheless, the markedly

low QT/RR regression residuals showed that the automatic QT interval measurement was fully reliable.

## CONCLUSION

Despite these limitations, the study shows that opposite QTc changes occur in both sexes during adolescent years. In the absence of detailed hormone level measurement, we can only speculate that while these QTc changes might be directly maintained by sex hormones in males, pure and direct sex hormone influence in females is less likely. The study also shows that tightly defined QT/RR patterns are achievable in children and adolescents by non-invasive postural testing. Since projection of such patterns may be used to compare the QT interval durations between different subjects, the described technique might be helpful in judging clinical cases of borderline QT interval abnormalities.

## DATA AVAILABILITY

All datasets generated for this study are included in the manuscript and/or the **Supplementary Files**.

## AUTHOR CONTRIBUTIONS

MM, TN, and IA conceived the study. IA, KHn, TN, and MM designed the study. IA, KHe, MŠ, and TN contributed to the clinical conduct. TN and PK supervised the clinical conduct. KHn and MM analyzed the data. IA, KHn, and MM drafted the manuscript. All authors approved the final manuscript.

## FUNDING

This research was supported in part by the British Heart Foundation New Horizons Grant NH/16/2/32499 and the Ministry of Health of the Czech Republic Grant NV19-02-00197.

## ACKNOWLEDGMENTS

We are grateful to the investigated subjects and their parents/guardians for their willingness to participate in this study. We are equally grateful for the kind help and support provided by the management and staff of the schools at which the recordings took place, namely Preparatory School Vedlejší, Brno; Preparatory School Údolní, Brno; Primary School Smetanův okruh, Krnov; Primary School Slovanské náměstí, Brno; Secondary and High School Smetanův okruh, Krnov; and Secondary and High School Slovanské náměstí, Brno.

## SUPPLEMENTARY MATERIAL

The Supplementary Material for this article can be found online at: <https://www.frontiersin.org/articles/10.3389/fphys.2019.00994/full#supplementary-material>

## REFERENCES

- Apter, D., Räisänen, I., Ylöstalo, P., and Vihko, R. (1987). Follicular growth in relation to serum hormonal patterns in adolescent compared with adult menstrual cycles. *Fertil. Steril.* 47, 82–88. doi: 10.1016/s0015-0282(16)49940-1
- Batchvarov, V. N., Ghuran, A., Smetana, P., Hnatkova, K., Harries, M., Dilaveris, P., et al. (2002). QT-RR relationship in healthy subjects exhibits substantial intersubject variability and high intrasubject stability. *Am. J. Physiol. Heart Circ. Physiol.* 282, H2356–H2363.
- Franz, M. R., Swerdlow, C. D., Liem, L. B., and Schaefer, J. (1988). Cycle length dependence of human action potential duration in vivo. Effects of single extrastimuli, sudden sustained rate acceleration and deceleration, and different steady-state frequencies. *J. Clin. Invest.* 82, 972–979. doi: 10.1172/jci113706
- Garnett, C. E., Zhu, H., Malik, M., Fossa, A. A., Zhang, J., Badilini, F., et al. (2012). Methodologies to characterize the QT/corrected QT interval in the presence of drug-induced heart rate changes or other autonomic effects. *Am. Heart J.* 163, 912–930. doi: 10.1016/j.ahj.2012.02.023
- Gravel, H., Jacquemet, V., Dahdah, N., and Curnier, D. (2018). Clinical applications of QT/RR hysteresis assessment: a systematic review. *Ann. Noninvasive Electrocardiol.* 23:e12514. doi: 10.1111/anec.12514
- Harlan, W. R., Grillo, G. P., Cornoni-Huntley, J., and Leaverton, P. E. (1979). Secondary sex characteristics of boys 12 to 17 years of age: the U.S. health examination survey. *J. Pediatr.* 95, 293–297.
- Harlan, W. R., Harlan, E. A., and Grillo, G. P. (1980). Secondary sex characteristics of girls 12 to 17 years of age: the U.S. health examination survey. *J. Pediatr.* 96, 1074–1078. doi: 10.1016/s0022-3476(80)80647-0
- Hnatkova, K., Johannesen, L., Vicente, J., and Malik, M. (2017). Heart rate dependency of JT interval sections. *J. Electrocardiol.* 50, 814–824. doi: 10.1016/j.jelectrocard.2017.08.005
- Hnatkova, K., Smetana, P., Toman, O., Bauer, A., Schmidt, G., and Malik, M. (2009). Systematic comparisons of electrocardiographic morphology increase the precision of QT interval measurement. *Pacing Clin. Electrophysiol.* 32, 119–130. doi: 10.1111/j.1540-8159.2009.02185.x
- Hnatkova, K., Vicente, J., Johannesen, L., Garnett, C., Stockbridge, N., and Malik, M. (2019). Errors of fixed QT heart rate corrections used in the assessment of drug-induced QTc changes. *Front. Physiol.* 10:635. doi: 10.3389/fphys.2019.00635
- Kohler, B. U., Henning, C., and Orglmeister, R. (2002). The principles of software QRS detection - Reviewing and comparing algorithms for detecting this important ECG waveform. *IEEE Eng. Med. Biol. Mag.* 21, 42–57.
- Kors, J. A., Talmon, J. L., and van Bommel, J. H. (1986). Multilead ECG analysis. *Comput. Biomed. Res.* 19, 28–46. doi: 10.1016/0010-4809(86)90004-2
- Kurokawa, J., Kodama, M., Clancy, C. E., and Furukawa, T. (2016). Sex hormonal regulation of cardiac ion channels in drug-induced QT syndromes. *Pharmacol. Ther.* 168, 23–28. doi: 10.1016/j.pharmthera.2016.09.004
- Lanfranchi, P. A., Shamsuzzaman, A. S., Ackerman, M. J., Kara, T., Jurak, P., Wolk, R., et al. (2002). Sex-selective QT prolongation during rapid eye movement sleep. *Circulation* 106, 1488–1492. doi: 10.1161/01.cir.0000030183.10934.95
- Lenton, E. A., Landgren, B. M., Sexton, L., and Harper, R. (1984). Normal variation in the length of the follicular phase of the menstrual cycle: effect of chronological age. *Br. J. Obstet. Gynaecol.* 91, 681–684. doi: 10.1111/j.1471-0528.1984.tb04830.x
- Linde, C., Bongiorno, M. G., Birgersdotter-Green, U., Curtis, A. B., Deisenhofer, I., Furokawa, T., et al. (2018). Sex differences in cardiac arrhythmia: a consensus document of the European Heart Rhythm Association, endorsed by the Heart Rhythm Society and Asia Pacific Heart Rhythm Society. *Europace* 20:1565–1565a0.
- Malik, M., Andreas, J.-O., Hnatkova, K., Hoekendörff, J., Cawello, W., Middle, W., et al. (2008a). Thorough QT/QTc study in patients with advanced Parkinson's disease: Cardiac safety of rotigotine. *Clin. Pharm. Therap.* 84, 595–603. doi: 10.1038/clpt.2008.143
- Malik, M., Hnatkova, K., Novotný, T., and Schmidt, G. (2008b). Subject-specific profiles of QT/RR hysteresis. *Am. J. Physiol. Heart Circ. Physiol.* 295, H2356–H2363. doi: 10.1152/ajpheart.00625.2008
- Malik, M., Hnatkova, K., Schmidt, A., and Smetana, P. (2008c). Accurately measured and properly heart-rate corrected QTc intervals show little daytime variability. *Heart Rhythm* 5, 1424–1431. doi: 10.1016/j.hrthm.2008.07.023
- Malik, M., Färbom, P., Batchvarov, V., Hnatkova, K., and Camm, A. J. (2002). Relation between QT and RR intervals is highly individual among healthy subjects: implications for heart rate correction of the QT interval. *Heart* 87, 220–228. doi: 10.1136/heart.87.3.220
- Malik, M., Garnett, C., Hnatkova, K., Johannesen, L., Vicente, J., and Stockbridge, N. (2018). Importance of QT/RR hysteresis correction in studies of drug-induced QTc interval changes. *J. Pharmacokin. Pharmacodyn.* 45, 491–503. doi: 10.1007/s10928-018-9587-8
- Malik, M., Garnett, C., Hnatkova, K., Vicente, J., Johannesen, L., and Stockbridge, N. (2019). Implications of individual QT/RR profiles - Part 1: Inaccuracies and problems of population-specific QT/heart rate corrections. *Drug Saf.* 42, 401–414. doi: 10.1007/s40264-018-0736-1
- Malik, M., Hnatkova, K., Batchvarov, V., Gang, Y., Smetana, P., and Camm, A. J. (2004). Sample size, power calculations, and their implications for the cost of thorough studies of drug induced QT interval prolongation. *Pacing Clin. Electrophysiol.* 27, 1659–1669. doi: 10.1111/j.1540-8159.2004.00701.x
- Malik, M., Hnatkova, K., Kowalski, D., Keirns, J. J., and van Gelderen, E. M. (2012a). Importance of subject-specific QT/RR curvatures in the design of individual heart rate corrections of the QT interval. *J. Electrocardiol.* 45, 571–581. doi: 10.1016/j.jelectrocard.2012.07.017
- Malik, M., van Gelderen, E. M., Lee, J. H., Kowalski, D. L., Yen, M., Goldwater, R., et al. (2012b). Proarrhythmic safety of repeat doses of mirabegron in healthy subjects: a randomized, double-blind, placebo-, and active-controlled thorough QT study. *Clin. Pharm. Therap.* 92, 696–706. doi: 10.1038/clpt.2012.181
- Malik, M., Hnatkova, K., Kowalski, D., Keirns, J. J., and van Gelderen, E. M. (2013). QT/RR curvatures in healthy subjects: sex differences and covariates. *Am. J. Physiol. Heart Circ. Physiol.* 305, H1798–H1806. doi: 10.1152/ajpheart.00577.2013
- Malik, M., Johannesen, L., Hnatkova, K., and Stockbridge, N. (2016). Universal correction for QT/RR hysteresis. *Drug Safety* 39, 577–588. doi: 10.1007/s40264-016-0406-0
- Mickey, E., and Brooke, R. B. (2019). *Tanner Stages*. Available at: <https://www.ncbi.nlm.nih.gov/books/NBK470280/> (accessed May 13, 2019).
- Novotný, T., Leinveber, P., Hnatkova, K., Reichlova, T., Matejkova, M., Sisakova, M., et al. (2014). Pilot study of sex differences in QTc intervals of heart transplant recipients. *J. Electrocardiol.* 47, 863–868. doi: 10.1016/j.jelectrocard.2014.07.015
- Pahlm, O., and Sornmo, L. (1984). Software QRS detection in ambulatory monitoring - a review. *Med. Biol. Eng. Comput.* 22, 289–297. doi: 10.1007/bf02442095
- Rautaharju, P. M., Mason, J. W., and Akiyama, T. (2014). New age- and sex-specific criteria for QT prolongation based on rate correction formulas that minimize bias at the upper normal limits. *Int. J. Cardiol.* 174, 535–540. doi: 10.1016/j.ijcard.2014.04.133
- Rautaharju, P. M., Zhou, S. H., Wong, S., Calhoun, H. P., Berenson, G. S., Prineas, R., et al. (1992). Sex differences in the evolution of the electrocardiographic QT interval with age. *Can. J. Cardiol.* 8, 690–695.
- Sarganas, G., Schaffrath Rosario, A., and Neuhauser, H. K. (2017). Resting heart rate percentiles and associated factors in children and adolescents. *J. Pediatr.* 187, 174–181. doi: 10.1016/j.jpeds.2017.05.021
- Smetana, P., and Malik, M. (2013). Sex differences in cardiac autonomic regulation and in repolarisation electrocardiography. *Pflugers Arch.* 465, 699–717. doi: 10.1007/s00424-013-1228-x
- Stramba-Badiale, M., Priori, S. G., Napolitano, C., Locati, E. H., Viñolas, X., Haverkamp, W., et al. (2000). Gene-specific differences in the circadian variation of ventricular repolarization in the long QT syndrome: a key to sudden death during sleep? *Ital. Heart J.* 1, 323–328.

**Conflict of Interest Statement:** The authors declare that the research was conducted in the absence of any commercial or financial relationships that could be construed as a potential conflict of interest.

Copyright © 2019 Andršová, Hnatkova, Helánová, Šišáková, Novotný, Kala and Malik. This is an open-access article distributed under the terms of the Creative Commons Attribution License (CC BY). The use, distribution or reproduction in other forums is permitted, provided the original author(s) and the copyright owner(s) are credited and that the original publication in this journal is cited, in accordance with accepted academic practice. No use, distribution or reproduction is permitted which does not comply with these terms.

### 3.4. Korekční vzorce v dětské populaci

S vědomím, že neexistuje žádný jednoduchý a univerzální vzorec pro korekci QT intervalu, se v klinické praxi využívají různé vzorce (Bazett,<sup>43</sup> Fridericia,<sup>44</sup> Framingham,<sup>49</sup> Hodges<sup>47</sup>) a lze je považovat za relativně dostatečné v případech, kdy se srdeční frekvence výrazně neliší od 60/min.<sup>62</sup> V ostatních případech je tedy nutná individuální korekce. A ačkoli je všeobecně známo, že klidová srdeční frekvence u malých dětí je výrazně vyšší než 60/min, korekční vzorce odvozené z dospělé populace se hojně užívají i v dětské populaci, přestože existují určité návrhy, jak korigovat QT interval u dětí (které stále vykazují stejné problémy jako u všech univerzálních korekcí<sup>63</sup>). Především užití Bazettovy korekce je v tomto případě zcela neadekvátní a chybné. To potvrdila i následující publikace, kdy jsme u 332 zdravých dětí (166 dívek) s věkovým průměrem  $10.7 \pm 2.6$  roky srovnávali 3 nejčastější korekční vzorce s individuální korekcí.

**Andršová I**, Hnatkova K, Helánová K, Šišáková M, Novotný T, Kala P, Malik M. Problems with Bazett QTc correction in paediatric screening of prolonged QTc interval. *BMC Pediatrics* 2020; 20:558. doi: 10.1186/s12887-020-02460-8.

IF 2,125. Počet citací ve Web of Science 5

Původní práce - kvantitativní podíl uchazečky 60%: Návrh projektu, návrh struktury publikace, sběr EKG signálů, elektrokardiologická měření, interpretace statistických výsledků, text publikace.




RESEARCH ARTICLE

Open Access



# Problems with Bazett QTc correction in paediatric screening of prolonged QTc interval

Irena Andršová<sup>1</sup>, Katerina Hnatkova<sup>2</sup>, Kateřina Helánová<sup>1</sup>, Martina Šišáková<sup>1</sup>, Tomáš Novotný<sup>1</sup>, Petr Kala<sup>1</sup> and Marek Malik<sup>2\*</sup> 

## Abstract

**Background:** Bazett formula is frequently used in paediatric screening for the long QT syndrome (LQTS) and proposals exist that using standing rather than supine electrocardiograms (ECG) improves the sensitivity of LQTS diagnosis. Nevertheless, compared to adults, children have higher heart rates (especially during postural provocations) and Bazett correction is also known to lead to artificially prolonged QTc values at increased heart rates. This study assessed the incidence of erroneously increased QTc values in normal children without QT abnormalities.

**Methods:** Continuous 12-lead ECGs were recorded in 332 healthy children (166 girls) aged  $10.7 \pm 2.6$  years while they performed postural manoeuvring consisting of episodes (in the following order) of supine, sitting, standing, supine, standing, sitting, and supine positions, each lasting 10 min. Detailed analyses of QT/RR profiles confirmed the absence of prolonged individually corrected QTc interval in each child. Heart rate and QT intervals were measured in 10-s ECG segments and in each segment, QTc intervals were obtained using Bazett, Fridericia, and Framingham formulas. In each child, the heart rates and QTc values obtained during supine, sitting and standing positions were averaged. QTc durations by the three formulas were classified to  $< 440$  ms, 440–460 ms, 460–480 ms, and  $> 480$  ms.

**Results:** At supine position, averaged heart rate was  $77.5 \pm 10.5$  beat per minute (bpm) and Bazett, Fridericia and Framingham QTc intervals were  $425.3 \pm 15.8$ ,  $407.8 \pm 13.9$ , and  $408.2 \pm 13.1$  ms, respectively. At sitting and standing, averaged heart rate increased to  $90.9 \pm 10.1$  and  $100.9 \pm 10.5$  bpm, respectively. While Fridericia and Framingham formulas showed only minimal QTc changes, Bazett correction led to QTc increases to  $435 \pm 15.1$  and  $444.9 \pm 15.9$  ms at sitting and standing, respectively. At sitting, Bazett correction identified 51, 4, and 0 children as having the QTc intervals 440–460, 460–480, and  $> 480$  ms, respectively. At standing, these numbers increased to 118, 11, and 1, while on standing these numbers were 151, 45, and 5, respectively. Irrespective of the postural position, Fridericia and Framingham formulas identified only a small number ( $< 7$ ) of children with QT interval between 440 and 460 ms and no children with longer QTc.

(Continued on next page)

\* Correspondence: [marek.malik@imperial.ac.uk](mailto:marek.malik@imperial.ac.uk)

<sup>2</sup>National Heart and Lung Institute, Imperial College, ICTEM, Hammersmith Campus, 72 Du Cane Road, Shepherd's Bush, London W12 0NN, England  
Full list of author information is available at the end of the article



© The Author(s). 2020 **Open Access** This article is licensed under a Creative Commons Attribution 4.0 International License, which permits use, sharing, adaptation, distribution and reproduction in any medium or format, as long as you give appropriate credit to the original author(s) and the source, provide a link to the Creative Commons licence, and indicate if changes were made. The images or other third party material in this article are included in the article's Creative Commons licence, unless indicated otherwise in a credit line to the material. If material is not included in the article's Creative Commons licence and your intended use is not permitted by statutory regulation or exceeds the permitted use, you will need to obtain permission directly from the copyright holder. To view a copy of this licence, visit <http://creativecommons.org/licenses/by/4.0/>. The Creative Commons Public Domain Dedication waiver (<http://creativecommons.org/publicdomain/zero/1.0/>) applies to the data made available in this article, unless otherwise stated in a credit line to the data.

(Continued from previous page)

**Conclusion:** During screening for LQTS in children, the use of Bazett formula leads to a high number of false positive cases especially if the heart rates are increased (e.g. by postural manoeuvring). The use of Fridericia formula can be recommended to replace the Bazett correction not only for adult but also for paediatric ECGs.

**Keywords:** Long QT screening, QTc prolongation in children, Bazett correction, Fridericia correction, Framingham correction

## Background

The fact that the QT interval duration shortens with increasing heart rate has been known practically from the beginning of electrocardiography. This knowledge only extended the observations of the heart rate influence on the duration of cardiac systole that were made more than 150 years ago, well before the first ever electrocardiogram was recorded [1].

Nevertheless, only some 2 decades ago, it was observed that the relationship between the QT interval and the underlying heart rate shows not only substantial inter-subject differences but also considerable intra-subject stability [2, 3]. The implications for clinical assessment of rate corrected QTc interval changes became well recognised [4] both in clinical practice and in the investigations of repolarisation changing properties of novel pharmaceutical compounds. The knowledge that no generic and universal heart rate correction formula can possibly exist that would reasonably correct the QT interval in all subjects led to the practice of using generic formulas (such as Bazett [5], Fridericia [6], Framingham [7], or Hodges [8] formulas) only in cases when the heart rate is not markedly different from baseline conditions, e.g. around 60 beats per minute (bpm) [9]. When QT correction is needed in other situations, individual QT/heart rate profiles need to be studied so that the individual-specific QT adaptation to rate changes can be taken into account.

In children, baseline heart rate is usually substantially higher than 60 bpm [10]. Consequently, the implications of the QT-heart rate individuality are little used in paediatric practice. Despite the knowledge that in adults, Bazett formula leads to artificially prolonged QTc values when applied to recordings of increased heart rate [11, 12], the formula is standardly used when judging paediatric electrocardiograms (ECG) e.g. when screening children for congenital long QT syndrome (LQTS). Recently, a proposal was published to use ECG during standing rather than supine position to increase the sensitivity of LQTS screening [13]. Bazett formula was used in the data supporting this proposal.

Nevertheless, the properties of the Bazett formula should also be considered when evaluating paediatric recordings since the erroneously prolonged QTc values at increased heart rate might lead to an increased number

of false positive LQTS diagnoses. To investigate this potential problem, we have studied Bazett corrected QTc intervals in a large set of long-term ECG recordings obtained in children during postural provocative manoeuvres [14].

## Methods

### Population and ECG recordings

The investigated population was reported in detail before [14]. In brief, continuous 12-lead ECGs sampled at 1000 Hz were obtained in 345 healthy children and adolescents aged from above 4 to below 15 years (174 girls). Each of the participants underwent a 70-min protocol of postural provocations that consisted of episodes (in the following order) of supine, sitting, standing, supine, standing, sitting, and supine positions, each lasting 10 min. The changes between the body positions were achieved within 20 s, the non-supine positions did not involve any external support. During the investigation, younger children listened to calming age-appropriate stories read by the investigator, others were investigated in an environment free of noise and of other external disturbances.

The source study excluded subjects on interfering drug therapy, cardiac structural congenital abnormalities (including those with a history of cardiac surgery), cardiac conduction abnormality, and (in one case) of a technical recording failure. The study was approved by the Ethics Committee of the University Hospital Brno. The parents or legal guardians of all participants gave informed written consent according to the Helsinki declaration.

In all subjects, the ECG recordings were longer than the 70-min of the investigated protocol since, for practical reasons, the recorders (SEER MC vers 2.0 of GE Healthcare, Milwaukee, WI, USA) were started before and switched off after the postural investigations which were organised in groups of up to 20 participants of similar ages.

### ECG measurements and heart rate correction

As previously described [14], the complete recordings were divided into consecutive 10-s ECG segments and in each segment, heart rate was measured based on the average of all RR intervals.

In each segment, representative median beat was also constructed, and QT interval duration was measured using previously published procedures [15, 16] in the image of the representative beats of all 12 leads superimposed on the same isoelectric axis. As previously described [14], appropriate validation including the measurements including systematic morphological interpretation [17] was employed.

For the purposes of the present investigation, only the 10-s ECG segments obtained during the individual postural positions were considered. To model a population screening strategy in which standard 10-s ECG recordings are obtained, we have not considered the correction for QT/RR hysteresis [18] in the present investigation. Rather, in each of the 10-s ECG segment, QT interval was corrected for the average of the RR intervals measured in the same segment. Three correction formulas were used:

- (a) Bazett correction [5]  $QTc = QT/\sqrt{RR}$ ,
- (b) Fridericia correction [6]  $QTc = QT/\sqrt[3]{RR}$ ,
- (c) Framingham correction [7]  $QTc = QT + 0.154(1 - RR)$ ,

where the QT, RR, and QTc intervals are expressed in seconds.

For each child, previously described individual QT/RR profiles including the QT/RR hysteresis correction was also available from previous investigations [14] but these were only used in this study to ascertain that none of the investigated children had any cardiac repolarisation abnormality.

### Models of long-QT screening

As a small minority of the children were unable to complete the whole protocol, only those children in whom repeated QT and heart rate readings were available during supine, sitting, and standing positions were included into the analyses presented here. For each child, the QTc values according to each of the correction formulas were averaged separately in each of the supine, sitting, and standing positions. Subsequently, for each of the positions, numbers of children in whom the averaged QTc values exceeded 440, 460, and 480 ms were identified and compared between the different correction formulas.

The threshold of 440 ms was selected as an upper borderline upper limit of normality [19], the threshold of 460 ms was selected as an indication of a clear abnormality, and the limit of 480 ms was selected as a definite diagnostic tool of a long QT syndrome [20] (especially if obtained as an average of repeated ECG recordings as was the case in this investigation).

### Individual QT/heart rate profiles

To elucidate the relationship between the correction formulas used in the study and the subject-specific profiles of QT/RR relationship, correlation coefficients were investigated between the averaged RR intervals in separate 10-s ECG segments and the theoretical QTc intervals given as  $QT/RR^\alpha$  and  $QT + \beta(1-RR)$ . These intra-subject correlations were investigated ranging the coefficients  $\alpha$  and  $\beta$  between 0 and 1 with the aim of studying the distribution of the coefficients that lead, for each child, to the zero correlation between repeated RR and QTc measurements. This was based on the principle that a successful heart rate correction eliminates the QT dependency on the underlying heart rate [2]. These calculations were made only using the measurements made in ECG segments recorded when the study subjects were in the pre-specified postural positions.

### Statistics

Descriptive data are presented as means  $\pm$  standard deviation. In addition to the categorical analysis based on upper QTc limits, heart rates and absolute QTc values at different postural positions, and their changes between supine and other positions were statistically summarised and compared between girls and boys. These comparisons were based on two-sample two-tail t-test assuming different variances of compared samples. The intra-subject differences in heart rate and in QTc intervals between postural positions were evaluated using paired two-tail t-test. Correlation between QTc changes and heart rate changes was evaluated using Pearson correlation coefficients. *P*-values below 0.05 were considered statistically significant. The statistical analyses were made using SPSS vers 26 (IBM, Armonk, NY, USA).

### Results

Complete heart rate and QT interval data of supine, sitting, and standing positions were available in 332 children (age range 4 years, 7 months to 14 years, 11 months). The population included 166 girls (aged  $10.7 \pm 2.7$  years) and 166 boys (aged  $10.8 \pm 2.6$  years). The previously reported study of full QT/RR profiles [14] confirmed that none of the children had any electrocardiographic repolarisation abnormality. That is, in each child, the full profile of individual QT/heart rate adaptation was measured and studied, and ECGs at different heart rates were visually reviewed to identify repolarisation pathologies. None of these were found.

### Postural changes

The absolute values of heart rates and of QTc intervals are shown in Table 1; their intra-subject differences associated with the postural changes are shown in Table 2. As expected, heart rate increased when changing the

**Table 1** Absolute values of ECG measurements

	Girls				Boys			
	Heart rate	QTc <sub>Bazett</sub>	QTc <sub>Fridericia</sub>	QTc <sub>Framingham</sub>	Heart rate	QTc <sub>Bazett</sub>	QTc <sub>Fridericia</sub>	QTc <sub>Framingham</sub>
Supine	78.00 ± 10.42	426.27 ± 15.36	408.3 ± 13.77	408.73 ± 13.01	76.96 ± 10.55	424.32 ± 16.26	407.27 ± 14.05	407.69 ± 13.17
Sitting	92.72 ± 9.55	436.93 ± 14.48	406.47 ± 12.98	405.47 ± 11.69	88.98 ± 10.36	433.00 ± 15.46	405.60 ± 13.44	405.17 ± 12.25
Standing	101.88 ± 10.19	445.9 ± 15.68	408.27 ± 13.57	405.08 ± 11.85	100.01 ± 10.75	443.97 ± 16.07	407.84 ± 13.81	405.13 ± 12.22

For individual postural positions, the table shows heart rate (in beats per minute) and QTc intervals according to the 3 considered correction formulas (in milliseconds). The only significant differences between girls and boys were for the sitting heart rate ( $p = 0.0007$ ) and for the sitting Bazett corrected QTc intervals ( $p = 0.018$ ). Note also that median values (not shown) were practically identical to the presented mean values

position from supine to standing. The extent of the heart rate change was perhaps less expected since the change from supine to sitting led, on average, to a heart rate increase by  $13.4 \pm 7.8$  bpm, whilst the position change from supine to standing increased heart rate, on average, by  $23.5 \pm 10.1$  bpm.

Importantly, while Fridericia and Framingham corrections led only to minimal and clinically clearly unimportant QTc changes (on average by small single milliseconds) from supine to sitting and to standing positions, Bazett corrected QTc intervals increased noticeably by, on average,  $9.7 \pm 8.1$  ms and  $19.6 \pm 11.4$  ms when the position was changed from supine to sitting and to standing, respectively.

The supine to sitting and supine to standing changes of Bazett corrected QTc intervals were highly significantly correlated to the corresponding changes of heart rate. The corresponding correlation coefficients were  $r = 0.817$  ( $p < 0.00001$ ) and  $r = 0.764$  ( $p < 0.00001$ ), respectively. No significant correlation was found between the heart rate changes and the changes of Fridericia corrected QTc intervals (correlation coefficients of  $r = -0.034$ , and  $r = 0.064$ , for changes to sitting and standing, respectively, both NS). The changes of the Framingham corrected QTc intervals were mildly negatively correlated to the corresponding changes of heart rate with correlation coefficients of  $r = -0.182$  ( $p = 0.001$ ) and  $r = -0.150$  ( $p = 0.008$ ) for changes to sitting and standing, respectively. The relationship between the heart rate changes and the QTc changes of the postural changes from supine to standing are shown in Fig. 1.

**Detection of children with a prolonged QTc interval**

Using the QTc intervals in supine, Bazett correction identified 51 children (15.36%) as having QTc interval between 440 and 460 ms, and 4 children (1.20%) as having QTc interval between 460 and 480 ms. When QTc intervals in sitting were used, Bazett correction found 118 children (35.54%) as having QTc interval between 440 and 460 ms, 11 children (3.31%) as having QTc interval between 460 and 480 ms, and 1 child (0.30%) as having the QTc interval above 480 ms. When QTc intervals in standing were used, the corresponding numbers of children identified with QTc prolongation increased to 156 (46.99%), 45 (13.55%), and 5 (1.51%), respectively.

Fridericia correction identified only 4 children (1.2%) in supine and 6 children (1.81%) in standing as having QTc interval between 440 and 460 ms. For Framingham correction, the corresponding numbers were 3 children (0.90%) and 1 child (0.30%), respectively. Using these corrections, no children were found to have the QTc interval above 440 ms in sitting recordings.

The summary of these observations is graphically displayed in Fig. 2.

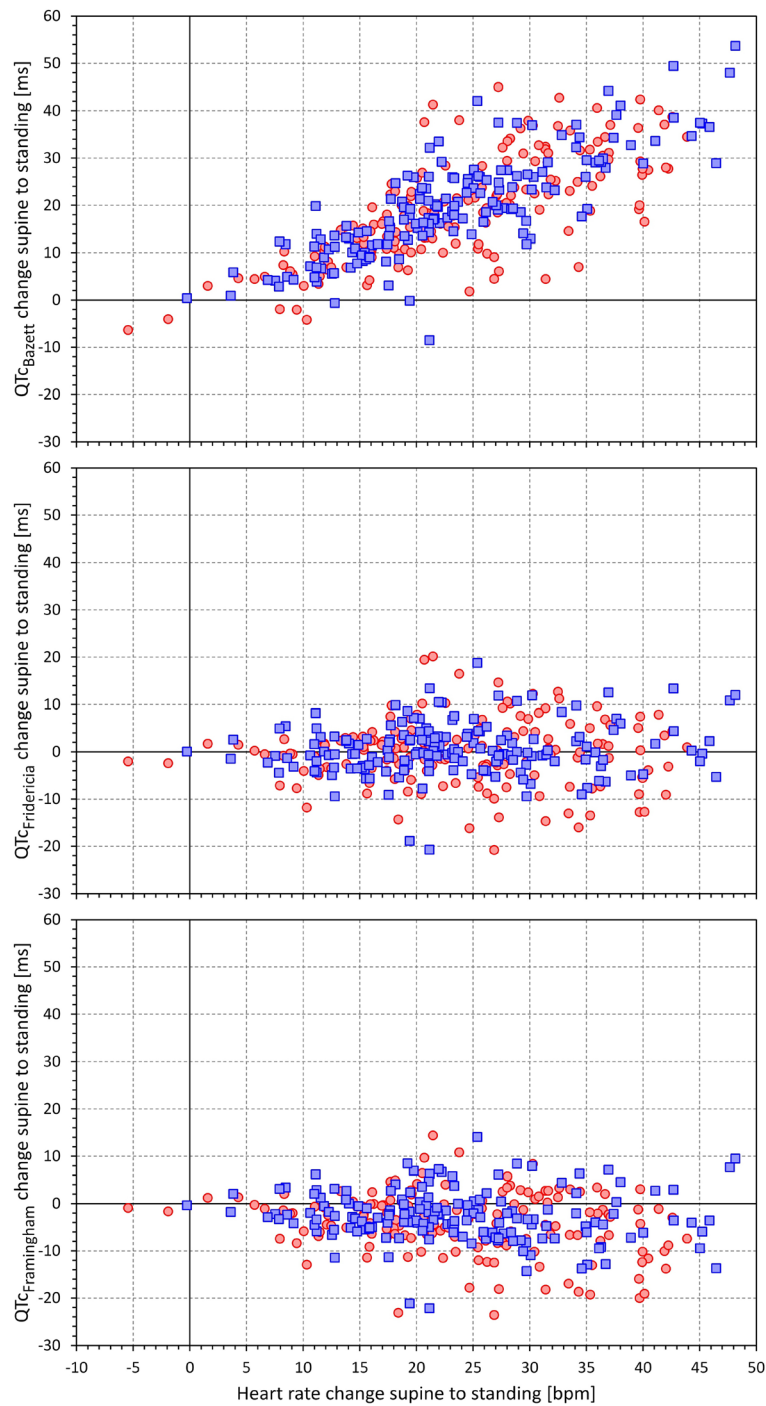
**Subject-specific QT/RR relationships**

The difference between Bazett formula and Fridericia and Framingham formulas is also shown in the displays of Fig. 3. While the Bazett correction coefficient of 0.5 is well outside the spread of the correction coefficients optimised for the study data in individual subjects, the correction coefficients of the Fridericia formula (0.333)

**Table 2** Postural changes of ECG measurements

	Girls				Boys			
	Heart rate	QTc <sub>Bazett</sub>	QTc <sub>Fridericia</sub>	QTc <sub>Framingham</sub>	Heart Rate	QTc <sub>Bazett</sub>	QTc <sub>Fridericia</sub>	QTc <sub>Framingham</sub>
Sitting-supine	14.72 ± 7.85	10.66 ± 8.14	-1.83 ± 4.70	-3.25 ± 5.06	12.02 ± 7.62	8.68 ± 7.90	-1.66 ± 3.65	-2.51 ± 3.65
	< 0.0001	< 0.0001	< 0.0001	< 0.0001	< 0.0001	< 0.0001	< 0.0001	< 0.0001
Standing-supine	23.87 ± 9.84	19.63 ± 11.69	-0.04 ± 7.50	-3.65 ± 7.27	23.06 ± 10.43	19.65 ± 11.22	0.57 ± 5.50	-2.55 ± 5.42
	< 0.0001	< 0.0001	NS	< 0.0001	< 0.0001	< 0.0001	NS	< 0.0001

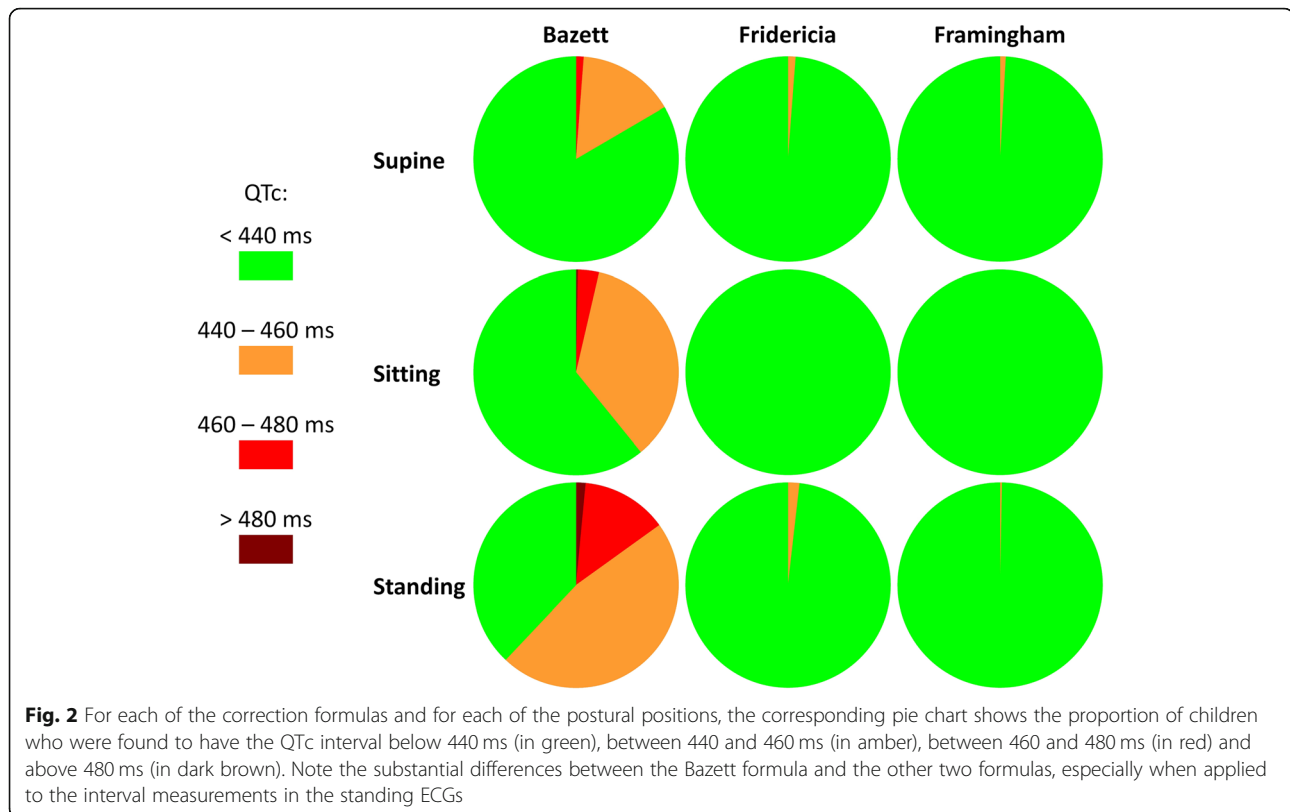
For the position changes from supine to sitting and supine to standing, the table shows changes in heart rate (in beats per minute) and in QTc intervals according to the considered QTc formulas (in milliseconds). For the positional changes, the table also shows  $p$ -value (bottom numbers) of the paired t-test comparing the sitting and standing values with the supine values. The only significant differences between girls and boys were for the sitting vs supine heart rates ( $p = 0.0017$ ) and for the sitting vs supine Bazett corrected QTc intervals ( $p = 0.025$ )



**Fig. 1** Scatter diagrams between heart rate changes from supine to standing (the same horizontal axis in all panels) and QTc changes reported by the Bazett formula (top panel) Fridericia formula (middle panel) and Framingham formula (bottom panel). In each panel, the red circles correspond to girls, and the blue squares to boys. Note the obvious positive correlation between the heart rate changes and the changes of the Bazett corrected QTc intervals as well as a slight negative correlation between the heart rate changes and the changes of the Framingham corrected QTc intervals

and of the Framingham formula (0.154) are well within the range of the inter-subject spread of the subject-specific optimisations of the log-linear and linear QT/RR regressions.

An example of the comparison of the effects of Bazett correction with the corrections of the other two formulas is also shown in Fig. 4 that shows the scatter diagrams of multiple 10-s QT and heart rate



measurements in a recording of an 8-year old healthy boy.

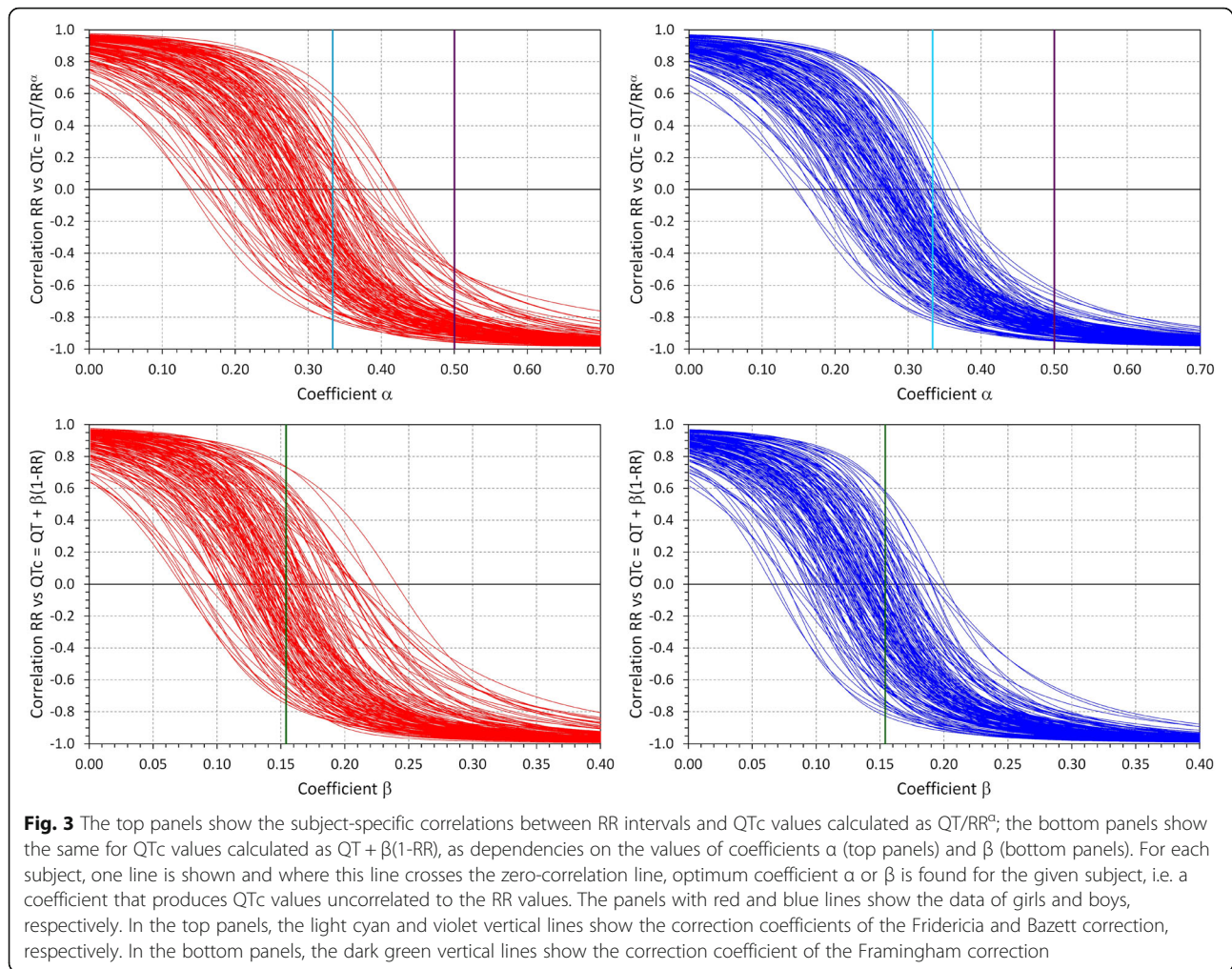
## Discussion

In adult electrocardiography, criticism of Bazett correction has been repeatedly published [11, 21] and some of these studies also referred to problems in children and adolescents [22, 23]. While in adult cardiology, the inaccuracies of Bazett correction might be mitigated by applying it only to recordings with heart rates not far from 60 bpm, this is hardly possible in children. The overestimation of Bazett corrected QTc intervals at higher heart rates thus need to be considered. This is of particular concern if the heart rate is further elevated, e.g. by exercise test or by postural manoeuvres, as was the case in the data that we presented. Therefore, while it is possible to agree with Reynisson et al. [13] that judging ECGs recorded in the standing position increases the sensitivity of LQTS diagnoses, our data show that this increase of sensitivity comes at a very high cost of substantially decreased specificity.

Indeed, all the children included in our study were previously confirmed to be free of QTc interval prolongation based on details of the QT/RR profiles [14]. This fits well with the applications of Fridericia and Framingham corrections that only occasionally identified small number of children with potentially moderate QTc

prolongation. On the contrary, Bazett correction identified 16.5% of children as having QTc above 440 ms when supine recordings were used, and this proportion increased to 25.7 and 61.7% (i.e. almost two thirds) when sitting and standing recordings were analysed, respectively. Projecting these results into clinical practice makes it clear that any screening strategy would easily be overwhelmed by a substantial number of false positive cases (these were probably not encountered by Reynisson et al. [13] because of the relatively small number of their control cases).

The Fridericia and Framingham corrections were originally developed by studying QT/heart-rate relationship in large populations [6, 7] while aiming at finding coefficients that would, in these populations, make the QTc values independent of the RR intervals. Bazett correction was not based on any such calculations [5]; indeed, when re-analysing the data available to Captain Bazett, a correction coefficient closer to Fridericia correction is found [24]. More importantly, however, the independence of QTc values of RR values in a population does not imply such an independence in individual subjects. Previous proposals of heart rate corrections were thus influenced by the investigated populations and large number of different formulas have been proposed [22, 25, 26]. Nevertheless, it is now understood that because of the inter-subject differences [3, 27], none of these universal

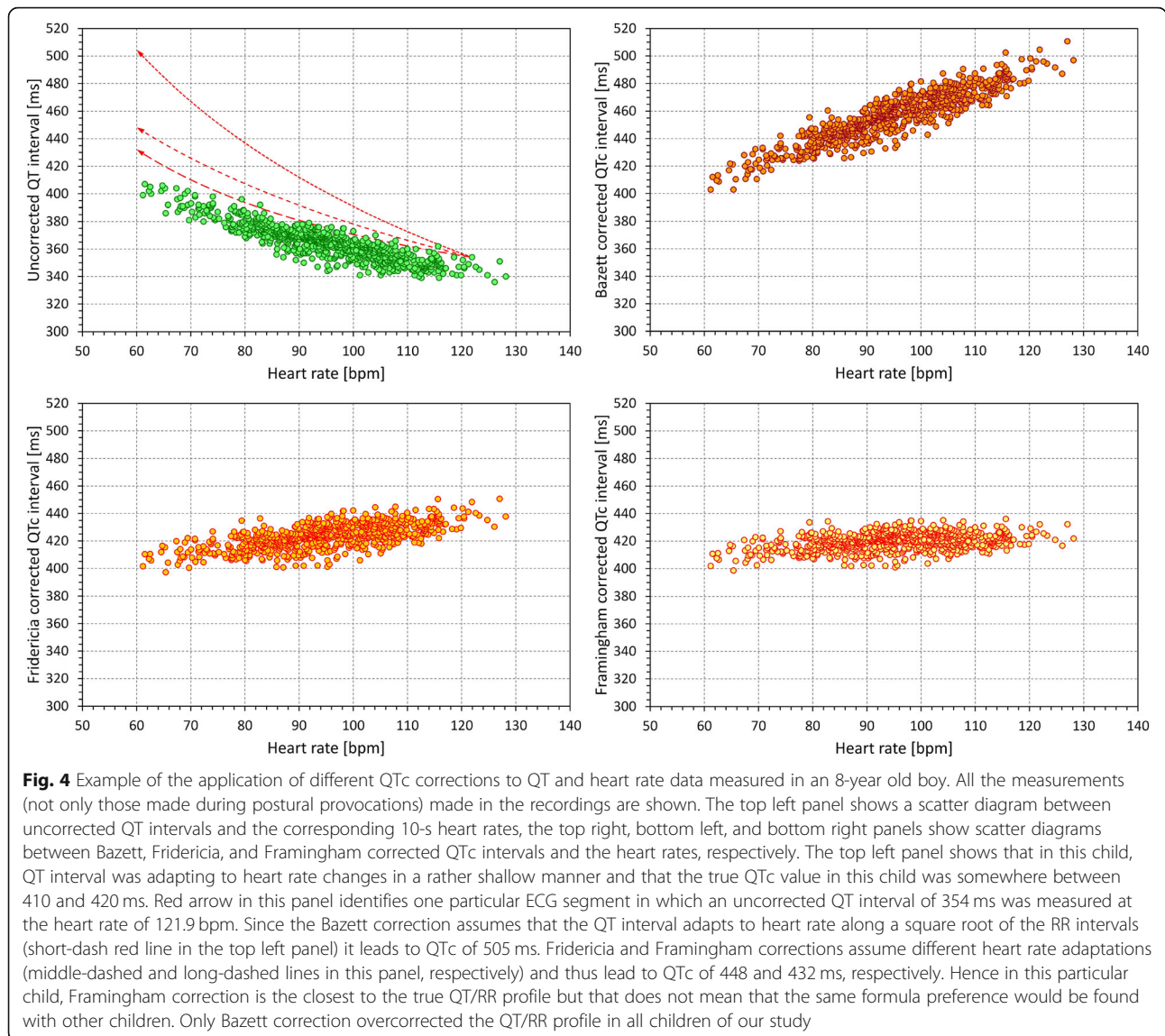


formulas can possibly make the QTc intervals independent of heart rate in each individual. Other problems with the “population-optimised” corrections have also been recognised [28]. This implies that excesses of heart rate are undesirable when making clinical judgements of QTc intervals and that formulas that are close to the “middle” of individual QT/RR profiles are preferable over the Bazett correction that is as far from the spread of the QT/RR profiles in adult subjects [29] as in our population of healthy children.

Superficially, our results might be perceived as contradicting all the studies that previously used Bazett formula in paediatric diagnostics. Of these, valid comparison between different formulas was published by Stramba-Badiale et al [30] finding little differences between different formulas with a slight preference for Bazett correction. Nevertheless, this study reported ECGs in newborns in whom the uncorrected QT values are numerically short and thus subject to different effects of logarithmic transformation [31]. Similar conclusions were reached by Phan et al. [32] but again in little

babies and children below 2 years of age. It is not known whether the individuality (that is, the combination of inter-subject differences with intra-subject stability) of QT/RR profiles exists already in newborns and small babies or whether it gradually develops and becomes detectable in school-aged children whom we investigated. Moreover, when considering only ECGs with strictly normal resting heart rates, we found lesser diagnostic differences between the compared formulas (see Fig. 2). The main problem highlighted by our study therefore relates to the elevated heart rates as recently advocated by Reynisson et al. [13].

Our results concerning Fridericia and Framingham formulas are in good agreement with the regulatory suggestions that show that these formulas are preferable to others when studying QTc stability under the conditions of heart rate changes. Superficially, the slight (and clinically clearly unimportant) decreases in QTc at sitting and standing compared to supine might create an impression that these formulas suffer from the opposite problem of the Bazett formula. Nevertheless, this is not justified



since Fig. 3 shows clearly that in the majority of the children of our population, both Fridericia and Framingham formulas led to a positive rather than to a negative correlation between QTc intervals and the RR intervals of the underlying heart rate. Detailed analysed of the data show that the minimally negative QTc changes were caused by a combination of the individual QT/RR curvatures (that were not fully reflected in the linear and log-linear regression models) and by the distribution of the heart rate changes in the population. The negative shallow correlations between the heart rate changes and QTc changes reported by the Framingham formula were also caused by the individual QT/RR profiles since in these children, the QT interval did not respond to the RR interval in a strictly linear fashion as expected by the formula. Our data thus suggest that Fridericia formula is

marginally preferable to Framingham formula in paediatric applications.

Since the Fridericia formula is now the method of choice when studying the drug-induced LQTS in regulatory analyses of clinical studies [4], we believe that the accuracy of LQTS diagnoses in children would also benefit from using Fridericia formula instead of the Bazett formula which, as we have shown, is likely to lead to an unacceptable number of false positive findings.

**Limitations**

Intentionally, we included only healthy children free of any electrocardiographic repolarisation abnormality in this study. That allows us to demonstrate the substantial problem of false positive QTc prolongation linked to the use of Bazett correction, but we are unable to assess the



incidence of false negative cases. Since a known proportion of children with congenital LQTS may present with normal QTc interval duration [33] even at heart rate close to 60 bpm (where any heart rate correction is of little importance) it is obvious that LQTS diagnosis cannot be solely based on ECG readings. To model a population screening strategy, we analysed our data only using separate 10-s ECG segments. That prevented us from considering QT/RR hysteresis [18] that is known to influence the accuracy of heart rate correction. The Fridericia and Framingham formulas were selected from a wide spectrum of other published formulas. Other correction possibilities might also eliminate the false positive problem associated with Bazett correction. Nevertheless, in adult data, Fridericia and Framingham formulas appeared to outperform other corrections [9].

## Conclusion

Despite these limitations, our data show that the use of Bazett correction in paediatric studies leads to problematic findings of artificially prolonged QTc intervals, especially if the recent suggestions are followed and if the underlying heart rates are increased by postural changes. Consistent with the diagnosis of acquired LQTS in adult subjects, Fridericia correction formula can be proposed for improved ECG evaluations.

## Abbreviations

bpm: Beats per minute; ECG: Electrocardiogram; LQTS: Long QT syndrome; ms: Millisecond

## Acknowledgements

We are grateful to the investigated subjects and their parents / guardians for their willingness to participate at the study. We are equally grateful for the kind help and support provided by the management and staff of the schools at which the recordings took place.

## Authors' contributions

MM, TN, and IA conceived the study. IA, KHn, TN, and MM designed the study. IA, KHe, MŠ, and TN contributed to the clinical conduct. TN and PK supervised the clinical conduct. KHn and MM analysed the data. IA, KHn, and MM drafted the manuscript. All authors approved the final manuscript.

## Funding

Supported in part by the British Heart Foundation New Horizons Grant NH/16/2/32499, and by Ministry of Health of the Czech Republic Grant NV19–02–00197. The funding bodies provided scientific grants but had no influence on the study conduct, data analysis, interpretations, or conclusions.

## Availability of data and materials

The data that support the findings of this study are available from the authors upon reasonable request.

## Ethics approval and consent to participate

The study was approved by the Ethics Committee of the University Hospital Brno. The parents or legal guardians of all participants gave informed written consent according to the Helsinki declaration.

## Consent for publication

The Informed consent provided by the parents or legal guardians of all participants included the agreement of scientific use of the data obtained. No data are presented that would allow individual study participants to be identified.

## Competing interests

The authors declare that they have no competing interests.

## Author details

<sup>1</sup>Department of Internal Medicine and Cardiology, Faculty of Medicine, University Hospital Brno, Masaryk University, Brno, Czech Republic. <sup>2</sup>National Heart and Lung Institute, Imperial College, ICTEM, Hammersmith Campus, 72 Du Cane Road, Shepherd's Bush, London W12 0NN, England.

Received: 1 October 2020 Accepted: 8 December 2020

Published online: 14 December 2020

## References

- Garrod AH. On the relative duration of the component parts of the radial sphygmograph trace in health. *J Anat Physiol.* 1870;18:351–4.
- Malik M, Färbom P, Batchvarov V, Hnatkova K, Camm AJ. Relation between QT and RR intervals is highly individual among healthy subjects: implications for heart rate correction of the QT interval. *Heart.* 2002;87:220–8.
- Batchvarov VN, Ghuran A, Smetana P, Hnatkova K, Harries M, Dilaveris P, Camm AJ, Malik M. QT-RR relationship in healthy subjects exhibits substantial intersubject variability and high intrasubject stability. *Am J Physiol Heart Circ Physiol.* 2002;282:H2356–63.
- Garnett CE, Zhu H, Malik M, Fossa AA, Zhang J, Badilini F, Li J, Darpo B, Sager P, Rodriguez I. Methodologies to characterize the QT/corrected QT interval in the presence of drug-induced heart rate changes or other autonomic effects. *Am Heart J.* 2012;163:912–30.
- Bazett JC. An analysis of time relations of electrocardiograms. *Heart.* 1920;7:353–67.
- Fridericia LS. Die Systolendauer im Elektrokardiogramm bei normalen Menschen und bei Herzkranken. *Acta Med Scand.* 1920;53:469–86.
- Sagie A, Larson MG, Goldberg RJ, Bengtson JR, Levy D. An improved method for adjusting the QT interval for heart rate (the Framingham study). *Am J Cardiol.* 1992;70:797–801.
- Hodges M, Salerno D, Erlie D. Bazett's QT correction reviewed: evidence that a linear QT correction for heart rate is better. *J Am Coll Cardiol.* 1983;1:694.
- Hnatkova K, Vicente J, Johannesen L, Garnett C, Stockbridge N, Malik M. Errors of fixed QT heart rate corrections used in the assessment of drug-induced QTc changes. *Front Physiol.* 2019;10:635. <https://doi.org/10.3389/fphys.2019.00635>.
- Grosso J, Groepenhoff H, Paridon SM, Brothers JA. Normative values for cardiopulmonary exercise stress testing using ramp cycle ergometry in children and adolescents. *J Pediatr.* 2020;S0022–3476(20)31146-X. <https://doi.org/10.1016/j.jpeds.2020.09.018>.
- Funck-Brentano C, Jaillon P. Rate-corrected QT interval: techniques and limitations. *Am J Cardiol.* 1993;72:17B–22B.
- Vinet A, Dubé B, Nadeau R, Mahiddine O, Jacquemet V. Estimation of the QT-RR relation: trade-off between goodness-of-fit and extrapolation accuracy. *Physiol Meas.* 2017;38:397–419.
- Reynisson B, Tanghöj G, Naumburg E. QTc interval-dependent body posture in pediatrics. *BMC Pediatr.* 2020;20:107. <https://doi.org/10.1186/s12887-020-1959-8>.
- Andršová I, Hnatkova K, Helánová K, Šišáková M, Novotný T, Kala P, Malik M. Individually rate corrected QTc intervals in children and adolescents. *Front Physiol.* 2019;10:994. <https://doi.org/10.3389/fphys.2019.00994>.
- Malik M, Andreas JO, Hnatkova K, Hoekendörff J, Cawello W, Middle M, Horstmann R, Braun M. Thorough QT/QTc study in patients with advanced Parkinson's disease: cardiac safety of rotigotine. *Clin Pharmacol Ther.* 2008;84:595–603.
- Malik M, van Gelderen EM, Lee JH, Kowalski DL, Yen M, Goldwater R, Mujais SK, Schaddelee MP, de Koning P, Kaibara A, Moy SS, Keirns JJ. Proarrhythmic risk of repeat doses of mirabegron in healthy subjects: a randomized, double-blind, placebo-, and active-controlled thorough QT study. *Clin Pharm Therap.* 2012;92:696–706.
- Hnatkova K, Smetana P, Toman O, Bauer A, Schmidt G, Malik M. Systematic comparisons of electrocardiographic morphology increase the precision of QT interval measurement. *Pacing Clin Electrophysiol.* 2009;32:119–30.
- Gravel H, Jacquemet V, Dahdah N, Curnier D. Clinical applications of QT/RR hysteresis assessment: a systematic review. *Ann Noninvasive Electrocardiol.* 2018;23:e12514. <https://doi.org/10.1111/anec.12514>.

19. Johnson JN, Ackerman MJ. QTc: how long is too long? *Br J Sports Med.* 2009;43:657–62.
20. Tester DJ, Will ML, Haglund CM, Ackerman MJ. Effect of clinical phenotype on yield of long QT syndrome genetic testing. *J Am Coll Cardiol.* 2006;47:764–8.
21. Malik M, Hnatkova K, Batchvarov V, Gang Y, Smetana P, Camm AJ. Sample size, power calculations, and their implications for the cost of thorough studies of drug induced QT interval prolongation. *Pacing Clin Electrophysiol.* 2004;27:1659–69.
22. Rautaharju PM, Warren JW, Calhoun HP. Estimation of QT prolongation. A persistent, avoidable error in computer electrocardiography. *J Electrocardiol.* 1990;23(Suppl):111–7.
23. Hazeke D, Yoshinaga M, Takahashi H, Tanaka Y, Haraguchi Y, Abe M, Koga M, Fukushima T, Nagashima M. Cut-offs for screening prolonged QT intervals from Fridericia's formula in children and adolescents. *Circ J.* 2010;74:1663–9.
24. Malik M. If Dr. Bazett had had a computer... *Pacing Clin Electrophysiol* 1996; 19:1635–1639.
25. Sarma JSM, Sarma RJ, Bilitch M, Katz D, Song SL. An exponential formula for heart rate dependence of QT interval during exercise and pacing in humans: reevaluation of Bazett's formula. *Am J Cardiol.* 1984;54:103–8.
26. van der Wall HEC, Gal P, Kemme MJB, van Westen GJP, Burggraaf J. Number of ECG replicates and QT correction formula influences the estimated QT prolonging effect of a drug. *J Cardiovasc Pharmacol.* 2019;73:257–64.
27. Gueta I, Klempfner R, Markovits N, Halkin H, Segev S, Rott D, Peled Y, Loebstein R. Clinically significant incidental QTc prolongation is subject to within-individual variability. *Ann Noninvasive Electrocardiol.* 2020;25:e12699. <https://doi.org/10.1111/anec.12699>.
28. Malik M, Garnett C, Hnatkova K, Vicente J, Johannesen L, Stockbridge N. Implications of individual QT/RR profiles-part 1: inaccuracies and problems of population-specific QT/heart rate corrections. *Drug Saf.* 2019;42:401–14.
29. Malik M, Johannesen L, Hnatkova K, Stockbridge N. Universal correction for QT/RR hysteresis. *Drug Saf.* 2016;39:577–88.
30. Stramba-Badiale M, Karnad DR, Goulene KM, Panicker GK, Dagradi F, Spazzolini C, Kothari S, Lokhandwala YY, Schwartz PJ. For neonatal ECG screening there is no reason to relinquish old Bazett's correction. *Eur Heart J.* 2018;39:2888–95.
31. Hnatkova K, Johannesen L, Vicente J, Malik M. Heart rate dependency of JT interval sections. *J Electrocardiol.* 2017;50:814–24.
32. Phan DQ, Silka MJ, Lan YT, Chang RK. Comparison of formulas for calculation of the corrected QT interval in infants and young children. *J Pediatr.* 2015;166:960–4.
33. Garson A Jr, Dick M 2nd, Fournier A, Gillette PC, Hamilton R, Kugler JD, van Hare GF 3rd, Vetter V, Vick GW 3rd. The long QT syndrome in children. An international study of 287 patients. *Circulation.* 1993;87:1866–72.

## Publisher's Note

Springer Nature remains neutral with regard to jurisdictional claims in published maps and institutional affiliations.

**Ready to submit your research? Choose BMC and benefit from:**

- fast, convenient online submission
- thorough peer review by experienced researchers in your field
- rapid publication on acceptance
- support for research data, including large and complex data types
- gold Open Access which fosters wider collaboration and increased citations
- maximum visibility for your research: over 100M website views per year

**At BMC, research is always in progress.**

Learn more [biomedcentral.com/submissions](https://biomedcentral.com/submissions)



### 3.5. Hystereze QT intervalu

Jedním z parametrů, který zásadně ovlivňuje hodnoty QTc při užití korekčních formulí (a při zvažování vztahu QT/SF obecně), je tzv. dynamická složka QT hystereze v průběhu změn SF. Od minulého století je znám fakt, že adaptace QT intervalu vykazuje jisté časové zpoždění za změnou SF a následným ustálením SF.<sup>64,65</sup> Výše uvedené studie zabývající se vztahem QT/RR toto zpoždění změn QT ku RR nemohly hodnotit, jelikož zkoumaly pouze 10-sekundové záznamy EKG. V takto krátkém záznamu se pak zpoždění QT hystereze ještě neobjeví. Teprve před necelými dvěma dekadami se objevily studie zaměřující se na tuto problematiku. Pueyo at al. v roce 2004 publikovali popis zpoždění QT/RR hystereze u pacientů po infarktu myokardu a ukázali, že prodloužené zpoždění je rizikovým faktorem.<sup>66</sup> Další práce dokazovala, že korekce s respektováním delší časové adaptace QT intervalu po změně SF vede k přesnějším hodnotám QTc.<sup>67</sup> Podrobnější charakteristiku tohoto dynamického vztahu QT/RR pak přinesla práce hodnotící hysterezi QT/RR u 40 zdravých jedinců (18 žen, průměrný věk  $30.4 \pm 8.1$  roků). Práce jasně prokázala intraindividuální specificitu, zároveň však interindividuální variabilitu tohoto parametru, obdobně, jak je tomu i u statického vztahu QT/RR. Statický vztah QT/RR vyjadřuje tedy, o kolik se QT interval prodlouží či zkrátí, jakmile se zrychlení či zpomalení SF ustálí, naproti tomu hystereze QT/RR zachycuje, jak rychle QT interval reaguje na zrychlení či zpomalení SF. Ze studie však také vyplývá, že tyto dvě veličiny jsou odlišné fyziologické pochody, které na sobě prakticky nezávisí.<sup>68</sup> Tato mezi subjektová variabilita QT intervalu k SF jde ruku v ruce i s adaptací ostatních EKG parametrů na změny SF.<sup>69</sup>

Nicméně tyto analýzy nepopisovaly, zda adaptace QT intervalu je stejně rychlá při zpomalení i zrychlení SF a pouze okrajově se dotkly otázky, zda je rychlost adaptace závislá na trvání změn SF nebo naopak na počtu srdečních cyklů, během kterých ke změnám SF dochází. S ohledem na výše popisované fyziologické prodlužování/zkracování QT intervalu během dětství a adolescence je jistě správné uvažovat i o možném vlivu věku na hysterezi QT/RR. Také stojí za zmínku i možnost rozdílné adaptace QT/RR u mužů a žen, jelikož mají ženy fyziologické hodnoty QTc ve větším rozmezí a bazální SF v průměru vyšší než muži. Vědomi si těchto nedostatků ve znalostech QT/RR hystereze, zpracovali jsme záznamy dlouhodobých EKG křivek u 751 zdravých dobrovolníků (336 žen) ve věku  $34,3 \pm 9,5$  let. K analýze jsme využili dvou různých exponenciálních matematických modelů popisujících adaptaci QT/RR. Výsledkem této studie bylo zjištění, že zpoždění QT/RR hystereze s přibývajícím věkem klesá, zatímco délka QTc s věkem roste. Ačkoli mají ženy delší QTc, rychlost adaptace QT intervalu k SF je oproti mužům rychlejší. I tento parametr vykazuje značnou interindividuální variabilitu, rozdíly QT/RR hystereze při zrychlení či zpomalení srdeční frekvence byly u jednotlivců navzájem odlišné, nicméně párový test nedosáhl statistické významnosti. Avšak v celé populaci byly tyto rozdíly statisticky významné. Analýza ukazuje, že rychlost adaptace QT intervalu při akceleraci SF byla pomalejší než při deceleraci SF.

**Andršová I**, Hnatkova K, Šišáková M, Toman O, Smetana P, Huster KM, Barthel P, Novotný T, Schmidt G, Malik M. Sex and rate change differences in QT/RR hysteresis in healthy subjects. *Front Physiol* 2022; 12:814542. doi: 10.3389/fphys.2021.814542.

IF 4,0. Počet citací ve Web of Science 1

Původní práce - kvantitativní podíl uchazečky 35%: Návrh struktury publikace, elektrokardiologická měření, interpretace statistických výsledků, text publikace.



# Sex and Rate Change Differences in QT/RR Hysteresis in Healthy Subjects

Irena Andršová<sup>1\*</sup>, Katerina Hnatkova<sup>2</sup>, Martina Šišáková<sup>1</sup>, Ondřej Toman<sup>1</sup>, Peter Smetana<sup>3</sup>, Katharina M. Huster<sup>4</sup>, Petra Barthel<sup>4</sup>, Tomáš Novotný<sup>1</sup>, Georg Schmidt<sup>4</sup> and Marek Malik<sup>2,5</sup>

<sup>1</sup> Faculty of Medicine, Department of Internal Medicine and Cardiology, University Hospital Brno, Masaryk University, Brno, Czechia, <sup>2</sup> National Heart and Lung Institute, Imperial College, London, United Kingdom, <sup>3</sup> Wilhelminenspital der Stadt Wien, Vienna, Austria, <sup>4</sup> Klinikum rechts der Isar, Technische Universität München, Munich, Germany, <sup>5</sup> Faculty of Medicine, Department of Internal Medicine and Cardiology, Masaryk University, Brno, Czechia

## OPEN ACCESS

### Edited by:

Richard Gary Trohman,  
Rush University, United States

### Reviewed by:

Alberto Porta,  
University of Milan, Italy  
Erick Andres Perez Alday,  
Emory University, United States

### \*Correspondence:

Irena Andršová  
andrsova.irena@fnbrno.cz

### Specialty section:

This article was submitted to  
Cardiac Electrophysiology,  
a section of the journal  
Frontiers in Physiology

**Received:** 13 November 2021

**Accepted:** 15 December 2021

**Published:** 07 February 2022

### Citation:

Andršová I, Hnatkova K, Šišáková M, Toman O, Smetana P, Huster KM, Barthel P, Novotný T, Schmidt G and Malik M (2022) Sex and Rate Change Differences in QT/RR Hysteresis in Healthy Subjects. *Front. Physiol.* 12:814542. doi: 10.3389/fphys.2021.814542

While it is now well-understood that the extent of QT interval changes due to underlying heart rate differences (i.e., the QT/RR adaptation) needs to be distinguished from the speed with which the QT interval reacts to heart rate changes (i.e., the so-called QT/RR hysteresis), gaps still exist in the physiologic understanding of QT/RR hysteresis processes. This study was designed to address the questions of whether the speed of QT adaptation to heart rate changes is driven by time or by number of cardiac cycles; whether QT interval adaptation speed is the same when heart rate accelerates and decelerates; and whether the characteristics of QT/RR hysteresis are related to age and sex. The study evaluated 897,570 measurements of QT intervals together with their 5-min histories of preceding RR intervals, all recorded in 751 healthy volunteers (336 females) aged  $34.3 \pm 9.5$  years. Three different QT/RR adaptation models were combined with exponential decay models that distinguished time-based and interval-based QT/RR hysteresis. In each subject and for each modelling combination, a best-fit combination of modelling parameters was obtained by seeking minimal regression residuals. The results showed that the response of QT/RR hysteresis appears to be driven by absolute time rather than by the number of cardiac cycles. The speed of QT/RR hysteresis was found decreasing with increasing age whilst the duration of individually rate corrected QTc interval was found increasing with increasing age. Contrary to the longer QTc intervals, QT/RR hysteresis speed was faster in females. QT/RR hysteresis differences between heart rate acceleration and deceleration were not found to be physiologically systematic (i.e., they differed among different healthy subjects), but on average, QT/RR hysteresis speed was found slower after heart rate acceleration than after rate deceleration.

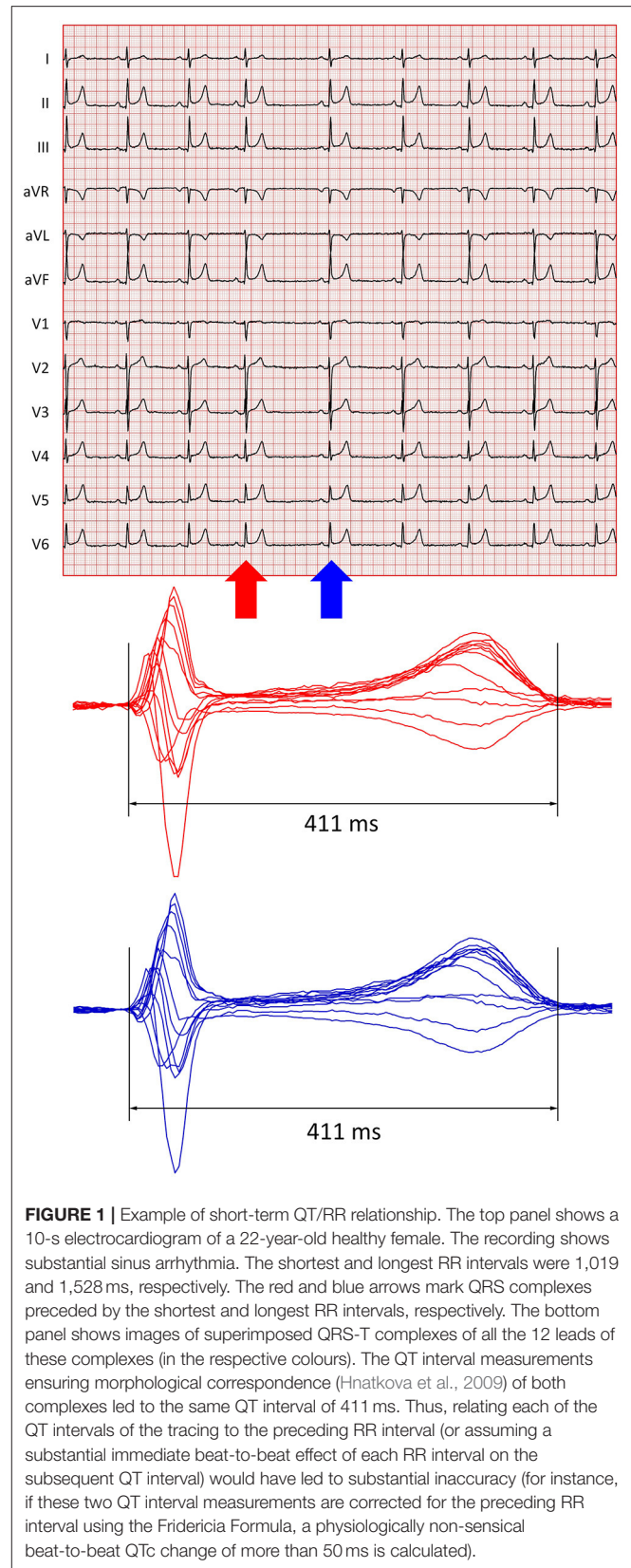
**Keywords:** QT/RR adaptation, QT/RR hysteresis, healthy subjects, non-linear regression modelling, best-fit models, sex differences, age influence

## INTRODUCTION

The dependency of QT interval duration on underlying heart rate has been known practically since the beginning of clinical electrocardiography (Waller, 1887; Einthoven, 1903). This dependency (the slower the heart rate, the longer the QT interval) also reflects even older knowledge of rate influence on the duration of mechanical systole, which was assessed by auscultation and mechanical apexograms well before the first recordings of electrical manifestation of cardiac activity. Indeed, in 1870, Garrod already suggested that the duration of systole changes with the cube root of the cardiac period (Garrod, 1870). Later, when using a mechanical cardiograph rather than a sphygmograph, Garrod proposed that the duration of systole relates to square root of the cardiac cycle (Garrod, 1875). This all happened almost half a century before corresponding proposals have been made concerning electrocardiographic QT interval measurements (Bazett, 1920; Fridericia, 1920).

During the subsequent century, however, much lesser, and much more recent attention has been given to the dynamics of the QT/heart-rate dependency. The knowledge that changes in heart rate lead to QT interval changes only after an appreciable time lag is only some decades-old (Franz et al., 1988; Lau et al., 1988). Although this dynamic aspect of the QT/heart rate relationship is now well-established and shown in repeated reports of solid data (Malik et al., 2008a; Jacquemet et al., 2014), some simplistic approaches to QT/heart-rate dependency still ignore the dynamic aspect, e.g., by proposing that QT interval duration measured on a beat-to-beat basis should be related solely to the duration of the preceding RR interval (Fossa, 2017), although this leads to substantial inaccuracies (example in **Figure 1**).

Despite these simplistic proposals, two components of the heart rate influence on QT duration are presently distinguished, and for the description of both, heart rate is usually expressed by corresponding durations of RR intervals. The *adaptation steepness* of the QT/heart rate relationship, i.e., how much QT interval changes when the underlying heart rate accelerates or decelerates, is usually described as QT/RR adaptation. This needs to be distinguished from the *speed* of QT/heart rate relationship, i.e., how quickly QT duration adapts to heart rate changes. The term *QT/RR hysteresis* is customarily (albeit perhaps somewhat inaccurately) used for this dynamic component (Malik, 2014; Zhang et al., 2014; Malik et al., 2016; Gravel et al., 2017, 2018). Previous studies suggested that both components are independent of each other. That is, a subject whose QT duration changes in response to heart rate changes more than in other subjects (i.e., who has a steeper QT/RR slope) may have the hysteresis speed both faster and slower than other subjects (Malik et al., 2008a). This makes the process of correcting the underlying heart rate for QT/RR hysteresis independent from the process of correcting the QT duration for the underlying heart rate. Indeed, different approaches to correcting the heart rate for hysteresis have previously been combined with different QT/heart rate corrections (Cassani González et al., 2012; Malik et al., 2016; Hnatkova et al., 2019a).



Although different studies have addressed the properties of QT/RR hysteresis, gaps still exist in the understanding of this phenomenon. Among others, the question remains open whether the delay needed to reach QT equilibrium after heart rate changes is driven by time or the number of cardiac cycles. In relation to this, it has not been fully established whether under physiologic conditions, the adaptation speed is the same when heart rate accelerates (and QT interval shortens) and when heart rate decelerates (and QT interval prolongs). Limited knowledge is also available on other physiologic characteristics of QT/RR hysteresis, including influence of sex and age.

Bearing these knowledge gaps in mind, we have investigated the properties of QT/RR hysteresis by QT interval and heart rate measurements in a large collection of long-term electrocardiographic (ECG) recordings collected in healthy subjects. The recordings were obtained in strictly physiologic conditions of controlled clinical studies and, thus, allowed to address the characteristics of the phenomenon without any pharmacologic or instrumental interventions.

## METHODS

### Investigated Population and Electrocardiographic Recordings

Clinical pharmacology studies enrolled 751 healthy volunteers including 336 females, with no statistical age differences between females and males ( $34.5 \pm 10.3$  vs.  $34.2 \pm 8.7$  years).

Before study enrolment, all the subjects had normal standard clinical ECG and normal clinical investigation. Standard inclusion and exclusion criteria mandated for phase I pharmacology studies (Guideline, 2001) were applied. These included negative tests for recreational substance tests and negative pregnancy tests in females. The studies were conducted at six different locations, and all were ethically approved by the institutional ethics bodies (Focus in Neuss; California Clinical Trials in Glendale; Parexel in Baltimore and Bloemfontein; PPD in Austin; and Spaulding in Milwaukee). The enrolled subjects gave informed written consent not only for study participation but also for scientific investigation of collected data. Parts of the same data have already been used in independent physiology studies assessing different electrocardiography aspects (Andršová et al., 2020; Toman et al., 2020; Hnatkova et al., 2021).

In every subject, repeated long-term 12-lead Holter ECG recordings with Mason-Likar electrode positions were obtained covering full day-time periods when the volunteers were on no medication and when they were not allowed to smoke and/or consume alcohol or caffeinated drinks. Because this investigation utilised only drug-free data either before the subjects received any investigative drug or after an appropriately long washout of the investigated drug and of its metabolites (Guideline, 2001), other specifics of the source pharmacology studies are unimportant.

### Electrocardiographic Measurement

Using previously described methods (Malik et al., 2008b, 2012), multiple 10-s sinus rhythm segments (i.e., segments without any ectopic beats) were extracted from the 12-lead Holter recordings.

The segments captured different heart rates available in the Holter recordings including different heart rate changes.

In each of these ECG segments, QT interval was measured following published procedures (Malik et al., 2008b, 2012) that included repeated visual controls of all the measurements and assurance that corresponding ECG morphologies were interpreted in a consistent way (Hnatkova et al., 2009). The visually verified QT interval measurements were made in representative median waveforms of the 10-s segments (sampled at 1,000 Hz) with superimposition of all the 12 leads on the same isoelectric axis.

For each 10-s segment, the RR interval sequence within the segment and within the preceding 5 min of the Holter recordings was also obtained. The positions of QRS complexes were determined automatically using different previously validated detection algorithms. When these algorithms disagreed, the QRS were localised manually by simultaneous display of all the 12 ECG leads.

### QT/RR Adaptation Models

Since QT/heart rate relationship is known to be different in different individuals, the description of QT/RR adaptation used mathematical forms with parameters optimised for different subjects. All the following formal descriptions of the models expect the QT and RR interval durations to be expressed in seconds.

The principal analysis was based on the previously published (Malik et al., 2013) non-linear curvature regression model

$$QT_i = X + \Psi \left[ (RR_i^H)^\gamma - 1 \right] + \varepsilon_i$$

where  $QT_i$  is the  $i$ -th measured QT interval;  $RR_i^H$  is the corresponding hysteresis-corrected (see the next section) duration of the RR interval representing the underlying heart rate;  $X$ ,  $\Psi$ , and  $\gamma$  are individually optimised parameters ( $\gamma$  is the curvature of the QT/RR relationship) and  $\varepsilon_i$  are zero-centred regression errors. As previously explained (Malik et al., 2013), the slope of regression is expressed as  $\Psi \times \gamma$  (where  $X$  and  $\Psi$  are obtained by simple linear regression modelling for a given value of  $\gamma \neq 0$ , whilst the value of  $\gamma$  is obtained by minimising the mean of  $\varepsilon_i$  squares).

With this curvature model, individually corrected QTc intervals were given by the formula

$$QTc = QT + \Psi \left[ 1 - (RR^H)^\gamma \right]$$

In addition to this primary curvature model of the QT/heart rate relationship, two simpler models were used to allow for comparisons with previous publications. The linear model was given by the formula

$$QT_i = \chi + \beta(RR_i^H - 1) + \varepsilon_i$$

while the log-log model was given by the formula

$$\log(QT_i) = \phi + \alpha \times \log(RR_i^H) + \varepsilon_i$$

where  $\beta$ ,  $\chi$ ,  $\alpha$ , and  $\phi$  are individually optimised parameters and other symbols have the same meaning as in the curvature model. The parameters  $\beta$  and  $\alpha$  are the slopes of the linear and log-log models, respectively.

The linear and log-log models led to QTc formulas:

$$QTc = QT + \beta(1 - RR^H) \text{ and } QTc = QT/(RR^H)^\alpha, \text{ respectively.}$$

### Expressions of QT/RR Hysteresis

To distinguish QT/RR hysteresis driven by absolute time and by the number of preceding cardiac cycles, two models of QT/RR hysteresis were used. Both derived hysteresis-corrected  $RR^H$  intervals as weighted averages of RR intervals preceding the QT measurement, and both used averaging weights based on previously proposed exponential decay, i.e., on the assumption that the influence of RR interval duration of the QT interval duration decreases exponentially when moving backward from the QT interval measurement (Malik et al., 2008a). That is, both models considered the history  $\{RR_i\}_{i=0}^N$  of  $N$  consecutive RR intervals preceding the QT measurement ( $RR_0$  being closest to the QT measurement) and expressed the hysteresis-corrected  $RR^H$  interval as:

$$RR^H = \sum_{i=0}^N \omega_i RR_i \text{ where } \sum_{i=0}^N \omega_i = 1.$$

The models differed in the definition of weights  $\{\omega_i\}_{i=0}^N$ . The model assuming the dependency on the number of preceding RR intervals used weights such that

$$\sum_{i=0}^k \omega_i = \frac{1 - e^{\mathcal{L}_I(\frac{k+1}{N+1})}}{1 - e^{\mathcal{L}_I}} \text{ for each } k, 0 \leq k \leq N,$$

while the model assuming the dependency on the absolute time preceding the QT interval measurement used the weights such that

$$\sum_{i=0}^k \omega_i = \frac{1 - e^{\mathcal{L}_T(\frac{T(k)}{T(N)})}}{1 - e^{\mathcal{L}_T}} \text{ where}$$

$$T(k) = \sum_{i=0}^k RR_i \text{ for each } k, 0 \leq k \leq N.$$

The coefficients  $\mathcal{L}_I$  and  $\mathcal{L}_T$  were individually optimised.

After the QT/RR hysteresis models were individually optimised (see the subsequent section), the coefficients  $\mathcal{L}_I$  and  $\mathcal{L}_T$  were, for the purposes of physiologic interpretation, converted to 95% hysteresis constants  $\mathcal{C}_I$  and  $\mathcal{C}_T$ , i.e., for each subject, the constant  $\mathcal{C}_I$  specified the number of RR intervals after which the dynamicity of QT interval duration reached 95% of the rate-corresponding change, and likewise, the constant  $\mathcal{C}_T$  specified the time needed for the 95% dynamic QT interval change. That is, the interval count  $\mathcal{C}_I$  and time span  $\mathcal{C}_T$  were identified such that:

$$\frac{1 - e^{\mathcal{L}_I(\frac{\mathcal{C}_I+1}{N+1})}}{1 - e^{\mathcal{L}_I}} = 0.95 \text{ and } \frac{1 - e^{\mathcal{L}_T(\frac{\mathcal{C}_T}{T(N)})}}{1 - e^{\mathcal{L}_T}} = 0.95.$$

This means that the lower the count  $\mathcal{C}_I$  or the shorter the time span  $\mathcal{C}_T$ , the faster the QT-interval adaptation to heart rate changes (or, in other words, the shorter the delay after which the QT interval reaches equilibrium after heart rate change).

### Residuals of QT/RR Models and Individual Model Optimisation

The combination of the three QT/RR adaptation models with the two QT/RR hysteresis models led to six different possibilities. In each subject, each of the six possibilities was optimised to achieve the closest fit of the QT/RR<sup>H</sup> regressions. That is, for each subject, parameters,  $\Psi$ ,  $\gamma$ ,  $\beta$ ,  $\alpha$ ,  $\mathcal{L}_I$ , and  $\mathcal{L}_T$  were optimised such that each of the models led to the lowest standard deviation of the corresponding QTc intervals. These values were expressed in milliseconds.

By definition of the QTc intervals, the QTc standard deviations constituted regression residuals of the intra-subject QT/RR<sup>H</sup> regression models, which were used to compare the closeness of fit among the six different modelling possibilities. This was based on the understanding that the closeness of data fit is an appropriate measure of the relevancy of any physiologic model. In other words, a combination of QT/RR adaptation and hysteresis models was considered physiologically more valid than another combination if it led to significantly lower regression residuals. Since the regression residuals were calculated for each subject separately, their intra-subject means were compared across the study population.

### Distinction Between Heart Rate Acceleration and Deceleration

To investigate whether QT/RR hysteresis speed differs between heart rate acceleration and deceleration, episodes of systematic rate increase and decrease were identified in the recordings of each study subject. For this purpose,  $\{RR_i\}_{i=0}^N$  histories of RR intervals preceding each QT measurement were considered and the slopes  $s_{0-30}$ ,  $s_{30-60}$ , and  $s_{0-60}$  of a linear regression between  $RR_i$  durations and their index numbers  $i$  were calculated between 0 and 30 s, 30 and 60 s, and 0 and 60 s preceding the QT measurement, respectively.

QT interval measurement was considered preceded by heart rate acceleration if  $s_{0-30} > 0$ ,  $s_{30-60} > 0$ , and if the lower 95% confidence intervals of  $s_{0-60}$  was positive. Likewise, QT interval measurement was considered preceded by heart rate deceleration if  $s_{0-30} < 0$ ,  $s_{30-60} < 0$ , and if the upper 95% confidence intervals of  $s_{0-60}$  was negative (note that  $RR_0$  interval was closest to the QT measurement, and that while 5-min histories of RR interval were available, the rate acceleration and deceleration episodes were defined using only the preceding 1 min. This is consistent with the asymptotic nature of the  $\omega_i$  coefficients in the exponential decay models).

In each subject, QT measurements preceded by heart rate acceleration and deceleration according to this definition were sorted according to the corresponding  $s_{0-60}$  slopes. A stepwise elimination algorithm was used to obtain subsets of these QT interval measurements that were as close as possible to a one-to-one correspondence between the absolute  $|s_{0-60}|$  values. This



eliminated the possibility of comparing QT/RR hysteresis speeds among data that showed faster rate acceleration than deceleration or vice versa.

In each of these balanced sets of heart rate acceleration and deceleration episodes, the optimisation of QT/RR hysteresis models, as described previously, was repeated (that is, separately for acceleration and deceleration episodes), and for each subject and for each of the six combinations of QT/RR adaptation and hysteresis models, separate rate acceleration and deceleration coefficients  $\mathfrak{L}_I$  and  $\mathfrak{L}_T$  were obtained and converted into acceleration and deceleration hysteresis constants  $\mathfrak{C}_I$  and  $\mathfrak{C}_T$ . Their statistical evaluations allowed for the comparison of QT/RR hysteresis speed between rate increase and decrease.

## Statistics and Data Presentation

Descriptive data are presented as means  $\pm$  SD. Comparisons between females and males were based on two-sample two-tail *t*-test assuming different variations between compared datasets, intra-subject comparisons (e.g., comparisons of regression residuals among the different QT/RR adaptation models) were based on paired two-tail *t*-test. The significance of linear regression slopes between age and investigated indices was tested by Fisher–Snedecor *F* distribution. Statistical tests used IBM SPSS package version 27. *P*-values below 0.05 were considered statistically significant. Because of interdependence among the different indices, no correction for multiplicity of statistical testing was performed.

## RESULTS

Relevant characteristics of the study population are summarised in **Figure 2**. As seen in this Figure, most of the subjects were aged between 20 and 50 years (87.8% females and 94.6% males).

In these subjects, altogether, 897,570 QT interval measurements in separate 10-s ECG segments were made, each with a 5-min history of preceding RR intervals. On average, there were  $1,195 \pm 293$  such measurements in the individual subjects. **Figure 2** also shows that in the individual subjects, broad ranges of heart rates were covered by these measurements, assuring that the data were suitable for stable regression analyses between QT interval and the underlying RR interval expressions (indeed, all the QT/RR models reported further led to significantly positive QT/RR slopes). Finally, **Figure 2** shows that in the individual subjects, the 5-min histories of preceding RR intervals covered sufficient ranges of heart rate acceleration and deceleration suitable for the QT/RR hysteresis estimates. On average,  $74.3 \pm 7\%$  of QT interval measurements in females and  $72.4 \pm 7.4\%$  of QT interval measurements in males were preceded by RR interval histories that showed statistically significant acceleration or deceleration (i.e., within 1 min preceding the QT interval measurement, the slope between RR interval durations and their order numbers was significantly different from zero).

## QT/RR Adaptation Models

**Figure 3** shows cumulative distributions of regression residual values for all the three types of QT/RR adaptation models. It

is clearly visible that for all the three models, the regression residuals were larger in females than in males. For the combination of curvature QT/RR adaptation with time-based and interval-based QT/RR hystereses, the residuals in females and males were  $5.68 \pm 1.1$  vs.  $5.31 \pm 1.08$  ms, and  $5.77 \pm 1.13$  vs.  $5.45 \pm 1.14$  ms, respectively, and both *p*-values were  $< 0.0001$ . The same strong statistical significance ( $p < 0.0001$ ) of sex differences was seen for all the other model combinations.

Comparison of the different panels in **Figure 3** also shows that, not surprisingly, regression residuals of the curvature QT/RR model were smaller than those of the linear QT/RR model, and that the residuals of the log-log QT/RR model were noticeably larger than those of the other models. In combination with the time-based QT/RR hysteresis, the residuals over the complete population were  $5.47 \pm 1.1$ ,  $5.65 \pm 1.14$ , and  $5.98 \pm 1.21$  ms for the curvature, linear, and log-log models, respectively. In combination with the interval-based QT/RR hysteresis, the corresponding values were  $5.59 \pm 1.15$ ,  $5.78 \pm 1.19$ , and  $6.1 \pm 1.25$  ms.

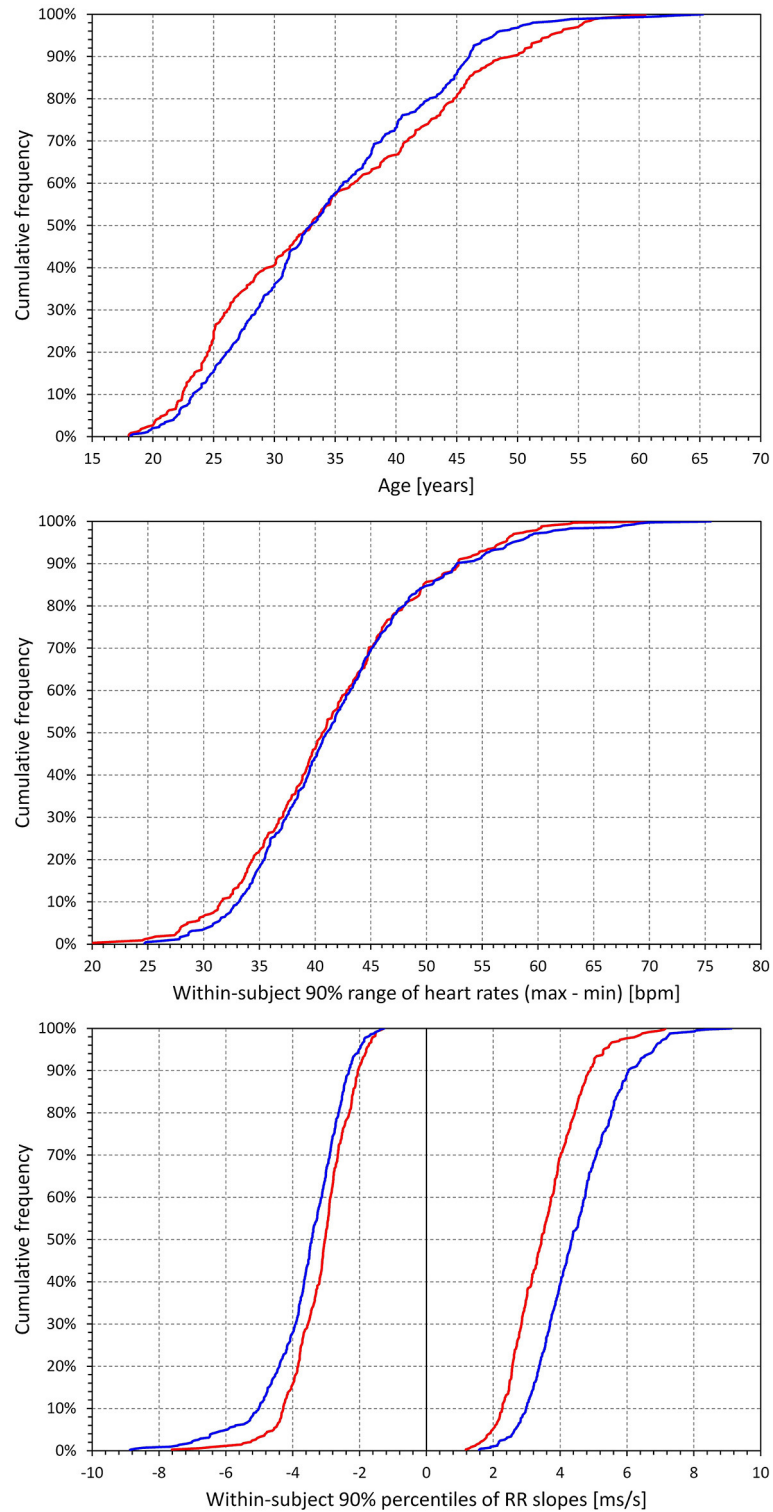
**Figure 4** shows scatter diagrams of intra-subject differences between the regression residuals of the different QT/RR adaptation models combined with the time-based QT/RR hysteresis model. The population averages of the intra-subject differences among the curvature and linear, curvature and log-log, and linear and log-log models were  $0.171 \pm 0.240$ ,  $0.509 \pm 0.317$ , and  $0.338 \pm 0.328$  ms, respectively (all significantly positive with  $p < 0.0001$ ). Similar statistical differences were also seen in each model separately for females and males, and for the combination with the interval-based QR/RR hysteresis model.

Using the curvature QT/RR adaptation model combined with the time-based QT/RR hysteresis model, **Figure 5** shows differences between females and males for the curvature parameter of the adaptation model ( $0.579 \pm 0.709$  vs.  $0.742 \pm 0.733$ ,  $p = 0.0021$ ), heart rate corresponding to the intra-subject mean  $RR^H$  intervals ( $73.3 \pm 6.8$  vs.  $68.3 \pm 6.4$  beats per minute,  $p < 0.0001$ ), and the intra-subject mean of QTc intervals ( $421 \pm 14$  vs.  $401 \pm 13$  ms,  $p < 0.0001$ ).

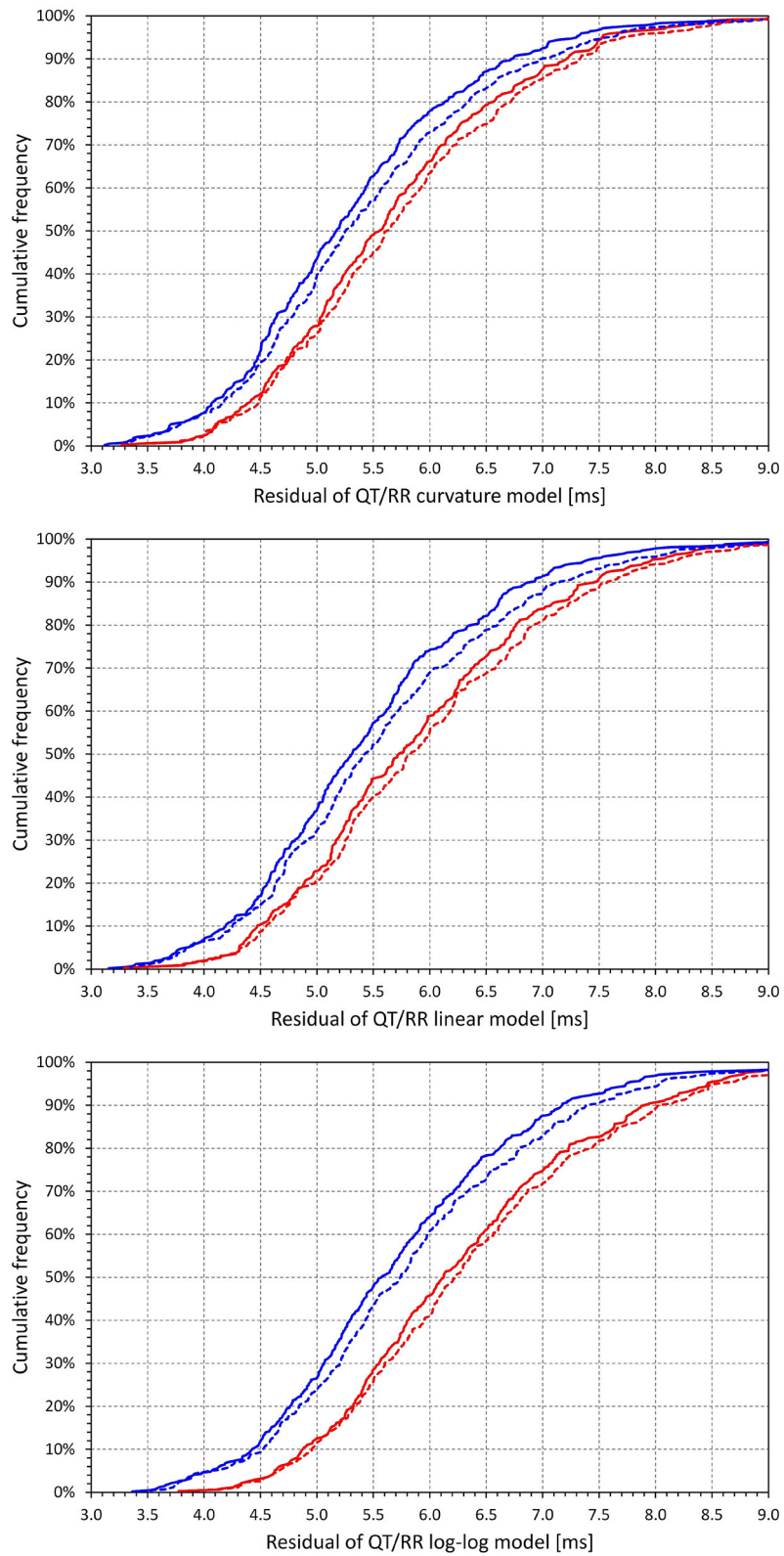
**Figure 6** confirms previously published observations that irrespective of adaptation and hysteresis models, the pattern of QT/RR relationship is steeper in females than in males (Malik et al., 2013) (for example, the slope of the curvature adaptation model combined with time-based hysteresis was  $0.161 \pm 0.033$  in females and  $0.142 \pm 0.026$  in males,  $p < 0.0001$ ).

## QT/RR Hysteresis Models

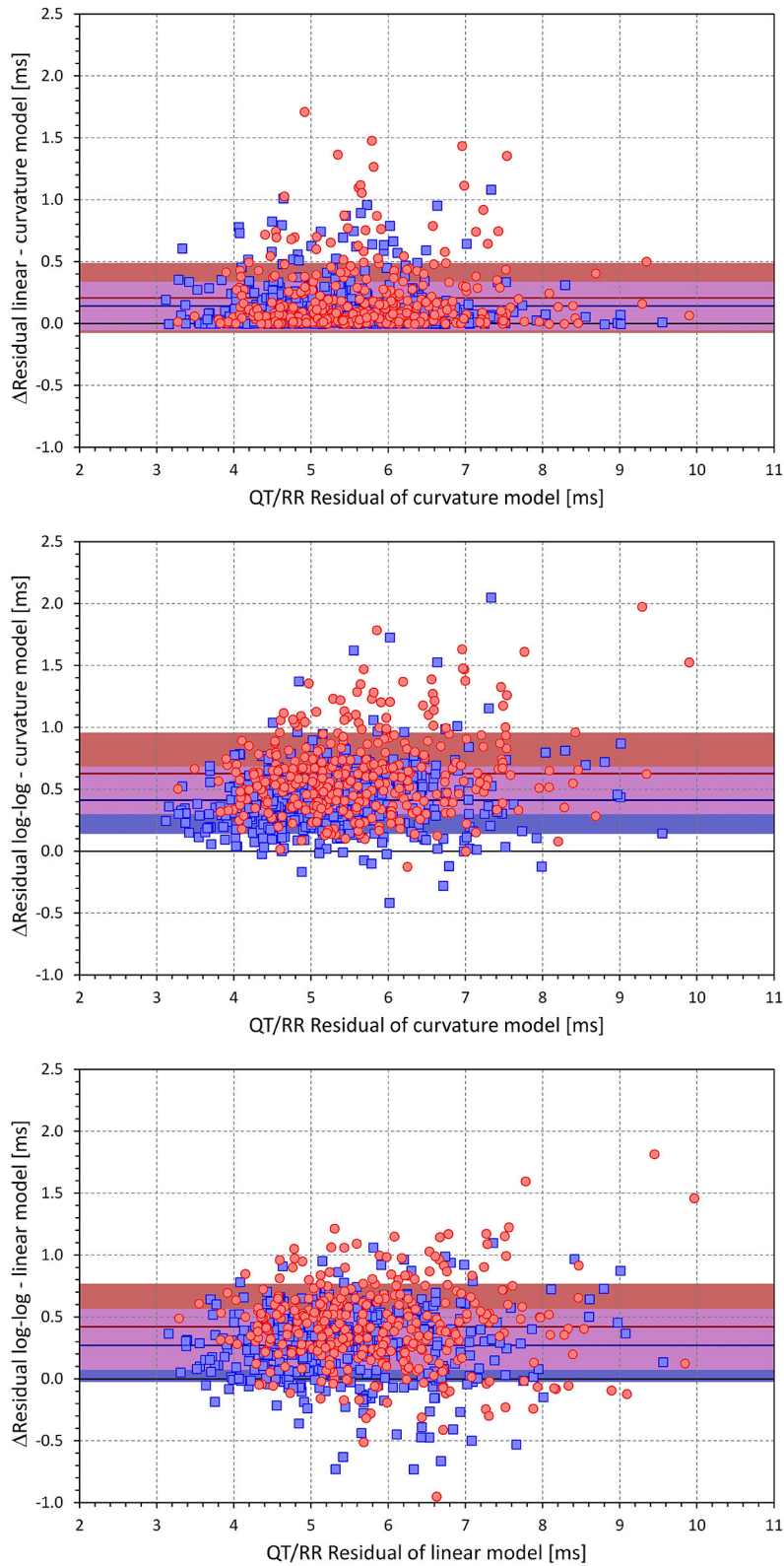
**Figure 7** shows that irrespective of the QT/RR adaptation model, the QT/RR hysteresis time-constants  $\mathfrak{C}_T$  were, on average, shorter in females than in males (e.g.,  $118 \pm 22$  vs.  $125 \pm 22$  s and  $p < 0.0001$  for the QT/RR curvature model). **Figure 8** shows that the same sex difference was also present for the hysteresis interval-constants  $\mathfrak{C}_I$  (e.g.,  $148 \pm 32$  vs.  $155 \pm 27$ ,  $p = 0.0027$ , also for the QT/RR curvature model). The somewhat lesser sex difference in the  $\mathfrak{C}_I$  constants compared to  $\mathfrak{C}_T$  constants needs to be interpreted together with the faster rates in females (as shown in **Figure 4**), which led to the same number of RR intervals representing shorter time in females than in males.



**FIGURE 2 |** Characteristic of the study population and electrocardiographic measurements. Top panel shows cumulative distributions of the ages of investigated subjects. The middle panel shows cumulative distributions of the 90% ranges of intra-subject heart rates in study subjects (that is, in each study subject, difference between the 5th and 95th percentiles of heart rates at which the QT interval was measured was calculated, and the panel shows the cumulative distribution of these differences). The bottom panel shows the cumulative distributions of the intra-subject 5th and 95th percentiles of the RR interval slopes preceding QT interval measurements (that is, for each subject, 60-s slopes of RR interval durations vs. their index numbers were obtained for each RR history of QT interval measurements, and the graphs show the distribution of the intra-subject 5th and 95th percentiles of these slopes. In each subject, the 5th percentile corresponded to heart rate deceleration, distributions below 0, and the 95th percentile corresponded to heart rate acceleration, distributions above 0). In each graph, the red and blue lines correspond to the female and male subjects, respectively.



**FIGURE 3 |** Cumulative distributions of intra-subject residuals of QT/RR<sup>H</sup> regression models for the curvature model (top panel), linear model (middle panel), and log-log model (bottom panel). In each of the panels, the red and blue lines correspond to females and males, respectively; the full and dashed lines correspond to the time-based and interval-based QT/RR hysteresis models, respectively.



**FIGURE 4** | Scatter diagrams of the intra-individual differences among the different QT/RR<sup>H</sup> regression models (all combined with the time-based QT/RR hysteresis model). The top panel shows the differences between the residuals of the linear and curvature models and the residuals of the curvature model, the middle panel (Continued)

**FIGURE 4** | shows the differences between the residuals of the log-log and curvature models and the residuals of the curvature model, and the bottom panel shows the differences between the residuals of the log-log and linear models and the residuals of the linear model. In each panel, the red circle and blue square marks correspond to females and males, respectively. The red and blue horizontal lines show the mean values of the residual differences in females and males, respectively. The light-coloured red and blue bands show the spans of mean  $\pm$  standard deviation of the residual differences in females and males, respectively; the light-coloured violet bands show the overlap of the mean  $\pm$  standard deviation bands between both sexes.

As already seen in **Figure 3**, a combination of any of the QT/RR adaptation models with the time-based QT/RR hysteresis led to lower regression residuals compared to the combination with the interval-based hysteresis. Confirmation of this observation with intra-subject differences is shown in **Figure 9**. The population averages of intra-subject differences in the residuals were  $0.119 \pm 0.198$ ,  $0.131 \pm 0.234$ , and  $0.119 \pm 0.186$  ms for the curvature, linear, and log-log adaptation models, respectively, and all were significantly positive ( $p < 0.0001$ ). In all the three adaptation models, these intra-subject differences were also smaller in females compared to males (e.g.,  $0.092 \pm 0.209$  vs.  $0.141 \pm 0.187$  ms and  $p = 0.001$  with the curvature adaptation model).

## Relationship to Age

**Figure 10** shows the relationship to age of selected indices derived from the curvature QT/RR adaptation model combined with the time-based QT/RR hysteresis model. The Figure shows that the curvature model was negatively moderately related to age in the males ( $p = 0.039$ ) but not in the females, and that hysteresis time constant was significantly increased with age ( $p < 0.0001$  for both sexes), as did the mean QTc interval ( $p < 0.0001$  in females and  $p = 0.001$  in males). Whilst there was little sex difference in QTc prolongation with increasing age, hysteresis time constant increased with age more steeply in males than in females ( $p = 0.03$ ). That is, the sex difference in the hysteresis time constant increased with age. No other index showed a relationship to age (including, perhaps surprisingly, the regression residuals).

The same observation of hysteresis constants and individually corrected QTc intervals increasing with age was made with other combinations of the QT/RR adaptation and QT/RR hysteresis models.

## QT/RR Hysteresis During Rate Acceleration and Deceleration

In individual study subjects, the close one-to-one matching between heart rate acceleration and deceleration instances selected  $66 \pm 20$  pairs of ECG segments with QT interval measurements.

The cumulative distributions of the differences between hysteresis time-constants  $\mathcal{C}_T$  optimised for rate acceleration and deceleration are shown in **Figure 11**; the same differences for the interval-constants  $\mathcal{C}_I$  are shown in **Figure 12**. Both Figures show that the subjects in whom the hysteresis speed was slower during heart rate acceleration than during heart rate deceleration were more numerous compared to the subjects showing the opposite relationship. The Figures also show that the difference in the proportion of subjects was more pronounced in males than in females.

The corresponding differences between hysteresis time and interval constants are shown in **Figures 13, 14** that present the constants optimised for rate acceleration and deceleration in a Bland-Altman type of scatter diagrams. The population means (as well as sex-specific population means) of all the differences were significantly positive, although the diagrams also show outliers of the overall data distribution (mainly seen in cases with only few acceleration-deceleration data pairs). When optimising the QT/RR hysteresis models with the curvature models of QT/RR dependency, the acceleration-deceleration differences in the  $\mathcal{C}_T$  constants were  $35.5 \pm 56.8$  and  $58.4 \pm 58.8$  s in females and males, respectively, both significantly positive ( $p < 0.0001$ ) and significantly different between sexes ( $p < 0.0001$ ). The corresponding differences in the  $\mathcal{C}_I$  constants were  $15.6 \pm 47.8$  and  $27.2 \pm 54.5$  cardiac cycles, again both significantly positive ( $p < 0.0001$ ) and significantly different between sexes ( $p = 0.0019$ ).

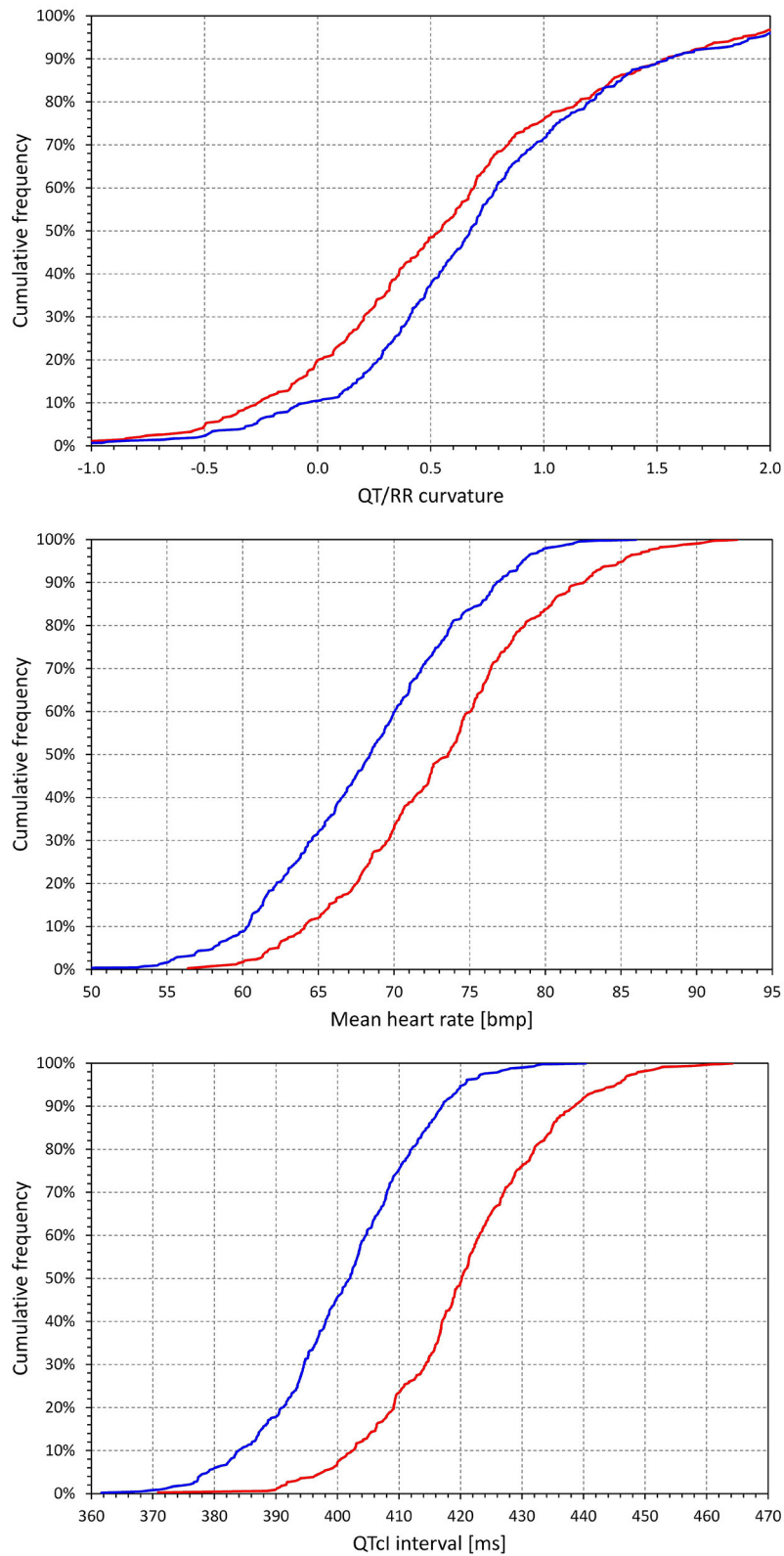
## DISCUSSION

The results of these analyses offer several conclusions of physiologic and, possibly, practical relevance. First, the profile of QT/RR hysteresis appears to be driven by absolute time rather than by the numbers of cardiac cycles. Second, the speed of QT/RR hysteresis is decreased with increase in age, and the duration of carefully and individually rate-corrected QTc interval is increased with increase in age. Third, QT/RR hysteresis differences between heart rate acceleration and deceleration are not physiologically systematic (i.e., they differ among different healthy subjects), but our data suggest that on average, QT/RR hysteresis speed is slower after heart rate acceleration than after heart rate deceleration. All these observations were based on the evaluation and comparisons of different combinations of the QT/RR adaptation and QT/RR hysteresis models.

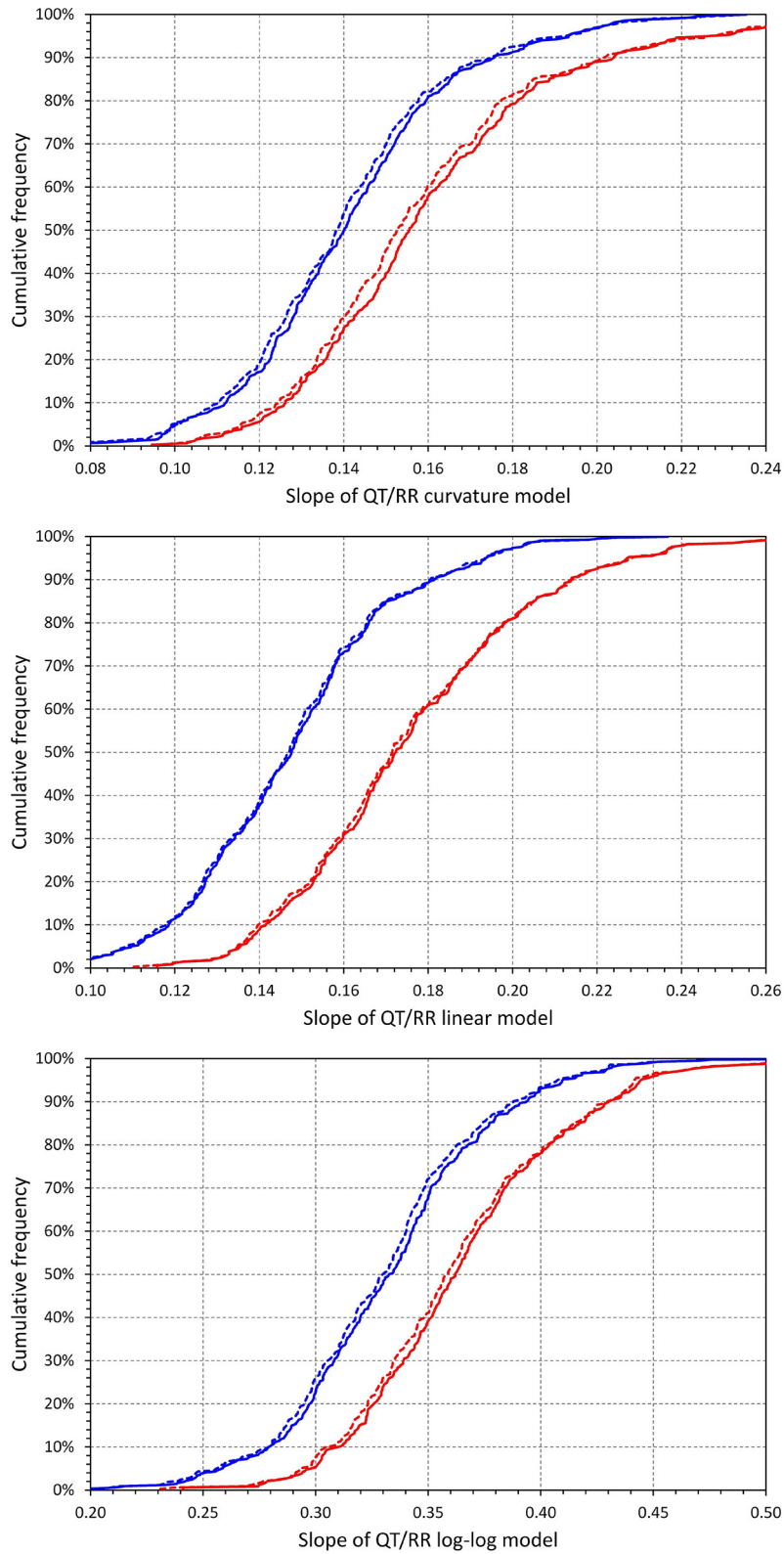
## QT/RR Hysteresis Properties

Repeated studies have previously described the implications of QT/RR hysteresis for the accuracy of the heart rate correction of QT interval measurement (Malik, 2014; Gravel et al., 2017, 2018). It has also been shown that incorporating hysteresis correction reduces the variability of QTc values significantly (Malik et al., 2008a,c). All the hysteresis estimates postulate that the RR interval duration used in the heart rate correction formulas of the QT interval cannot be directly measured but needs to be derived from a longer history of cardiac cycles preceding the QT measurement. This increases the compactness of the QT/RR relationship and allows for characterisation of the relationship in each subject with a greater precision and increased confidence (example in **Figure 15**).

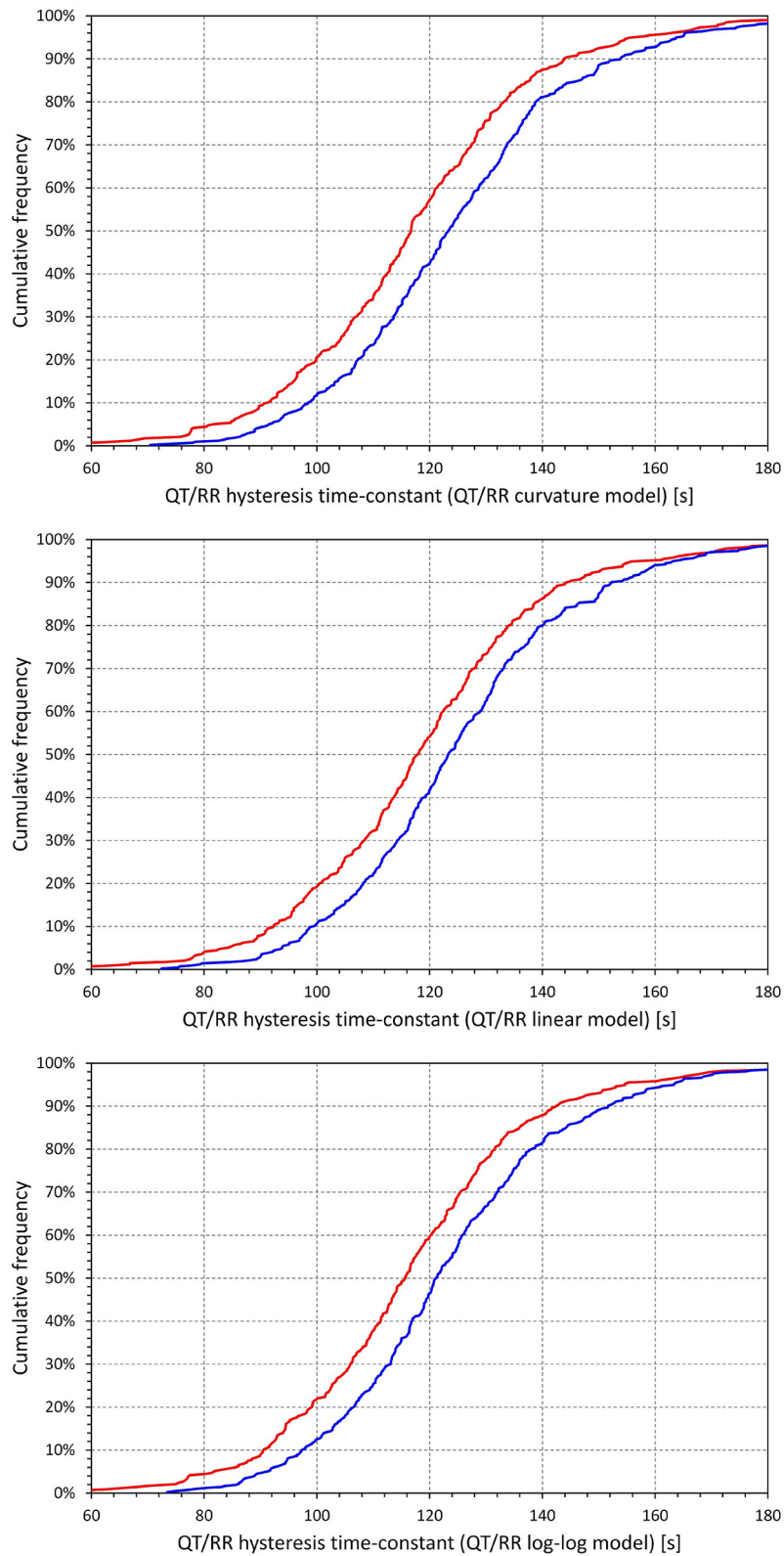
Whilst the exponential decay model used in this study allowed us to distinguish the time-based and interval-based hysteresis



**FIGURE 5 |** Cumulative distributions of the subject-specific characteristics of the curvature  $QT/RR^H$  model combined with time-based curvature  $QT/RR$  hysteresis model. The distributions of model curvature (parameter  $\gamma$ ), mean heart rate derived from the  $RR^H$  values, and mean individually corrected  $QT_c$  intervals are shown in the top, middle, and bottom panels, respectively. The red and blue lines correspond to females and males, respectively.

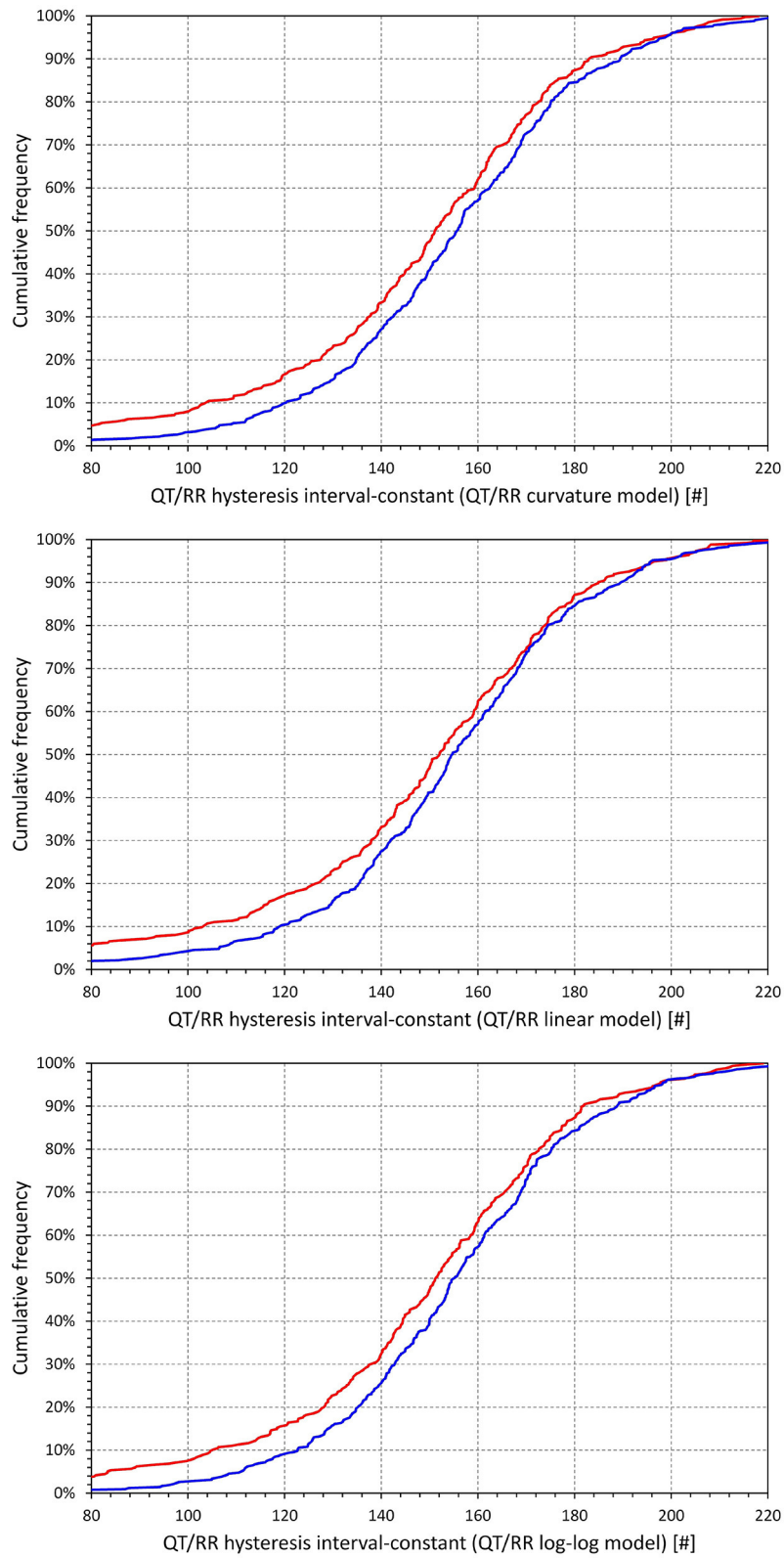


**FIGURE 6 |** Cumulative distributions of intra-subject slopes of QT/RR<sup>H</sup> regression models for the curvature model (top panel), linear model (middle panel), and log-log model (bottom panel). In each of the panels, the red and blue lines correspond to females and males, respectively; the full and dashed lines correspond to the time-based and interval-based QT/RR hysteresis models, respectively.

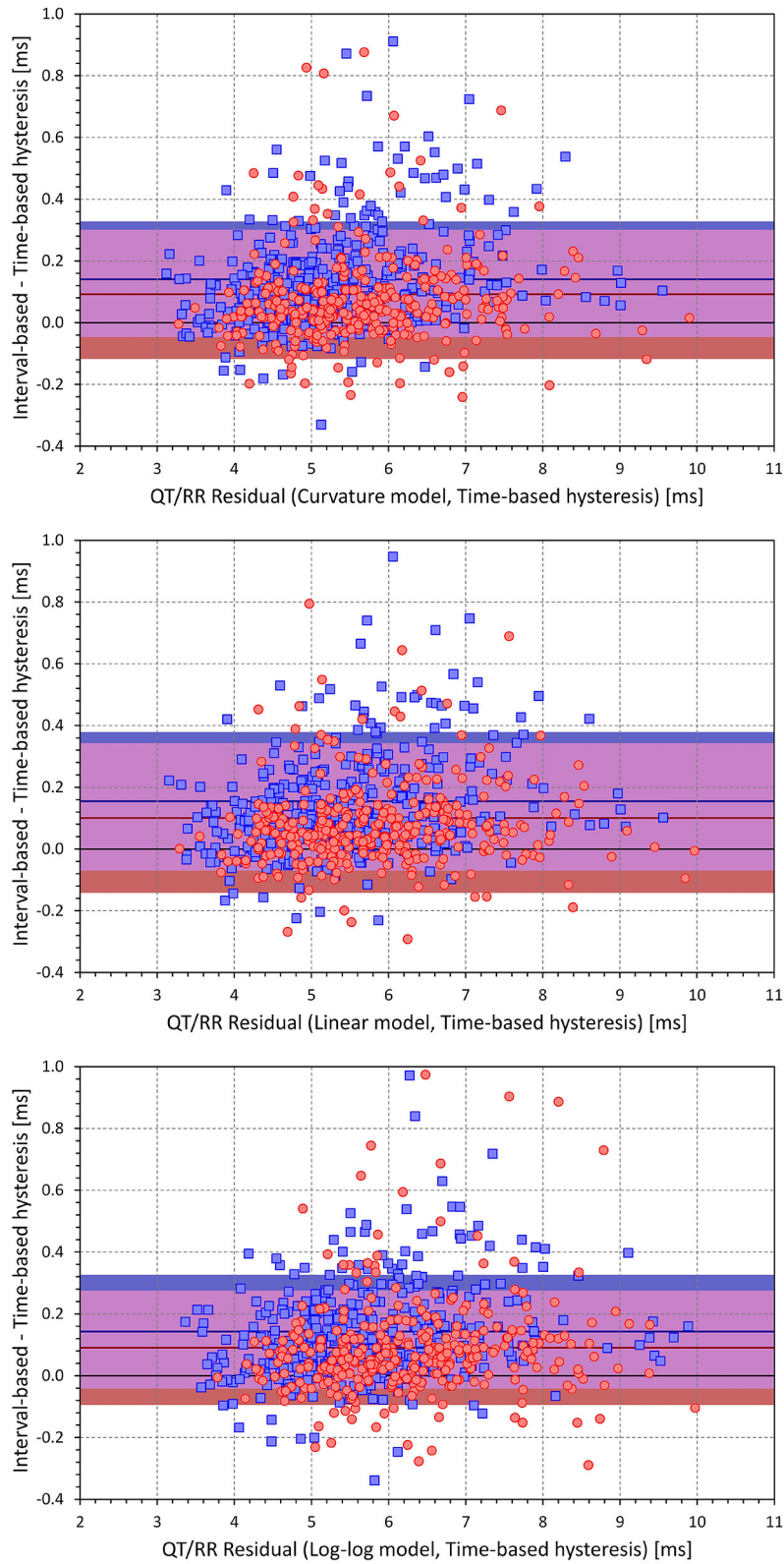


**FIGURE 7 |** Cumulative distributions of QT/RR hysteresis time-constants derived from the combination with the QT/RR<sup>H</sup> curvature model (top panel), linear model (middle panel), and log-log model (bottom panel). In each of the panels, the red and blue lines correspond to females and males, respectively.





**FIGURE 8** | Cumulative distributions of QT/RR hysteresis interval constants derived from the combination with the QT/RR<sup>H</sup> curvature model (top panel), linear model (middle panel), and log-log model (bottom panel). In each of the panels, the red and blue lines correspond to females and males, respectively.



**FIGURE 9** | Scatter diagrams of the intra-individual differences among regression residuals comparing the interval-based and time-different QT/RR hysteresis models. The differences between the residuals and the residuals of the time-based QT/RR hysteresis model are shown for the QT/RR<sup>H</sup> curvature model in the top panel, linear  
(Continued)

**FIGURE 9** | model in the middle panel, and log-log model in the bottom panel. In each panel, the red circle and blue square marks correspond to females and males, respectively. The red and blue horizontal lines show the mean values of the residual differences in females and males, respectively. The light-coloured red and blue bands show the spans of mean  $\pm$  standard deviation of the residual differences in females and males, respectively; the light-coloured violet bands show the overlap of the mean  $\pm$  standard deviation bands between both sexes.

expressions, other approaches have been proposed (Jacquemet et al., 2014), e.g., the autoregressive filter approach which, for beat-to-beat consecutive measurements of RR intervals  $\{RR_i\}_{i=0}^N$ , optimises a parameter  $\vartheta$  so that QT interval measurement following the interval  $RR_j$  (for  $j \gg 0$ ) is corrected for  $RR_j^H = \vartheta RR_j + (1 - \vartheta)RR_{j-1}^H$ . It is easy to demonstrate that this autoregressive approach differs minimally from the interval-based exponential decay model (Malik, 2014). Making the parameter  $\vartheta$  cycle-by-cycle dependent on the duration of RR intervals would lead to an approach closely corresponding to the time-based approach that our study found significantly (albeit numerically only slightly) more accurate. Therefore, implementation of our observation of the preference of the time-based QT/RR hysteresis models needs to be further tested in other mathematical implementations.

In addition to separate estimates of QT/RR hysteresis, i.e., corrections of the RR interval values to be used in QT/heart-rate corrections, more complex autoregressive models involve both beat-to-beat RR interval history and QT interval history (Porta et al., 2010, 2020; El-Hamad et al., 2019). These approaches were shown useful in providing estimates of QT interval changes and variability that cannot be explained by heart rate and cardiac period influence (Baumert et al., 2016). We were not able to employ any of these methods, since QT interval measurements of the source clinical studies were not performed on a consecutive beat-to-beat basis. The combination of both QT and RR histories in the same model also does not allow for a clear separation between QT/RR adaptation steepness and speed of QT/RR hysteresis.

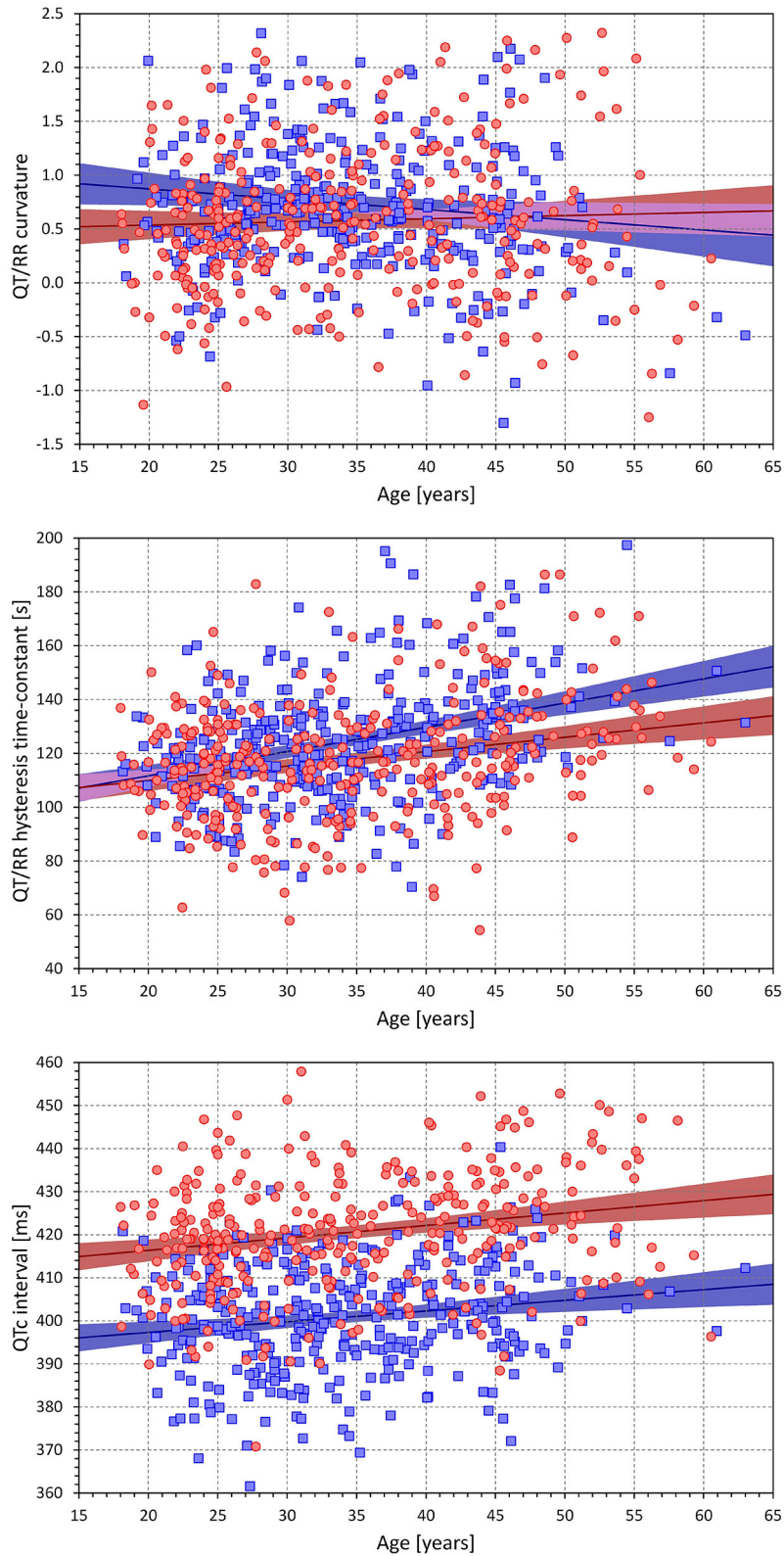
Estimates of QT/RR hysteresis in the data derived from long-term ECG recordings are based on the assumption that the profile of the hysteresis (i.e., influence of the sequence of RR intervals preceding the measured QT interval) remains the same throughout the recordings. Such an assumption is an obvious simplification. Following rhythm abnormalities including supraventricular abnormalities, e.g., compensatory pauses of atrial ectopic beats, noticeable sinus pauses, abrupt vagal withdrawal, etc., noticeable QT interval changes might be detected on a beat-to-beat basis (the term “immediate effect” is occasionally used). In other situations, e.g., marked respiratory and other physiologic sinus arrhythmia, little or no beat-to-beat effects of heart period changes on the subsequent QT interval can frequently be detected (as in the example in **Figure 1**). It is therefore appropriate to study QT/RR hysteresis under different conditions, which led to our differentiation between heart rate acceleration and deceleration, which might be expected to reflect different sympatho-vagal reactions.

Our observation of, on average, slower hysteresis speed during heart rate acceleration contradicts a recent report by

Axelsson et al. (2021) who observed the opposite. Nevertheless, they investigated the phenomenon in patients with permanent pacemakers and, thus, abnormalities in cardiac electrophysiology in whom QT/RR hysteresis might be different to that in the healthy subjects who were investigated in this study. The observations that we report were also based on heart rate changes due to physiologic reactions during drug-free days of pharmacologic investigations (i.e., due to movement and other responses to the environment in clinical research laboratories). Such situations might lead to electrophysiologic processes very different from responses to constant atrial or ventricular pacing at different fixed frequencies.

Initial studies on QT/RR hysteresis characterised the phenomenon by measuring the differences between QT intervals at the same instantaneous heart rate reached during rate acceleration (i.e., when QT interval duration is still influenced by slower heart rate in the past and, thus, is longer than it would correspond to the instantaneous heart rate under fully stabilised conditions) and deceleration (i.e., when QT interval duration is still influenced by previously faster rate and, thus, is shorter than the instantaneous heart rate would indicate) (Watanabe, 2007; Pelchovitz et al., 2012). These approaches led to measurements of the area of the “hysteresis window,” which was also used to study the influence of autonomic status and reflexes. Nevertheless, it is easy to understand that the measurements of hysteresis window area are highly problematic, since they depend on the speed of heart rate change (the faster the acceleration or deceleration of the rate, the greater the difference between the instantaneous rate and the rate derived from the history profile that influences QT duration). The reports of autonomic influences on the area of hysteresis window are consequently very difficult to interpret, since the speed of heart rate change (e.g., during and after physical exercise) is also subject to autonomic influence.

Because of these problems, the previous observations of autonomic influence on hysteresis window are difficult to compare with our observations that hysteresis speed declines with age, and that females show statistically faster hysteresis speed. These results might be interpreted as manifestations of cardiac autonomic status. Indeed, cardiac autonomic modulations are well-known to decrease with advancing age, and females have been shown to exhibit higher baseline parasympathetic modulations than males (Huikuri et al., 1996; Kuch et al., 2001; Hnatkova et al., 2019b). Thus, while QT/RR hysteresis might be influenced by cardiac autonomic status, other possibilities also exist that might explain our observations. These include a gradual buildup of myocardial fibrosis and an age-related increase in subclinical cardiac risk factors that might be expected to be more pronounced in males than in females.



**FIGURE 10 |** Scatter diagrams showing age influence on the subject-specific curvatures of the QT/RR<sup>H</sup> curvature model combined with time-based QT/RR hysteresis (top panel), on the subject-specific hysteresis time-constants of the QT/RR<sup>H</sup> curvature model (middle panel), and on the mean of individually corrected QTC intervals (Continued)

**FIGURE 10** | of the QT/RR<sup>H</sup> curvature model combined with time-based QT/RR hysteresis (bottom panel). In each panel, the red circle and blue square marks correspond to females and males, respectively. The red and blue lines show the linear regression models between the displayed characteristics and age, the light-coloured red and blue bands show the 95% confidence intervals of the linear regressions, and the light-coloured violet areas show the overlaps among the regression confidence intervals of both sexes.

## QT/QTc Variability

Although correcting QT interval duration for heart rate (or corresponding RR interval) derived from QT/RR hysteresis assessment leads to a substantial reduction in QTc variability (Malik et al., 2008a; Jacquemet et al., 2011, 2014; Hnatkova and Malik, 2020), the variability is not entirely eliminated as also demonstrated by the positive (i.e., > 0) regression residuals that we report (also note that the vertical width of the scatter diagram shown in **Figure 15** spans some 10 ms). There are different sources of such a variability. In addition to long-term QTc changes [e.g., due to postprandial effects (Hnatkova et al., 2014; Taubel et al., 2014)], the short-term beat-to-beat variability of QT interval duration (Baumert et al., 2016) also play a role, since this QT instability cannot frequently be explained by underlying cardiac cycle variations. The details of the properties of short-term QT variability (Baumert et al., 2008; Malik, 2008; El-Hamad et al., 2015) and of the underlying mechanisms of repolarisation instability (Kenttä et al., 2011; Bauer et al., 2019) are beyond the scope of this text, but it needs to be noted that, because of rate independence, this variability cannot be addressed by correction of QT/RR hysteresis. This also explain the frequent absence (or even occasional reversal) of the so-called immediate effect of each RR interval, as we have already discussed in the previous section.

## Open Questions

Some studies suggested QT/RR hysteresis models that include a fixed immediate effect coefficient (Halámek et al., 2007), i.e., assume that the RR interval immediately preceding the QT interval measurement has always a substantially larger influence than the preceding RR intervals. As already discussed, such larger influence does not correspond to many observations, since the reproducibility of the immediate effect might be questioned. Nevertheless, it is also possible that hysteresis profiles differ under different physiologic circumstances. The duration of the subsequent QT interval might, thus, respond differently to atrial premature contraction than to a sinus nodal cycle with the same coupling interval. In this sense, atrial and ventricular pacing experiments and/or pharmacologically induced rapid heart rate changes (e.g., those by intravenous atropine or phenylephrine) might not be fully relevant to study the mechanisms that determine QT/RR hysteresis during physiologically regulated sinus rhythm. Rather, different physiologic reflexes leading to heart rate changes might need to be compared, e.g., heart rate changes during postural manoeuvres, head-up tilt, or mental stress testing.

Studies on specific clinical populations might provide further insight into the mechanisms of QT/RR hysteresis as well as into processes that influence it, especially since differences in hysteresis profiles have previously been linked to the difference in survival of cardiac patients. Little is presently

known about QT/RR hysteresis in patients with abnormalities in autonomic and other cardiac regulation, e.g., patients with diabetic neuropathy, end-stage renal disease, thyroid dysfunction, or epilepsy. The role of cardiac structure would be better understood if QT/RR hysteresis was studied on patients with cardiac sarcoidosis, amyloidosis, lipomatosis, and cellular transplant rejection.

Presently, it is not known whether the sex difference in hysteresis speed occurs, similar to the differences in the individually corrected QTc intervals, around puberty (Andršová et al., 2019). Focused extensions of previous investigations in children and adolescents are needed to address this question.

## Additional Findings

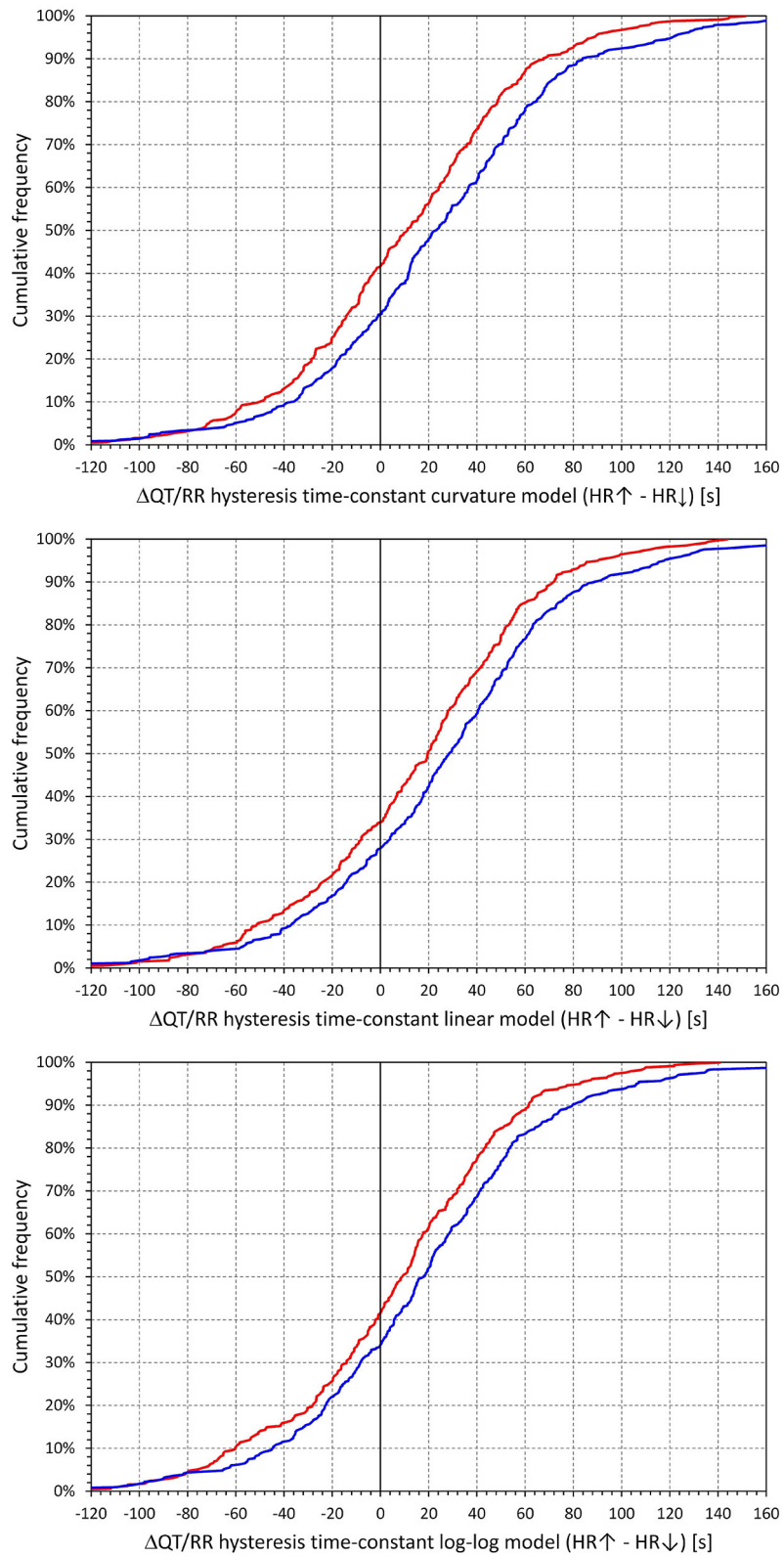
In addition to the findings related to QT/RR hysteresis, our study also led to further observations. Consistent with previous reports (Malik, 2018), the data of the study show that the somewhat popular intra-subject QT/RR regression modelling based on logarithm transformation (i.e., the modelling that leads to individually corrected QTc intervals in the form QT/RR<sup>α</sup>) is less accurate than simple linear regressions. While the differences in the residuals of the QT/RR models are numerically small, they still play a role in power sample calculations of studies that depend on accurate QTc estimates (Malik et al., 2004).

QTc interval increases related to advancing age have previously been described (Rautaharju et al., 2014; Linde et al., 2018). Our study thus contributes only the observation that these age-related increases are also present when considering individually corrected QTc intervals rather than QTc values based on less accurate universal (i.e., not subject-specific) rate corrections. Somewhat surprisingly, we have not observed age influence on mean heart rate. However, this might have been affected by the calculation of the means across heart rates derived from the episodes when QT interval was measured rather than across the complete profile of the source Holter recordings.

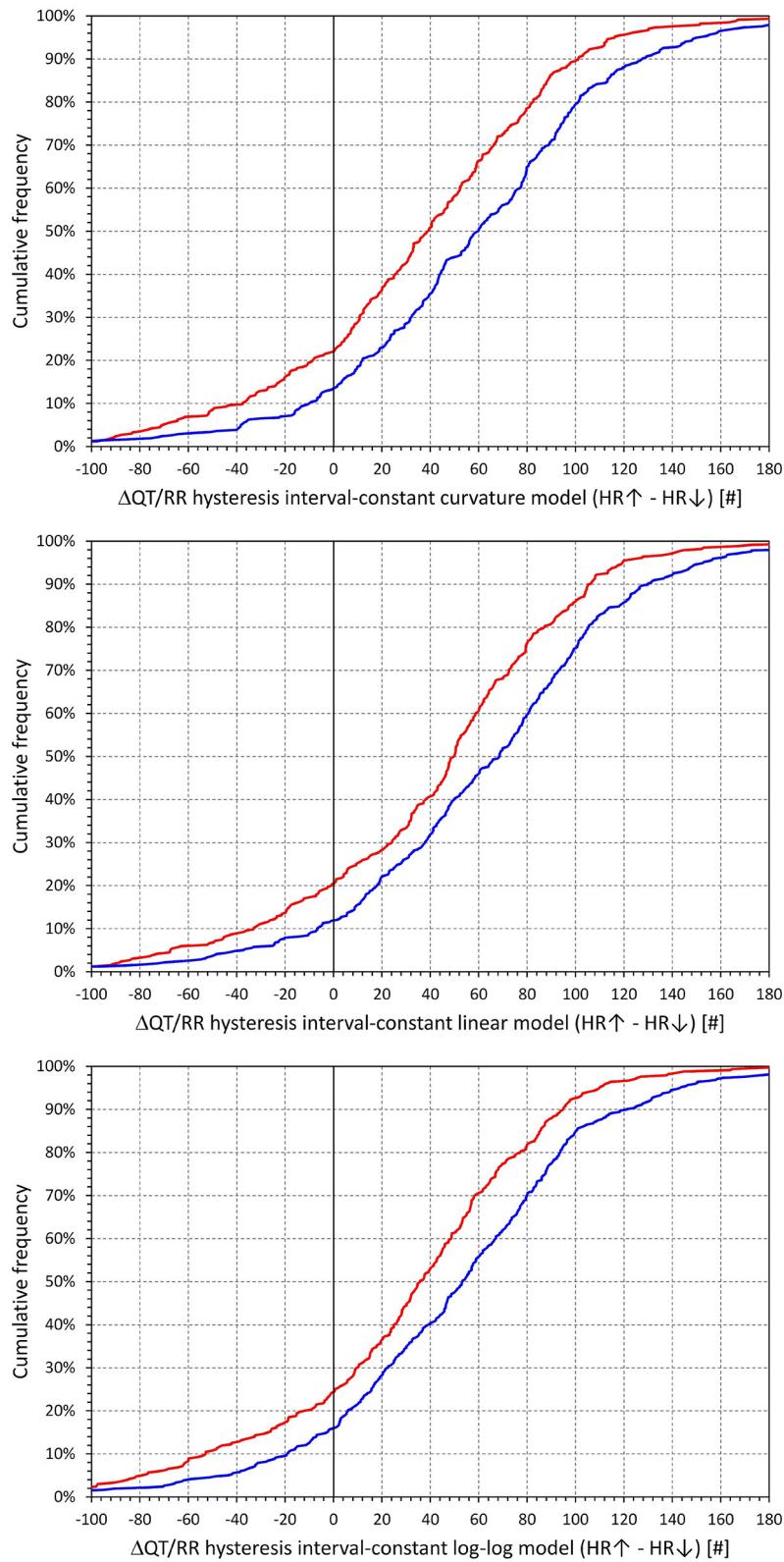
The study data also agree with published observations that the slope of QT/RR adaptation is steeper in females than in males (Linde et al., 2018), which means that the marked sex difference in QT intervals observed at slower heart rates gradually diminishes as the heart rate increases. Other characters of the data [e.g., sex differences in the QT/RR curvatures (Malik et al., 2013)] also agree with existing reports, giving credibility to the analysed data collection.

## Limitations

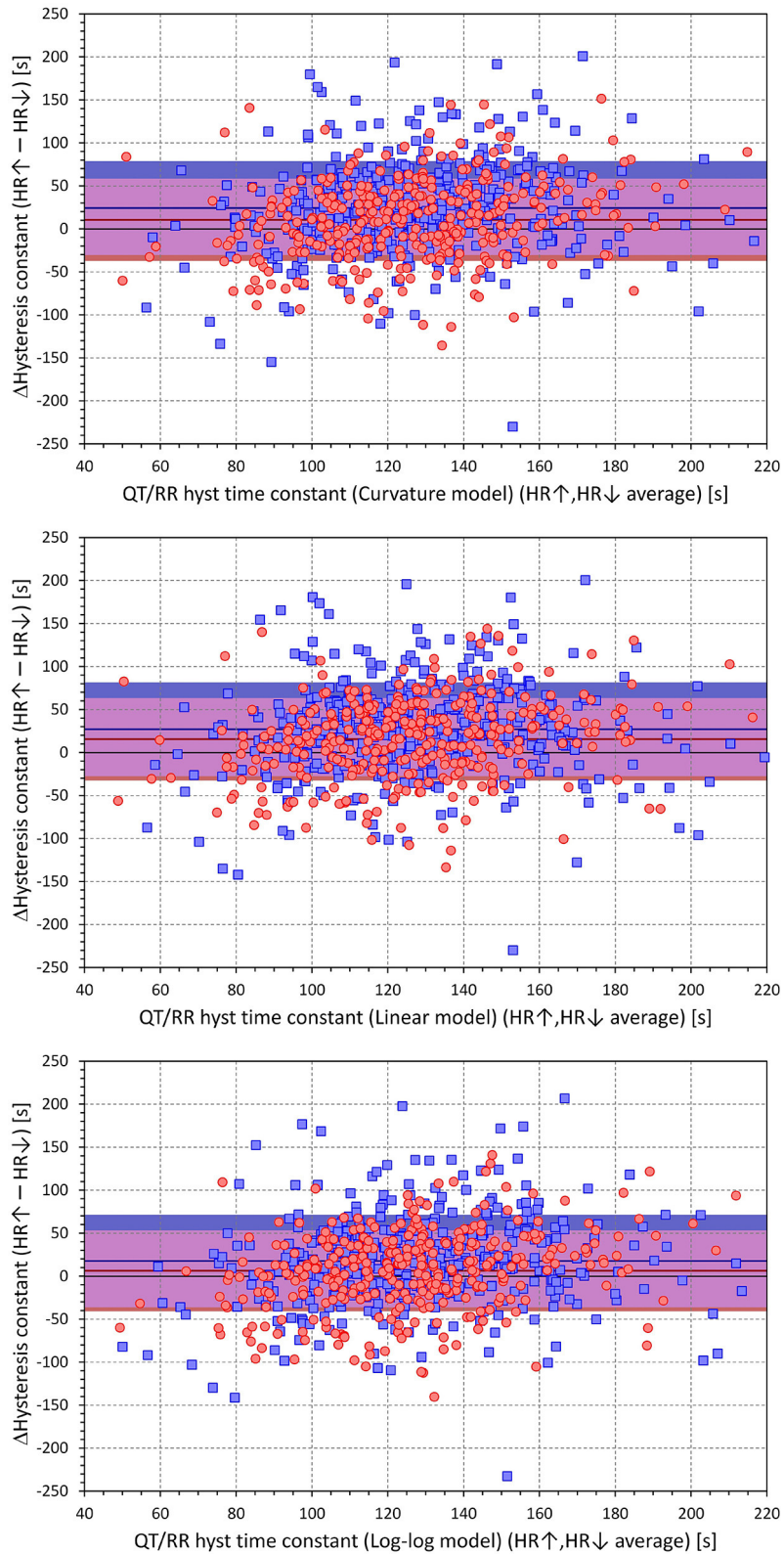
The use of the exponential decay model of QT/RR hysteresis is the main limitation of the study. While it might be argued that the regression residuals are numerically so small that any improvement of the model could only lead to miniscule differences, we cannot be sure whether other hysteresis models



**FIGURE 11 |** Cumulative densities of subject-specific differences among hysteresis time constants during heart rate acceleration and deceleration. The top, middle, and bottom panels show the differences for the curvature, linear, and log-log QT/RRH models, respectively. In each panel, the red and blue lines correspond to females and males, respectively.

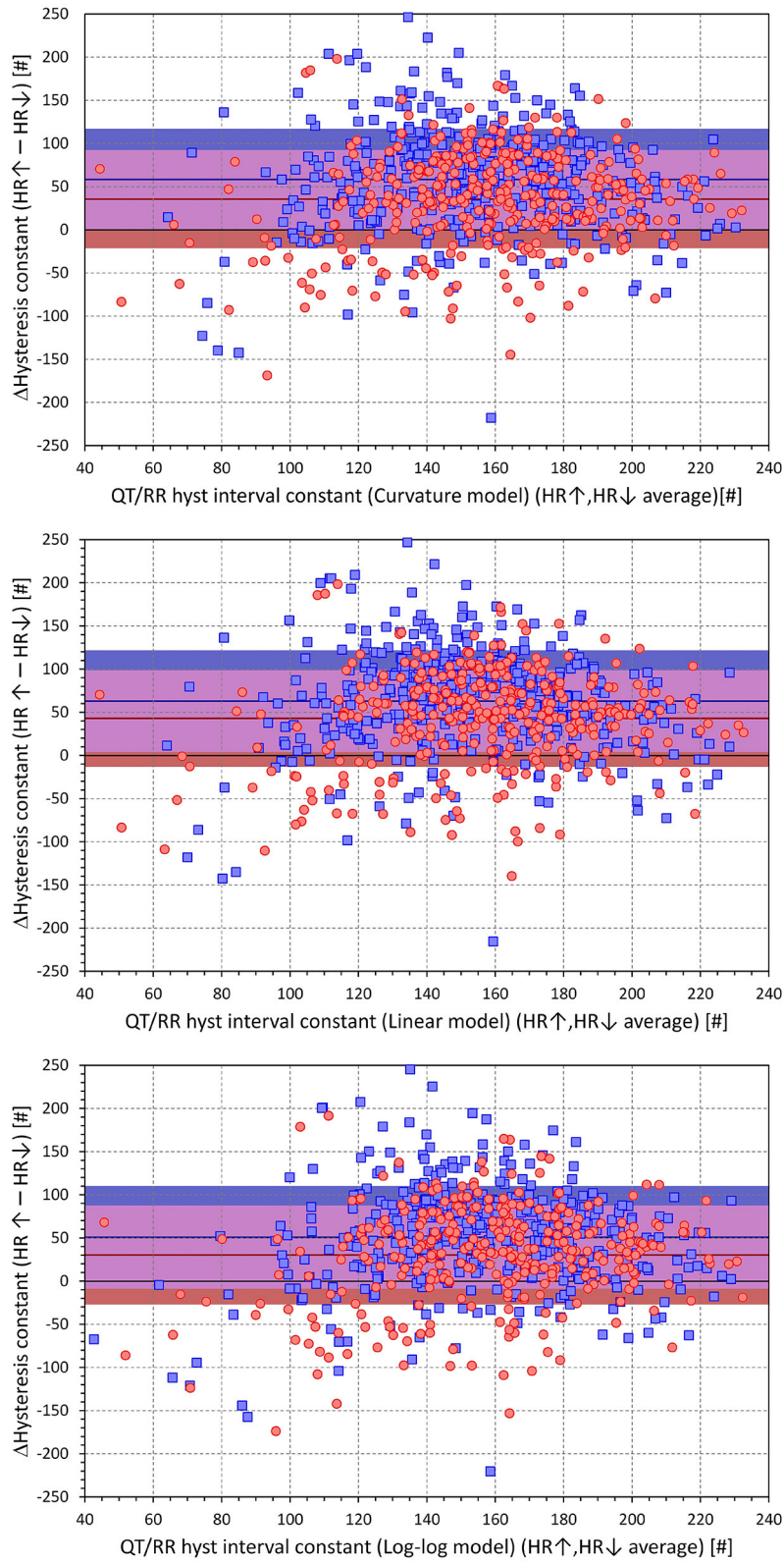


**FIGURE 12 |** Cumulative densities of subject-specific differences among hysteresis interval constants during heart rate acceleration and deceleration. The top, middle, and bottom panels show the differences for the curvature, linear, and log-log QT/RR<sup>H</sup> models, respectively. In each panel, the red and blue lines correspond to females and males, respectively.



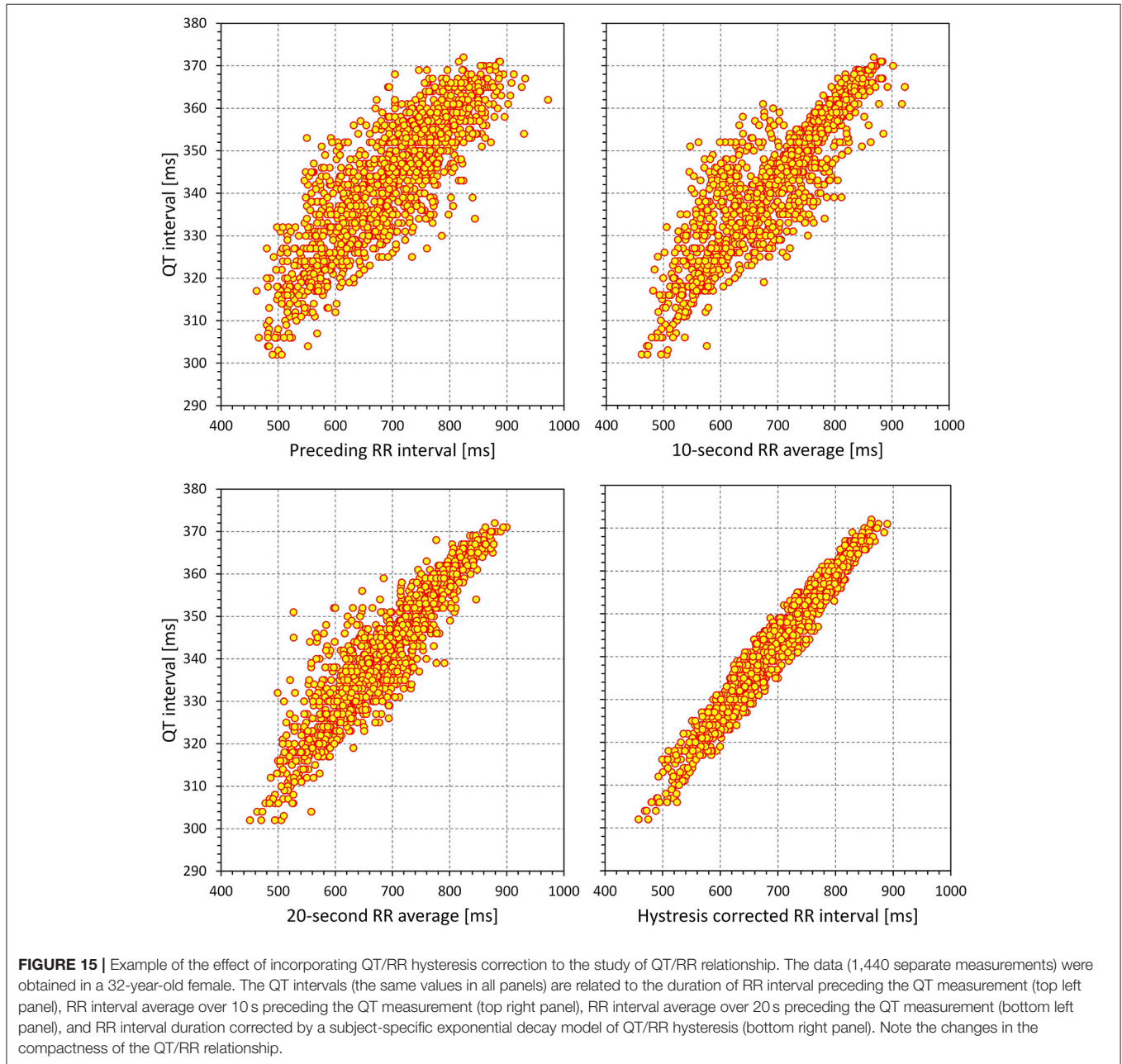
**FIGURE 13 |** Scatter diagrams of subject-specific differences among hysteresis time constants during heart rate acceleration and deceleration plotted against their intra-subject averages. The top, middle, and bottom panels show the differences for the curvature, linear, and log-log QT/RR<sup>H</sup> models, respectively. In each panel, the red circle and blue square marks correspond to females and males, respectively. The red and blue horizontal lines show the mean values of the residual differences in females and males, respectively. The light-coloured red and blue bands show the spans of mean  $\pm$  standard deviation of the residual differences in females and males, respectively; the light-coloured violet bands show the overlap of the mean  $\pm$  standard deviation bands between both sexes.





**FIGURE 14 |** Scatter diagrams of subject-specific differences among hysteresis interval constants during heart rate acceleration and deceleration plotted against their intra-subject averages. The top, middle, and bottom panels show the differences for the curvature, linear, and log-log QT/RR<sup>H</sup> models, respectively. In each panel, *(Continued)*

**FIGURE 14** | the red circle and blue square marks correspond to females and males, respectively. The red and blue horizontal lines show the mean values of the residual differences in females and males, respectively. The light-coloured red and blue bands show the spans of mean  $\pm$  standard deviation of the residual differences in females and males, respectively; the light-coloured violet bands show the overlap of the mean  $\pm$  standard deviation bands between both sexes.



would lead to the same results regarding the time-based and interval-based comparisons, sex differences in hysteresis speed, and differentiation between heart rate acceleration and deceleration. Since the study investigated Holter recordings of healthy subjects, we cannot comment on corresponding aspects in other well-defined clinical populations. The age range of the investigated subjects was limited; the population included

only three subjects older than 60 years old. It is possible that with broader age ranges, other indices would also be found significantly age-dependent. Finally, we have not considered other data, such as body mass index, cognition function, or physical fitness characteristics, that might all also influence the investigated indices. The equations of linear regression analysis are based on the assumptions that independent and dependent

variables (RR interval expressions and QT interval durations in this study) and the residual errors are normally distributed. This has not been tested in the study data; the test would be needed for each subject and each regression model separately (since all the regressions were performed for each subject separately). However, the number of ECG readings in each subject was large, thus minimising the effects of potential (albeit unlikely) departures from normal distributions (Schmidt and Finan, 2018). Also, normality tests have not been performed in the vast majority of studies investigating QT/RR regressions (Davey et al., 2000; Maury et al., 2013; Robyns et al., 2017; Yodogawa et al., 2021).

## CONCLUSION

The study provides further details on the physiology of QT/RR hysteresis. Analyses of the closeness of fit of the regression models between QT interval durations and RR intervals representing the underlying heart rate suggest that the response profile of QT/RR hysteresis appears to be driven by absolute time rather than the number of cardiac cycles over which the QT interval reacts to heart rate changes. We also observed that the speed of QT/RR hysteresis, contrary to the duration of individually rate-corrected QTc intervals, is decreased with increase in age. The slope of this increase was significantly steeper in females and thus, sex difference in hysteresis speed (which was faster in females) increases with age. In majority of the subjects, hysteresis speed was slower after heart rate acceleration than deceleration. The study also supported previous suggestions that the regression modelling between the QT and RR interval durations should not be based on logarithmic transformation (which has been popular in some studies on subject-specific QT heart rate corrections), since this transformation leads to poorer regression fit of data.

## REFERENCES

- Andršová, I., Hnatkova, K., Helánová, K., Šišáková, M., Novotný, T., Kala, P., et al. (2019). Individually rate corrected QTc intervals in children and adolescents. *Front. Physiol.* 10:994. doi: 10.3389/fphys.2019.00994
- Andršová, I., Hnatkova, K., Šišáková, M., Toman, O., Smetana, P., Huster, K. M., et al. (2020). Heart rate dependency and inter-lead variability of the T peak – T end intervals. *Front. Physiol.* 11:595815. doi: 10.3389/fphys.2020.595815
- Axelsson, K. J., Gransberg, L., Lundahl, G., Vahedi, F., and Bergfeldt, L. (2021). Adaptation of ventricular repolarization time following abrupt changes in heart rate: comparisons and reproducibility of repeated atrial and ventricular pacing. *Am. J. Physiol. Heart Circ. Physiol.* 320, H381–H392. doi: 10.1152/ajpheart.00542.2020
- Bauer, A., Klemm, M., Rizas, K. D., Hamm, W., von Stülpnagel, L., Dommasch, M., et al. (2019). Prediction of mortality benefit based on periodic repolarisation dynamics in patients undergoing prophylactic implantation of a defibrillator: a prospective, controlled, multicentre cohort study. *Lancet* 394, 1344–1351. doi: 10.1016/S0140-6736(19)31996-8
- Baumert, M., Lambert, G. W., Dawood, T., Lambert, E. A., Esler, M. D., McGrane, M., et al. (2008). QT interval variability and cardiac norepinephrine spillover in patients with depression and panic disorder. *Am. J. Physiol. Heart Circ. Physiol.* 295, H962–H968. doi: 10.1152/ajpheart.00301.2008
- Baumert, M., Porta, A., Vos, M. A., Malik, M., Couderc, J. P., Laguna, P., et al. (2016). variability in body surface ECG: measurement, physiological

## DATA AVAILABILITY STATEMENT

The raw data supporting the conclusions of this article will be made available by the authors, without undue reservation but pending the approval by the sponsors of the source clinical studies.

## ETHICS STATEMENT

The studies involving human participants were reviewed and approved by Focus in Neuss California Clinical Trials in Glendale Parexel in Baltimore Parexel in Bloemfontein PPD in Austin Spaulding in Milwaukee. The patients/participants provided their written informed consent to participate in this study.

## AUTHOR CONTRIBUTIONS

IA, KH, and MM: study design and initial manuscript draft. KH and MM: software development and statistics and figures. GS, IA, KMH, MŠ, OT, PB, PS, and TN: ECG interpretation and ECG measurement. GS, TN, OT, and PS: supervision of the measurements. GS, MM, and TN: quality control of the measurements. GS, IA, KH, KMH, MM, MŠ, OT, PB, PS, and TN: final manuscript and approval of submission. All authors contributed to the article and approved the submitted version.

## FUNDING

This study was supported in part by the Ministry of Health, Czech Republic, conceptual development of research organization (Grant FNBr/65269705), by the British Heart Foundation New Horizons Grant NH/16/2/32499, and by the Specific Research of Masaryk University MUNI/A/1437/2020.

- basis, and clinical value: position statement and consensus guidance endorsed by the European Heart Rhythm Association jointly with the ESC Working Group on Cardiac Cellular Electrophysiology. *Europace* 18, 925–944. doi: 10.1093/europace/euv405
- Bazett, J. C. (1920). An analysis of time relations of electrocardiograms. *Heart* 7, 353–367.
- Cassani González, R., Engels, E. B., Dubé, B., Nadeau, R., Vinet, A., LeBlanc, A. R., et al. (2012). Assessment of the sensitivity of detecting drug-induced QTc changes using subject-specific rate correction. *J. Electrocardiol.* 45, 541–545. doi: 10.1016/j.jelectrocard.2012.07.004
- Davey, P. P., Barlow, C., and Hart, G. (2000). Prolongation of the QT interval in heart failure occurs at low but not at high heart rates. *Clin. Sci.* 98, 603–610. doi: 10.1042/CS19990261
- Einthoven, W. (1903). Die galvanometrische Registrierung des menschlichen Elektrokardiogramms, zugleich eine Beurteilung der Anwendung des Kapillar-Elektrometers in der Physiologie. *Pflügers Arch.* 99, 472–480. doi: 10.1007/BF01811855
- El-Hamad, F., Javorka, M., Czipelova, B., Krohova, J., Turianikova, Z., Porta, A., et al. (2019). Repolarization variability independent of heart rate during sympathetic activation elicited by head-up tilt. *Med. Biol. Eng. Comput.* 57, 1753–1762. doi: 10.1007/s11517-019-01998-9
- El-Hamad, F., Lambert, E., Abbott, D., and Baumert, M. (2015). Relation between QT interval variability and muscle sympathetic nerve activity in

- normal subjects. *Am. J. Physiol. Heart Circ. Physiol.* 309, H1218–H1224. doi: 10.1152/ajpheart.00230.2015
- Fossa, A. A. (2017). Beat-to-beat ECG restitution: a review and proposal for a new biomarker to assess cardiac stress and ventricular tachyarrhythmia vulnerability. *Ann. Noninvasive Electrocardiol.* 22:e12460. doi: 10.1111/anec.12460
- Franz, M. R., Swerdlow, C. D., Liem, L. B., and Schaefer, J. (1988). Cycle length dependence of human action potential duration *in vivo*. Effects of single extrastimuli, sudden sustained rate acceleration and deceleration, and different steady-state frequencies. *J. Clin. Invest.* 82, 972–979. doi: 10.1172/JCI113706
- Fridericia, L. S. (1920). Die Systolendauer im Elektrokardiogramm bei normalen Menschen und bei Herzkranken. *Acta Med. Scand.* 53, 469–486. doi: 10.1111/j.0954-6820.1920.tb18266.x
- Garrod, A. H. (1870). On the relative duration of the component parts of the radial sphygmograph trace in health. *J. Anat. Physiol.* 18, 351–354. doi: 10.1098/rspl.1869.0079
- Garrod, A. H. (1875). On some points connected with circulation of the blood, arrived at from study of the sphygmograph-trace. *J. Anat. Physiol.* 23, 140–151. doi: 10.1098/rspl.1874.0019
- Gravel, H., Curnier, D., Dahdah, N., and Jacquemet, V. (2017). Categorization and theoretical comparison of quantitative methods for assessing QT/RR hysteresis. *Ann. Noninvasive Electrocardiol.* 22:e12463. doi: 10.1111/anec.12463
- Gravel, H., Jacquemet, V., Dahdah, N., and Curnier, D. (2018). Clinical applications of QT/RR hysteresis assessment: a systematic review. *Ann. Noninvasive Electrocardiol.* 23:e12514. doi: 10.1111/anec.12514
- Guideline, ICH. (2001). Safety pharmacology studies for human pharmaceuticals S7A. *Fed. Regist.* 66, 36791–36792.
- Haláček, J., Jurák, P., Villa, M., Soucek, M., Frána, P., Nykodým, J., et al. (2007). Dynamic coupling between heart rate and ventricular repolarisation. *Biomed. Tech.* 52, 255–263. doi: 10.1515/BMT.2007.044
- Hnatkova, K., Andršová, I., Toman, O., Smetana, P., Huster, K. M., Šišáková, M., et al. (2021). Spatial distribution of physiologic 12-lead QRS complex. *Sci. Rep.* 11:4289. doi: 10.1038/s41598-021-83378-8
- Hnatkova, K., Kowalski, D., Keirns, J. J., van Gelderen, E. M., and Malik, M. (2014). QTc changes after meal intake: sex differences and correlates. *J. Electrocardiol.* 47, 856–862. doi: 10.1016/j.jelectrocard.2014.07.026
- Hnatkova, K., and Malik, M. (2020). Sources of QTc variability: implications for effective ECG monitoring in clinical practice. *Ann. Noninvasive Electrocardiol.* 25:e12730. doi: 10.1111/anec.12730
- Hnatkova, K., Šišáková, M., Smetana, P., Toman, O., Huster, K. M., Novotný, T., et al. (2019b). Sex differences in heart rate responses to postural provocations. *Int. J. Cardiol.* 297, 126–134. doi: 10.1016/j.ijcard.2019.09.044
- Hnatkova, K., Smetana, P., Toman, O., Bauer, A., Schmidt, G., and Malik, M. (2009). Systematic comparisons of electrocardiographic morphology increase the precision of QT interval measurement. *Pacing Clin. Electrophysiol.* 32, 119–130. doi: 10.1111/j.1540-8159.2009.02185.x
- Hnatkova, K., Vicente, J., Johannesen, L., Garnett, C., Stockbridge, N., and Malik, M. (2019a). Errors of fixed QT heart rate corrections used in the assessment of drug-induced QTc changes. *Front. Physiol.* 10:635. doi: 10.3389/fphys.2019.00635
- Huikuri, H. V., Pikkujämsä, S. M., Airaksinen, K. E., Ikäheimo, M. J., Rantala, A. O., Kauma, H., et al. (1996). Sex-related differences in autonomic modulation of heart rate in middle-aged subjects. *Circulation* 94, 122–125. doi: 10.1161/01.CIR.94.2.122
- Jacquemet, V., Cassani González, R., Sturmer, M., Dubé, B., Sharestan, J., Vinet, A., et al. (2014). Interval measurement and correction in patients with atrial flutter: a pilot study. *J. Electrocardiol.* 47, 228–235. doi: 10.1016/j.jelectrocard.2013.11.002
- Jacquemet, V., Dubé, B., Knight, R., Nadeau, R., LeBlanc, A. R., Sturmer, M., et al. (2011). Evaluation of a subject-specific transfer-function-based nonlinear QT interval rate-correction method. *Physiol. Meas.* 32, 619–635. doi: 10.1088/0967-3334/32/6/001
- Kenttä, T., Karsikas, M., Junttila, M. J., Perkiömäki, J. S., Seppänen, T., Kiviniemi, A., et al. (2011). Morphology measured from exercise electrocardiogram as a predictor of cardiac mortality. *Europace* 13, 701–707. doi: 10.1093/europace/euq461
- Kuch, B., Hense, H. W., Sinnreich, R., Kark, J. D., von Eckardstein, A., Sapoznikov, D., et al. (2001). Determinants of short-period heart rate variability in the general population. *Cardiology* 95, 131–138. doi: 10.1159/000047359
- Lau, C. P., Freeman, A. R., Fleming, S. J., Malik, M., Camm, A. J., and Ward, D. E. (1988). Hysteresis of the ventricular paced QT interval in response to abrupt changes in pacing rate. *Cardiovasc. Res.* 22, 67–72. doi: 10.1093/cvr/22.1.67
- Linde, C., Bongiorno, M. G., Birgersdotter-Green, U., Curtis, A. B., Deisenhofer, I., Furokawa, T., et al. (2018). Sex differences in cardiac arrhythmia: a consensus document of the European Heart Rhythm Association, endorsed by the Heart Rhythm Society and Asia Pacific Heart Rhythm Society. *Europace* 20, 1565–1565. doi: 10.1093/europace/euy067
- Malik, M. (2008). Beat-to-beat QT variability and cardiac autonomic regulation. *Am. J. Physiol. Heart Circ. Physiol.* 295, H923–H925. doi: 10.1152/ajpheart.00709.2008
- Malik, M. (2014). QT/RR hysteresis. *J. Electrocardiol.* 47, 236–239. doi: 10.1016/j.jelectrocard.2014.01.002
- Malik, M. (2018). Methods of subject-specific heart rate corrections. *J. Clin. Pharmacol.* 58, 1020–1024. doi: 10.1002/jcph.1269
- Malik, M., Hnatkova, K., Batchvarov, V., Gang, Y., Smetana, P., and Camm, A. J. (2004). Sample size, power calculations, and their implications for the cost of thorough studies of drug induced QT interval prolongation. *Pacing Clin. Electrophysiol.* 27, 1659–1669. doi: 10.1111/j.1540-8159.2004.00701.x
- Malik, M., Hnatkova, K., Kowalski, D., Keirns, J. J., and van Gelderen, E. M. (2013). QT/RR curvatures in healthy subjects: sex differences and covariates. *Am. J. Physiol. Heart Circ. Physiol.* 305, H1798–H1806. doi: 10.1152/ajpheart.00577.2013
- Malik, M., Hnatkova, K., Novotny, T., and Schmidt, G. (2008a). Subject-specific profiles of QT/RR hysteresis. *Am. J. Physiol. Heart Circ. Physiol.* 295, H2356–H2363. doi: 10.1152/ajpheart.00625.2008
- Malik, M., Andreas, J.-O., Hnatkova, K., Hoekendorff, J., Cawello, W., et al. (2008b). Thorough QT/QTc Study in patients with advanced Parkinson's disease: cardiac safety of rotigotine. *Clin. Pharmacol. Ther.* 84, 595–603. doi: 10.1038/clpt.2008.143
- Malik, M., Hnatkova, K., Schmidt, A., and Smetana, P. (2008c). Accurately measured and properly heart-rate corrected QTc intervals show little daytime variability. *Heart Rhythm* 5, 1424–1431. doi: 10.1016/j.hrthm.2008.07.023
- Malik, M., Johannesen, L., Hnatkova, K., and Stockbridge, N. (2016). Universal correction for QT/RR hysteresis. *Drug Saf.* 39, 577–588. doi: 10.1007/s40264-016-0406-0
- Malik, M., van Gelderen, E. M., Lee, J. H., Kowalski, D. L., Yen, M., Goldwater, R., et al. (2012). Safety of repeat doses of mirabegron in healthy subjects: a randomized, double-blind, placebo-, and active-controlled thorough QT study. *Clin. Pharm. Therap.* 92, 696–706. doi: 10.1038/clpt.2012.181
- Maury, P., Caudron, G., Bouisset, F., Fourcade, J., Duparc, A., Mondoly, P., et al. (2013). Slower heart rate and altered rate dependence of ventricular repolarization in patients with lone atrial fibrillation. *Arch. Cardiovasc. Dis.* 106, 12–18. doi: 10.1016/j.acvd.2012.10.001
- Pelchovitz, D. J., Ng, J., Chicos, A. B., Bergner, D. W., and Goldberger, J. J. Q. T.-. R. R. (2012). Hysteresis is caused by differential autonomic states during exercise and recovery. *Am. J. Physiol. Heart Circ. Physiol.* 302, H2567–H2573. doi: 10.1152/ajpheart.00041.2012
- Porta, A., Cairo, B., De Maria, B., and Bari, V. (2020). Complexity of spontaneous QT variability unrelated to RR variations and respiration during graded orthostatic challenge. *Comput. Cardiol.* 47:9. doi: 10.22489/CinC.2020.009
- Porta, A., Tobaldini, E., Gnecchi-Ruscone, T., and Montano, N. (2010). RT variability unrelated to heart period and respiration progressively increases during graded head-up tilt. *Am. J. Physiol. Heart Circ. Physiol.* 298, H1406–H1414. doi: 10.1152/ajpheart.01206.2009
- Rautaharju, P. M., Mason, J. W., and Akiyama, T. (2014). New age- and sex-specific criteria for QT prolongation based on rate correction formulas that minimize bias at the upper normal limits. *Int. J. Cardiol.* 174, 535–540. doi: 10.1016/j.ijcard.2014.04.133
- Robyns, T., Willems, R., Vandenberg, B., Ector, J., Garweg, C., Kuiperi, C., et al. (2017). Individualized corrected QT interval is superior to QT interval corrected using the Bazett formula in predicting mutation carriage in families with long QT syndrome. *Heart Rhythm* 14, 376–382. doi: 10.1016/j.hrthm.2016.11.034
- Schmidt, A. F., and Finan, C. (2018). Linear regression and the normality assumption. *J. Clin. Epidemiol.* 98, 146–151. doi: 10.1016/j.jclinepi.2017.12.006

- Taubel, J., Ferber, G., Lorch, U., Batchvarov, V., Savelieva, I., and Camm, A. J. T. (2014). study of the effect of oral moxifloxacin on QTc interval in the fed and fasted state in healthy Japanese and Caucasian subjects. *Br. J. Clin. Pharmacol.* 77, 170–179. doi: 10.1111/bcp.12168
- Toman, O., Hnatkova, K., Smetana, P., Huster, K. M., Šišáková, M., Barthel, P., et al. (2020). Physiologic heart rate dependency of the PQ interval and its sex differences. *Sci. Rep.* 10:2551. doi: 10.1038/s41598-020-59480-8
- Waller, A. D. A. (1887). demonstration on man of electromotive changes accompanying the heart's beat. *J. Physiol.* 8, 229–234. doi: 10.1113/jphysiol.1887.sp000257
- Watanabe, M. A. (2007). Lissajous curves and QT hysteresis: a critical look at QT/RR slope analysis techniques. *Heart Rhythm* 4, 1006–1008. doi: 10.1016/j.hrthm.2007.05.010
- Yodogawa, K., Aiba, T., Sumitomo, N., Yamamoto, T., Murata, H., Iwasaki, Y. K., et al. (2021). Differential diagnosis between LQT1 and LQT2 by QT/RR relationships using 24-hour Holter monitoring: a multicenter cross-sectional study. *Ann. Noninvasive Electrocardiol.* 26:e12878. doi: 10.1111/anec.12878
- Zhang, Y., Bao, M., Dai, M., Zhong, H., Li, Y., and Tan, T. (2014). QT hysteresis index improves the power of treadmill exercise test in the screening of coronary artery disease. *Circ. J.* 78, 2942–2949. doi: 10.1253/circj.CJ-14-0697
- Conflict of Interest:** The authors declare that the research was conducted in the absence of any commercial or financial relationships that could be construed as a potential conflict of interest.
- Publisher's Note:** All claims expressed in this article are solely those of the authors and do not necessarily represent those of their affiliated organizations, or those of the publisher, the editors and the reviewers. Any product that may be evaluated in this article, or claim that may be made by its manufacturer, is not guaranteed or endorsed by the publisher.
- Copyright © 2022 Andršová, Hnatkova, Šišáková, Toman, Smetana, Huster, Barthel, Novotný, Schmidt and Malik. This is an open-access article distributed under the terms of the Creative Commons Attribution License (CC BY). The use, distribution or reproduction in other forums is permitted, provided the original author(s) and the copyright owner(s) are credited and that the original publication in this journal is cited, in accordance with accepted academic practice. No use, distribution or reproduction is permitted which does not comply with these terms.*

### 3.6. Prostorový úhel QRS-T

Při snaze lépe pochopit fyziologii repolarizačního procesu byla navržena celá řada numerických charakteristik, jejichž cílem je rozlišení mezi normální a abnormální repolarizací v klinicky dobře definovaných populacích. Jedná se o nejrůznější matematické metody od jednoduchých kalkulací plochy pod vlnou T<sup>70</sup> až po trojrozměrné rekonstrukce vektorokardiografických smyček vln T a jejich kvantifikace (s nutností využití algoritmů dekompozice na singulární hodnoty a rekonstrukce ve vícerozměrných algebraických prostorech).<sup>71,72</sup>

Jednou z takovýchto charakteristik je i trojrozměrný úhel mezi vektory QRS komplexu a T vlny. Existence tohoto úhlu vychází ze známého faktu, že se srdeční repolarizace nešíří stejnou prostorově orientovanou cestou jako předchozí depolarizace.<sup>73</sup> Matematickou definici této charakteristiky určili Geselowitz et al., avšak tzv. ventrikulární gradient měl v následujících letech jen velmi malý praktický dopad.<sup>74</sup> Až v roce 2000 bylo prokázáno, že úhel ventrikulárního gradientu (tedy prostorový úhel QRS-T) má predikční potenciál mortality u pacientů, kteří přežili akutní IM.<sup>75</sup> Následně byla stratifikační síla tohoto parametru prokázána nejen u pacientů s různým strukturálním onemocněním srdce, ale i u pacientů například s diabetem mellitem, renálním selháním a dalších, včetně běžné populace.<sup>76,77,78,79,80</sup> Jelikož se jedná o dynamický parametr reagující na změny SF, obdobně jako QT/RR hystereze, opět vystávaly nejasnosti ohledně intraindividuální variability či věkově a pohlavně vázaných rozdílů. S týmem technicky zaměřených kolegů jsme se na tyto otázky pokusili odpovědět pomocí různých matematických výpočtů velikosti prostorového QRS-T úhlu. K výpočtům byly použity až 4krát opakované 14 až 16 hodin dlouhé 12-ti svodové EKG záznamy u 523 zdravých dobrovolníků (z toho 259 žen). Získaný záznam byl přetransformován do tří ortogonálních svodů XYZ a následně k výpočtům byla použita metoda plochy, metoda maximálních vektorů a metoda integrálu možných úhlů QRS a T. Pro podrobnější popis viz doloženou publikaci. Následně byly hodnoty změn úhlu hodnoceny v závislosti na změnách SF a akceptace její hystereze. Opět byla prokázána intraindividuální variabilita úhel/RR hystereze, tedy žádná univerzální formule popisující závislost QRS-T prostorového úhlu na ustálené SF nebyla nalezena. Stejně jako již publikoval Smetana et al.,<sup>81</sup> i v naší práci jsme zaznamenali rozdíl v QRS-T úhlu mezi muži a ženami, v průměru vyšel úhel u žen o 10° až 20° menší než v mužské populaci. Zároveň jsme neprokázali zpoždění adaptace úhlu v závislosti ke změnám SF, jak je tomu u jiných dynamických repolarizačních parametrů. Toto chování QRS-T úhlu spíše odráží přímý vliv autonomní a neurohumorální regulace komor než vliv samotné srdeční frekvence.

**Andršová I**, Hnatkova K, Toman O, Šišáková M, Smetana P, Huster KM, Barthel P, Novotný T, Schmidt G and Malik M. Intra-subject stability of different expressions of spatial QRS-T angle and their relationship to heart rate. *Front. Physiol* 2022; 13:939633. doi: 10.3389/fphys.2022.939633

IF 4,0. Počet citací ve Web of Science 0

Původní práce - kvantitativní podíl uchazečky 35%: Návrh struktury publikace, elektrokardiologická měření, interpretace statistických výsledků, text publikace.



## OPEN ACCESS

## EDITED BY

Vijay S. Chauhan,  
Peter Munk Cardiac Centre, Canada

## REVIEWED BY

Juan Pablo Martínez,  
University of Zaragoza, Spain  
Marcel van der Heyden,  
University Medical Center Utrecht,  
Netherlands

## \*CORRESPONDENCE

Katerina Hnatkova,  
k.hnatkova@imperial.ac.uk

## SPECIALTY SECTION

This article was submitted to Cardiac Electrophysiology, a section of the journal Frontiers in Physiology

RECEIVED 09 May 2022

ACCEPTED 18 July 2022

PUBLISHED 30 August 2022

## CITATION

Andršová I, Hnatkova K, Toman O, Šišáková M, Smetana P, Huster KM, Barthel P, Novotný T, Schmidt G and Malik M (2022), Intra-subject stability of different expressions of spatial QRS-T angle and their relationship to heart rate. *Front. Physiol.* 13:939633. doi: 10.3389/fphys.2022.939633

## COPYRIGHT

© 2022 Andršová, Hnatkova, Toman, Šišáková, Smetana, Huster, Barthel, Novotný, Schmidt and Malik. This is an open-access article distributed under the terms of the [Creative Commons Attribution License \(CC BY\)](https://creativecommons.org/licenses/by/4.0/). The use, distribution or reproduction in other forums is permitted, provided the original author(s) and the copyright owner(s) are credited and that the original publication in this journal is cited, in accordance with accepted academic practice. No use, distribution or reproduction is permitted which does not comply with these terms.

# Intra-subject stability of different expressions of spatial QRS-T angle and their relationship to heart rate

Irena Andršová<sup>1,2</sup>, Katerina Hnatkova<sup>3\*</sup>, Ondřej Toman<sup>1,2</sup>, Martina Šišáková<sup>1,2</sup>, Peter Smetana<sup>4</sup>, Katharina M. Huster<sup>5</sup>, Petra Barthel<sup>5</sup>, Tomáš Novotný<sup>1,2</sup>, Georg Schmidt<sup>5</sup> and Marek Malik<sup>2,3</sup>

<sup>1</sup>Department of Internal Medicine and Cardiology, University Hospital Brno, Brno, Czech, <sup>2</sup>Department of Internal Medicine and Cardiology, Faculty of Medicine, Masaryk University, Brno, Czech, <sup>3</sup>National Heart and Lung Institute, Imperial College, London, England, <sup>4</sup>Wilhelminenspital der Stadt Wien, Vienna, Austria, <sup>5</sup>Klinikum Rechts der Isar, Technische Universität München, Munich, Germany

Three-dimensional angle between the QRS complex and T wave vectors is a known powerful cardiovascular risk predictor. Nevertheless, several physiological properties of the angle are unknown or poorly understood. These include, among others, intra-subject profiles and stability of the angle relationship to heart rate, characteristics of angle/heart-rate hysteresis, and the changes of these characteristics with different modes of QRS-T angle calculation. These characteristics were investigated in long-term 12-lead Holter recordings of 523 healthy volunteers (259 females). Three different algorithmic methods for the angle computation were based on maximal vector magnitude of QRS and T wave loops, areas under the QRS complex and T wave curvatures in orthogonal leads, and weighted integration of all QRS and T wave vectors moving around the respective 3-dimensional loops. These methods were applied to orthogonal leads derived either by a uniform conversion matrix or by singular value decomposition (SVD) of the original 12-lead ECG, giving 6 possible ways of expressing the angle. Heart rate hysteresis was assessed using the exponential decay models. All these methods were used to measure the angle in 659,313 representative waveforms of individual 10-s ECG samples and in 7,350,733 individual beats contained in the same 10-s samples. With all measurement methods, the measured angles fitted second-degree polynomial regressions to the underlying heart rate. Independent of the measurement method, the angles were found significantly narrower in females ( $p < 0.00001$ ) with the differences to males between 10° and 20°, suggesting that in future risk-assessment studies, different angle dichotomies are needed for both sexes. The integrative method combined with SVD leads showed the highest intra-subject reproducibility ( $p < 0.00001$ ). No reproducible delay between heart rate changes and QRS-T angle changes was found. This was interpreted as a suggestion that the measurement of QRS-T angle might offer direct assessment of cardiac autonomic responsiveness at the ventricular level.



## KEYWORDS

healthy volunteers, long-term ECG, ECG measurements, spatial QRS-T angle, heart rate, heart rate hysteresis, polynomial regression, sex differences

## 1 Introduction

The observations that the myocardial repolarisation sequence cannot follow the same spatial path as the preceding depolarisation sequence was made not long after the invention of electrocardiography. Already in 1934, [Wilson et al. \(1934\)](#) proposed the measurements of areas under the electrocardiogram (ECG) deflections to quantify the disparity between spatial orientations of the QRS complex and the T wave. This disparity was subsequently refined by [Geselowitz \(Geselowitz, 1983\)](#) who proposed mathematical forms of the so-called ventricular gradient. The concept was subsequently further elaborated but with little practical implications. Indeed, in 1989, [Macfarlane and Lawrie](#) wrote in their substantial ECG book ([Macfarlane and Lawrie, 1989](#)) that “the most exciting thing about the ventricular gradient is its name”.

In 2000, however, the seminal report by [Zabel et al., \(2000\)](#) showed that the angle of the ventricular gradient, that is the 3-dimensional angle between the QRS and T wave orientations, is a potent predictor of mortality risk in survivors of acute myocardial infarction. Subsequently, the risk stratification strength of the QRS-T angle has been confirmed in a large number of studies including investigations of other ischaemic heart disease populations ([de Torbal et al., 2004](#); [Malik et al., 2004](#)), acute coronary syndrome ([Lown et al., 2012](#)), heart failure ([Gotsman et al., 2013](#); [Selvaraj et al., 2014](#); [Sweda et al., 2020](#)), hypertrophic ([Cortez et al., 2017a](#); [Cortez et al., 2017b](#); [Jensen et al., 2021](#)) and dilated cardiomyopathy ([Li et al., 2016](#)), diabetic patients ([Voulgari et al., 2010](#); [Cardoso et al., 2013](#); [May et al., 2017](#); [May et al., 2018](#)), renal patients on haemodialysis ([de Bie et al., 2013](#); [Poulikakos et al., 2018](#)); and many other populations and conditions ranging from systemic sclerosis ([Gialafos et al., 2012](#)) and Chagas disease ([Zampa et al., 2014](#)) to overall hospital ([Yamazaki et al., 2005](#)) and general populations ([Kardys et al., 2003](#); [Kors et al., 2003](#); [Walsh et al., 2013](#)). It has also recently been shown that QRS-T angle might be meaningfully combined with other ECG-based risk factors ([Hnatkova et al., 2022](#)).

The risk-prediction properties of the QRS-T angle are thus now proven beyond any reasonable doubt. The strength of the QRS-T angle-based prediction of cardiovascular risk and/or of cardiovascular death has been shown comparable if not exceeding that of established risk factors including left ventricular ejection fraction, QRS complex width, and heart rate ([Hnatkova et al., 2022](#)). Nevertheless, several physiological aspects of the parameter are either unknown or poorly understood. While population-based relationship of the angle to the underlying heart rate has previously been reported ([Smetana et al., 2004](#); [Kenttä et al., 2010](#)), little is known about the individual intra-subject profiles of this relationship and of its

relationship to sex and age. Simple comparison with the hysteresis loops of the QT interval adaptation to the changes in the underlying heart rate suggested that the QRS-T angle changes follow the heart rate changes more rapidly ([Hnatkova et al., 2010](#)) but no details on the possible angle/heart-rate hysteresis are known. Practical comparisons of different possibilities of calculating the angle were reported ([Hnatkova et al., 2018](#)) but it is unknown whether these possibilities differ in the intra-subject reproducibility when the relationship to heart rate is considered.

Concentrating on these knowledge gaps, we utilised ECG measurements made in long-term 12-lead Holter recordings obtained in a large population of normal healthy volunteers who were investigated during clinical pharmacology studies. For the comparison of the possibilities of the angle calculations, we used three different methods, namely the measurements based on the so-called maximum and area calculations ([Cortez and Schlegel, 2010](#); [Oehler et al., 2014](#)) as well as a measurement variant derived from the initial reports of the clinical usefulness of the angle measurement ([Zabel et al., 2000](#)). The initial report of the risk-prediction value expressed the angle as an integral of cosines of angles between the QRS complex directions and the maximum T wave direction. Since this was not mathematically consistent, we introduce a method that uses the integral method applied to both the QRS complex and the T wave directions.

## 2 Materials and methods

### 2.1 Investigated population and electrocardiographic recordings

The ECG recordings used in the study have been reported previously in studies that investigated very different electrophysiology factors ([Hnatkova et al., 2021](#); [Andršová et al., 2022](#); [Toman et al., 2022](#)). For the purposes of the present investigation, we applied very different data processing methods.

In brief, clinical pharmacology studies were conducted at 3 different clinical research sites. These studies enrolled 523 healthy volunteers including 259 females. Before study enrolment, all the volunteers had a normal standard clinical ECG and normal clinical investigation. All the source studies used the same standard inclusion and exclusion criteria mandated for Phase I pharmacology investigations ([ICH Guideline, 2001](#)) including negative recreational substances tests and negative pregnancy tests for females. All the source studies were ethically approved by the institutional ethics bodies (Parexel in Baltimore; California Clinical Trials in Glendale; and

Spaulding in Milwaukee). All subjects gave informed written consent to study participation including scientific investigation of collected data.

Demographic data including age, sex, racial classification, body height, and body weight were collected. Lean body mass (LBM) was calculated as  $LBM = 0.29569 \cdot W + 41.813 \cdot H - 43.2933$  for females and  $LBM = 0.3281 \cdot W + 33.929 \cdot H - 29.5336$  for males, where  $W$  is body weight in kilograms and  $H$  is body height in metres (Hume, 1966); it was expressed in kilograms. Body mass index (BMI) was calculated as  $BMI = W/H^2$ .

In each study participant, repeated three to four long-term 12-lead Holter ECG recordings with Mason-Likar electrode positions were obtained during full day-time periods (i.e., each recording was approximately 14–16 h long) while the subjects were not allowed to smoke and/or consume alcohol or caffeinated drinks and/or to sleep. No medication was administered during these recordings and, where appropriate, sufficient wash-out periods after previous treatment periods were used. The study protocols were mutually consistent in respect of the conduct during the drug-free baseline days. Since only drug-free data were used in the investigation reported here, further details of source studies are immaterial.

As previously reported (Malik et al., 2008a; Malik et al., 2012), multiple non-adjacent 10-s ECG segments were extracted from the long-term ECGs. All these 10-s segments contained only sinus rhythm free of ectopic beats and were extracted (a) from pre-specified time-points of the source pharmacologic studies, (b) from recording scans aimed at finding representative spectrum of different underlying heart rates of selected ECG segments distinguishing those that were and were not preceded by heart rate changes exceeding  $\pm 2$  beat per minute. That is, the complete day-time recordings were searched to identify ECG segments that were preceded by stable or variable heart rates and the extractions were made from these segments while keeping the distinction between stable and variable preceding rates. The ECG segments were pre-selected for further processing only if satisfactory algorithmic measurement of QT interval was possible (Malik et al., 2008a; Malik et al., 2012). This was judged by similarities in the measured QT intervals of partially overlapping and adjacent ECG segments. Nevertheless, since all ECG interval measurements were subsequently visually verified and, where appropriate, manually corrected (see the next section) the judgement details of algorithmic measurements are of no importance.

## 2.2 Electrocardiographic measurements

In each of these ECG segments, QRS complex (i.e., the Q wave onset and J point) and the T wave offset were identified following published procedures (Malik et al., 2008a; Malik et al., 2012) that included repeated visual controls, manual corrections of all the measurements, and intra- and inter-subject repeatability and stability of the measurements. Consistency of

the interpretation of corresponding ECG morphologies was also assured (Hnatkova et al., 2009). The visually verified QT interval measurements were made in the representative median waveforms of the 10-s segments (sampled at 1,000 Hz) with the superimposition of all 12 leads on the same isoelectric axis (Malik, 2004; Xue, 2009).

Using a previously proposed technique (Berger et al., 1997; Baumert et al., 2008), QT interval was projected to individual beats within the 10-s ECG by finding the maximum correlation between the median waveform and the signal of individual QRS-T complexes. The maximum correlations were identified separately for the surroundings of the QRS onset and of the T wave offset. Since it has previously been observed that this process might lead to slightly different results when applied to different ECG leads (Malik, 2008), the cross-correlation technique was applied to the vector magnitude of algebraically reconstructed orthogonal leads (Guldenring et al., 2012).

Subsequently, Pearson correlation coefficients were calculated between the analysed beat and representative median waveform in (a) a window surrounding the QRS onset by  $\pm 40$  ms and (b) a window surrounding the T wave offset by  $\pm 50$  ms. The QRS-T pattern of the given beat was accepted for further analysis only if both these correlation coefficients exceeded 0.9. This assured that beats substantially distorted by pollution noise were excluded. No other restrictions were applied. This made the data selection/exclusion less stringent compared to previous investigations of beat-to-beat QT interval analyses (Toman et al., 2022).

The source clinical studies included episodes of per-protocol changes of postural positions. This allowed to capture measurable ECG segments at broad heart rate ranges (Malik et al., 2012).

## 2.3 RR interval histories

For each analysed ECG segment, a 5-min history of preceding RR intervals was obtained. This was combined with the positions of the individual beats within the segment, allowing to obtain a beat-specific history of RR intervals in a 5-min history of each analysed beat. That is, the RR interval of the histories also included the positions of all QRS complexes regardless of whether these were or were not accepted for further analysis.

## 2.4 Expressions of spatial QRS-T angle

### 2.4.1 Orthogonal leads

The assessment of spatial QRS-T angle requires to derive 3 orthogonal leads from the 12-lead ECG signal. This was performed in two different ways.

Firstly, previously published conversion matrix suitable for Mason-Likar electrode positions (Guldenring et al., 2012) was used to derive orthogonal leads XYZ for each of the median representative waveforms and for each QRS-T beat accepted for further analysis.

Subsequently, the same 12-lead ECG signals (i.e., the representative waveforms and the beats accepted for analysis) were processed by singular value decomposition (Acar et al., 1999; Acar and Köymen, 1999; Yana et al., 2006; Hnatkova et al., 2021) between the QRS onset and T wave offset. This derived three dominant and mutually orthogonal leads S<sub>1</sub>, S<sub>2</sub>, and S<sub>3</sub> (as if the system of orthogonal axes was optimally rotated for the given 12-lead signal).

### 2.4.2 QRS-T angle measurement

Three principal algorithmic methods of deriving the 3-dimensional QRS-T angle were considered. The following notations is used in their descriptions:

A triplet of values  $[\varphi, \phi, \psi]$  is considered to represent a vector between the zero point  $[0, 0, 0]$  and the point determined by the triplet. Such a vector will be denoted as  $\mathfrak{B}[\varphi, \phi, \psi]$ . Vector magnitude of vector  $\mathbb{W} = \mathfrak{B}[\varphi, \phi, \psi]$  is given by formula  $\sqrt{\varphi^2 + \phi^2 + \psi^2}$  and will be denoted as  $\|\mathbb{W}\|$ . Symbol  $\mathfrak{U}(\mathbb{G}, \mathbb{H})$  will represent the 3-dimensional angle between vectors  $\mathbb{G}$  and  $\mathbb{H}$ . Finally, orthogonal  $\mathcal{XYZ}$  system of ECG leads will be considered defining functions  $\mathcal{X}(t)$ ,  $\mathcal{Y}(t)$ , and  $\mathcal{Z}(t)$ , which assign the voltage values of each of the orthogonal leads to each instance  $t$  of the ECG recording. A vector  $\mathfrak{B}[\mathcal{X}(t), \mathcal{Y}(t), \mathcal{Z}(t)]$  will be denoted as  $\mathcal{E}(t)$ .

#### 2.4.2.1 Area method

The area-based QRS-T angle method uses the integrals of the orthogonal ECG leads (van Oosterom, 2014). That is, using the described notation, the orientation of the QRS complex is defined by a vector.

$$\mathcal{V}_{QRS} = \mathfrak{B} \left[ \int_Q^J \mathcal{X}(t) dt, \int_Q^J \mathcal{Y}(t) dt, \int_Q^J \mathcal{Z}(t) dt \right]$$

and similarly, the orientation of the T wave is defined by a vector

$$\mathcal{V}_T = \mathfrak{B} \left[ \int_J^{T_e} \mathcal{X}(t) dt, \int_J^{T_e} \mathcal{Y}(t) dt, \int_J^{T_e} \mathcal{Z}(t) dt \right]$$

where  $Q$ ,  $J$ , and  $T_e$  specify QRS onset, QRS offset, and T wave offset, respectively. The 3-dimensional QRS-T angle is subsequently computed as the spatial angle  $\mathfrak{U}(\mathcal{V}_{QRS}, \mathcal{V}_T)$  between these two vectors.

#### 2.4.2.2 Maximum method

The maximum vector-based QRS-T angle calculation is based on the notion that QRS and T wave orientations are defined by the maxima of the vector magnitudes within the

corresponding orthogonal loops (Cortez et al., 2017a). That is, within the orthogonal  $\mathcal{XYZ}$  system of ECG leads, time points  $t_{QRS}$  and  $t_T$  are selected such that  $\|\mathcal{E}(t_{QRS})\| = \max_{Q \leq t \leq J} \|\mathcal{E}(t)\|$  and similarly  $\|\mathcal{E}(t_T)\| = \max_{J \leq t \leq T_e} \|\mathcal{E}(t)\|$ , where  $Q$ ,  $J$ , and  $T_e$  again specify QRS onset, QRS offset, and T wave offset, respectively.

The QRS-T angle is then computed as the spatial angle  $\mathfrak{U}(\mathcal{E}(t_{QRS}), \mathcal{E}(t_T))$  between the maximum magnitude vectors  $\mathcal{E}(t_{QRS})$  and  $\mathcal{E}(t_T)$ .

#### 2.4.2.3 Integral method

The integral-based QRS-T angle calculation is based on a weighted average of all angles between all points within the QRS loop and all points within the T wave loop, weighted by the product of the magnitudes of the vectors represented by these points. That is, within the orthogonal  $\mathcal{XYZ}$  system of ECG leads, the integral based QRS-T angle is given by the formula

$$\left( \int_{t=Q}^J \int_{u=J}^{T_e} \mathfrak{U}(\mathcal{E}(t), \mathcal{E}(u)) * \|\mathcal{E}(t)\| * \|\mathcal{E}(u)\| du dt \right) / \left( \int_{t=Q}^J \int_{u=J}^{T_e} \|\mathcal{E}(t)\| * \|\mathcal{E}(u)\| du dt \right)$$

### 2.4.3 QRS-T angle expressions

The two possibilities of obtaining orthogonal lead system and the three possibilities of computing the QRS-T angle led to six combinations that were investigated in this study. We shall term these combinations Area<sub>XYZ</sub>, Maximum<sub>XYZ</sub>, Integral<sub>XYZ</sub>, Area<sub>SVD</sub>, Maximum<sub>SVD</sub>, and Integral<sub>SVD</sub> – all with obvious meanings. All the values of the angles were expressed in degrees with values between 0° and 180°.

## 2.5 Data analyses

For each 10-s ECG segment analysed in the study, the six different computations of the QRS-T angle were applied to the median representative waveform and to each of the individual beats accepted for the analysis. For each of the six computations, the values obtained for the individual beats were also averaged.

### 2.5.1 Comparisons of QRS-T angle expressions

Three different types of comparisons of different QRS-T angle expressions were made. Firstly, for each algorithmic method, the values obtained based on a combination with the XYZ conversion matrix were compared with the values obtained for the same ECG signal based on the combination of the SVD-based orthogonal leads. The comparison was made for both individual beats and representative median waveforms of ECG segments. Secondly, for each of the six QRS-T angle expressions, comparisons were made between the values derived from representative median waveforms of ECG segments and the

averages of the values obtained from individual beats within the same ECG segments. Finally, for both the representative median waveforms and individual beats, comparisons were made between Maximum<sub>XYZ</sub> and Area<sub>XYZ</sub> results, Maximum<sub>XYZ</sub> and Integral<sub>XYZ</sub> results, and Area<sub>XYZ</sub> and Integral<sub>XYZ</sub> results. The same comparisons were also made for the three different measurements combined with the SVD-based orthogonal leads.

For each of the comparisons, Bland-Altman-type (Bland and Altman, 1986) of scatter diagram was constructed relating the differences between compared values to their mean. These diagrams were based on data pooled from all ECG segments in all subjects and were judged visually. Cumulative distributions of the pooled differences between compared measurements were also constructed for visual judgement.

To allow statistical evaluation of these comparisons, in each of the analyses and in each of the study subjects, intra-subject mean of absolute differences of the compared QRS-T angle values and intra-subject standard deviation of these differences were also obtained.

## 2.5.2 Relationship to heart rate

### 2.5.2.1 Regression model between QRS-T angle and heart rate

For an initial assessment, intra-subject relationships between measured QRS-T angles were investigated based on graphical representations. As an initial approximation of the dependency, second degree polynomial regression model between QRS-T angles and underlying heart rate (or reciprocals of the RR intervals) was used in subsequent investigations.

### 2.5.2.2 Average estimates of rate hysteresis

To replicate the procedures that were previously used in the estimates of the QT/RR hysteresis (Malik et al., 2016), QRS-T angle measurements in individual beats were related to preceding heart rate derived from different durations of the RR interval history of each beat in which the angle measurement was performed. The duration of the history that leads to the closest fit in the regression analysis approximates the hysteresis constant, i.e., the delay with which the QRS-T angle reacts to heart rate changes.

In more detail, for each individual beat  $\ell$  at which the QRS-T angle  $\Theta_\ell$  was measured, underlying heart rate  $\mathcal{R}_\ell(d)$  was obtained from the average of  $d$  RR intervals preceding the beat  $\ell$ . Subsequently, in each study subject, polynomial regression analysis was evaluated in form

$$\Theta_\ell = \beta_0 + \beta_1 \mathcal{R}_\ell(d) + \beta_2 \mathcal{R}_\ell^2(d) + \varepsilon_\ell$$

Where  $\beta_0$ ,  $\beta_1$ , and  $\beta_2$  are subject-specific regression coefficients and  $\varepsilon_\ell$  are zero centred regression errors. The coefficient  $d$  that led to the lowest regression residual, that is to the minimal value of  $\sqrt{\sum \beta \varepsilon_\ell^2}$  approximated the heart rate hysteresis of the QRS-T angle  $\Theta$ .

For this purpose, a geometric progression sequence of 50 values between 1 and 300 was used to vary the coefficient  $d$ . Subsequently, standard golden search algorithm was used to determine the “optimal” value of  $d$  for each study subject.

The analysis was subsequently repeated deriving the heart rate  $\mathcal{R}_\ell(d)$  not from  $d$  preceding RR intervals but from the RR intervals within the preceding  $d$  seconds. Both types of analysis (i.e., heart rate derived from preceding number of RR intervals of the preceding time window) were performed for all QRS-T angle measurements in a study subject as well as in only those measurements that were preceded by variable heart rate.

All these steps were performed for each study subject and for all six QRS-T angle expressions.

### 2.5.2.3 Exponential decay model of rate hysteresis

The expressions of underlying heart rate based on a simple average of preceding RR intervals does not reflect gradual decrease of the influence of heart rate changes in more remote history. Therefore, exponential decay models were also used, in the same form as previously developed for the purposes of estimating QT/RR hysteresis (Malik et al., 2008b; Malik et al., 2016; Andršová et al., 2022).

That means that the same form of polynomial regression analysis as described with the experiments of average estimates of rate hysteresis (see previous section) were used replacing the  $\mathcal{R}_\ell(d)$  calculations of underlying heart rate with expressions  $\mathcal{H}_\ell(\lambda)$  derived from exponential decay models where the parameter  $\lambda$  specifies the speed of the adaptation (see further).

In more detail, if beat  $\ell$  is preceded by a sequence  $\{\text{RR}_i\}_{i=0}^N$  of  $N$  consecutive RR intervals ( $\text{RR}_0$  being the closest to the beat  $\ell$ ) the underlying heart rate  $\mathcal{H}_\ell(\lambda)$  is derived from a weighted average of the RR intervals as  $\mathcal{H}_\ell(\lambda) = 60/\sum_{i=0}^N \omega_i \text{RR}_i$ , where  $\sum_{i=0}^N \omega_i = 1$  and individual RR intervals are measured in second.

Two different exponential decay models were considered which differed in the definition of the weights  $\{\omega_i\}_{i=0}^N$ . The model assuming the dependency on the number of preceding RR intervals used weights such that

$$\sum_{i=0}^k \omega_i = \frac{1 - e^{\lambda \left(\frac{k+1}{N+1}\right)}}{1 - e^\lambda}$$

for each  $k, 0 \leq k \leq N$ ,

While the model assuming the dependency on the absolute time preceding the beat  $\ell$  measurement used the weights such that

$$\sum_{i=0}^k \omega_i = \frac{1 - e^{\lambda \left(\frac{\mathbb{T}(k)}{\mathbb{T}(N)}\right)}}{1 - e^\lambda}$$

where

$$\mathbb{T}(k) = \sum_{i=0}^k \text{RR}_i$$

for each  $k, 0 \leq k \leq N$ .

While the parameter  $\lambda$  specifies the speed of the adaptation to heart rate changes, it does not have obvious physiologic interpretation. Therefore, the models were characterised by the so-called hysteresis constant, i.e., by the number of RR intervals or by the time-elapsed at which the adaptation to changed heart rate reaches 95%, i.e., by either a number  $y$  of RR intervals or by time delay  $\mathbb{T}(y)$  such that  $\sum_{i=0}^y \omega_i = 0.95$ .

As with the experiments of average estimates of rate hysteresis, the search of optimal subject-specific hysteresis time constant started with a geometric progression sequence of 50 values specifying the hysteresis constant between 1 and 277 (the upper limit determined by the duration of 300 s of the RR interval histories). Subsequently, standard golden search algorithm was used to determine the “optimal” hysteresis constant for each study subject.

### 2.5.3 Intra-subject characteristics and reproducibility

Physiologic characteristics of QRS-T angle in individual study subjects were investigated in the same way for all six QRS-T angle expressions. For each subject and for each angle expression, setting of the optimal hysteresis constant (and of the optimal interval for heart rate measurement) was used for the assessment of physiologic characteristics. The QRS-T angle measurements at individual beats were therefore used.

#### 2.5.3.1 Curvatures of the relationship to the underlying heart rate

For each subject and for each QRS-T angle expression  $\Theta^{(a)}$ , higher degree polynomial regressions were investigated. That is, for different polynomial degree  $\varphi$ , regression forms

$$\Theta_{\varphi}^{(a)} = \sum_{i=0}^{\varphi} \beta_i^{(a)} [\mathcal{H}_{\varphi}(\lambda)]^i + \varepsilon_{\varphi}^{(a,\varphi)}$$

were used, leading to residual error estimates  $\mathfrak{E}^{(a,\varphi)} = \sqrt{\sum_{\varphi} (\varepsilon_{\varphi}^{(a,\varphi)})^2}$ . Clearly, with increasing degree  $\varphi$ , the residual errors decrease, i.e.,  $\mathfrak{E}^{(a,\varphi)} \geq \mathfrak{E}^{(a,\varphi+1)}$ . The search for the optimum polynomial degree was driven by the criterion  $\mathfrak{E}^{(a,\varphi+1)}/\mathfrak{E}^{(a,\varphi)} > 0.95$  for all six QRS-T angle expression in at least 95% of study population. Polynomial degree  $\varphi_o$  was defined in this way.

#### 2.5.3.2 Sex and race differences

For each subject and for each QRS-T angle expression  $\Theta^{(a)}$ , the  $\varphi_o$ -degree polynomial regressions provided projections of the  $\Theta^{(a)}$  values at heart rate of 60 and 120 beats per minute (bpm). These were subsequently statistically compared between sexes and different subject races.

In addition, for each angle expression ( $a$ ), subject-specific polynomial curvatures

$$\sum_{i=0}^{\varphi_o} \beta_i^{(a)} h^i$$

Were computed for  $h$  ranging between 50 and 120 bpm and at each value of  $h$  (with a step of 1 bpm) median, inter-quartile range, and a 10% to 90% range were calculated for females and males separately.

#### 2.5.3.3 Relationship to Body mass index and Lean body mass

The projections of the  $\Theta^{(a)}$  values at heart rate of 60 and 120 bpm were related to body mass index and to lean body mass. The relationship was studied separately in female and male sub-populations.

#### 2.5.3.4 Intra-subject reproducibility

The dependency of QRS-T angle measurements on the underlying heart rate makes it non-sensical to investigate intra-subject reproducibility of the measurements without considering the relationship to heart rate. Therefore, to investigate the reproducibility of the different QRS-T angle expressions, residual errors  $\mathfrak{E}^{(a,\varphi_o)}$  of the optimal-degree polynomial regression to the underlying heart rate were used.

#### 2.5.3.5 Slope and curvature of heart rate relationship

In the higher degree polynomial regressions, coefficients  $\beta_i^{(a)}$  influence each other. Therefore, to compare the slope of the heart rate relationship between different QRS-T angle expressions, simple linear model was used in the form  $\Theta_{\varphi}^{(a)} = \beta_0^{(a)} + \beta_1^{(a)} \mathcal{H}_{\varphi}(\lambda) + \varepsilon_{\varphi}$  and parameters  $\beta_1^{(a)}$  were used to estimate the slope of the heart rate relationship.

The intra-subject degree of the polynomial curvature of the heart rate relationship was estimated by the differences  $\mathfrak{E}^{(a,\varphi_o)} - \mathfrak{E}^{(a,\varphi_o-1)}$ . That is, after the intra-subject optimum degree  $\varphi_o$  of the polynomial curvature was established defining the relationship to the hysteresis corrected heart rate, the regression residual of this polynomial curvature was compared to the regression residual of a polynomial curvature in which the polynomial degree was lowered by one.

## 2.6 Statistics and data presentation

Computation of the matrix-based conversion of 12-lead ECG signals to the orthogonal XYZ leads, the SVD of the signals, and the computation of the QRS-T angles utilised purpose developed software written in C++. Microsoft visual studio (version 16.11.8) implementation of Microsoft Visual C++ 2019 compiler (version 00435-60000-00000-AA114) was used.

Descriptive data are presented as means  $\pm$  SD. Comparison between study groups, e.g., between female and male sub-populations, were tested by two-sample two-tail  $t$ -test assuming different variances of the compared samples. Intra-

subject comparisons, e.g., the comparisons between  $\mathcal{C}^{(a,\varphi_0)}$  and  $\mathcal{C}^{(b,\varphi_0)}$  values, were tested by the paired two-tail *t*-test.

Pearson correlation coefficients and linear regressions were used to study the relationship between BMI and LBM and the QRS-T angle values. The linear regressions were computed together with their 95% confidence bands.

Statistical tests used IBM SPSS package, version 27. *p* values below 0.05 were considered statistically significant. Because of interdependence between the different indices, no correction for multiplicity of statistical testing was made.

## 3 Results

### 3.1 Population and electrocardiographic data

As stated, the source clinical pharmacology studies enrolled 523 healthy volunteers including 259 females. There were no statistical age differences between females ( $33.4 \pm 9.1$  years, range 18.1–55.4 years) and males ( $33.7 \pm 7.8$  years, range 18.2–54.5 years). Similarly, the body mass index was not different between females ( $25.2 \pm 2.9$  kg/m<sup>2</sup>, range 20.0–30.0 kg/m<sup>2</sup>) and males ( $25.6 \pm 2.7$  kg/m<sup>2</sup>, range 20.2–30.1 kg/m<sup>2</sup>). As expected, lean body mass was lower in females ( $45.3 \pm 5.0$  kg) than in males ( $57.1 \pm 5.3$  kg,  $p < 0.0001$ ). Among females, 38.6% and 56.7% of the subjects classified themselves as of African origin and of White Caucasian origin, respectively. Among males, these proportions were 51.3% and 42.8%, respectively. The remainder of the population classified themselves as of Asian, American Indian/Alaska Native, Native Hawaiian/Pacific Islander, or Other.

The study was based on the total of 659,313 individual 10-s ECG samples and the total of 7,350,733 individual beats accepted for the analysis. On average, there were  $1,252 \pm 220$  and  $1,269 \pm 217$  ECG segments, and  $14,298 \pm 2,983$  and  $13,825 \pm 2,981$  individual beats processed per each female and male subject, respectively (no statistical differences between sexes).

### 3.2 Comparisons of QRS-T angle expressions

#### 3.2.1 Differences between orthogonal lead systems

Scatter diagrams of the differences between QRS-T angle measurements made in conversion matrix based orthogonal XYZ leads and in orthogonal SVD-based leads are shown in **Figure 1**. Visual judgement of the images in **Figure 1** suggests that the difference between the two orthogonal leads systems influenced the Integral method less than the other two methods while the Maximum method was influenced more than the other two methods. This applied to both the images based on individual

ECG beats (top panels in **Figure 1**) and on representative median ECG waveforms (bottom panels in **Figure 1**).

This visual observation was confirmed statistically as shown in the top panels **A** and **B** of **Figure 5**. (Note that **Figure 5** shows statistical summaries also of subsequent **Figures 2–4**). All the differences between different QRS-T angle methods (and their applications to single beats and representative waveforms) seen in panel **A** of **Figure 5** (intra-subject means of absolute values of the differences shown in **Figure 1**) were statistically significant (all  $p < 0.00001$ ). The sex difference was only significant for the Integral method applied to individual beats ( $p = 0.0011$ ). The intra-subject standard deviations of the differences shown in **Figure 1** (see panel **B** of **Figure 5**) were also highly statistically different between different methods (and their applications to single beats and representative waveforms –  $p < 0.00001$  for all). Sex differences seen in this panel of **Figure 5** were also all statistically significantly different ( $p < 0.0001$ ) except for both cases of the Maximum method.

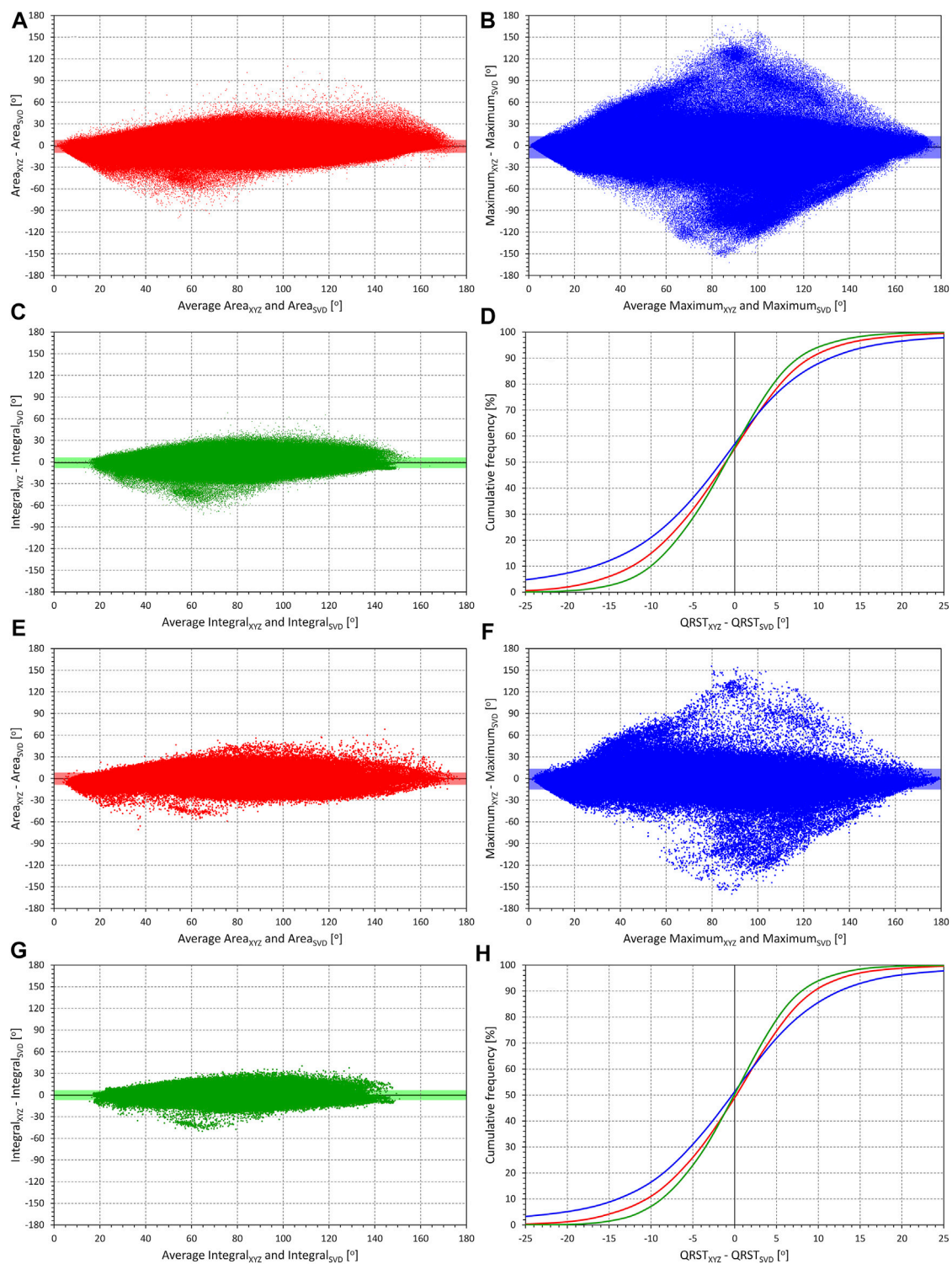
#### 3.2.2 Differences between individual beats and representative waveforms

Similar visual comparisons between the methods are also seen in **Figure 2** which shows the differences between QRS-T angle methods applied to representative waveforms and to the individual beats with results averaged over the same ECG segment. Regardless of whether the methods are applied to the matrix-based XYZ leads or to the SVD leads, the Integral method and the Maximum method appear least and most influenced, respectively.

Statistical analyses shown in panels **C** and **D** of **Figure 5** confirm these observations. With the exception of the two variants (XYZ and SVD) of the Maximum method, all the between-method differences seen in panel **C** of **Figure 5** were statistically significant ( $p < 0.0001$  to  $p < 0.001$ ). The results of the Maximum methods were also only those that showed no similar significant difference between females and males. The intra-subject standard deviations of the differences (panel **D** of **Figure 5**) showed the same results of comparisons with closely similar statistical significances.

#### 3.2.3 Differences between measurement algorithms

Scatter diagrams of the comparison between QRS-T angle calculation methods are shown in **Figure 3** (XYZ matrix-based orthogonal leads) and **4** (SVD-based orthogonal leads). Generally, the Maximum method leads to lower values of the angle compared to the other two methods while on average, the Integral method leads to slightly higher results compared to the Area method. The statistical summaries of the absolute values and standard deviations of these differences are shown in panels **E** and **F** of **Figure 5** (XYZ matrix-based orthogonal leads) and panels **G** and **H** of **Figure 5** (SVD-based orthogonal leads). The difference between the Area and Integral methods was



**FIGURE 1**  
 Comparison of QRS-T angle measurements in XYZ and SVD orthogonal projections. The matrix (XYZ) and the singular value decomposition (SVD) methods are used to derive orthogonal leads. In individual panels, the measurements in all subjects are pooled and the difference between XYZ and SVD angle expressions is plotted against their averaged value. The mean difference is shown by a bold horizontal line while the light-coloured band (along the horizontal axis) shows the spread of mean  $\pm$  standard deviation. Panels (A) (comparisons of  $Area_{XYZ}$  and  $Area_{SVD}$ ), (B) (comparisons of  $Maximum_{XYZ}$  and  $Maximum_{SVD}$ ), and (C) (comparisons of  $Integral_{XYZ}$  and  $Integral_{SVD}$ ) show data derived from individual beats. Panel (D) shows cumulative distributions of the  $Method_{XYZ} - Method_{SVD}$  values shown in panels (A), (B), and (C) (the colours of the graphs in this panel (Continued)

**FIGURE 1**

correspond to the colours of the scatter diagram panels). Panels (E), (F), and (G) show corresponding comparisons of the methods applied to representative waveforms of individual 10-s ECG segments. Panel (H) again shows the cumulative distributions of the method differences shown in panels (E), (F), and (G). Note that the trapezoidal shape of the images (noticeable especially in panels (B) and (F) is caused by the measurements strictly between 0° and 180° (the difference of 180° is only possible if one of the methods gives 0° and the other 180°, in which case the average of the methods is 90°).

substantially and significantly lower compared to the Area—Maximum or Maximum—Integral differences and showed also lower intra-subject standard deviations (all  $p < 0.00001$ ).

### 3.3 Heart rate dependency and hysteresis assessment

Figures 6, 7 show examples of the relationship between QRS-T angle measurements and the underlying heart rate assessed in 1-min intervals preceding each single-beat angle measurements. The figures show clear correlation between the angles and the heart rate as well as an obvious non-linear nature of the relationship.

#### 3.3.1 Interval-based heart rate estimates

The results of the experiments investigating interval-based QRS-T-angle/heart-rate hysteresis estimates are shown in Figure 8. Unexpectedly, the results do not suggest any physiologic range of heart-rate hysteresis estimates.

When tested considering only measurements preceded by variable heart rates, Maximum<sub>XYZ</sub> and Maximum<sub>SVD</sub> angle expressions reach closes fit to heart rate measured approximately over preceding 20 s or a similar number of RR intervals. With the other angle expressions, the result is much less clear since heart rate measurements of intervals longer than 20 s or 20 RR intervals do not appear to make any difference in the closeness of fit until approximately rate measurements over the preceding 3 min.

When testing the hysteresis effect in the complete data of each subject, the results are even less expected. When measuring the effect of heart rate assessed in an interval longer than approximately 30 s, the closeness of fit of the regressions between Area and Integral expressions and heart rate remains stable while the Maximum expressions show only minimal gradual increases of the regression residuals.

The intra-subject optimisation of the heart rate measurement was similarly inconclusive since no clearly defined minima of regression residuals were found in substantial majority of study subjects.

#### 3.3.2 Exponential decay estimates

These rather unexpected observations were replicated in experiment with exponential decay optimisation as seen in

Figure 9. Only the Maximum expressions show some albeit very loosely defined minima in the search for optimum hysteresis constant. Both the Area and Integral expressions reach a stable level of regression residuals from approximately 30 to 40 s (panels in right part of Figure 9) or 30 to 40 beats (panels in the left part of Figure 9) onwards, regardless of whether the investigation is made using only beats preceded by variable heart rates or all study data.

Similar to the optimisation of heart rate measurements, no defined optimal hysteresis constants were found for almost all study subjects. With the Area and Integral expressions, the intra-subject golden cut searches converged to the maximum available scale of available data.

### 3.4 Physiologic characteristics

#### 3.4.1 Polynomial regression to heart rate

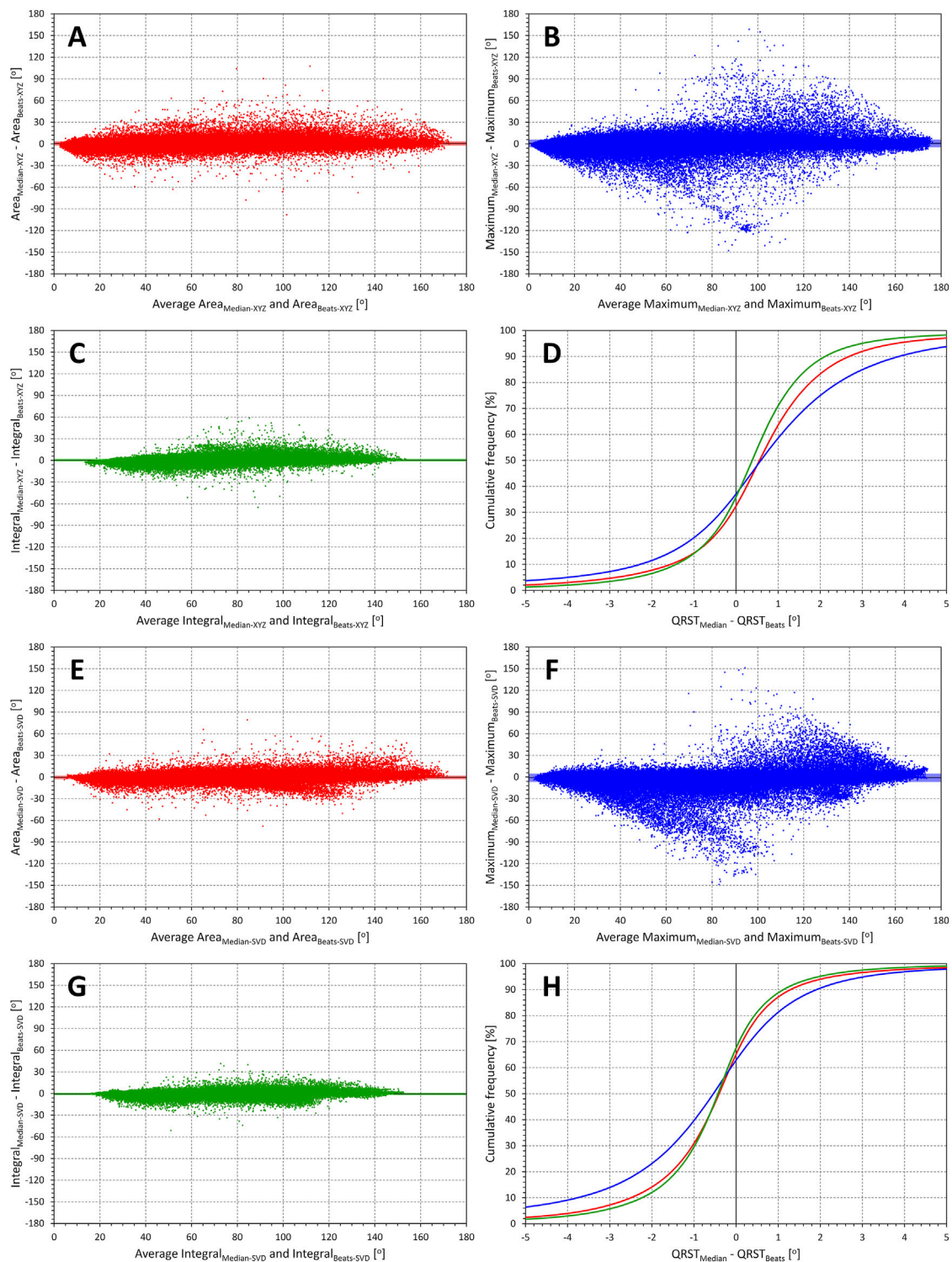
The optimum degree of polynomial regression between QRS-T angle and underlying heart rate was found to be  $\varphi = 2$ . Specifically, the proportions  $\mathfrak{C}^{(a,2)}/\mathfrak{C}^{(a,1)}$  were below 0.95 in 17.7, 14.2, 13.2, 19.2, 14.4, and 14.0% of the population for Area<sub>XYZ</sub>, Maximum<sub>XYZ</sub>, Integral<sub>XYZ</sub>, Area<sub>SVD</sub>, Maximum<sub>SVD</sub>, and Integral<sub>SVD</sub>, respectively. The corresponding proportions of  $\mathfrak{C}^{(a,3)}/\mathfrak{C}^{(a,2)}$  were below 0.95 in only 2.1, 2.9, 2.7, 2.5, 1.9, and 2.1% of the population.

Pooling female and male subjects together, the regression residuals of the second-degree polynomial regression between QRS-T angle and optimum (hysteresis-optimisation based) measurement of heart rate were  $11.37 \pm 3.26$ ,  $13.36 \pm 5.55$ ,  $8.93 \pm 2.38$ ,  $10.20 \pm 2.71$ ,  $13.11 \pm 7.28$ , and  $7.97 \pm 1.77^\circ$  for Area<sub>XYZ</sub>, Maximum<sub>XYZ</sub>, Integral<sub>XYZ</sub>, Area<sub>SVD</sub>, Maximum<sub>SVD</sub>, and Integral<sub>SVD</sub>, respectively. (See also the subsequent section on intra-subject reproducibility for the comparison between sexes.)

#### 3.4.2 Sex differences

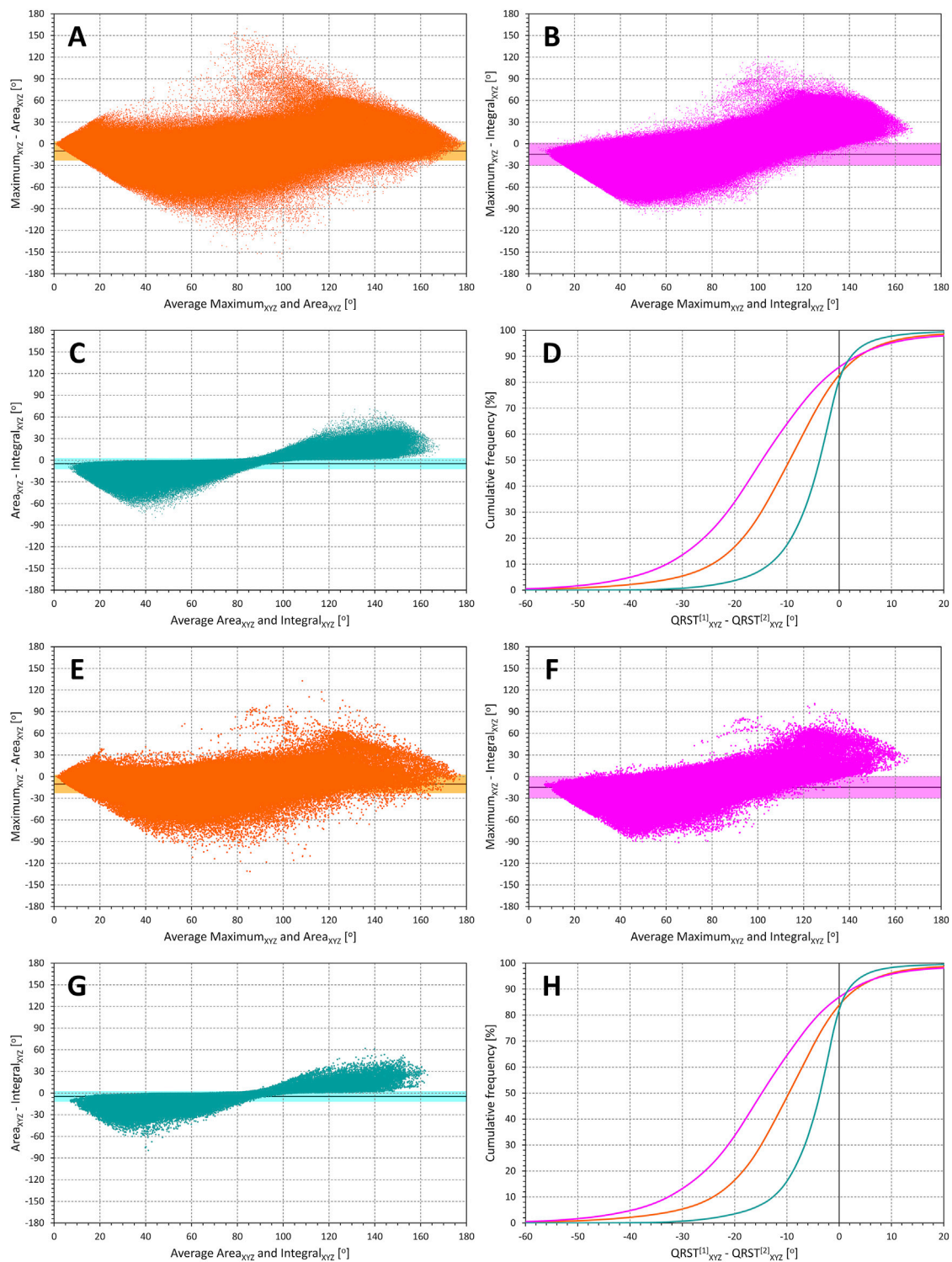
The intra-subject curvatures of second-degree polynomial regressions between QRS-T angle expressions and the underlying heart rate were used to construct images in Figure 10. Although, as seen in this Figure, there was a noticeable overlap between both sexes, the figure shows that irrespective of the underlying heart rate and irrespective of the QRS-T angle expression, females showed lower QRS-T angle than males. Dependent of



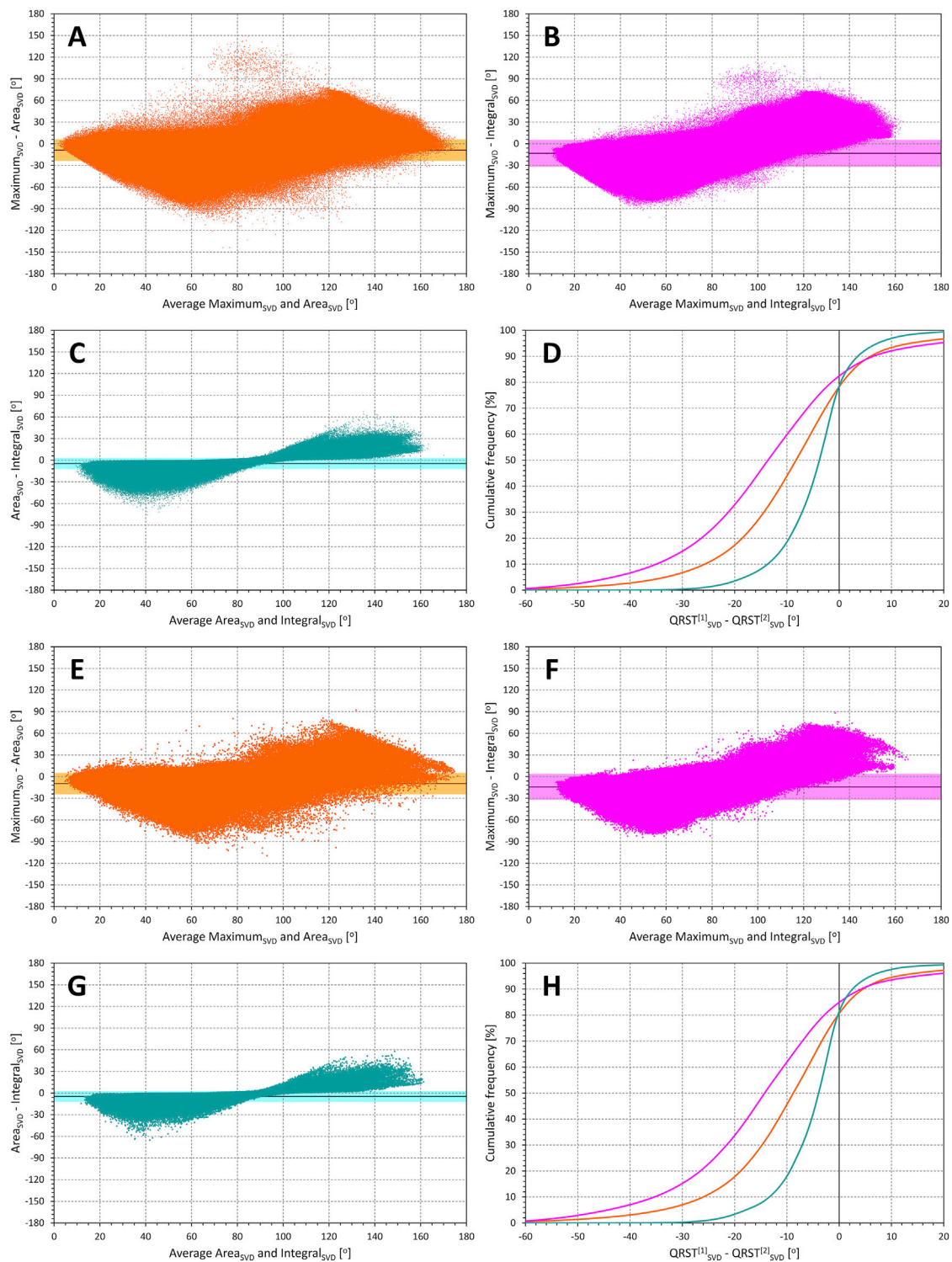


**FIGURE 2**

Comparisons of QRS-T angle measurements in individual beats and representative waveforms. Bland-Altman type of comparisons between QRS-T angle expressions measured at the representative waveform of 10-s ECG segments with the averages of the same angle expressions measured at individual beats of the same ECG segment. The layout of the figure and of the individual panels corresponds to that of Figure 1, with all the measurements in all study subjects pooled. In the method indicators, additional subscripts Median and Beats indicate measurement value derived from representative median waveform and obtained as an average of individual beats of the ECG segment, respectively. Panels (A,B) and (C) show the comparisons for the  $Area_{XYZ}$ ,  $Maximum_{XYZ}$ , and  $Integral_{XYZ}$  angle measurements, respectively; panel (D) again shows the cumulative distributions of the measurement differences shown in panels (A), (B), and (C). The same analysis of the results of methods  $Area_{SVD}$ ,  $Maximum_{SVD}$ , and  $Integral_{SVD}$  is shown in panels (E,F) and (G), respectively; corresponding cumulative distributions are shown in panel (H).



**FIGURE 3**  
 Comparisons of methods of QRS-T angle measurements in XYZ orthogonal projections. Bland-Altman type of comparisons between different QRS-T angle methods applied to the matrix-derived orthogonal leads XYZ. The layout of the figure and of the individual panels corresponds to that of Figure 1, with all the measurements in all study subjects pooled. Panels (A–C) shows the comparisons of Maximum<sub>XYZ</sub> with Area<sub>XYZ</sub>, Maximum<sub>XYZ</sub> with Integral<sub>XYZ</sub>, and Area<sub>XYZ</sub> with Integral<sub>XYZ</sub>, respectively, all values are derived from individual beat measurements. Panel (D) shows corresponding cumulative distributions, i.e., of pooled values Maximum<sub>XYZ</sub>–Area<sub>XYZ</sub>, Maximum<sub>XYZ</sub>–Integral<sub>XYZ</sub>, and Area<sub>XYZ</sub>–Integral<sub>XYZ</sub>. Panels (E–H) show the same analysis applied to the measurements derived from representative median waveforms of 10-s ECG segments (again pooled over all study subjects).



**FIGURE 4**  
 Comparisons of methods of QRS-T angle measurements in SVD orthogonal projections. Bland-Altman type of comparisons between different QRS-T angle methods applied to the orthogonal leads derived by singular value decomposition of the original 12-lead ECG signals. The layout of the Figure and the meaning of individual panels is the same as in Figure 3 but methods Maximum<sub>SVD</sub>, Area<sub>SVD</sub>, and Integral<sub>SVD</sub> were analysed instead of Maximum<sub>XYZ</sub>, Area<sub>XYZ</sub>, and Integral<sub>XYZ</sub>, respectively.

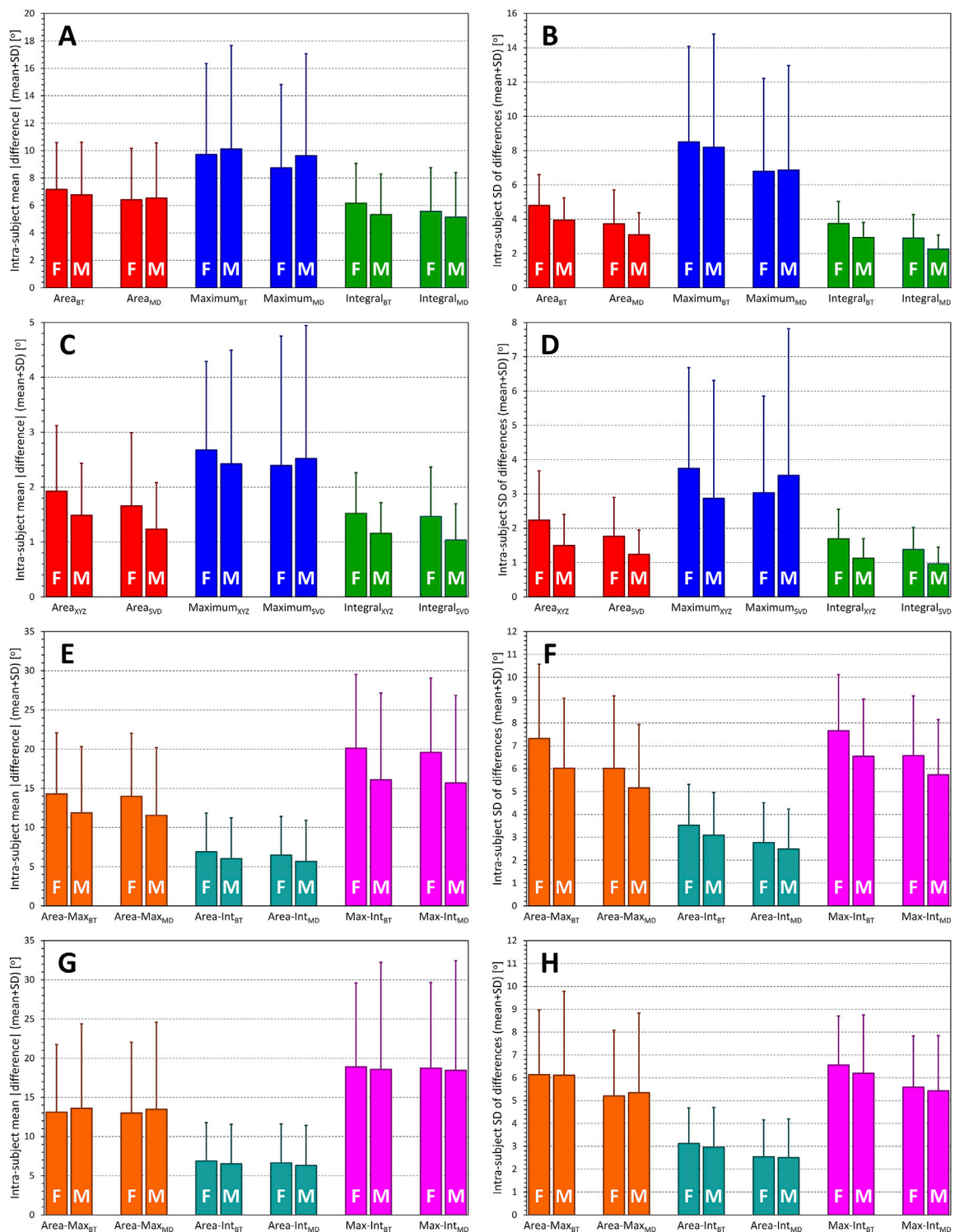


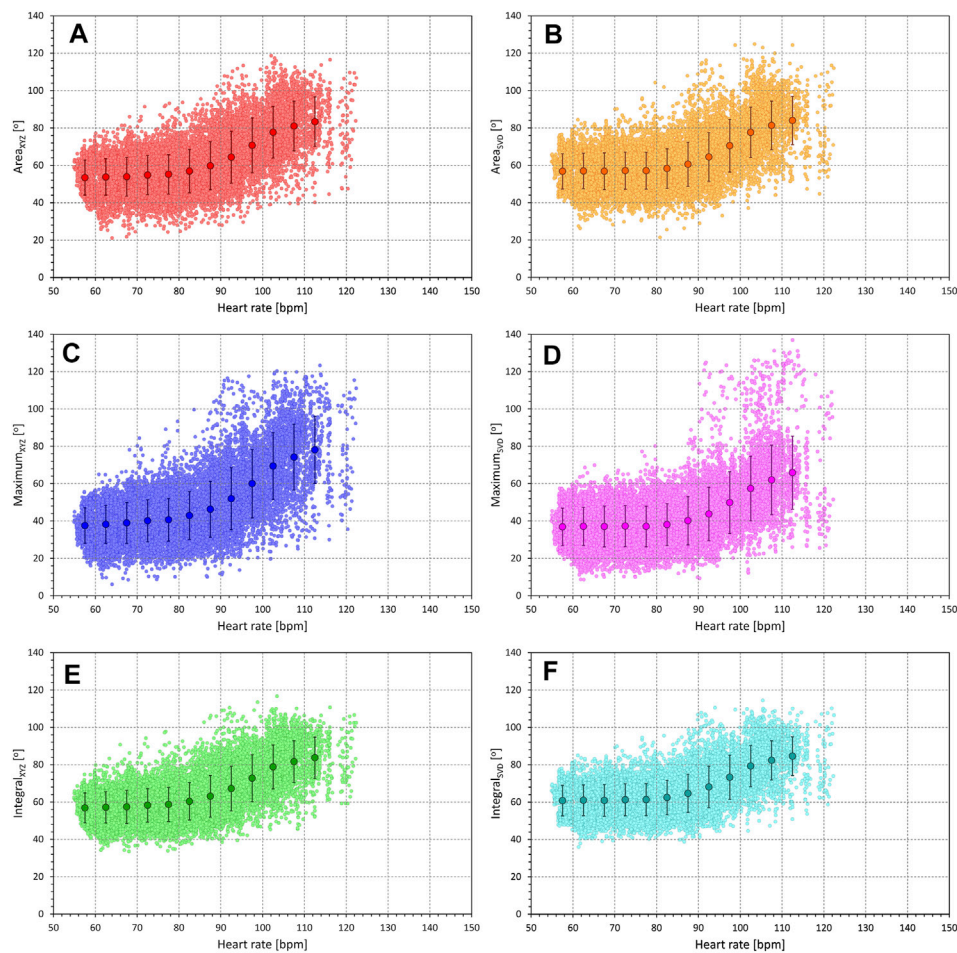
FIGURE 5

Statistical summaries of the differences between QRS-T angle measurements shown in Figures 1–4. Panel (A) shows the summary of intra-subject means of absolute values of the differences between the angle measurements in conversion matrix-derived XYZ orthogonal leads and SVD-derived optimised orthogonal leads; panel (B) shows the summary of intra-subject standard deviations of these differences. Panel (C) shows the summary of intra-subject means of absolute values of the differences between measurements in median waveforms of an ECG segment and the averages of measurements in individual beats of the same segment; panel (D) shows the summary of intra-subject standard deviations of these differences. Panels (E) and (G) show the summary of the intra-subject means of absolute values of the differences between different measurement

(Continued)

**FIGURE 5**

methods applied to the matrix-derived XYZ orthogonal leads (panel **E**) and to the measurements SVD-derived optimised orthogonal leads (panel **G**); panels **(F)** and **(H)** show the summary of intra-subject standard deviations of these differences. In each panel, statistics of female (F) and male (M) sub-populations are shown separately. See the text for the definition of measurement methods (Max – Maximum, Int – Integral). Subscripts Method<sub>BT</sub> and Method<sub>MD</sub> indicate measurements performed in individual beats and in the median waveforms, respectively. See the text for *p*-values of statistical comparisons.



**FIGURE 6**

Example of the relationship of beat-based measurements of QRS-T angle and the heart rate measured over 1 min preceding each angle measurements. The data were obtained from the recordings of a 21.2-year-old female subject. Individual panels of the figure correspond to different QRS-T angle expressions; results corresponding to, Area<sub>XYZ</sub>, Area<sub>SVD</sub>, Maximum<sub>XYZ</sub>, Maximum<sub>SVD</sub>, Integral<sub>XYZ</sub>, and Integral<sub>SVD</sub> angle expressions are shown in panels **(A–F)**, respectively. In each panel, the individual light-colour small marks correspond to the individual ECG beats data, the larger full-colour marks correspond to the averages of the QRS-T angle values in 5 beat per minute (BPM) bins, the error bars of the larger full-colour marks show the spread of  $\pm 1$  standard deviation in the corresponding 5-BPM bins.

the angle expression, values in females were approximately 10° to 20° lower than those in males.

Statistical evaluations of the sex differences are demonstrated in panels **A** and **B** of **Figure 11** which show the sex-specific averages of QRS-T angles at heart rate of 60 and 120 bpm. All the sex differences shown in both these figure

panels were highly statistically significant ( $p < 0.00001$  for all sex comparisons).

Statistically significant differences were also noted between the different QRS-T angle expressions (corresponding to the measurement differences that were described previously). At the heart rate of 60 bpm (panel **A**

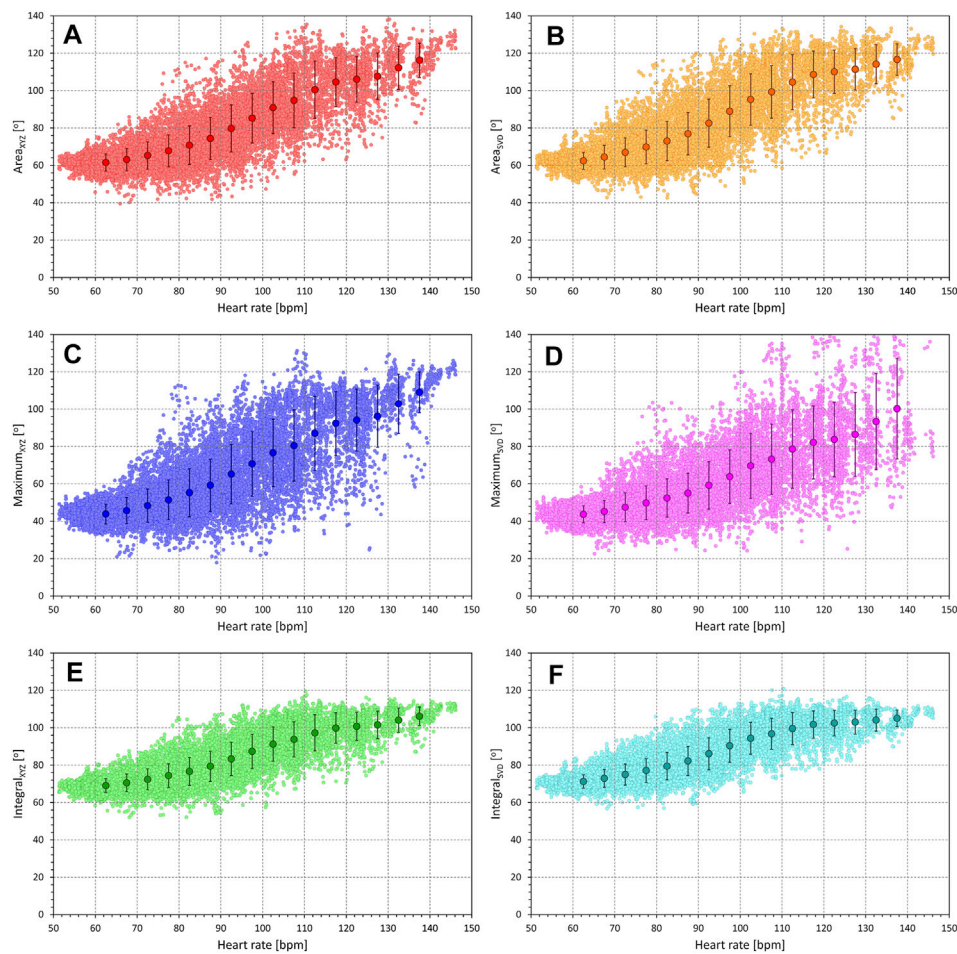


FIGURE 7

Example of the relationship of beat-based measurements of QRS-T angle and the heart rate measured over 1 min preceding each angle measurements. The data were obtained from the recordings of a 24.4-year-old male subject. The layout of the figure and the meaning of the symbols correspond to those in Figure 6.

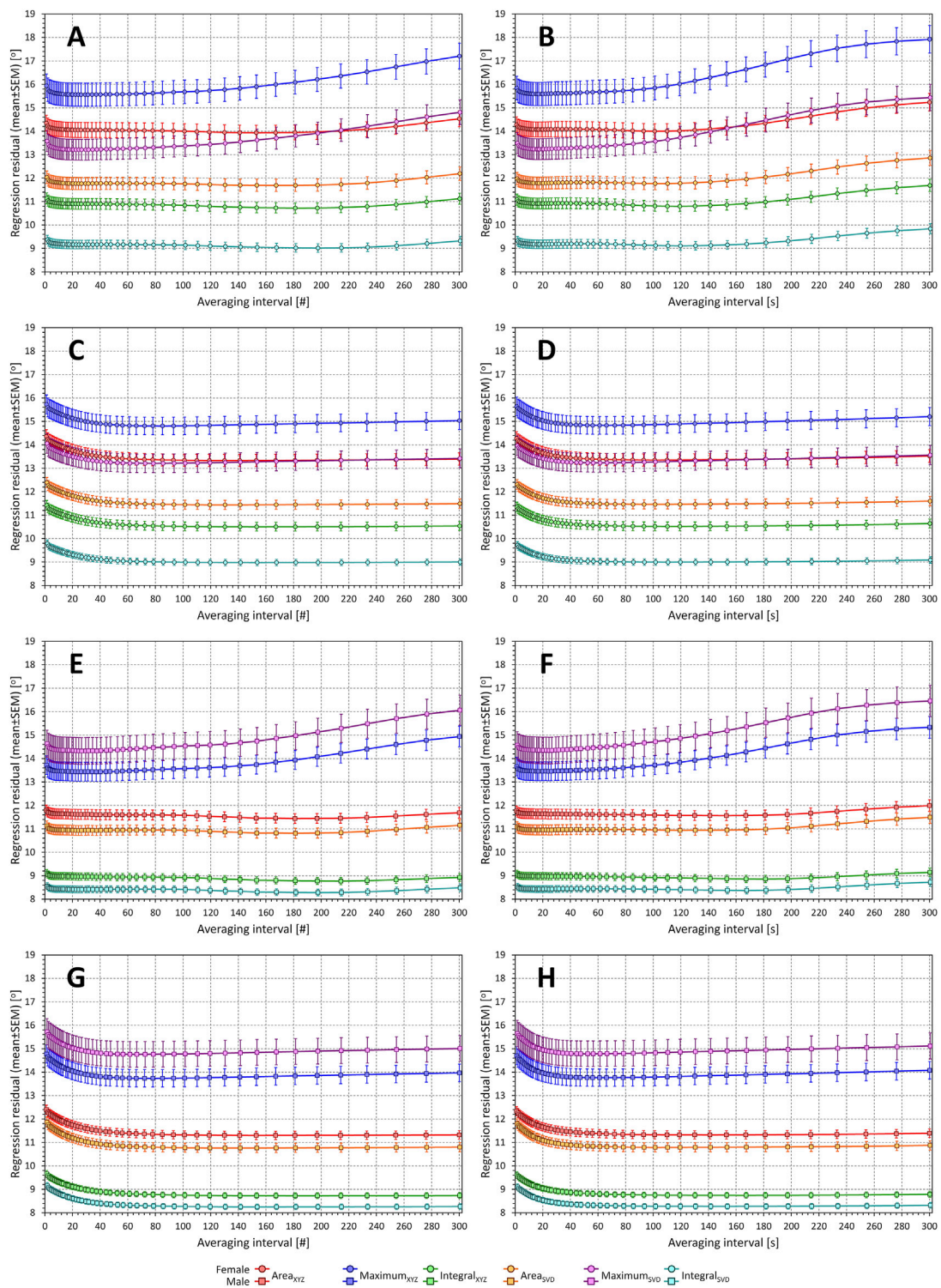
of Figure 11), the results of the methods showed, on average, the following sequence:  $\text{Maximum}_{XYZ} < \text{Maximum}_{SVD} < \text{Area}_{XYZ} < \text{Area}_{SVD} < \text{Integral}_{XYZ} < \text{Integral}_{SVD}$  with all these differences between QRS-T angle expressions being highly statistically significant ( $p < 0.00001$  in all pairs). At the heart rate of 120 bpm (panel B of Figure 11), the measurements by the  $\text{Maximum}_{XYZ}$  expression were, on average, still statistically significantly smaller than those by the  $\text{Maximum}_{SVD}$  expression ( $p = 0.007$ ) which were, in turn, significantly smaller than the results by the other expressions ( $p < 0.00001$ ). There were, however, no significant differences between the other angle expressions.

### 3.4.3 Intra-subject reproducibility

Panel C of Figure 11 shows the regression residuals of second-degree polynomial regressions between QRS-T angles and the heart rate measurement derived by the intra-subject

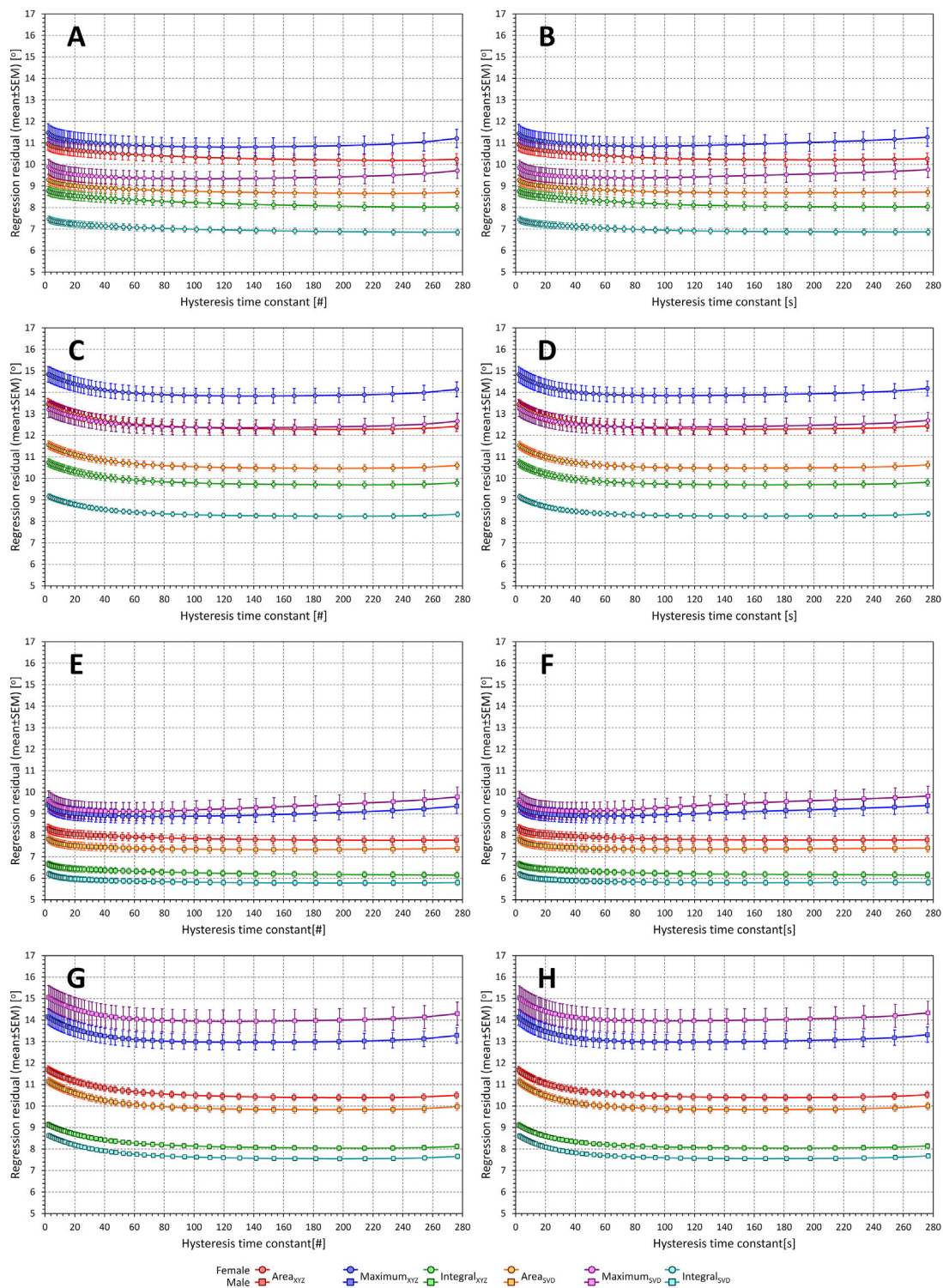
hysteresis optimisation. Despite the females showing lower QRS-T angle values, they also showed marginally but statistically significantly ( $p$ -value between 0.004 and  $<0.00001$ ) higher regression residuals, i.e., lower intra-subject reproducibility of the QRS-T angle values “corrected for the underlying heart rate” when the Area or Integral expressions were used. The sex difference for the  $\text{Maximum}_{XYZ}$  expression did not reach statistical significance while the sex difference for the  $\text{Maximum}_{SVD}$  expression showed the opposite sex difference ( $p = 0.015$ ).

More importantly, there were substantial disagreements between the different QRS-T angle expressions. In the total population, the highest residuals ( $13.31 \pm 5.64^\circ$ ) were seen with  $\text{Maximum}_{XYZ}$  expression while the lowest residuals ( $7.82 \pm 1.74^\circ$ ) were seen with the  $\text{Integral}_{SVD}$  expression. The averaged order of the residuals contrasted with the order measurement values since it was the opposite what was observed for the values



**FIGURE 8**

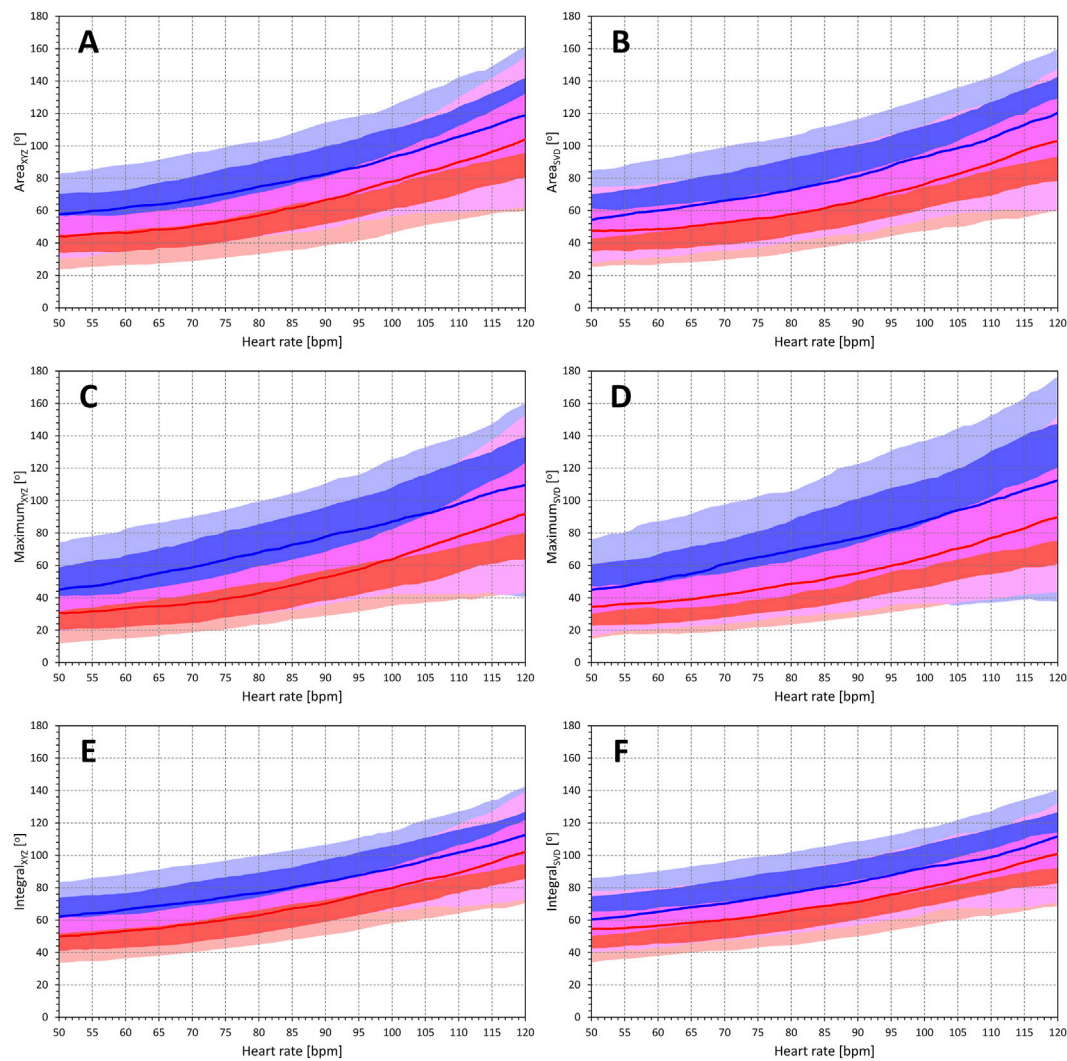
Regression residuals of QRS-T angle related to averaged preceding heart rate. In each panel, the individual graphs correspond to different QRS-T angle expressions and show the mean  $\pm$  standard deviation of intra-subject residuals of second-degree polynomial regressions between QRS-T angle measurements and heart rates measured in preceding intervals of a given number of RR intervals [(#)—panels on the left] or a given number of seconds [(s)—panels on the right]. Panels (A) and (B) show the results in females with regressions involving only measurements preceded by variable heart rates; panels (C) and (D) show the results in females with regressions involving all measurements; panels (E) and (F) show the results in males with regressions involving only measurements preceded by variable heart rates; panels (G) and (H) show the results in males with regressions involving all measurements. Results related to the QRS-T angle expressions  $Area_{XYZ}$ ,  $Maximum_{XYZ}$ ,  $Integral_{XYZ}$ ,  $Area_{SVD}$ ,  $Maximum_{SVD}$ , and  $Integral_{SVD}$  are shown in red, blue, green, amber, violet, and cyan, respectively. See the text for the definitions of the angle expressions.



**FIGURE 9**

Regression residuals of QRS-T angle related to exponential decay of preceding heart rate. In each panel, the individual graphs correspond to different QRS-T angle expressions and show the mean  $\pm$  standard deviation of intra-subject residuals of second-degree polynomial regressions between QRS-T angle measurements and heart rates derived by exponential decay hysteresis constants of a given number of RR intervals [(#)—panels on the left] or a given number of seconds [(s)—panels on the right]. Panels (A,B) show the results in females with regressions involving only measurements preceded by variable heart rates; panels (C,D) show the results in females with regressions involving all measurements; panels (E) and (F) show the results in males with regressions involving only measurements preceded by variable heart rates; panels (G) and (H) show the results in males with regressions involving all measurements. Results related to the QRS-T angle expressions  $Area_{XYZ}$ ,  $Maximum_{XYZ}$ ,  $Integral_{XYZ}$ ,  $Area_{SVD}$ ,  $Maximum_{SVD}$ , and  $Integral_{SVD}$  are shown in red, blue, green, amber, violet, and cyan, respectively. See the text for the definitions of the angle expressions.





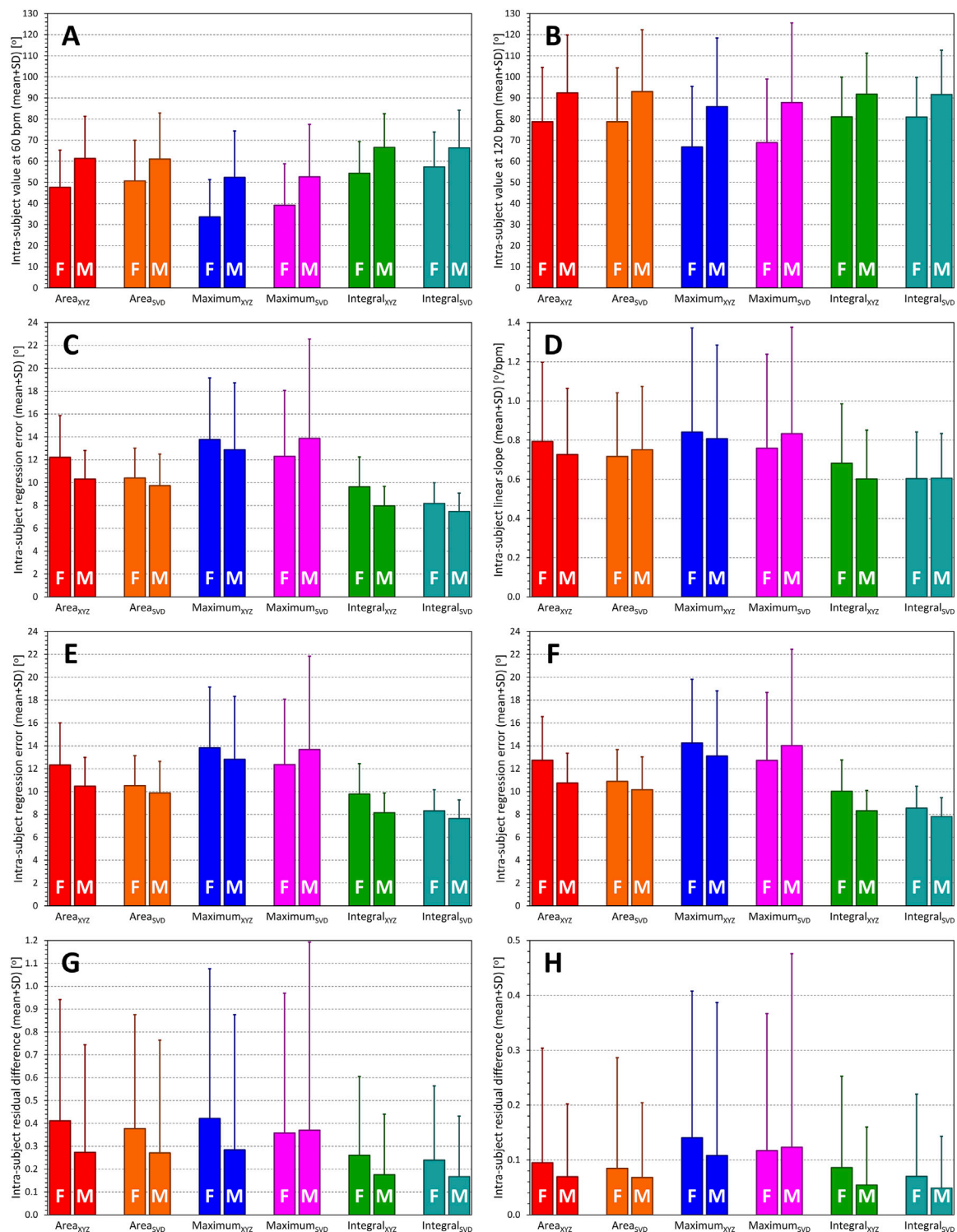
**FIGURE 10**

Population profiles of QRS-T angle relationship to underlying heart rate. Each panel of the figure corresponds to a different QRS-T angle expression and shows the summary of population distributions of intra-subject curvatures of second-degree polynomial regressions between QRS-T angle measurements and heart rate measured over the preceding 1 min. Bold red and blue lines show point-by-point median values of the regression curvatures in female and male subjects, respectively. The red and blue bands show the point-by-point inter-quartile ranges of the curvature values in females and males, respectively; the violet bands show the overlaps between the inter-quartile ranges between both sexes. The light red and light blue bands show the 10%–90% ranges of the curvature values in females and males, respectively; the light violet bands show the overlaps between the 10%–90% ranges between both sexes. The bands of inter-quartile ranges including their sex overlap are shown overlaying the 10%–90% bands. Panels (A–F) correspond to  $Area_{XYZ}$ ,  $Area_{SVD}$ ,  $Maximum_{XYZ}$ ,  $Maximum_{SVD}$ ,  $Integral_{XYZ}$ , and  $Integral_{SVD}$  QRS-T angle expressions, respectively.

measured at 60 bpm, that is the residuals were ordered  $Maximum_{XYZ} > Maximum_{SVD} > Area_{XYZ} > Area_{SVD} > Integral_{XYZ} > Integral_{SVD}$  with the individual step differences highly statistically significant ( $p < 0.00001$ ) apart from the difference between  $Maximum_{XYZ}$  and  $Maximum_{SVD}$  which was only marginal ( $13.31 \pm 5.64^\circ$  vs.  $13.11 \pm 7.45^\circ$ ) and not statistically different.

### 3.4.4 Curvatures of regression to heart rate

Panel D of Figure 11 shows the comparisons of intra-subject linear slopes between QRS-T angle expressions and the underlying heart rate. Sex differences are inconsistent but importantly, these slopes of the Integral expressions were significantly lower than those of the other expressions ( $p < 0.00001$ ).



**FIGURE 11**

Summaries of QRS-T angle/rate regression residuals. Statistical evaluation of the characteristics of different QRS-T angle expressions (see the labels of the horizontal axes in each panel). Panels (A,B) show the intra-subject QRS-T angle values measured at the heart rate of 60 and 120 bpm, respectively (as derived by the second-degree polynomial regressions between QRS-T angle measurements and heart rate measured over the preceding 1 min). Panel (C) shows intra-subject residuals of the second-degree polynomial regression between QRS-T angle measurements and heart rate expressed by intra-subject optimum hysteresis model. Panel (D) shows intra-subject slopes of linear regressions between QRS-T angle measurements and heart rate measured during the preceding 1 min. Panels (E,F) show the intra-subject residuals of the

(Continued)

**FIGURE 11**

second-degree (panel E) and linear (panel F) regressions between QRS-T angle measurements and heart rate measured over the preceding 1 min. Panels (G,H) show the decrease in regression residuals between second-degree and linear (panel G) and third-degree and second-degree (panel H) polynomial regression between QRS-T angle measurements and heart rate expressed by intra-subject optimum hysteresis model. In each panel, statistics of female (F) and male (M) sub-populations are shown separately. See the text for  $p$ -values of statistical comparisons.

For comparison with the intra-subject reproducibility as illustrated in panel C of Figure 11, panels E and F of the same Figure show regression residuals of second-degree (panel E) and first degree, i.e., linear (panel F) regression analysis relating the QRS-T angle expressions to heart rate calculated based on a simple average of preceding 1-min RR intervals. While there are numerically slight (albeit statistically significant) increases in the displayed values from panel C to panel E as well as from panel E to panel F, the patterns are practically the same, highlighting the absence of any clearly detectable hysteresis-type delays between the changes of heart rate and of QRS-T angles.

Panel G of Figure 11 shows  $\mathfrak{C}^{(a,2)} - \mathfrak{C}^{(a,1)}$  values, interpreted as the curvatures of the relationship between different QRS-T angle expressions and heart rate. As seen in the display, the QRS-T angle/heart-rate profiles were, on average, more curved in females compared to males ( $p$ -values between 0.01 and 0.001) for all angle expressions except of Maximum<sub>SVD</sub>.

Finally, panel H of Figure 11 shows  $\mathfrak{C}^{(a,3)} - \mathfrak{C}^{(a,2)}$  values. Similar trends as observed in panel G can be seen, although without statistical significances. The panel also shows that these residual differences were very tiny compared to those shown in panel G (note the difference in the vertical axes of both panels).

None of the characteristics summarised in Figure 11 appeared to be correlated with age.

### 3.4.5 Relationship to race, body mass index and lean body mass

The race categories others than African or White Caucasian origin were too infrequent for any meaningful analysis. Therefore, the race comparison was only possible between subjects of African and White Caucasian origin. Neither statistically significant differences nor trends towards borderline statistical differences were found.

The projections of the  $\Theta^{(a)}$  values at heart rate of 60 and 120 bpm were borderline correlated with BMI in females ( $p$ -values of the significance of the Pearson correlations ranged between 0.039 and 0.337) and were systematically significantly correlated with BMI in males ( $p$ -values of the significance of the Pearson correlations ranged between 0.012 and <0.0001). The corresponding scatter diagrams and linear regressions of the projected  $\Theta^{(a)}$  values are shown in Figure 12 (projections to the heart rate of 60 bpm) and Figure 13 (projections to the heart rate of 120 bpm). In females, the correlation coefficients relating the BMI to the two projections of different QRS-T angle expressions ranged

between  $-0.136$  and  $-0.062$ , and the projected  $\Theta^{(a)}$  values were decreasing by between 0.32 and 1.13 degrees per one unit of BMI. In males, the correlations ranged between  $-0.260$  and  $-0.155$  and the projected  $\Theta^{(a)}$  values were decreasing by between 1.27 and 2.48 degrees per one unit of BMI.

No such significant or borderline significant correlations were found when studying the relationship to LBM (investigations in females and males made separately).

## 4 Discussion

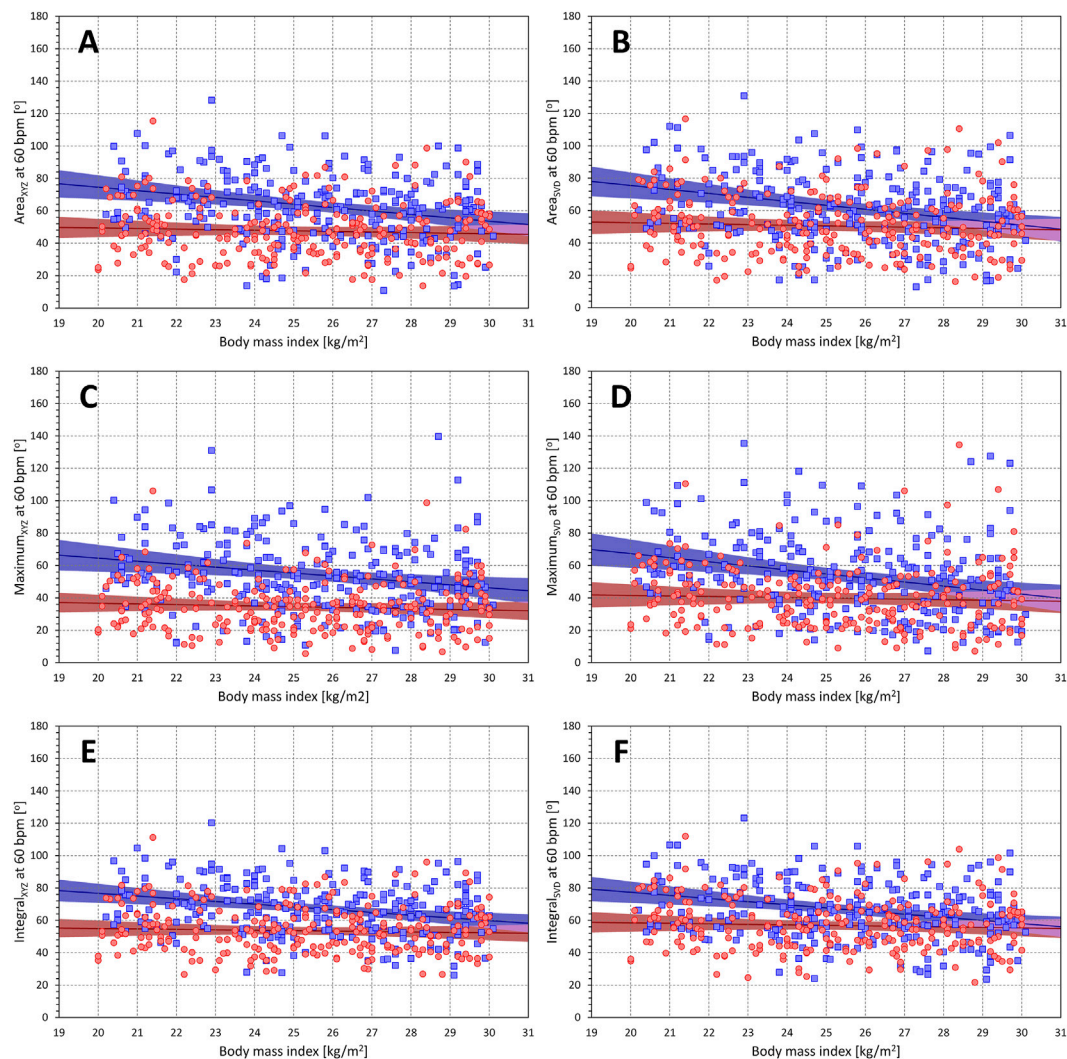
The study led to several observations of which three appeared of physiologic and practical importance.

First, despite dealing with very substantial datasets, we were unable to determine any clear hysteresis-type delay between heart rate changes and QRS-T angle changes. The most likely explanation of this observation is that QRS-T angle does not react to heart rate (e.g., in a similar way as the duration of the QT interval does) but that it is influenced directly by mechanisms and regulatory processes that simultaneously influence the heart rate. Second, we show important practical differences between the methods of the QRS-T angle measurement. Third, we confirm that under normal circumstances, female hearts show lesser differences between QRS and T wave loop orientations.

### 4.1 Cardiac autonomic and neurohumoral status

Our first observation likely suggests that the QRS-T angle is directly influenced by cardiac autonomic and neurohumoral status (Malik and Camm, 1990; Task Force, 1996; Puglisi et al., 2013; MacDonald et al., 2020) rather than driven by the frequency of ventricular depolarisations. The initial 30–40 s period of regression instability might be interpreted as a predominant sympathetic influence with less clear vagal modulations.

If this observation is confirmed in independent data, it would offer a substantial advance in the assessment of cardiac autonomic status at the level of ventricular myocardium, e.g., through the paraventricular ganglia (Zaglia and Mongillo, 2017), rather than at the level of sinus node. Measurement of cardiac autonomic responsiveness at the sinus nodal level has long been available by the heart rate variability (HRV) techniques (Task Force, 1996; Malik et al., 2019) and although new approaches are



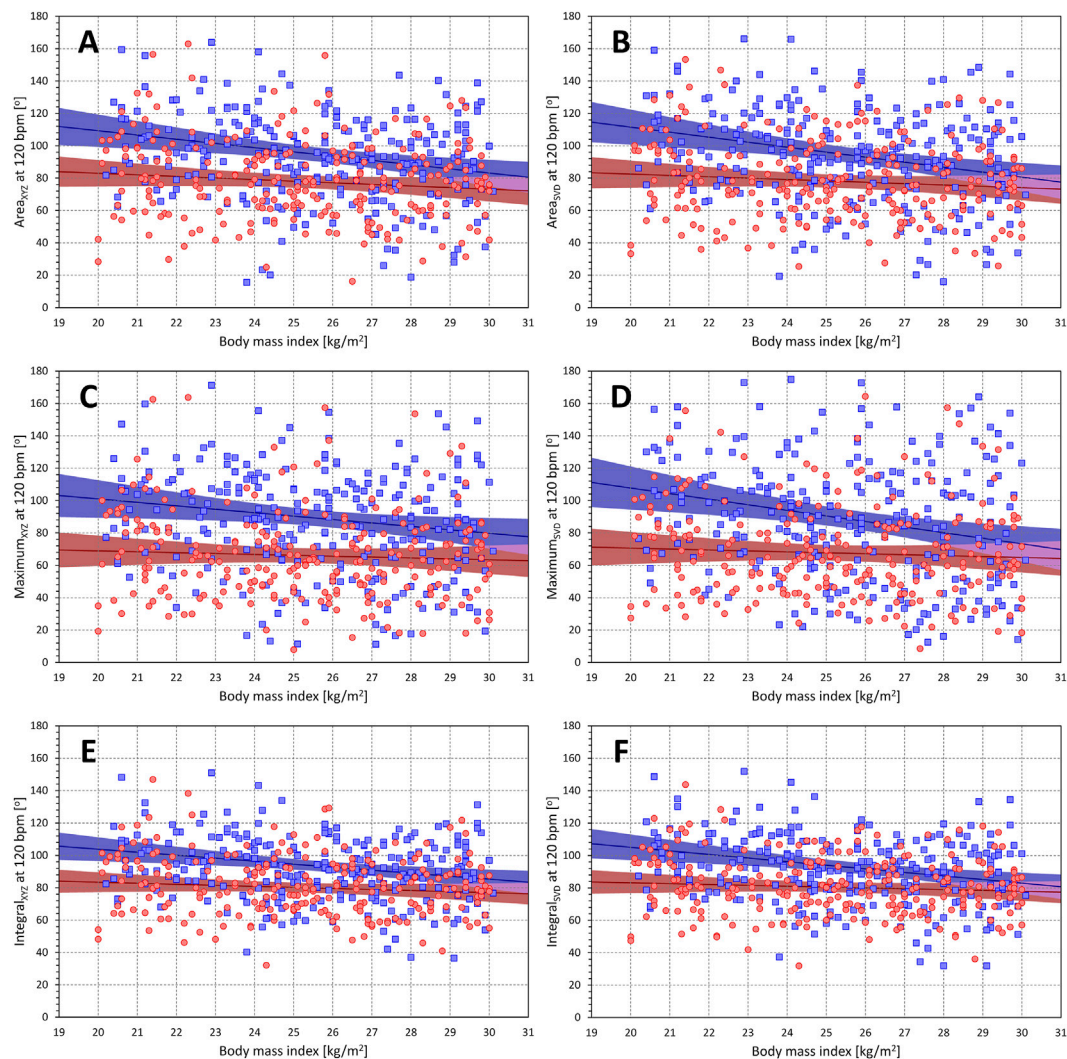
**FIGURE 12**

Relationship of QRS-T angle (projections to heart rate of 60 bpm) to body mass index. The different panels of the figure show scatter diagrams between body mass index and subject-specific projections of different QRS-T angle expressions to the heart rate of 60 bpm. Panels (A–F) show QRS-T angle data of Area<sub>XYZ</sub>, Area<sub>SVD</sub>, Maximum<sub>XYZ</sub>, Maximum<sub>SVD</sub>, Integral<sub>XYZ</sub>, and Integral<sub>SVD</sub>, respectively. In each panel, the red circles and blue squares show the data of female and male subjects, respectively. The red and blue bold lines are linear regression of QRS-T angle to body mass index in female and male sub-populations, respectively. The light red and light blue areas are the 95% confidence bands of the sex-specific regressions, the light violet areas are the overlaps between the regression confidence bands of both sexes.

still being developed, most with the aim of more accurately distinguishing sympathetic and parasympathetic influence (Valenza et al., 2018), all the heart-period-based techniques fail when sinus nodal periodicity is absent (e.g., in atrial fibrillation) or disturbed (e.g. by pacing, frequent ectopic activity, sinoatrial blocks, etc.). In addition to these situations, it would also be beneficial to accompany HRV-based assessment of cardiac autonomic status by independent technique, especially if the results could be obtained on beat-to-beat basis which is the case with QRS-T angle. This would offer advances to cardiac risk stratification as well as to early assessment systemic neuropathies

(May et al., 2018). Linking the QRS-T angle to cardiac sympathetic status would also help explaining its risk prediction properties.

The possibility that the assessment of QRS-T angle might serve this purpose is supported by some of the previous observations. The predictive value of QRS-T angle was reported additive to HRV-based risk stratification (Poulikakos et al., 2018) in a multivariate analysis of the follow-up cardiac events and mortality in a population of end-stage renal disease patients on haemodialysis. QRS-T angle was also reported predictive of mortality in atrial fibrillation patients who had



**FIGURE 13**

Relationship of QRS-T angle (projections to heart rate of 120 bpm) to body mass index. The different panels of the figure show scatter diagrams between body mass index and subject-specific projections of different QRS-T angle expressions to the heart rate of 120 bpm. The layout of the figure and the meaning of the individual symbols is the same as in Figure 12.

an automatic cardioverter-defibrillator implanted for primary prophylactic reasons (Hnatkova et al., 2022). At the same time, however, our observations of the absence of any clearly measurable time lag between heart rate changes and QRS-T angle changes, while in agreement with previous observations of rapid changes (Hnatkova et al., 2010), are somewhat at odds with the report by Kenttä et al. (2010) who described hysteresis-type differences between RR interval changes and QRS-T angle changes during exercise testing in a relatively small study of healthy volunteers undergoing exercise testing. Their report of hysteresis-type patterns is rather descriptive than quantitative and therefore not necessary in complete disagreement with our findings. They also used measurement techniques close to the

Maximum method which, as described subsequently, we consider to be the least suitable of the measurement possibilities and which is also influenced by postural and other changes of T wave morphology. The conjecture that the QRS-T angle might reflect cardiac sympathetic status might also be potentially challenged by the lack of the relationship to age that we were unable to document. However, this needs to be considered together with the appreciable spread of intra-subject values as seen in Figures 6, 7, and with the limited range of ages of investigated subjects.

Further studies are needed to verify our conjecture of the direct sympathetic influence on QRS-T angle. Among others, atrial pacing during electrophysiology studies with abrupt

changes of the stimulation rate [i.e., investigations similar to the seminal studies of QT/RR hysteresis (Franz et al., 1988; Lau et al., 1988)] would be helpful to elucidate whether the observed relationship of the QRS-T angle to heart rate is driven solely by the changes in the ventricular depolarisation frequency or whether inducement of autonomic changes is needed to influence the angle. Spectral analysis of beat-to-beat measurement of the QRS-T angle during distinctly different autonomic conditions (Pomeranz et al., 1985; Hnatkova et al., 2019) might also help in the assessment of our conjecture, especially if accompanied by the estimates of the coherence between the QRS-T angle and RR interval spectra.

## 4.2 Technology of QRS-T angle measurement

Our second observation relates to the differences between the methods used for QRS-T angle assessment. Not only were the results by the three methods significantly different but the reproducibility of the methods was also substantially and significantly distinct. Of the three algorithmic methods tested, the Maximum approach appeared least reliable. Regardless of which orthogonal lead system was used, the results of the Maximum method differed from the other two methods both in the terms of mean values but also in terms of the spread, i.e., standard deviations of the differences. The intra-beat and intra-median waveform differences between Maximum<sub>XYZ</sub> and Maximum<sub>SVD</sub> results were also significantly larger compared to the other two methods and, in terms of the relationship to the underlying heart rate, the Maximum method also appeared to show significantly lower intra-subject reproducibility which is well known to be of substantial practical importance for any risk assessment method (Malik et al., 1992). This poor performance of the Maximum method agrees with lesser risk prediction power reported in independent clinical data (Hnatkova et al., 2018).

The Area method is well known (van Oosterom, 2014) but, as far as we are aware, the Integral method has not been reported previously. At the same time, the philosophy of these two methods is similar. It is easy to see that in the Area method, the QRS complex and T wave loop 3-dimensional orientations are derived as averages of vectors moving around the QRS complex and T wave loops, with the contribution of each vector weighted by its magnitude. The Integral method takes this philosophy one step forward and computes the QRS-T angle and an average of all angles between all pairs of vectors moving around the QRS complex and T wave loops, with the contribution of each vector pairs weighted by the product of their magnitudes. It is therefore not surprising that these two methods were significantly closer to each other compared to their differences from the Maximum method. The significantly tighter

intra-subject reproducibility of the Integral method offers clear advantage over the Area method.

With both Area and Integral computation methods, we have also observed reduction of intra-subject regression residuals (i.e., increase in intra-subject reproducibility) when using SVD-based rather than conversion matrix-based XYZ orthogonal leads. This is not surprising since SVD leads to optimally constructed orthogonal leads for individual QRS-T patterns of each beat or each representative waveform. On the contrary, using the same conversion matrix for all ECG is likely to lead to some signal loss of the orthogonal components that might be of importance for the valid assessment of the angle.

Considering all this together, the study suggests that the Integral<sub>SVD</sub> is the optimum expression of the 3-dimensional QRS-T angle. It showed not only the tightest intra-subject reproducibility but also the closest correspondence between the averaged measurements of individual beats within a 10-s ECG segment and the measurement performed at the representative waveform of the same segment.

The six different QRS-T angle expressions that we have investigated are naturally not the only possibilities. In addition to simplistic measurements that can be performed “by hand” using standard 12-lead ECG images (Rautaharju et al., 2007), different conversion matrices might be used (Schreurs et al., 2010), and even simple quasi-orthogonal leads considered (Cortez et al., 2014). Combination of different approaches is also possible. The very first studies that showed the clinical usefulness of the QRS-T angle (Acar et al., 1999; Zabel et al., 2000) utilised the so-called TCRT measurement of the angle which was, in principle, a combination of the Integral (from the QRS side) and of the Maximum (from the T wave side) measurement algorithms.

## 4.3 Orthogonal lead systems

There is a principal difference between the orthogonal lead systems that we used for the conversion of the 12-lead ECGs into 3-dimensional representations in which the QRS-T spatial angles can be computed. The conversion to the XYZ leads was based on a published transformation matrix (Guldenring et al., 2012) that was originally derived from simultaneous recordings of standard 12-lead Mason-Likar recordings and Frank orthogonal electrocardiograms. In this system, the orientation of the XYZ axes is determined anatomically and the conversion thus approximates signals that would have been collected, for a given ECG, in the standard right → left, front → back, and head → foot directions. In this sense, the XYZ leads are anatomically orthogonal and, dependent on the position of the heart in the thorax, are related to the physical geometry of the organ. On the contrary, the S1, S2, and S3 leads derived from the SVD transformation do not have defined relationship to the physical geometry of the thorax or the organ but are made

algebraically orthogonal by the SVD-based matrix manipulation. SVD also produces a conversion matrix to approximate the original ECG leads from the S1, S2, and S3 signals (Acar and Köymen, 1999; Hnatkova et al., 2021) but these conversion matrices differ for different ECGs.

Because of the transformation differences, the orthogonal system of leads S1, S2, and S3 cannot be considered as a simple rotation of the XYZ axes. Both the SVD and the XYZ conversion matrix utilise the information from all original ECG leads (both transformations involve only the 8 algebraically independent leads I, II, V1, V2, . . . , V6). However, since both transformations act differently, the 3-dimensional morphology of the QRS complex and T wave loops are not identical (even if spatially rotated) and thus, the angles measured between these loops are not the same. Nevertheless, as shown in Figure 1, the differences between the orthogonal representations are not large when considering the Area and the Integral methods (the Maximum method is clearly affected by the differences in the morphology of the QRS complex and T wave loops in both representations). This is because the information in the signals of the different ECG leads differs only little from the projection of “ideal” 3-dimensional QRS and T wave loops. Indeed, it was shown (Acar et al., 1999; Hnatkova et al., 2021) that in normal ECGs, the power of the ECG signal beyond three orthogonal leads is in small single percentages. Hence, although the 3-dimensional morphology of the QRS complex and T wave loops is not the same in both representations, it is not diametrically different either.

As already discussed, the results of the study give some preference to the SVD-based conversion to the orthogonal leads. This likely because both the XYZ matrix conversion and the SVD-based orthogonal representation involve certain level of numerical imprecision. The XYZ matrix conversion applies the same transformation matrix to every ECG. Although the matrix was derived from a regression analysis involving more than 500 separate ECG signals (Guldenring et al., 2012), it cannot be assumed that the relationship between the 12-lead signals and true orthogonal Frank leads would be the same in every subject and every recording. The SVD-based conversion to S1, S2, and S3 leads omits the signals that project into the 4th to 8th algebraic orthogonal dimensions. The tight intra-subject reproducibility and beat-to-beat stability of the Integral<sub>SVD</sub> method might suggest that, on average, the errors of the 3-dimensional XYZ reconstruction might be marginally larger than the errors due to the omission of the higher algebraic components derived by SVD.

## 4.4 Sex differences

While differences between sexes have been described before (Smetana et al., 2004), the projected differences

between females and males (as seen in Figure 10) appeared, somewhat surprisingly, practically constant at different heart rates. The sex differences were also confirmed with all QRS-T angle expressions, although the extent of the differences appeared larger with the Maximum method and smaller with the Integral method. Both the sex and the influence by the different expressions were likely contributed by the sex differences in ECG morphology (Macfarlane, 2020). Despite the lower mean values of the QRS-T values in females, we also observed marginally larger spread of the values in the female sub-population and lower intra-subject reproducibility in females.

From a practical point of view, using the same normal value and/or the same dichotomy of the QRS-T angle for both females and males seems inappropriate for clinical risk assessment studies. Such studies either need to use different normality limits or, preferably, include sex of the patients as well as heart rates of the analysed QRS-T angle values in multivariable analyses. Our data also suggest that the Integral<sub>SVD</sub> expression might be the optimum way of assessing the QRS-T angle in both females and males. With this expression, sex differences of around 10° might be expected.

Similar to other electrocardiographic sex differences (Linde et al., 2018), it seems reasonable to hypothesise that the QRS-T angle is influenced by sex hormones. Further studies of the phenomenon, e.g., of the differences during menstrual cycle or of pubertal development (Andršová et al., 2019), might provide more detailed understanding. Wider QRS-T angles in males might also be contributed by wider spread of repolarisation across ventricular myocardium that is seen in longer Tpeak-Tend intervals in males (Andršová et al., 2020).

## 4.5 Relation to BMI

Although statistically significant in males and borderline significant in females, the decreases in the QRS-T angles with increasing BMI were only modest. Perhaps, this is partially because per protocol of the source clinical studies, only subjects with BMI between 20 and 30 were included. Still, two possible explanations for such a population trend might be proposed.

First, even a marginal increase in BMI might signify modest thickening in the chest fatty layers that likely act as electrical capacitors with slight effects on the difference between epicardial potentials and surface ECG signals. Investigations of ECGs recorded in substantially obese subjects might be helpful to investigate this phenomenon further. Second, even within this narrow range of the BMI values, their differences might be related to the different levels of athletic training and physical activity that was not

systematically assessed in the study subjects. Such differences might manifest by different levels of autonomic activity (Guo et al., 1999) as well as by moderate increases in ventricular mass (Augustine and Howard, 2018). Both factors might affect the values of the QRS-T angles.

When using the QRS-T angle assessment in future risk-prediction studies, relation to BMI might need to be considered, especially when dealing with very lean or markedly obese patients.

## 4.6 Limitations

Limitations of our study also need to be considered. Importantly, as our data were obtained in healthy volunteers participating at clinical pharmacology studies, we are not able to relate our QRS-T angle measurement to any cardiac risk and/or follow-up events. While the Maximum and Area method have previously been shown to be potent risk predictors, the Integral method still needs to be investigated in this way although the so-called TCRT method of the very first risk-studies of the angle is a combination of the integral approach applied to the QRS complex with the maximum approach applied to the T wave (Zabel et al., 2000; Zabel and Malik, 2001; Malik et al., 2004; Hnatkova et al., 2018). The restriction to healthy subjects also does not allow us to comment on whether the same or similar findings would be found in patient populations recorded under different clinical conditions (e.g., heart failure patients, survivors of acute myocardial infarction, heart transplant recipients, etc.). Nevertheless, assessment methods that are lesser reproducible in healthy volunteers are unlikely more stable in patients with ECG abnormalities. The SVD analysis of the source 12-lead ECGs would also allow to measure the QRS-T angle in more than three orthogonal directions. All three analytical methods might be applied in SVD-derived orthogonal systems of four or more dimensions although it is questionable whether the gradually decreasing amplitudes of the ECG components in the additional dimensions would change the 3-dimensional measurements noticeably. The age ranges of the study population were some 35 years wide and did not include any subjects over 60 years of age. Nevertheless, an obvious and statistically significant age relationship of heart rate variability, QT/RR hysteresis profiles, and of individually corrected QTc intervals was previously observed over similar or even narrower age ranges (Andršová et al., 2022; Toman et al., 2022). Finally, the data of the study were derived from ECG recordings obtained using Mason-Likar electrode positions. As far as we are aware, no direct comparison is available of QRS-T angles measured in simultaneously recorded ECGs using standard and Mason-Likar electrode positions. Nevertheless, when the same dichotomy limits were applied to the TCRT data derived from recordings of standard and Mason-Likar electrode configurations, similarly strong risk prediction was obtained

(Hnatkova et al., 2022). We therefore consider it likely that the method comparisons presented here would also apply to standard ECG recordings. The demographic measurements of body weight and height as well as the ages of the subjects were determined objectively. The study did not include any sex-transversal subjects and the sex differentiation was therefore also objective. On the contrary, the race classification was self-declarative and no genetic or other data are available to confirm the subjective race declarations objectively.

## 5 Conclusion

Despite these limitations, the study shows that it is plausible to speculate that spatial QRS-T angle measurement might allow direct assessment of cardiac autonomic responsiveness at the ventricular level. Further evaluations and confirmations of this hypothesis are needed but if confirmed, it would not only explain the risk-prediction properties of the angle but also allow employing the angle measurement in focused profiling of cardiovascular risk. The study also shows that the newly proposed Integral measurement of the angle offers increased measurement stability especially if the measurement is performed using the SVD-derived orthogonal leads optimised for each analysed ECG recording. Finally, the study confirms sex differences in physiologic QRS-T angle measurement with values in females lower than values in males irrespective of the heart rate at which the measurement is performed.

## Data availability statement

The raw data supporting the conclusions of this article will be made available by the authors, without undue reservation, but pending the approval by the sponsors of the source clinical studies.

## Ethics statement

The studies involving human participants were reviewed and approved by Parexel in Baltimore; California Clinical Trials in Glendale; and Spaulding in Milwaukee. The patients/participants provided their written informed consent to participate in this study.

## Author contributions

Study design IA, KH, and MM; Software development KH and MM; ECG interpretation GS, IA, KMH, MA OT, PB, PS, and TN; ECG measurement GS, IA, KMH, MA, OT, PB, PS, and TN;



Supervision of the measurements GS, TN, OT, and PS; Quality control of the measurements GS, MM, and TN; Statistics and figures KH and MM; Initial manuscript draft IA, KH, and MM; Final manuscript GS, IA, KH, KMH, MM, MA, OT, PB, PS, and TN; Approval of the submission GS, IA, KH, KMH, MM, MA, OT, PB, PS, and TN.

## Funding

Supported in part by the British Heart Foundation New Horizons Grant NH/16/2/32499, by Ministry of Health, Czech Republic, conceptual development of research organization (Grant FNBr/65269705), and by the Specific Research of Masaryk University MUNI/A/1450/2021.

## References

- Acar, B., and Köymen, H. (1999). SVD-based on-line exercise ECG signal orthogonalization. *IEEE Trans. Biomed. Eng.* 46, 311–321. doi:10.1109/10.748984
- Acar, B., Yi, G., Hnatkova, K., and Malik, M. (1999). Spatial, temporal and wavefront direction characteristics of 12-lead T-wave morphology. *Med. Biol. Eng. Comput.* 37, 574–584. doi:10.1007/BF02513351
- Andršová, I., Hnatkova, K., Helánová, K., Šišáková, M., Novotný, T., Kala, P., et al. (2019). Individually rate corrected QTc intervals in children and adolescents. *Front. Physiol.* 10, 994. doi:10.3389/fphys.2019.00994
- Andršová, I., Hnatkova, K., Šišáková, M., Toman, O., Smetana, P., Huster, K. M., et al. (2020). Heart rate dependency and inter-lead variability of the T peak - T end intervals. *Front. Physiol.* 11, 595815. doi:10.3389/fphys.2020.595815
- Andršová, I., Hnatkova, K., Šišáková, M., Toman, O., Smetana, P., Huster, K. M., et al. (2022). Sex and rate change differences in QT/RR hysteresis in healthy subjects. *Front. Physiol.* 12, 814542. doi:10.3389/fphys.2021.814542
- Augustine, D. X., and Howard, L. (2018). Left ventricular hypertrophy in athletes: Differentiating physiology from pathology. *Curr. Treat. Options Cardiovasc. Med.* 20, 96. doi:10.1007/s11936-018-0691-2
- Baumert, M., Lambert, G. W., Dawood, T., Lambert, E. A., Esler, M. D., McGrane, M., et al. (2008). QT interval variability and cardiac norepinephrine spillover in patients with depression and panic disorder. *Am. J. Physiol. Heart Circ. Physiol.* 295, H962–H968. doi:10.1152/ajpheart.00301.2008
- Berger, R. D., Kasper, E. K., Baughman, K. L., Marban, E., Calkins, H., and Tomaselli, G. F. (1997). Beat-to-beat QT interval variability: Novel evidence for repolarization lability in ischemic and nonischemic dilated cardiomyopathy. *Circulation* 96, 1557–1565. doi:10.1161/01.cir.96.5.1557
- Bland, J. M., and Altman, D. G. (1986). Statistical methods for assessing agreement between two methods of clinical measurement. *Lancet* 8476, 307–310. doi:10.1016/s0140-6736(86)90837-8
- Cardoso, C. R., Leite, N. C., and Salles, G. F. (2013). Factors associated with abnormal T-wave axis and increased QRS-T angle in type 2 diabetes. *Acta Diabetol.* 50, 919–925. doi:10.1007/s00592-013-0483-9
- Cortez, D., Schlegel, T. T., Ackerman, M. J., and Bos, J. M. (2017). ECG-derived spatial QRS-T angle is strongly associated with hypertrophic cardiomyopathy. *J. Electrocardiol.* 50, 195–202. doi:10.1016/j.jelectrocard.2016.10.001
- Cortez, D., Sharma, N., Cavanaugh, J., Tuozio, F., Derk, G., Lundberg, E., et al. (2017). Lower spatial QRS-T angle rules out sustained ventricular arrhythmias in children with hypertrophic cardiomyopathy. *Cardiol. Young* 27, 354–358. doi:10.1017/S1047951116000640
- Cortez, D., Sharma, N., Devers, C., Devers, E., and Schlegel, T. T. (2014). Visual transform applications for estimating the spatial QRS-T angle from the conventional 12-lead ECG: Kors is still most Frank. *J. Electrocardiol.* 47, 12–19. doi:10.1016/j.jelectrocard.2013.09.003
- Cortez, D. L., and Schlegel, T. T. (2010). When deriving the spatial QRS-T angle from the 12-lead electrocardiogram, which transform is more Frank:

## Conflict of interest

The authors declare that the research was conducted in the absence of any commercial or financial relationships that could be construed as a potential conflict of interest.

## Publisher's note

All claims expressed in this article are solely those of the authors and do not necessarily represent those of their affiliated organizations, or those of the publisher, the editors and the reviewers. Any product that may be evaluated in this article, or claim that may be made by its manufacturer, is not guaranteed or endorsed by the publisher.

Regression or inverse dower? *J. Electrocardiol.* 43, 302–309. doi:10.1016/j.jelectrocard.2010.03.010

de Bie, M. K., Koopman, M. G., Gaasbeek, A., Dekker, F. W., Maan, A. C., Swenne, C. A., et al. (2013). Incremental prognostic value of an abnormal baseline spatial QRS-T angle in chronic dialysis patients. *Europace* 15, 290–296. doi:10.1093/europace/eus306

de Torbal, A., Kors, J. A., van Herpen, G., Meij, S., Nelwan, S., Simoons, M. L., et al. (2004). The electrical T-axis and the spatial QRS-T angle are independent predictors of long-term mortality in patients admitted with acute ischemic chest pain. *Cardiology* 101, 199–207. doi:10.1159/000076697

Franz, M. R., Swerdlow, C. D., Liem, L. B., and Schaefer, J. (1988). Cycle length dependence of human action potential duration *in vivo*. Effects of single extrastimuli, sudden sustained rate acceleration and deceleration, and different steady-state frequencies. *J. Clin. Invest.* 82, 972–979. doi:10.1172/JCI113706

Geselowitz, D. B. (1983). The ventricular gradient revisited: Relation to the area under the action potential. *IEEE Trans. Biomed. Eng.* 30, 76–77. doi:10.1109/tbme.1983.325172

Gialafos, E., Konstantopoulou, P., Voulgari, C., Giavri, I., Panopoulos, S., Vaiopoulos, G., et al. (2012). Abnormal spatial QRS-T angle, a marker of ventricular repolarisation, predicts serious ventricular arrhythmia in systemic sclerosis. *Clin. Exp. Rheumatol.* 30, 327–331.

Gotsman, I., Keren, A., Hellman, Y., Banker, J., Lotan, C., and Zwas, D. R. (2013). Usefulness of electrocardiographic frontal QRS-T angle to predict increased morbidity and mortality in patients with chronic heart failure. *Am. J. Cardiol.* 111, 1452–1459. doi:10.1016/j.amjcard.2013.01.294

Guldenring, D., Finlay, D. D., Strauss, D. G., Galeotti, L., Nugent, C. D., Donnelly, M. P., et al. (2012). Transformation of the mason-likar 12-lead electrocardiogram to the Frank vectorcardiogram. *Annu. Int. Conf. IEEE Eng. Med. Biol. Soc.* 2012, 677–680. doi:10.1109/EMBC.2012.6346022

Guo, X. H., Yi, G., Batchvarov, V., Gallagher, M. M., and Malik, M. (1999). Effect of moderate physical exercise on noninvasive cardiac autonomic tests in healthy volunteers. *Int. J. Cardiol.* 69, 155–168. doi:10.1016/s0167-5273(99)00029-7

Hnatkova, K., Smetana, P., Toman, O., Bauer, A., Schmidt, G., and Malik, M. (2009). Systematic comparisons of electrocardiographic morphology increase the precision of QT interval measurement. *Pacing Clin. Electrophysiol.* 32, 119–130. doi:10.1111/j.1540-8159.2009.02185.x

Hnatkova, K., Andršová, I., Toman, O., Smetana, P., Huster, K. M., Šišáková, M., et al. (2021). Spatial distribution of physiologic 12-lead QRS complex. *Sci. Rep.* 11, 4289. doi:10.1038/s41598-021-83378-8

Hnatkova, K., Andršová, I., Novotný, T., Britton, A., Shipley, M., Vandenberg, B., et al. (2022). QRS micro-fragmentation as a mortality predictor. *Eur. Heart J.* 2022, ehac085. In press. doi:10.1093/eurheartj/ehac085

Hnatkova, K., Seegers, J., Barthel, P., Novotný, T., Smetana, P., Zabel, M., et al. (2018). Clinical value of different QRS-T angle expressions. *Europace* 20, 1352–1361. doi:10.1093/europace/eux246

- Hnatkova, K., Šišáková, M., Smetana, P., Toman, O., Huster, K. M., Novotný, T., et al. (2019). Sex differences in heart rate responses to postural provocations. *Int. J. Cardiol.* 297, 126–134. doi:10.1016/j.ijcard.2019.09.044
- Hnatkova, K., Toman, O., Sisakova, M., Novotny, T., and Malik, M. (2010). Dynamic properties of selected repolarization descriptors. *J. Electrocardiol.* 43, 588–594. doi:10.1016/j.jelectrocard.2010.06.003
- Hume, R. (1966). Prediction of lean body mass from height and weight. *J. Clin. Pathol.* 19, 389–391. doi:10.1136/jcp.19.4.389
- ICH Guideline (2001). Safety pharmacology studies for human pharmaceuticals 57A. *Fed. Regist.* 66, 36791–36792.
- Jensen, C. J., Lambers, M., Zadeh, B., Wambach, J. M., Nassenstein, K., and Witteman, J. C. (2003). Spatial QRS-T angle predicts cardiac death in a general population with cardiac magnetic resonance imaging. *Int. J. Med. Sci.* 18, 821–825. doi:10.7150/ijms.52415
- Kardys, I., Kors, J. A., van der Meer, I. M., Hofman, A., van der Kuip, D. A., and Witteman, J. C. (2003). Spatial QRS-T angle predicts cardiac death in a general population. *Eur. Heart J.* 24, 1357–1364. doi:10.1016/s0195-668x(03)00203-3
- Kenttä, T., Karsikas, M., Kiviniemi, A., Tulppo, M., Seppänen, T., and Huikuri, H. V. (2010). Dynamics and rate-dependence of the spatial angle between ventricular depolarization and repolarization wave fronts during exercise ECG. *Ann. Noninvasive Electrocardiol.* 15, 264–275. doi:10.1111/j.1542-474X.2010.00374.x
- Kors, J. A., Kardys, I., van der Meer, I. M., van Herpen, G., Hofman, A., van der Kuip, D. A., et al. (2003). Spatial QRS-T angle as a risk indicator of cardiac death in an elderly population. *J. Electrocardiol.* 36 (1), 113–114. doi:10.1016/j.jelectrocard.2003.09.033
- Lau, C. P., Freeman, A. R., Fleming, S. J., Malik, M., Camm, A. J., and Ward, D. E. (1988). Hysteresis of the ventricular paced QT interval in response to abrupt changes in pacing rate. *Cardiovasc. Res.* 22, 67–72. doi:10.1093/cvr/22.1.67
- Li, S. N., Zhang, X. L., Cai, G. L., Lin, R. W., Jiang, H., Chen, J. Z., et al. (2016). Prognostic significance of frontal QRS-T angle in patients with idiopathic dilated cardiomyopathy. *Chin. Med. J.* 129, 1904–1911. doi:10.4103/0366-6999.187844
- Linde, C., Bongiorni, M. G., Birgersdotter-Green, U., Curtis, A. B., Deisenhofer, I., Furokawa, T., et al. (2018). Sex differences in cardiac arrhythmia: A consensus document of the European heart rhythm association, endorsed by the heart rhythm society and asia pacific heart rhythm society. *Europace* 20, 1565. doi:10.1093/europace/euy067
- Lown, M. T., Munyombwe, T., Harrison, W., West, R. M., Hall, C. A., Morrell, C., et al. (2012). Association of frontal QRS-T angle-age risk score on admission electrocardiogram with mortality in patients admitted with an acute coronary syndrome. *Am. J. Cardiol.* 109, 307–313. doi:10.1016/j.amjcard.2011.09.014
- MacDonald, E. A., Rose, R. A., and Quinn, T. A. (2020). Neurohumoral control of sinoatrial node activity and heart rate: Insight from experimental models and findings from humans. *Front. Physiol.* 11, 170. doi:10.3389/fphys.2020.00170
- Macfarlane, P. W., and Lawrie, T. D. V. (1989). *Comprehensive electrocardiology*. New York, Oxford, Beijing, Frankfurt, São Paulo, Sydney, Tokyo, Toronto: Pergamon Press.
- Macfarlane, P. W. (2020). "Morphology of normal resting electrocardiogram," in *Sex and cardiac electrophysiology*. Editor M. Malik (London: Elsevier), 63–72.
- Malik, M., Andreas, J.-O., Hnatkova, K., Hoekendorff, J., Cawello, W., Middle, M., et al. (2008). Thorough QT/QTc Study in patients with advanced Parkinson's disease: Cardiac safety of rotigotine. *Clin. Pharmacol. Ther.* 84, 595–603. doi:10.1038/clpt.2008.143
- Malik, M. (2008). Beat-to-beat QT variability and cardiac autonomic regulation. *Am. J. Physiol. Heart Circ. Physiol.* 295, H923–H925. doi:10.1152/ajpheart.00709.2008
- Malik, M., and Camm, A. J. (1990). Heart rate variability. *Clin. Cardiol.* 13, 570–576. doi:10.1002/clc.4960130811
- Malik, M. (2004). Errors and misconceptions in ECG measurement used for the detection of drug induced QT interval prolongation. *J. Electrocardiol.* 37 (1), 25–33. doi:10.1016/j.jelectrocard.2004.08.005
- Malik, M., Hnatkova, K., and Batchvarov, V. N. (2004). Post infarction risk stratification using the 3-D angle between QRS complex and T-wave vectors. *J. Electrocardiol.* 37 (1), 201–208. doi:10.1016/j.jelectrocard.2004.08.058
- Malik, M., Hnatkova, K., Huikuri, H. V., Lombardi, F., Schmidt, G., and Zabel, M. (2019). CrossTalk proposal: Heart rate variability is a valid measure of cardiac autonomic responsiveness. *J. Physiol.* 597, 2595–2598. doi:10.1113/JP277500
- Malik, M., Hnatkova, K., Novotny, T., and Schmidt, G. (2008). Subject-specific profiles of QT/RR hysteresis. *Am. J. Physiol. Heart Circ. Physiol.* 295, H2356–H2363. doi:10.1152/ajpheart.00625.2008
- Malik, M., Johannesen, L., Hnatkova, K., and Stockbridge, N. (2016). Universal correction for QT/RR hysteresis. *Drug Saf.* 39, 577–588. doi:10.1007/s40264-016-0406-0
- Malik, M., Kulakowski, P., Poloniecki, J., Staunton, A., Odemuyiwa, O., Farrell, T., et al. (1992). Frequency versus time domain analysis of signal-averaged electrocardiograms. I. Reproducibility of the results. *J. Am. Coll. Cardiol.* 20, 127–134. doi:10.1016/0735-1097(92)90148-g
- Malik, M., van Gelderen, E. M., Lee, J. H., Kowalski, D. L., Yen, M., Goldwater, R., et al. (2012). Proarrhythmic safety of repeat doses of mirabegron in healthy subjects: A randomized, double-blind, placebo-and active-controlled thorough QT study. *Clin. Pharmacol. Ther.* 92, 696–706. doi:10.1038/clpt.2012.181
- May, O., Graversen, C. B., Johansen, M. Ø., and Arildsen, H. (2017). A large frontal QRS-T angle is a strong predictor of the long-term risk of myocardial infarction and all-cause mortality in the diabetic population. *J. Diabetes Complicat.* 31, 551–555. doi:10.1016/j.jdiacomp.2016.12.001
- May, O., Graversen, C. B., Johansen, M. Ø., and Arildsen, H. (2018). The prognostic value of the frontal QRS-T angle is comparable to cardiovascular autonomic neuropathy regarding long-term mortality in people with diabetes. A population based study. *Diabetes Res. Clin. Pract.* 142, 264–268. doi:10.1016/j.diabres.2018.05.018
- Oehler, A., Feldman, T., Henrikson, C. A., and Tereshchenko, L. G. (2014). QRS-T angle: A review. *Ann. Noninvasive Electrocardiol.* 19, 534–542. doi:10.1111/anec.12206
- Pomeranz, B., Macaulay, R. J. B., Caudill, M. A., Kutz, I., Adam, D., Gordon, D., et al. (1985). Assessment of autonomic function in humans by heart rate spectral analysis. *Am. J. Physiol.* 248, H151–H153. doi:10.1152/ajpheart.1985.248.1.H151
- Poulikakos, D., Hnatkova, K., Banerjee, D., and Malik, M. (2018). Association of QRS-T angle and heart rate variability with major cardiac events and mortality in hemodialysis patients. *Ann. Noninvasive Electrocardiol.* 23, e12570. doi:10.1111/anec.12570
- Puglisi, J. L., Negroni, J. A., Chen-Izu, Y., and Bers, D. M. (2013). The force-frequency relationship: Insights from mathematical modeling. *Adv. Physiol. Educ.* 37, 28–34. doi:10.1152/advan.00072.2011
- Rautaharju, P. M., Prineas, R. J., and Zhang, Z. M. (2007). A simple procedure for estimation of the spatial QRS/T angle from the standard 12-lead electrocardiogram. *J. Electrocardiol.* 40, 300–304. doi:10.1016/j.jelectrocard.2006.11.003
- Schreurs, C. A., Algra, A. M., Man, S. C., Cannegieter, S. C., van der Wall, E. E., Schalij, M. J., et al. (2010). The spatial QRS-T angle in the Frank vectorcardiogram: Accuracy of estimates derived from the 12-lead electrocardiogram. *J. Electrocardiol.* 43, 294–301. doi:10.1016/j.jelectrocard.2010.03.009
- Selvaraj, S., Ilkhanoff, L., Burke, M. A., Freed, B. H., Lang, R. M., Martinez, E. E., et al. (2014). Association of the frontal QRS-T angle with adverse cardiac remodeling, impaired left and right ventricular function, and worse outcomes in heart failure with preserved ejection fraction. *J. Am. Soc. Echocardiogr.* 27, 74–82. doi:10.1016/j.echo.2013.08.023
- Smetana, P., Batchvarov, V. N., Hnatkova, K., Camm, A. J., and Malik, M. (2004). Ventricular gradient and nonpolar repolarization components increase at higher heart rate. *Am. J. Physiol. Heart Circ. Physiol.* 286, H131–H136. doi:10.1152/ajpheart.00479.2003
- Sweda, R., Sabti, Z., Strebel, I., Kozhuharov, N., Wussler, D., Shrestha, S., et al. (2020). Diagnostic and prognostic values of the QRS-T angle in patients with suspected acute decompensated heart failure. *Esc. Heart Fail.* 7, 1817–1829. doi:10.1002/ehf2.12746
- Task Force, E. S. C/N. A. S. P. E. (1996). Heart rate variability: Standards of measurement, physiological interpretation and clinical use. *Circulation* 93, 1043–1065. doi:10.1161/01.cir.93.5.1043
- Toman, O., Hnatkova, K., Šišáková, M., Smetana, P., Huster, K. M., Barthel, P., et al. (2022). Short-term beat-to-beat QT variability appears influenced more strongly by recording quality than by beat-to-beat RR variability. *Front. Physiol.* 13, 863873. doi:10.3389/fphys.2022.863873
- Valenza, G., Citi, L., Saul, J. P., and Barbieri, R. (2018). Measures of sympathetic and parasympathetic autonomic outflow from heartbeats dynamics. *J. Appl. Physiol.* 125, 19–39. doi:10.1152/jappphysiol.00842.2017
- van Oosterom, A. (2014). The case of the QRS-T angles versus QRST integral maps. *J. Electrocardiol.* 47, 144–150. doi:10.1016/j.jelectrocard.2013.10.006
- Voulgari, C., Moysakakis, I., Perrea, D., Kyriaki, D., Katsilambros, N., and Tentolouris, N. (2010). The association between the spatial QRS-T angle with cardiac autonomic neuropathy in subjects with Type 2 diabetes mellitus. *Diabet. Med.* 27, 1420–1429. doi:10.1111/j.1464-5491.2010.03120.x
- Walsh, J. A., 3rd, Soliman, E. Z., Ilkhanoff, L., Ning, H., Liu, K., Nazarian, S., et al. (2013). Prognostic value of frontal QRS-T angle in patients without clinical evidence of cardiovascular disease (from the Multi-Ethnic Study of Atherosclerosis). *Am. J. Cardiol.* 112, 1880–1884. doi:10.1016/j.amjcard.2013.08.017
- Wilson, F. N., Macleod, A. G., Barker, P. S., and Johnston, F. D. (1934). The determination and the significance of the areas of the ventricular deflections of the electrocardiogram. *Am. Heart J.* 10, 46–61. doi:10.1016/s0002-8703(34)90303-3

- Xue, J. Q. (2009). Robust QT interval estimation - from algorithm to validation. *Ann. Noninvasive Electrocardiol.* 14 (1), S35–S41. doi:10.1111/j.1542-474X.2008.00264.x
- Yamazaki, T., Froelicher, V. F., Myers, J., Chun, S., and Wang, P. (2005). Spatial QRS-T angle predicts cardiac death in a clinical population. *Heart rhythm.* 2, 73–78. doi:10.1016/j.hrthm.2004.10.040
- Yana, K., Shichiku, H., Satoh, T., Mizuta, H., and Ono, T. (2006). An improved QT interval measurement based on singular value decomposition. *Conf. Proc. IEEE Eng. Med. Biol. Soc.* 2006, 3990–3993. doi:10.1109/IEMBS.2006.259959
- Zabel, M., Acar, B., Klingenhöben, T., Franz, M. R., Hohnloser, S. H., and Malik, M. (2000). Analysis of 12-lead T-wave morphology for risk stratification after myocardial infarction. *Circulation* 102, 1252–1257. doi:10.1161/01.cir.102.11.1252
- Zabel, M., and Malik, M. (2001). Predictive value of T-wave morphology variables and QT dispersion for postmyocardial infarction risk assessment. *J. Electrocardiol.* 34 (1), 27–35. doi:10.1054/jelc.2001.28822
- Zaglia, T., and Mongillo, M. (2017). Cardiac sympathetic innervation, from a different point of (re)view. *J. Physiol.* 595, 3919–3930. doi:10.1113/JP273120
- Zampa, H. B., Moreira, D. A., Ferreira Filho, C. A., Souza, C. R., Menezes, C. C., Hirata, H. S., et al. (2014). Value of the Qrs-T angle in predicting the induction of ventricular tachyarrhythmias in patients with Chagas disease. *Arq. Bras. Cardiol.* 103, 460–467. doi:10.5935/abc.20140162

### 3.7. Tpeak – Tend interval

Nejen popis vztahu QRS-T, ale i morfologie samotné vlny T jsou parametry, které skrývají velké množství informací potřebných k pochopení fyziologie či patofyziologie repolarizačního procesu. Ačkoli již víme mnohé o metodologii měření QT intervalu včetně korekčních metod k SF,<sup>82</sup> stále neumíme dobře uchopit a vysvětlit tzv. „nespecifické“ repolarizační změny vlny T. Tato definice je často používaná v rámci popisu EKG, ve kterém se vlna T nejeví jako normální, ale pro kterou současné znalosti neumožňují přesný popis její elektrofyziologické abnormality. Jelikož je známo, že prostorové a časové odchylky repolarizace mohou mít proarytmogenní potenciál, je snaha nalézt jednoduchou metodu vycházející z EKG křivky k popisu této repolarizační heterogenity. Nicméně navržené metody, jako například disperze QT intervalu poukazující na variabilitu QT intervalu v jednotlivých EKG svodech,<sup>83,84</sup> se ukázaly spíše jako nepřesnosti měření než jako odraz patofyziologických procesů.<sup>85,86</sup> Tsee et al. shrnuli práce, které zkoumaly jako užitečný parametr vystihující heterogenitu repolarizace a tedy vhodný stratifikační marker délku intervalu mezi vrcholem a koncem T vlny, tzv Tpe interval.<sup>87</sup> Studie vycházela z již dříve prokazaného pozorování na histologických vzorcích psí srdeční tkáně, kde tento interval popisoval rozdílnost šíření akčního potenciálu (AP) napříč různými vrstvami srdeční svaloviny. Tyto rozdílnosti pak byly vysvětleny odlišnou délkou trvání AP tzv. M buněk (hlubokých myokardiálních) oproti buňkám uložených v epi- a endokardiálních vrstvách.<sup>88,89</sup> Použitelnost tohoto parametru však při dalším zkoumání vykazuje zásadní nesrovnalosti. V lidské srdeční tkáni existence tzv. vrstvy M buněk doposud nebyla prokázána. Dalším faktem je, že tvar T vlny na povrchovém EKG je ovlivněn nejen transmurálním gradientem AP, ale také gradienty mezi jednotlivými oblastmi srdečních komor, atd. Navíc studie ARIC (Association Between QT-Interval Components and Sudden Cardiac Death) poukázala na to, že predikční hodnotu NSS má spíše prodloužení trvání T vlny ještě před jejím vrcholem než po něm.<sup>90</sup> Neméně důležité je, že neexistuje shoda na tom, který svod resp. která kombinace EKG svodů by měla být použita pro měření Tpe. Morfologie vlny T v jakémkoli svodu je totiž výsledkem projekce šíření smyčky T vlny.<sup>91</sup> Tak jako u předchozích popisovaných charakteristik (QT interval, úhel QRS-T, atd.) chybí data o přesnějším popisu reakce Tpe intervalu na změnu a následné ustálení SF.

S vědomím těchto nejasností jsme provedli analýzu Tpe intervalů v různých svodech EKG ve velkém souboru dlouhodobých 12-ti svodových EKG u zdravých jedinců. Jelikož tyto EKG záznamy obsahovaly dostatečné množství různých změn SF, byli jsme schopni zhodnotit také vztah těchto dvou parametrů v jednotlivých svodech. Analýzou zmíněných parametrů jsme provedli u 639 zdravých dobrovolníků (311 žen) průměrného věku  $33,8 \pm 9,4$ . Došli jsme k závěrům, že Tpe intervaly se v EKG svodech liší, což souvisí se složitou prostorovou orientací trojrozměrné smyčky T vlny. Dalším zjištěním bylo, že bez ohledu na výběr EKG svodu není Tpe interval systematicky závislý na srdeční frekvenci, tedy korekce k SF v klinické praxi není

potřebná. Ve srovnání s jinými repolarizačními parametry vykazuje Tpe interval značnou intraindividuální variabilitu. Závěrem lze tedy říci, že hodnocení Tpe intervalu v různých svodech nelze kombinovat. Naše studie také souhlasí s předchozími názory, že prediktivní hodnota intervalu Tpe je v současnosti poněkud sporná.<sup>92,93</sup>

**Andršová I**, Hnatkova K, Šišáková M, Toman O, Smetana P, Huster KM, Barthel P, Novotny T, Schmidt G, Malik M. Heart rate dependency and interlead variability of the T peak - T end intervals. *Front Physiol* 2020; 11:595815. doi: 10.3389/fphys.2020.595815

IF 4,566. Počet citací ve Web of Science 5

Původní práce - kvantitativní podíl uchazečky 35%: Návrh struktury publikace, elektrokardiologická měření, interpretace statistických výsledků, diskuze výsledků, text publikace.



# Heart Rate Dependency and Inter-Lead Variability of the T Peak – T End Intervals

Irena Andršová<sup>1</sup>, Katerina Hnatkova<sup>2</sup>, Martina Šišáková<sup>1</sup>, Ondřej Toman<sup>1</sup>, Peter Smetana<sup>3</sup>, Katharina M. Huster<sup>4</sup>, Petra Barthel<sup>4</sup>, Tomáš Novotný<sup>1</sup>, Georg Schmidt<sup>4</sup> and Marek Malik<sup>2\*</sup>

<sup>1</sup> Department of Internal Medicine and Cardiology, University Hospital Brno, Faculty of Medicine, Masaryk University, Brno, Czechia, <sup>2</sup> National Heart and Lung Institute, Imperial College London, London, United Kingdom, <sup>3</sup> Wilhelminenspital der Stadt Wien, Vienna, Austria, <sup>4</sup> Klinikum rechts der Isar, Technische Universität München, Munich, Germany

## OPEN ACCESS

### Edited by:

Ademuyiwa S. Aromolaran,  
Masonic Medical Research Institute  
(MMRI), United States

### Reviewed by:

John Pearce Morrow,  
Columbia University, United States  
Ioana Mozos,  
Victor Babes University of Medicine  
and Pharmacy, Romania

### \*Correspondence:

Marek Malik  
marek.malik@imperial.ac.uk

### Specialty section:

This article was submitted to  
Cardiac Electrophysiology,  
a section of the journal  
Frontiers in Physiology

**Received:** 17 August 2020

**Accepted:** 14 October 2020

**Published:** 15 December 2020

### Citation:

Andršová I, Hnatkova K, Šišáková M, Toman O, Smetana P, Huster KM, Barthel P, Novotný T, Schmidt G and Malik M (2020) Heart Rate Dependency and Inter-Lead Variability of the T Peak – T End Intervals. *Front. Physiol.* 11:595815. doi: 10.3389/fphys.2020.595815

The electrocardiographic (ECG) assessment of the T peak–T end (Tpe) intervals has been used in many clinical studies, but several related physiological aspects have not been reported. Specifically, the sources of the Tpe differences between different ECG leads have not been systematically researched, the relationship of Tpe duration to underlying heart rate has not been firmly established, and little is known about the mutual correspondence of Tpe intervals measured in different ECG leads. This study evaluated 796,620 10-s 12-lead ECGs obtained from long-term Holters recorded in 639 healthy subjects (311 female) aged  $33.8 \pm 9.4$  years. For each ECG, transformation to orthogonal XYZ lead was used to measure Tpe in the orthogonal vector magnitude (used as a reference for lead-to-lead comparisons) and to construct a three-dimensional T wave loop. The loop roundness was expressed by a ratio between its circumference and length. These ratios were significantly related to the standard deviation of Tpe durations in different ECG leads. At the underlying heart rate of 60 beats per minute, Tpe intervals were shorter in female than in male individuals ( $82.5 \pm 5.6$  vs  $90.0 \pm 6.5$  ms,  $p < 0.0001$ ). When studying linear slopes between Tpe intervals measured in different leads and the underlying heart rate, we found only minimal heart rate dependency, which was not systematic across the ECG leads and/or across the population. For any ECG lead, positive Tpe/RR slope was found in some subjects (e.g., 79 and 25% of subjects for V2 and V4 measurements, respectively) and a negative Tpe/RR slope in other subjects (e.g., 40 and 65% for V6 and V5, respectively). The steepest positive and negative Tpe/RR slopes were found for measurements in lead V2 and V4, respectively. In all leads, the Tpe/RR slope values were close to zero, indicating, on average, Tpe changes well below 2 ms for RR interval changes of 100 ms. On average, longest Tpe

intervals were measured in lead V<sub>2</sub>, the shortest in lead III. The study concludes that the T<sub>pe</sub> intervals measured in different leads cannot be combined. Irrespective of the measured ECG lead, the T<sub>pe</sub> interval is not systematically heart rate dependent, and no heart rate correction should be used in clinical T<sub>pe</sub> investigations.

**Keywords:** T wave peak, T wave spatial loop, heart rate dependency, ECG lead comparison, sex differences

## INTRODUCTION

Detailed classification and quantification of repolarization abnormalities is one of the unmet needs of contemporary electrocardiography. While noticeable progress has been made in the understanding of the electrocardiogram (ECG) manifestations of congenital channelopathies (Zareba, 2006) and of drug-induced ion channel abnormalities (Fenichel et al., 2004) as well as in the methodology of QT interval measurement and of its heart rate correction (Garnett et al., 2012), comprehension of the details of T wave changes due to ischemic heart disease and nonischemic cardiomyopathies remains elusive. The terms of “nonspecific T wave changes” is frequently used to describe ECGs in which the T wave does not appear normal but for which the present knowledge does not allow the details of the underlying electrophysiological abnormality to be identified.

Since both spatial and temporal repolarization abnormalities are linked to arrhythmogenesis, different methods have previously been proposed to quantify repolarization heterogeneity based on simple measurements applicable to standard 12-lead ECG recordings. Some three decades ago, the concept of the so-called QT dispersion (that is the lead-to-lead variability of QT interval duration) became very popular (Day et al., 1990; Okin et al., 2000) only to be quickly recognized as a mere expression of measurement inaccuracies and errors more frequent with abnormal rather than normal recordings (Kors and van Herpen, 1998; Kors et al., 1999; Rautaharju, 1999; Malik and Batchvarov, 2000) but without any physiological link to repolarization heterogeneity (Malik et al., 2000; Smetana et al., 2011).

More recently, previous observations made with canine wedge preparations (Sicouri and Antzelevitch, 1991; Antzelevitch, 2008) have been interpreted as a suggestion that the interval between the peak and the end of the T wave (T<sub>pe</sub> interval) can serve as a measure of repolarization heterogeneity. A recent, albeit somewhat limited meta-analysis concluded that the T<sub>pe</sub> interval is “a useful risk stratification tool in different diseases and in the general population” (Tse et al., 2017). Nevertheless, a closer inspection of the different studies published on the usefulness of the T<sub>pe</sub> interval shows substantial inconsistencies in the measurement (e.g., different ECG leads and/or different combinations of measurements across several leads) as well as in the use of both heart rate uncorrected and heart rate corrected T<sub>pe</sub> intervals (Malik et al., 2018). There is no consensus on whether the measurements in different ECG leads are mutually equivalent. In addition, systematic data are lacking on the heart rate dependency of T<sub>pe</sub> intervals measured in different leads.

To address these questions, we have analyzed T<sub>pe</sub> measurements in different ECG leads across a large collection of long-term 12-lead ECG recordings in healthy subjects. As

these recordings included episodes of different heart rates, we were also able to study not only the heart rate dependency of the T<sub>pe</sub> intervals but also the heart rate dependency of lead-to-lead differences.

## MATERIALS AND METHODS

### Investigated Population and Electrocardiographic Recordings

A collection of Holter recordings previously analyzed for a different purpose was used (Toman et al., 2020). Altogether, 639 healthy adult subjects participated at six clinical pharmacology studies. All subjects had a normal resting ECG and normal clinical investigation before enrollment as mandated in clinical pharmacology research (Guideline, 2001). Standard inclusion and exclusion criteria applicable to Phase I pharmacology studies applied (Guideline, 2001). Among others, negative tests of recreational substances and negative pregnancy tests for female subjects were required. All the source studies were ethically approved by the institutional ethics bodies (Focus in Neuss; Parexel in Baltimore, Bloemfontein, and Glendale; PPD in Austin; and Spaulding in Milwaukee). All subjects gave informed written consent to the participation according to the Helsinki declaration.

As previously described (Toman et al., 2020), each of the studies included repeated 12-lead day-time Holter recordings. In each participant, the recordings were made during multiple baseline days when the subjects were off any medication, did not smoke, and refrained from consuming caffeinated drinks. During these baseline days, study protocols included repeated positioning maneuvers aiming at capturing wide heart rates ranges in each participant. The Holter recordings used Mason–Likar electrode positions. The right arm (RA) and left arm (LA) electrodes were placed on top of or close to the acromioclavicular joints; the left foot (LF) and neutral electrodes were placed on top of or close to the iliac crests.

Clinical conduct of the baseline days did not include any aspects that would make the data incompatible or incomparable between the source studies. As the investigation described in this text utilized only drug-free baseline recordings, details of the clinical pharmacology investigations are not relevant.

### Electrocardiographic JT Interval Measurements

Using previously developed technology combining computerized signal processing with visual checks and manual corrections of the measurements (Malik et al., 2008a, 2012; Toman et al., 2020), multiple 10-s segments were extracted from each of the Holter

recordings aiming at the inclusion of segments with different underlying heart rates. For each extracted segment, a 5-min history of preceding RR intervals was obtained.

Each extracted 10-s ECG segment was filtered to reduce noise pollution and to eliminate baseline wander (Malik et al., 2008a, 2012). Subsequently, a representative median beat was constructed (Xue, 2009), sampled at 1,000 Hz. In this representative beat, all 12 leads were superimposed on the same isoelectric axis, and QRS offset and T offset points were identified using algorithms that were previously developed and described (Malik et al., 2008a, 2012). The quality control of the measurement of these points included visual verification and manual correction of computerized ECG processing by at least two independently working cardiologists with subsequent independent reconciliation in case of measurement disagreement. Pattern matching algorithms (Hnatkova et al., 2009) were also applied. This ensured that comparable morphologies of QRS offset and T offset were measured systematically. The visual verification and manual correction of the T offset measurements also distinguished between T and U waves. The shallow U waves frequently seen in precordial leads of normal ECGs were excluded from subsequent T wave analyses.

## T Wave Loop Construction

Using the previously published conversion matrix suitable for the Mason–Likar electrode positions (Guldenring et al., 2012), the voltage values of the representative beats of each ECG sample were used to derive orthogonal XYZ leads. From these, vector magnitude lead  $VM$  was constructed using the standard formula of  $VM(t) = (X_t^2 + Y_t^2 + Z_t^2)^{1/2}$ , where  $W_t$  is the voltage of the orthogonal lead  $W$  at the time instant  $t$ .

The orthogonal XYZ leads were also used to construct the T wave loop as a three-dimensional curvature starting and ending at the (0, 0, 0) point and passing sequentially through the points  $[X(t), Y(t), Z(t)]$  for  $t$  ranging from  $J$  (the QRS offset) to  $T$  (the T wave offset). The length of the T wave loop was calculated as a simple sample-to-sample sum of the distances between neighboring points  $\mathcal{L} = VM(J) + \sum_{t=J}^{T-1} [(X_{t+1} - X_t)^2 + (Y_{t+1} - Y_t)^2 + (Z_{t+1} - Z_t)^2]^{1/2} + VM(T)$ . [Note that the formula ensures that the loop starts and end at the (0, 0, 0) point.] To express the roundness of the loop, the T loop ratio was calculated as  $\mathcal{L}/[2 \times \max_{J \leq t \leq T} VM(t)]$ .

This ratio is 1 for T wave loops that are strictly unidimensional and collapsed into a line, while an increasing value of the ratio signifies loops of increasing roundness (or of even more complex morphology).

## T Peak Measurements

In each ECG lead, in the orthogonal vector magnitude as well as in the derived nonstandard ECG dipoles (see the details described further), the same previously published algorithm (Johannesen et al., 2016) was used to detect the peak of the T wave within the interval between the QRS offset and T wave offset.

Objective noise assessment algorithms (Batchvarov et al., 2002) were used to eliminate ECG leads in which the T wave

morphology was too noise polluted to allow the T peak detection with sufficient confidence. To exclude leads with flat T waves in which the result of T peak detection algorithms might have been questioned, measurements were accepted only in those leads in which the voltage of the detected T peak differed from the line connecting the QRS offset and T wave offset by at least 100  $\mu V$  and in which the T peak detection was stable. When dual peaks of opposite orientation were detected in biphasic T waves, the peak with the highest absolute voltage was used. Nevertheless, biphasic T waves were seen almost exclusively only in the derived precordial bipoles (as explained further in this text).

In each lead, the Tpe interval was measured as the difference between the T peak and the T wave offset (common to all leads of the same ECG sample).

## Underlying Heart Rate

To study the relationship of the Tpe durations to the underlying heart rate, hysteresis-corrected RR interval values were used. Based on existing experience, previously published exponential decay hysteresis model (Malik et al., 2008b) was used based on the following considerations: For a Tpe interval measurement, the sequence of preceding RR intervals  $\{RR_i\}_{i=0}^N$  ( $RR_0$  closest to the Tpe measurement) is considered. The RR interval representing the heart rate underlying the Tpe measurement is then calculated as

$$RR' = \sum_{i=0}^N \omega_i RR_i$$

where for each  $j = 0, \dots, N$ ,

$$\omega_j = \frac{\left(1 - e^{-\lambda \frac{\sum_{i=0}^j RR_i}{\sum_{i=0}^N RR_i}}\right)}{(1 - e^{-\lambda})}$$

The coefficient  $\lambda$  characterizes the profile of the Tpe/RR hysteresis, i.e., the speed with which Tpe interval adapts to changing heart rate. While subject-specific optimization of the coefficient  $\lambda$  is possible, the lead-to-lead comparison would become problematic if such a subject-specific optimization was performed since it would need to be applied to different ECG leads separately. We have therefore used a common value of  $\lambda = 7.4622$ , which corresponds to the 95% adaptation after a 2-min period (Malik et al., 2016). Note also that the majority of the extracted ECG segments were preceded by a stable heart rate; when all preceding RR intervals are of practically the same duration, the hysteresis-corrected  $RR'$  value corresponds to the common RR duration.

## Data Investigations

To analyze the relationship of the Tpe intervals measured in different ECG leads and to investigate their heart rate relationship, we utilized the available data in three separate facets of the study.



## Spread of the Lead-to-Lead Tpe Values

The principles of electrocardiography suggest that any lead-to-lead differences are caused, especially in normal physiologic situations, by different vector projections of the same spatial distribution of electrophysiological processes rather than by associations of different ECG leads with different myocardial regions. When applied to the lead-to-lead differences of the Tpe intervals, this principle suggests that Tpe spread across leads increases with the spatial spread of the T wave loop.

To test this suggestion, we investigated the relationship between the standard deviation (SD) of Tpe durations in different leads and the T loop ratio. Specifically, for each study subject, the mean value of the T loop ratio of all extracted ECG segments was related to the mean of SD of Tpe durations in different ECG leads. This use of subject-specific average avoided the problem of influencing the relationships by multiple data from the same subject that could not be considered as mutually independent.

For the purpose of this investigation, six different sets of ECG leads were considered (**Figure 1**):

- All the 12 standard leads of the ECG,
- Six bipolar leads between the V1 to V6 electrodes and the RA electrode,
- Six bipolar leads between the V1 to V6 electrodes and the LA electrode,
- Six bipolar leads between the V1 to V6 electrodes and the LF electrode,
- Bipolar leads V1–V2, V1–V3, . . . , V1–V6, and V–V3, V2–V4, . . . , V2–V6, forming a group of nine “wide” precordial dipoles, and
- Bipolar leads V3–V4, V3–V5, V3–V6, V4–V5, V5–V6, and V5–V6, forming a group of six “narrow” precordial dipoles.

The nonstandard bipolar leads were derived from the standard 12 leads using trivial algebraic equations.

## Heart Rate Dependency of the Tpe Values

Because of the known subject-specific relationship between the QT intervals and the underlying heart rate, the heart rate dependency of the Tpe intervals measured in different leads was investigated in each study subject separately. That is, for each subject, linear regressions between Tpe intervals measured in different standard ECG leads and the underlying heart rate were calculated. The slopes of these intrasubject regressions were statistically summarized for each standard ECG lead.

The intrasubject linear regressions also allowed to project the Tpe intervals in the given subject to heart rates of 60 and 120 beats per minute (bpm). These projections were repeated for the different leads and statistically summarized to express the influence of the heart rate changes on the Tpe durations.

The residuals of the linear regressions also allowed us to study intrasubject reproducibility of Tpe interval measurements. Since the residuals are influenced by the magnitude of the dependent variable, we used the relative residuals that we defined, in each study subject, as the proportion between the Tpe/RR residual and the projected value of Tpe at the heart rate of 60 bpm.

The same study of linear regressions was also repeated for the Tpe interval measured in the orthogonal XYZ vector magnitude and for the interval between the QRS offset and T wave offset (the JT interval), which is lead independent.

To investigate whether the heart rate influence on the Tpe intervals measured in different leads is physiologically driven by similar processes as those underlying the heart rate influence on the JT interval, the 60–120-bpm changes in the Tpe intervals were related to the 60–120-bpm changes in the JT intervals in the corresponding subjects.

## Reconstruction of Orthogonal Vector Magnitude Tpe From Standard ECG Leads

Consistent with previous studies (Johannesen et al., 2014; Hnatkova et al., 2019a), it seems reasonable to propose that the peak of the T wave detected on the vector magnitude of orthogonal XYZ leads represents the instance of maximum repolarization changes across ventricular myocardium. This point might therefore be possibly proposed for the gold standard expression of the Tpe interval.

Consequently, we have investigated whether the Tpe interval measured in the vector magnitude of orthogonal XYZ leads can be reasonably approximated by an algebraic combination of Tpe intervals measured in standard ECG leads. For this purpose, we selected those standard ECG leads in which the T peak was measurable in a majority of the analyzed ECG segments. Multivariable regression analysis was subsequently performed to calculate linear regression coefficients that would allow to estimate the Tpe interval of the XYZ vector magnitude from the measurements in standard leads. Two calculations of this multivariable regression analysis were performed that did and did not include underlying heart rates and a constant intercept value.

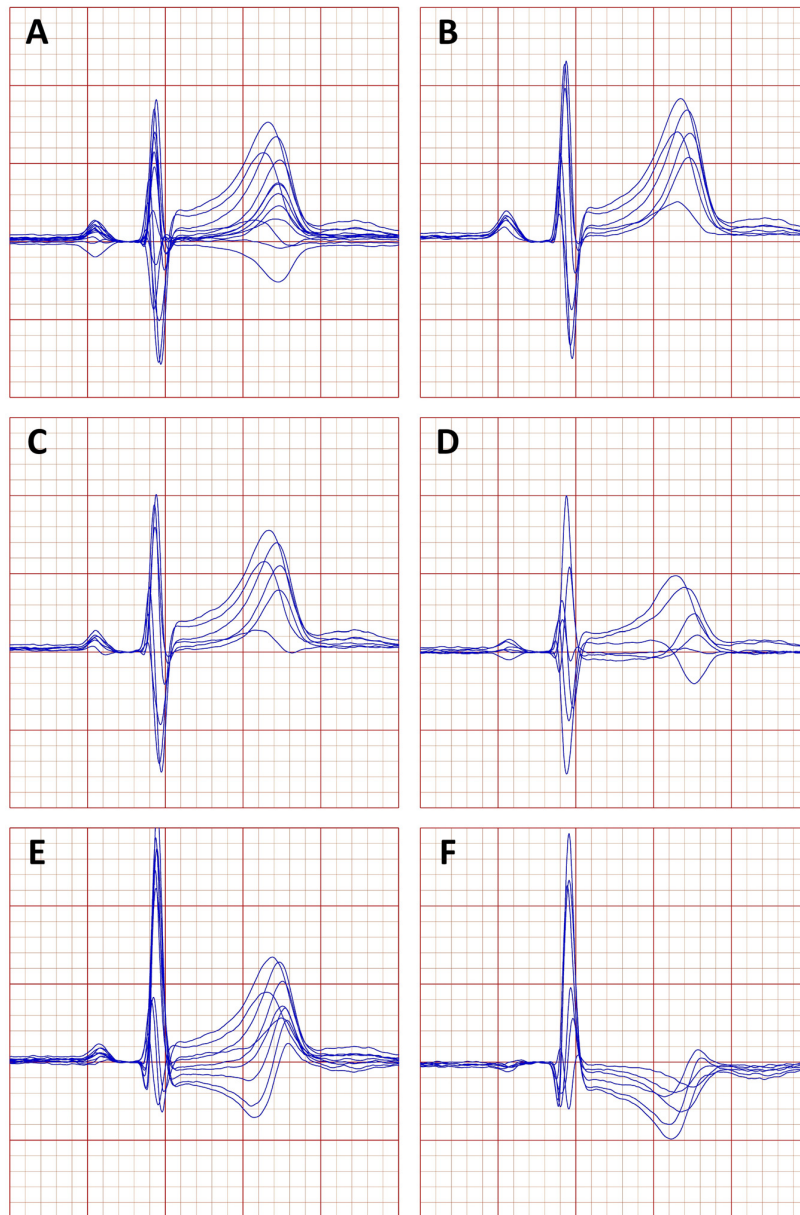
The multivariable regression coefficients were obtained based on the analysis of all ECG samples in which the Tpe interval was measurable in all selected standard ECG leads. Subsequently, the actual precision of the Tpe of XYZ vector magnitude reconstruction was assessed in each study subject separately by obtaining the mean and the SD of the differences between actual measurements and the corresponding reconstructed values.

## Sex Differences

Because of the known sex differences between QT intervals and QT/RR relationships, all the statistical summaries of the study were performed separately for the subgroups of female and male participants.

## Statistics and Data Presentation

Data are presented as means  $\pm$  SD. Differences between female and male subjects were evaluated using two-sample, two-tail *t*-test assuming different variances of compared samples. Intrasubject comparisons (e.g., comparisons between Tpe intervals projected to heart rates of 60 and 120 bpm) were evaluated using two-tail paired *t*-test. *p*-Values above 0.05 were considered statistically nonsignificant (NS). Because of the interdependency of evaluated data, no correction for multiplicity of testing was performed, and all statistical tests



**FIGURE 1** | Example of a representative beatform of an electrocardiogram (ECG) obtained in a 33-year-old male. **(A)** Standard leads of the 12 lead ECG, **(B)** the bipolar leads between the precordial electrodes and the right arm electrode, **(C)** the bipolar leads between the precordial electrodes and the left arm electrode, **(D)** the bipolar leads between the precordial electrodes and the left foot electrode, **(E)** the “wide” precordial dipoles, and **(F)** the “narrow” precordial electrodes (see the text for explanation of the precordial dipoles).

performed are presented. Statistical evaluation used the IBM SPSS package version 25.

## RESULTS

### Population and Electrocardiographic Measurements

The source clinical pharmacology studies investigated 639 subjects (311 female). The ages of sex-defined subgroups

were practically identical (female,  $33.8 \pm 10.1$  years; male,  $33.9 \pm 8.7$  years, NS).

The study involved measurement of 796,620 ECG samples of which 385,135 and 411,485 were obtained in female and male subjects, respectively. The subject-specific counts of ECG samples were practically the same in female and male subjects ( $1,238 \pm 253$  vs  $1,262 \pm 240$ , respectively).

Both the intrasubject maximum and minimum heart rates (hysteresis corrected) of the ECG segments in female subjects ( $115.0 \pm 13.0$  and  $53.7 \pm 6.3$  bpm, respectively) were

significantly faster than those in male subjects ( $109.0 \pm 13.1$  and  $50.3 \pm 5.5$  bpm, respectively, both  $p < 0.0001$  for comparison with female subjects). The intrasubject ranges between minimum and maximum heart rates were also wider in female compared to male subjects ( $61.3 \pm 12.6$  vs  $58.7 \pm 12.6$ ,  $p = 0.009$ ). Nevertheless, these intrasubject ranges were sufficiently wide so that regression projections to heart rates of 60 and 120 bpm involved, where necessary, stable extrapolations.

While the Tpe interval of XYZ vector magnitude was measurable in all selected segments (since the selection excluded noise polluted segments), **Figure 2** shows that the measurability of the T peak differed substantially in different leads. Failed localization of T peak due to flat and/or too widely spread T waves was frequent in leads III, aVL, and V1 in which the T peak was measurable only in 48.8, 17.4, and 30.8% of ECG segments in female subjects and in 57.8, 28.5, and 46.4% of ECG segments in male subjects, respectively. (While it was possible to identify T wave peaks in these leads, the number of the accepted measurements was reduced by failed consistency and repeatability checks.) In leads II, aVR, V2, V3, V4, V5, and V6, T peak was measurable in more than 90% of all ECG segments, and as seen in **Figure 2**, T peak was more frequently measurable in male compared to female subjects. As also seen in **Figure 2**, the proportions of T peak measurability observed in the complete data were replicated also in the data of individual study subjects.

## Spread of the Lead-to-Lead Tpe Values

**Figure 3** shows the scatter diagrams between the intrasubject means of T wave loop ratio and the corresponding intrasubject means of the ECG-specific SDs of the Tpe intervals in the standard 12 leads (**Figure 3A**), in bipolar leads between precordial electrodes and the RA, LA, and LF electrodes (**Figures 3B–D**, respectively), in the wide precordial bipolar leads (**Figure 3E**), and in the narrow precordial bipolar leads (**Figure 3F**). Corresponding cumulative frequencies of the intrasubject means of the ECG-specific SDs of the Tpe intervals are shown in **Figure 4**.

As seen in **Figure 3**, all sets of the ECG leads, except for the narrow precordial bipoles, showed statistically significant positive relationship with the T wave loop ratio. The result for the set of narrow precordial bipolar leads was the opposite with statistically significant negative relationship. This might possibly be surprising but is likely caused by restricted projections of the T wave loop combined with isoelectric projections of narrow loops.

**Figure 3** also shows that the relationship to the T wave loop ratio was steeper in male compared to female subjects (again with the exception of narrow precordial bipoles). **Figure 4** shows that the interlead spread of Tpe intervals (i.e., of the T peak positions) among the standard ECG leads as well as among the precordial bipoles was more compact in female compared to male subjects. While the SDs of Tpe intervals in the precordial–LF dipoles were similar between female and male subjects, in other lead groups, the

spread of the Tpe intervals was larger in male compared to female subjects.

## Heart Rate Dependency of the Tpe Values

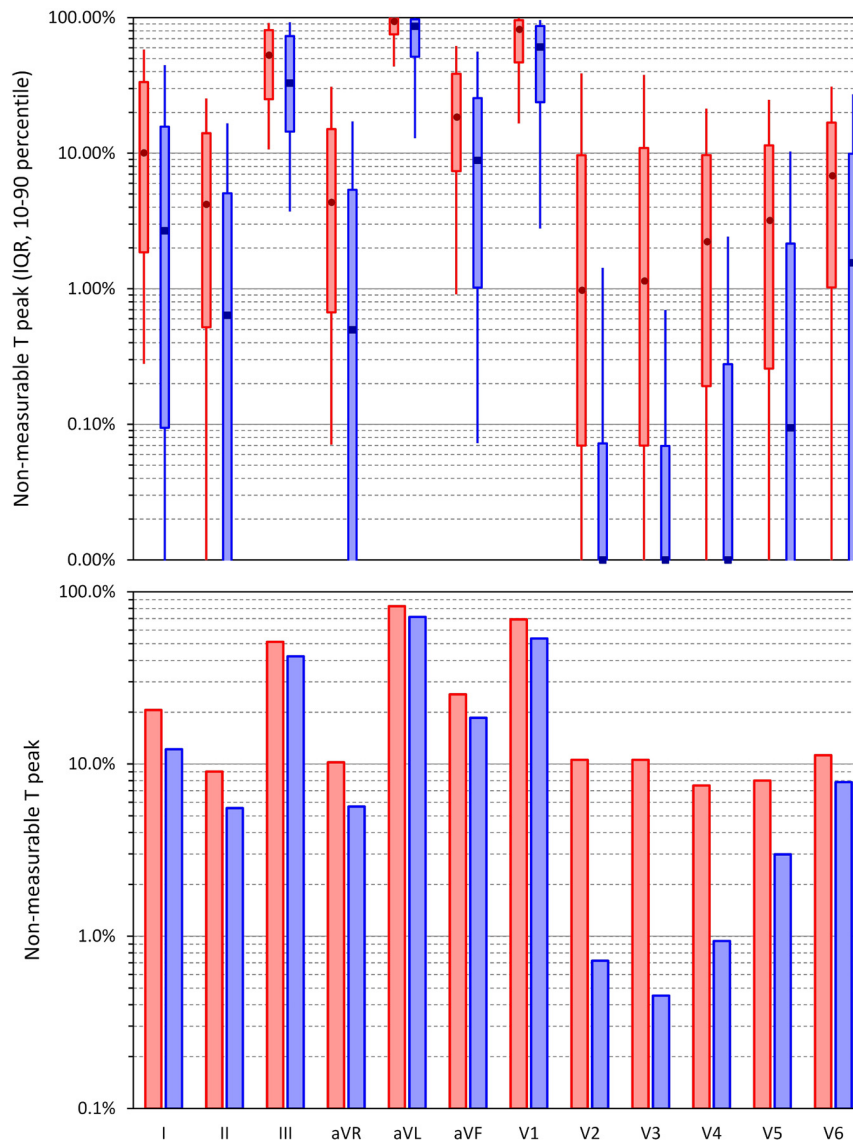
**Figure 5A** shows cumulative distributions of the subject-specific linear JT/RR slopes. These were steeper in female compared to male subjects ( $0.175 \pm 0.028$  vs  $0.145 \pm 0.023$ ,  $p < 0.0001$ ).

The other panels of **Figure 5** show corresponding cumulative distributions of the subject-specific Tpe/RR slopes (**Figure 5B** corresponds to the Tpe measured in XYZ vector magnitude, the other panels to the Tpe measured in different standard ECG leads). In different leads, these slopes fluctuated around zero. On average, the steepest positive Tpe/RR slopes were found in lead V2 ( $0.0171 \pm 0.0266$  and  $0.0176 \pm 0.0203$  in female and male subjects, respectively), the steepest negative Tpe/RR slopes were found in lead V4 ( $-0.0124 \pm 0.0245$  and  $-0.0174 \pm 0.0205$  in female and male subjects, respectively). Note that the absolute values of even these steepest slopes were approximately only 10% of the JT/RR slopes. In leads III, aVL, V1, V2, and V3, the Tpe/RR slopes were not statistically different between female and male subjects; in all other standard leads, the slope values were higher in female compared to male subjects. In lead V6, the slopes were, on average, positive in female subjects while negative in male subjects ( $0.0052 \pm 0.0128$  vs  $-0.0040 \pm 0.0163$ ,  $p = 0.0005$ ).

The effects of the heart rate influence are summarized in **Figure 6**. While the heart rate change from 60 to 120 bpm led to JT interval shortening by an average of  $87.4 \pm 14.1$  ms in female and  $72.7 \pm 11.5$  ms in male subjects ( $p < 0.00001$ , **Figure 6A**), Tpe interval in the XYZ vector magnitude prolonged, on average, by  $1.77 \pm 11.19$  ms in female subjects and  $3.86 \pm 9.04$  ms in male subjects ( $p = 0.01$ ). In the standard ECG leads, the averaged changes in the Tpe interval again fluctuated around zero. Consistent with the maximum and minimum Tpe/RR slopes, largest averaged shortening of the Tpe interval was found in lead V2 (by  $8.55 \pm 13.32$  and  $8.79 \pm 10.17$  ms in female and male subjects, respectively,  $p = \text{NS}$  for sex comparison), while the largest averaged prolongation was found in lead V4 (by  $6.20 \pm 12.25$  and  $8.71 \pm 10.25$  ms in female and male subjects, respectively,  $p = 0.006$  for sex comparison).

**Figure 6** also shows that while JT interval was significantly longer in female compared to male subjects ( $322.3 \pm 14.0$  vs  $297.0 \pm 12.6$  ms at 60 bpm, and  $234.8 \pm 11.9$  vs  $224.3 \pm 10.5$  ms at 120 bpm,  $p < 0.00001$  for both), the opposite was the case for the Tpe interval measured at the XYZ vector magnitude where, on average, the Tpe interval was shorter in female than in male subjects ( $82.5 \pm 5.6$  vs  $90.0 \pm 6.5$  ms at 60 bpm, and  $84.3 \pm 10.3$  vs  $93.9 \pm 10.0$  ms at 120 bpm,  $p < 0.00001$  for both). In no other lead was the average Tpe interval at either 60 or 120 bpm longer in female than in male subjects, although in some leads (e.g., V2 and V6), the difference between sexes was not statistically significant.

Finally, **Figure 7A** shows that the intrasubject Tpe interval projections at 60 bpm (measured in the XYZ vector magnitude) were unrelated to the corresponding projections of JT intervals. The same was true for Tpe intervals measured in other ECG leads as well as for the 120-bpm projections (results not shown).



**FIGURE 2 |** Incidence of non-measurable peaks of the T wave in standard electrocardiogram (ECG) leads. The bottom panel shows the incidence among all ECG segments investigated in the study pooled together; the top panel shows the summary of the incidence in individual study subjects—the bars show the interquartile ranges, and the error bars the spreads between the 10th and 90th percentiles of the population. The dark marks in the middle of the bars are the population medians. In both panels, the displays in red and blue show the data in female and male subjects, respectively. Note the logarithmic vertical axes (in the top panel, there were only 0 display values below 0.01%).

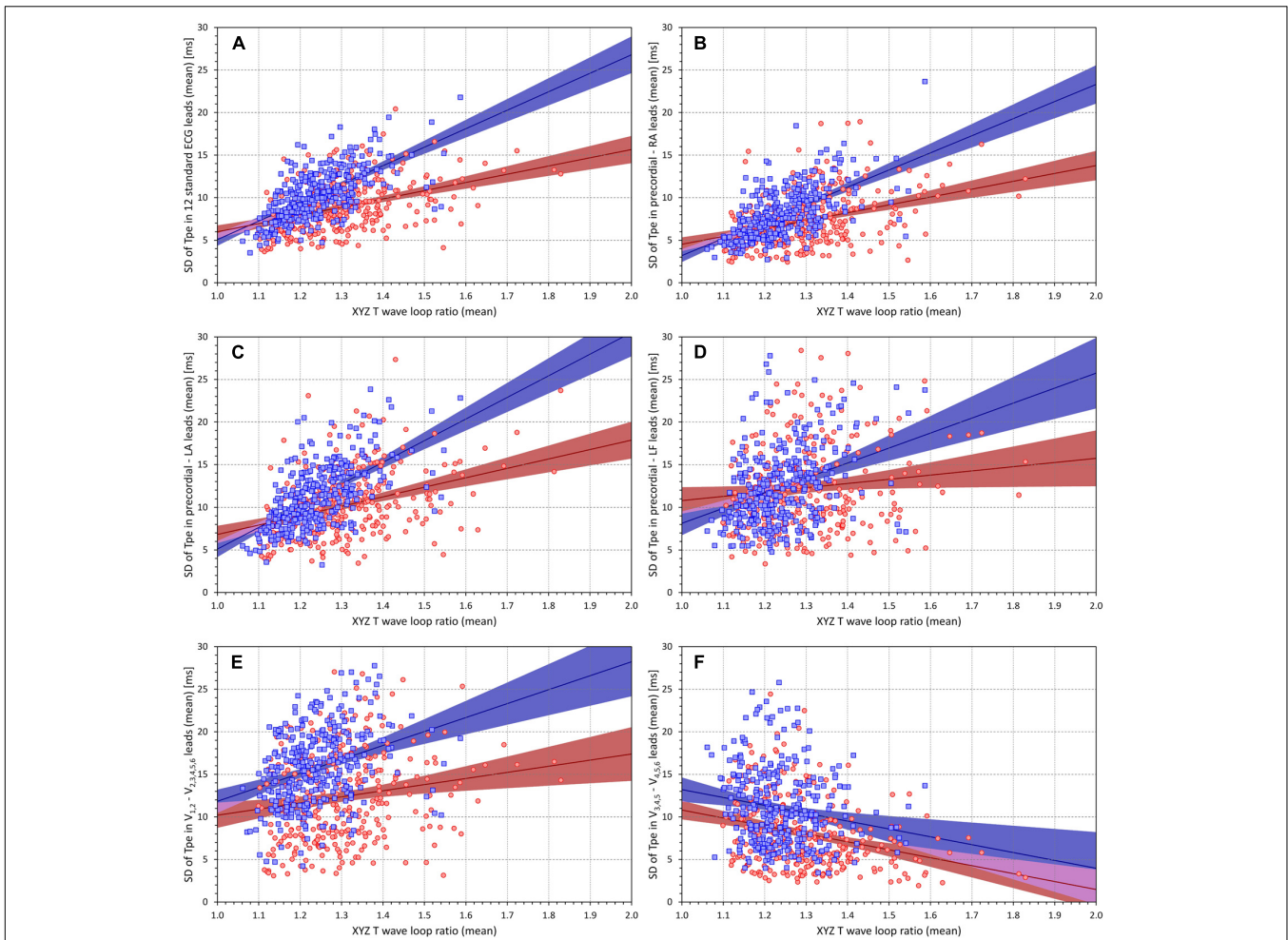
The other panels of **Figure 7** show that there was no systematic relationship between the 60- and 120-bpm changes of the JT intervals and the corresponding changes in the Tpe intervals measured in different leads. For some leads, the scatter diagrams show positive but weak correlations, while for other leads, weak negative correlations were observed.

### Intrasubject Reproducibility

**Figure 8** shows the comparison of relative Tpe/RR residuals with the relative JT/RR residuals. It is clearly visible that the relative JT/RR residuals were almost one magnitude smaller compared to the Tpe/RR residuals. The smallest relative Tpe/RR residual was

seen with the measurements based on lead I ( $7.24 \pm 2.51\%$  and  $7.17 \pm 2.20\%$  in female and male subjects, respectively,  $p = \text{NS}$  for sex comparison), which was markedly larger ( $p < 0.00001$ ) compared to the relative JT/RR residuals ( $1.84 \pm 0.36\%$  and  $1.88 \pm 0.39\%$  in female and male subjects, respectively,  $p = \text{NS}$  for sex comparison).

**Figure 8** also shows that, while the relative Tpe/RR residuals measured in XYZ vector magnitude were significantly larger in female ( $7.41 \pm 3.86\%$ ) than in male subjects ( $6.09 \pm 2.96\%$ ,  $p < 0.0001$ ), the same direction of difference existed in some leads (e.g., in lead V2, the residuals were  $8.24 \pm 3.25\%$  and  $5.74 \pm 2.33\%$  in female and male subjects, respectively,



**FIGURE 3 |** Scatter diagrams between the T wave loop ratios (mean values in individual subjects) and the standard deviations of the Tpe intervals in groups of electrocardiogram (ECG) leads (mean values in individual subjects). Different panels of the figure correspond to different groups of ECG leads—the association of the panels with the lead groups is the same as in **Figure 1**. In each panel [please see the labels of vertical axes for the explanation of panels **(A–F)**], the red circles and blue squares correspond to female and male subjects, respectively. The solid red and solid blue lines show the linear regressions between the measured standard deviations of Tpe intervals and the T wave loop ratios in female and male subjects, respectively. The red- and blue-shaded areas are the 95% confidence intervals of the regression lines; the violet areas are the overlaps between the confidence intervals of the sex-specific regressions. SD, standard deviation; RA, right arm; LA, left arm; LF, left foot.

$p < 0.0001$ ) but was reversed in other leads (e.g., the residuals in lead V6 were  $5.89 \pm 1.88\%$  and  $6.96 \pm 2.68\%$  in female and male subjects, respectively,  $p < 0.0001$ ).

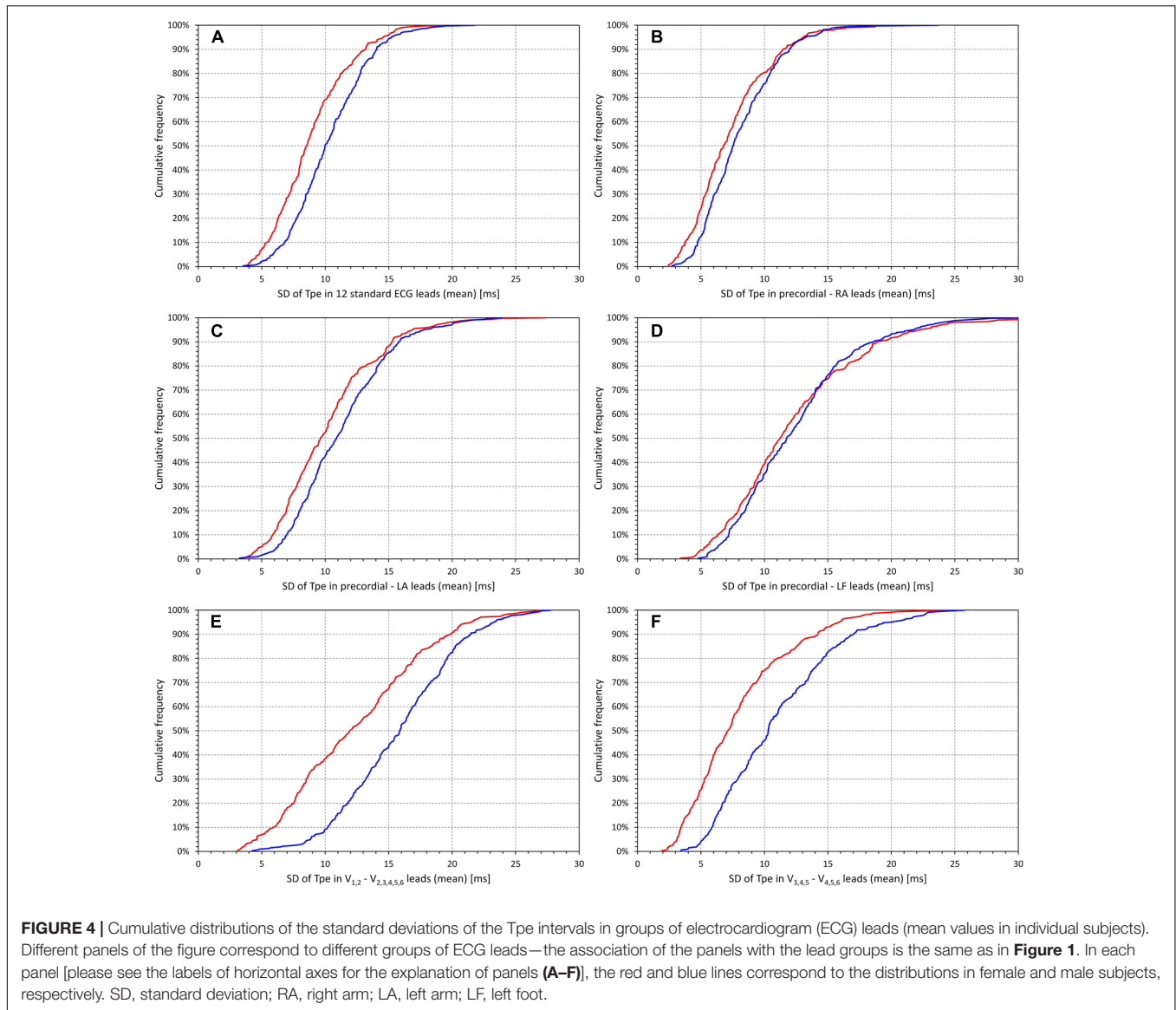
### Reconstruction of Orthogonal Vector Magnitude Tpe From Standard ECG Leads

**Figure 9** shows Bland–Altman-like scatter diagram comparing the Tpe interval projections at 60 bpm measured in the XYZ vector magnitude and in standard ECG leads. The figure shows that, while Tpe intervals measured in some leads are closer to the measurement in the XYZ vector magnitude, the relationship to other leads is less clear. The same comparison is shown in **Figure 10** that demonstrates the projections at 120 bpm. The spread of corresponding Tpe projections is wider. Hence,

there is no standard ECG lead that could be used to obtain a close approximation of the Tpe interval measured in the XYZ vector magnitude.

Of the 796,620 ECG segments investigated in the study, full measurement of the Tpe intervals (i.e., accepted detection of T peaks) in all leads I, II, V2, V3, V4, V5, and V6 was available in 580,430 ECG segments (72.9%). Of these segments, 243,489 were obtained in female subjects (63.2% of all segments in female subjects) and 336,941 were obtained in male subjects (81.9% of all segments in male subjects). Note also that this restriction of the complete measurements was only used in the multivariable regression analyses, while all the previously described results used full datasets of all accepted measurements.

**Figure 11A** shows the summary of the comparison of the lead measurements of Tpe with the Tpe measurement in XYZ vector magnitude. Although this summary is potentially problematic



since it was based on multiples of measurements in the same subjects, trends are seen corresponding to the intrasubject comparisons shown in **Figures 9, 10**. In some leads (mainly in V2 and V3), the T peak precedes that of the XYZ vector magnitude (making the Tpe interval longer), while in other leads (e.g., II, V5, and V6), the T peak follows that of the XYZ vector magnitude.

Restricted multivariable regression analysis without involving underlying heart rate or an onset constant suggested the following approximation of Tpe interval in XYZ vector magnitude in female subjects:

$$0.0706\mathfrak{B}_I + 0.2879\mathfrak{B}_{II} - 0.0052\mathfrak{B}_{V2} + 0.0313\mathfrak{B}_{V3} + 0.2240\mathfrak{B}_{V4} + 0.2331\mathfrak{B}_{V5} + 0.1625\mathfrak{B}_{V6}$$

while the form for male subjects was:

$$0.1468\mathfrak{B}_I + 0.1212\mathfrak{B}_{II} + 0.0639\mathfrak{B}_{V2}$$

$$+ 0.1047\mathfrak{B}_{V3} + 0.3339\mathfrak{B}_{V4} + 0.2145\mathfrak{B}_{V5} + 0.0241\mathfrak{B}_{V6}$$

where  $\mathfrak{B}_L$  represents the Tpe interval measured in ECG lead L (in ms).

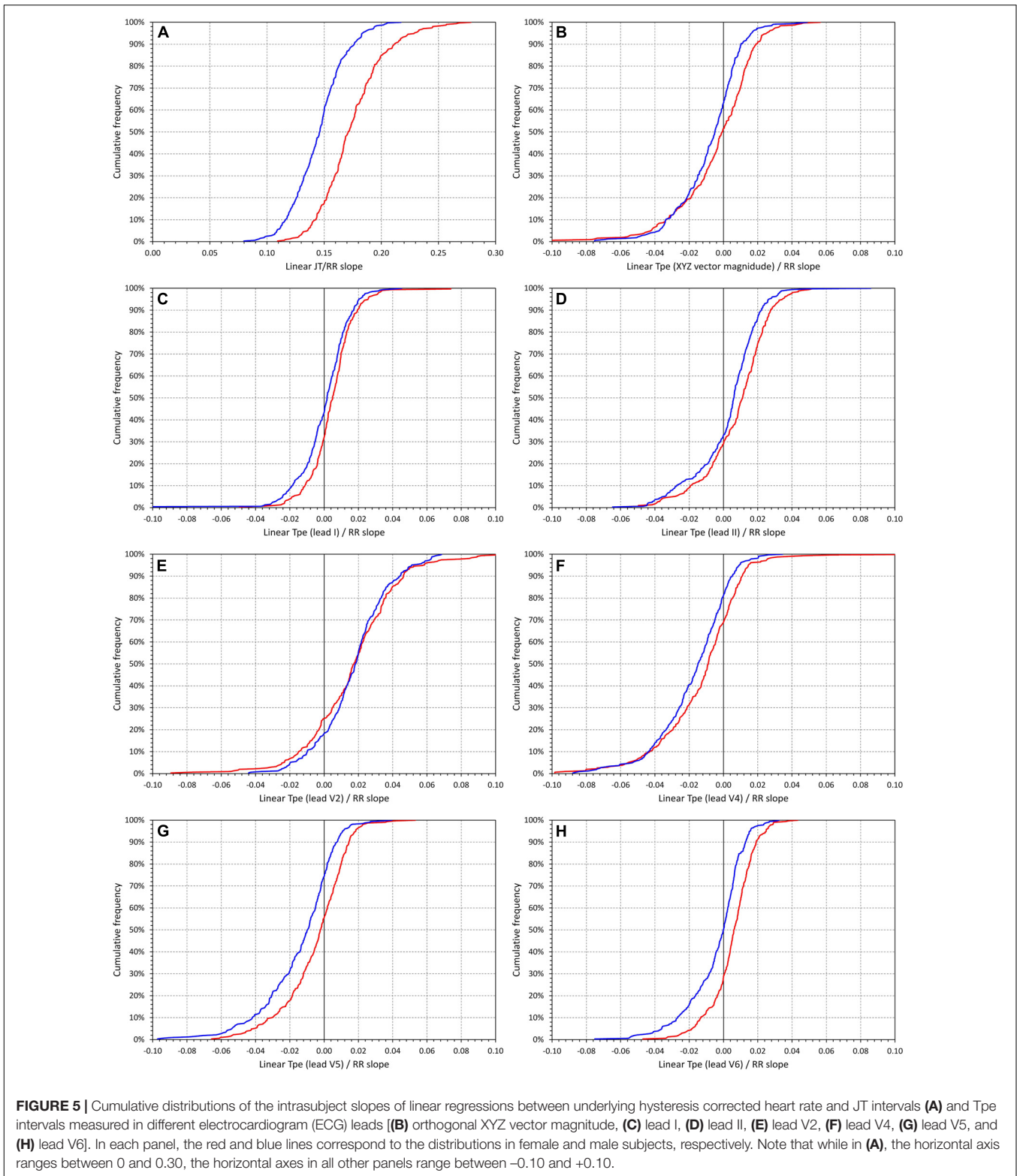
Complete regression analysis proposed the following approximation for female subjects:

$$17.9237 + 0.0012\mathfrak{Q} + 0.0120\mathfrak{B}_I + 0.2475\mathfrak{B}_{II} - 0.0164\mathfrak{B}_{V2} + 0.0328\mathfrak{B}_{V3} + 0.2108\mathfrak{B}_{V4} + 0.2021\mathfrak{B}_{V5} + 0.0894\mathfrak{B}_{V6}$$

and for male subjects:

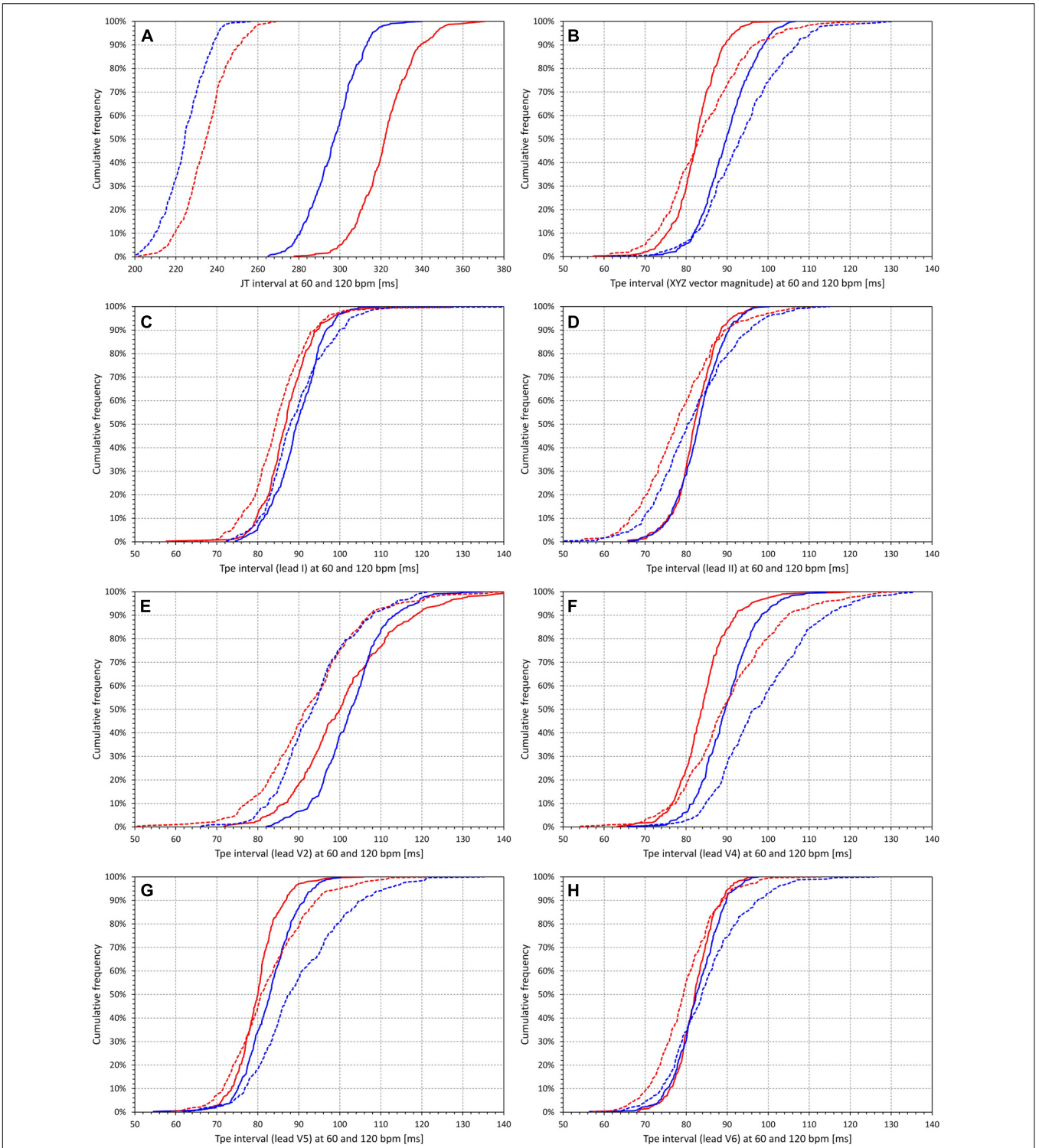
$$23.7813 - 0.0002\mathfrak{Q} + 0.0924\mathfrak{B}_I + 0.0855\mathfrak{B}_{II} + 0.0005\mathfrak{B}_{V2} + 0.1032\mathfrak{B}_{V3} + 0.3122\mathfrak{B}_{V4} + 0.1855\mathfrak{B}_{V5} - 0.0310\mathfrak{B}_{V6}$$

where  $\mathfrak{Q}$  is the RR interval corresponding to the underlying heart rate (in ms).



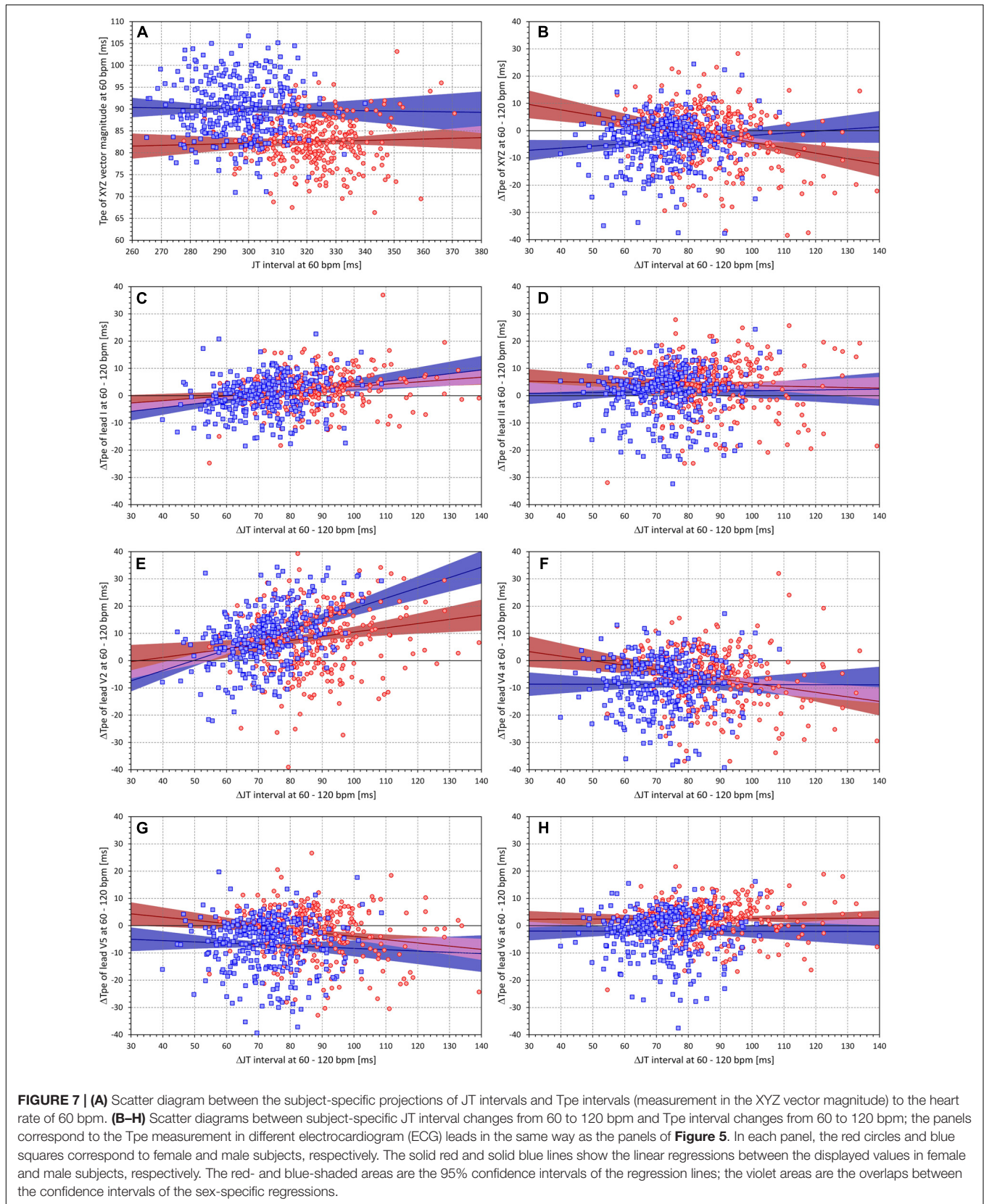
While in the complete data pooled of all subjects together, these formulae provided close approximations (SD of the differences of 4.089 and 5.606 ms for female and male subjects in the restricted regression and 3.859 and 5.339 ms for female

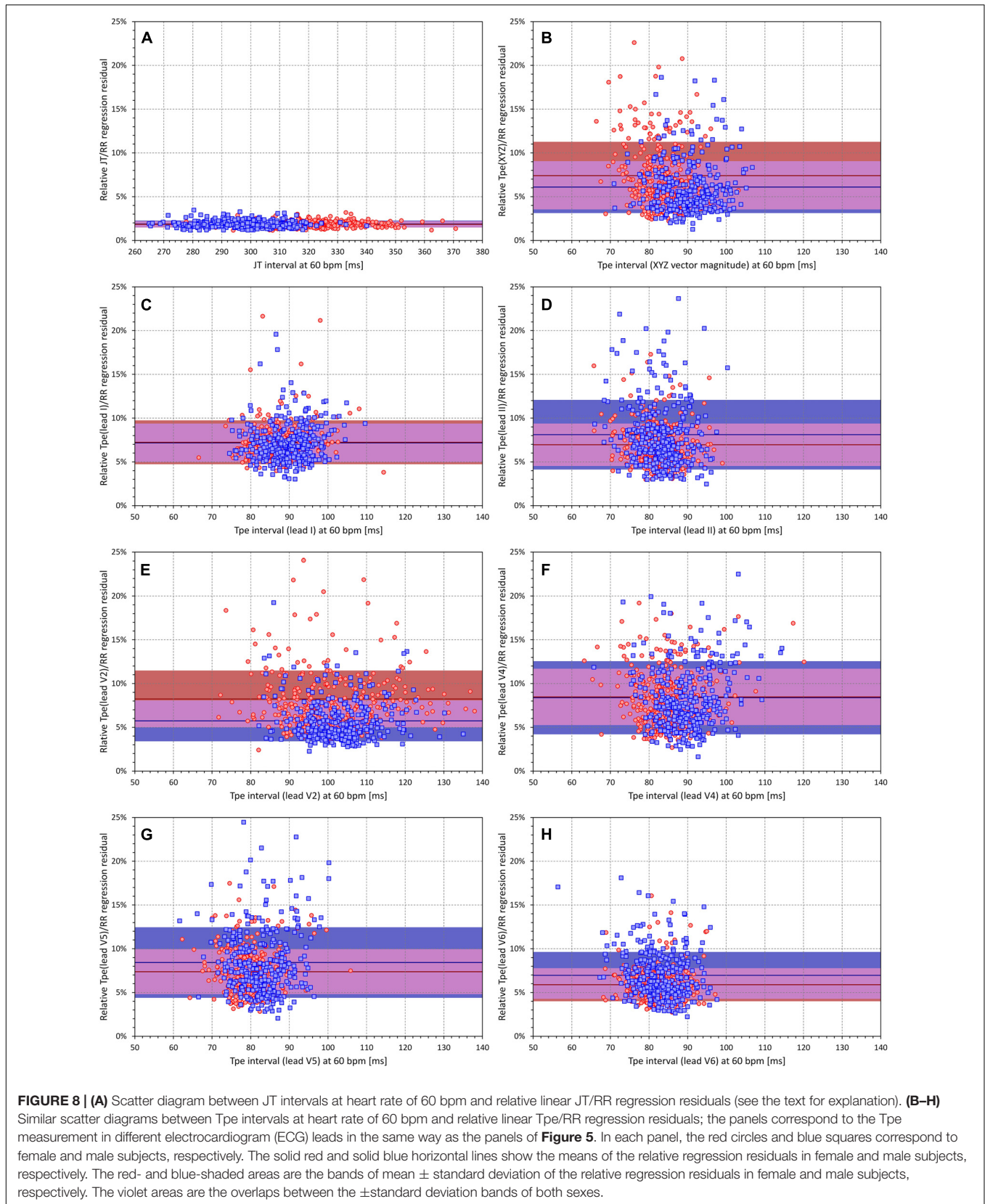
and male subjects in the complete regression), the intrasubject approximations were much less tight. **Figures 11B,D** show the cumulative distribution of mean approximation differences for the restricted and complete regressions, respectively (i.e., the

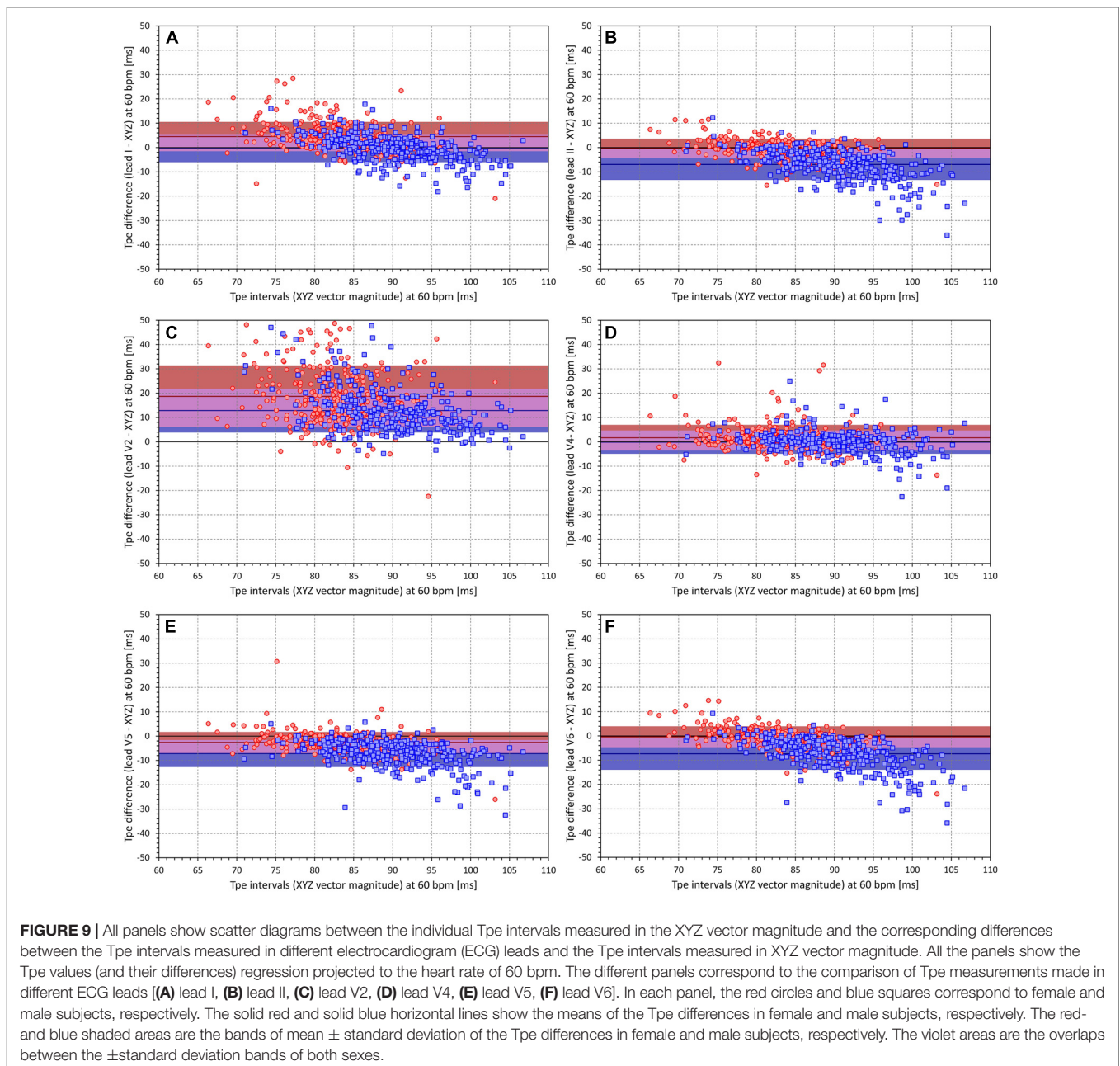


**FIGURE 6 |** Cumulative distributions of intrasubject regression projections of the (A) JT intervals and (B–H) Tpe intervals corresponding to heart rate of 60 beats per minute (bpm) (solid lines) and to heart rate of 120 bpm (dashed lines). (B–H) correspond to different electrocardiogram (ECG) leads in the same way as the panels of **Figure 5**. In each panel, the red and blue lines correspond to the distributions in female and male subjects, respectively. Note that while in (A), the horizontal axis ranges between 200 and 380 ms, the horizontal axes in all other panels range between 50 and 140 ms.







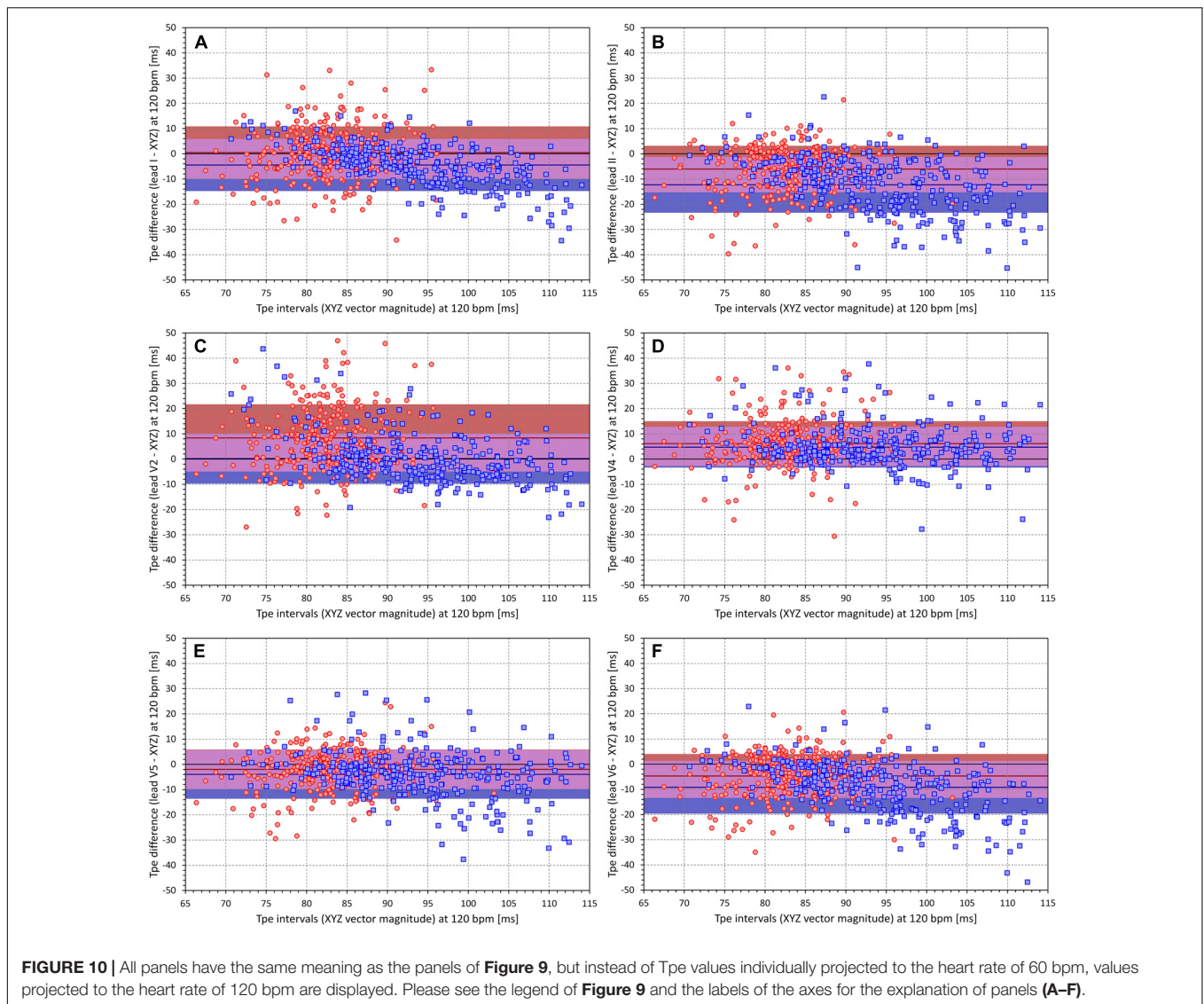


panels show the distribution of intrasubject errors of these formulae). Corresponding scatter diagrams of the intrasubject means and SDs of the differences between the approximated Tpe intervals measured in the XYZ vector magnitude are shown in **Figures 11C,E**.

## DISCUSSION

The study leads to four distinct observations and conclusions that appear to be of possible importance for future investigations of the Tpe interval including the assessment of its risk predictive properties.

First, and not surprisingly, the timing of the T peak (and thus the duration of the Tpe intervals) differs in different ECG leads. The spread of the Tpe intervals across ECG leads is related to the spatial width and morphological complexity of the three-dimensional T wave loop. Since T wave loop abnormalities are, together with other T wave morphology indices, known risk predictors (Huang et al., 2009; Hasan et al., 2012; Seegers et al., 2017), it can be expected that in high-risk patients, the lead-to-lead differences in the Tpe interval duration would be larger than in low-risk subjects. Theoretically, it might thus be proposed that a spread of Tpe intervals across leads would approximate T wave loop abnormalities. Nevertheless, since such an approach would have the same technical disadvantages as QT dispersion (Kors

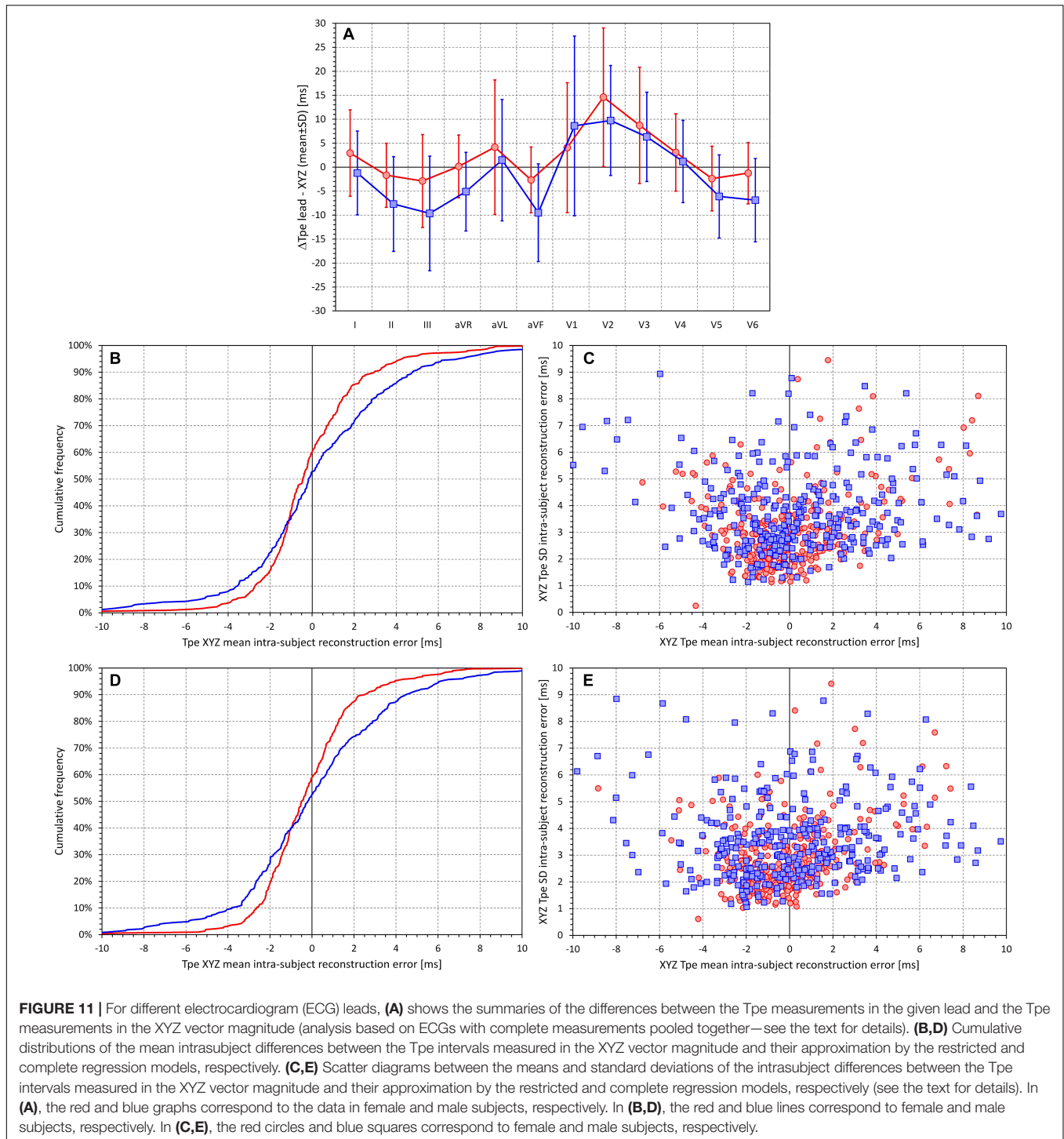


and van Herpen, 1998; Malik and Batchvarov, 2000) and since there are more effective and more accurate ways of assessing T wave loop (Acar et al., 1999), this possibility cannot be advocated.

Second, regardless of which ECG lead was used for measurement, we have not found any heart rate dependency of Tpe intervals that would, for practical purposes, require heart rate correction similar to those used for QT or JT intervals. While it has previously been shown that not only the JT intervals but also the J–T peak intervals are substantially and systematically heart rate dependent (Hnatkova et al., 2019b), this is not the case with the Tpe intervals. Using the measurements of any lead, we have found subjects in whom the Tpe correlation with RR of the underlying heart rate was positive and other subjects in whom the correlation was negative (see **Figure 5**). Proposals have previously been made to correct the Tpe interval using the Bazett formula, arguing that this improves the risk-prediction capabilities of the measurement (Chua et al., 2016). However, such argumentation is misplaced. Resting heart rate is a powerful

risk predictor in its own rights (Copie et al., 1996; Böhm et al., 2020) and thus correcting even practically random values by the Bazett formula might lead to significant risk-related population differences (Malik and Camm, 1997).

Third, our results shown in **Figure 8** demonstrated substantially poorer intrasubject reproducibility of the Tpe intervals compared to JT intervals (when their durations are related to the underlying heart rate). The intrasubject reproducibility of Tpe measurements is also similarly poorer than that of the QT intervals (results not shown). This is not necessarily surprising since the definition of the end of the T wave is, apart from isoelectric projections of the terminal part of the T wave, independent of the angle projecting the T wave loop into a given ECG lead; the spatial orientation of the T wave loop (and hence the projection of the T wave peak) is influenced by the position of the heart in the thorax, which changes with posture, meal intake, and other circumstances. Since alternative expressions of the distribution of the T wave



power were reported to be less variable compared to the T peak identification (Vicente et al., 2017; Hnatkova et al., 2019b), these other expressions are likely worth investigating further. The relatively poor reproducibility of the Tpe interval measurement might also be the reason for inconsistencies in the literature. For instance, while Shenthar et al. (2015) reported Tpe of  $200 \pm 110$  and  $100 \pm 20$  ms in STEMI patients who suffered and did not

suffer from ventricular fibrillation, Yu et al. (2018) described Tpe differences of  $92.6 \pm 11.7$  vs  $86.8 \pm 11.5$  ms also among STEMI patients who experienced and did not experience ventricular tachycardia and/or fibrillation.

Finally, our failed attempt of proposing a generally applicable approximation the Tpe intervals in the XYZ vector magnitude based on measurements in standard ECG leads suggests that

the interlead differences in the T loop projection are different in different subjects. Considering the individuality of many other repolarization indices, this observation is not surprising. Importantly, the differences in the comparisons of individual lead measurements with those in XYZ vector magnitude (see **Figures 9, 10, 11A**) show that measurements in different leads should not be mixed. Strategies such as “*If lead V6 was not suitable, leads V5 and V4 were measured.*” (Shenthar et al., 2015) might decrease the stability of measurements, especially if frontal and lateral precordial leads are fused in the same dataset. Our results suggest that, apart from the theoretical considerations that suggest the preference of the XYZ vector magnitude, there are no physiological reasons to prefer one lead over another as long as the same lead is always used. It should also be noted that a number of publications on the Tpe interval stated that V6 is preferable because it best reflects the transmural axis of the left ventricle (Shenthar et al., 2015; Yu et al., 2018). Frequently, a study by El-Sherif et al. (1976) is referenced to support this concept, while surprisingly, this publication by El Sherif et al. does not deal with the topic and provides no credence to the conjecture. Apart from these considerations, the full regression models also showed that RR intervals of underlying heart rate have very little influence on the composite of the Tpe intervals in different leads (note the minimal regression constants of the  $\Omega$  value contributions).

## Limitations

A number of limitations of our investigation need to be listed. To obtain orthogonal XYZ representation of the ECG signals, we have used previously published conversion matrix optimized for the Mason–Likar electrode positions. Other conversion matrices have also been proposed (Edenbrandt and Pahlm, 1988; Kors et al., 1990) albeit not necessarily suitable for the electrode configuration that was used with the Holter recordings during the source clinical studies. Since the detailed relationship of standard ECG leads to the orthogonal XYZ leads is likely to be subject specific, it might be also possible to use singular value decomposition (Damen and van der Kam, 1982; Acar and Köymen, 1999) and to create an orthogonal lead system specific for each ECG segment. That would, however, potentially complicate the assessment of the relationship to heart rate since different ECGs of the same subject are likely to have different optimal orthogonal projections. When studying the spread of T peak measurements across groups of ECG leads, we have, in addition to standard ECG leads, considered bipolar leads between pairs of electrodes. Other possibilities also exist, e.g., the RA – (V1 + V2)/2 or (V1 + V2)/2 – (V5 + V6)/2, etc. Nevertheless, we believe that considering such possibilities would have been superfluous. While investigating the proportions of the T wave loop, we have not considered T wave amplitude in separate T wave leads. Although the measurements of the end of the T wave were visually validated and manually corrected where appropriate, the identification of T peak positions was based on validated robust algorithm. While the T wave offset was determined in the images of all standard ECG leads superimposed on the same isoelectric axis (Malik, 2004), visual

checks of T peak positions would be needed in every lead separately. With the number of ECG segments analyzed in the study, this would have been impossible to achieve. Using the T wave offset common for all ECG leads also eliminated the problems associated with the concept of QT dispersion. We have also not investigated the circadian profile of the Tpe interval duration (Mozos and Filimon, 2013). We have also used a rather simple universally applicable model of Tpe/RR hysteresis (Malik et al., 2016), while other models of hysteresis adaptation were also proposed (Haláček et al., 2010; Gravel et al., 2018). However, it is highly doubtful whether these would have made any difference even if separately applied to the Tpe assessment in different ECG leads. Assessing the hysteresis of RR interval influence properly requires a clear and robust heart rate dependency (Malik et al., 2008b), which we have not found with the Tpe interval. When we repeated the same data analyses using only ECG segments preceded by stable heart rate (results not shown), the same absence of any systematic heart rate dependency was found. The fact that, in individual leads, the Tpe measurements were more frequently accepted in male compared to female individuals reflects the slightly higher noise pollution of Holter recordings in female individuals, which, compared to male individuals, leads also to marginally lower intrasubject QTc variability (Malik et al., 2013).

## CONCLUSION

Despite these limitations, the study leads to the following conclusions. First, even in normal healthy recordings, the Tpe intervals differ across ECG leads, and the spread of their durations is related to the spatial width and morphological complexity of the three-dimensional T wave loop. Second, irrespective of the measured ECG lead, the duration of Tpe interval is not systematically heart rate dependent; no heart rate correction should be used in the clinical Tpe investigations. Third, compared to other repolarization-related intervals, the Tpe measurement suffers from poorer intrasubject reproducibility. Finally, the relationship between Tpe intervals measured in different ECG leads is different in different subjects; studies of the Tpe intervals should therefore avoid combining measurements in different ECG leads.

## DATA AVAILABILITY STATEMENT

The raw data supporting the conclusions of this article will be made available by the authors, without undue reservation but pending the approval by the sponsors of the source clinical studies.

## ETHICS STATEMENT

The studies involving human participants were reviewed and approved by the Focus in Neuss; Parexel in Baltimore;

Bloemfontein, and Glendale; PPD in Austin; and Spaulding in Milwaukee. The patients/participants provided their written informed consent to participate in the source studies.

## AUTHOR CONTRIBUTIONS

IA, KH, and MM: study design and initial manuscript draft. KH and MM: software development and, statistics and figures. GS, IA, KMH, MŠ, OT, PB, PS, and TN: ECG interpretation and measurement. GS, TN, OT, and PS: supervision of the

measurements. GS, MM, and TN: quality control of the measurements. All authors contributed to the article and approved the submitted version.

## FUNDING

This study was supported in part by the British Heart Foundation New Horizons Grant NH/16/2/32499 and by Ministry of Health, Czechia, conceptual development of research organization (Grant FNBr/65269705).

## REFERENCES

- Acar, B., and Köymen, H. (1999). SVD-based on-line exercise ECG signal orthogonalization. *IEEE Trans. Biomed. Eng.* 46, 311–321. doi: 10.1109/10.748984
- Acar, B., Yi, G., Hnatkova, K., and Malik, M. (1999). Spatial, temporal and wavefront direction characteristics of 12-lead T-wave morphology. *Med. Biol. Eng. Comput.* 37, 574–584. doi: 10.1007/bf02513351
- Antzelevitch, C. (2008). Drug-induced spatial dispersion of repolarization. *Cardiol. J.* 15, 100–121.
- Antzelevitch, C., and Di Diego, J. M. (2019). Tpeak-Tend interval as a marker of arrhythmic risk. *Heart Rhythm.* 16, 954–955. doi: 10.1016/j.hrthm.2019.01.017
- Batchvarov, V., Hnatkova, K., and Malik, M. (2002). Assessment of noise in digital electrocardiograms. *Pacing Clin. Electrophysiol.* 25, 499–503. doi: 10.1046/j.1460-9592.2002.00499.x
- Böhm, M., Schumacher, H., Teo, K. K., Lonn, E. M., Mahfoud, F., Ukena, C., et al. (2020). Resting heart rate and cardiovascular outcomes in diabetic and non-diabetic individuals at high cardiovascular risk analysis from the ONTARGET/TRANSCEND trials. *Eur. Heart J.* 41, 231–238. doi: 10.1093/eurheartj/ehy808
- Chua, K. C., Rusinaru, C., Reinier, K., Uy-Evanado, A., Chugh, H., Gunson, K., et al. (2016). Tpeak-to-Tend interval corrected for heart rate: a more precise measure of increased sudden death risk? *Heart Rhythm.* 13, 2181–2185. doi: 10.1016/j.hrthm.2016.08.022
- Copie, X., Hnatkova, K., Staunton, A., Fei, L., Camm, A. J., and Malik, M. (1996). Predictive power of increased heart rate versus depressed left ventricular ejection fraction and heart rate variability for risk stratification after myocardial infarction. Results of a two-year follow-up study. *J. Am. Coll. Cardiol.* 27, 270–276. doi: 10.1016/0735-1097(95)00454-8
- Damen, A. A., and van der Kam, J. (1982). The use of the singular value decomposition in electrocardiography. *Med. Biol. Eng. Comput.* 20, 473–482. doi: 10.1007/bf02442409
- Day, C. P., McComb, L. M., and Campbell, R. W. F. (1990). QT dispersion: an indication of arrhythmia risk in patients with long QT intervals. *Br. Heart J.* 63, 342–344. doi: 10.1136/hrt.63.6.342
- Edenbrandt, L., and Pahlm, O. (1988). Vectorcardiogram synthesized from a 12-lead ECG: superiority of the inverse Dower matrix. *J. Electrocardiol.* 21, 361–367. doi: 10.1016/0022-0736(88)90113-6
- El-Sherif, N., Myerburg, R. J., Scherlag, B. J., Befeler, B., Aranda, J. M., Castellanos, A., et al. (1976). Electrocardiographic antecedents of primary ventricular fibrillation. Value of the R-on-T phenomenon in myocardial infarction. *Br. Heart J.* 38, 415–422. doi: 10.1136/hrt.38.4.415
- Fenichel, R. R., Malik, M., Antzelevitch, C., Sanguinetti, M., Roden, D. M., Priori, S. G., et al. (2004). Drug-induced Torsades de Pointes and implications for drug development. *J. Cardiovasc. Electrophysiol.* 15, 475–495.
- Garnett, C. E., Zhu, H., Malik, M., Fossa, A. A., Zhang, J., Badilini, F., et al. (2012). Methodologies to characterize the QT/corrected QT interval in the presence of drug-induced heart rate changes or other autonomic effects. *Am. Heart J.* 163, 912–930. doi: 10.1016/j.ahj.2012.02.023
- Gravel, H., Jacquemet, V., Dahdah, N., and Curnier, D. (2018). Clinical applications of QT/RR hysteresis assessment: a systematic review. *Ann. Noninvasive Electrocardiol.* 23, e12514. doi: 10.1111/anec.12514
- Guideline, I. C. H. (2001). Safety pharmacology studies for human pharmaceuticals S7A. *Fed. Regist.* 66, 36791–36792.
- Guldenring, D., Finlay, D. D., Strauss, D. G., Galeotti, L., Nugent, C. D., Donnelly, M. P., et al. (2012). Transformation of the Mason-Likar 12-lead electrocardiogram to the Frank vectorcardiogram. *Conf. Proc. IEEE Eng. Med. Biol. Soc.* 2012, 677–680.
- Haláček, J., Jurák, P., Bunch, T. J., Lipoldová, J., Novák, M., Vondra, V., et al. (2010). Use of a novel transfer function to reduce repolarization interval hysteresis. *J. Interv. Card Electrophysiol.* 29, 23–32. doi: 10.1007/s10840-010-9500-x
- Hasan, M. A., Abbott, D., and Baumert, M. (2012). Beat-to-beat vectorcardiographic analysis of ventricular depolarization and repolarization in myocardial infarction. *PLoS One* 7:e49489. doi:10.1371/journal.pone.0049489
- Hnatkova, K., Smetana, P., Toman, O., Bauer, A., Schmidt, G., and Malik, M. (2009). Systematic comparisons of electrocardiographic morphology increase the precision of QT interval measurement. *Pacing Clin. Electrophysiol.* 32, 119–130. doi: 10.1111/j.1540-8159.2009.02185.x
- Hnatkova, K., Vicente, J., Johannesen, L., Garnett, C., Strauss, D. G., Stockbridge, N., et al. (2019a). Detection of T wave peak for serial comparisons of JTp interval. *Front. Physiol.* 10:934. doi: 10.3389/fphys.2019.00934
- Hnatkova, K., Vicente, J., Johannesen, L., Garnett, C., Strauss, D. G., Stockbridge, N., et al. (2019b). Heart rate correction of the J-to-Tpeak interval. *Sci. Rep.* 9:15060. doi: 10.1038/s41598-019-51491-4
- Huang, H. C., Lin, L. Y., Yu, H. Y., and Ho, Y. L. (2009). Risk stratification by T-wave morphology for cardiovascular mortality in patients with systolic heart failure. *Europace* 11, 1522–1528. doi: 10.1093/europace/eup294
- Johannesen, L., Vicente, J., Hosseini, M., and Strauss, D. G. (2016). Automated algorithm for J-Tpeak and Tpeak-Tend assessment of drug-induced proarrhythmia risk. *PLoS One* 11:e0166925. doi: 10.1371/journal.pone.0166925
- Johannesen, L., Vicente, J., Mason, J. W., Sanabria, C., Waite-Labott, K., Hong, M., et al. (2014). Differentiating drug-induced multichannel block on the electrocardiogram: randomized study of dofetilide, quinidine, ranolazine, and verapamil. *Clin. Pharmacol. Ther.* 96, 549–558. doi: 10.1038/clpt.2014.155
- Kors, J. A., and van Herpen, G. (1998). Measurement error as a source of QT dispersion: a computerised analysis. *Heart* 80, 453–458. doi: 10.1136/hrt.80.5.453
- Kors, J. A., van Herpen, G., Sittig, A. C., and van Bommel, J. H. (1990). Reconstruction of the Frank vectorcardiogram from standard electrocardiographic leads: diagnostic comparison of different methods. *Eur. Heart J.* 11, 1083–1092. doi: 10.1093/oxfordjournals.eurheartj.a059647
- Kors, J. A., van Herpen, G., and van Bommel, J. H. (1999). QT dispersion. *Circulation* 99, 1458–1463.
- Malik, M. (2004). Errors and misconceptions in ECG measurement used for the detection of drug induced QT interval prolongation. *J. Electrocardiol.* 37(Suppl.), 25–33. doi: 10.1016/j.jelectrocard.2004.08.005
- Malik, M., Acar, B., Gang, Y., Yap, Y. G., Hnatkova, K., and Camm, A. J. (2000). QT dispersion does not represent electrocardiographic interlead heterogeneity of ventricular repolarization. *J. Cardiovasc. Electrophysiol.* 11, 835–843. doi: 10.1111/j.1540-8167.2000.tb00061.x
- Malik, M., Andreas, J.-O., Hnatkova, K., Hoekendorff, J., Cawello, W., Middle, M., et al. (2008a). Thorough QT/QTc study in patients with advanced Parkinson's disease: cardiac safety of rotigotine. *Clin. Pharmacol. Ther.* 84, 595–603. doi: 10.1038/clpt.2008.143

- Malik, M., and Batchvarov, V. N. (2000). Measurement, interpretation, and clinical potential of QT dispersion. *J. Am. Coll. Cardiol.* 36, 1749–1766. doi: 10.1016/s0735-1097(00)00962-1
- Malik, M., and Camm, A. J. (1997). Mystery of QTc interval dispersion. *Am. J. Cardiol.* 79, 785–787.
- Malik, M., Hnatkova, K., Kowalski, D., Keirns, J. J., and van Gelderen, E. M. Q. T. (2013). /RR curvatures in healthy subjects: sex differences and covariates. *Am. J. Physiol. Heart Circ. Physiol.* 305, H1798–H1806.
- Malik, M., Hnatkova, K., Novotny, T., and Schmidt, G. (2008b). Subject-specific profiles of QT/RR hysteresis. *Am. J. Physiol. Heart Circ. Physiol.* 295, H2356–H2363.
- Malik, M., Huikuri, H., Lombardi, F., Schmidt, G., and Zabel, M. (2018). Conundrum of the Tpeak-Tend interval. *J. Cardiovasc. Electrophysiol.* 29, 767–770. doi: 10.1111/jce.13474
- Malik, M., Johannesen, L., Hnatkova, K., and Stockbridge, N. (2016). Universal correction for QT/RR hysteresis. *Drug Saf.* 39, 577–588. doi: 10.1007/s40264-016-0406-0
- Malik, M., van Gelderen, E. M., Lee, J. H., Kowalski, D. L., Yen, M., Goldwater, R., et al. (2012). Proarrhythmic safety of repeat doses of mirabegron in healthy subjects: a randomized, double-blind, placebo-, and active-controlled thorough QT study. *Clin. Pharm. Therap.* 92, 696–706. doi: 10.1038/clpt.2012.181
- Mozos, I., and Filimon, L. (2013). QT and Tpeak-Tend intervals in shift workers. *J. Electrocardiol.* 46, 60–65. doi: 10.1016/j.jelectrocard.2012.10.014
- Okin, P. M., Devereux, R. B., Howard, B. V., Fabsitz, R. R., Lee, E. T., and Welty, T. K. (2000). Assessment of QT interval and QT dispersion for prediction of all-cause and cardiovascular mortality in American Indians. The Strong Heart Study. *Circulation* 101, 61–66. doi: 10.1161/01.cir.101.1.61
- Rautaharju, P. M. (1999). QT and dispersion of ventricular repolarization: the greatest fallacy in electrocardiography in the 1990s. *Circulation* 18, 2477–2478.
- Rautaharju, P. M. (2002). Why did QT dispersion die? *Card Electrophysiol. Rev.* 6, 295–301.
- Seegers, J., Hnatkova, K., Friede, T., Malik, M., and Zabel, M. (2017). T-wave loop area from a pre-implant 12-lead ECG is associated with appropriate ICD shocks. *PLoS One* 12:e0173868. doi:10.1371/journal.pone.0173868
- Shenthar, J., Deora, S., Rai, M., and Nanjappa Manjunath, C. (2015). Prolonged Tpeak-end and Tpeak-end/QT ratio as predictors of malignant ventricular arrhythmias in the acute phase of ST-segment elevation myocardial infarction: a prospective case-control study. *Heart Rhythm.* 12, 484–489. doi: 10.1016/j.hrthm.2014.11.034
- Sicouri, S., and Antzelevitch, C. (1991). A subpopulation of cells with unique electrophysiological properties in the deep subepicardium of the canine ventricle. The M cell. *Circ. Res.* 68, 1729–1741. doi: 10.1161/01.res.68.6.1729
- Smetana, P., Schmidt, A., Zabel, M., Hnatkova, K., Franz, M., Huber, K., et al. (2011). Assessment of repolarization heterogeneity for prediction of mortality in cardiovascular disease: peak to the end of the T wave interval and nondipolar repolarization components. *J. Electrocardiol.* 44, 301–308. doi: 10.1016/j.jelectrocard.2011.03.004
- Toman, O., Hnatkova, K., Smetana, P., Huster, K. M., Šišáková, M., Barthel, P., et al. (2020). Physiologic heart rate dependency of the PQ interval and its sex differences. *Sci. Rep.* 10:2551. doi: 10.1038/s41598-020-59480-8
- Tse, G., Gong, M., Wong, W. T., Georgopoulos, S., Letsas, K. P., Vassiliou, V. S., et al. (2017). The Tpeak - Tend interval as an electrocardiographic risk marker of arrhythmic and mortality outcomes: a systematic review and meta-analysis. *Heart Rhythm.* 14, 1131–1137.
- Vicente, J., Hosseini, M., Johannesen, L., and Strauss, D. G. (2017). Electrocardiographic biomarkers to confirm drug's electrophysiological effects used for proarrhythmic risk prediction under CiPA. *J. Electrocardiol.* 50, 808–813. doi: 10.1016/j.jelectrocard.2017.08.003
- Xue, J. Q. (2009). Robust QT interval estimation - from algorithm to validation. *Ann. Noninvasive Electrocardiol.* 14(Suppl. 1), S35–S41.
- Yu, Z., Chen, Z., Wu, Y., Chen, R., Li, M., Chen, X., et al. (2018). Electrocardiographic parameters effectively predict ventricular tachycardia/fibrillation in acute phase and abnormal cardiac function in chronic phase of ST-segment elevation myocardial infarction. *J. Cardiovasc. Electrophysiol.* 29, 756–766. doi: 10.1111/jce.13453
- Zareba, W. (2006). Genotype-specific ECG patterns in long QT syndrome. *J. Electrocardiol.* 39, S101–S106.

**Conflict of Interest:** The authors declare that the research was conducted in the absence of any commercial or financial relationships that could be construed as a potential conflict of interest.

Copyright © 2020 Andršová, Hnatkova, Šišáková, Toman, Smetana, Huster, Barthel, Novotný, Schmidt and Malik. This is an open-access article distributed under the terms of the Creative Commons Attribution License (CC BY). The use, distribution or reproduction in other forums is permitted, provided the original author(s) and the copyright owner(s) are credited and that the original publication in this journal is cited, in accordance with accepted academic practice. No use, distribution or reproduction is permitted which does not comply with these terms.



### 3.8. QT variabilita

V poslední době je v rámci rizikové stratifikace hodně propagovaná variabilita QT intervalu (QTV). Jedná se o změny QT intervalu tep od tepu, ať už při několikasekundovém či několikahodinovém jedno- až 12-ti svodovém EKG záznamu. Zvýšené hodnoty variability QT intervalu jsou považovány za ukazatel výrazné heterogenity srdeční repolarizace, což poukazuje na možnou arytmogenní nestabilitu. Tomuto tématu se věnuje nemalé množství prací zabývajících se hodnotou QTV a dalšími odvozenými parametry, jako jsou index variability QT (QTVi), směrodatná odchylka QT (SDQT) atd., u skupin pacientů s různou kardiologickou diagnózou a předpokládaným vyšším rizikem NSS či mortalitou obecně.<sup>94,95,96</sup> Dokonce nedávné stanovisko Evropské asociace srdečního rytmu (EHRA) považuje zvýšenou QTV a především QTVi za významný rizikový marker NSS a tato asociace vydala i doporučený postup hodnocení, tzv. Standardizační dokument.<sup>97</sup> Nicméně jednotlivé práce nemají konzistentní metodiku. Například studie u pacientů s DKMP analyzovala tyto parametry z EKG dlouhého 30 minut a QTV hodnotila v 256-ti sekundových segmentech RR.<sup>94</sup> Naopak studie u pacientů s primárně preventivně implantovaným ICD provedla hodnocení QTV z 24 hodinových záznamů z ICD a zjistila, že ke zvýšení QTV dochází cca 30 až 60 s před maligní arytmií.<sup>98</sup> Naproti tomu práce popisující fyziologické hodnoty QTV a odvozených parametrů vycházela z 10-sekundových EKG záznamů.<sup>99</sup> Některé práce tedy určují QTV jako podíl mezi absolutními změnami intervalu QT cyklus od cyklu k variabilitě RR intervalu, na druhou stranu je pak QTV uváděna jako absolutní hodnota QT mezi jednotlivými RR bez zajištění ustálené SF.<sup>100,101,102</sup> S vědomím existence zpoždění hystereze QT intervalu za ustálenou SF a její intraindividuální stabilitou vyvstává otázka o ustálenosti intraindividuální variability QTV a zda je QTV ovlivňována ustálenou srdeční frekvencí a/nebo krátkodobou variabilitou RR intervalu. Některé studie pak naznačují sníženou reprodukovatelnost tohoto parametru.<sup>103</sup>

Protože tyto neprozkoumané fyziologické vlastnosti QTV mohou ovlivnit postupy v měření a výslednou interpretaci v rámci rizikové stratifikace, rozhodli jsme se hodnotit reproducibilitu QTV a dalších odvozených parametrů v závislosti k SF. K výpočtům jsme použili jednotlivé 10-ti sekundové vzorové záznamy získané z dlouhodobé EKG monitorace provedené v rámci klinických farmakologických studií u zdravých dobrovolníků. Tímto postupem jsme mohli hodnotit vztah QTV k předešlým RR a současně i zhodnotit vliv ustálené srdeční frekvence. Analýzou jsme zjistili, že reproducibilita těchto parametrů je malá, zvyšuje se však zahrnutím variability SF (HRV). Tedy převážně HRV je dominantní složkou QTVi, oproti tomu samotná QTV má mnohem menší vliv. Parametr QTVi je závislý na věku, stejně jako HRV. Je tedy otázkou, zda síla stratifikace je vskutku ukryta v samotné QTV či naopak v již dobře známé HRV. Podrobnou metodiku vypracovanou ve spolupráci s technicky zaměřenou částí našeho týmu přináší následující publikace.

**Andršová I**, Hnatkova K, Šišáková M, Toman O, Smetana P, Huster KM, Barthel P, Novotný T, Schmidt G, Malik M. Heart rate influence on the QT variability risk factors. *Diagnostics* 2020; 10:1096; doi:10.3390/diagnostics10121096.

IF 3,706. Počet citací ve Web of Science 1

Původní práce - kvantitativní podíl uchazečky 45%: Návrh struktury publikace, elektrokardiologická měření, interpretace statistických výsledků, diskuze výsledků, text publikace.

Article

# Heart Rate Influence on the QT Variability Risk Factors

Irena Andršová<sup>1</sup>, Katerina Hnatkova<sup>2</sup>, Martina Šišáková<sup>1</sup>, Ondřej Toman<sup>1</sup>, Peter Smetana<sup>3</sup>, Katharina M. Huster<sup>4</sup>, Petra Barthel<sup>4</sup>, Tomáš Novotný<sup>1</sup>, Georg Schmidt<sup>4</sup> and Marek Malik<sup>2,5,\*</sup> 

<sup>1</sup> Department of Internal Medicine and Cardiology, University Hospital Brno, Faculty of Medicine, Masaryk University, Jihlavská 20, 625 00 Brno, Czech Republic; Andrsova.Irena@fnbrno.cz (I.A.); sisakova.martina@fnbrno.cz (M.Š.); Toman.Ondrej@fnbrno.cz (O.T.); Novotny.Tomas3@fnbrno.cz (T.N.)

<sup>2</sup> National Heart and Lung Institute, Imperial College, 72 Du Cane Road, Shepherd's Bush, London W12 0NN, UK; K.Hnatkova@imperial.ac.uk

<sup>3</sup> Wilhelminenspital der Stadt Wien, Montleartstraße 37, 1160 Vienna, Austria; psmetana@hotmail.com

<sup>4</sup> Klinikum rechts der Isar, Technische Universität München, Ismaninger Straße 22, D-81675 Munich, Germany; Katharina.Huster@mri.tum.de (K.M.H.); barthel@tum.de (P.B.); gschmidt@tum.de (G.S.)

<sup>5</sup> Department of Internal Medicine and Cardiology, Faculty of Medicine, Masaryk University, Jihlavská 20, 625 00 Brno, Czech Republic

\* Correspondence: marek.malik@imperial.ac.uk

Received: 27 November 2020; Accepted: 14 December 2020; Published: 16 December 2020



**Abstract:** QT interval variability, mostly expressed by QT variability index (QTVi), has repeatedly been used in risk diagnostics. Physiologic correlates of QT variability expressions have been little researched especially when measured in short 10-second electrocardiograms (ECGs). This study investigated different QT variability indices, including QTVi and the standard deviation of QT interval durations (SDQT) in 657,287 10-second ECGs recorded in 523 healthy subjects (259 females). The indices were related to the underlying heart rate and to the 10-second standard deviation of RR intervals (SDRR). The analyses showed that both QTVi and SDQT (as well as other QT variability indices) were highly statistically significantly ( $p < 0.00001$ ) influenced by heart rate and that QTVi showed poor intra-subject reproducibility (coefficient of variance approaching 200%). Furthermore, sequential analysis of regression variance showed that SDQT was more strongly related to the underlying heart rate than to SDRR, and that QTVi was influenced by the underlying heart rate and SDRR more strongly than by SDQT ( $p < 0.00001$  for these comparisons of regression dependency). The study concludes that instead of QTVi, simpler expressions of QT interval variability, such as SDQT, appear preferable for future applications especially if multivariable combination with the underlying heart rate is used.

**Keywords:** QT variability; RR variability; QT variability index; underlying heart rate; sequential analysis of regression variance

## 1. Introduction

Despite all the recent technological and biochemical advances, evaluation of a standard 12-lead electrocardiogram (ECG) remains an essential diagnostic procedure. Among other aspects, the importance of ECG-based diagnostic tools is evident in population wide screening programmes in which the ease and low cost of ECG acquisition offers many practical advantages compared to more innovative investigations [1–3]. Naturally, electrocardiography also benefits from technological progress and different signal processing methods are being developed to assist ECG-based diagnoses well beyond the conventional visual interpretation [4–6].

One of these ECG processing technologies is based on the temporal measurement of beat-to-beat QT interval variability. The recent position statement by the European Heart Rhythm Association has shown that increased QT interval variability appears to be a risk marker of arrhythmic and cardiovascular death [7]. Indeed, the risk diagnostic value of QT interval variability has been reported in patients with cardiomyopathy [8,9], in long QT syndrome patients [10,11], in recipients of automatic implantable cardioverter defibrillators [12,13] as well as in a variety of other clinically and pathologically defined conditions [14–16].

In a number of previous studies, longer ECG recordings have been used [7]. Nevertheless, such recordings are not entirely realistic for wide screening purposes or indeed for day-to-day clinical practice. This is well recognised [17] and studies using ECG of standard 10-second duration for the investigation of QT variability have been reported including a proposal of normal physiologic values [18,19].

Lesser attention has been paid to the physiologic intra-subject variability of 10-second QT variability and to the physiologic correlates of different indices used to express short-term QT variability although reports have been published of poorer reproducibility of 10-second QT variability in comparison to the stability of other short-term ECG indices [18]. In particular, it has not been systematically researched whether the underlying heart rate and/or the underlying short-term variability of beat-to-beat intervals influences the QT variability and whether, in these respects, any noticeable differences exist between different measurement metrics that have previously been proposed to express the QT interval variability. The lack of understanding of heart rate influence on QT beat-to-beat variability contrasts the overwhelming knowledge on heart rate influence on QT interval duration. While corrections of QT interval duration for the underlying heart rate have now existed for a century [20,21], no such methodology exists for beat-to-beat QT variability.

Since such physiologic correlates of QT interval variability may influence the diagnostic and risk-prediction potency of the measurements and, since such correlates might need to be considered in future clinical studies, we have conducted a study investigating the rhythm-related correlates and reproducibility of 10-second QT variability in a large dataset of ECG recordings obtained during clinical pharmacology studies of healthy volunteers.

## 2. Methods

### 2.1. Investigated Population and Electrocardiographic Recordings

Clinical pharmacology studies conducted at 3 different locations enrolled 523 healthy volunteers including 259 females, with no statistical age differences between females and males ( $33.4 \pm 9.1$  years vs.  $33.7 \pm 7.8$  years). Before study enrolment, all the volunteers had a normal standard clinical ECG and normal clinical investigation. Standard inclusion and exclusion criteria mandated for Phase I pharmacology studies [22] were used including negative recreational substances tests and negative pregnancy tests for females. The populations of the studies were based on standard calls for participation at pharmacology studies; no requirements on physical fitness and/or athletic training were made. All the source studies were ethically approved by the institutional ethics bodies (Parexel in Baltimore; California Clinical Trials in Glendale; and Spaulding in Milwaukee) and all subjects gave informed written consent to study participation and to scientific investigation of data collected during the studies.

In all volunteers, repeated long-term 12-lead Holter ECG recordings with Mason–Likar electrode positions were obtained covering the full day-time periods during which the subjects were not allowed to smoke and/or consume alcohol or caffeinated drinks. Those Holter recordings that were collected during days when the subjects were on no medication were analysed in the present study. The protocols of the different studies were also mutually consistent in respect of the clinical conduct during the drug-free baseline days. Since only drug-free data were used in the present investigation, further details of the source pharmacology studies are of no relevance.

Using previously described methods [23,24], multiple 10-second ECG segments were extracted from the long-term ECGs. The segments were selected with the aim of capturing different heart rates available in the Holter recording. That is, in addition to ECG segments obtained during protocol pre-specified study time-points, the complete day-time Holter recordings were scanned to obtain heart rates of all measurable 10-second extractions. From these, ECG segments were selected so that in each recording, the complete range of heart rates was uniformly covered [24]. All the extracted 10-second segments contained only sinus rhythm recordings and were free of any ectopic beats.

In each of these ECG segments, the QT interval was measured following published procedures [23,24] that included repeated visual controls of all the measurements and assurance that corresponding ECG morphologies were interpreted in a consistent way [25]. The visually verified QT interval measurements were made in the representative median waveforms of the 10-second segments (sampled at 1000 Hz) with the superimposition of all 12 leads on the same isoelectric axis [26,27]. In more detail: The QRS onset and T wave offset points were initially generated by validated signal processing algorithms applied to each extracted 10-second ECG segment. Subsequently, these positions were projected on the superimposed representative waveforms and their positions were checked by two independently working cardiologists. These checks were made on computer screens with a display resolution of 1 millisecond per 1 pixel. Where necessary, the cardiologists used the graphics displays to correct the QRS onset and T wave offset positions manually. When the two cardiologists disagreed, a senior third cardiologist reconciled their differences. In this way, systematically consistent positions of the QRS onset and T wave offset were obtained for the representative waveform of each extracted ECG segment.

### 2.2. Beat-to-Beat QT Interval Measurements

Using a previously proposed technique [28,29], QT interval was projected to individual beats within the 10-second ECG by finding the maximum correlation between the representative waveform (in which the original measurement was made) and the signal of individual QRS-T complexes. The maximum correlations were identified separately for the surroundings of the QRS onset and of the T wave offset. Since it has previously been observed that this process might lead to slightly different results when applied to different ECG leads [30], the cross-correlation technique was applied to the vector magnitude of algebraically reconstructed orthogonal leads [31]. ECG segments were excluded from analysis if noise pollution prevented the beat-to-beat measurements of the QT interval to be made reliably.

### 2.3. QT Interval Variability Expressions

In each 10-second ECG, heart rate was measured in beats per minute (bpm) based on the average duration of all RR intervals. For the purposes of investigating the QT interval variability and its physiological correlates, a further 6 indices were obtained for each 10-second ECG:

- Standard deviation of all RR intervals (SDRR),
- Coefficient of variance of RR intervals ( $RR_{cvar} = SDRR/\overline{RR}$ , where  $\overline{RR}$  is the average of all RR intervals),
- Standard deviation of all QT intervals in individual beats (SDQT),
- Coefficient of variance of QT intervals ( $QT_{cvar} = SDQT/\overline{QT}$ , where  $\overline{QT}$  is the average of all QT intervals),
- Proportion of QT and RR interval variances ( $QT_{var}/RR_{var} = SDQT^2/SDRR^2$ ),
- QT variability index ( $QTVi = QT_{cvar}^2/RR_{cvar}^2$ ).

Of these indices, the QT variability index was the first index to be introduced [28] and is perhaps the most frequently used QT variability expression [7] although it includes not only QT interval but also the RR interval variability.

#### 2.4. Data Investigations

To investigate the heart rate effects and the correlates of the different indices, the available data of the described indices were used in the following investigations.

##### 2.4.1. Effects of Heart Rate

To investigate the effect of heart rate in principle, averages of the 6 indices were obtained, in each study subject separately, for ECGs with heart rate between 50 and 75 bpm and for ECGs with heart rates between 75 and 100 bpm. Cumulative distributions of these averages were produced.

##### 2.4.2. Influence of Age

For each index, the intra-subject averages of the indices obtained for heart rate ranges of 50–75 and 75–100 bpm were related to the age of the subjects. Linear regressions were used to investigate the relationship.

##### 2.4.3. Intra-Subject Variability

In each study subject, standard deviations of the indices were also obtained for heart rate ranges of 50–75 and 75–100 bpm. These were used to obtain the intra-subject coefficient of variances of each index in these heart rate bands. Similar to the intra-subject means of the indices, the cumulative distributions of the intra-subject coefficient of variances were constructed.

##### 2.4.4. Intra-Subject and Inter-Subject Relationship between the Indices

Firstly, within the data of each subject separately, Spearman rank correlations were calculated between selected pairs of the indices. The cumulative distributions of the correlation coefficients were constructed.

Secondly, to investigate the proportional relationship between different indices (including the heart-rate relationship), sequential analysis of regression variance was used. That is, when investigating how a combination of indices A and B relates to index Z, we considered a multivariable linear regression  $Z = \beta_0 + \beta_1A + \beta_2B + e_{AB}$ , and compared the regression residuals  $e_{AB}$  of this regression model with the residuals of univariable regressions  $Z = \xi_0 + \xi_1A + e_A$  and  $Z = \zeta_0 + \zeta_1B + e_B$  (where  $\beta_i$ ,  $\xi_i$ , and  $\zeta_i$  are numerical coefficients obtained by solving the standard linear regression equations, and  $e_{\bullet}$  are zero centred normally distributed residuals). These linear regressions were obtained for each subject separately. If, in the study population, the proportions  $(e_A - e_{AB})/e_A$  were smaller than the proportions  $(e_B - e_{AB})/e_B$ , it was concluded that the index Z was influenced by index A more than by index B. This is because the proportion  $(e_A - e_{AB})/e_A$  shows how much of the residual  $e_A$  (i.e., a residual left after applying the regression of Z to A) can be explained by further regression to B. Where dictated by the definition of index Z, the values of indices A or B were replaced by their reciprocal values  $1/A$  or  $1/B$  in the regression equations.

Similar considerations were made when considering three predictor indices A, B, and C. Residuals  $e_{ABC}$  of linear regression  $Z = \beta_0 + \beta_1A + \beta_2B + \beta_3C + e_{ABC}$  were used as a reference in comparisons between  $(e_A - e_{ABC})/e_A$  and  $(e_B - e_{ABC})/e_B$ , between  $(e_{AB} - e_{ABC})/e_{AB}$  and  $(e_{AC} - e_{ABC})/e_{AC}$ , and likewise for further combinations of predictor indices.

### 2.5. Statistics and Data Presentation

Descriptive data are presented as means  $\pm$  SD. Comparisons between females and males were based on a two-sample two-tail *t*-test assuming different variations between compared datasets. Within-subject comparisons (e.g., comparisons of the indices between the two heart rate bands, or comparisons between coefficients of variance of different indices) were based on a paired two-tail *t*-test. The significance of linear regression slopes between age and the investigated indices was tested using the Fisher–Snedecor F distribution. The comparisons between the proportions of regression residuals used non-parametric paired Wilcoxon test. The calculation of the multivariable linear regressions repeated in different study subjects utilised in-house matrix manipulation software package programmed in C++. Statistical tests used IBM SPSS package, version 27. *p* values below 0.05 were considered statistically significant. Because of interdependence between the different indices, no correction for multiplicity of statistical testing was made.

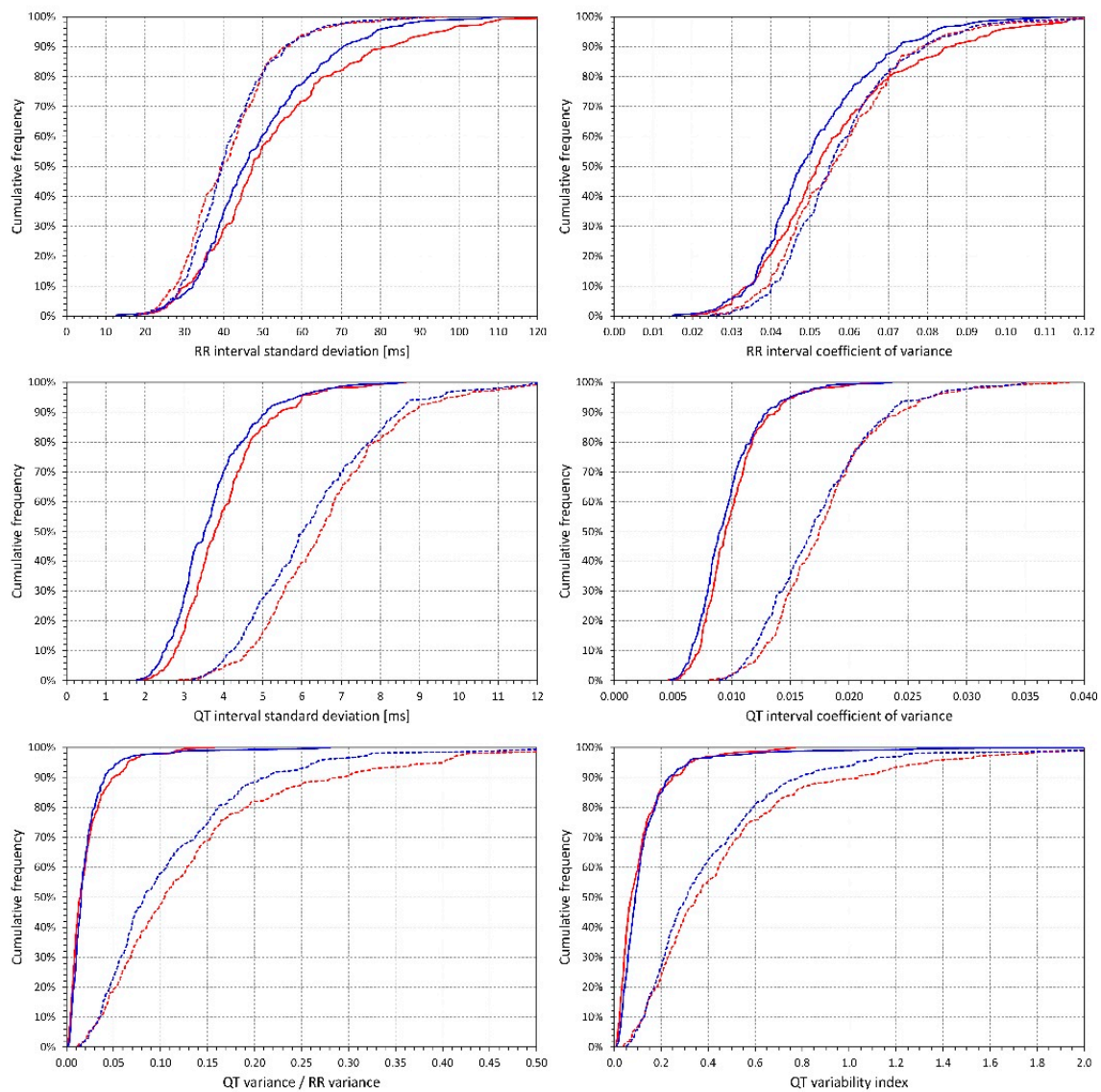
### 3. Results

The analyses of the study were based on the total of 657,287 individual 10-second ECG samples in which reliable beat-to-beat QT interval measurements were made (only 1.1% of the original data in which QT interval measurement was made and visually confirmed in the representative waveform had to be excluded because of problems with beat-to-beat measurements). On average, there were  $1247 \pm 221$  and  $1266 \pm 218$  ECG segments processed in female and male subjects (no significant differences between the sex groups).

Figure 1 shows the cumulative distributions of the 6 indices measured in ECGs of the two heart rate bands. In all indices with the exception of 10-second RR interval coefficient of variance, the heart rate effect was highly statistically significant in both sexes ( $p < 0.00001$  for all the comparisons). The difference of the  $RR_{cvar}$  values in the two heart rate bands was only significant in males ( $p < 0.00001$ ) but was not significant in females. The only significant sex differences were larger SDRR and  $RR_{cvar}$  in females at heart rates 50–75 bpm ( $p = 0.02$  and  $0.002$ , respectively) and larger SDQT in females at both heart rate bands ( $p = 0.002$  for 50–75 bpm, and  $p = 0.02$  for 75–100 bpm).

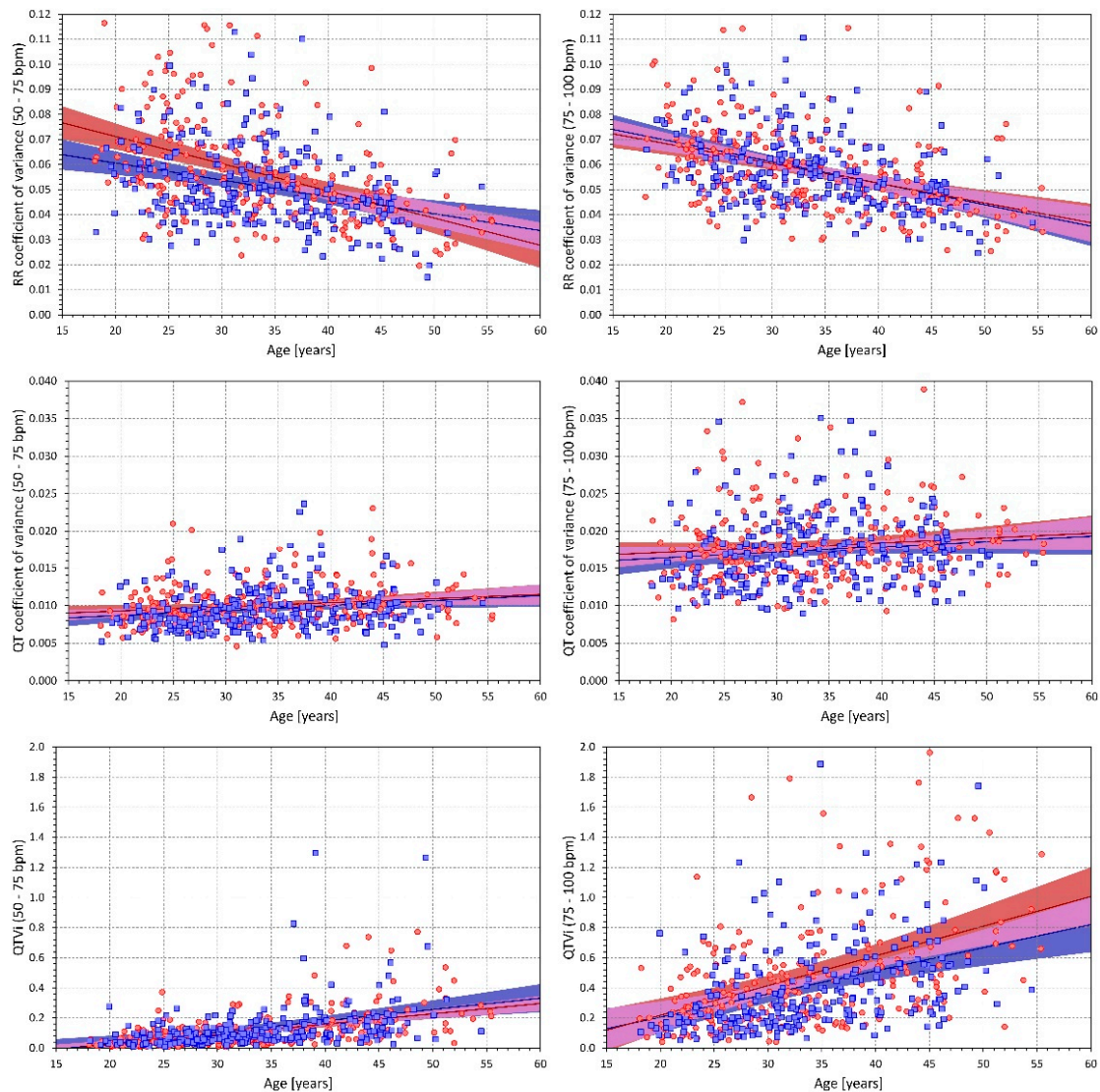
All the indices, except for  $QT_{cvar}$  at heart rates of 75–100 bpm, were statistically significantly related to age (both in females and males, with *p* values ranging from 0.005 to  $<0.00001$ ). While RR variability (both SDRR and  $RR_{cvar}$ ) decreased with age, the other QT variability indices increased with age. While generally, the increase of QT variability with advancing age was moderate, it was stronger for the data measured at 75–100 bpm compared to 50–75 bpm. Figure 2 shows scatter diagrams of the relationship with age for  $RR_{cvar}$ ,  $QT_{cvar}$ , and QT variability index. From the practical point of view, a steep relationship to age was observed for the QT variability index measured at heart-rates of 75–100 bpm where it reached 0.020 and 0.015 increases of the index for each year of age in females and males, respectively. While the slopes of the SDQT related to age were statistically significant, they were rather shallow.

The distributions of intra-subject coefficients of variance of the different indices are shown in Figure 3. As seen in the figure, the measurements of SDQT and  $QT_{cvar}$  were, within individual subjects, more reproducible than the measurements of SDRR and  $RR_{cvar}$  which, in turn, were more reproducible than the  $QT_{var}/RR_{var}$  ratio or the QT variability index. All these differences were highly statistically significant in both sexes (all  $p < 0.00001$ ). In addition to these principal reproducibility results, we also observed that SDRR,  $RR_{cvar}$ ,  $QT_{var}/RR_{var}$  ratio, and the QT variability index were less reproducible at the higher heart rates 75–100 bpm compared to the lower heart rates of 50–75 bpm (again, all  $p < 0.00001$ ). At the slower heart rate of 50–75 bpm, the  $QT_{var}/RR_{var}$  ratio, and QT variability index were also less reproducible in males compared to females (both  $p < 0.00001$ ) but this difference was not present at the higher heart rates. Further differences shown in the distribution graphs of Figure 3 were occasionally also statistically significant but were numerically minimal and, thus, without obvious implications.

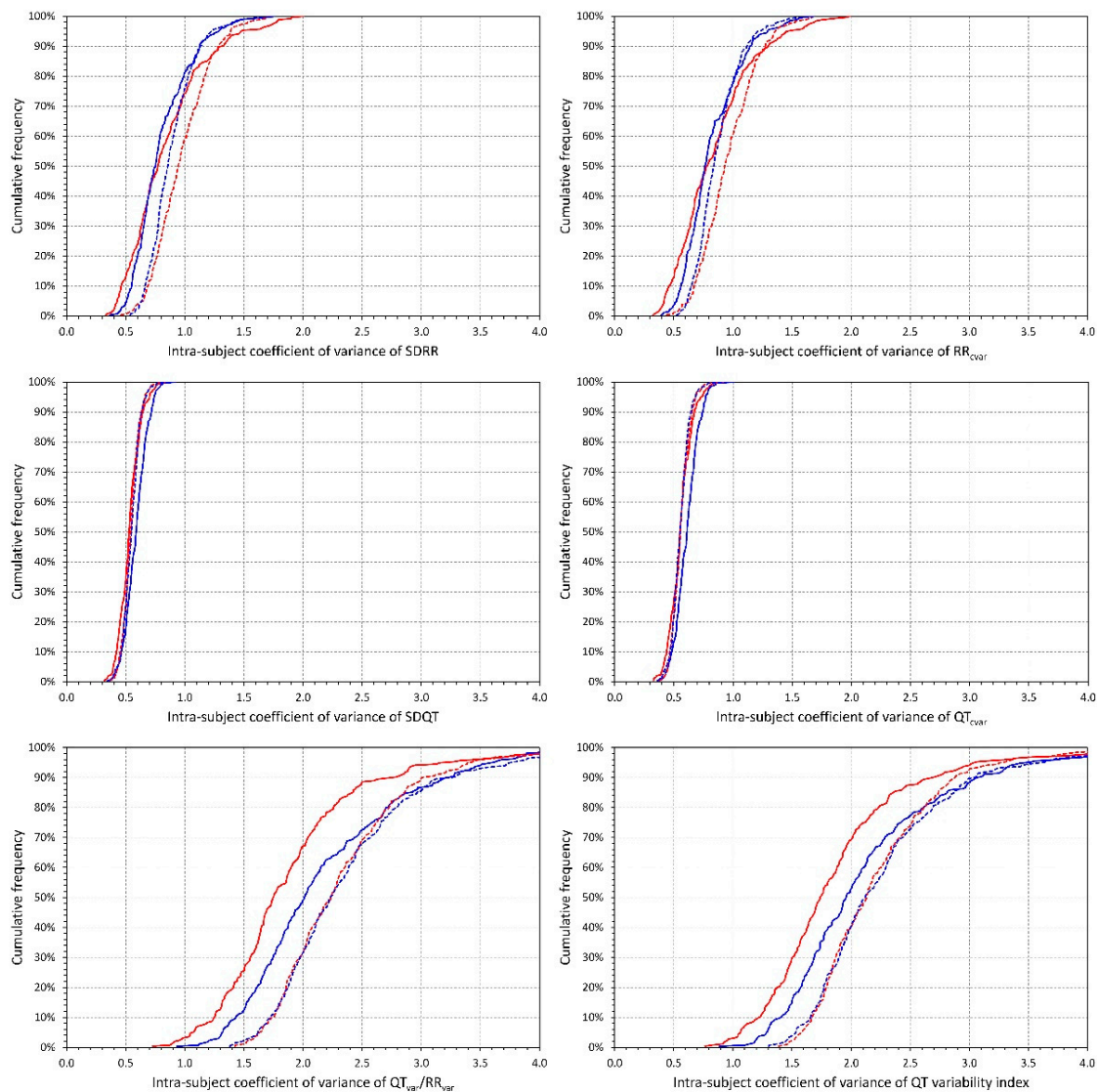


**Figure 1.** Values of measured indices. For each of the investigated indices (see the labels of the horizontal axes of individual panels) the figure shows the cumulative distributions of intra-subject means calculated over electrocardiograms (ECGs) with heart rate between 50 and 75 bpm (full lines) and between 75 and 100 bpm (dashed lines). The red and blue lines correspond to female and male subjects, respectively.



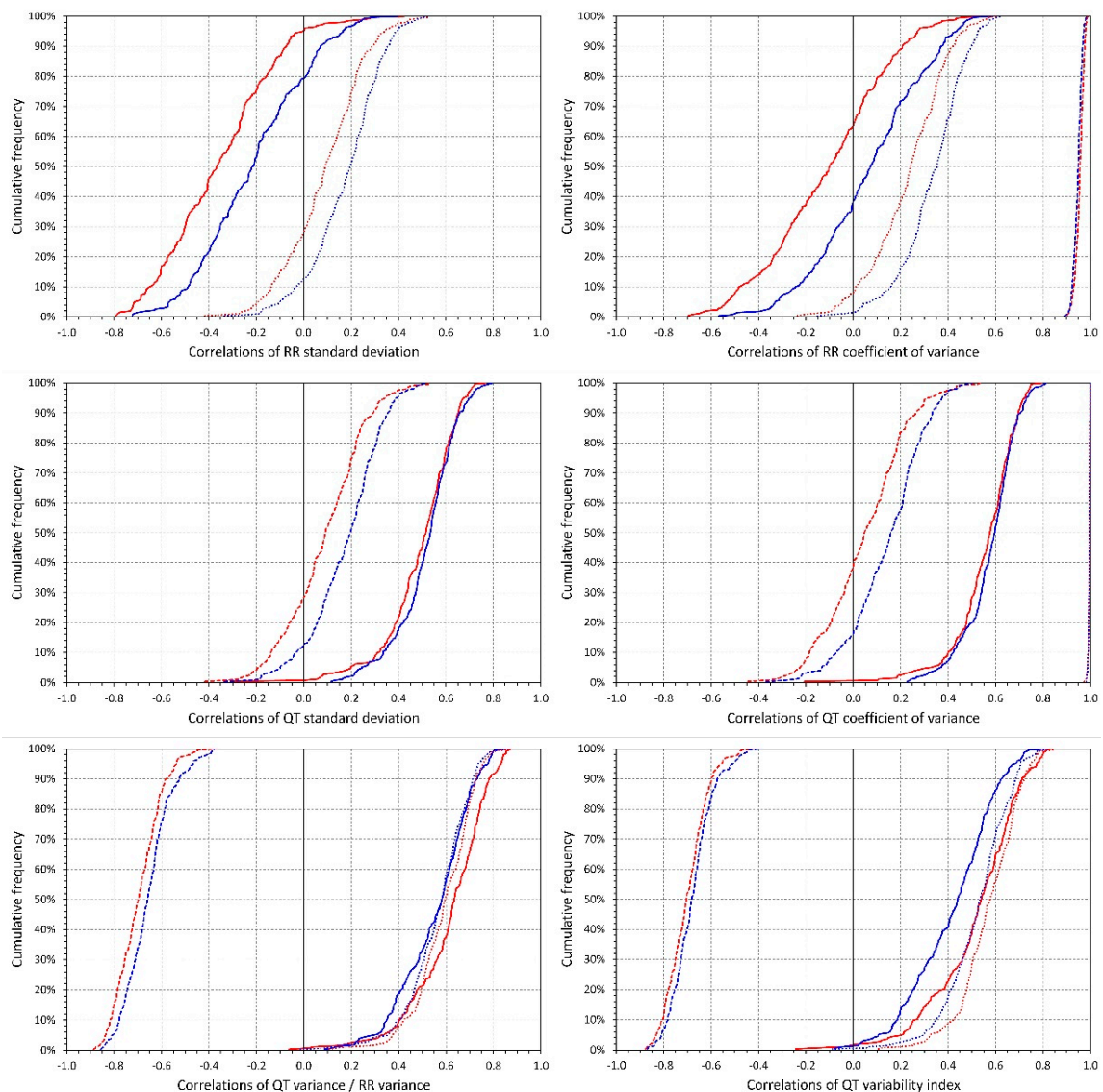


**Figure 2.** Relationship to age. Scatter diagrams of the relationship between age of the study subjects (horizontal axes) and RR interval coefficient of variance (top panels), QT coefficients of variance (middle panels), and QT variability index (bottom panels). The panels on the left and on the right show the relationship of age to intra-subject means calculated over ECG with heart rate between 50 and 75 bpm and between 75 and 100 bpm, respectively. In each panel, the red circles and blue squares correspond to female and male subjects, respectively. The solid red and solid blue lines show the linear regressions between the ages and the intra-subject mean values. The red shaded and blue shaded areas are the 95% confidence bands of the regression lines; the violet areas are the overlaps between the confidence bands of the sex-specific regressions.



**Figure 3.** Intra-subject coefficients of variance. For each of the investigated indices (see the labels of the horizontal axes of individual panels) the figure shows the cumulative distributions of intra-subject coefficient of variance of the given index calculated over ECGs with heart rate between 50 and 75 bpm (full lines) and between 75 and 100 bpm (dashed lines). The red and blue lines correspond to female and male subjects, respectively.

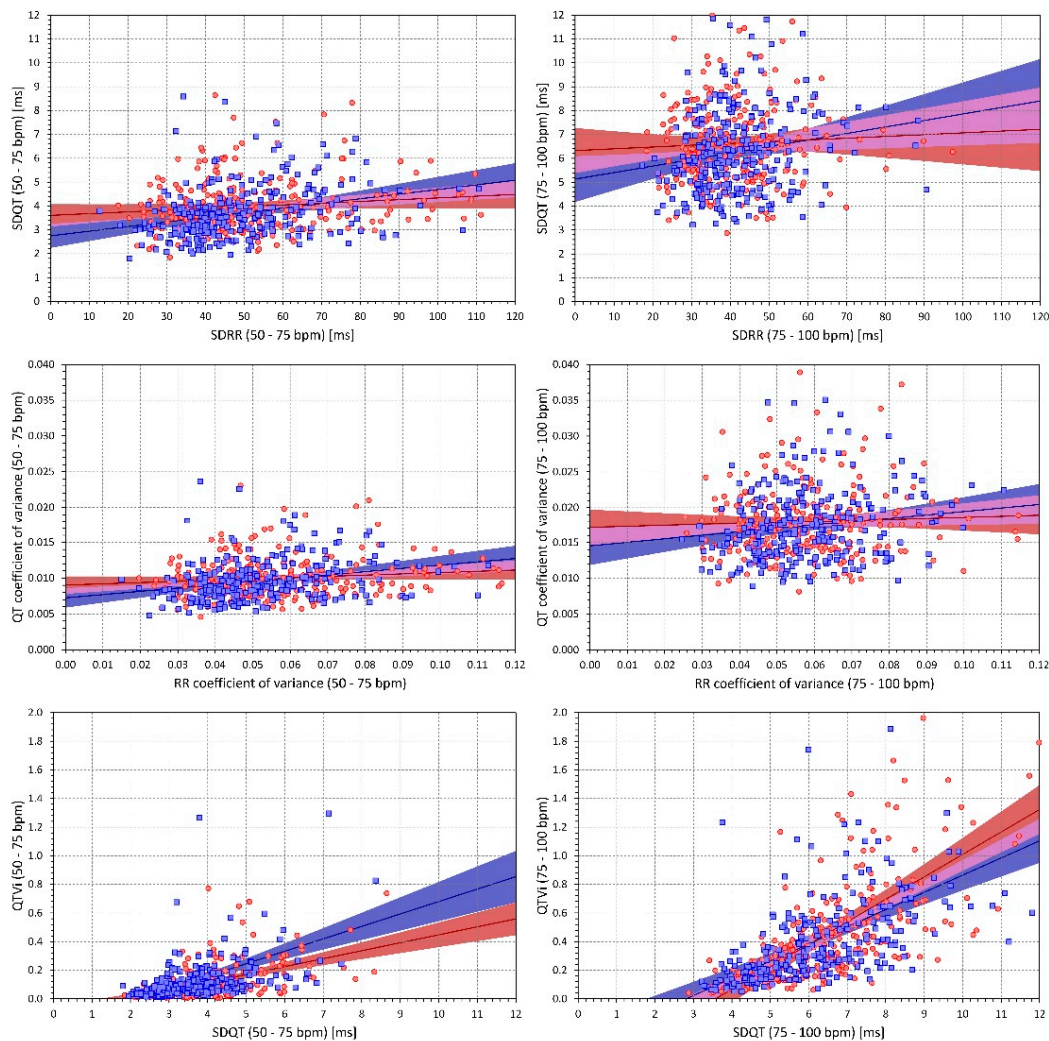
Figure 4 shows the distributions of intra-subject rank correlation coefficients between selected indices. Importantly, with the exception of  $RR_{cvar}$ , all the indices were systematically related to heart rate. While the SDRR decreased with increasing rate, SDQT,  $QT_{cvar}$ ,  $QT_{var}/RR_{var}$  ratio, and the QT variability index were all systematically increasing with increasing heart rate. As expected,  $QT_{var}/RR_{var}$  ratio and QT variability index were also, within each subject, positively correlated with SDQR and negatively correlated with SDRR. Figure 5 shows scatter diagrams between intra-subject means of selected indices. (Note that while the data shown in Figure 5 are individual means—each subject is represented by one marker—the correlation coefficients summarised in Figure 4 were calculated within each subject separately). Again, as expected, a strong relationship between SDQT and the QT variability index is seen also at the population level—especially at the higher heart rates 75–100 bpm. Figure 5 should not be interpreted as a suggestion of “correctable” relationships (note the large spreads of the individual points). Rather, the figure demonstrates the differences in the strength of the relationships between different indices and the heart rate influence on these relationships.



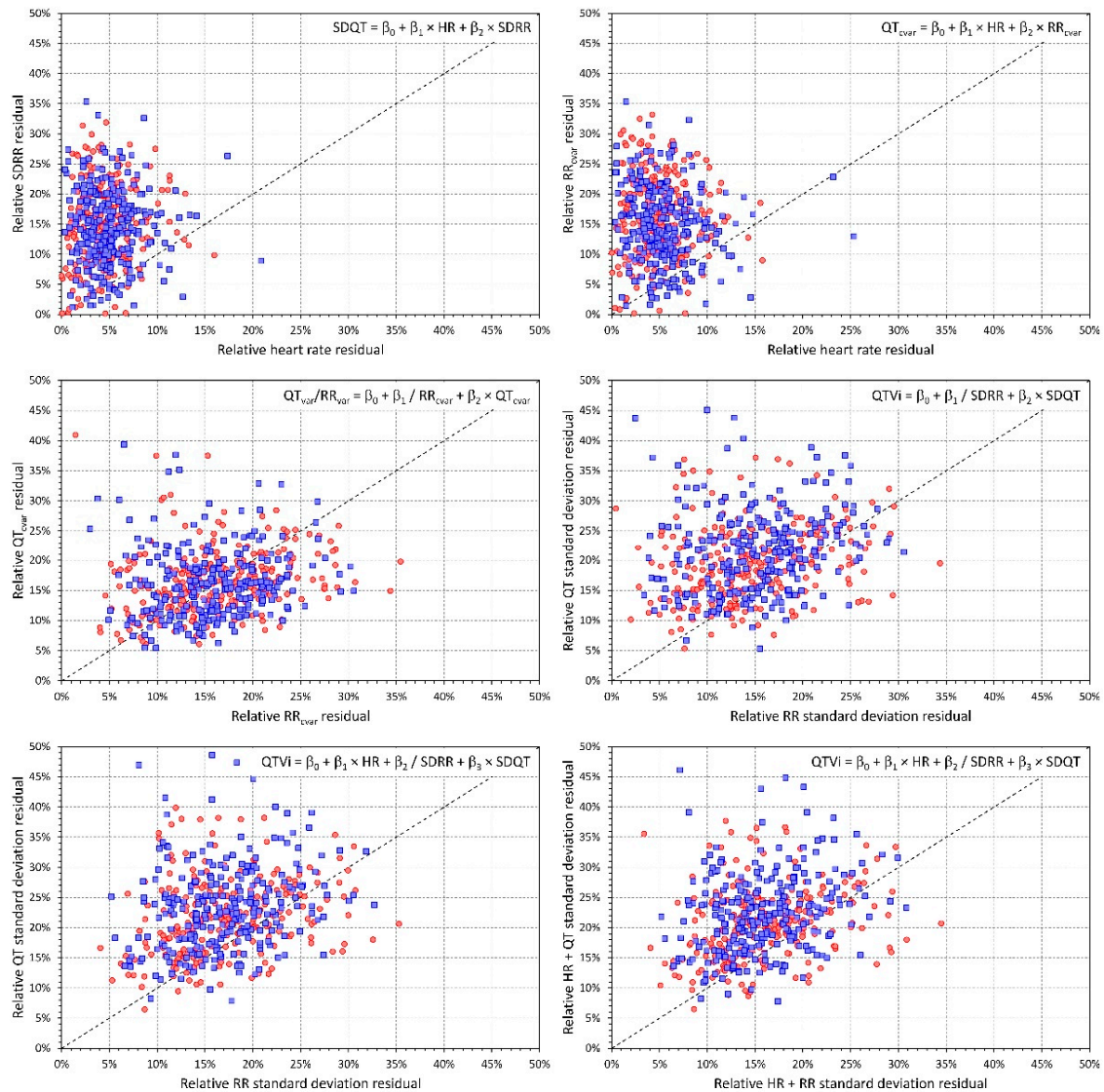
**Figure 4.** Intra-subject rank correlations. For each of the investigated indices (see the labels of the horizontal axes of individual panels) the figure shows the cumulative distributions of intra-subject Spearman rank correlation coefficients (calculated over all available ECGs in the given subject) between the given index and the underlying heart rate (full lines), standard deviation of RR intervals (dashed line), and standard deviation of QT intervals (dotted line). The red and blue lines correspond to female and male subjects, respectively.

The results of the sequential analysis of the regression variance are shown in Figure 6. The top panels of the figure show that within individual subjects, the SDRR and  $QT_{cvar}$  are more strongly influenced by heart rate than by the short-term RR variability represented by SDRR and  $RR_{cvar}$ . In both cases, the relative regression residuals were much larger for SDRR than for heart rate ( $p < 0.00001$  for both sexes in both cases). The same results with the same strong statistical significances were obtained when considering regressions  $QT_{cvar} = \beta_0 + \beta_1 \times HR + \beta_2 \times SDRR$  and  $SDQT = b_0 + b_1 \times HR + b_2 \times RR_{cvar}$ . The left middle panel of the figure shows that when relating the  $QT_{var}/RR_{var}$  ratio to both  $QT_{cvar}$  and the reciprocal of  $RR_{cvar}$ , there was only a non-significant trend towards larger relative residuals left by  $QT_{cvar}$ . The middle right panel shows that the QT variability index was more strongly influenced by the reciprocal of SDRR than by SDQT ( $p < 0.00001$  in both sexes). Similar results were obtained when relating the QT variability index to a combination of heart rate, reciprocal of SDRR and SDQT

(the bottom panels of Figure 6). Relative residuals left by the reciprocal of SDRR were lower than those left by SDQT and similarly, relative residuals left by a regression combination of heart rate and the reciprocal of SDRR were lower than those left by a combination of heart rate and SDQT (all the comparisons in these cases gave  $p < 0.00001$  for both sexes). Note that the panels of Figure 6 also allow visual comparisons—when the majority of the points (each representing the relative residuals in the ECGs of one individual subject) appear above the line of identity, the influence of the predictor (or predictors) shown on the horizontal axis is stronger than the influence of the predictor(s) shown on the vertical axis.



**Figure 5.** Inter-subject relationship of the measured indices. Scatter diagrams of the inter-subject relationships between intra-subject means of SDRR and SDQT (panels on the top),  $RR_{cvar}$  and  $QT_{cvar}$  (panels in the middle), and SDQT and QT variability index (panels at the bottom). Panels at the left and on the right show the indices calculated over ECGs with heart rates 50–75 bpm and 75–100 bpm, respectively. In each panel, the red circles and blue squares correspond to female and male subjects, respectively. The solid red and solid blue lines show the linear regressions between the intra-subject mean values of the compared indices. The red shaded and blue shaded areas are the 95% confidence bands of the regression lines; the violet areas are the overlaps between the confidence bands of the sex-specific regressions.



**Figure 6.** Sequential analysis of the regression variance. Results of the sequential analysis of the regression variance (see the text for details). Each panel corresponds to a given linear regression estimate (see the formulas at the top right of the panels) and shows the relative residuals, that is the proportions  $(e_A - e_{AB})/e_A$  or  $(e_{AB} - e_{ABC})/e_{AB}$  as explained in the text. Scatter diagrams in the separate panels show the relationship between relative residuals of predictors used in the multivariable regression. The labels of the axes have the form “Relative A residuals” or “Relative A+B residuals” meaning the proportions  $(e_A - e_{AB})/e_A$  or  $(e_{AB} - e_{ABC})/e_{AB}$ . In each panel the dashed line shows the line of identity. In each panel, the red circles and blue squares correspond to female and male subjects, respectively (note that the multivariable linear regressions and their residuals regressions were evaluated in each subject separately using all the ECGs available for the given subject).

#### 4. Discussion

The study leads to three distinct observations that all appear to be of practical importance. Firstly, the study shows convincingly that in healthy subjects, the different indices used in the vast majority of studies reporting QT interval variability [7] are all strongly related to the underlying heart rate. Secondly, while the QT variability index is the most popular numerical expression of QT interval variability, we have also observed that it is substantially less reproducible compared to the simpler expressions such as the standard deviation of the QT intervals. Finally, we have also noted that among the investigated indices of QT variability, the QT variability index was most strongly related to age

of healthy subjects. The reason for this age dependency is likely based on the age-related decline of RR variability.

Since its inception [28], it has been understood that QTVi is a combination of both QT and RR interval variability. The somewhat surprising aspect of our results is the proportion of the influences based on the sequential analysis of the regression variance. As shown in Figure 6, the RR interval variability is the dominant determinant of QTVi while the QT interval variability provides only a secondary influence. This needs to be considered together with our other finding that shows that the underlying heart rate rather than RR variability drives the QT variability measured by SDQT or QT<sub>cvar</sub>. These observations have clear implications for further utility and research of QTVi. Many studies have repeatedly shown the risk-prediction capability of QTVi [32–36]. Nevertheless, both increased heart rate [37,38] and decreased heart rate variability [39,40] are well recognised strong risk factors. Since, as we demonstrated, both increased heart rate and decreased RR variability increase the QTVi values, it is legitimate to ask to which extent the QTVi-based risk prediction is driven by true QT variability. While combinations of different factors into composite measures and/or scoring systems are valid methods for prospective diagnostic and risk studies, physiologic understanding and diagnostic utility of QT interval variability can be masked by its combination with other risk factors especially if these factors influence the combined values as strongly as we have shown. Still, if QTVi values are used in future prospective studies, the strong relationship to age needs to be considered; different diagnostic dichotomy limits are needed for different age groups.

Therefore, we are of the opinion that future investigative studies of QT variability would be better served by using simpler expressions of QT variability, such as the standard deviation of individual QT interval durations. This is also supported by our observation that SDQT showed substantially tighter intra-subject reproducibility compared to QTVi. (Note, however, that intra-subject coefficients of variance of around 50% to 60% as shown in Figure 3 for SDQT indicate still fairly variable results albeit much more stable compared to coefficient of variance around 200% that we observed for QTVi). Nevertheless, even with SDQT or QT<sub>cvar</sub>, the influence of heart rate still needs to be considered. Multivariable analyses involving the QT variability indices together with the underlying heart rate may be proposed.

QT variability assessment has already been implemented in commercial Holter systems [41]. It can, therefore, be advocated that future clinical risk-assessment studies combine the simpler QT variability indices with other risk-stratification techniques ranging from heart rate variability [42] and heart rate turbulence [43,44] to deceleration capacity [45] and T wave alternans [46]. As all these indices can be obtained from the same Holter recordings, their multivariable comparisons and combinations might be applied to a variety of clinically well-defined populations. Implementation of the simpler expressions of QT variability should also be possible in standard bedside models of ECG equipment (which already report the underlying rate).

There is little independent data available which we could use to validate our principal results, especially those obtained by the sequential analysis of the regression variance. Other observations made in the study appear to agree with previous publications. The observation of larger SDRR in females compared to males that we observed at slower but not faster heart rates is consistent with reports of sex differences in frequency components of heart rate variability during resting but not during sympathetically stimulating conditions [47]. The larger SDQT values in females are likely related to the sex difference in QT interval duration since there was comparatively lesser difference observed with QT<sub>cvar</sub>. Because of the substantial heart rate influence on the measured QT variability indices, we are also unable to compare our measurements with previously published normal values [19]. Ranges and distributions of the values that we have measured for the different indices are shown in Figure 1 including their changes due to the heart rate differences.

Since the QT variability index is predominantly influenced by beat-to-beat RR interval differences, its relationship to age most likely expresses the age-related decline of heart rate variability [42] rather than the age-associated changes of QT interval duration [48].

## 5. Limitations

Limitations of our study also need to be considered. While a number of previous QT variability studies used longer ECGs, we concentrated on 10-second ECG segments because these are more relevant for practical purposes. This also means that we are unable to comment on whether the very same observations would be obtained also with longer recordings. Nevertheless, since every longer recording is, in principle, a series of shorter segments, it is unlikely that with longer ECGs, our results would be very different. Although we have accepted beat-to-beat QT interval measurements only when a closed fit was found between the individual beat images and the representative median waveforms, some residual influence of ECG noise cannot be excluded entirely. Since ECG noise can be expected to increase with physical activity which, in turn, leads to increased heart rates, our observations of heart rate influence might have been overestimated. However, since positive intra-subject correlations between heart rate and the QT variability indices were found in practically every subject of the study (see Figure 4) any noise-related overestimating of the heart rate dependency might have only been marginal. The investigated population included neither very young nor very old subjects. The investigations of the relationship to age were, therefore, limited to the available age ranges. Finally, since the study data were obtained from clinical pharmacology investigations in healthy subjects, we are unable to comment on whether the same results would have been found if researching populations with clinically well-defined pathological characteristics. Nevertheless, our observations still have an impact on clinical studies in the same way as other physiologic characteristics influence clinical investigations and diagnoses. In particular, while increased QT variability has previously been reported in different studies of congenital long QT syndrome patients [7], we cannot comment on the heart rate influence of QT variability in these patients. Similarly, we cannot comment on whether multivariable QT variability and heart rate assessment could serve the diagnostics of acquired (e.g., drug-induced) long QT syndrome [49] and whether it might increase the power of relevant clinical studies [50].

## 6. Conclusions

Despite these limitations, the study shows that the underlying heart rate and the underlying RR interval variability are crucial determinants of the standard indices of QT interval variability. This influence is of particular importance for future applications of the popular QT variability index which is less influenced by true QT variability than it is by the heart rate and RR interval characteristics. The QT variability index also shows substantially low intra-subject reproducibility. Simpler expressions of QT interval variability such as the standard deviation of QT interval duration in individual beats might be preferable in future applications especially if multivariable combination with the underlying heart rate is used.

**Author Contributions:** Study design—I.A., K.H., M.M., Software development—K.H., M.M., ECG interpretation—G.S., I.A., K.M.H., M.Š., O.T., P.B., P.S., T.N. ECG measurement—G.S., I.A., K.M.H., M.Š., O.T., P.B., P.S., T.N. Supervision of the measurements—G.S., T.N., O.T., P.S. Quality control of the measurements—G.S., M.M., T.N. Statistics and figures—K.H., M.M. Initial manuscript draft—I.A., K.H., M.M. Final manuscript—G.S., I.A., K.H., K.M.H., M.M., M.Š., O.T., P.B., P.S., T.N. Approval of the submission—G.S., I.A., K.H., K.M.H., M.M., M.Š., O.T., P.B., P.S., T.N. All authors have read and agreed to the published version of the manuscript.

**Funding:** Supported in part by the British Heart Foundation New Horizons Grant NH/16/2/32499, by Ministry of Health, Czech Republic, conceptual development of research organization (Grant FNBr/65269705), and by the Specific Research of Masaryk University MUNI/A/1446/2019.

**Conflicts of Interest:** The authors declare no conflict of interest.

## References

1. US Preventive Services Task Force; Curry, S.J.; Krist, A.H.; Owens, D.K.; Barry, M.J.; Caughey, A.B.; Davidson, K.W.; Doubeni, C.A.; Epling, J.W., Jr.; Kemper, A.R.; et al. Screening for cardiovascular disease risk with electrocardiography: US Preventive Services Task Force recommendation statement. *JAMA* **2018**, *319*, 2308–2314. [[PubMed](#)]
2. Somsen, G.A. The role of ECG screening in primary care; a call for collaboration between general practitioner and cardiologist. *Neth. Heart J.* **2020**, *28*, 190–191. [[CrossRef](#)] [[PubMed](#)]
3. Campbell, M.J.; Zhou, X.; Han, C.; Abrishami, H.; Webster, G.; Miyake, C.Y.; Sower, C.T.; Anderson, J.B.; Knilans, T.K.; Czosek, R.J. Pilot study analyzing automated ECG screening of hypertrophic cardiomyopathy. *Heart Rhythm* **2017**, *14*, 848–852. [[CrossRef](#)] [[PubMed](#)]
4. Lyons, M.M.; Kraemer, J.F.; Dhingra, R.; Keenan, B.T.; Wessel, N.; Glos, M.; Penzel, T.; Gurubhagavatula, I. Screening for obstructive sleep apnea in commercial drivers using EKG-derived respiratory power index. *J. Clin. Sleep Med.* **2019**, *15*, 23–32. [[CrossRef](#)] [[PubMed](#)]
5. Yao, X.; McCoy, R.G.; Friedman, P.A.; Shah, N.D.; Barry, B.A.; Behnken, E.M.; Inselman, J.W.; Attia, Z.I.; Noseworthy, P.A. ECG AI-guided screening for low ejection fraction (EAGLE): Rationale and design of a pragmatic cluster randomized trial. *Am. Heart J.* **2020**, *219*, 31–36. [[CrossRef](#)] [[PubMed](#)]
6. Proietti, M.; Farcomeni, A.; Goethals, P.; Scavee, C.; Vijgen, J.; Blankoff, I.; Vandekerckhove, Y.; Lip, G.Y.; Mairesse, G.H. Belgian Heart Rhythm Week Investigators. Cost-effectiveness and screening performance of ECG handheld machine in a population screening programme: The Belgian Heart Rhythm Week screening programme. *Eur. J. Prev. Cardiol.* **2019**, *26*, 964–972. [[CrossRef](#)] [[PubMed](#)]
7. Baumert, M.; Porta, A.; Vos, M.A.; Malik, M.; Couderc, J.P.; Laguna, P.; Piccirillo, G.; Smith, G.L.; Tereshchenko, L.G.; Volders, P.G. QT interval variability in body surface ECG: Measurement, physiological basis, and clinical value: Position statement and consensus guidance endorsed by the European Heart Rhythm Association jointly with the ESC Working Group on Cardiac Cellular Electrophysiology. *Europace* **2016**, *18*, 925–944.
8. Fischer, C.; Seeck, A.; Schroeder, R.; Goernig, M.; Schirdewan, A.; Figulla, H.R.; Baumert, M.; Voss, A. QT variability improves risk stratification in patients with dilated cardiomyopathy. *Physiol. Meas.* **2015**, *36*, 699–713. [[CrossRef](#)]
9. Orosz, A.; Baczkó, I.; Nagy, V.; Gavallér, H.; Csanády, M.; Forster, T.; Papp, J.G.; Varró, A.; Lengyel, C.; Sepp, R. Short-term beat-to-beat variability of the QT interval is increased and correlates with parameters of left ventricular hypertrophy in patients with hypertrophic cardiomyopathy. *Can. J. Physiol. Pharmacol.* **2015**, *93*, 765–772. [[CrossRef](#)]
10. Porta, A.; Girardengo, G.; Bari, V.; George, A.L., Jr.; Brink, P.A.; Goosen, A.; Crotti, L.; Schwartz, P.J. Autonomic control of heart rate and QT interval variability influences arrhythmic risk in long QT syndrome type 1. *J. Am. Coll. Cardiol.* **2015**, *65*, 367–374. [[CrossRef](#)]
11. Seethala, S.; Singh, P.; Shusterman, V.; Ribe, M.; Haugaa, K.H.; Němec, J. QT adaptation and intrinsic QT variability in congenital long QT syndrome. *J. Am. Heart Assoc.* **2015**, *4*, e002395. [[CrossRef](#)] [[PubMed](#)]
12. Monasterio, V.; Martínez, J.P.; Laguna, P.; McNitt, S.; Polonsky, S.; Moss, A.J.; Haigney, M.; Zareba, W.; Couderc, J.P. Prognostic value of average T-wave alternans and QT variability for cardiac events in MADIT-II patients. *J. Electrocardiol.* **2013**, *46*, 480–486. [[CrossRef](#)] [[PubMed](#)]
13. Smoczyńska, A.; Loen, V.; Sprenkeler, D.J.; Tuinenburg, A.E.; Ritsema van Eck, H.J.; Malik, M.; Schmidt, G.; Meine, M.; Vos, M.A. Short-term variability of the QT interval can be used for the prediction of imminent ventricular arrhythmias in patients with primary prophylactic implantable cardioverter defibrillators. *J. Am. Heart Assoc.* **2020**, *9*, e018133. [[CrossRef](#)] [[PubMed](#)]
14. Orosz, A.; Csajbók, É.; Czékus, C.; Gavallér, H.; Magony, S.; Valkusz, Z.; Várkonyi, T.T.; Nemes, A.; Baczkó, I.; Forster, T.; et al. Increased short-term beat-to-beat variability of QT interval in patients with acromegaly. *PLoS ONE* **2015**, *10*, e0125639. [[CrossRef](#)] [[PubMed](#)]
15. Viigimae, M.; Karai, D.; Pilt, K.; Pirn, P.; Huhtala, H.; Polo, O.; Meigas, K.; Kaik, J. QT interval variability index and QT interval duration during different sleep stages in patients with obstructive sleep apnea. *Sleep Med.* **2017**, *37*, 160–167. [[CrossRef](#)] [[PubMed](#)]
16. Nussinovitch, U.; Rubin, S.; Levy, Y.; Lidar, M.; Livneh, A. QT variability index in patients with systemic sclerosis. *Eur. J. Rheumatol.* **2018**, *6*, 179–183. [[PubMed](#)]



17. Niemeijer, M.N.; van den Berg, M.E.; Eijgelsheim, M.; van Herpen, G.; Stricker, B.H.; Kors, J.A.; Rijnbeek, P.R. Short-term QT variability markers for the prediction of ventricular arrhythmias and sudden cardiac death: A systematic review. *Heart* **2014**, *100*, 1831–1836. [[CrossRef](#)]
18. Feeny, A.; Han, L.; Tereshchenko, L.G. Repolarization lability measured on 10-second ECG by spatial TT' angle: Reproducibility and agreement with QT variability. *J. Electrocardiol.* **2014**, *47*, 708–715. [[CrossRef](#)]
19. van den Berg, M.E.; Kors, J.A.; van Herpen, G.; Bots, M.L.; Hillege, H.; Swenne, C.A.; Stricker, B.H.; Rijnbeek, P.R. Normal values of QT variability in 10-s electrocardiograms for all ages. *Front. Physiol.* **2019**, *10*, 1272. [[CrossRef](#)]
20. Bazett, J.C. An analysis of time relations of electrocardiograms. *Heart* **1920**, *7*, 353–367. [[CrossRef](#)]
21. Fridericia, L.S. Die Systolendauer im Elektrokardiogramm bei normalen Menschen und bei Herzkranken. *Acta Med. Scand.* **1920**, *53*, 469–486. [[CrossRef](#)]
22. ICH Guideline. Safety pharmacology studies for human pharmaceuticals S7A. *Fed. Regist.* **2001**, *66*, 36791–36792.
23. Malik, M.; Andreas, J.-O.; Hnatkova, K.; Hoeckendorff, J.; Cawello, W.; Middle, M.; Horstmann, R.; Braun, M. Thorough QT/QTc Study in patients with advanced Parkinson's disease: Cardiac safety of rotigotine. *Clin. Pharmacol. Ther.* **2008**, *84*, 595–603. [[CrossRef](#)] [[PubMed](#)]
24. Malik, M.; van Gelderen, E.M.; Lee, J.H.; Kowalski, D.L.; Yen, M.; Goldwater, R.; Mujais, S.K.; Schaddelee, M.P.; de Koning, P.; Kaibara, A.; et al. Proarrhythmic safety of repeat doses of mirabegron in healthy subjects: A randomized, double-blind, placebo-, and active-controlled thorough QT study. *Clin. Pharm. Ther.* **2012**, *92*, 696–706. [[CrossRef](#)] [[PubMed](#)]
25. Hnatkova, K.; Smetana, P.; Toman, O.; Bauer, A.; Schmidt, G.; Malik, M. Systematic comparisons of electrocardiographic morphology increase the precision of QT interval measurement. *Pacing Clin. Electrophysiol.* **2009**, *32*, 119–130. [[CrossRef](#)] [[PubMed](#)]
26. Malik, M. Errors and misconceptions in ECG measurement used for the detection of drug induced QT interval prolongation. *J. Electrocardiol.* **2004**, *37*, 25–33. [[CrossRef](#)]
27. Xue, J.Q. Robust QT interval estimation—From algorithm to validation. *Ann. Noninvasive Electrocardiol.* **2009**, *14* (Suppl. 1), S35–S41. [[CrossRef](#)]
28. Berger, R.D.; Kasper, E.K.; Baughman, K.L.; Marban, E.; Calkins, H.; Tomaselli, G.F. Beat-to-beat QT interval variability: Novel evidence for repolarization lability in ischemic and nonischemic dilated cardiomyopathy. *Circulation* **1997**, *96*, 1557–1565. [[CrossRef](#)]
29. Baumert, M.; Lambert, G.W.; Dawood, T.; Lambert, E.A.; Esler, M.D.; McGrane, M.; Barton, D.; Nalivaiko, E. QT interval variability and cardiac norepinephrine spillover in patients with depression and panic disorder. *Am. J. Physiol. Heart Circ. Physiol.* **2008**, *295*, H962–H968. [[CrossRef](#)]
30. Malik, M. Beat-to-beat QT variability and cardiac autonomic regulation. *Am. J. Physiol. Heart Circ. Physiol.* **2008**, *295*, H923–H925. [[CrossRef](#)]
31. Guldenring, D.; Finlay, D.D.; Strauss, D.G.; Galeotti, L.; Nugent, C.D.; Donnelly, M.P.; Bond, R.R. Transformation of the Mason-Likar 12-lead electrocardiogram to the Frank vectorcardiogram. *Annu. Int. Conf. IEEE Eng. Med. Biol. Soc.* **2012**, *2012*, 677–680. [[PubMed](#)]
32. Hiromoto, K.; Shimizu, H.; Mine, T.; Masuyama, T.; Ohyanagi, M. Correlation between beat-to-beat QT interval variability and impaired left ventricular function in patients with previous myocardial infarction. *Ann Noninvasive Ann. Noninvasive Electrocardiol.* **2006**, *11*, 299–305. [[CrossRef](#)] [[PubMed](#)]
33. Oosterhoff, P.; Tereshchenko, L.G.; van der Heyden, M.A.; Ghanem, R.N.; Fetics, B.J.; Berger, R.D.; Vos, M.A. Short-term variability of repolarization predicts ventricular tachycardia and sudden cardiac death in patients with structural heart disease: A comparison with QT variability index. *Heart Rhythm* **2011**, *8*, 1584–1590. [[CrossRef](#)] [[PubMed](#)]
34. Haigney, M.C.; Zareba, W.; Gentlesk, P.J.; Goldstein, R.E.; Illovsky, M.; McNitt, S.; Andrews, M.L.; Moss, A., Jr. Multicenter Automatic Defibrillator Implantation Trial II investigators. QT interval variability and spontaneous ventricular tachycardia or fibrillation in the Multicenter Automatic Defibrillator Implantation Trial (MADIT) II patients. *J. Am. Coll. Cardiol.* **2004**, *44*, 1481–1487. [[CrossRef](#)]
35. Dobson, C.P.; Kim, A.; Haigney, M. QT Variability Index. *Prog. Cardiovasc. Dis.* **2013**, *56*, 186–194. [[CrossRef](#)]
36. Heravi, A.S.; Etkorn, L.H.; Urbanek, J.K.; Crainiceanu, C.M.; Punjabi, N.M.; Ashikaga, H.; Brown, T.T.; Budoff, M.J.; D'Souza, G.; Magnani, J.W.; et al. HIV infection is associated with variability in ventricular repolarization: The Multicenter AIDS Cohort Study (MACS). *Circulation* **2020**, *141*, 176–187. [[CrossRef](#)]

37. Copie, X.; Hnatkova, K.; Staunton, A.; Fei, L.; Camm, A.J.; Malik, M. Predictive power of increased heart rate versus depressed left ventricular ejection fraction and heart rate variability for risk stratification after myocardial infarction. Results of a two-year follow-up study. *J. Am. Coll. Cardiol.* **1996**, *27*, 270–276. [[CrossRef](#)]
38. Seravalle, G.; Grassi, G. Heart rate as cardiovascular risk factor. *Postgrad. Med.* **2020**, *132*, 358–367. [[CrossRef](#)]
39. Malik, M.; Hnatkova, K.; Huikuri, H.V.; Lombardi, F.; Schmidt, G.; Zabel, M. CrossTalk proposal: Heart rate variability is a valid measure of cardiac autonomic responsiveness. *J. Physiol.* **2019**, *597*, 2595–2598. [[CrossRef](#)]
40. Goldenberg, I.; Goldkorn, R.; Shlomo, N.; Einhorn, M.; Levitan, J.; Kuperstein, R.; Klempfner, R.; Johnson, B. Heart rate variability for risk assessment of myocardial ischemia in patients without known coronary artery disease: The HRV-DETECT (Heart Rate Variability for the Detection of Myocardial Ischemia) study. *J. Am. Heart Assoc.* **2019**, *8*, e014540. [[CrossRef](#)]
41. Dobson, C.P.; La Rovere, M.T.; Pinna, G.D.; Goldstein, R.; Olsen, C.; Bernardinangeli, M.; Veniani, M.; Midi, P.; Tavazzi, L.; Haigney, M. GISSI-HF Investigators. QT variability index on 24-hour Holter independently predicts mortality in patients with heart failure: Analysis of Gruppo Italiano per lo Studio della Sopravvivenza nell'Insufficienza Cardiaca (GISSI-HF) trial. *Heart Rhythm* **2011**, *8*, 1237–1242. [[CrossRef](#)] [[PubMed](#)]
42. ESC/NASPE Task Force. Heart rate variability—Standards of measurement, physiological interpretation, and clinical use. *Circulation* **1996**, *93*, 1043–1065. [[CrossRef](#)]
43. Schmidt, G.; Malik, M.; Barthel, P.; Schneider, R.; Ulm, K.; Rolnitzky, L.; Camm, A.J.; Bigger, J.T., Jr.; Schömig, A. Heart rate turbulence after ventricular premature beats as a predictor of mortality after acute myocardial infarction. *Lancet* **1999**, *353*, 1390–1396. [[CrossRef](#)]
44. Bauer, A.; Malik, M.; Schmidt, G.; Barthel, P.; Bonnemeier, H.; Cygankiewicz, I.; Guzik, P.; Lombardi, F.; Müller, A.; Oto, A.; et al. Heart rate turbulence: Standards of measurement, physiological interpretation, and clinical use. International Society for Holter and Noninvasive Electrophysiology Consensus. *J. Am. Coll. Cardiol.* **2008**, *52*, 1353–1365. [[CrossRef](#)]
45. Bauer, A.; Kantelhardt, J.W.; Barthel, P.; Schneider, R.; Mäkikallio, T.; Ulm, K.; Hnatkova, K.; Schömig, A.; Huikuri, H.; Bunde, A.; et al. Deceleration capacity of heart rate as a predictor of mortality after myocardial infarction: Cohort study. *Lancet* **2006**, *367*, 1674–1681. [[CrossRef](#)]
46. Verrier, R.L.; Klingenhoben, T.; Malik, M.; El-Sherif, N.; Exner, D.V.; Hohnloser, S.H.; Ikeda, T.; Martinez, J.P.; Narayan, S.M.; Nieminen, T.; et al. Microvolt T-wave alternans: Physiological basis, methods of measurement, and clinical utility consensus guideline by International Society for Holter and Noninvasive Electrocardiology. *J. Am. Coll. Cardiol.* **2011**, *58*, 1309–1324. [[CrossRef](#)]
47. Hnatkova, K.; Šišáková, M.; Smetana, P.; Toman, O.; Huster, K.M.; Novotný, T.; Schmidt, G.; Malik, M. Sex differences in heart rate responses to postural provocations. *Int. J. Cardiol.* **2019**, *297*, 126–134. [[CrossRef](#)]
48. Linde, C.; Bongiorni, M.G.; Birgersdotter-Green, U.; Curtis, A.B.; Deisenhofer, I.; Furokawa, T.; Gillis, A.M.; Haugaa, K.H.; Lip, G.Y.H.; Van Gelder, I.; et al. ESC Scientific Document Group. Sex differences in cardiac arrhythmia: A consensus document of the European Heart Rhythm Association, endorsed by the Heart Rhythm Society and Asia Pacific Heart Rhythm Society. *Europace* **2018**, *20*, 1565–1565ao. [[CrossRef](#)]
49. Garnett, C.E.; Zhu, H.; Malik, M.; Fossa, A.A.; Zhang, J.; Badilini, F.; Li, J.; Darpö, B.; Sager, P.; Rodriguez, I. Methodologies to characterize the QT/corrected QT interval in the presence of drug-induced heart rate changes or other autonomic effects. *Am. Heart J.* **2012**, *163*, 912–930. [[CrossRef](#)]
50. Malik, M.; Hnatkova, K.; Batchvarov, V.; Gang, Y.; Smetana, P.; Camm, A.J. Sample size, power calculations, and their implications for the cost of thorough studies of drug induced QT interval prolongation. *Pacing Clin. Electrophysiol.* **2004**, *27*, 1659–1669. [[CrossRef](#)]

**Publisher's Note:** MDPI stays neutral with regard to jurisdictional claims in published maps and institutional affiliations.



© 2020 by the authors. Licensee MDPI, Basel, Switzerland. This article is an open access article distributed under the terms and conditions of the Creative Commons Attribution (CC BY) license (<http://creativecommons.org/licenses/by/4.0/>).

Koncept okamžitého vlivu RR intervalu na trvání následného intervalu QT je sporný, protože okamžitá QTV je málo závislá na výchozím stavu RR intervalu. Mnohem více, i dle výše demonstrované práce, závisí na ustáleném stavu RR. Následující publikace pak popisuje, že ačkoli použijeme k hodnocení QTV aktuální RR interval z ustálené SF, tak výsledek okamžité QTV bude stále výrazně ovlivněn biologickým a technickým hlukem zdrojového signálu. Při dalších studiích QTV je potřeba brát v úvahu i šum obsažený v EKG signálu.

Toman O, Hnatkova K, Šišáková M, Smetana P, Huster KM, Barthel P, Novotný T, **Andršová I**, Schmidt G, Malik M. Short-term beat-to-beat QT variability appears influenced more strongly by recording quality than by beat-to-beat RR variability. *Front Physiol* 2022; 12: 863873. doi: 10.3389/fphys.2022.863873

IF 4,0. Počet citací ve Web of Science 0

Původní práce - kvantitativní podíl uchazečky 30 %: Návrh struktury publikace, elektrokardiologická měření, interpretace statistických výsledků, diskuze výsledků, text publikace.



# Short-Term Beat-to-Beat QT Variability Appears Influenced More Strongly by Recording Quality Than by Beat-to-Beat RR Variability

Ondřej Toman<sup>1,2</sup>, Katerina Hnatkova<sup>3</sup>, Martina Šišáková<sup>1,2</sup>, Peter Smetana<sup>4</sup>, Katharina M. Huster<sup>5</sup>, Petra Barthel<sup>5</sup>, Tomáš Novotný<sup>1,2</sup>, Irena Andršová<sup>1,2\*</sup>, Georg Schmidt<sup>5</sup> and Marek Malik<sup>2,3</sup>

<sup>1</sup> Department of Internal Medicine and Cardiology, University Hospital Brno, Brno, Czechia, <sup>2</sup> Department of Internal Medicine and Cardiology, Faculty of Medicine, Masaryk University, Brno, Czechia, <sup>3</sup> National Heart and Lung Institute, Imperial College, London, United Kingdom, <sup>4</sup> Wilhelminenspital der Stadt Wien, Vienna, Austria, <sup>5</sup> Klinikum rechts der Isar, Technische Universität München, Munich, Germany

## OPEN ACCESS

### Edited by:

Veronique Meijborg,  
Academic Medical  
Center, Netherlands

### Reviewed by:

Frida Sandberg,  
Lund University, Sweden  
Alberto Porta,  
University of Milan, Italy

### \*Correspondence:

Irena Andršová  
andrsova.irena@fnbrno.cz

### Specialty section:

This article was submitted to  
Cardiac Electrophysiology,  
a section of the journal  
Frontiers in Physiology

Received: 27 January 2022

Accepted: 28 February 2022

Published: 01 April 2022

### Citation:

Toman O, Hnatkova K, Šišáková M, Smetana P, Huster KM, Barthel P, Novotný T, Andršová I, Schmidt G and Malik M (2022) Short-Term Beat-to-Beat QT Variability Appears Influenced More Strongly by Recording Quality Than by Beat-to-Beat RR Variability. *Front. Physiol.* 13:863873. doi: 10.3389/fphys.2022.863873

Increases in beat-to-beat variability of electrocardiographic QT interval duration have repeatedly been associated with increased risk of cardiovascular events and complications. The measurements of QT variability are frequently normalized for the underlying RR interval variability. Such normalization supports the concept of the so-called immediate RR effect which relates each QT interval to the preceding RR interval. The validity of this concept was investigated in the present study together with the analysis of the influence of electrocardiographic morphological stability on QT variability measurements. The analyses involved QT and RR measurements in 6,114,562 individual beats of 642,708 separate 10-s ECG samples recorded in 523 healthy volunteers (259 females). Only beats with high morphology correlation ( $r > 0.99$ ) with representative waveforms of the 10-s ECG samples were analyzed, assuring that only good quality recordings were included. In addition to these high correlations, SDs of the ECG signal difference between representative waveforms and individual beats expressed morphological instability and ECG noise. In the intra-subject analyses of both individual beats and of 10-s averages, QT interval variability was substantially more strongly related to the ECG noise than to the underlying RR variability. In approximately one-third of the analyzed ECG beats, the prolongation or shortening of the preceding RR interval was followed by the opposite change of the QT interval. In linear regression analyses, underlying RR variability within each 10-s ECG sample explained only 5.7 and 11.1% of QT interval variability in females and males, respectively. On the contrary, the underlying ECG noise contents of the 10-s samples explained 56.5 and 60.1% of the QT interval variability in females and males, respectively. The study concludes that the concept of stable and uniform immediate RR interval effect on the duration of subsequent QT interval duration is highly questionable. Even if only stable beat-to-beat measurements of QT

interval are used, the QT interval variability is still substantially influenced by morphological variability and noise pollution of the source ECG recordings. Even when good quality recordings are used, noise contents of the electrocardiograms should be objectively examined in future studies of QT interval variability.

**Keywords:** healthy volunteers, long-term ECG, short-term ECG measurements, QT variability, RR variability, ECG noise contents, immediate RR interval effect, regression-based correction

## INTRODUCTION

The temporal dynamics of ventricular myocardial repolarisation are of interest since increases in beat-to-repolarisation variability have been reported to signify an increased risk of arrhythmic complications and cardiovascular death (Baumert et al., 2016; Hasan and Abbott, 2016). While other possibilities of electrocardiographic measurements have been published (Hasan et al., 2012; Schmidt et al., 2016; Rahola et al., 2021), most frequent expressions of ventricular repolarisation variability are based on beat-to-beat changes in QT interval duration. Risk prediction based on QT variability and its diagnostic utility has been reported in patients with ischaemic heart disease (Hasan et al., 2013), in cardiomyopathy patients (Fischer et al., 2015; Orosz et al., 2015a), in patients with long QT syndrome (Porta et al., 2015; Seethala et al., 2015), in recipients of automatic implantable cardioverter-defibrillators (Monasterio et al., 2013; Smoczyńska et al., 2020) as well as in a variety of other clinically and pathologically defined conditions (Orosz et al., 2015b; Viigimae et al., 2017; Nussinovitch et al., 2018).

Frequently, QT variability is expressed by the so-called QT variability index that was proposed by Berger et al. (1997) in the seminal publication on the topic of QT variability. This index, as repeatedly reviewed (Dobson et al., 2013), relates the beat-to-beat variance of QT interval durations to the simultaneously measured variance of RR interval durations.

In principle, the QT variability index aims at normalizing the beat-to-beat changes of QT interval duration for the underlying changes in the RR intervals, reflecting approximately the concept that QT interval duration needs to be corrected (or normalized) for the duration of the preceding RR interval [i.e., the concept of the so-called immediate RR interval effect (Fossa et al., 2002)]. The QT variability index is therefore a combined measure; its increases may be caused both by increases in the QT variance and by decreases of RR variance, both of which are known indicators of increased risk of cardiovascular events and complications (Malik and Camm, 1990; ESC/NASPE Task Force, 1996; Baumert et al., 2016).

QT interval variability without any correction for the RR variability has also been researched (Niemeijer et al., 2014; Baumert et al., 2016; van den Berg et al., 2019) including the reports of normal values in short-term ECG. While such studies might still have included data influenced by the underlying RR variability, physiologically important technical studies were also reported, investigating the QT interval variability with RR interval effects removed by regression modeling (Porta et al., 2010, 2020; El-Hamad et al., 2019). These studies have been

based on shorter ECG recordings that allowed QT interval measurements on every beat basis.

Our experience suggests that in long-term ECG recordings, beat-to-beat QT interval measurements might be influenced by the quality of the signals, even if the measurement is performed only in carefully selected segments of the recordings. We have therefore conducted a study that compared the influence of underlying RR variability and of signal quality on beat-to-beat QT interval variability in segments extracted from long-term 12-lead Holter recordings obtained in a large population of normal healthy volunteers who were investigated during clinical pharmacology studies.

## METHODS

### Investigated Population and Electrocardiographic Recordings

Clinical pharmacology studies enrolled 523 healthy volunteers including 259 females, with no statistical age differences between females and males ( $33.4 \pm 9.1$  vs.  $33.7 \pm 7.8$  years). Before study enrollment, all the volunteers had a normal standard clinical ECG and normal clinical investigation. The studies were conducted at 3 different clinical research sites that used the same standard inclusion and exclusion criteria mandated for Phase I pharmacology studies (ICH Guideline, 2001), including negative recreational substances tests and negative pregnancy tests for females. All the source studies were ethically approved by the institutional ethics bodies (Parexel in Baltimore; California Clinical Trials in Glendale; and Spaulding in Milwaukee) and all subjects gave informed written consent to study participation and to the scientific investigation of data collected during the studies. The population used in this investigation was the same as reported in a previous study in which we reported the influence of underlying heart rate on QT interval variability (Andršová et al., 2020). However, for the purposes of this investigation, we applied different data processing techniques.

In each study participant, repeated three to four long-term 12-lead Holter ECG recordings with Mason-Likar electrode positions were obtained covering the full day-time periods, i.e., ~14-h periods during which the subjects were not allowed to sleep [to eliminate the influence of sleep on the QT interval duration (Browne et al., 1983; Lanfranchi et al., 2002; Viigimae et al., 2015)]. During these periods, the subjects were not allowed to smoke and/or consume alcohol or caffeinated drinks. No medication was administered during the day of the analyzed Holter recordings and if any medication was administered previously, the recordings were made after appropriate wash-out

gaps. The protocols of the different studies were also mutually consistent in respect of the clinical conduct during the drug-free baseline days. Thus, only drug-free data are presented here making further details of source pharmacology studies irrelevant.

Using previously described methods (Malik et al., 2008a, 2012a), multiple non-overlapping and non-adjacent 10-s ECG segments were extracted from the long-term ECGs. The segments were selected with the aim of capturing different heart rates available in the Holter recording. All the extracted 10-s segments contained only sinus rhythm recordings and were free of any ectopic beats. In more detail, the selected segments were extracted (a) from pre-specific time-points of the source pharmacologic studies, (b) from scans of the recordings aimed at finding a representative spectrum of different underlying heart rates of selected ECG segments that were not preceded by heart rate changes exceeding  $\pm 2$  beat per minute, and (c) from scans of the recordings aimed at finding representative spectrum of heart rate changes preceding the selected ECG segments. A minimum 20-s gap between selected segments was maintained. The ECG segments were selected only if a satisfactory algorithmic measurement of QT interval was possible (Malik et al., 2008a, 2012a).

In each of these ECG segments, QT interval was measured following published procedures (Malik et al., 2008a, 2012a) that included repeated visual controls of all the measurements. Consistency of the interpretation of corresponding ECG morphologies was also assured (Hnatkova et al., 2009). The visually verified QT interval measurements were made in the representative median waveforms of the 10-s segments (sampled at 1,000 Hz) with the superimposition of all 12 leads on the same isoelectric axis (Malik, 2004; Xue, 2009). For each ECG segment, computerized QT interval measurement in the representative median waveform was visually verified and, where necessary, manually corrected by two independently working cardiologists. In case of their disagreement, the final measurement decision was made by a senior member of the team. All visual decisions included the possibility of excluding an ECG segment if the QT interval measurement was considered not reliable (e.g., because of low voltage T waves or because of visible noise pollution that interfered with the measurement).

## Beat-to-Beat QT Interval Measurements

Using a previously proposed technique (Berger et al., 1997; Baumert et al., 2008), QT interval was projected to individual beats within the 10-s ECG by finding the maximum correlation between the representative waveform (in which the original measurement was made) and the signal of the individual QRS-T complexes. The maximum correlations were identified separately for the surroundings of the QRS onset and of the T wave offset. Since it has previously been observed that this process might lead to slightly different results when applied to different ECG leads (Malik, 2008), the cross-correlation technique was applied to the vector magnitude of algebraically reconstructed orthogonal leads (Guldenring et al., 2012).

After the cross-correlation techniques were applied and the corresponding positions of QRS onset and T wave offset were identified in each beat of the analyzed 10-s ECG segment,

Pearson correlation coefficients were calculated between the analyzed beat and representative median waveform in windows of  $\pm 40$  ms surrounding the QRS onset and  $\pm 50$  ms surrounding the T wave offset. The QT interval measurement on the given beat was accepted only if both these correlation coefficients exceeded 0.99. This assured that substantially noisy beats were excluded.

A 10-s ECG segment in which the QT measurement of the representative waveform was previously performed was accepted for the data analysis of this study if it contained at least two beats with accepted QT interval measurements.

For each beat with accepted QT interval measurement (i.e., an accepted beat in an accepted 10-s segment), the duration of the preceding RR interval was obtained. For each 10-s segment, the median duration of the accepted QT interval measurements and the median duration of the accepted preceding RR intervals were obtained. The heart rate of the 10-s ECG segment was also obtained from all RR intervals regardless of whether the subsequent QT interval measurements were accepted.

## ECG Noise and Morphological Variability

Although the strict acceptance limit imposed on the cross-correlation coefficients between the individual beats and the representative median waveform assured that beats substantially polluted by noise were eliminated from the analysis, it was still proper to investigate the morphological differences between the individual beats and the 10-s representative waveform.

For this purpose, in each accepted beat, the SD of the voltage differences between the representative waveform and the individual leads was calculated, for each ECG lead, in the windows of  $\pm 100$  ms surrounding the aligned QRS onsets and T wave offset (possible overlaps between subsequent beats during fast heart rate were eliminated). In each ECG lead and each beat, the average of these two standard deviations of voltage differences was calculated and the median value of these measurements across all 12 ECG leads represented the morphological departure of the measured beat from the 10-s representative waveform. Although these signal differences might have been caused by biologically determined signal variability [e.g., respiration induced (Noriega et al., 2012)] we shall use the term “beat noise” for the purpose of this investigation.

In each 10-s ECG segment, the median value of the beat noise, termed here the “10-s median beat noise,” was calculated over all accepted beats and used to characterize the morphological stability of the complete 10-s segment.

## Individual Beat Analysis

For each accepted beat, the difference  $\Delta QT$  between the measured QT interval and the median of accepted QT interval durations in the 10-s ECG segment was calculated and correspondingly, the difference  $\Delta RR$  was obtained between the RR interval preceding an accepted beat and the median of RR interval preceding accepted beats in the same 10-s ECG segment.

The concept of the “immediate RR interval effect” postulates that a longer RR interval should be followed by a longer QT interval. To assess the validity of this concept, we pooled, in each

study subject separately, all the  $\Delta$ QT and  $\Delta$ RR pairs from all accepted beats in all processed 10-s ECG segments.

Three different analyses of the  $\Delta$ QT and  $\Delta$ RR pairs were performed: Firstly, in each study subject, a linear regression between  $\Delta$ QT and  $\Delta$ RR was calculated. Secondly, the data  $\Delta$ QT and  $\Delta$ RR pair was called concordant if either ( $\Delta$ RR > 0 and  $\Delta$ QT > 0) or ( $\Delta$ RR < 0 and  $\Delta$ QT < 0) and likewise, it was called discordant if ( $\Delta$ RR < 0 and  $\Delta$ QT > 0) or ( $\Delta$ RR > 0 and  $\Delta$ QT < 0). We have calculated the proportions of concordant and discordant  $\Delta$ QT,  $\Delta$ RR pairs among all accepted beats (in each study subject separately) and, to eliminate minimal data fluctuations, repeated the calculations of the proportions of concordant and discordant  $\Delta$ QT,  $\Delta$ RR pairs considering only those concordant and discordant beats for which the absolute value  $|\Delta$ RR| exceeded 20 ms, and 50 ms. Thirdly, in each study subject, the Spearman correlation coefficient between  $|\Delta$ QT| and  $|\Delta$ RR| pairs were compared with the Spearman correlation coefficient between  $|\Delta$ QT| values and the beat-wise corresponding values of the beat noise.

## ECG Segment Analysis

In each ECG segment, the SD of  $\Delta$ QT and  $\Delta$ RR values was obtained (it is easy to see that these values were identical to the within segments SD of QT and RR interval values—we shall use the abbreviations SDQT and SDRR to denote these within-segment measurements).

The intra-subject averages of SDQT and SDRR values as well as of median beat noise values were compared between female and male study participants, and also related to the subject ages.

Within each subject, Spearman correlations were computed between SDQT, SDRR, and median beat noise obtained from the same ECG segments. Similar Spearman correlations were also calculated between SDQT and heart rate of the ECG segment, and SDQT and the median QT interval duration in the ECG segment. The median QT duration of an ECG segment was calculated using only the accepted beats.

## Correction of SDQT

To investigate the covariates of SDQT, intra-subject linear regressions were performed. That is, in each subject in whom  $N$  accepted 10-s ECG segments were available, values  $\{\mathfrak{S}_i^{QT}\}_{i=1}^N$ ,  $\{\mathfrak{S}_i^{RR}\}_{i=1}^N$ ,  $\{\mathcal{U}_i\}_{i=1}^N$ ,  $\{\mathcal{H}_i\}_{i=1}^N$ , and  $\{\mathcal{Q}_i\}_{i=1}^N$  of serial measurements of SDQT, SDRR, 10-s median beat noise, 10-s heart rate, and 10-s median QT interval, respectively, were used to construct linear regressions:

$$\mathfrak{S}_i^{QT} = \alpha_1 + \alpha_2 \mathfrak{S}_i^{RR} + \epsilon_i^{(1)} \quad (1)$$

$$\mathfrak{S}_i^{QT} = \beta_1 + \beta_2 \mathcal{U}_i + \epsilon_i^{(2)} \quad (2)$$

$$\mathfrak{S}_i^{QT} = \vartheta_1 + \vartheta_{21} \mathfrak{S}_i^{RR} + \vartheta_{22} \mathcal{U}_i + \epsilon_i^{(3)} \quad (3)$$

$$\mathfrak{S}_i^{QT} = \zeta_1 + \zeta_{21} \mathfrak{S}_i^{RR} + \zeta_{22} \mathcal{U}_i + \zeta_{23} \mathcal{H}_i + \epsilon_i^{(4)} \quad (4)$$

$$\mathfrak{S}_i^{QT} = \xi_1 + \xi_{21} \mathfrak{S}_i^{RR} + \xi_{22} \mathcal{U}_i + \xi_{23} \mathcal{H}_i + \xi_{24} \mathcal{Q}_i + \epsilon_i^{(5)} \quad (5)$$

where the regression coefficients were obtained by standard matrix equations to obtain zero centered  $\epsilon_i^{(\bullet)}$  errors with minimal sums of their squares.

Using these equations, regression intercepts  $\alpha_1$ ,  $\beta_1$ , and  $\vartheta_1$  were interpreted as intra-subject central values of SDQT “corrected” for the influence of SDRR, the influence of 10-s median beat noise, and the combined influence of SDRR and 10-s median beat noise. That is, using the same principles as used in subject-specific heart rate corrections of QT interval and of other interval measurements (Hnatkova et al., 2017) that produce correction values for RR interval of 1 s, the intercepts  $\alpha_1$ ,  $\beta_1$ , and  $\vartheta_1$  were used as estimates of intra-subject SDQT values corrected for zero SDRR, zero beat noise, and combined zero SDRR and zero beat noise. No such correction of SDQT was based on equations (4) and (5).

For all regression equations (1) through (5), the values  $\sqrt{\sum_{i=1}^N (\epsilon_i^{(\bullet)})^2}$ , that is the residuals of the equations, were compared with the SD of all SDQT measurements (i.e., SD of all  $\mathfrak{S}_i^{QT}$  values). This comparison of the residuals allowed us to study the effects of combined co-variates on the intra-subject reproducibility of SDQT. This allowed studying the intra-subject variability of SDQT measurements made in different 10-s ECGs and the reduction of such variability by eliminating the influence of SDRR, of 10-s median beat noise, and of the combinations of SDRR and 10-s median beat noise with 10-s heart rate and 10-s median QT interval.

## Statistics and Data Presentation

Descriptive data are presented as means  $\pm$  SD. Distributions of Spearman correlation coefficients computed in individual subjects are presented as medians and inter-quartile ranges (IQR). Comparisons between females and males were based on a two-sample two-tail  $t$ -test assuming different variations between compared datasets and subsequently confirmed by the non-parametric Kolmogorov-Smirnov test. The significance of linear regression slopes between age and the investigated indices was tested using the Fisher-Snedecor  $F$  distribution.

The comparisons between the proportions of regression residuals and other intra-subject comparisons used non-parametric paired Wilcoxon test. The calculation of the multivariable linear regressions repeated in different study subjects utilized an in-house matrix manipulation software package programmed in C++. The differences between the measured intra-subject means of SDQT values and the values corrected for zero SDRR and/or for zero beat noise were expressed in relative terms, that is by calculating the proportions of  $(\text{SDQT} - \text{SDQT}_{\text{corrected}}) / \text{SDQT}$ , where the  $\text{SDQT}_{\text{corrected}}$  is the regression corrected value. We term these proportions the “SDQT reductions” and express them in per-cent. Using the same proportions between intra-subject SDQT variability and the residuals of regressions (1) to (5), we obtained regression-based reductions of intra-subject SDQT variability which we term the “residual reductions” and express them again in per-cent.

Statistical tests used IBM SPSS package, version 27 (IBM, Armonk, New York, USA).  $P$ -values below 0.05 were considered statistically significant. Because of the interdependence between the different indices, no correction for the multiplicity of statistical testing was made.

## RESULTS

The study was based on a total of 642,708 individual 10-s ECG samples and a total of 6,114,562 individual beats accepted for the analysis. On average, there were  $1,208 \pm 228$  and  $1,248 \pm 224$  ECG segments, and  $11,610 \pm 2,821$  and  $11,768 \pm 2,831$  individual beats processed in female and male subjects, respectively (no statistical differences between sexes).

**Figures 1, 2** show examples of the distribution and inter-dependency of ECG measurements in two study subjects. The relationships between the measurements seen in the figures appeared visually representative of the data in other subjects.

### Analysis of Individual Beats

#### Immediate RR Interval Effect

**Figure 3** shows the distribution of intra-subject linear-regression  $\Delta QT/\Delta RR$  slopes calculated when pooling, in each study subject separately, all individual analyzed beats. These slopes were  $0.0171 \pm 0.0076$  and  $0.0174 \pm 0.0066$  in females and males, respectively (no statistical difference between sexes).

Pooling all accepted beats together, the intra-subject standard deviation of  $\Delta QT$  was  $4.88 \pm 1.05$  ms in females and  $4.52 \pm 0.94$  ms in males ( $p < 0.0001$ ). This was very similar to the  $\Delta QT/\Delta RR$  regression residuals which were  $4.78 \pm 1.08$  ms in females and  $4.42 \pm 0.96$  ms in males ( $p < 0.0001$ ). Thus, relating  $\Delta QT$  linearly to  $\Delta RR$  reduced the intra-subject standard deviations only (median, IQR) by 1.59% (0.80–2.87%) in females and by 1.99% (1.14–3.11%) in males.

#### Concordant and Discordant Beats

The intra-subject frequencies of concordant and discordant beats are shown in **Figure 4**. In relation to all beats accepted for analysis, the intra-subject frequencies of concordant beats were  $43.1 \pm 3.5\%$  and  $41.9 \pm 2.7\%$  in females and males ( $p < 0.0001$ ), the frequencies of discordant beats were  $25.7 \pm 4.1\%$  and  $24.8 \pm 3.5\%$  in females and males ( $p = 0.008$ ). When considering only beats with  $|\Delta RR| > 20$  ms, the frequencies of concordant and discordant beats were  $23.6 \pm 5.7$  and  $10.6 \pm 3.0\%$ , respectively (no sex difference); with  $|\Delta RR| > 50$  ms, the corresponding frequencies were  $10.2 \pm 4.9$  and  $3.3 \pm 1.8\%$ , respectively (no sex difference). **Figure 5** presents cumulative distributions of the data shown in **Figure 4**.

#### Correlations

The intra-subject correlations between  $|\Delta RR|$  and  $|\Delta QT|$ , and between beat noise and  $|\Delta QT|$  are also shown in **Figure 4**. The  $|\Delta QT|$  vs.  $|\Delta RR|$  correlation coefficients were (median and IQR)  $0.056$  (0.034–0.087) and  $0.075$  (0.050–0.102) in females and males, respectively ( $p < 0.0001$  for the sex differences). In 53 females (20.9%) and 27 males (10.0%), the correlation between  $|\Delta QT|$  vs.  $|\Delta RR|$  was not significantly positive. The  $|\Delta QT|$  vs. beat noise correlation coefficients were  $0.309$  (0.278–0.336) and  $0.333$  (0.306–0.355) in females and males, respectively ( $p < 0.0001$  for the sex differences). The  $|\Delta QT|$  vs. beat noise correlation was stronger than the  $|\Delta QT|$  vs.  $|\Delta RR|$  correlation in every study subject. See also **Figure 5** for the cumulative distributions of these correlation data.

### Analysis of 10-S ECG Segments

#### Sex Comparisons

As expected (see **Figure 6**), the intra-subject mean heart rate of the analyzed 10-s ECG samples was faster in females ( $75.6 \pm 6.8$  beats per minute — bpm) than in males ( $71.5 \pm 6.0$  bpm,  $p < 0.0001$ ). The mean 10-s SDRR was not different between sexes ( $43.7 \pm 15.4$  and  $43.5 \pm 12.8$  ms in females and males, respectively). Somewhat unexpectedly, the intra-subject means of 10-s median beat noise were smaller in females ( $16.8 \pm 3.0 \mu V$ ) than in males ( $20.1 \pm 3.9 \mu V$ ,  $p < 0.0001$ ). Despite the heart rate differences, the mean duration of the uncorrected QT interval was longer in females ( $386.9 \pm 18.4$  ms) than in males ( $379.5 \pm 16.0$  ms,  $p < 0.0001$ ).

#### Relationship to Age

As again expected (see **Figure 7**), intra-subject mean SDRR was significantly decreasing with increasing age ( $p < 0.0001$  in both sexes). The intra-subject means of 10-s median beat noise were significantly decreasing with age in males ( $p = 0.0003$ ) but were only non-significantly decreasing with advancing age in females. The age-related increase in mean 10-s SDQT was significant in males ( $p = 0.007$ ) but was only statistically borderline in females ( $p = 0.092$ ).

#### Correlations

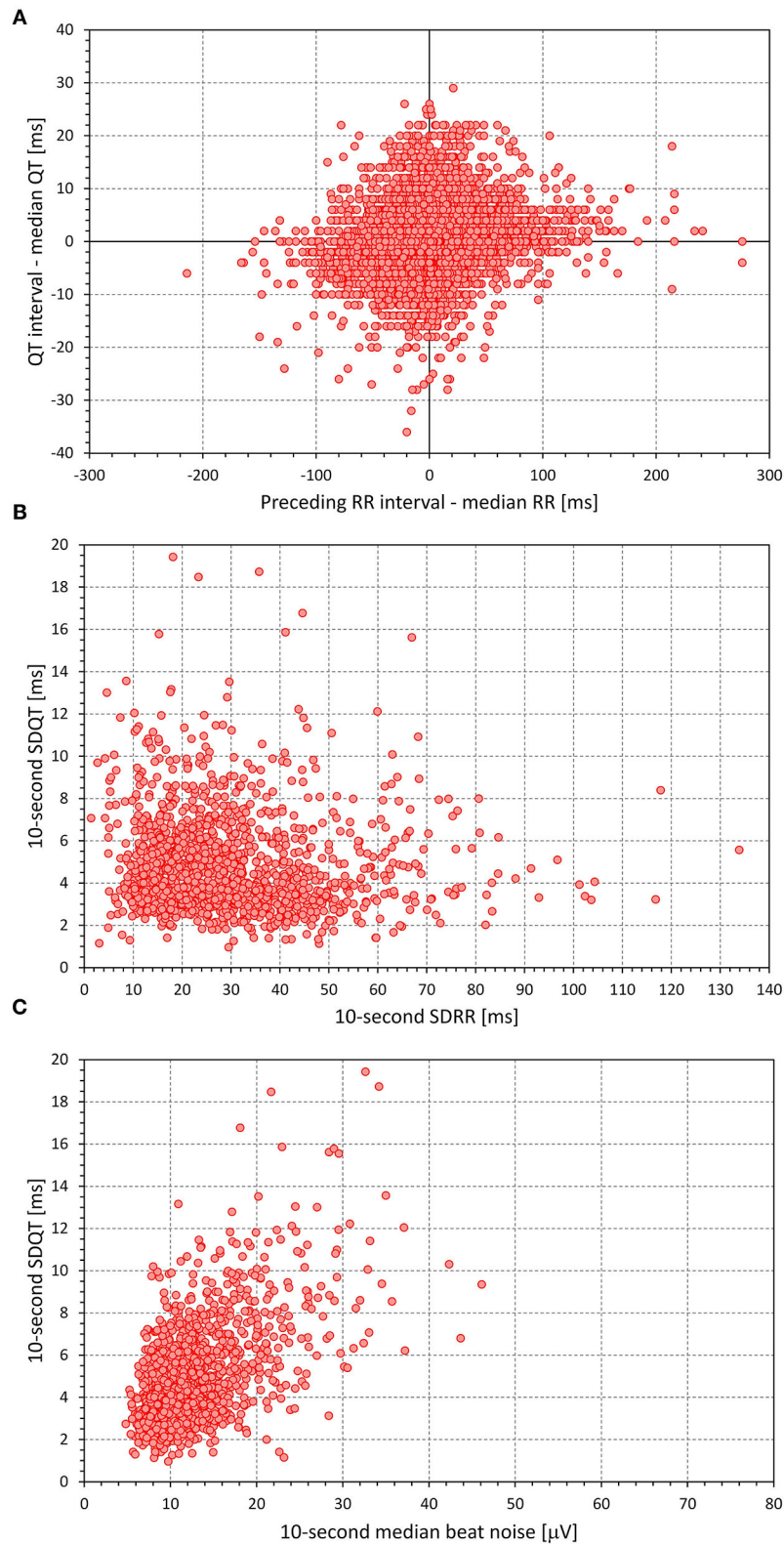
The intra-subject correlations between the 10-s ECG measurements are graphically summarized in **Figure 8**. Similar to the individual beat measurements, the correlations between SDQT and SDRR were modest,  $0.073$  (–0.016–0.158) in females and  $0.146$  (0.057–0.235) in males (sex comparison  $p < 0.0001$ ). The correlations between SDQT and 10-s median beat noise were substantially stronger,  $0.498$  (0.432–0.549) in females and  $0.549$  (0.497–0.596) in males ( $p < 0.0001$ ). The correlations between 10-s heart rate and 10-s median beat noise were  $0.464$  (0.398–0.538) in females and  $0.511$  (0.444–0.569) in males ( $p < 0.0001$ ) and influenced the correlations between SDQT and 10-s heart rate which were  $0.413$  (0.323–0.515) in females and  $0.492$  (0.392–0.565) in males ( $p < 0.0001$ ). These were very similar (albeit with opposite signs) to the correlations between SDQT and 10-s median QT interval,  $-0.390$  (–0.490––0.296) on females and  $-0.427$  (–0.504––0.329) in males ( $p = 0.0016$ ). As expected, the correlations between 10-s heart rate and SDRR were mostly (but not exclusively) negative,  $-0.387$  (–0.548––0.241) in females and  $-0.246$  (–0.397––0.073) in males ( $p < 0.0001$ ).

Cumulative distributions of the data presented in **Figure 8** are shown in **Figure 9**.

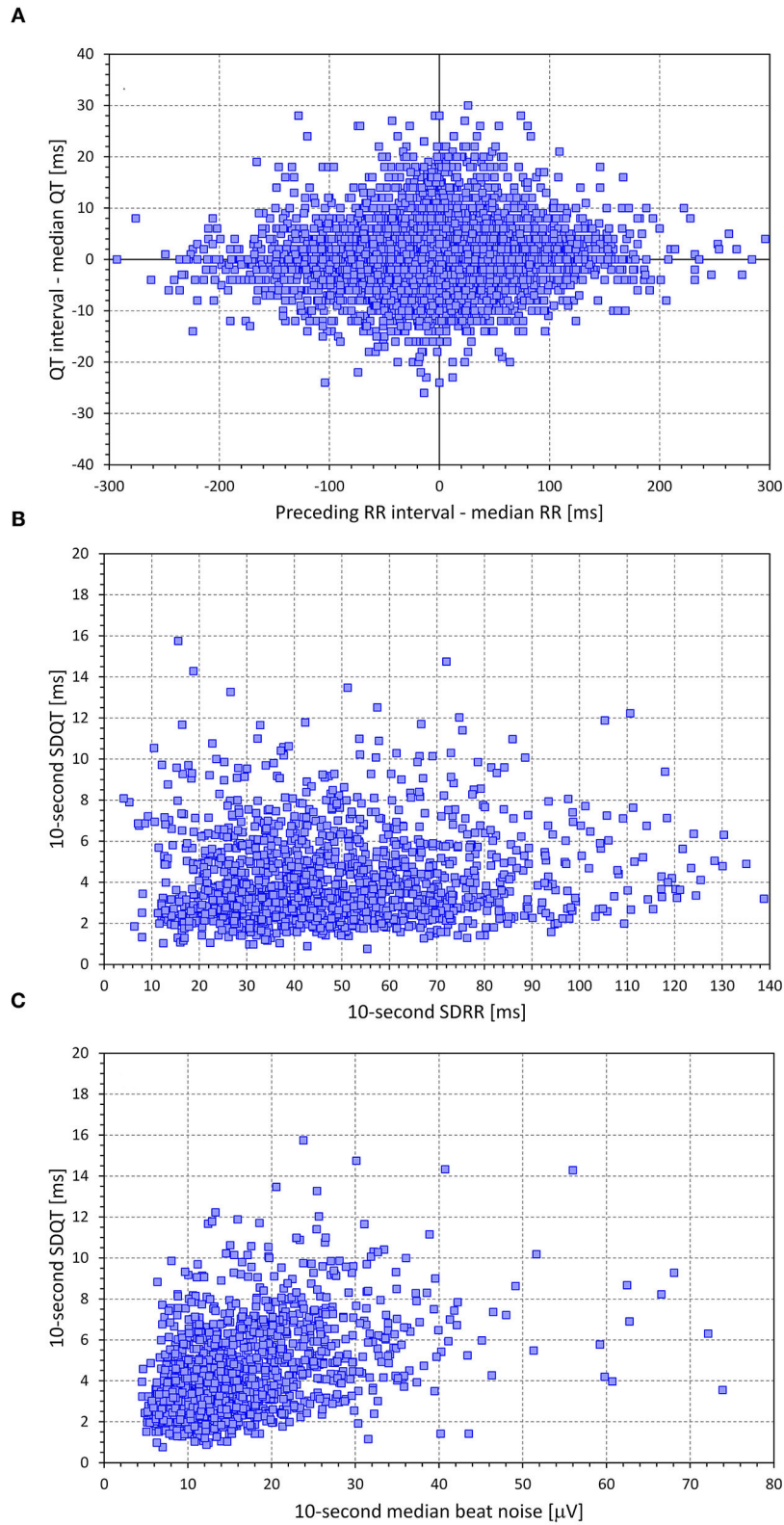
Contrary to these intra-subject correlations, some of the inter-subject correlations between the intra-subject mean values were very shallow (**Figure 10**). The intra-subject means of SDQT were not related to the intra-subject means of SDRR; the intra-subject means of SDQT were related to means of 10-s median noise in males ( $p < 0.0001$ ) but not in females.

As expected, the intra-subject means of SDQT were very strongly related to the intra-subject variability of SDQT.

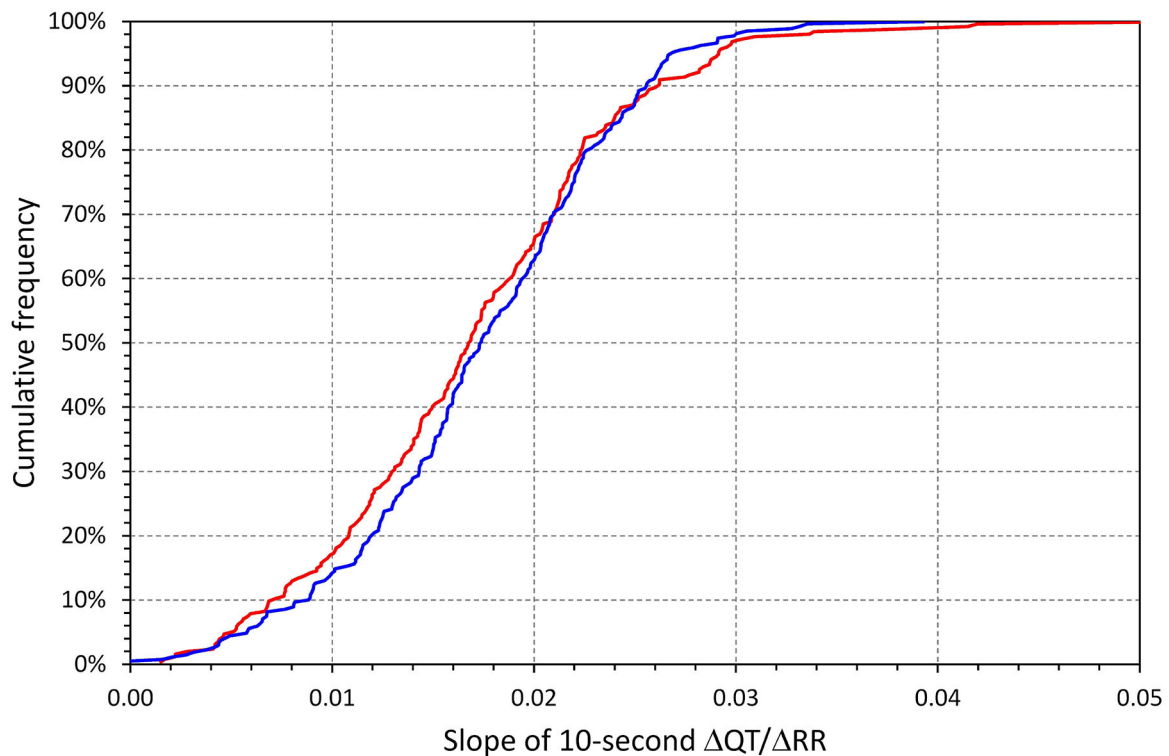




**FIGURE 1** | Example of data distribution in a 36-year-old female. The top **(A)** shows a scatter diagram between the  $\Delta\text{RR}$  and the  $\Delta\text{QT}$  value measured in all individual beats accepted in the data analysis of this subject. The middle **(B)** and bottom **(C)** were derived from the data of accepted 10-s ECG segments of the Holter recordings of the subject. The middle **(B)** shows a scatter diagram between SDRR and SDQT values, the bottom **(C)** shows a scatter diagram between median beat noise and the SDQT values. Note the wide spread of the data in all panels and the visible data trend in the bottom panel.



**FIGURE 2** | Example of data distribution in a 34-year-old male. The layout of the figure is the same as in **Figure 1**.



**FIGURE 3** | Cumulative distributions of intra-subject linear  $\Delta\text{QT}/\Delta\text{RR}$  regression slopes. In each subject, the regression involved all individual beats accepted for the given subject. The red and blue lines correspond to females and males, respectively.

### Regression-Based Corrections of SDQT

**Figure 11** shows that the intra-subject mean SDQT values were significantly larger in females ( $4.51 \pm 0.96$  ms) than in males ( $4.05 \pm 0.88$  ms,  $p < 0.0001$ ). The intra-subject variabilities, that is standard deviations of SDQT, were also larger in females ( $2.61 \pm 0.67$  ms) than in males ( $2.46 \pm 0.66$  ms,  $p = 0.01$ ).

**Figure 11** further shows that regression-based correction of intra-subject SDQT values for the underlying SDRR values reduces SDQT (median, IQR) by only 5.7% (2–10.3%) in females and 11.1% (6.2–16.8%) in males. On the contrary, the correction for the underlying 10-s median noise reduces SDQT by 56.5% (48.7–62.3%) in females and by 60.1% (50.9–66.6%) in males. Additional combined correction for both the underlying SDRR and 10-s median noise reduces SDQT only a little bit more by 59.7% (51.8–66.8%) in females and by 65.0% (56.3–72.6%) in males. All these relative corrections show significant sex differences ( $p$  between  $<0.0001$  and 0.001). The comparisons of these corrections are shown in **Figures 12, 13**.

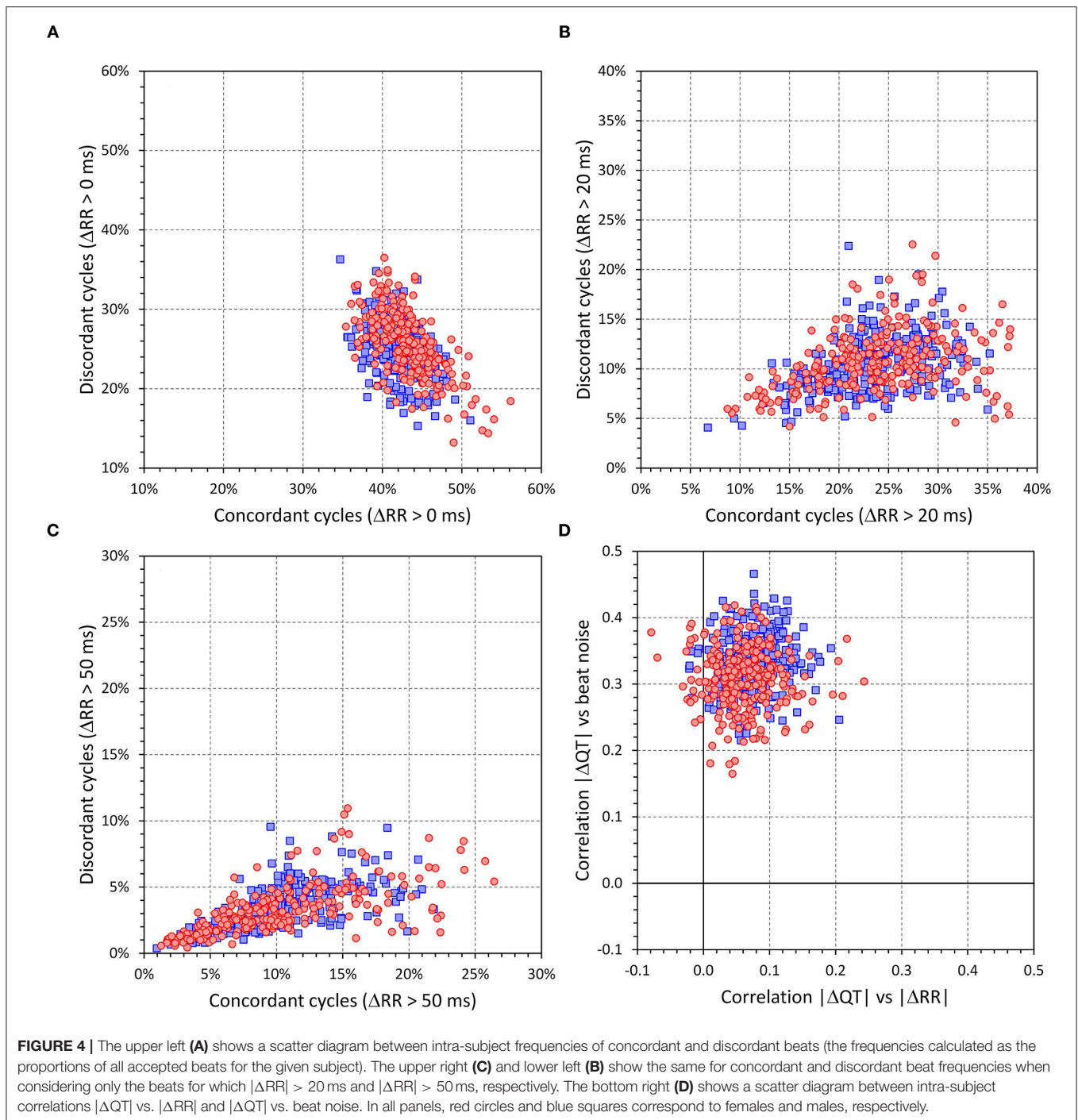
**Figure 11** also shows a reduction of the intra-subject variability of SDQT. The reduction by correction for underlying SDRR values is only minimal, by 0.54% (0.10–1.32%) in females and by 1.33% (0.46–2.68%) in males. The correction for the underlying 10-s median noise led to a larger reduction in the intra-subject SDQT variability by 13.3% (9.5–16.7%) in females and by 16.5% (13.1–19.7%) in males. Combined correction for both the underlying SDRR and 10-s median noise reduced

SDQT variability only a tiny bit more by 13.7% (10.3–17.4%) in females and by 17.4% (13.7–20.7%) in males. As with the corrections of the SDQT values, all these corrections of SDQT variability show significant sex differences (all  $p < 0.0001$ ).

**Figures 14, 15** show the comparison of these SDQT variability reductions and also show that additional multi-variable regression involving also underlying 10-s heart rate and the 10-s median QT interval duration led only to further marginal corrections of SDQT variability.

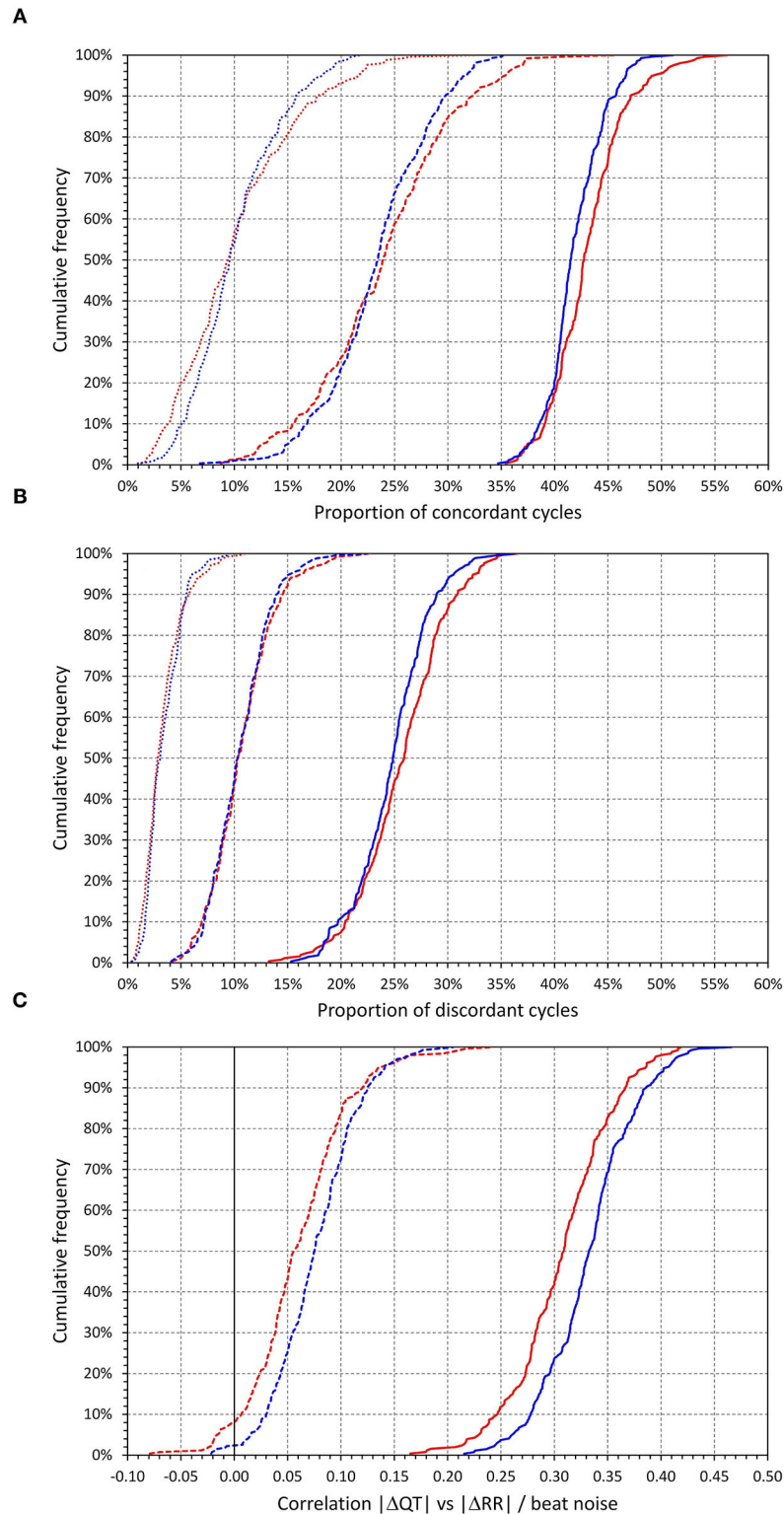
## DISCUSSION

The study leads to two principal observations that are of importance for both physiologic understandings of cardiac repolarisation variability and practical interpretation of ECG measurements. Firstly, our observations contradict the concept of systematic and reproducible immediate RR interval effect on QT interval duration. Secondly, the data analyses suggest that the standard approaches to the assessment of beat-to-beat QT interval variability might overestimate true QT variability if the noise within the source ECG recordings is not carefully controlled or if the QT variability is not corrected for the extent of biological and technical noise.

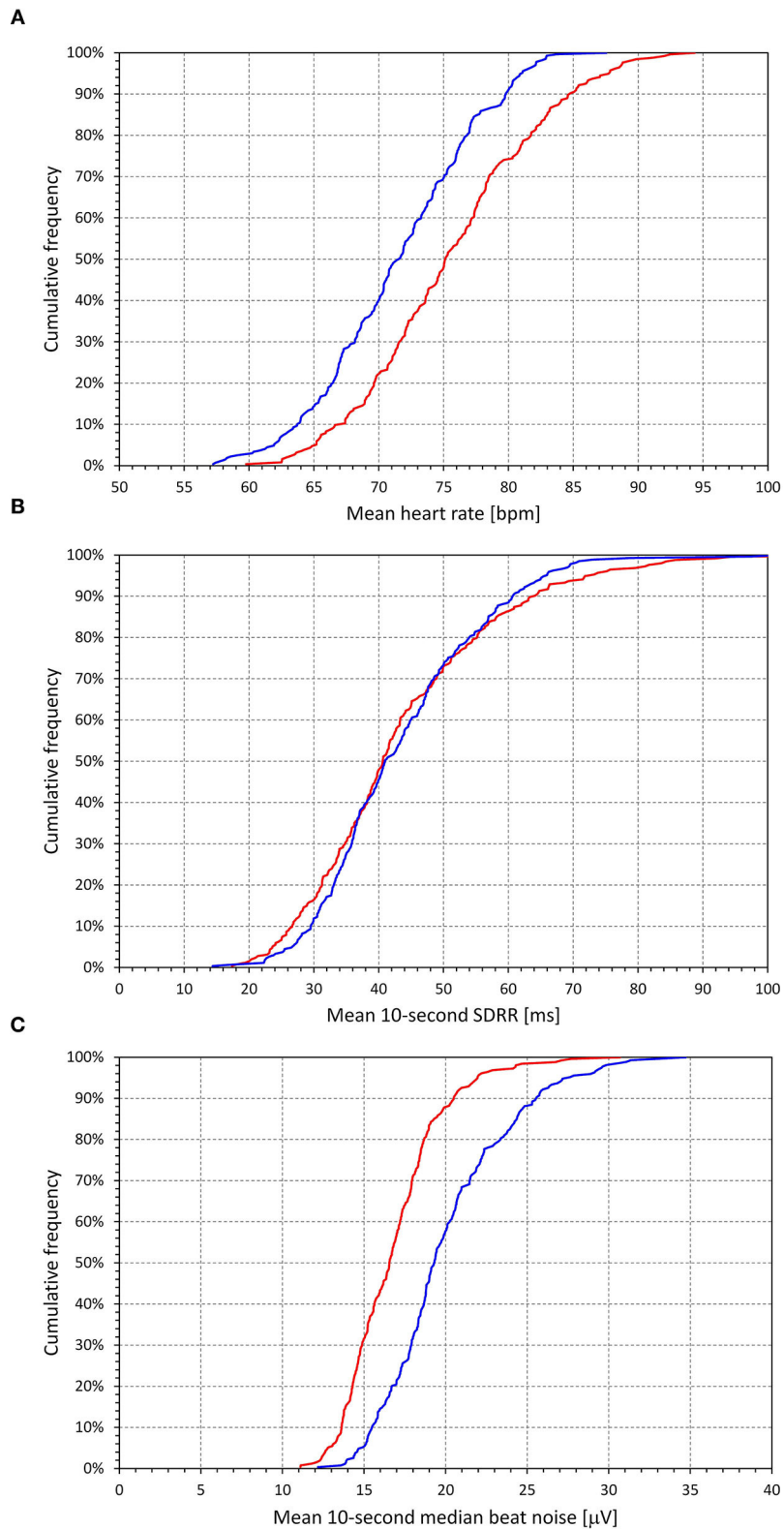


As seen in the examples in **Figures 1, 2**, as well as in the analysis of individual beat data, the relationship between  $\Delta QT$  and  $\Delta RR$  was not only shallow but also largely non-reproducible. Indeed, the linear relation of QT interval changes to RR interval changes accounted only for a small number of single percentages of the intra-subject beat-to-beat  $\Delta QT$  variability. This non-systematic relationship between QT interval changes and RR interval changes was further confirmed by the

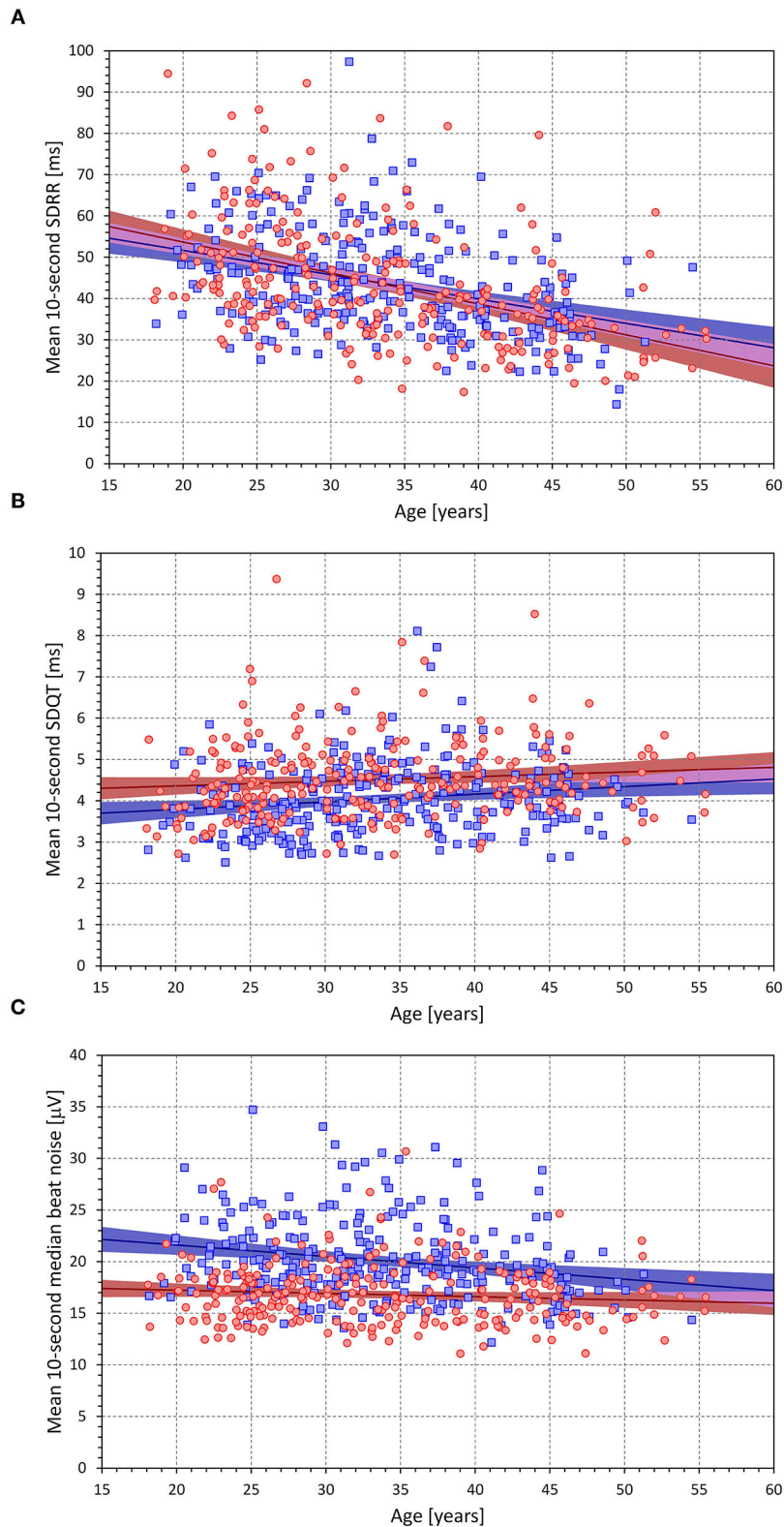
remarkably low intra-subject correlations between SDQT and SDRR (see **Figure 7**). Hence this study is very much in agreement with a number of previous studies that challenged that concept of immediate RR interval effect on the QT interval. While beat-to-beat RR interval prolongation and shortening is more frequently followed by QT interval prolongation and shortening than by the opposite QT interval changes, the opposite changes appear in approximately one-third of the beats (as seen by the



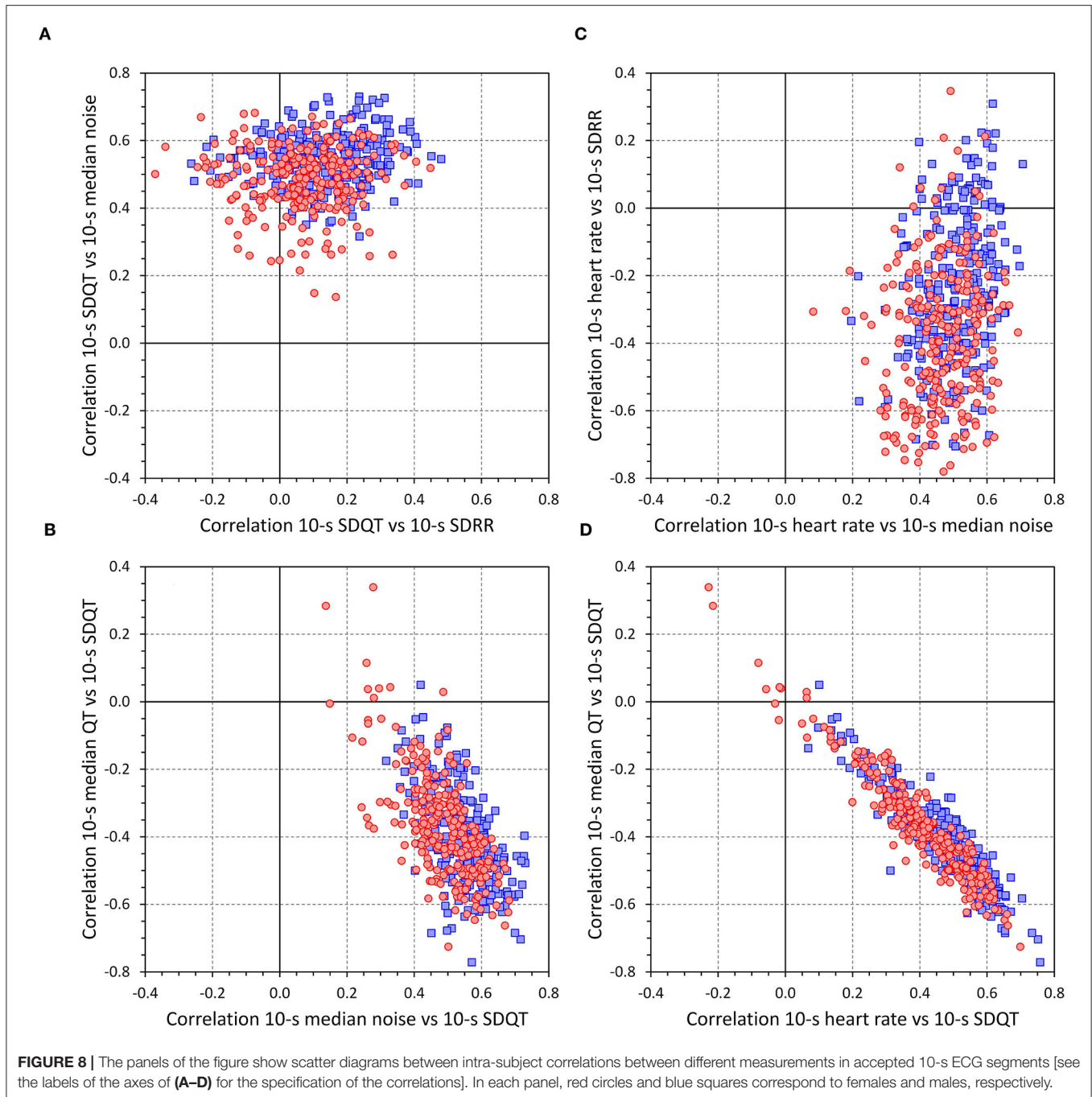
**FIGURE 5 |** Cumulative distributions of the intra-subject proportions of concordant beats [top (A)], the proportions of discordant beats [middle (B)], and of the intra-subject correlations between  $|\Delta QT|$  and  $|\Delta RR|$ , and between  $|\Delta QT|$  and beat noise [bottom (C)]. In the upper two panels, the solid lines, dashed lines, and dotted lines correspond to all concordant/discordant beats, concordant/discordant beats for which  $|\Delta RR| > 20$  ms, and concordant/discordant beats for which  $|\Delta RR| > 50$  ms, respectively. In the bottom panel, the solid and dashed lines correspond to intra-subject correlations  $|\Delta QT|$  vs. beat noise, and intra-subject correlations  $|\Delta QT|$  vs.  $|\Delta RR|$ , respectively. In all panels, the red and blue lines correspond to females and males, respectively.



**FIGURE 6 |** Population distributions of principal ECG measurements (intra-subject means of measurements obtained in individual 10-s ECG segments accepted in the recordings of the given subject). The top **(A)**, middle **(B)**, and bottom **(C)** show the distributions of mean heart rates, mean values of SDRR, and mean values of 10-s median beat noise, respectively. In each panel, the red and blue lines show the distributions among females and males, respectively.



**FIGURE 7 |** The figure shows age influence on intra-subject means of 10-s SDRR [upper **(A)**], 10-s SDQT [middle **(B)**], and 10-s median beat noise [bottom **(C)**]. In each panel, the red circle and blue square marks correspond to females and males, respectively. The red and blue lines show the linear regression models between the displayed characteristics and age, the light colored red and blue bands show the 95% confidence intervals of the linear regressions, the light-colored violet areas show the overlaps between the regression confidence intervals of both sexes.

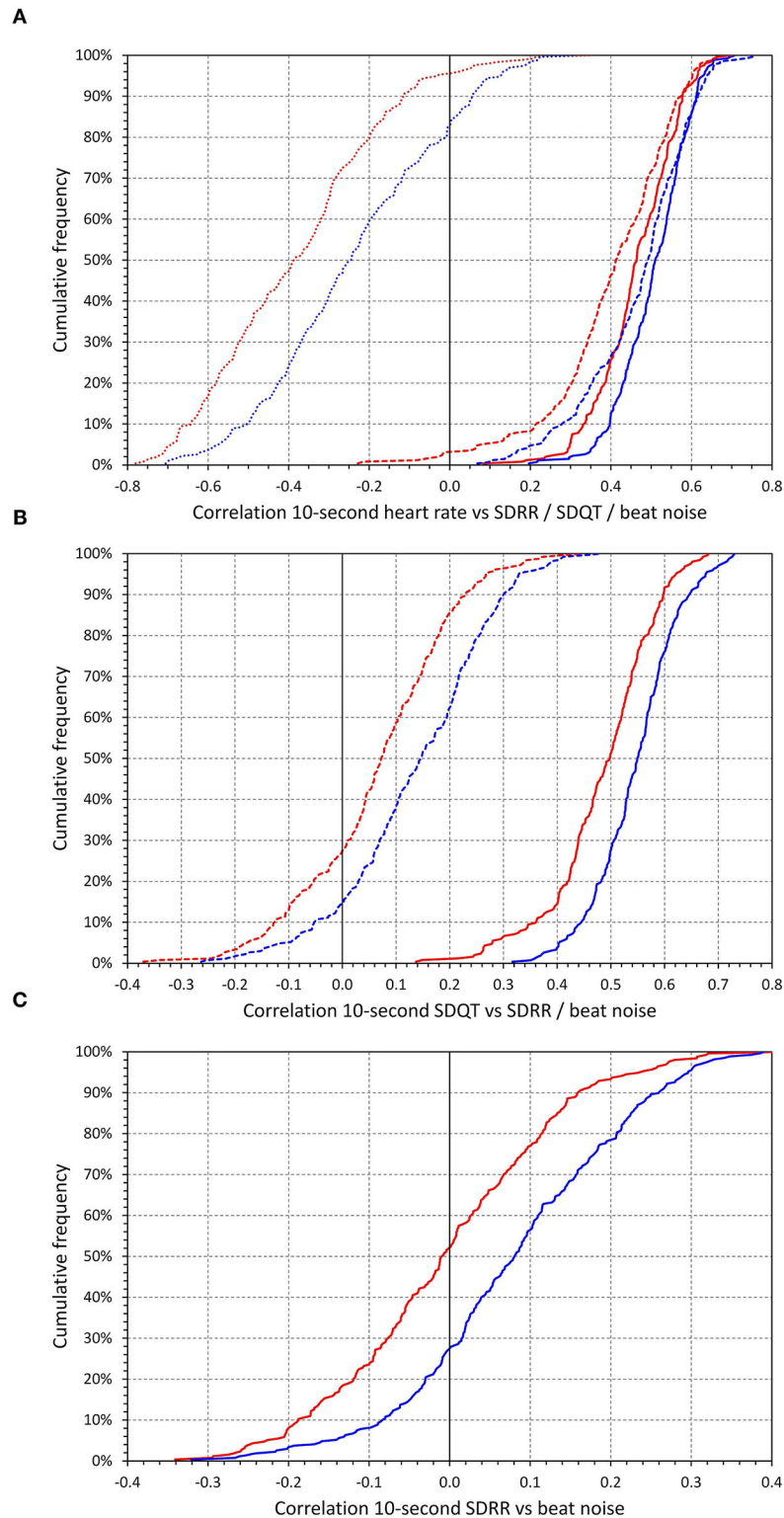


analysis of concordant and discordant beat frequency as shown in **Figure 4**).

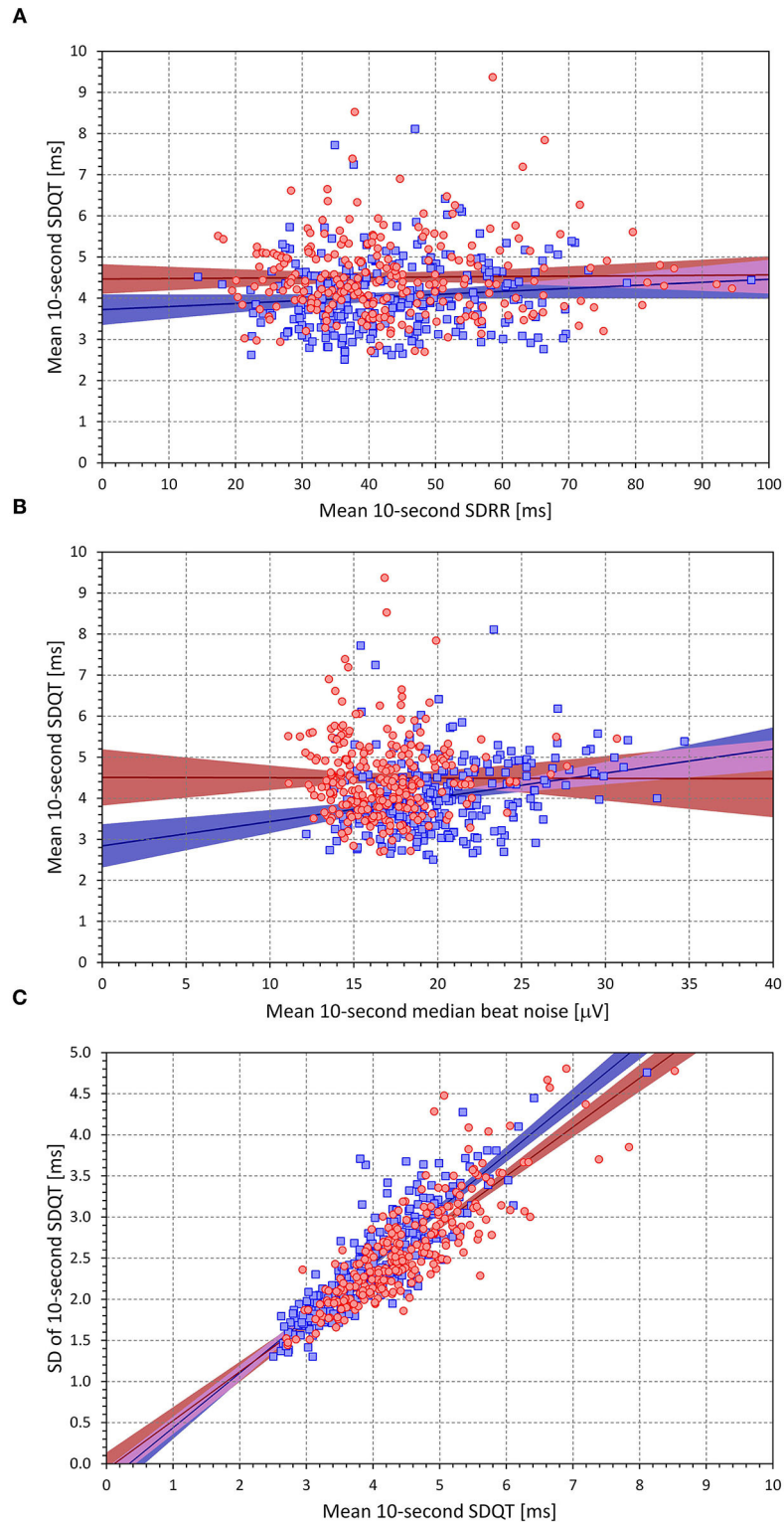
This challenge to the concept of immediate RR interval effect has two practical implications. Firstly, as repeatedly confirmed in previous publications, QT intervals duration should not be corrected for the preceding RR interval, and the complete history of preceding heart rate should be taken into account (Franz et al., 1988; Lau et al., 1988; Malik et al., 2004, 2008b, 2016; Jacquemet et al., 2014; Gravel et al., 2017). Indeed,

the intra-subject slopes of  $\Delta\text{QT}/\Delta\text{RR}$  linear regressions were approximately one-tenth of the QT/RR regressions used in population-based QTc corrections (Sagie et al., 1992). This is in good agreement with the previously established profiles of QT/RR hysteresis. While the need of considering the longer heart rate history of any QT interval measurement is now largely accepted and incorporated into the design of studies investigating heart rate corrected QT interval, it is regrettable when statements that “QT and RR value for each beat will be used

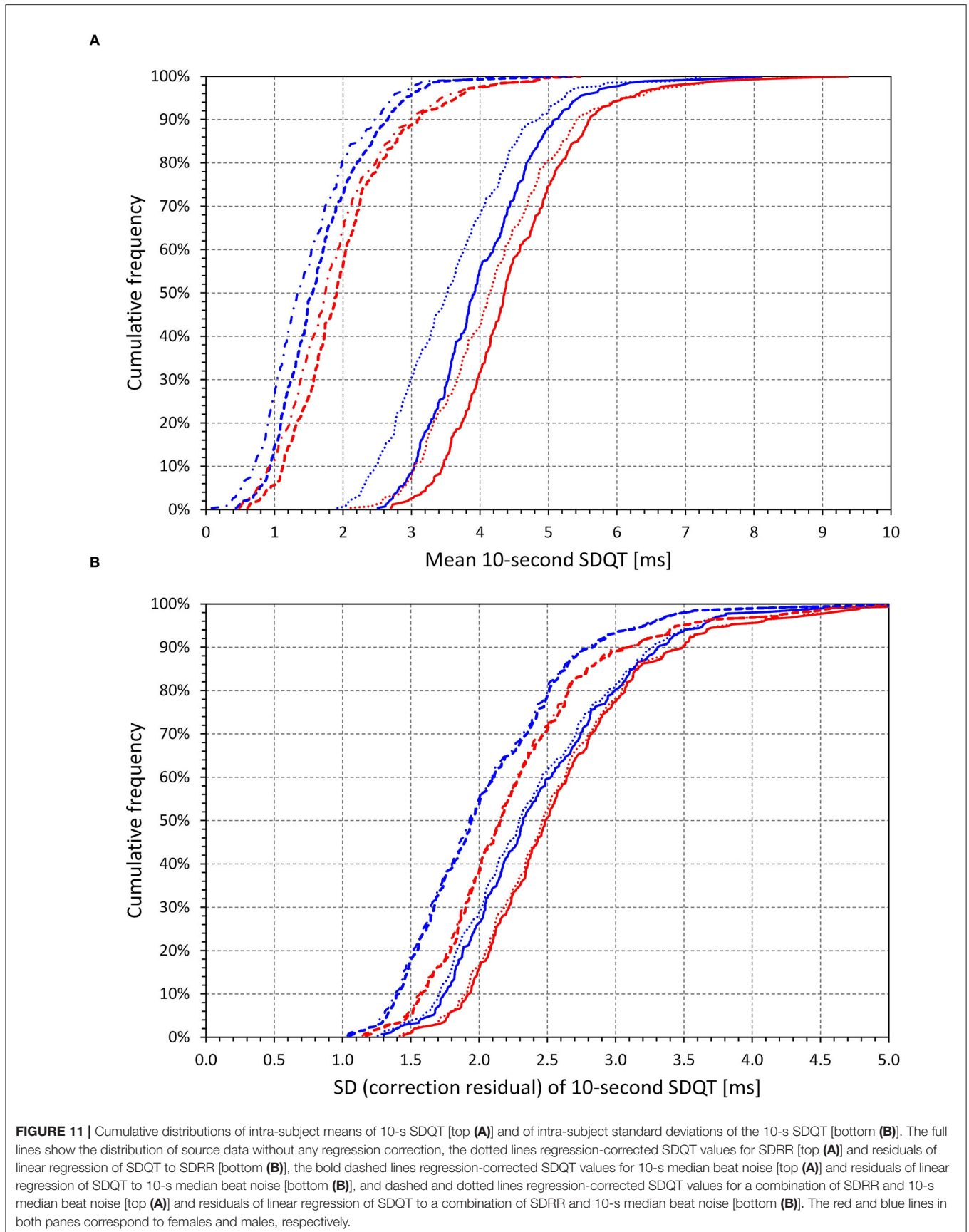


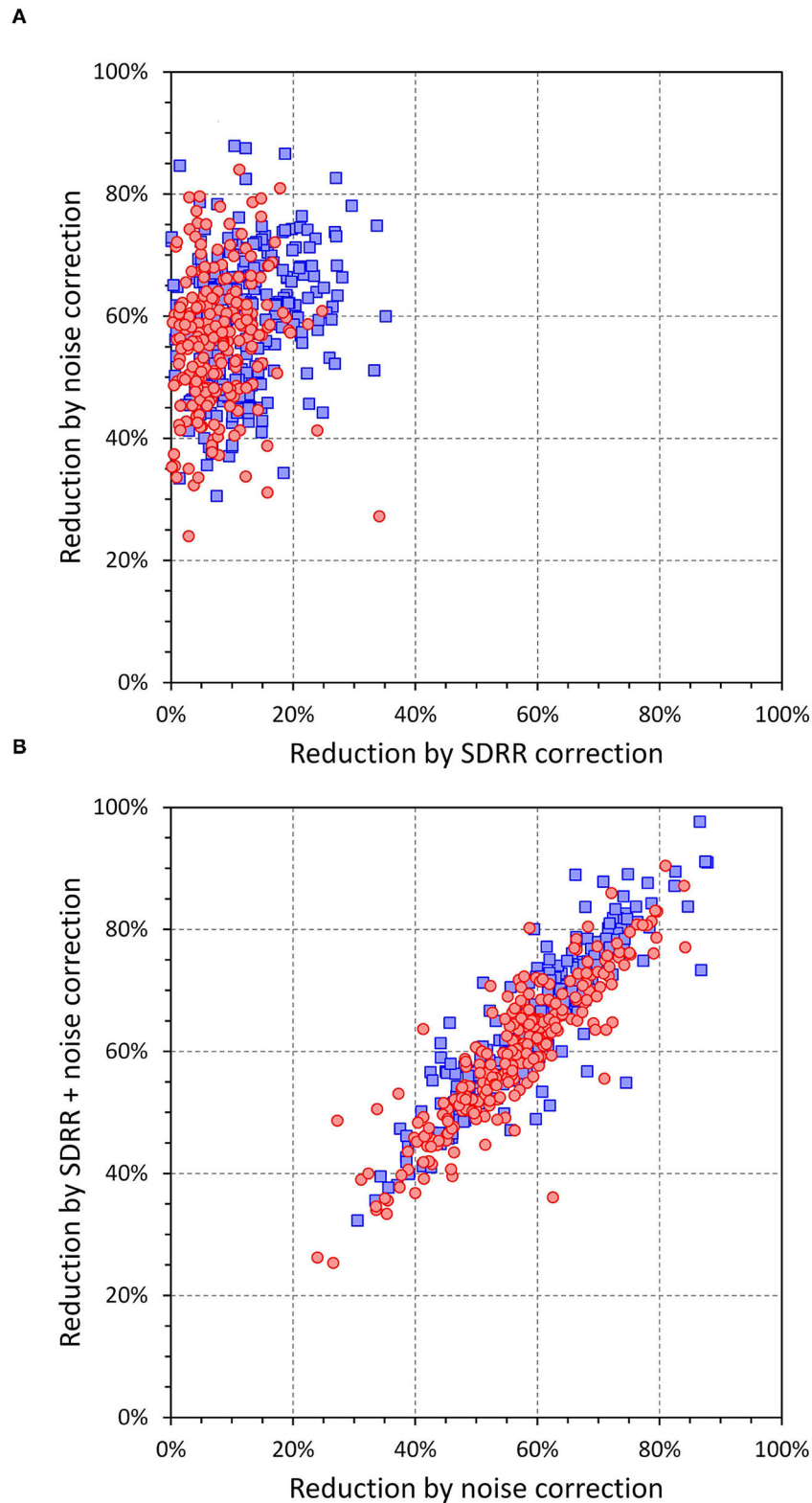


**FIGURE 9 |** The top **(A)** shows cumulative distributions of intra-subject correlations between 10-s heart rate and 10-s median beat noise (solid lines), intra-subject correlations between 10-s heart rate and 10-s SDQT (dashed lines), and intra-subject correlations between 10-s heart rate and 10-s SDRR (dotted lines). The middle **(B)** shows cumulative distributions of intra-subject correlations between 10-s SDQT and 10-s median beat noise (solid lines) and intra-subject correlations between 10-s SDQT and 10-s SDRR (dashed lines). The bottom **(C)** shows cumulative distributions of intra-subject correlations between 10-s SDRR and 10-s median beat noise. In each panel, the red and blue lines show the distributions in females and males, respectively.

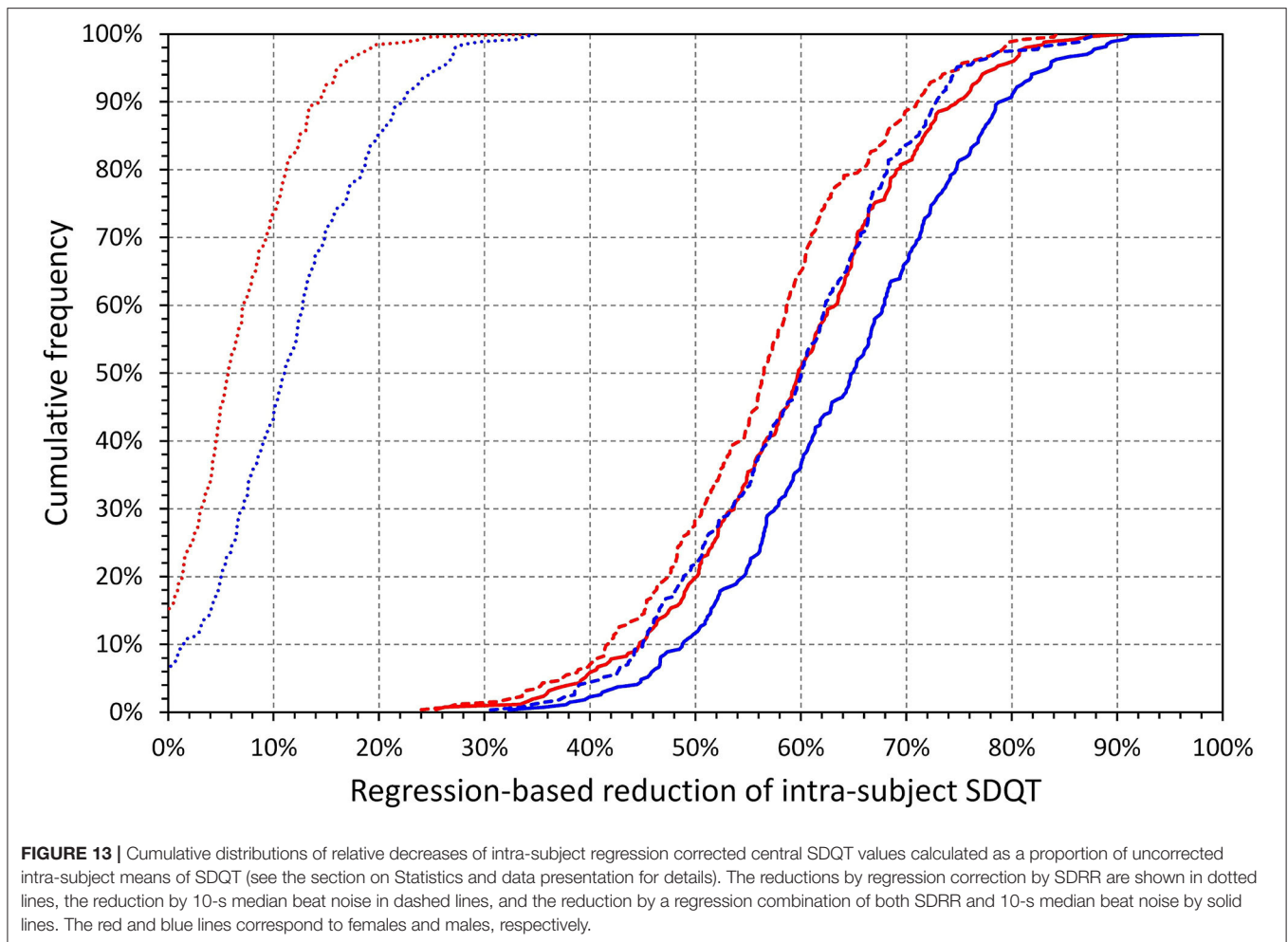


**FIGURE 10 |** Scatter diagrams showing population relationship between intra-subject means of 10-s SDRR and 10-s SDQT [top **(A)**], intra-subject means of 10-s median beat noise, and 10-s SDQT [middle **(B)**], and intra-subject means of 10-s SDQT and intra-subject standard deviations of 10-s SDQT [bottom **(C)**]. In each panel, the red circle and blue square marks correspond to females and males, respectively. The red and blue lines show the linear regression models between the displayed characteristics, the light colored red and blue bands show the 95% confidence intervals of the linear regressions, the light-colored violet areas show the overlaps between the regression confidence intervals of both sexes.





**FIGURE 12 |** The reduction values shown in this figure are defined as values of relative decrease of intra-subject regression corrected central SDQT values calculated as a proportion of uncorrected intra-subject means of SDQT. The top **(A)** shows a scatter diagram of the reductions involving regression to SDRR vs. those involving 10-s median beat noise; the bottom **(B)** shows a scatter diagram of the reductions involving 10-s median beat noise vs. those involving regression to a combination of SDRR and 10-s median beat noise. In both panels, red circles and blue squares correspond to female and males, respectively.

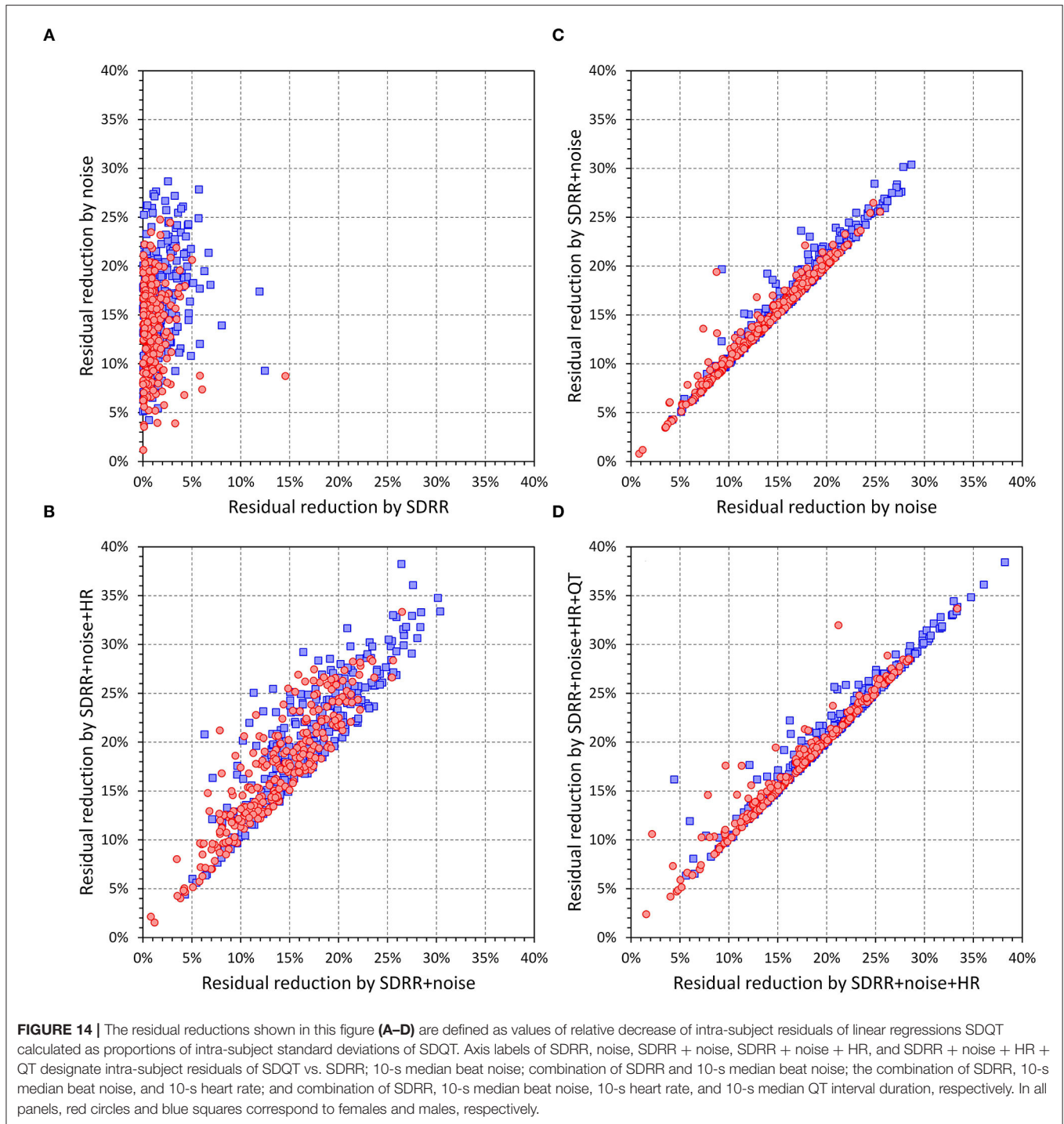


for heart rate correction” are written in rather recent analysis plans of laboratories providing ECG services for pharmaceutical industry (ERT, 2020). Secondly, the lack of immediate RR interval effect has implications for the physiologic interpretation of the QT variability index (Berger et al., 1997; Baumert et al., 2016). As we have previously discussed (Andršová et al., 2020), increases in the QT variability index might be caused both by increases in beat-to-beat QT variability and by decreases in heart rate variability which the index cannot distinguish (Tereshchenko et al., 2012). It can only be suggested that in future studies of diagnostic and prognostic implications of QT variability, separate measurements of QT variability and RR variability are investigated separately so that the implications of increased QT variability are not confused with heart rate variability reduction.

The immediate RR interval effect needs to be distinguished from general QT interval dependency on the underlying heart rate which is indisputable. Dependent on the degree of sinus arrhythmia, a single RR interval measurement offers a more or a less imprecise estimate of underlying heart rate. It is therefore not surprising that repeated studies have found some dependency of QT interval, QTpeak interval,

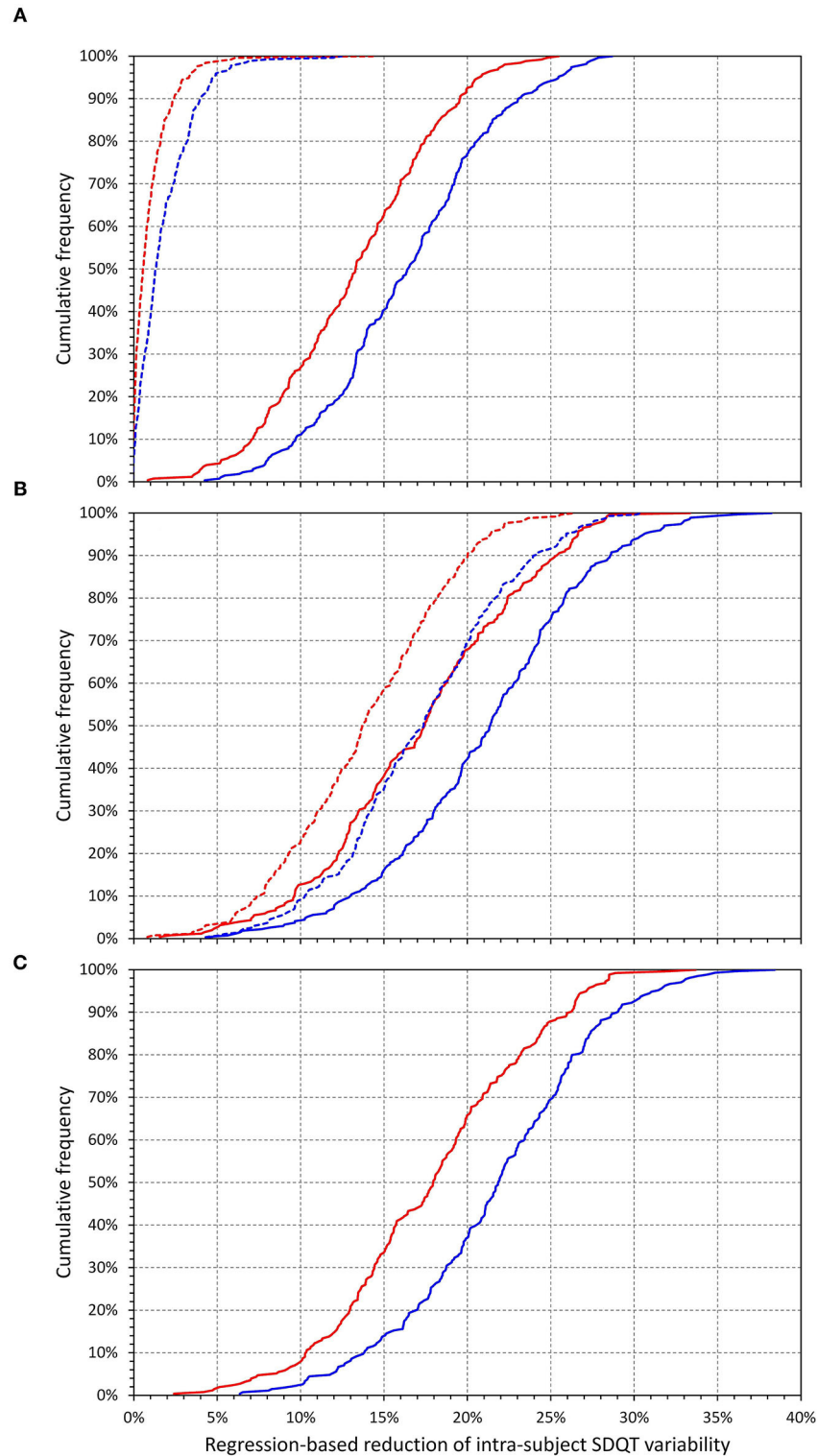
and of other repolarisation characteristics on the preceding RR interval (Funck-Brentano and Jaillon, 1993; Porta et al., 1998a). However, the concept of immediate RR interval effect postulates something different since it proposes that beat-to-beat shortening and prolongation of RR interval leads to consistent shortening and prolongation of the immediately following QT interval. This concept is clearly invalidated by this study.

Our finding of the association of beat-to-beat QT variability with the morphological instability (which, for simplicity’s sake, we call “noise”) of the source ECG tracing should not be interpreted as a suggestion that there are no beat-to-beat QT changes and that only morphology changes influence the beat-to-beat measurements. Morphological ECG changes might also have valid biological basis [e.g., related to respiration (Noriega et al., 2012; Sadiq et al., 2021), posture (Markendorf et al., 2018), food intake (Täubel et al., 2019), mental stress (Hwang et al., 2018), and other external inputs and physiologic reflexes]. While some of these mechanisms might not be fast enough to contribute beat-to-beat changes in QT interval measurements, it seems clear that the measurement of the differences between individual beats and the global representative waveform is not



necessarily reflecting only technical ECG imperfection. Still, the association of short-term QT variability with the “noise” measurements was so surprisingly strong, that we are of the opinion that some truly technical noise levels were involved and their influence on the beat-to-beat QT interval measurement needs to be considered. This is in good agreement with the old observations that the so-called QT dispersion was highly

contributed by ECG signal imperfections (Kautzner et al., 1994; Kors and van Herpen, 1998; Rautaharju, 1999; Malik and Batchvarov, 2000). Our observations were made despite the careful selection of only beats with very high correlations between the individual beat morphologies and the representative waveforms (i.e., despite using only good quality recordings). Therefore, it seems appropriate to suggest that in future studies



**FIGURE 15 |** Cumulative distributions of the relative decrease of intra-subject residuals of linear regressions SDQT calculated as proportions of intra-subject standard deviations of SDQT (see the section on Statistics and data presentation for details). The top **(A)** shows the reductions by 10-s median beat noise correction (solid lines) and by SDRR correction (dashed lines). The middle **(B)** shows reductions by a correction for a combination of 10-s median beat noise and SDRR (dashed lines) and for a combination of 10-s median beat noise, SDRR, and 10-s heart rate (solid lines). The bottom **(C)** shows reductions by a correction for a combination of 10-s median beat noise, SDRR, 10-s heart rate, and 10-s median QT interval duration. In each panel, the red and blue lines show the distributions among females and males, respectively.

of beat-to-beat QT variability, the objective assessment of ECG noise contents is incorporated (Batchvarov et al., 2002; Lee et al., 2012; Abreu et al., 2017; Everss-Villalba et al., 2017) so that it can be shown that any reported QT variability changes are independent of ECG noise pollution.

Two further comments are important for the practical implications of our findings of the influence of signal variability which we, for simplicity, call the noise. Firstly, the noise levels that we have observed were only tiny (see the bottom panel of **Figure 6**) in comparison to what would be called noise-polluted ECG in clinical and/or experimental practice as well as tiny in comparison to technical studies that previously investigated the effects of ECG noise on the ECG measurement and diagnostic accuracy (Porta et al., 1998b; Chang, 2010; Li et al., 2014; Tayel et al., 2018). Indeed, the median noise levels well below 20  $\mu\text{V}$  (see **Figure 6**) would be practically invisible on standard ECG prints. Secondly, and perhaps more importantly, our observation of the noise influence calls for careful interpretations of data obtained by the simple correlation matching algorithm (Berger et al., 1997; Baumert et al., 2016) that has been the basis for many if not the majority of previous studies of beat-to-beat QT variability. Regardless of whether the signal morphological variability is caused by biological or technical factors, it is not surprising that even tiny morphological changes influence the correlation matching algorithm. Hence, comparisons of beat-to-beat QT variability between different data sets might be problematic (if not entirely misleading) unless the QT variability data are corrected for the underlying morphological variability. Establishing an algorithm that would not only allow beat-to-beat QT measurements but would also produce results independent of measurable morphological variability remains a challenge.

The concept of correction of the SDQT values replicated the intra-subject regressions-based corrections of QT, JT, and JTp intervals for the underlying heart rate (Garnett et al., 2012; Panicker et al., 2018; Hnatkova et al., 2019). Since the intra-subject spreads of the data were rather wide (see examples in **Figures 1, 2**) we have not attempted to use any curvilinear regressions (Malik et al., 2012b) and used linear regression as the least biased approach. Contrary to the QT heart rate correction that, by the usual definition, estimates the duration of the QT interval at RR interval of 1 s, we used corrections estimating the SDQT values at the zero level of SDRR and/or zero level of ECG morphological variability. Possibly, similar corrections might be used in future studies of QT variability if, for some reason, multivariable regressions also involving heart rate variability and ECG signal-to-noise ratio do not appear appropriate.

It is not surprising that we found increased ECG morphological variability during faster heart rates (see **Figure 7**). It is thus possible that previous observations of increased QT variability at faster heart rates (Hnatkova et al., 2013) were influenced by measurement bias. The relationship between heart rate and QT variability also explains the somewhat counterintuitive observation of the negative correlation between QT interval duration and QT variability (see **Figure 7**). As heart rate increases,

uncorrected QT interval decreases which leads to this somewhat unexpected observation. Since it has been observed that faster heart rates lead to increased morphological variability, it remains challenging to investigate whether short-term SDQT is influenced by autonomic conditions independently of the autonomic influence on SDQT measurement accuracy.

## Limitations

The limitations of our study also need to be considered. While a number of previous QT variability studies used longer ECGs, we analyzed 10-s ECG segments since these are more relevant for practical purposes. We are unable to comment on whether the very same observations would be obtained with longer recordings. Nevertheless, since every longer ECG recording is, in principle, a series of shorter ECG segments, it is unlikely that with longer recordings, our observations would be principally different. The investigated population included neither very young nor very old subjects. The investigations of the relationship to age were therefore limited to the available age ranges. Finally, since the study data were obtained from clinical pharmacology investigations in healthy subjects, we are unable to comment on whether the same results would have been found if researching populations with clinically well-defined pathological characteristics. Nevertheless, our observations on the influence of recording quality and morphological instability still have implications for clinical investigations since anecdotal experience from clinical investigations suggests that poorer ECG quality is related to worsened outcomes.

## CONCLUSION

Despite these limitations, the study shows that the concept of immediate RR interval effect on the duration of subsequent QT interval duration is questionable since the beat-to-beat QT interval variability is little dependent on the underlying RR interval variability. Importantly, the analyzed data provide substantial evidence that even if only stable beat-to-beat measurements of QT interval are used, the QT interval variability is still substantially influenced by morphological variability and noise pollution of the source ECG recordings. The quality and signal-to-noise ratio thus needs to be carefully considered in future studies of QT interval variability.

## DATA AVAILABILITY STATEMENT

The raw data supporting the conclusions of this article will be made available by the authors, without undue reservation but pending the approval by the sponsors of the source clinical studies.

## ETHICS STATEMENT

The studies involving human participants were reviewed and approved by Parexel in Baltimore, California Clinical Trials in Glendale, and Spaulding in Milwaukee. The patients/participants



provided their written informed consent to participate in the source clinical studies.

## AUTHOR CONTRIBUTIONS

IA, KH, MM, and OT: study design and initial manuscript draft. KH and MM: software development and statistics and figures. GS, IA, KMH, MŠ, OT, PB, PS, and TN: ECG interpretation and ECG measurement. GS, TN, OT, and PS: supervision of the measurements. GS, MM, and TN: quality control of the

measurements. All authors approved the final manuscript of the submission.

## FUNDING

This work was supported in part by the British Heart Foundation New Horizons Grant NH/16/2/32499, by Ministry of Health, Czech Republic, Conceptual Development of Research Organization (Grant FNBr/65269705), and by the Specific Research of Masaryk University MUNI/A/1450/2021.

## REFERENCES

- Abreu, R., Nunes, S., Leal, A., and Figueiredo, P. (2017). Physiological noise correction using ECG-derived respiratory signals for enhanced mapping of spontaneous neuronal activity with simultaneous EEG-fMRI. *Neuroimage* 154, 115–127. doi: 10.1016/j.neuroimage.2016.08.008
- Andršová, I., Hnatkova, K., Šišáková, M., Toman, O., Smetana, P., Huster, K. M., et al. (2020). Heart rate influence on the QT variability risk factors. *Diagnostics* 10, 1096. doi: 10.3390/diagnostics10121096
- Batchvarov, V., Hnatkova, K., and Malik, M. (2002). Assessment of noise in digital electrocardiograms. *Pacing Clin. Electrophysiol.* 25, 499–503. doi: 10.1046/j.1460-9592.2002.00499.x
- Baumert, M., Lambert, G. W., Dawood, T., Lambert, E. A., Esler, M. D., McGrane, M., et al. (2008). QT interval variability and cardiac norepinephrine spillover in patients with depression and panic disorder. *Am. J. Physiol. Heart Circ. Physiol.* 295, H962–H968. doi: 10.1152/ajpheart.00301.2008
- Baumert, M., Porta, A., Vos, M. A., Malik, M., Couderc, J. P., Laguna, P., et al. (2016). variability in body surface ECG: measurement, physiological basis, and clinical value: position statement and consensus guidance endorsed by the European heart rhythm association jointly with the ESC working group on cardiac cellular electrophysiology. *Europace* 18, 925–944. doi: 10.1093/europace/euv405
- Berger, R. D., Kasper, E. K., Baughman, K. L., Marban, E., Calkins, H., and Tomaselli, G. F. (1997). Beat-to-beat QT interval variability: novel evidence for repolarization lability in ischemic and nonischemic dilated cardiomyopathy. *Circulation* 96, 1557–1565. doi: 10.1161/01.CIR.96.5.1557
- Browne, K. F., Prystowsky, E., Heger, J. J., Chilson, D. A., and Zipes, D. P. (1983). Prolongation of the Q-T interval in man during sleep. *Am. J. Cardiol.* 52, 55–59. doi: 10.1016/0002-9149(83)90068-1
- Chang, K. M. (2010). Arrhythmia ECG noise reduction by ensemble empirical mode decomposition. *Sensors* 10, 6063–6080. doi: 10.3390/s100606063
- Dobson, C. P., Kim, A., and Haigney, M. (2013). QT variability index. *Prog. Cardiovasc. Dis.* 56, 186–194. doi: 10.1016/j.pcad.2013.07.004
- El-Hamad, F., Javorka, M., Czippelova, B., Krohova, J., Turianikova, Z., Porta, A., et al. (2019). Repolarization variability independent of heart rate during sympathetic activation elicited by head-up tilt. *Med. Biol. Eng. Comput.* 57, 1753–1762. doi: 10.1007/s11517-019-01998-9
- ERT (2020). *Statistical Analysis Plan. Single-Dose and Randomized, Single-Center, Placebo- and Active Controlled, Crossover Study to Assess the Effect of Omecamtiv Mecarbil (OM) on QT/QTc Intervals in Healthy Subjects*. Available online at: [https://clinicaltrials.gov/ProvidedDocs/08/NCT04175808/SAP\\_002.pdf](https://clinicaltrials.gov/ProvidedDocs/08/NCT04175808/SAP_002.pdf)
- ESC/NASPE Task Force (1996). Heart rate variability: standards of measurement, physiological interpretation and clinical use. *Circulation* 93, 1043–1065. doi: 10.1161/01.CIR.93.5.1043
- Evers-Villalba, E., Melgarejo-Meseguer, F. M., Blanco-Velasco, M., Gimeno-Blanes, F. J., Sala-Pla, S., Rojo-Álvarez, J. L., et al. (2017). Noise maps for quantitative and clinical severity towards long-term ECG monitoring. *Sensors* 17, 2448. doi: 10.3390/s17112448
- Fischer, C., Seeck, A., Schroeder, R., Goernig, M., Schirdewan, A., Figulla, H. R., et al. (2015). QT variability improves risk stratification in patients with dilated cardiomyopathy. *Physiol. Meas.* 36, 699–713. doi: 10.1088/0967-3334/36/4/699
- Fossa, A. A., DePasquale, M. J., Raunig, D. L., Avery, M. J., and Leishman, D. J. (2002). The relationship of clinical QT prolongation to outcome in the conscious dog using a beat-to-beat QT-RR interval assessment. *J. Pharmacol. Exp. Ther.* 302, 828–833. doi: 10.1124/jpet.102.035220
- Franz, M. R., Swerdlow, C. D., Liem, L. B., and Schaefer, J. (1988). Cycle length dependence of human action potential duration *in vivo*. Effects of single extrastimuli, sudden sustained rate acceleration and deceleration, and different steady-state frequencies. *J. Clin. Invest.* 82, 972–979. doi: 10.1172/JCI113706
- Funck-Brentano, C., and Jaillon, P. (1993). Rate-corrected QT interval: techniques and limitations. *Am. J. Cardiol.* 72, 17B–22B. doi: 10.1016/0002-9149(93)90035-B
- Garnett, C. E., Zhu, H., Malik, M., Fossa, A. A., Zhang, J., Badilini, F., et al. (2012). Methodologies to characterize the QT/corrected QT interval in the presence of drug-induced heart rate changes or other autonomic effects. *Am. Heart J.* 163, 912–930. doi: 10.1016/j.ahj.2012.02.023
- Gravel, H., Curnier, D., Dahdah, N., and Jacquemet, V. (2017). Categorization and theoretical comparison of quantitative methods for assessing QT/RR hysteresis. *Ann. Noninvasive Electrocardiol.* 22, e12463. doi: 10.1111/anec.12463
- Guldenring, D., Finlay, D. D., Strauss, D. G., Galeotti, L., Nugent, C. D., Donnelly, M. P., et al. (2012). Transformation of the Mason-Likar 12-lead electrocardiogram to the frank vectorcardiogram. *Annu. Int. Conf. IEEE Eng. Med. Biol. Soc.* 2012, 677–680. doi: 10.1109/EMBC.2012.6346022
- Hasan, M. A., and Abbott, D. (2016). A review of beat-to-beat vectorcardiographic (VCG) parameters for analyzing repolarization variability in ECG signals. *Biomed. Tech.* 61, 3–17. doi: 10.1515/bmt-2015-0005
- Hasan, M. A., Abbott, D., and Baumert, M. (2012). Beat-to-beat spatial and temporal analysis for QRS-T morphology. *Annu. Int. Conf. IEEE Eng. Med. Biol. Soc.* 2012, 4193–4195. doi: 10.1109/EMBC.2012.6346891
- Hasan, M. A., Abbott, D., and Baumert, M. (2013). Beat-to-beat QT interval variability and T-wave amplitude in patients with myocardial infarction. *Physiol. Meas.* 34, 1075–1083. doi: 10.1088/0967-3334/34/9/1075
- Hnatkova, K., Johannesen, L., Vicente, J., and Malik, M. (2017). Heart rate dependency of JT interval sections. *J. Electrocardiol.* 50, 814–824. doi: 10.1016/j.jelectrocard.2017.08.005
- Hnatkova, K., Kowalski, D., Keirns, J. J., van Gelderen, E. M., and Malik, M. (2013). Relationship of QT interval variability to heart rate and RR interval variability. *J. Electrocardiol.* 46, 591–596. doi: 10.1016/j.jelectrocard.2013.07.007
- Hnatkova, K., Smetana, P., Toman, O., Bauer, A., Schmidt, G., and Malik, M. (2009). Systematic comparisons of electrocardiographic morphology increase the precision of QT interval measurement. *Pacing Clin. Electrophysiol.* 32, 119–130. doi: 10.1111/j.1540-8159.2009.02185.x
- Hnatkova, K., Vicente, J., Johannesen, L., Garnett, C., Strauss, D. G., Stockbridge, N., et al. (2019). Heart rate correction of the J-to-Tpeak interval. *Sci. Rep.* 9, 15060. doi: 10.1038/s41598-019-51491-4
- Hwang, B., You, J., Vaessen, T., Myin-Germeys, I., Park, C., and Zhang, B. T. (2018). Deep ECGNet: an optimal deep learning framework for monitoring mental stress using ultra short-term ECG signals. *Telemed. J. E Health* 24, 753–772. doi: 10.1089/tmj.2017.0250
- ICH Guideline (2001). Safety pharmacology studies for human pharmaceuticals S7A. *Fed. Regist.* 66, 36791–36792.
- Jacquemet, V., Cassani González, R., Sturmer, M., Dubé, B., Sharestan, J., Vinet, A., et al. (2014). QT interval measurement and correction in

- patients with atrial flutter: a pilot study. *J. Electrocardiol.* 47, 228–235. doi: 10.1016/j.jelectrocard.2013.11.002
- Kautzner, J., Yi, G., Camm, A. J., and Malik, M. (1994). Short- and long-term reproducibility of QT, QTc, and QT dispersion measurement in healthy subjects. *Pacing Clin. Electrophysiol.* 17, 928–937. doi: 10.1111/j.1540-8159.1994.tb01435.x
- Kors, J. A., and van Herpen, G. (1998). Measurement error as a source of QT dispersion: a computerised analysis. *Heart* 80, 453–458. doi: 10.1136/hrt.80.5.453
- Lanfranchi, P. A., Shamsuzzaman, A. S., Ackerman, M. J., Kara, T., Jurak, P., Wolk, R., et al. (2002). Sex-selective QT prolongation during rapid eye movement sleep. *Circulation* 106, 1488–1492. doi: 10.1161/01.CIR.0000030183.10934.95
- Lau, C. P., Freeman, A. R., Fleming, S. J., Malik, M., Camm, A. J., and Ward, D. E. (1988). Hysteresis of the ventricular paced QT interval in response to abrupt changes in pacing rate. *Cardiovasc. Res.* 22, 67–72. doi: 10.1093/cvr/22.1.67
- Lee, J., McManus, D. D., Merchant, S., and Chon, K. H. (2012). Automatic motion and noise artifact detection in holter ECG data using empirical mode decomposition and statistical approaches. *IEEE Trans. Biomed. Eng.* 59, 1499–1506. doi: 10.1109/TBME.2011.2175729
- Li, Q., Rajagopalan, C., and Clifford, G. D. (2014). A machine learning approach to multi-level ECG signal quality classification. *Comput. Methods Prog. Biomed.* 117, 435–447. doi: 10.1016/j.cmpb.2014.09.002
- Malik, M. (2004). Errors and misconceptions in ECG measurement used for the detection of drug induced QT interval prolongation. *J. Electrocardiol.* 37, 25–33. doi: 10.1016/j.jelectrocard.2004.08.005
- Malik, M. (2008). Beat-to-beat QT variability and cardiac autonomic regulation. *Am. J. Physiol. Heart Circ. Physiol.* 295, H923–H925. doi: 10.1152/ajpheart.00709.2008
- Malik, M., Andreas, J.-O., Hnatkova, K., Hoekendorff, J., Cawello, W., Middle, M., et al. (2008a). Thorough QT/QTc Study in patients with advanced Parkinson's disease: cardiac safety of rotigotine. *Clin. Pharmacol. Ther.* 84, 595–603. doi: 10.1038/clpt.2008.143
- Malik, M., and Batchvarov, V. N. (2000). Measurement, interpretation, and clinical potential of QT dispersion. *J. Am. Coll. Cardiol.* 36, 1749–1766. doi: 10.1016/S0735-1097(00)00962-1
- Malik, M., and Camm, A. J. (1990). Heart rate variability. *Clin. Cardiol.* 13, 570–576. doi: 10.1002/clc.4960130811
- Malik, M., Hnatkova, K., Batchvarov, V., Gang, Y., Smetana, P., and Camm, A. J. (2004). Sample size, power calculations, and their implications for the cost of thorough studies of drug induced QT interval prolongation. *Pacing Clin. Electrophysiol.* 27, 1659–1669. doi: 10.1111/j.1540-8159.2004.0701.x
- Malik, M., Hnatkova, K., Kowalski, D., Keirns, J. J., and van Gelderen, E. M. (2012b). Importance of subject-specific QT/RR curvatures in the design of individual heart rate corrections of the QT interval. *J. Electrocardiol.* 45, 571–581. doi: 10.1016/j.jelectrocard.2012.07.017
- Malik, M., Hnatkova, K., Novotny, T., and Schmidt, G. (2008b). Subject-specific profiles of QT/RR hysteresis. *Am. J. Physiol. Heart Circ. Physiol.* 295, H2356–H2363. doi: 10.1152/ajpheart.00625.2008
- Malik, M., Johannesen, L., Hnatkova, K., and Stockbridge, N. (2016). Universal correction for QT/RR hysteresis. *Drug Saf.* 39, 577–588. doi: 10.1007/s40264-016-0406-0
- Malik, M., van Gelderen, E. M., Lee, J. H., Kowalski, D. L., Yen, M., Goldwater, R., et al. (2012a). Proarrhythmic safety of repeat doses of mirabegron in healthy subjects: a randomized, double-blind, placebo-, and active-controlled thorough QT study. *Clin. Pharm. Ther.* 92, 696–706. doi: 10.1038/clpt.2012.181
- Markendorf, S., Lüscher, T. F., Gerds-Li, J. H., Schönrrath, F., and Schmied, C. M. (2018). Clinical impact of repolarization changes in supine versus upright body position. *Cardiol. J.* 25, 589–594. doi: 10.5603/CJ.a2017.0138
- Monasterio, V., Martínez, J. P., Laguna, P., McNitt, S., Polonsky, S., Moss, A. J., et al. (2013). Prognostic value of average T-wave alternans and QT variability for cardiac events in MADIT-II patients. *J. Electrocardiol.* 46, 480–486. doi: 10.1016/j.jelectrocard.2013.08.004
- Niemeijer, M. N., van den Berg, M. E., Eijgelsheim, M., van Herpen, G., Stricker, B. H., Kors, J. A., et al. (2014). Short-term QT variability markers for the prediction of ventricular arrhythmias and sudden cardiac death: a systematic review. *Heart* 100, 1831–1836. doi: 10.1136/heartjnl-2014-305671
- Noriega, M., Martínez, J. P., Laguna, P., Bailón, R., and Almeida, R. (2012). Respiration effect on wavelet-based ECG T-wave end delineation strategies. *IEEE Trans. Biomed. Eng.* 59, 1818–1828. doi: 10.1109/TBME.2011.2157824
- Nussinovitch, U., Rubin, S., Levy, Y., Lidar, M., and Livneh, A. (2018). QT variability index in patients with systemic sclerosis. *Eur. J. Rheumatol.* 6, 179–183. doi: 10.5152/eurjrheum.2019.19074
- Orosz, A., Baczkó, I., Nagy, V., Gavallér, H., Csanády, M., Forster, T., et al. (2015a). Short-term beat-to-beat variability of the QT interval is increased and correlates with parameters of left ventricular hypertrophy in patients with hypertrophic cardiomyopathy. *Can. J. Physiol. Pharmacol.* 93, 765–772. doi: 10.1139/cjpp-2014-0526
- Orosz, A., Csajbók, É., Czékus, C., Gavallér, H., Magony, S., Valkusz, Z., et al. (2015b). Increased short-term beat-to-beat variability of QT interval in patients with acromegaly. *PLoS ONE* 10, e0125639. doi: 10.1371/journal.pone.0125639
- Panicker, G. K., Kadam, P., Chakraborty, S., Kothari, S., Turner, J. R., and Karnad, D. R. (2018). Individual-specific QT interval correction for drugs with substantial heart rate effect using Holter ECGs extracted over a wide range of heart rates. *J. Clin. Pharmacol.* 58, 1013–1019. doi: 10.1002/jcph.1258
- Porta, A., Baselli, G., Caiani, E., Malliani, A., Lombardi, F., and Cerutti, S. (1998a). Quantifying electrocardiogram RT-RR variability interactions. *Med. Biol. Eng. Comput.* 36, 27–34. doi: 10.1007/BF02522854
- Porta, A., Baselli, G., Lombardi, F., Cerutti, S., Antolini, R., Del Greco, M., et al. (1998b). Performance assessment of standard algorithms for dynamic R-T interval measurement: comparison between R-Tapex and R-T(end) approach. *Med. Biol. Eng. Comput.* 36, 35–42. doi: 10.1007/BF02522855
- Porta, A., Cairo, B., De Maria, B., and Bari, V. (2020). Complexity of spontaneous QT variability unrelated to RR variations and respiration during graded orthostatic challenge. *Comput. Cardiol.* 47. doi: 10.22489/CinC.2020.009
- Porta, A., Girardengo, G., Bari, V., George, A. L. Jr., Brink, P. A., Goosen, A., et al. (2015). Autonomic control of heart rate and QT interval variability influences arrhythmic risk in long QT syndrome type 1. *J. Am. Coll. Cardiol.* 65, 367–374. doi: 10.1016/j.jacc.2014.11.015
- Porta, A., Tobaldini, E., Gnecchi-Ruscone, T., and Montano, N. (2010). RT variability unrelated to heart period and respiration progressively increases during graded head-up tilt. *Am. J. Physiol. Heart Circ. Physiol.* 298, H1406–H1414. doi: 10.1152/ajpheart.01206.2009
- Rahola, J. T., Kiviniemi, A. M., Ukkola, O. H., Tulppo, M. P., Junttila, M. J., Huikuri, H. V., et al. (2021). Temporal variability of T-wave morphology and risk of sudden cardiac death in patients with coronary artery disease. *Ann. Noninvasive Electrocardiol.* 26, e12830. doi: 10.1111/anec.12830
- Rautaharju, P. M. (1999). QT and dispersion of ventricular repolarization: the greatest fallacy in electrocardiography in the 1990s. *Circulation* 99, 2477–2478. doi: 10.1161/circ.99.18.2476/c
- Sadiq, I., Perez-Alday, E. A., Shah, A. J., and Clifford, G. D. (2021). Breathing rate and heart rate as confounding factors in measuring T wave alternans and morphological variability in ECG. *Physiol. Meas.* 42, 015002. doi: 10.1088/1361-6579/abd237
- Sagie, A., Larson, M. G., Goldberg, R. J., Bengtson, J. R., and Levy, D. (1992). An improved method for adjusting the QT interval for heart rate (the framingham heart study). *Am. J. Cardiol.* 70, 797–801. doi: 10.1016/0002-9149(92)90562-D
- Schmidt, M., Baumert, M., Malberg, H., and Zaunseider, S. T. (2016). Wave amplitude correction of QT interval variability for improved repolarization lability measurement. *Front. Physiol.* 7, 216. doi: 10.3389/fphys.2016.00216
- Seethala, S., Singh, P., Shusterman, V., Ribe, M., Haugaa, K. H., and Nèmec, J. (2015). QT adaptation and intrinsic QT variability in congenital long QT syndrome. *J. Am. Heart Assoc.* 4, e002395. doi: 10.1161/JAHA.115.002395
- Smoczyńska, A., Loen, V., Sprenkeler, D. J., Tuinenburg, A. E., Ritsema van Eck, H. J., Malik, M., et al. (2020). Short-term variability of the QT interval can be used for the prediction of imminent ventricular arrhythmias in patients with primary prophylactic implantable cardioverter defibrillators. *J. Am. Heart Assoc.* 2020, e018133. doi: 10.1161/JAHA.120.018133
- Täubel, J., Ferber, G., Van Langenhoven, L., Del Bianco, T., Fernandes, S., Djumanov, D., et al. (2019). The cardiovascular effects of a meal: J-Tpeak and tpeak-tend assessment and further insights into the physiological effects. *J. Clin. Pharmacol.* 59, 799–810. doi: 10.1002/jcph.1374
- Tayel, M. B., Eltrass, A. S., and Ammar, A. I. (2018). A new multi-stage combined kernel filtering approach for ECG noise removal. *J. Electrocardiol.* 51, 265–275. doi: 10.1016/j.jelectrocard.2017.10.009

- Tereshchenko, L. G., Cygankiewicz, I., McNitt, S., Vazquez, R., Bayes-Genis, A., Han, L., et al. (2012). Predictive value of beat-to-beat QT variability index across the continuum of left ventricular dysfunction: competing risks of noncardiac or cardiovascular death and sudden or nonsudden cardiac death. *Circ. Arrhythm. Electrophysiol.* 5, 719–727. doi: 10.1161/CIRCEP.112.970541
- van den Berg, M. E., Kors, J. A., van Herpen, G., Bots, M. L., Hillege, H., Swenne, C. A., et al. (2019). Normal values of QT variability in 10-s electrocardiograms for all ages. *Front. Physiol.* 10, 1272. doi: 10.3389/fphys.2019.01272
- Viigimae, M., Karai, D., Pilt, K., Pirn, P., Huhtala, H., Polo, O., et al. (2017). QT variability index and QT interval duration during different sleep stages in patients with obstructive sleep apnea. *Sleep Med.* 37, 160–167. doi: 10.1016/j.sleep.2017.06.026
- Viigimae, M., Karai, D., Pirn, P., Pilt, K., Meigas, K., and Kaik, J. (2015). QT interval variability index and QT Interval duration in different sleep stages: analysis of polysomnographic recordings in nonapneic male patients. *Biomed. Res. Int.* 2015, 963028. doi: 10.1155/2015/963028
- Xue, J. Q. (2009). Robust QT interval estimation - from algorithm to validation. *Ann. Noninvasive Electrocardiol.* 14 (Suppl. 1), S35–S41. doi: 10.1111/j.1542-474X.2008.00264.x

**Conflict of Interest:** The authors declare that the research was conducted in the absence of any commercial or financial relationships that could be construed as a potential conflict of interest.

**Publisher's Note:** All claims expressed in this article are solely those of the authors and do not necessarily represent those of their affiliated organizations, or those of the publisher, the editors and the reviewers. Any product that may be evaluated in this article, or claim that may be made by its manufacturer, is not guaranteed or endorsed by the publisher.

Copyright © 2022 Toman, Hnatkova, Šišáková, Smetana, Huster, Barthel, Novotný, Andršová, Schmidt and Malik. This is an open-access article distributed under the terms of the Creative Commons Attribution License (CC BY). The use, distribution or reproduction in other forums is permitted, provided the original author(s) and the copyright owner(s) are credited and that the original publication in this journal is cited, in accordance with accepted academic practice. No use, distribution or reproduction is permitted which does not comply with these terms.

O QTV lze tedy zatím jen říci, že i přes její popisovaný silný stratifikační potenciál se jedná o hodnotu výrazně ovlivněnou hlukem v signálu s obtížnou a složitou metodikou získání.

## 4. Prostorové komponenty a fragmentace QRS komplexu

Jak již bylo zmíněno v kapitole 3.6, repolarizace se nešíří po stejné dráze jako předešlá depolarizace. Nicméně je logické, že repolarizace bude depolarizační disperzí ovlivněna, a proto má ve stratifikaci NSS opodstatněné místo. Mnohé dříve publikované studie dokazují závislost mortality z kardiálních příčin na trvání QRS komplexu u pacientů po infarktu myokardu s nebo i bez srdečního selhání.<sup>104,105,106</sup> Pacienti indikovaní k primárně preventivní implantaci ICD s trváním QRS minimálně 120 ms profitují z této terapie více než pacienti s nepatologickými hodnotami šíře QRS.<sup>107</sup> Přesto pozitivní předpovědní hodnota rizika NSS dle šířky QRS je nízká, a to především u pacientů s ICHS léčených beta-blokátory.<sup>108</sup> Analýza podskupin studie MADIT II prokázala nejvyšší prospěch z primárně preventivní implantace ICD u pacientů s trváním QRS komplexu nad 150 ms. V této podskupině vedla implantace ICD k 36% absolutní a 63% relativní redukci rizika.<sup>109</sup>

V dospělé populaci máme dobře definovanou šířku QRS komplexu.<sup>110</sup> Je známý i fakt, že existují rozdíly mezi muži a ženami, a že trvání QRS je rozdílné i u různých ras.<sup>111,112,113</sup> Důvod těchto odlišností není zcela jasný a jen obtížně se dá vysvětlit pouhou velikostí srdce.<sup>112,114</sup>

### 4.1. Prostorové komponenty QRS komplexu

Depolarizace komor je popisována jako nekontrolovatelný tok iontových proudů myokardem šířících se podél svalových vláken přes mezibuněčné spoje. Šířka QRS musí být z velké části způsobena heterogenitou v šíření depolarizační sekvence včetně anizotropních rozdílů mezi podélným a příčným přenosem jednotlivých vrstev tkáně.<sup>115</sup> Je potřeba však zdůraznit, že délka trvání QRS komplexu je u zdravých jedinců při bazální SF prakticky neměnná, což naznačuje intraindividuální stabilitu i přes interindividuální variabilitu.<sup>112,115</sup> Depolarizace je tedy u zdravých jedinců velmi složitý proces, nicméně s jasnými intraindividuálními pravidly.

K pochopení odlišného individuálního trvání QRS a pochopení interindividuálních rozdílů šíření depolarizace byla navržena technologie ve spolupráci s technicky orientovanými spoluautory, kterou popisuje následující článek. Metoda je založená na dekompozici EKG signálu na singulární hodnoty a poté rekonstrukci původního QRS signálu do ortogonálních složek.<sup>116,117,118</sup> Základem je tedy trojrozměrná orientace signálu QRS komplexu ze svodů I, II, V1 až V6 (zbylé svody jsou pouze algebraickou kombinací předešlých) zkonstruovaná do 8 komponent včetně parametrů přesahujících svými rozměry tři ortogonální dimenze (v algebraickém spíše než geometrickém vícerozměrném smyslu). Sloučením QRS komplexů z osmi nezávislých svodů dostaneme plochu pod QRS křivkou, která vystihuje podíl jednotlivých algebraických komponent k celkovému QRS signálu. Porovnáním této sumace s jednotlivými zrekonstruovanými komponentami získáme představu o toku depolarizace a také o jeho homogenitě (viz obrázek 1 následující publikace). V podstatě je šíření relativně

homogenní depolarizační vlny srdeční tkání charakterizováno pohybem vektoru v trojrozměrném prostoru (stejným způsobem, který používá vektorokardiografie). Lokální abnormality narušující homogenitu srdeční depolarizace jsou pak promítány do komponent obsažených ve vyšších algebraických dimenzích.

V tomto smyslu má zásadní význam rozlišení mezi algebraickými a geometrickými dimenzemi. Ačkoliv hovoříme o více než třech dimenzích, máme na mysli algebraické dimenze. Netvrdíme tedy, že depolarizační vlny existují mimo standardní trojrozměrný prostor. Lokalizované heterogenity, které se objevují během depolarizace, spíše vedou k lokálním signálům, které nejsou synchronní s jinými lokálními signály z různých oblastí myokardu. Kvůli geometrii hrudníku přispívají takové lokální signály k morfologii QRS v různých svodech EKG odlišně. Když je signál ze všech nezávislých svodů zpracován rozkladem singulární hodnoty, tyto lokalizované signály nejsou geometricky (ve trojrozměrném smyslu) konzistentní s jinými lokalizovanými signály, a proto nemohou být reprezentovány trojrozměrným pohybem vektoru. V důsledku toho analýza komplexu QRS přiřazuje lokální signály do vyšších dimenzí (v čistě algebraickém smyslu).

Práce představuje novou metodu v analýze QRS a hodnocení heterogenity depolarizace. Pomocí metody jsme potvrdili, že šíření depolarizace je individuálně rozdílné. Neboli, šíření repolarizace je v podstatě u každého jedince různé, nicméně stabilní. Dalším zjištěním je, že vliv na kratší trvání QRS komplexu u žen je způsoben pravděpodobně plynulejším a méně komplikovaným šířením depolarizace srdeční tkání v porovnání s muži.

Hnatkova K, **Andršová I**, Toman O, Smetana P, Huster KM, Šišáková, Barthel P, Novotný T, Schmidt G, Malik M. Spatial distribution of physiologic 12-lead QRS complex. Scientific Reports 2021; 11:4289. doi: 10.1038/s41598-021-83378-8.

IF 4,997. Počet citací ve Web of Science 3

Původní práce - kvantitativní podíl uchazečky 25%: Elektrokardiologická měření, fyziologická interpretace metody, interpretace statistických výsledků, diskuze výsledků.



OPEN

# Spatial distribution of physiologic 12-lead QRS complex

Katerina Hnatkova<sup>1</sup>, Irena Andršová<sup>2</sup>, Ondřej Toman<sup>2</sup>, Peter Smetana<sup>3</sup>, Katharina M. Huster<sup>4</sup>, Martina Šišáková<sup>2</sup>, Petra Barthel<sup>4</sup>, Tomáš Novotný<sup>2</sup>, Georg Schmidt<sup>4</sup> & Marek Malik<sup>1</sup>✉

The normal physiologic range of QRS complex duration spans between 80 and 125 ms with known differences between females and males which cannot be explained by the anatomical variations of heart sizes. To investigate the reasons for the sex differences as well as for the wide range of normal values, a technology is proposed based on the singular value decomposition and on the separation of different orthogonal components of the QRS complex. This allows classification of the proportions of different components representing the 3-dimensional representation of the electrocardiographic signal as well as classification of components that go beyond the 3-dimensional representation and that correspond to the degree of intricate convolutions of the depolarisation sequence. The technology was applied to 382,019 individual 10-s ECG samples recorded in 639 healthy subjects (311 females and 328 males) aged  $33.8 \pm 9.4$  years. The analyses showed that QRS duration was mainly influenced by the proportions of the first two orthogonal components of the QRS complex. The first component demonstrated statistically significantly larger proportion of the total QRS power (expressed by the absolute area of the complex in all independent ECG leads) in females than in males ( $64.2 \pm 11.6\%$  vs  $59.7 \pm 11.9\%$ ,  $p < 0.00001$ —measured at resting heart rate of 60 beats per minute) while the second component demonstrated larger proportion of the QRS power in males compared to females ( $33.1 \pm 11.9\%$  vs  $29.6 \pm 11.4\%$ ,  $p < 0.001$ ). The analysis also showed that the components attributable to localised depolarisation sequence abnormalities were significantly larger in males compared to females ( $2.85 \pm 1.08\%$  vs  $2.42 \pm 0.87\%$ ,  $p < 0.00001$ ). In addition to the demonstration of the technology, the study concludes that the detailed convolution of the depolarisation waveform is individual, and that smoother and less intricate depolarisation propagation is the mechanism likely responsible for shorter QRS duration in females.

As well known, the physiologically normal adult QRS complex is 80–125 ms wide<sup>1,2</sup>. It has also been long understood<sup>3</sup> that in addition to the heart size and to the ventricular myocardial mass<sup>4</sup>, the duration of the QRS complex is influenced by the myocyte geometry and layer orientation<sup>5</sup>, Purkinje fibre tree structure<sup>6</sup>, and depolarising ion currents<sup>7</sup>. It is also known that compared to males, females have shorter QRS complex<sup>8,9</sup>, and that QRS duration disparities exist between races<sup>9,10</sup>.

The electrophysiologic reasons for the sex and race differences are poorly understood but they cannot be explained by the differences in heart sizes and myocardial volume alone. In proportional terms, adult heart sizes are less variable compared to the QRS duration<sup>11</sup> and while heart size reasonably correlates with body size<sup>12</sup>, the QRS duration does not<sup>9</sup>. This all potentially makes the broad range of the normal QRS complex durations somewhat unexpected.

The usual understanding of cardiac electrophysiology considers depolarisation sequence as a rather simple ion exchange reaction that propagates along myocardial fibre bands with practically uncontrolled cell to cell excitation transmission across gap junctions. The contribution of the differences in myocyte geometric composition and of the details in Purkinje fibre distribution must thus be rather substantial to explain the appreciable spread of myocardial depolarization duration. Considering these histology factors, the inter-subject differences in the QRS width have to be largely caused by heterogeneity in the propagation of the depolarization sequence including the anisotropic differences between longitudinal and cross-fibre excitation transmission combined with gap junction discontinuities<sup>13,14</sup>. At the same time, while showing substantial inter-subject differences, QRS complex duration is reasonably stable within each healthy subject, especially when considering repeated measurements at

<sup>1</sup>National Heart and Lung Institute, Imperial College, ICTEM, Hammersmith Campus, 72 Du Cane Road, Shepherd's Bush, London W12 0NN, England. <sup>2</sup>Department of Internal Medicine and Cardiology, Faculty of Medicine, University Hospital Brno, Masaryk University, Jihlavská 20, 625 00 Brno, Czech Republic. <sup>3</sup>Wilhelminenspital der Stadt Wien, Montleartstraße 37, 1160 Vienna, Austria. <sup>4</sup>Klinikum Rechts der Isar, Technische Universität München, Ismaninger Straße 22, 81675 Munich, Germany. ✉email: marek.malik@imperial.ac.uk

corresponding underlying heart rates<sup>9,15</sup>. Thus, the anisotropy of excitation propagation is likely to show similar intra-subject stability combined with appreciable inter-subject variability.

To allow clinical assessment of the myocardial depolarisation anisotropy and to permit investigation of its implication among clinically defined populations, a non-invasive method for the assessment of the spatial distribution of myocardial excitation waveforms is needed, preferably based on standard 12-lead electrocardiograms (ECG). Having this need in mind, we have tested the application of singular value decomposition (SVD)<sup>16</sup> to the 12-lead QRS complex electrocardiograms. SVD was previously successfully used in a broad spectrum of electrocardiographic studies including, among others, ECG compression<sup>17,18</sup>, noise removal<sup>19</sup>, interval measurement<sup>20</sup>, and ECG component complexity analyses<sup>21–23</sup>. For the purposes of the present study, we have extended SVD algorithms as well as the interpretation of their results applied to the QRS signal complexity analysis. In addition to testing the application of the technology, we aimed at investigating whether the SVD signal analysis would help explaining the differences in QRS complex duration among healthy subjects and whether, similar to the differences in the QRS duration, it would show differences in QRS composition between the sexes. We have researched this using data that have previously been collected in a battery of clinical pharmacology studies.

## Methods

**Investigated population and electrocardiographic recordings.** A collection of Holter recordings previously analysed for a different purpose was used<sup>24</sup>. Altogether 639 healthy subjects participated at six different clinical pharmacology studies. All subjects were screened before enrolment and all had a normal resting ECG and normal clinical investigation as mandated in clinical pharmacology research<sup>25</sup>. Clinical conduct of the studies including the procedures of electrocardiogram acquisition adhered strictly to the relevant guidelines and regulations<sup>25,26</sup>. All these studies were ethically approved by the institutional ethics bodies (Focus in Neuss; Parexel in Baltimore, Bloemfontein, and Glendale; PPD in Austin; and Spaulding in Milwaukee). All subjects gave informed written consent to the participation. All the source studies were conducted in accordance with the Helsinki declaration.

As previously described<sup>24</sup>, each of the studies included repeated 12-lead day-time Holter recordings in each participant. The recordings were made during multiple baseline days. During these baseline days, study protocols included repeated provocative manoeuvres with the aim of capturing wide heart rates ranges in each participant. The postural provocative manoeuvres included time-points during which the study subjects were, per protocol, in undisturbed supine, unsupported sitting, and unsupported standing positions. In addition to these, other study per-protocol time-points required the subjects to maintain strict supine positions. The Holter recordings used Mason-Likar electrode positions. Clinical conduct of the baseline days did not differ between individual units. The investigation described in this text utilized the baseline Holter recordings when the subjects were off any medication, did not smoke, and refrained from consuming caffeinated drinks. Further details of the clinical pharmacology studies are therefore irrelevant.

**Electrocardiographic measurements.** Using previously developed technology combining computerized signal processing with visual checks and manual corrections of the measurements<sup>24,27,28</sup>, multiple 10-s segments were extracted from each of the Holter recordings aiming at the inclusion of segments with different underlying heart rates. That is, in addition to the extractions at pre-specified study time-points described in the previous section, instantaneous heart rate was measured throughout the complete day-time Holters and additional segments were extracted to cover the range of captured heart rates uniformly. These additional extractions were made during times when the study subjects were not restricted by study protocols although the standard clinical pharmacology research requirements were observed<sup>20</sup>. Apart from the postural provocative manoeuvres, the source studies did not include any physical or mental challenges. During the day-time Holter recordings, the subjects were allowed neither to sleep nor to leave the confined area of the clinical unit.

For each extracted segment, 2-min history of preceding RR interval was obtained and within these 2-min intervals, heart rate was measured in non-overlapping 30-s sections. Extracted segments were used in this study only if they were preceded by reasonably stable heart rates which were defined as the range between minimum to maximum heart rate measured in the 30-s sections not exceeding 5 beats per minute (bpm).

Each extracted 10-s ECG segment was filtered to reduce noise pollution and to eliminate baseline wander<sup>27,28</sup>. Subsequently, a representative median beat was constructed, as previously used in other ECG studies<sup>28,29</sup>. Specifically, in the waveforms of the original recording sampled at 1000 Hz, QRS complexes were identified, superimposed by obtaining autocorrelation maxima across all independent leads, and sample by sample medians of all superimposed P-QRS-T morphologies were used to form the representative beat (our unpublished experience suggests that by eliminating outlier values, the sample-by-sample medians reduce the noise of the representative beat compared to sample-by-sample averages). In this representative beat, all 12 leads were superimposed on the same isoelectric axis and QRS onset and offset points were identified using previously developed algorithms<sup>27,28</sup>. The quality control of the identification of these points included visual verification and manual correction of computerized measurements by at least two independently working cardiologists with subsequent independent reconciliation in case of measurement disagreement. Pattern matching algorithms<sup>30</sup> were also applied to ensure that comparable morphologies of QRS onset and offset were measured systematically.

In each measured ECG segment, the QRS width was defined as the time distance between the QRS onset and offset. The underlying heart rate was defined as the heart rate calculated from the averaged duration of the RR intervals in the preceding 2-min (which also included the 10 s of the measured ECG segment itself).

**Singular value decomposition.** The SVD principles of ECG signal were published in detail many times before<sup>16,20,22</sup>. In brief, the 12-lead ECG contains only 8 algebraically independent leads I, II, V1, V2, ..., V6 since



the unipolar limb leads are only simple algebraic combinations of leads I and II. Hence, the ECG signal may be considered to constitute a matrix  $\mathbb{M}^{8,n}$  of voltage values which has 8 rows  $\gg_i$  corresponding to individual leads, and  $n$  columns, each corresponding to one time-instant. That is, each row  $\gg_i$  is a function of time and the values  $\gg_i(t)$ , where  $0 \leq t < n$ , create the image of the  $i$ -th lead of the original ECG recording. The decomposition is based on an algorithm that creates a diagonal matrix  $\Sigma^{8,n}$  and matrices  $\mathbb{U}^{8,8}$  and  $\mathbb{V}^{n,n}$  such that  $\Sigma = \mathbb{U}^T \mathbb{M} \mathbb{V}$ , which means  $\mathbb{M} = \mathbb{U} \mathbb{W}$ , where  $\mathbb{W}^{8,n} = \Sigma \mathbb{V}^T$ .  $\Sigma$  is a diagonal matrix with non-zero values only in the left-most diagonal. These elements of  $\Sigma$  (all  $> 0$ ) are the eigenvalues  $\{\sigma_i\}_{i=1}^8$  of the decomposition while the columns of matrices  $\mathbb{U}$  and  $\mathbb{V}$  are the left and right singular vectors. The rows of matrix  $\mathbb{W}$  are the algebraically orthogonal components  $\{\lambda_i\}_{i=1}^8$  of the decomposition.

**Orthogonal ECG signal reconstruction.** In previous electrocardiographic SVD applications, the orthogonal components of matrix  $\mathbb{W}$  were standardly sorted according to the corresponding values of eigenvalues. For the purposes of the present investigation, we used a different approach.

Original ECG signal in matrix  $\mathbb{M}$  can be reconstructed using only subset of components of orthogonal signal matrix  $\mathbb{W}$ . Specifically, for any subset of the 8 orthogonal components (i.e. any selection of one, two, or more of the components  $\lambda_i$ ), a matrix  $\mathbb{X}^{8,n}$  can be created, for which the rows of the subset are the same as the corresponding rows of  $\mathbb{W}$  while other rows contain zeros. The original matrix  $\mathbb{M}$  can then be approximated by matrix  $\mathbb{N}^{8,n} = \mathbb{U} \mathbb{X}$ . Each of the 8 rows of matrix  $\mathbb{N}$  correspond to the approximation of the corresponding ECG lead that originally constituted the matrix  $\mathbb{M}$ .

Various ways of quantifying the difference between  $\mathbb{M}$  and  $\mathbb{N}$  ECG signal can be proposed. In this study, we used the perhaps simplest possibility which was to calculate the area between the signals of individual leads of  $\mathbb{M}$  and  $\mathbb{N}$ . That is for each lead  $l \in \{I, II, V1, V2, \dots, V6\}$ , we calculated the difference  $\Delta_l$  between original lead  $\gg_l$  and its approximation  $\times_l$  as  $\Delta_l = \sum_{t=0}^{n-1} |\gg_l(t) - \times_l(t)|$  and quantified the difference  $\Delta$  between  $\mathbb{M}$  and  $\mathbb{N}$  as the average of all  $\Delta_l$  (i.e. the average over different leads).

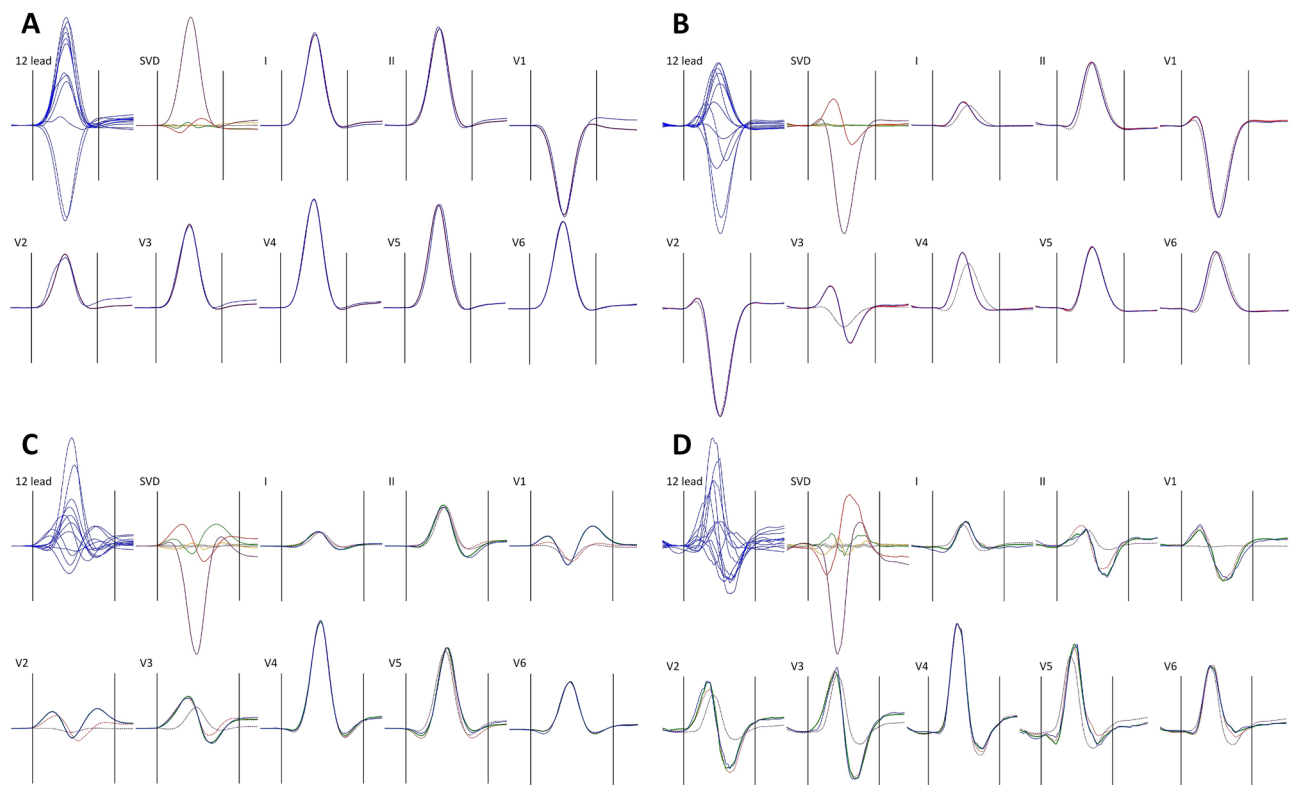
Obviously, if the selected subset of the 8 orthogonal components was empty (i.e. if no orthogonal components were used), the matrix  $\mathbb{N}$  contained only zeros and all  $\Delta_l = \sum_{t=0}^{n-1} |\gg_l(t)|$ .

This allowed to order the orthogonal components  $\{\lambda_i\}_{i=1}^8$  according to their contribution to the original ECG signal. That is, we firstly selected a single component  $\lambda_{1st}$  such that if only this component was used in matrix  $\mathbb{X}$ , the corresponding  $\mathbb{N}$  to  $\mathbb{M}$  difference  $\Delta$  was the smallest among all single components  $\lambda_i$ . Subsequently, we selected a second component  $\lambda_{2nd}$  such that if the matrix  $\mathbb{X}$  was composed of components  $(\lambda_{1st} \oplus \lambda_{2nd})$ —i.e. if the matrix  $\mathbb{X}$  had only two non-zero rows, the corresponding  $\mathbb{N}$  to  $\mathbb{M}$  difference  $\Delta$  was the smallest among all two component combinations  $(\lambda_{1st} \oplus \lambda_i)$ , where  $\lambda_i \neq \lambda_{1st}$ . The same process was repeated and  $\lambda_{3rd}$  was selected for minimum approximation difference based on  $(\lambda_{1st} \oplus \lambda_{2nd} \oplus \lambda_{3rd})$ , and so on, up to the selection of the last  $\lambda_{8th}$  orthogonal component.

This selection of  $\lambda$  components results in a sequence of  $\mathbb{N}$  to  $\mathbb{M}$  differences  $\{\Delta_i\}_{i=0}^8$  where  $\Delta_i$  corresponds to the approximation signals  $\mathbb{N}$  composed of the first  $i$  components selected during the described selection process. Clearly  $\Delta_0 \geq \Delta_1 \geq \Delta_2 \geq \dots \geq \Delta_8 = 0$ . The absolute contribution of the  $i$ -th component to the reconstruction of original ECG signal  $\mathbb{M}$  is equal to  $\Delta_{i-1} - \Delta_i$ . Clearly, the value of this absolute contribution depends on the magnitude of the original ECG and cannot be directly used for comparisons of different ECGs. For that purpose, it is appropriate to consider the contribution of the  $i$ -th component in relative terms, i.e. as a value  $\nabla_i = (\Delta_{i-1} - \Delta_i) / \Delta_0$ .

**Geometric interpretation.** When applying the SVD algorithm to the QRS complex, i.e. having the columns of matrix  $\mathbb{M}$  spanning sample-by-sample between QRS onset and QRS offset,  $\Delta_0$  becomes the absolute area under the QRS waveforms, i.e. the total “power” of the QRS signal (averaged over all 8 independent leads) and is measured in milliseconds\*millivolts. The relative contribution of the first component  $\nabla_1$  specifies the proportion of the signal that can be explained by projection of the depolarisation waveform only in one direction along (and backwards) of the main spatial QRS vector. There are only rare ECGs (example in Fig. 1A) in which almost all the QRS signal is explained by the first component, i.e. for which the electrocardiographic projection of the depolarisation waveform is practically only unidirectional. By the SVD principles, the second component corresponds to a projection of the depolarisation waveform that is perpendicular to the vector of the first component. That is, the sum  $\nabla_1 + \nabla_2$  specifies how much of the QRS signal can be explained by depolarisation projection onto a 2-dimensional plane (defined by the perpendicular vectors of components  $\lambda_{1st}$  and  $\lambda_{2nd}$ ). In some ECGs in which the total QRS power is far from explained by the first component, projection onto a single plane explains most of the QRS signal (example in Fig. 1B). In other ECGs, even the sum of  $\nabla_1 + \nabla_2$  is still substantially below 1 and the third component needs to be added, i.e. more faithful reconstruction of the original signal is obtained by considering the electrocardiographic projection of depolarisation in 3-dimensional space (example in Fig. 1C). Nevertheless, once the QRS signal is fractionated differently in different leads, further components algebraically perpendicular to the 3-dimensional space of the first 3 components (well beyond mental spatial imagination) are needed to reconstruct the original signal (example in Fig. 1D).

For these reasons, the decomposition components  $\nabla_i$  allow expressing the “proportion” of the ECG signal that is represented by electrical field changes in one vector direction, by changes along a combination of two perpendicular vectors, three perpendicular vectors, and so on. Similar attempts of quantifying these proportions were previously made based on decomposition eigenvalues  $\{\sigma_i\}_{i=1}^8$ <sup>21,22,31</sup>. To study the differences between these approaches, we applied the analysis to the QRS complex signals of the data analysed in this study and compared the  $\nabla_i$  values with corresponding eigenvalue proportions  $\varrho_i = \frac{\sigma_i}{\sum_{k=1}^8 \sigma_k}$ . The comparison was based on their relative differences, i.e. values  $(\nabla_i - \varrho_i) / \frac{\nabla_i + \varrho_i}{2}$  which allowed to judge the comparisons independent of the dimension  $i$ .



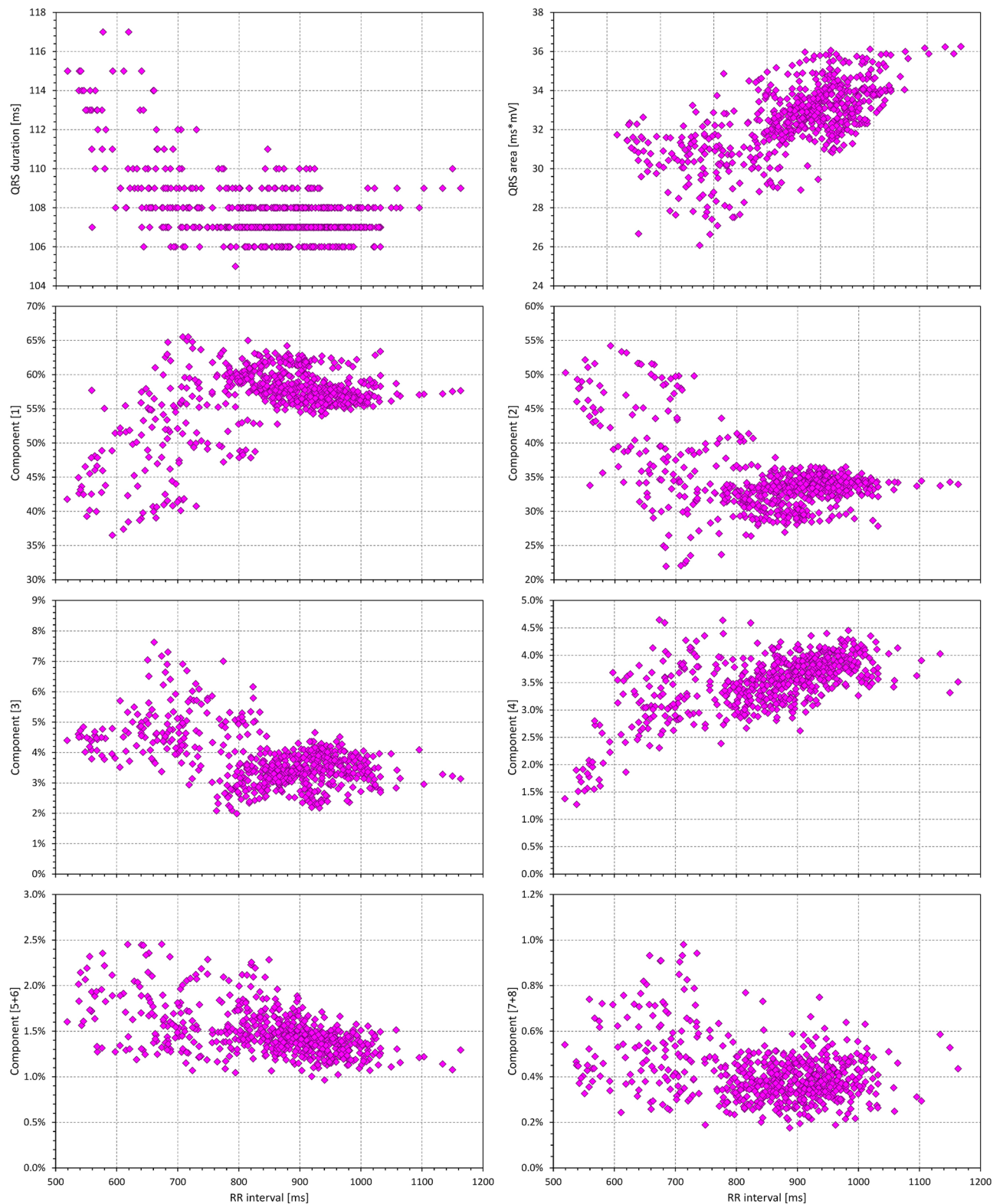
**Figure 1.** Examples of QRS reconstruction by orthogonal components. In all panels, superimposition of all 12 leads of the filtered representative median image of the QRS complex (12 lead) is shown together with the orthogonal components of matrix  $\mathbb{W}$  (SVD) and with individual independent leads (I, II, V1, V2, ..., V6) superimposed with the reconstruction. In all panels, the original ECG waveforms are shown in blue, the first, second, third, and fourth orthogonal components in violet, red, green, and amber, respectively (with all further components shown in grey). Panel (A) shows an ECG of a 51-year old female in which the reconstruction by the first component (full violet lines in the images of individual leads) explained 91.15% of the QRS area. Panel (B) shows an ECG of a 22-year old female in which the reconstruction by the first component (dotted violet lines in the lead images) explained 73.46% of the QRS area but the combination of the first and second component (full red lines in the lead images) explained 97.93% of the QRS area. Panel (C) shows an ECG of a 28-year old male in which the first and first + second component (dotted violet and red lines in the lead images, respectively) explained 58.49% and 72.56% of the QRS area but in which the combination of the first 3 components (full green lines in the lead images) explained 93.17% of the QRS area. Panel (D) shows an ECG of a 37-year old male in which the first, first + second, and first + second + third components (the same colour coding as in panel (C)) explained 42.83%, 80.27%, and 87.76% of the QRS area, respectively.

**Covariates.** In each study subject, covariate analysis was performed using data obtained from all ECGs of the given subject. The relative values of individual components as well as the values of their different combinations (i.e. values  $\nabla_i + \nabla_j + \dots$ ) were related to the RR intervals representative of the underlying heart rate of the corresponding ECG as well as to the duration of the QRS complex in the ECG. For this purpose, both linear and log-linear regression models were employed. As previously observed<sup>9</sup>, log-linear model fitted the relationship between QRS duration and the RR intervals better than the linear model. The intra-subject fits of the linear and log-linear models between the relative components and RR intervals and QRS duration were similar (i.e. for some of the components, linear model provided somewhat lower regression residua while for others, the fit by the log-linear model was tighter). For consistency, we have therefore used the log-linear regression models for all the intra-subject dependencies. Although some cases showed noticeable spread of the measured values (example in Figs. 2 and 3) the patterns of the regressions were still clearly detected.

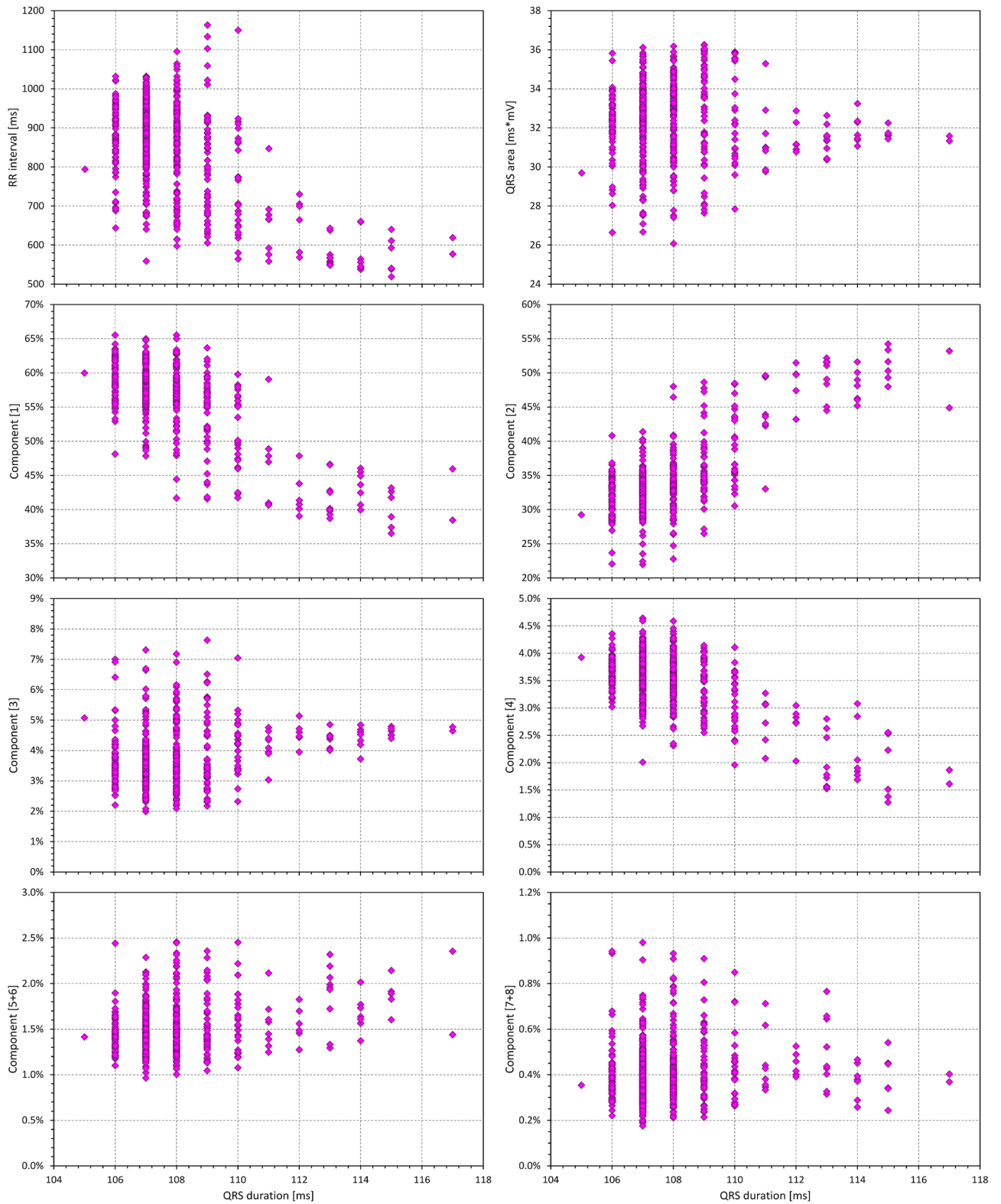
To allow comparisons across subjects, these log-linear regression models were used to project the individual components and their combinations to the heart rate of 60 and 120 bpm, as well as to the QRS duration of 100 ms.

In each subject, Spearman correlation coefficients were also calculated between the values of the relative components and their combinations, and the RR intervals of the underlying heart rate, and the QRS durations.

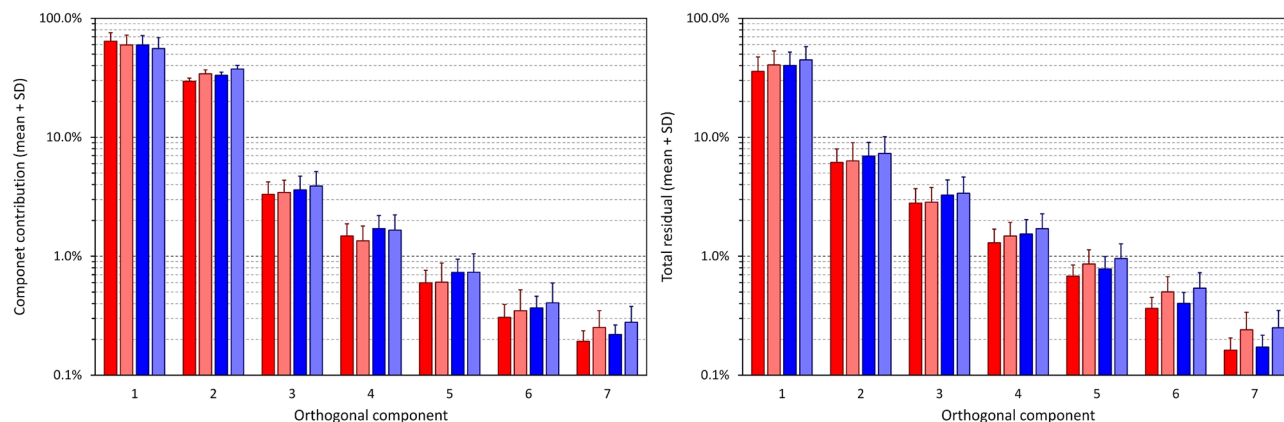
**Statistics and data presentation.** Data are presented as means  $\pm$  standard deviation. Differences between subject groups (mainly between female and male participants) were evaluated using two-sample two-tail t-test assuming different variances of compared samples. Intra-subject comparisons (e.g. comparisons between components projected to heart rates of 60 and 120 bpm) were evaluated using two-tail paired t-test. P-values above



**Figure 2.** Example of relationship between values measured in a 23-year old male. Individual panels show the dependency of QRS duration, of absolute QRS area, and of selected orthogonal components and their combination on the RR intervals of the underlying heart rate.



**Figure 3.** Example of relationship between measured values in the same 23-year old male as presented in Fig. 2. Individual panels show the dependency of absolute QRS area and of selected orthogonal components and their combination on the QRS duration. For completeness, the inverse relationship between the QRS duration and the RR interval of the underlying heart rate is also shown. The layout of the panels corresponds to that of Fig. 2.



**Figure 4.** Summary of measured QRS components in individual study subjects. The right panel shows the contribution of individual components to the absolute QRS area, the left panel shows the proportion of the absolute QRS area remaining after the first, first + second, first + second + third, etc., component have been used to recompose the original electrocardiograms. The data in females and males are shown in red and blue, respectively; the dark and light columns correspond to the data projected to heart rates of 60 and 120 bpm, respectively. Mean values  $\pm$  standard deviations are shown (note the logarithmic vertical axes). The 8th component is not shown since the combination of all 8 components covers the absolute QRS area fully and therefore, the contribution of the 8th component corresponds to the remainder after the use of the first 7 components.

0.05 were considered statistically non-significant (NS). Because of the inter-dependency of evaluated data, no correction for multiplicity of testing was performed and all statistical tests performed are presented.

In each ECG, SVD calculations were made covering the interval between QRS onset and QRS offset. To avoid the possibility of the SVD results being influenced by QRS duration, the calculation was also repeated using a fixed width of the interval covered by matrix  $\mathbb{M}$  in all ECGs. Specifically, this repeated calculation spanned the interval starting 5 ms before QRS onset and finishing 130 ms later. (The results of the fixed width calculations were only used to confirm the stability of the main analyses that are presented).

The SVD calculations were made using a custom software package developed in C++ (compiler of Microsoft Visual Studio version 15.4.0). Statistical evaluation used IBM SPSS package version 25.

## Results

**Population and electrocardiographic measurements.** The source clinical pharmacology studies investigated 639 subjects (311 females). The ages of sex-defined sub-groups were practically identical (females  $33.8 \pm 10.1$  years; males  $33.9 \pm 8.7$  years, NS). The numbers of analysed ECG samples were also not different between females ( $609 \pm 192$ ) and males ( $591 \pm 200$ , NS). The complete study evaluated 382,019 ECG samples.

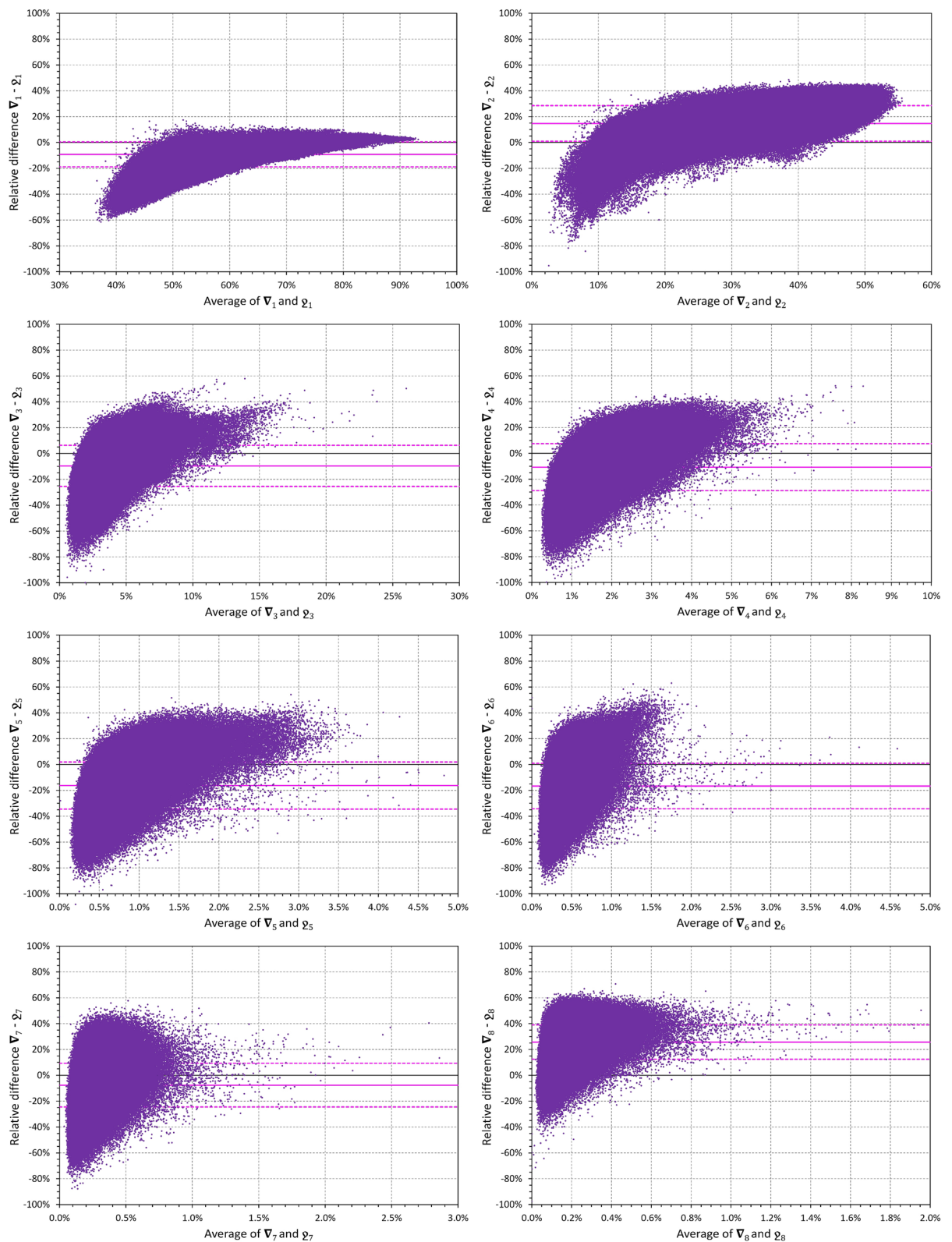
The spread (i.e. the minimum to maximum range) of heart rates of the analysed ECG segments was also similar in females and males ( $57.8 \pm 12.7$  vs  $56.2 \pm 12.7$  bpm, NS). Nevertheless, the spread of measured QRS widths was narrower in females ( $8.7 \pm 5.8$  ms) compared to that in males ( $10.2 \pm 5.5$  ms,  $p < 0.001$ ). The regression-based extrapolation to the QRS width of 100 ms have thus involved some marginal extrapolations beyond available values, especially for females with markedly short QRS complexes.

Summaries of individual ECG measurements are shown Fig. 4, their numerical values are listed in the Supplementary Table. The observations made with the repeated SVD analyses using the fixed 130 ms intervals were practically the same (not shown here). That is, albeit the numerical values were little different, their proportions and sex comparisons led to the very same conclusions as described further.

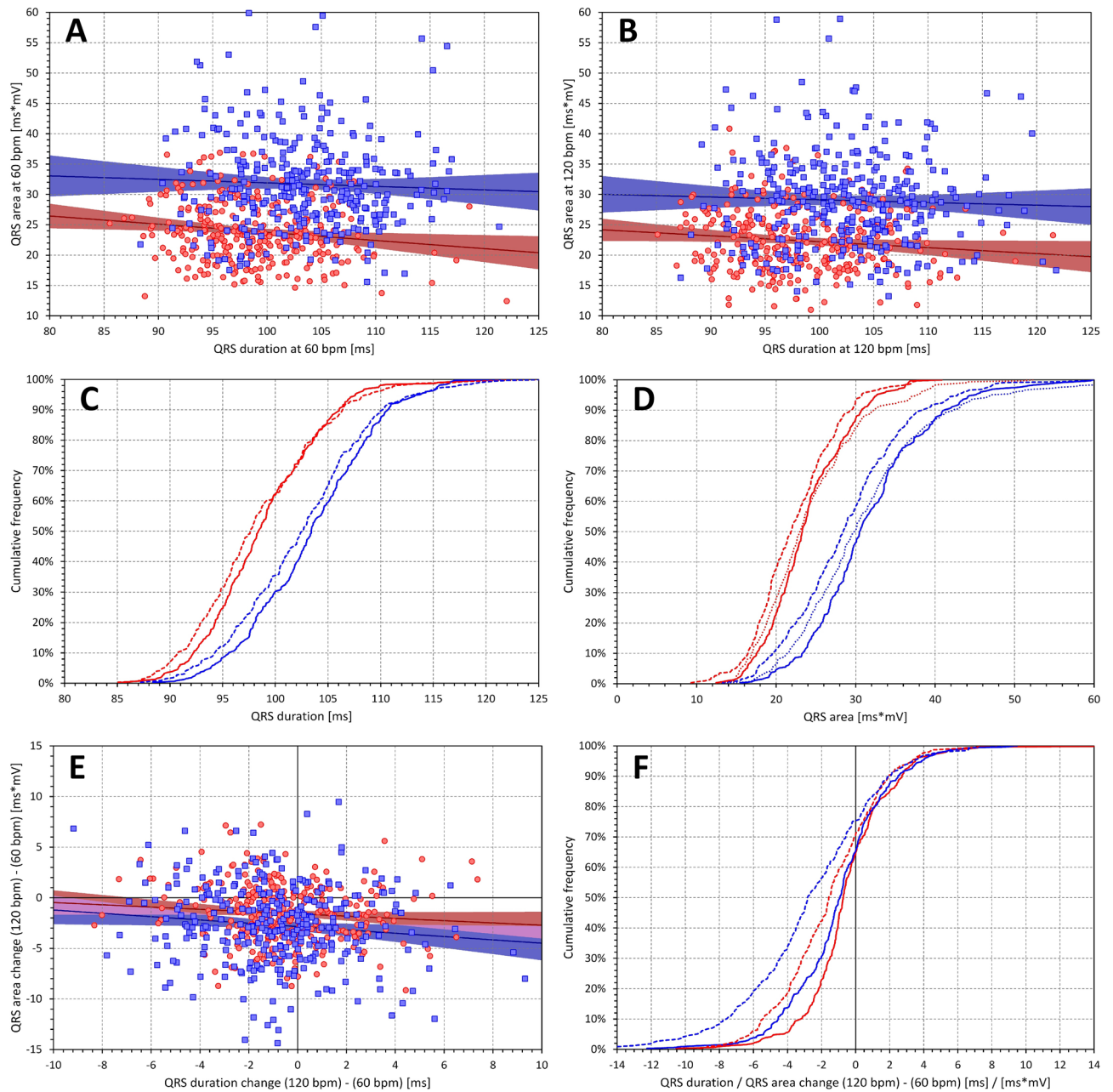
**Comparison with eigenvalue proportions.** In 8.27% of the analysed ECG samples, the order of the decomposition components  $\nabla_i$  was different from the order of SVD eigenvalues  $\sigma_i$  that are standardly used for component ordering<sup>16</sup>. In 1.40% and 4.10% of the samples, this difference of the order occurred in the first 3 and in the 4th to 6th dimensions, respectively. More important, however, were the numerical differences between components  $\nabla_i$  and the corresponding eigenvalue proportions  $\varrho_i$ . These are displayed in Fig. 5 which shows that with higher dimensions, these numerical differences spanned between approximately  $-80$  to  $+40\%$ .

**Absolute area under the QRS waveform.** Consistent with previous observations<sup>9</sup>, QRS durations were significantly shorter in females than in males ( $98.9 \pm 5.5$  vs  $103.5 \pm 5.9$  ms,  $p < 0.00001$ , at 60 bpm, Fig. 6). As also seen in Fig. 6, total QRS area, i.e. the  $\Delta_0$  value, was also significantly smaller in females compared to males but this difference was unrelated to the differences in QRS durations (when projected to 100 ms of QRS duration, the  $\Delta_0$  areas were  $24.21 \pm 6.52$  and  $31.26 \pm 9.26$  ms $\cdot$ mV in female and males, respectively,  $p < 0.00001$ ).

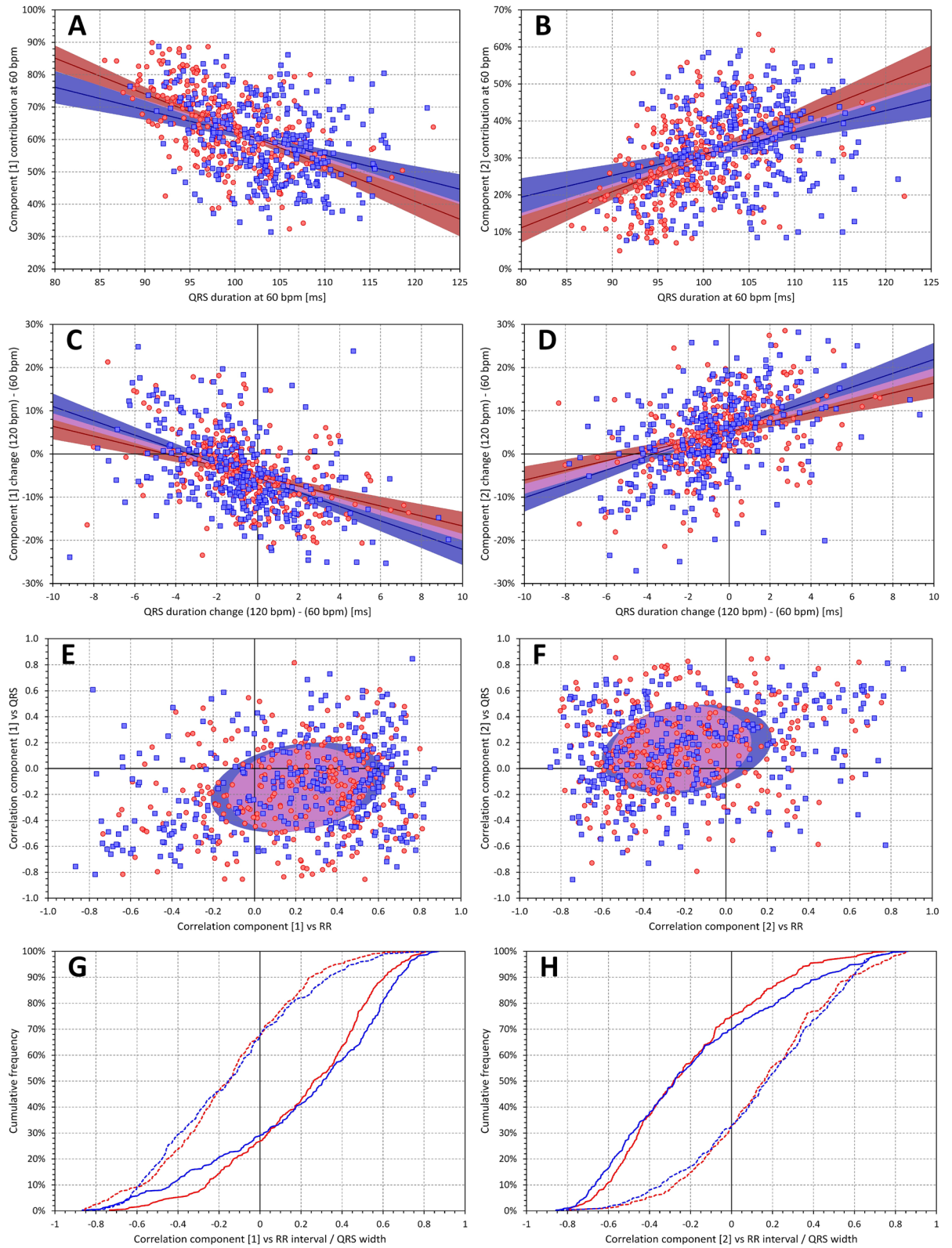
Also consistent with previous observations<sup>9</sup>, we observed QRS widening with increasing heart rate in approximately 30% of the subjects while QRS was shortening with increasing heart rate in others. Similar proportions



**Figure 5.** To demonstrate the differences between the decompositions approach that we used and the usual order of eigenvalues, the figure shows Bland–Altman type comparisons of relative eigenvalue proportions  $\varrho_i = \sigma_i / (\sum_{k=1}^8 \sigma_k)$  and  $\nabla_i$  for all  $i, 1 \leq i \leq 8$ . To allow comparison between different components, the vertical values show relative differences, that is values  $(\nabla_i - \varrho_i) / (\nabla_i + \varrho_i)$ . The scatter diagrams show the data of all evaluated 10-s ECG samples, the bold horizontal lines are the means of the relative  $\nabla_i - \varrho_i$  values, the dashed lines are their means  $\pm$  standard deviations. Note that the individual data include multiple readings in different subjects and that the values shown in the scatter diagrams are not fully mutually independent.



**Figure 6.** Data of QRS duration and of absolute QRS area. Panels (A) and (B) show the scatter diagrams of the relationship between the QRS duration and the absolute QRS area at heart rates of 60 and 120 bpm, respectively. Panels (C) and (D) show the cumulative distributions of QRS duration and of absolute QRS area. Panel (E) shows the scatter diagram of the relationship between intra-subject changes of QRS duration and of absolute QRS area corresponding to heart rate changes between 60 and 120 bpm and panel (F) shows the cumulative distributions of these intra-subject changes. In panels (A), (B), and (E), the red circles and blue squares show data of female and male subjects, respectively. The solid red and solid blue lines show the linear regressions between the displayed values in females and males, respectively. The red shaded and blue shaded areas are the 95% confidence intervals of the regression lines; the violet areas are the overlaps between the confidence intervals of the sex-specific age-regressions. In panels (C), (D), and (F), the red and blue lines correspond to female and male subjects, respectively. In panels (C) and (D), the full lines and dashed lines correspond to the values at 60 and 120 bpm, respectively. The dotted lines in panel (D) show the values at QRS duration of 100 ms. The full and dashed lines in panel (F) show the changes of QRS duration and of absolute QRS area, respectively.





◀ **Figure 7.** Data of first two components  $\nabla_1$  and  $\nabla_2$ . On the left side, panel (A) shows the scatter diagram of the relationship of  $\nabla_1$  to QRS duration at heart rate of 60 bpm. Panel (C) shows the scatter diagram of the  $\nabla_1$  changes between 120 and 60 bpm to the corresponding changes of QRS duration. Panel (E) shows the scatter diagram of the relationship between intra-subject correlation coefficients  $\nabla_1$  versus RR interval and  $\nabla_1$  versus QRS duration. Panel (G) shows the cumulative distributions of these correlation coefficients. On the right side, panels (B), (D), (F) and (H) show the same data comparisons for  $\nabla_2$  component. The meaning of the symbols in scatter diagrams in panels (A), (B), (C), and (D) is the same as in the scatter diagrams of Fig. 6. In panels (E) and (F), the red circles and blue squares again correspond to the female and male subjects, respectively. The light red and light blue elliptical shapes show the mean  $\pm$  standard deviation of the correlation coefficients (the elliptical shapes are oriented to represent the optimal orthogonal projection of the data). The violet areas are the overlaps between the sex-specific elliptical shapes. In panels (G) and (H), the red and blue lines correspond to females and males, respectively; the full and dashed lines show the intra-subject correlation coefficients of the orthogonal components to heart rate and to the QRS duration, respectively.

of subjects showed QRS area to increase and decrease with increasing heart rate but the heart rate influences of QRS duration and of QRS area were practically independent of each other (Fig. 6).

**Components of the 3-dimensional space.** Within individual subjects, the first relative component (i.e. the  $\nabla_1$  value) was, on average, negatively but moderately correlated with QRS duration (intra-subject Spearman correlation  $r$  of  $-0.159 \pm 0.327$  and  $-0.146 \pm 0.347$  in females and males, respectively). It was therefore somewhat surprising that the population correlations between  $\nabla_1$  and QRS duration assessed at specific heart rates were noticeably stronger ( $-0.529$  and  $-0.346$  at the rate of 60 bpm, and  $-0.528$  and  $-0.309$  at 120 bpm, in females and males, respectively). There was also a noticeable discrepancy between intra-subject relationship of  $\nabla_1$  to QRS duration and to the underlying heart rate. While the intra-subject correlation to QRS was positive in approximately 30% of the subjects, the intra-subject correlation to heart rate was positive in approximately 70% of the subjects. All this is shown in the left panels of Fig. 7 (note the cumulative distributions in panel G of the figure).

The right panels of Fig. 7 show that the relationship of  $\nabla_2$  to heart rate and QRS duration was almost exactly the opposite to that of the  $\nabla_1$ . Note that the cumulative distributions shown in panels G and H of the figure are practically mirror images of each other. While the intra-subject correlation with QRS width was only moderately positive (intra-subject  $r$  of  $0.155 \pm 0.330$  and  $0.149 \pm 0.345$  in females and males) the population correlation assessed at 60 bpm led to  $r$  of  $0.474$  and  $0.290$  in females and males, respectively. At 120 bpm, the corresponding  $r$  values were  $0.443$  and  $0.234$ .

Left part of Fig. 8 shows that  $\nabla_3$  values were much less related to QRS duration with averages of intra-subject correlations close to 0 and population correlations at 60 bpm with  $r$  of  $0.188$  and  $0.140$  in females and males, respectively. When all first three components were combined (i.e. values of  $\nabla_1 + \nabla_2 + \nabla_3$  considered) more than 90% of the QRS absolute area was covered and the population dependency on QRS duration almost disappeared (right part of Fig. 8).

**QRS fractionation components.** On average, there were no meaningful intra-subject correlations of  $\nabla_4$ ,  $\nabla_5$ , or  $\nabla_6$  to QRS duration (the absolute values of all  $r$  averages were below 0.02). This contrasted with the positive population correlations which, at 60 bpm, led to  $r$  values of  $0.294$  and  $0.295$  in females and males, respectively, for  $\nabla_4$ . For  $\nabla_5$ , the corresponding  $r$  values were  $0.329$  and  $0.292$ , while for  $\nabla_6$ , the  $r$  values were  $0.388$  and  $0.305$ . Similar gradual increase of  $r$  from  $\nabla_4$  to  $\nabla_6$  was also seen at heart rate of 120 bpm (Fig. 9).

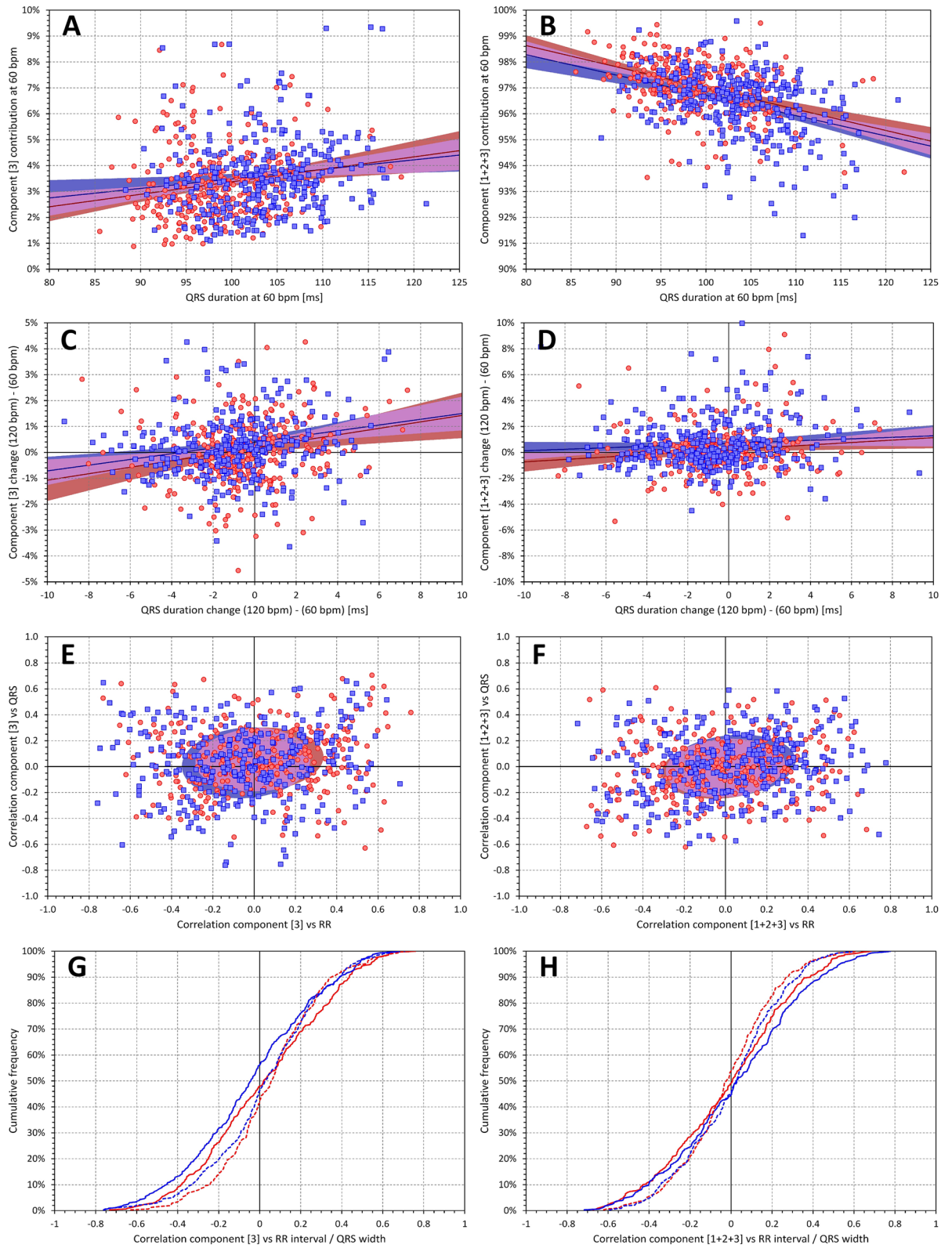
As expected, the contribution of components  $\nabla_4$  to  $\nabla_6$  was gradually decreasing and in the majority of cases, the component combination  $\nabla_4 + \nabla_5 + \nabla_6$  represented less than 3% of the absolute QRS area. Compared to  $\nabla_4 + \nabla_5$ , the combination  $\nabla_4 + \nabla_5 + \nabla_6$  showed only a small albeit noticeable increase while still maintaining relatively strong correlation with QRS duration (Fig. 10). On the contrary, the population heart rate dependency of components  $\nabla_4$ ,  $\nabla_5$ , and  $\nabla_6$  and of their combinations was practically absent (Figs. 9 and 10).

**Decomposition residuals.** The situation was different with the combination of final components  $\nabla_7 + \nabla_8$  (Fig. 11). On average, this combination showed no intra-subject correlation with QRS complex ( $r$  of  $0.001 \pm 0.151$  and  $-0.014 \pm 0.157$  for females and males, respectively). However, in population data, significant correlations with QRS complex were observed. At the rate of 60 bpm,  $r$  values of  $0.521$  and  $0.409$  were observed for females and males, respectively. At 120 bpm, these  $r$  values decreased to  $0.332$  and  $0.237$ , respectively. Substantial intra-subject effect of heart rate was also noted. Although numerically rather small, the value  $\nabla_7 + \nabla_8$  increased from  $0.364 \pm 0.087$  and  $0.402 \pm 0.093\%$  in females and males at 60 bpm, to  $0.501 \pm 0.172$  and  $0.538 \pm 0.189\%$  at 120 bpm ( $p < 0.00001$  and  $p = 0.012$  in females and males, respectively).

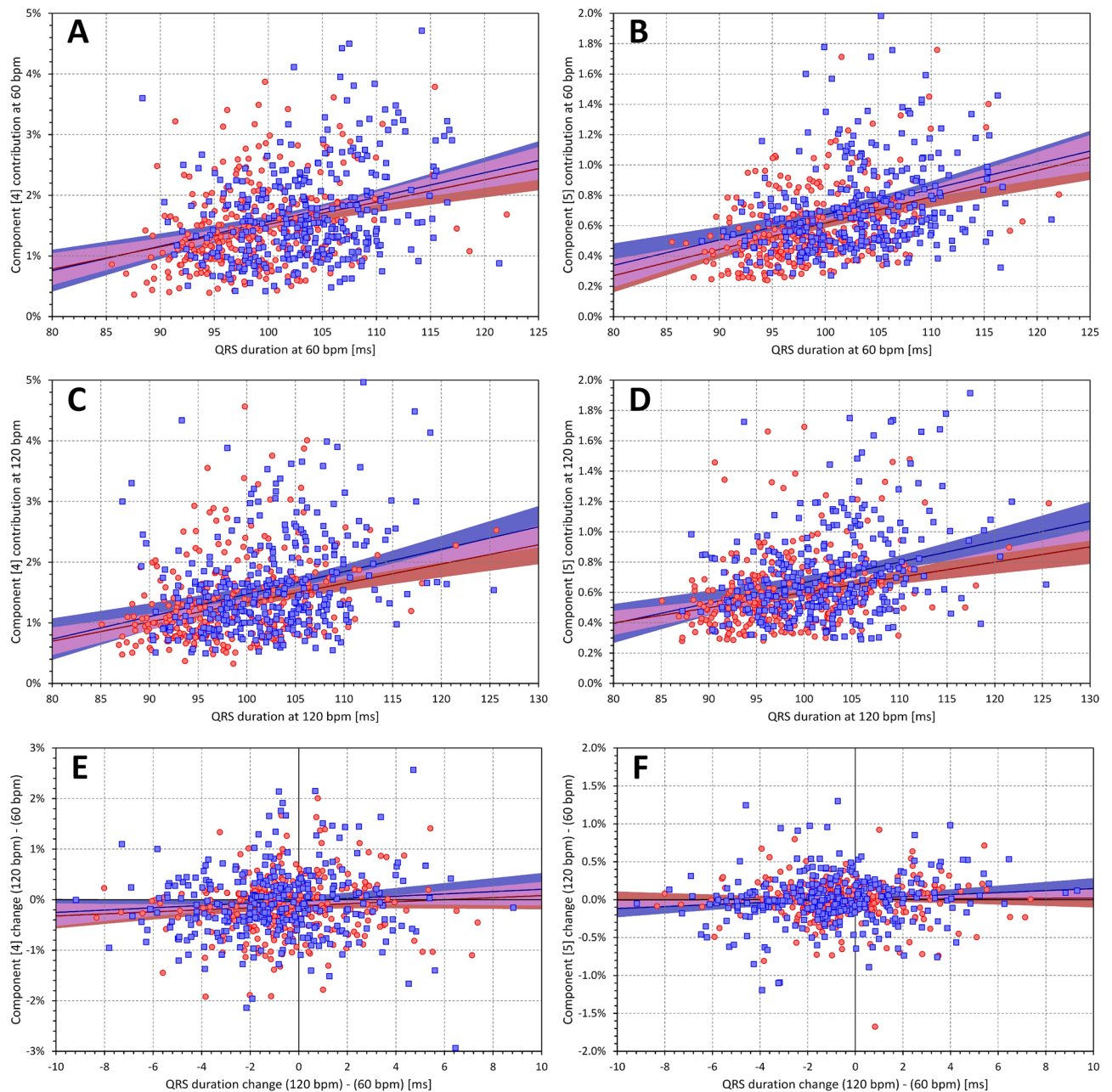
**Sex comparisons.** Since these observations suggest the electrophysiologic basis for shorter QRS duration in females compared to males, Fig. 12 summarises the observed sex differences.

The results were similar for components values projected to 60 bpm and to 120 bpm. Females showed larger  $\nabla_1$  compared to males (e.g.  $64.2 \pm 11.6$  vs  $59.7 \pm 11.9\%$  at 60 bpm,  $p < 0.00001$ ) while all  $\nabla_2$  to  $\nabla_7$  are larger in males with different levels of statistical significance.  $\nabla_8$  were also larger in males than in females but we observed statistically significant differences only at 60 bpm while at 120 bpm, the values were still numerically smaller in females ( $0.241 \pm 0.096$  vs  $0.250 \pm 0.099\%$ ) but not significantly different.

When eliminating the influence of different QRS durations by using data projected to the same level of 100 ms, the sex comparison was different. The components  $\nabla_1$  to  $\nabla_3$  were practically the same between sexes.  $\nabla_4$  to  $\nabla_7$



**Figure 8.** The layout and meaning of panels of the figure is the same as in Fig. 7. The left panels (A), (C), (E), and (G) correspond to the component  $\nabla_3$ , whilst the right panels (B), (D), (F), and (H) correspond to the combination of components  $\nabla_1 + \nabla_2 + \nabla_3$ .



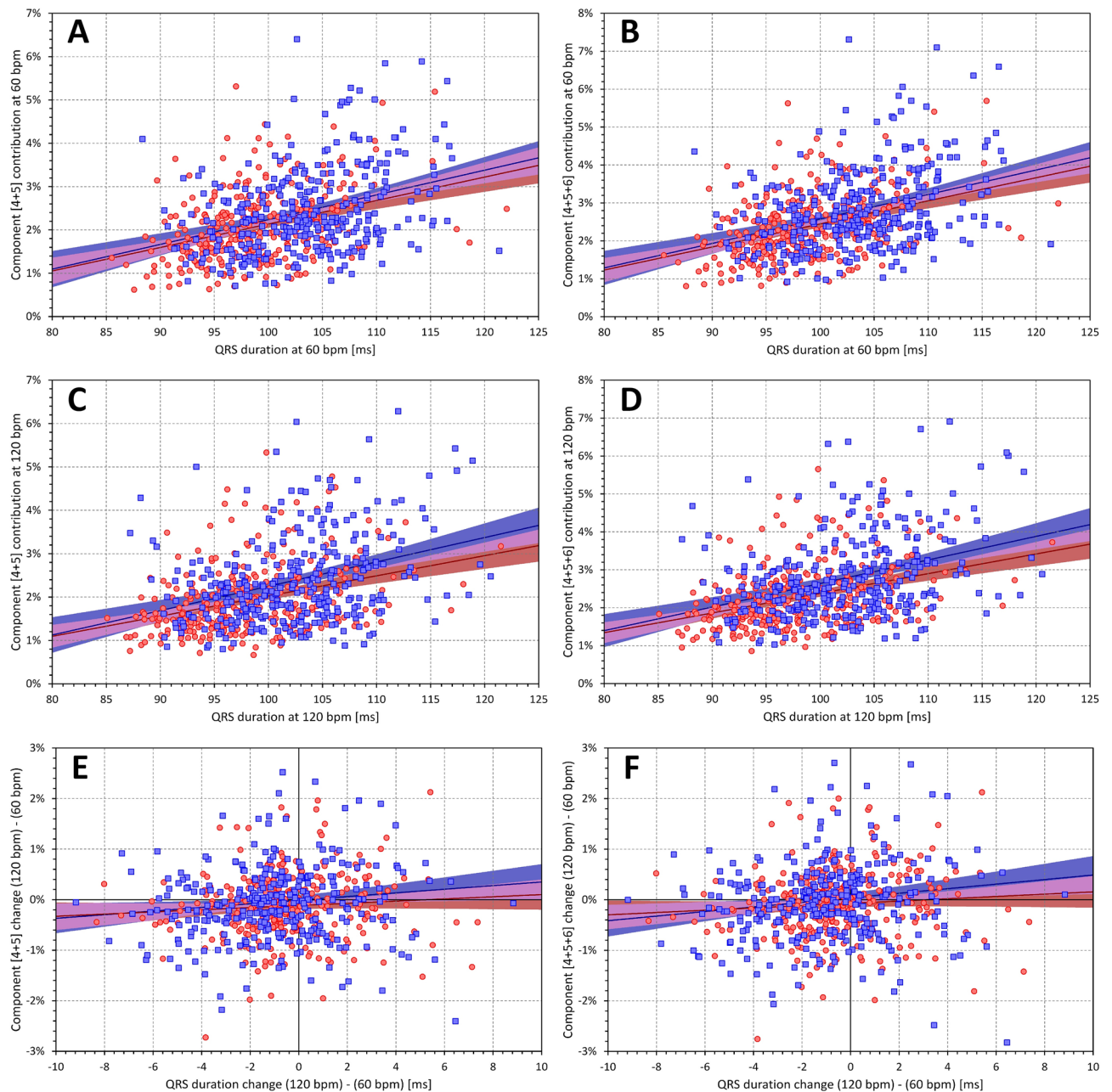
**Figure 9.** The left panels (A) and (C) show scatter diagrams of the intra-subject relationship of component  $\nabla_4$  to QRS duration at heart rate of 60 and 120 bpm, respectively. The panel (E) shows the scatter diagram of the  $\nabla_4$  changes between 120 and 60 bpm to the corresponding changes of QRS duration. The right panels B, D, and F show the same for component  $\nabla_5$ . The meaning of the symbols in scatter diagrams is the same as in the scatter diagrams of Fig. 6.

were larger in males than in females (the difference did not reach statistical significance for  $\nabla_4$ , likely because large spread of projected values in females) while  $\nabla_8$  showed again no difference between sexes.

## Discussion

In addition to the setup of the technology, these data analyses offer electrophysiological insights and lead to potentially unexpected observations.

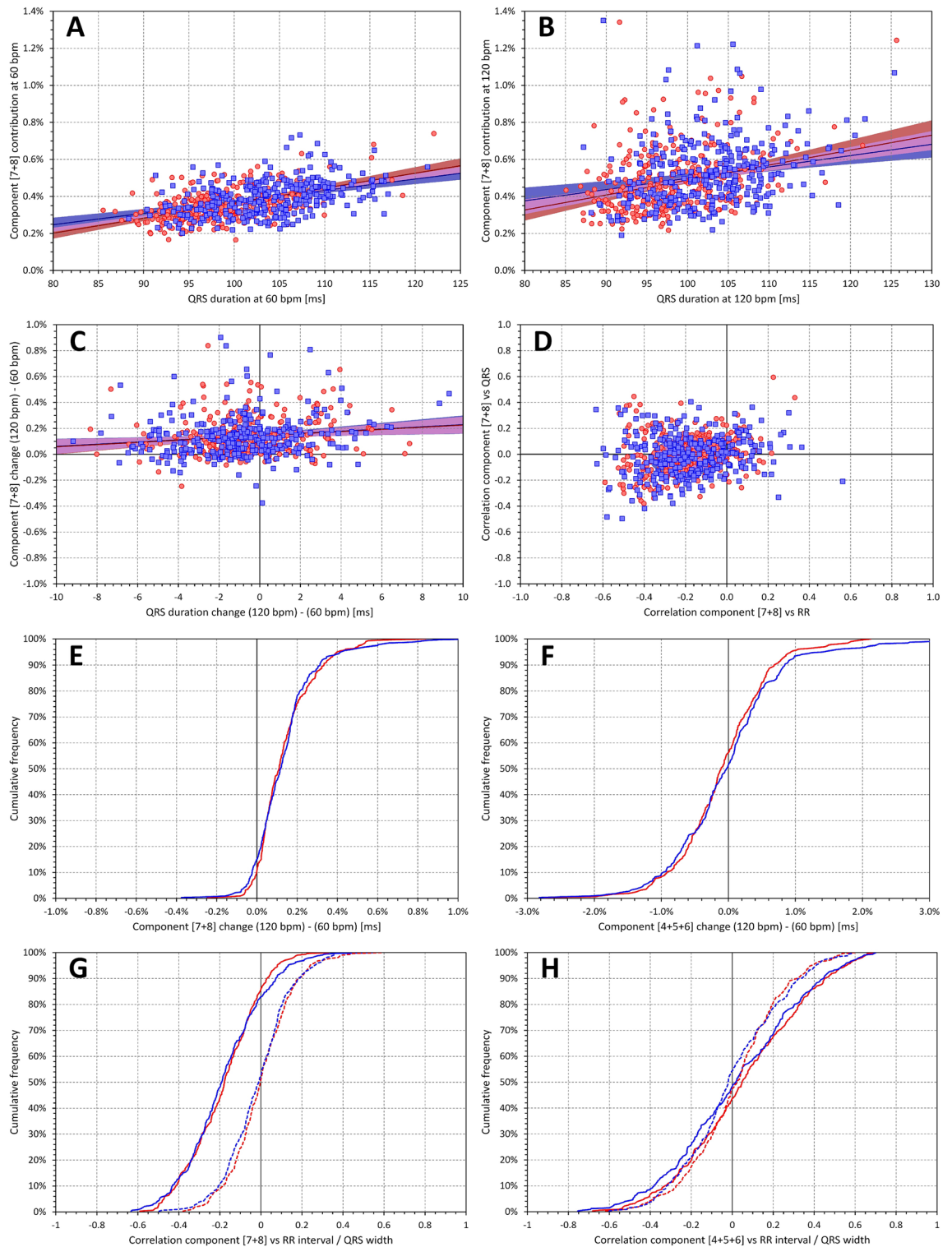
Previous clinical experience with vectorcardiography<sup>32–34</sup> might lead to expectations that the first two (if not the first three) components  $\nabla_1$  to  $\nabla_2$  (or, in some cases, to  $\nabla_3$ ) would contribute similarly to the 3-dimensional composite of the QRS complex. Indeed, the directions of the projections of the first 3 components also create an orthogonal 3-dimensional system which can be represented as an optimal rotation of the XYZ coordinate system so that the maximum QRS power projects into the first direction, the maximum of the remainder into the perpendicular second direction, and so on. Nevertheless, the optimum orientation of coordinates by SVD



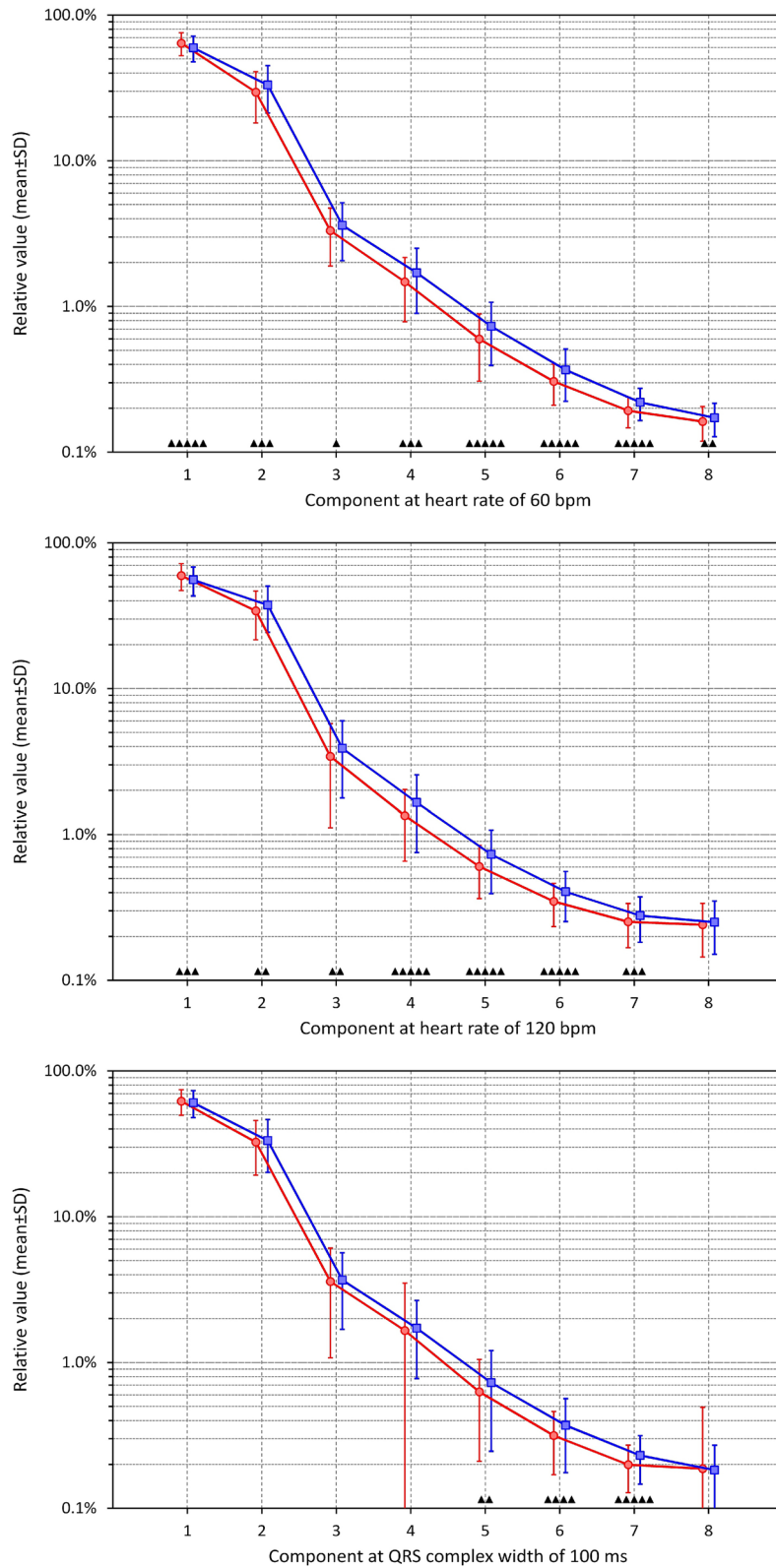
**Figure 10.** The layout and meaning of panels of the figure is the same as in Fig. 9. The left panels (A), (C), and (E) correspond to the combination of components  $\nabla_4+\nabla_5$ , whilst the right panels (B), (D), and (F) correspond to the combination of components  $\nabla_4+\nabla_5+\nabla_6$ .

results in different proportions of the components. It is easy to understand that, in principle,  $\nabla_3$  is a measure of QRS planarity<sup>33,35</sup>. Since it is known that electrophysiology of normal hearts is characterised by an almost perfect planarity of the spatial QRS loop<sup>36,37</sup>, the contribution of  $\nabla_3$  only around 3% to 4% of the total QRS absolute area is not surprising. Nevertheless, the practically 2:1 proportion between  $\nabla_1$  to  $\nabla_2$  was somewhat unexpected as was the proportion of subjects in whom  $\nabla_1$  exceeded 80% and  $\nabla_2$  was below 20% (see top panels of Fig. 7). Although similar proportion has previously been described for the eigenvalues of resting ECGs<sup>23</sup> we initially assumed that similar to the vectorcardiography images, the contributions of  $\nabla_1$  and  $\nabla_2$  would not be this different since the proportions of this decomposition are not similar those of eigenvalues (see Fig. 5).

The marked differences between the intra-subject and inter-subject relationship of the components to the QRS complex duration suggest that the proportions of the components (perhaps except for  $\nabla_7$  and  $\nabla_8$ ) are not determined dynamically by physiologic regulatory processes but are driven by individual anatomic and histologic composites of the ventricular myocardium. Our observations also strongly support the physiologic expectation that even in healthy subjects, narrower QRS complex is a consequence of a more direct and less convoluted path of the depolarisation sequence.



**Figure 11.** Panels (A) and (B) show scatter diagrams of the intra-subject relationship of component combination  $\nabla_7+\nabla_8$  to QRS duration at heart rate of 60 and 120 bpm, respectively. Panel (C) shows the scatter diagram of the  $\nabla_7+\nabla_8$  changes between 120 and 60 bpm to the corresponding changes of QRS duration. The meaning of the symbols in these scatter diagrams is the same as in the scatter diagrams of Fig. 6. Panel (D) shows the scatter diagram of the relationship between intra-subject correlation coefficients  $\nabla_7+\nabla_8$  versus RR interval and  $\nabla_7+\nabla_8$  versus QRS duration. The layout of this panel is the same as panels (E) and (F) in Fig. 7 (note that the data points are clustered so compactly that the underlying elliptical shapes are not easily visible). Panel (E) shows the cumulative distribution of  $\nabla_7+\nabla_8$  changes between heart rates of 120 and 60 bpm; for comparison, panel (F) shows the same for  $\nabla_4+\nabla_5+\nabla_6$  changes. Panel (G) shows the cumulative distribution of intra-subject correlations of  $\nabla_7+\nabla_8$  versus RR interval (full lines) and versus QRS duration (dashed lines). For comparison, panel (H) shows the same for intra-subject  $\nabla_4+\nabla_5+\nabla_6$  correlations. In panels (E), (F), (G), and (H), the red and blue lines correspond to female and male subjects, respectively.



**Figure 12.** The panels show the mean ( $\pm$  standard deviation) values of decomposition components  $\nabla_1$  to  $\nabla_8$  for female (red graphs) and male (blue graphs) subjects. The top, middle, and bottom panels show the values of components assessed at 60 bpm heart rate, 120 bpm heart rate, and 100 ms of QRS duration, respectively. For each component showing statistically significant difference between females and males, the level of significance is shown above the horizontal axis (▲— $p < 0.05$ , ▲▲— $p < 0.01$ , ▲▲▲— $p < 0.001$ , ▲▲▲▲— $p < 0.0001$ , ▲▲▲▲▲— $p < 0.00001$ ). Note the logarithmic scale of the vertical axes.

Although the ECG signals were not only filtered but also processed by the construction of median representative beat (which, we believe, also has noise-reduction properties) before applying the SVD analysis, the component  $\nabla_8$ , and perhaps also the component  $\nabla_7$ , represents mainly the residual noise in the recordings. This is consistent with the marked increase of these components between rates of 60 and 120 bpm which is frequently accompanied by some decrease of signal quality especially if the heart rate increase reflects physical activity.

The observation of the likely relationship between QRS duration and the convolutedness of the depolarisation sequence might also provide insight into the sex difference of QRS complex. The shorter QRS complex duration in females has previously been repeatedly described<sup>38</sup>. It has also been repeatedly proposed that this sex difference might reflect differences in heart sizes. Nevertheless, this has not been confirmed<sup>9</sup>. Rather, the sex differences might be driven by the depolarisation sequence initiated by the His-Purkinje system. Our results seem to indicate that compared to males, the propagation of the depolarisation sequence in females is more direct and less curled and twisted. This is not supported only by the proportions between  $\nabla_1$  (larger in females) and  $\nabla_2$  (larger in males) but also by the sex differences in the higher components above the 3-dimensional projections as shown in Fig. 12. Such a lesser complexity of the female depolarisation sequence might also be the basis for the known decreased incidence of ventricular tachyarrhythmias in females<sup>39–41</sup> (with the exception of channelopathy-based arrhythmias<sup>42</sup> that are unrelated to the depolarisation abnormalities). Since the present study evaluated healthy adults with females largely of pre-menopausal ages, we cannot comment on whether the observed sex differences are a consequence of hormonal influence. Electrocardiography studies in children and adolescents<sup>43</sup> as well as studies of the influence of menstrual cycle are needed to address these details.

SVD analyses have previously been applied also to body surface maps and multi-lead ECGs<sup>44,45</sup>. These analyses showed that larger number of independent ECG components can be detected. Nevertheless, since we had only 12-lead ECG available, we were unable to decompose the signals to more than 8 algebraic dimensions corresponding to the number of independent leads. While a system analysing standard 10-s 12-lead ECGs is more practical for further applications of the technology that we have described here, application of the same principles to multi-lead ECG recordings would be of research interest.

Visible fragmentation of the QRS complex has repeatedly been described as an indicator of increased risk of adverse cardiac events<sup>46–49</sup>. It has also been observed that fragmented QRS complex is more often present in males compared to females<sup>50</sup> and that, in cardiac patients, QRS abnormalities were more predictive in patients with prolonged QRS complex<sup>51</sup>. Having used data of healthy subjects, we cannot link our methodological results to these studies directly. Nevertheless, the logic of the analysis suggests that the comparison between the orthogonal components  $\nabla_1$  to  $\nabla_3$  and the value of the  $\nabla_4$  to  $\nabla_6$  (or perhaps  $\nabla_4$  to  $\nabla_7$ ) components might offer automatic detection of fragmented QRS complex including the distinction of micro-fragmented cases that are not directly apparent during standard visual judgement and diagnosis. Further studies are needed in this respect, but the data presented here might suggest prospectively defined normality limits (e.g. 3.5% for the combination of  $\nabla_4 + \nabla_5 + \nabla_6$  – see Fig. 10). The so-called non-dipolar components (based on eigenvalue proportions) of the T wave have previously been proposed as risk indicators in cardiac patients<sup>52</sup>. It seems therefore logical to extend this technology also to repolarisation signals.

QRS complex duration, its morphological characteristics, and ECG-based depolarisation abnormalities are also used to optimise and to predict the outcome of cardiac resynchronisation therapy<sup>53,54</sup>. We are again unable to comment on the possible use of the described technology for these purposes but, based on the electrophysiologic understanding of the analysis, it appears feasible to suggest that studies of this kind might be worth conducting.

Intentionally, we analysed only ECG segments preceded by stable heart rate. This allowed avoiding potential problems with heart rate hysteresis and led to inter-subject differences in the number of analysed ECG segments. Hysteresis-driven disparity between ECG indices and simultaneously measured heart rate occurs when the adaptation to heart rate changes is delayed. This is a known property of repolarisation-related intervals<sup>55–57</sup> which has important practical implications<sup>58,59</sup>. Nevertheless, it is not known whether QRS duration exhibits any delayed heart rate adaptation<sup>9</sup>. Similarly, based on the analysed data, we cannot address the question of how quickly the decomposition components alter in response to abrupt heart rate changes.

**Limitations.** Further limitations of the analytical technique also need to be considered. The algebraic process of SVD is based on signal reconstruction analysis and therefore cannot map the depolarisation wave propagation directly. The ECG images of localised depolarisation abnormalities might cancel each other and thus be beyond SVD detection. The presented analysis might therefore underestimate but not overestimate depolarisation abnormalities. As already stated, while the span of heart rates covered by different ECGs in individual subjects was reasonably wide, the span of the QRS durations was limited in some subjects. In such cases, the regression projections to 100 ms of QRS duration might have involved substantial extrapolation beyond available data and might thus have polluted the estimates by some errors. The source clinical studies did not involve echocardiographic examinations and we are thus unable to relate the observations to anatomical heart sizes. The original Holter recordings used Mason-Likar electrode positions. We cannot answer the question of whether this influenced the measured values and whether any derived normality limits would be different if standard ECG leads were used. The spans of the ages of the subjects were not wide enough to investigate age influence. Although the ECG signal quality might be influenced by obesity, we have not related the measurements to body mass index.

## Conclusion

Despite these limitations, the presented technology and data analyses suggest that components of QRS complex beyond the 3-dimensional reconstruction can reliably be estimated and that they have an electrophysiologic role in judging the propagation of the depolarisation waveform through the myocardium. It appears that the detailed

convolution of the depolarisation waveform is individual, and that smoother and less intricate depolarisation propagation is the mechanism responsible for shorter QRS duration in females.

Received: 19 July 2020; Accepted: 2 February 2021

Published online: 22 February 2021

## References

- Macfarlane, P. W. & Lawrie, T. D. V. The normal electrocardiogram and vectorcardiogram. In *Comprehensive Electrocardiology* (eds Macfarlane, P. W. *et al.*) (Springer, London, 2010).
- Rijnbeek, P. R. *et al.* Normal values of the electrocardiogram for ages 16–90 years. *J. Electrocardiol.* **47**, 914–921 (2014).
- Boineau, J. P. & Spach, M. S. The relationship between the electrocardiogram and the electrical activity of the heart. *J. Electrocardiol.* **1**, 117–124 (1968).
- Mincholé, A., Zacur, E., Ariga, R., Grau, V. & Rodriguez, B. MRI-based computational torso/biventricular multiscale models to investigate the impact of anatomical variability on the ECG QRS complex. *Front. Physiol.* **10**, 1103. <https://doi.org/10.3389/fphys.2019.01103> (2019).
- Weiss, D. L., Keller, D. U., Seemann, G. & Dössel, O. The influence of fibre orientation, extracted from different segments of the human left ventricle, on the activation and repolarization sequence: a simulation study. *Europace Suppl.* **6**, 96–104 (2007).
- Mehdirad, A. A., Nelson, S. D., Love, C. J., Schaal, S. F. & Tchou, P. J. QRS duration widening: reduced synchronization of endocardial activation or transseptal conduction time?. *Pacing Clin. Electrophysiol.* **21**, 1589–1594 (1998).
- Carmeliet, E. Conduction in cardiac tissue. Historical reflections. *Physiol Rep.* **7**, e13860. <https://doi.org/10.14814/phy2.13860> (2019).
- Macfarlane, P. W., McLaughlin, S. C., Devine, B. & Yang, T. F. Effects of age, sex, and race on ECG interval measurements. *J. Electrocardiol.* **27**(Suppl), 14–19 (1994).
- Hnatkova, K., Smetana, P., Toman, O., Schmidt, G. & Malik, M. Sex and race differences in QRS duration. *Europace* **18**, 1842–1849 (2016).
- Sia, C. H. *et al.* A population-wide study of electrocardiographic (ECG) norms and the effect of demographic and anthropometric factors on selected ECG characteristics in young, Southeast Asian males—results from the Singapore armed forces ECG (SAFE) study. *Ann. Noninvasive Electrocardiol.* **24**, e12634. <https://doi.org/10.1111/anec.12634> (2019).
- Mohammadi, S. *et al.* Study of the normal heart size in northwest part of Iranian population: a cadaveric study. *J. Cardiovasc. Thorac. Res.* **8**, 119–125 (2016).
- Vanhaebost, J., Faouzi, M., Mangin, P. & Michaud, K. New reference tables and user-friendly Internet application for predicted heart weights. *Int. J. Legal Med.* **128**, 615–620 (2014).
- Klabunde, R. E. *Cardiovascular Physiology Concepts* (Lippincott, Philadelphia, 2012).
- Veeraraghavan, R., Gourdie, R. G. & Poelzing, S. Mechanisms of cardiac conduction: a history of revisions. *Am. J. Physiol. Heart Circ. Physiol.* **306**, H619–H627 (2014).
- Mason, J. W. *et al.* A fundamental relationship between intraventricular conduction and heart rate. *J. Electrocardiol.* **49**, 362–370 (2016).
- Acar, B. & Köymen, H. SVD-based on-line exercise ECG signal orthogonalization. *IEEE Trans. Biomed. Eng.* **46**, 311–321 (1999).
- Ahmed, S. M., Al-Zoubi, Q. & Abo-Zahhad, M. A hybrid ECG compression algorithm based on singular value decomposition and discrete wavelet transform. *J. Med. Eng. Technol.* **31**, 54–61 (2007).
- Kumar, R., Kumar, A. & Singh, G. K. Hybrid method based on singular value decomposition and embedded zero tree wavelet technique for ECG signal compression. *Comput. Methods Programs. Biomed.* **129**, 135–148 (2016).
- Jung, W. H. & Lee, S. G. An R-peak detection method that uses an SVD filter and a search back system. *Comput. Methods Programs. Biomed.* **108**, 1121–1132 (2012).
- Yana, K., Shichiku, H., Satoh, T., Mizuta, H. & Ono, T. An improved QT interval measurement based on singular value decomposition. *Conf. Proc. IEEE Eng. Med. Biol. Soc.* **2006**, 3990–3993 (2006).
- Priori, S. G. *et al.* Evaluation of the spatial aspects of T-wave complexity in the long-QT syndrome. *Circulation* **96**, 3006–3012 (1997).
- Acar, B., Yi, G., Hnatkova, K. & Malik, M. Spatial, temporal and wavefront direction characteristics of 12-lead T-wave morphology. *Med. Biol. Eng. Comput.* **37**, 574–584 (1999).
- Schlegel, T. T. *et al.* Accuracy of advanced versus strictly conventional 12-lead ECG for detection and screening of coronary artery disease, left ventricular hypertrophy and left ventricular systolic dysfunction. *BMC Cardiovasc. Disord.* **10**, 28. <https://doi.org/10.1186/1471-2261-10-28> (2010).
- Toman, O. *et al.* Physiologic heart rate dependency of the PQ interval and its sex differences. *Sci. Rep.* **10**, 2551. <https://doi.org/10.1038/s41598-020-59480-8> (2020).
- Guideline, I. C. H. Safety pharmacology studies for human pharmaceuticals S7A. *Fed. Regist.* **66**, 36791–36792 (2001).
- Guideline, I. C. H. 1E14 Clinical evaluation of QT/QTc interval prolongation and proarrhythmic potential for non-antiarrhythmic drugs. Guidance to industry. *Fed. Regist.* **70**, 61134–61135 (2005).
- Malik, M. *et al.* Thorough QT/QTc study in patients with advanced Parkinson's disease: cardiac safety of rotigotine. *Clin. Pharmacol. Therap.* **84**, 595–603 (2008).
- Malik, M. *et al.* Proarrhythmic safety of repeat doses of mirabegron in healthy subjects: a randomized, double-blind, placebo-, and active-controlled thorough QT study. *Clin. Pharm. Therap.* **92**, 696–706 (2012).
- Perez-Alday, E. A. *et al.* Importance of the heart vector origin point definition for an ECG analysis: the Atherosclerosis Risk in Communities (ARIC) study. *Comput. Biol. Med.* **104**, 127–138 (2019).
- Hnatkova, K. *et al.* Systematic comparisons of electrocardiographic morphology increase the precision of QT interval measurement. *Pacing Clin. Electrophysiol.* **32**, 119–130 (2009).
- Malik, M. *et al.* QT dispersion does not represent electrocardiographic interlead heterogeneity of ventricular repolarization. *J. Cardiovasc. Electrophysiol.* **11**, 835–843 (2000).
- Sur, S., Han, L. & Tereshchenko, L. G. Comparison of sum absolute QRST integral, and temporal variability in depolarization and repolarization, measured by dynamic vectorcardiography approach, in healthy men and women. *PLoS ONE* **8**, e57175. <https://doi.org/10.1371/journal.pone.0057175> (2013).
- Ray, D., Hazra, S., Goswami, D. P., Macfarlane, P. W. & Sengupta, A. An evaluation of planarity of the spatial QRS loop by three dimensional vectorcardiography: its emergence and loss. *J. Electrocardiol.* **50**, 652–660 (2017).
- Jaros, R., Martinek, R. & Danyš, L. Comparison of different electrocardiography with vectorcardiography transformations. *Sensors* **19**, 3072. <https://doi.org/10.3390/s19143072> (2019).
- Choudhuri, S., Ghosal, T., Goswami, D. P. & Sengupta, A. Planarity of the spatial QRS loop of vectorcardiogram is a crucial diagnostic and prognostic parameter in acute myocardial infarction. *Med Hypotheses* **130**, 109251. <https://doi.org/10.1016/j.mehy.2019.109251> (2019).



36. Hiraoka, M., Kawano, S., Sawanobori, T. & Kokusho, S. QRS planarity studies in the vectorcardiogram. Clinical and experimental studies. *Jpn. Heart J.* **23**, 39–48 (1982).
37. Arnaud, P., Morlet, D. & Rubel, P. Planarity of the spatial QRS loop Comparative analysis in normals, infarcts, ventricular hypertrophies, and intraventricular conduction defects. *J. Electrocardiol.* **22**, 143–152 (1989).
38. Linde, C. *et al.* Sex differences in cardiac arrhythmia: a consensus document of the European Heart Rhythm Association, endorsed by the Heart Rhythm Society and Asia Pacific Heart Rhythm Society. *Europace* **20**, 1565–1565ao (2018).
39. Ubrich, R. *et al.* (2017) Sex differences in long-term mortality among acute myocardial infarction patients: Results from the ISAR-RISK and ART studies. *PLoS ONE* **12**, e0186783. <https://doi.org/10.1371/journal.pone.0186783> (2017).
40. Zaman, S., Deshmukh, T., Aslam, A., Martin, C. & Kovoov, P. Sex differences in electrophysiology, ventricular tachyarrhythmia, cardiac arrest and sudden cardiac death following acute myocardial infarction. *Heart Lung Circ.* **29**, 1025–1031 (2020).
41. Gasparini, M. *et al.* Sex differences in implantable cardiac defibrillator therapy according to arrhythmia detection times. *Heart* **106**, 520–526 (2020).
42. Johannesen, L. *et al.* Quantitative understanding of QTc prolongation and gender as risk factors for Torsade de Pointes. *Clin. Pharmacol. Ther.* **103**, 304–309 (2018).
43. Andršová, I. *et al.* Individually rate corrected QTc intervals in children and adolescents. *Front Physiol.* **10**, 994. <https://doi.org/10.3389/fphys.2019.00994> (2019).
44. Uijen, G. J. & van Oosterom, A. On the detection of the number of signals in multi-lead ECGs. *Methods Inf. Med.* **31**, 247–255 (1992).
45. Uijen, G. J. & van Oosterom, A. The performance of information-theoretic criteria in detecting the number of independent signals in multi-lead ECGs. *Methods Inf. Med.* **31**, 256–262 (1992).
46. Das, M. K. *et al.* Fragmented QRS on a 12-lead ECG: A predictor of mortality and cardiac events in patients with coronary artery disease. *Heart Rhythm* **4**, 1385–1392 (2007).
47. Cheema, A. *et al.* Fragmented QRS and mortality risk in patients with left ventricular dysfunction. *Circ. Arrhythm Electrophysiol.* **3**, 339–344 (2010).
48. Pietrasik, G. & Zareba, W. QRS fragmentation: Diagnostic and prognostic significance. *Cardiol. J.* **19**, 114–121 (2012).
49. Xu, S., Yang, L., Hong, D., Chen, L. & Wang, X. Predictive value of fragmented QRS for ventricular tachyarrhythmias in patients with acute myocardial infarction: a meta-analysis. *Eur. J. Clin. Invest.* **50**, e13182. <https://doi.org/10.1111/eci.13182> (2020).
50. Haukilahti, M. A. E. *et al.* Gender differences in prevalence and prognostic value of fragmented QRS complex. *J. Electrocardiol.* **61**, 1–9 (2020).
51. Reichlin, T. *et al.* Automated electrocardiographic quantification of myocardial scar in patients undergoing primary prevention implantable cardioverter-defibrillator implantation: association with mortality and subsequent appropriate and inappropriate therapies. *Heart Rhythm* **17**, 1664–1671 (2020).
52. Zabel, M. *et al.* Analysis of T-wave morphology from the 12-lead electrocardiogram for prediction of long-term prognosis in male US veterans. *Circulation* **105**, 1066–1070 (2002).
53. van Stipdonk, A. M. W. *et al.* QRS area is a strong determinant of outcome in cardiac resynchronization therapy. *Circ. Arrhythm. Electrophysiol.* **11**, 006767. <https://doi.org/10.1161/circep.118.006767> (2018).
54. Emerek, K. *et al.* Vectorcardiographic QRS area is associated with long-term outcome after cardiac resynchronization therapy. *Heart Rhythm* **16**, 213–219 (2019).
55. Malik, M., Johannesen, L., Hnatkova, K. & Stockbridge, N. Universal correction for QT/RR hysteresis. *Drug Saf.* **39**, 577–588 (2016).
56. Gravel, H., Jacquemet, V., Dahdah, N. & Curnier, D. Clinical applications of QT/RR hysteresis assessment: a systematic review. *Ann. Noninvasive Electrocardiol.* **23**, e12514. <https://doi.org/10.1111/anec.12514> (2018).
57. Hnatkova, K. *et al.* Heart rate correction of the J-to-Tpeak interval. *Sci. Rep.* **9**, 15060. <https://doi.org/10.1038/s41598-019-51491-4> (2019).
58. Malik, M. *et al.* Sample size, power calculations, and their implications for the cost of thorough studies of drug induced QT interval prolongation. *Pacing Clin. Electrophysiol.* **27**, 1659–1669 (2004).
59. Malik, M. *et al.* Importance of QT/RR hysteresis correction in studies of drug-induced QTc interval changes. *J. Pharmacokin. Pharmacodyn.* **45**, 491–503 (2018).

## Author contributions

Study design: I.A., K.H., M.M., Software development: K.H., M.M., ECG interpretation: I.A., G.S., K.M.H., M.Š., O.T., P.B., P.S., T.N., ECG measurement: I.A., G.S., K.M.H., M.Š., O.T., P.B., P.S., T.N., Supervision of the measurements: G.S., T.N., O.T., P.S., Quality control of the measurements: I.A., G.S., M.M., T.N., Statistics and figures: K.H., M.M., Initial manuscript draft: I.A., K.H., M.M., T.N., Final manuscript: I.A., G.S., K.H., K.M.H., M.M., M.Š., O.T., P.B., P.S., T.N., Approval of the submission: I.A., G.S., K.H., K.M.H., M.M., M.Š., O.T., P.B., P.S., T.N.

## Funding

Supported in part by the British Heart Foundation New Horizons Grant NH/16/2/32499 and by Ministry of Health, Czech Republic, conceptual development of research organization (Grant FNBr/65269705).

## Competing interests

The authors declare no competing interests.

## Additional information

**Supplementary Information** The online version contains supplementary material available at <https://doi.org/10.1038/s41598-021-83378-8>.

**Correspondence** and requests for materials should be addressed to M.M.

**Reprints and permissions information** is available at [www.nature.com/reprints](http://www.nature.com/reprints).

**Publisher's note** Springer Nature remains neutral with regard to jurisdictional claims in published maps and institutional affiliations.



**Open Access** This article is licensed under a Creative Commons Attribution 4.0 International License, which permits use, sharing, adaptation, distribution and reproduction in any medium or format, as long as you give appropriate credit to the original author(s) and the source, provide a link to the Creative Commons licence, and indicate if changes were made. The images or other third party material in this article are included in the article's Creative Commons licence, unless indicated otherwise in a credit line to the material. If material is not included in the article's Creative Commons licence and your intended use is not permitted by statutory regulation or exceeds the permitted use, you will need to obtain permission directly from the copyright holder. To view a copy of this licence, visit <http://creativecommons.org/licenses/by/4.0/>.

© The Author(s) 2021

# Spatial distribution of physiologic 12-lead QRS complex

by

Katerina Hnatkova, Irena Andršová, Ondřej Toman, Peter Smetana, Katharina M Huster,  
Martina Šišáková, Petra Barthel, Tomáš Novotný, Georg Schmidt, Marek Malik

## Supplementary table of measured values

		Females	Males	p-value
QRS Area [ms*mV]	RR slope	0.104 ± 0.187	0.137 ± 0.201	0.031
	RR correlation	0.163 ± 0.322	0.278 ± 0.333	
	QRS slope	0.958 ± 2.055	1.242 ± 2.007	NS
	QRS correlation	0.132 ± 0.264	0.214 ± 0.273	
	60 bpm projection	23.90 ± 5.11	31.70 ± 7.55	<0.00001
	120 bpm projection	22.36 ± 5.27	29.01 ± 7.61	<0.00001
	100 ms projection	24.21 ± 6.52	31.26 ± 9.26	<0.00001
QRS [ms]	RR slope	0.008 ± 0.037	0.014 ± 0.040	0.038
	RR correlation	0.106 ± 0.327	0.140 ± 0.340	
	60 bpm projection	98.9 ± 5.5	103.5 ± 5.9	<0.00001
	120 bpm projection	98.4 ± 6.2	102.5 ± 6.5	<0.00001
∇ <sub>1</sub> [%]	RR slope	0.114 ± 0.208	0.107 ± 0.273	NS
	RR correlation	0.214 ± 0.340	0.212 ± 0.423	
	QRS slope	-1.048 ± 2.120	-1.104 ± 2.179	NS
	QRS correlation	-0.159 ± 0.327	-0.146 ± 0.347	
	60 bpm projection	64.2 ± 11.6	59.7 ± 11.9	<0.00001
	120 bpm projection	59.6 ± 12.5	55.7 ± 12.6	<0.001
	100 ms projection	62.0 ± 12.3	60.5 ± 12.7	NS
∇ <sub>2</sub> [%]	RR slope	-0.215 ± 0.357	-0.184 ± 0.422	NS
	RR correlation	-0.218 ± 0.341	-0.190 ± 0.412	
	QRS slope	1.829 ± 4.270	1.582 ± 4.159	NS
	QRS correlation	0.155 ± 0.330	0.149 ± 0.345	
	60 bpm projection	29.6 ± 11.4	33.1 ± 11.9	<0.001
	120 bpm projection	34.2 ± 12.5	37.4 ± 13.1	0.001
	100 ms projection	32.5 ± 13.2	33.3 ± 13.1	NS
∇ <sub>3</sub> [%]	RR slope	-0.002 ± 0.588	-0.066 ± 0.482	NS
	RR correlation	0.026 ± 0.310	-0.039 ± 0.311	
	QRS slope	1.016 ± 5.964	0.206 ± 5.282	NS
	QRS correlation	0.055 ± 0.246	0.029 ± 0.274	
	60 bpm projection	3.32 ± 1.42	3.61 ± 1.55	0.013
	120 bpm projection	3.43 ± 2.32	3.89 ± 2.12	0.009
	100 ms projection	3.59 ± 2.52	3.68 ± 1.99	NS

		Females	Males	p-value
$\nabla_4$ [%]	RR slope	0.142 ± 0.595	0.062 ± 0.560	NS
	RR correlation	0.077 ± 0.290	0.038 ± 0.319	
	QRS slope	0.842 ± 6.53	-0.097 ± 5.28	0.047
	QRS correlation	0.020 ± 0.216	-0.013 ± 0.246	
	60 bpm projection	1.48 ± 0.69	1.70 ± 0.81	<0.001
	120 bpm projection	1.35 ± 0.69	1.66 ± 0.90	<0.00001
	100 ms projection	1.66 ± 1.84	1.72 ± 0.94	NS
$\nabla_5$ [%]	RR slope	-0.045 ± 0.568	0.005 ± 0.564	NS
	RR correlation	-0.012 ± 0.236	-0.007 ± 0.252	
	QRS slope	-0.106 ± 5.461	0.429 ± 5.641	NS
	QRS correlation	-0.004 ± 0.166	0.024 ± 0.199	
	60 bpm projection	0.598 ± 0.291	0.731 ± 0.338	<0.00001
	120 bpm projection	0.604 ± 0.241	0.732 ± 0.339	<0.00001
	100 ms projection	0.629 ± 0.419	0.727 ± 0.481	0.006
$\nabla_6$ [%]	RR slope	-0.185 ± 0.485	-0.143 ± 0.500	NS
	RR correlation	-0.065 ± 0.187	-0.058 ± 0.210	
	QRS slope	-0.228 ± 4.722	-0.131 ± 4.574	NS
	QRS correlation	-0.001 ± 0.142	-0.002 ± 0.158	
	60 bpm projection	0.306 ± 0.096	0.367 ± 0.144	<0.00001
	120 bpm projection	0.348 ± 0.115	0.406 ± 0.153	<0.00001
	100 ms projection	0.316 ± 0.146	0.370 ± 0.195	<0.0001
$\nabla_7$ [%]	RR slope	-0.353 ± 0.403	-0.306 ± 0.453	NS
	RR correlation	-0.127 ± 0.153	-0.124 ± 0.178	
	QRS slope	-0.333 ± 4.434	-0.281 ± 4.405	NS
	QRS correlation	-0.001 ± 0.127	-0.011 ± 0.137	
	60 bpm projection	0.193 ± 0.046	0.220 ± 0.055	<0.00001
	120 bpm projection	0.252 ± 0.084	0.278 ± 0.096	<0.001
	100 ms projection	0.199 ± 0.071	0.230 ± 0.084	<0.00001
$\nabla_8$ [%]	RR slope	-0.497 ± 0.592	-0.485 ± 0.451	NS
	RR correlation	-0.192 ± 0.140	-0.192 ± 0.159	
	QRS slope	-0.197 ± 7.666	-0.056 ± 6.216	NS
	QRS correlation	0.004 ± 0.141	-0.010 ± 0.135	
	60 bpm projection	0.162 ± 0.043	0.172 ± 0.045	0.004
	120 bpm projection	0.241 ± 0.096	0.250 ± 0.099	NS
	100 ms projection	0.187 ± 0.305	0.183 ± 0.088	NS

For the total QRS area (average of all 8 independent ECG leads), QRS duration, and each of the decomposition components, the table shows the slopes of the log-linear regressions to the RR intervals of the underlying heart rate and to the QRS durations, corresponding Spearman correlation coefficients, and the regression-based projections to the heart rate of 60 and 120 beats per minute (bpm) and to the QRS duration of 100 ms. The values shown are mean ± standard deviation displayed separately for female and male subjects. The log-linear regression slopes and the regression projected values were compared between females and males using two-sample, two-tail t-test assuming different standard deviations of compared samples.

## 4.2. Fragmentace QRS komplexu

Nejen délka trvání QRS komplexu může značit poruchu depolarizace, ale i jeho tvar. Tzv. fragmentace QRS komplexu na povrchovém EKG záznamu je považována za rizikový marker arytmiické příhody u různých kardiologických pacientů ať již se získaným či vrozeným srdečním onemocněním.<sup>119,120,121</sup> Například u hereditárního arytmiického syndromu jako je Brugada syndrom tyto jakési vícenásobné zářezy narušující raménka QRS komplexu značí vysoké riziko maligní komorové arytmie.<sup>122,123</sup> Tyto malformace QRS komplexu jsou vidět pouhým okem, jistě proto musí existovat i mikro-malformace, které jsou díky filtrům EKG odstraněny, či zaniknou v hluku, a přitom jejich přítomnost může mít velký prediktivní potenciál. Výše zmíněná metoda detekce mikrofragmentací QRS komplexu (QRS- $\mu f$ ) pak byla podkladem podrobnější analýzy QRS komplexů z povrchového EKG na třech rozdílných populačních skupinách.

Jak již bylo vysvětleno, lokální heterogenity depolarizační vlny nemohou být reprezentovány trojrozměrným vektorovým pohybem a jsou přiřazeny k vyšším algebraickým dimenzím. Proto jsme navrhli kvantifikovat fragmentaci QRS komplexu součtem 4. až 6. dimenze. Vyšší, 7. a 8. dimenze, představují morfologickou variabilitu QRS komplexu v různých EKG svodech, která se v jiných svodech nereplikuje. Proto tyto 7. a 8. algebraické dimenze QRS komplexu představují nepřesnost záznamu a biologický šum. Fragmentace QRS odvozená ze 4. až 6. dimenze je do značné míry neviditelná pouhým okem, a proto jsme navrhli termín mikrofragmentace QRS (QRS- $\mu f$ ). Prospektivně jsme také navrhli, že by toto měření mohlo představovat rizikový marker.

Srovnání zrekonstruovaných komponent QRS komplexu s komplexem původním, tedy vyhodnocení QRS- $\mu f$ , pak bylo provedeno u pacientů s implantovaným ICD, u těžkých kardiaků a v neposlední řadě i u vzorku běžné populace. Jak popisuje následující publikace, QRS- $\mu f$  prokázala značnou mortalitní prediktivní hodnotu nezávisle na již dříve stanovených rizikových faktorech. K přesné predikci charakteru mortality (arytmická příhoda či srdeční selhání) bude potřeba dalších analýz.

Hnatkova K, **Andršová I**, Novotný T, Britton A, Shipley M, Vandenberg B, Sprenkeler DJ, Junttila J, Reichlin T, Schlögl S, Vos MA, Friede T, Bauer A, Huikuri HV, Willems R, Schmidt G, Franz MR, Sticherling C, Zabel M, Malik M. QRS micro-fragmentation as a mortality predictor. *Eur Heart J* 2022; 43:4177–4191.

IF 39,3. Počet citací ve Web of Science 7

Původní práce - kvantitativní podíl uchazečky 20%: Elektrokardiologická měření a jejich reprodukovatelnost, fyziologická interpretace metody, interpretace statistických výsledků, diskuze výsledků.

# QRS micro-fragmentation as a mortality predictor

Katerina Hnatkova <sup>1</sup>, Irena Andršová <sup>2,3</sup>, Tomáš Novotný <sup>2,3</sup>, Annie Britton<sup>4</sup>, Martin Shipley<sup>4</sup>, Bert Vandenberg <sup>5</sup>, David J. Sprenkeler <sup>6</sup>, Juhani Junttila <sup>7</sup>, Tobias Reichlin <sup>8</sup>, Simon Schlögl<sup>9,10</sup>, Marc A. Vos<sup>6</sup>, Tim Friede <sup>10,11</sup>, Axel Bauer <sup>12</sup>, Heikki V. Huikuri<sup>7</sup>, Rik Willems <sup>5</sup>, Georg Schmidt <sup>13,14</sup>, Michael R. Franz<sup>15</sup>, Christian Sticherling <sup>16</sup>, Markus Zabel <sup>9,10</sup>, and Marek Malik <sup>1,3\*</sup>

<sup>1</sup>National Heart and Lung Institute, Imperial College, ICTEM, Hammersmith Campus, 72 Du Cane Road, Shepherd's Bush, London W12 0NN, UK; <sup>2</sup>Department of Internal Medicine and Cardiology, University Hospital Brno, Brno, Czech Republic; <sup>3</sup>Department of Internal Medicine and Cardiology, Masaryk University, Brno, Czech Republic; <sup>4</sup>Research Department of Epidemiology and Public Health, University College London, UK; <sup>5</sup>Department of Cardiovascular Sciences, University of Leuven, Leuven, Belgium; <sup>6</sup>Department of Medical Physiology, University Medical Center Utrecht, Utrecht, The Netherlands; <sup>7</sup>Medical Research Center Oulu, University Central Hospital of Oulu and University of Oulu, Oulu, Finland; <sup>8</sup>Department of Cardiology, Inselspital, Bern University Hospital, Bern, Switzerland; <sup>9</sup>Department of Cardiology and Pneumology, University Medical Center, Göttingen, Germany; <sup>10</sup>German Center of Cardiovascular Research (DZHK), Partner Site Göttingen, Göttingen, Germany; <sup>11</sup>Department of Medical Statistics, University Medical Center Göttingen, Göttingen, Germany; <sup>12</sup>University Hospital for Internal Medicine III, Medical University Innsbruck, Innsbruck, Austria; <sup>13</sup>Klinikum rechts der Isar, Technical University of Munich, Munich, Germany; <sup>14</sup>German Center for Cardiovascular Research Partner Site Munich Heart Alliance, Munich, Germany; <sup>15</sup>Veteran Affairs and Georgetown University Medical Centers, Washington, DC, USA; and <sup>16</sup>Department of Cardiology, University Hospital of Basel, Basel, Switzerland

Received 27 August 2021; revised 5 January 2022; accepted 8 February 2022; online publish-ahead-of-print 21 February 2022

See the editorial comment for this article 'The fractionated QRS complex for cardiovascular risk assessment', by Richard N. W. Hauer, <https://doi.org/10.1093/eurheartj/ehac198>.

## Aims

Fragmented QRS complex with visible notching on standard 12-lead electrocardiogram (ECG) is understood to represent depolarization abnormalities and to signify risk of cardiac events. Depolarization abnormalities with similar prognostic implications likely exist beyond visual recognition but no technology is presently suitable for quantification of such invisible ECG abnormalities. We present such a technology.

## Methods and results

A signal processing method projects all ECG leads of the QRS complex into optimized three perpendicular dimensions, reconstructs the ECG back from this three-dimensional projection, and quantifies the difference (QRS 'micro'-fragmentation, QRS- $\mu f$ ) between the original and reconstructed signals. QRS 'micro'-fragmentation was assessed in three different populations: cardiac patients with automatic implantable cardioverter-defibrillators, cardiac patients with severe abnormalities, and general public. The predictive value of QRS- $\mu f$  for mortality was investigated both univariably and in multivariable comparisons with other risk factors including visible QRS 'macro'-fragmentation, QRS- $Mf$ . The analysis was made in a total of 7779 subjects of whom 504 have not survived the first 5 years of follow-up. In all three populations, QRS- $\mu f$  was strongly predictive of survival ( $P < 0.001$  univariably, and  $P < 0.001$  to  $P = 0.024$  in multivariable regression analyses). A similar strong association with outcome was found when dichotomizing QRS- $\mu f$  prospectively at 3.5%. When QRS- $\mu f$  was used in multivariable analyses, QRS- $Mf$  and QRS duration lost their predictive value.

## Conclusion

In three populations with different clinical characteristics, QRS- $\mu f$  was a powerful mortality risk factor independent of several previously established risk indices. Electrophysiologic abnormalities that contribute to increased QRS- $\mu f$  values are likely responsible for the predictive power of visible QRS- $Mf$ .

\* Corresponding author. Tel: +44 2086602112, Email: [marek.malik@imperial.ac.uk](mailto:marek.malik@imperial.ac.uk)

© The Author(s) 2022. Published by Oxford University Press on behalf of European Society of Cardiology.

This is an Open Access article distributed under the terms of the Creative Commons Attribution License (<https://creativecommons.org/licenses/by/4.0/>), which permits unrestricted reuse, distribution, and reproduction in any medium, provided the original work is properly cited.

### Key question

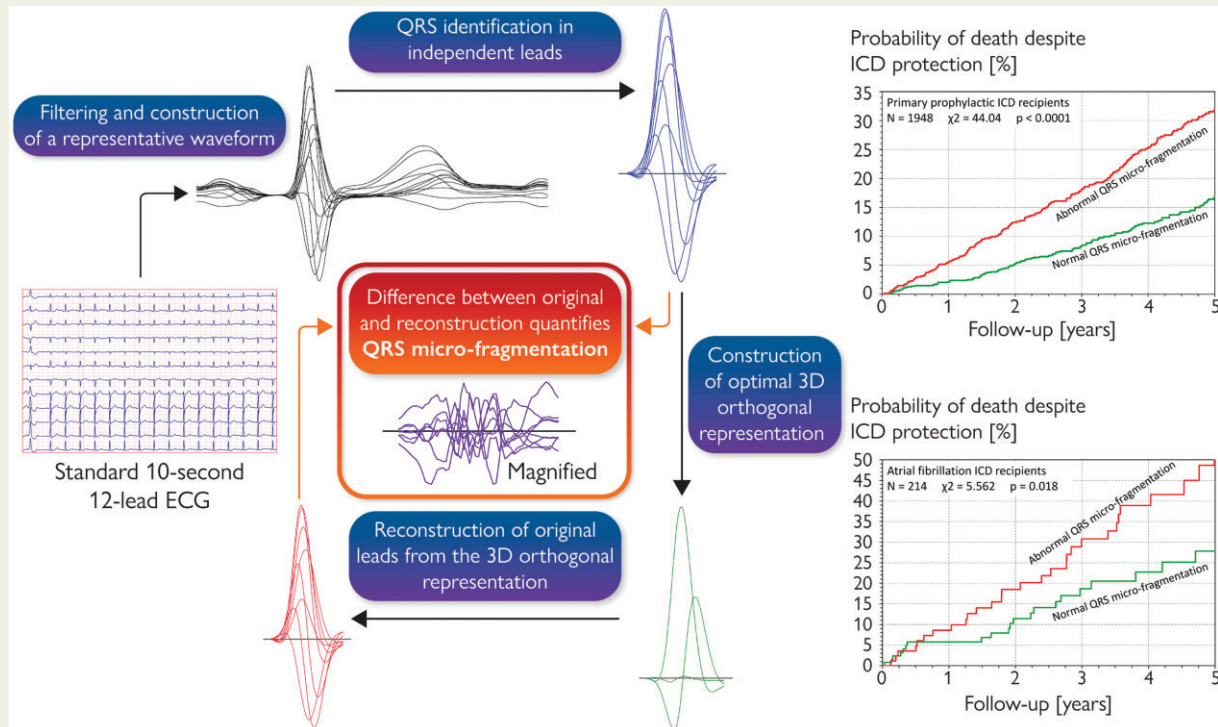
- The cardiac risk associated with visually diagnosed QRS fragmentation suggests that important QRS abnormalities might exist below the resolution of visual detection. Nevertheless, at present, little possibility exists to detect 'invisible' abnormalities of myocardial depolarization.

### Key finding

- QRS 'micro-fragmentation', QRS- $\mu f$  analysis quantifies 'invisible' abnormalities of myocardial depolarization. It was found to independently predict death in three different populations of a total of 7779 subjects of whom 504 have not survived the first 5 years of follow-up.

### Take-home message

QRS- $\mu f$  is a strong predictor of worsened survival. It can be assessed in standard short-term 12-lead electrocardiograms.



**Structured Graphical Abstract** Principles of QRS micro-fragmentation.

**Keywords** Electrocardiogram • QRS complex • Fragmentation • Mortality prediction

## Introduction

Abnormalities of the electrocardiographic QRS complex reflect intramyocardial conduction pathologies. Such abnormalities include not only the typical bundle branch block patterns but also forms due to less specific intraventricular conduction abnormalities. Prolonged QRS complex duration has long been a recognized risk factor for adverse cardiac events.<sup>1,2</sup> More recently, the so-called QRS complex fragmentation, defined by visually detected splits of QRS waves,<sup>3,4</sup> has also been found to predict poor outcome in both cardiac patients and other well-defined groups<sup>5–7</sup> including the general population.<sup>4</sup> This increased risk due to visible QRS fragmentation appears independent of the overall QRS complex duration.<sup>8</sup>

Visual diagnosis of QRS fragmentation leads to a yes/no classification although quantitative sums of QRS splits detected in different leads and probabilistic approaches have also been proposed.<sup>9</sup> This categorical distinction suggests that similarly important QRS abnormalities might exist below the resolution of visual detection. Such a concept is not new. Already some decades ago, spectral analyses of signal-averaged QRS complex were proposed, albeit with variable success, to identify abnormalities hidden within the overall QRS pattern.<sup>10,11</sup> Nevertheless, so far, little success has been achieved when trying to detect 'invisible' abnormalities of myocardial depolarization in standard clinical 10-s electrocardiograms (ECG).

We have recently reported a method for QRS complex analysis that might be used for this purpose.<sup>12</sup> Briefly, the method is based

on projecting the 12-lead ECG signal (i.e. its eight independent leads) into an optimized three-dimensional orthogonal representation, reconstructing the 12-lead signal back from the orthogonal leads, and measuring the difference between the original and the reconstructed signal. As also recently reported, the ECG reconstruction methods allow to differentiate between noise and signal components that might be attributed to localized heterogeneities of the depolarization wavefront.<sup>12</sup> Only small proportions (single-digit percentages) of the original ECG signal are attributable to such localized heterogeneities but we propose that these measurements might be interpreted as invisible QRS ‘micro-fragmentation’ (QRS- $\mu f$ ).

We have tested the predictive value of QRS- $\mu f$  in three independent populations with different risk of cardiac adverse events. We show here that in these tests, QRS- $\mu f$  not only significantly predicted adverse outcome during follow-up but that the risk prediction was also independent of other recognized risk factors including the visually detected QRS fragmentation (that, for the distinction purposes, we call ‘macro-fragmentation’, QRS-Mf).

## Methods

### Investigated populations and electrocardiographic recordings

All three sources of analysed ECGs and follow-up data have previously been published.<sup>13–15</sup>

#### Retrospective part of EU-CERT-ICD

The European Commission supported study EU-CERT-ICD included a retrospective part that recorded patients in whom automatic implantable cardioverter-defibrillators (ICDs) were implanted for primary prophylaxis between 2002 and 2014. All details of this part of EU-CERT-ICD were reported previously.<sup>13</sup> In five contributing centres (Basel, Göttingen, Leuven, Oulu, and Utrecht) short-term (8- or 10-s) digital 12-lead ECG recordings were also collected in the patients on median of 1 day [interquartile range (IQR) 1–6 days] before ICD implantation.

As previously described,<sup>13</sup> clinical data in this registry included, among others, pre-implantation assessment of left ventricular ejection fraction (LVEF), rhythm classification of the recorded ECG, and the distinction between ischaemic and non-ischaemic heart disease.

#### VA Washington

A collection of digital 10-s 12-lead ECGs of US male veterans with ischaemic and non-ischaemic heart disease was made available for testing the predictive value of QRS- $\mu f$ . As previously described,<sup>14</sup> these were the historical data of patients recorded between 1984 and 1991 at the VA Medical Center in Washington, DC. All ECG recordings were stored within the hospital information system of the clinical centre. For the purposes of a previous study,<sup>14</sup> least noise-polluted ECG recording was selected for each patient. These recordings were available for the present investigation.

#### Whitehall II study

The Whitehall II programme is an ongoing epidemiologic study with repeated calls during which series of medical investigations are performed in British civil servants of a broad spectrum of employment levels and positions.<sup>15</sup> During the call between 2007 and 2009, participants in sinus rhythm had a digital 5-min 12-lead ECG recorded.<sup>16</sup> To

model short-term 10-s ECG acquisition, a 10-s section was extracted starting 100 s from the beginning of the 5-min signal.

### Electrocardiogram analyses

Supplementary material online, Table S1 shows the technical details of the analysed ECGs. In each short-term ECG, the locations of QRS complexes were detected automatically and, where necessary, checked and corrected visually. Subsequently, the ECG signals were filtered (100 Hz low pass Butterworth filter with cubic spline baseline wander elimination—see Supplementary material online, Figure S1 for details). Using these filtered signals, representative median beats were constructed in each lead and superimposed on the same isoelectric axis. All these pre-processing used algorithms and their software implementation that were repeatedly used and validated in previous studies.<sup>12,17</sup>

### Electrocardiogram measurements

For each of the analysed ECGs, the image of the superimposed patterns of representative beats of different leads was visually interpreted and global 12-lead QRS onset and offset, and T wave offset points were identified. Supplementary material online, Figure S1 also shows an example of measured ECG patterns. The visual analyses were made by team members who had neither access to any clinical and/or follow-up data nor information of a study from which individual ECGs originated. To assure consistency of the visual ECG interpretation, the recordings of each of the data sources were interpreted by the same team member.

In each ECG, heart rate was measured based on the total duration of the short-term recording. QT interval was measured from the global onset of the QRS complex to the global offset of the T wave, and spatial angle between the QRS complex and the T wave loops was measured by the previously published method<sup>18,19</sup> of the total cosine R to T (TCRT) and expressed in degrees. To obtain QTc values, the QT interval was corrected for the heart rate using Fridericia formula.

Since the construction of representative median beat eliminates patterns not synchronized with QRS complexes, the interval measurements were also reliable in atrial fibrillation recordings that were present in the EU-CERT-ICD data—note Supplementary material online, Figure S1. (This was consistent with previously published analyses of ECGs polluted by other types of biological noise not phase-locked with QRS complexes.<sup>17</sup>) Similarly, correction of the QT interval to the heart rate derived from the complete 10-s recordings made QTc calculations also applicable to atrial fibrillation ECGs.

### QRS macro-fragmentation

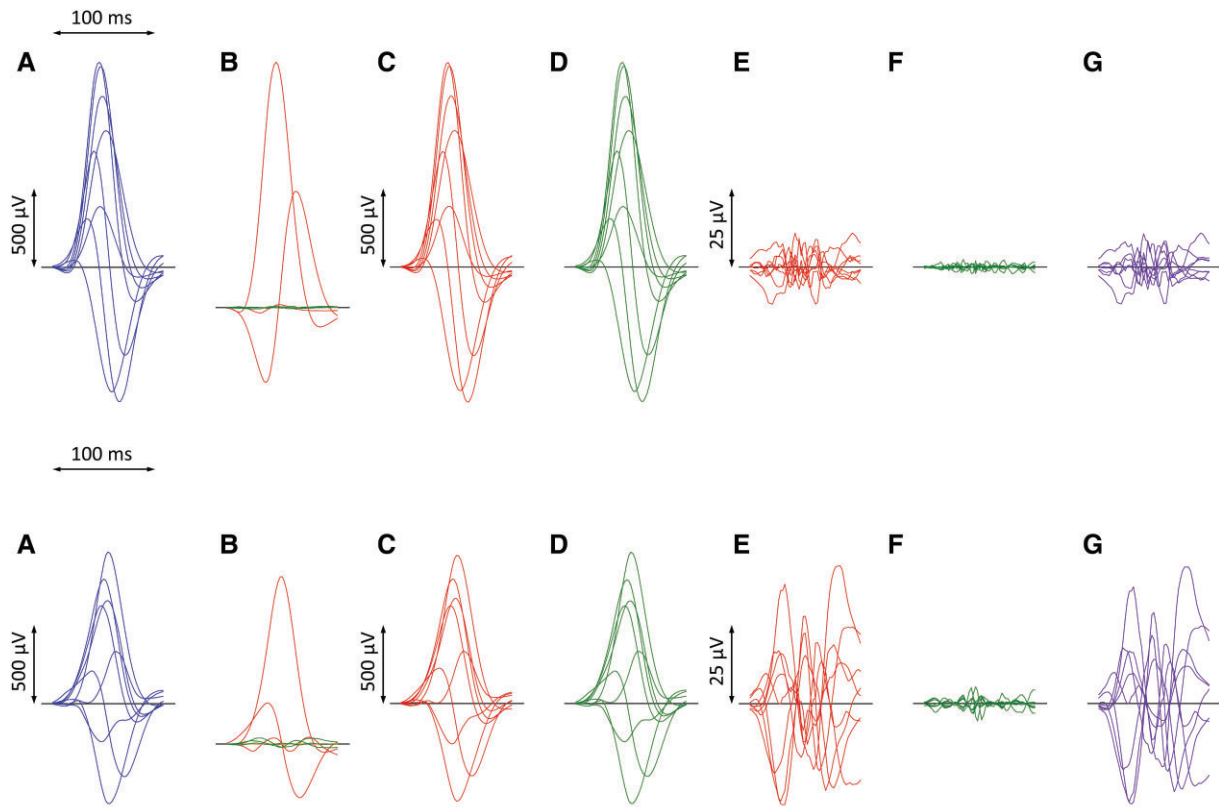
Using the filtered median beat images of the individual ECG leads, QRS-Mf was defined as additional QRS local maxima,<sup>3–5</sup> i.e. as a visible notching in the pattern of the R or S waves, including additional waves, if present in more than one lead.

### QRS micro-fragmentation

The term *micro-fragmentation* should not be interpreted as an increased precision of the ‘standard’ visible macro-fragmentation. Rather, we propose this term since the analysis detects signal characteristics that are largely inaccessible by the naked eye and which are, in principle, independent of the visually detected QRS-Mf.

Individual steps of the QRS- $\mu f$  analysis are summarized in Figure 1: QRS- $\mu f$  was quantified using the published method based on singular value decomposition (SVD) of the QRS complex signal (that is, between the visually detected and manually verified QRS onset and offset). Singular value decomposition considers the signals of all eight





**Figure 1** Example of ECG processing of a recordings in a 69-year-old male survivor (top row) and a 60-year-old patient who died 11 months later (bottom row). In both cases, the QRS duration was 109 ms. Filtered QRS complex patterns of independent Leads I, II, V1, V2, ..., V6 are considered together as if on the same isoelectric axis (A). Singular value decomposition transforms the signals into eight algebraically orthogonal signals which are sorted according to their contribution to the original ECG leads (Components 1–3 are shown in red, 4–6 in green, and 7 and eight in amber in panels (B); the 7th and 8th components are almost invisible in these cases). The Components 1–3 create the optimized three-dimensional QRS vector projection. When these components are used to reconstruct the original ECG, patterns in panels (C) are obtained while reconstruction based on Components 1–6 gives patterns in panels (D). (E) and (F) show the differences between the original ECG are the reconstruction based on 1–3 and 1–6 components, respectively (i.e.  $E = A - C$ ,  $F = A - D$ ). The residuals shown in panels (F) (corresponding to the contribution of 7th and 8th components) are considered noise and eliminated. QRS micro-fractionation is calculated as the averaged absolute area under contribution by Components 4–6 shown in panels G ( $G = D - C = E - F$ ). This area is related to the absolute area under the original ECG signal and was 0.887 and 5.754% in the top and bottom row ECGs, respectively. Note that the differences between panels (A) and (C) cannot be visually quantified.

algebraically independent leads of 12-lead ECG (Leads I, II, V1, V2, ..., V6) and examines the multi-lead signal in a theoretical eight-dimensional space. Within this representation, it composes eight algebraically orthogonal signals which are sorted according to their contribution to the original ECG. The 1st, 2nd, and 3rd components correspond to a three-dimensional representation of the ECG (as if the XYZ leads were rotated to contain the maximum signal in lead X, most of the signal perpendicular to X in Lead Y, and the remainder of the three-dimensional representation in Lead Z). When the ECG is reconstructed back from these rotated XYZ components, the reconstruction differs from the original ECG and the difference is represented by the 4th–8th components of the original SVD decomposition.

The numerical values of QRS- $\mu f$  are the sums of 4th, 5th, and 6th decomposition fractions while the 7th and 8th fractions are attributed to recording noise. As previously explained, micro-fragmentation values are expressed in percentages of the total area under the absolute QRS complex curves and averaged over all eight independent leads of the analysed ECG.<sup>12</sup> A certain level of micro-fragmentation is found

within each ECG (i.e. each ECG differs from its optimized XYZ reconstruction) but the observed distribution of QRS- $\mu f$  estimates among healthy subjects proposed that values above 3.5% might be considered abnormal.<sup>12</sup>

The same method for micro-fragmentation calculation (including the same ECG pre-processing) as previously published<sup>12</sup> was used in all three studies. The QRS- $\mu f$  estimates were based on the initial assessment of QRS onset and offset points that were not changed during the analysis. Since the analysis was based on the processing of median representative beats, the method was also applicable to atrial fibrillation recordings (note [Supplementary material online, Figure S1](#)).

### Follow-up events

For the purposes of this study, all-cause mortality data were available from EU-CERT-ICD and VA Washington studies. In the Whitehall II study, mortality data were available including the distinction between cardiovascular and non-cardiovascular deaths. This distinction was

based on the cause of death in the death certificates (i.e. cardiovascular death was defined as death due to the ICD-10 coded diseases of the circulatory system).

Consequently, in the analyses of the predictive value of QRS- $\mu f$  assessment, all-cause mortality was considered in the cardiac patients of EU-CERT-ICD and of VA Washington studies while cardiovascular death was considered in the general-population Whitehall II study (we have not aimed at predicting the substantial proportion of Whitehall II mortality due to neoplasms). In all these studies, follow-up from the date of the ECG acquisition was considered, restricted to a maximum of 5 years.

When using the terms survivors, non-survivors, and mortality in this text, we shall mean the follow-up distinction between those who did not and did die in the EU-CERT-ICD and VA Washington populations and those who did not and did die of cardiovascular death in the Whitehall II population.

## Statistics and data presentation

Categorical data are presented as percentages with absolute counts where appropriate, continuous data are shown as medians and IQR. In each of the populations, differences in continuous risk predictors between survivors and non-survivors were tested by non-parametric Mann–Whitney *U*-test with cumulative distributions of QRS- $\mu f$  values displayed. Differences between cumulative distributions were further evaluated using Kolmogorov–Smirnov test which was also used to compare the QRS- $\mu f$  distributions between subjects with and without QRS-*Mf* diagnosed. Relationships between different continuous risk factors were investigated using Kendall's  $\tau$  coefficients.

Associations between QRS- $\mu f$  measurements and mortality during the follow-up were compared with other risk predictors of age, heart rate, QRS duration, QTc duration, TCRT, and the presence of QRS-*Mf*. In the EU-CERT-ICD study, comparison with LVEF was also included. Using univariable and multivariable Cox regression models with backward stepwise elimination, hazard ratios (HRs) and their 95% confidence intervals (CIs) of each risk factor were estimated for each of the source studies twice—with continuous and dichotomized risk predictors. In the models using continuous risk factors, numerical measurements of QRS- $\mu f$  were used after logarithmic transformation. The dichotomized models also included the presence of QRS-*Mf*. The same dichotomies of the risk factors were used in all three source studies: dichotomy of 3.5% of QRS- $\mu f$  was prospectively applied<sup>12</sup>; age was dichotomized at >65 years; heart rate at >75 b.p.m.; QRS duration at >120 ms; QTc duration at >450 ms and TCRT at >110°. In the analysis of EU-CERT-ICD study, LVEF was dichotomized at <25% since this value was close to the median of the population and, in supplementary analyses, creatinine level was dichotomized at 1.35 mg/dL. For QRS- $\mu f$  and other continuous variables, Harrell's C-index values were calculated<sup>20</sup> together with areas under the receiver operating characteristic (ROC) curve and their Mann–Whitney standard errors. Receiver operating characteristic curves considered deaths during complete follow-up.

To investigate the additional predictive value of QRS- $\mu f$  in comparison with QRS-*Mf*, the univariable predictive value of QRS- $\mu f$  was assessed in sub-populations of subjects without diagnosed QRS-*Mf*.

Comparison of the probability of mortality in dichotomized populations was displayed using Kaplan–Meier curves that were compared by log-rank test. The statistical testing was performed using SPSS package version 27 (IBM, Armonk, NY, USA). *P*-values < 0.05 were considered statistically significant; all tests were two-sided, no test multiplicity correction was used.

The EU-CERT-ICD study was also used to test the stability of the mortality risk prediction in different subsets of the data, by repeating

the analyses in the data of different clinical centres, and in the data of patients diagnosed with ischaemic vs. non-ischaemic heart disease. In supplementary analyses, the predictive value of QRS- $\mu f$  was also assessed among atrial fibrillation patients. Survival of subjects with QRS- $\mu f$  above and below 3.5% was also compared in different population subgroups.

## Results

Table 1 shows the characteristics of the investigated populations. Taking these together, QRS- $\mu f$  was investigated in 7779 subjects of whom 504 have not survived during the first 5 years of follow-up. Nevertheless, mortality was very different between the populations. In the ICD-protected cardiac patients of EU-CERT-ICD, the cumulative 5-year death rate was 15.1%, while it was 21.3% in the cardiac VA Washington patients. In the general population of the Whitehall II study, the 5-year rate of cardiovascular mortality was 0.95% (while that of non-cardiovascular mortality, mainly due to neoplasms, was 2.3%). The prevalence of QRS- $\mu f$  > 3.5% among the EU-CERT-ICD, VA Washington, and Whitehall II subjects was 45.7, 23.3, and 10.9%, respectively.

Supplementary material online, Table S2 shows that in all three populations, the relationship between QRS- $\mu f$  and other risk factors considered in the analysis was very weak although it was, not surprisingly, frequently statistically significant because of the large sample sizes. In all populations, the relation of QRS- $\mu f$  to QRS duration was stronger than to other risk factors but this was still weak with the correlation  $\tau$  coefficients well below 0.4. Since QRS- $\mu f$  is calculated as a proportion to the total area under the QRS waves, the relation to the QRS complex duration is not caused by its mathematical definition.<sup>12</sup>

## Outcome prediction

The left panels of individual sections of Figure 2 show, for each of the investigated populations, cumulative distributions of QRS- $\mu f$  in survivors and non-survivors. In all three cases, the distributions were highly statistically different. The right panels of the figure show the survival probabilities in sub-populations with QRS- $\mu f$  > 3.5 and  $\leq$ 3.5%. In all three populations, the differences were highly statistically significant.

Tables 2 and 3 show the results of the Cox regression models using continuous and dichotomized risk predictors. In both models, QRS- $\mu f$  was found to be an independent highly significant outcome predictor in all three populations. Harrell's C-index values and univariable areas under the ROC curves of continuous risk predictors are shown in Supplementary material online, Figure S2. Supplementary material online, Table S3 shows multivariable C-index statistics. Selected multivariable ROC curves are shown in Supplementary material online, Figure S3.

## Stability of outcome prediction

The top part of Figure 3 shows that when the distinction between QRS- $\mu f$  > 3.5 and  $\leq$ 3.5% was applied separately to ischaemic and non-ischaemic patients of EU-CERT-ICD, highly significant differences in the survival probability were seen in both groups. Supplementary material online, Table S4 shows that in both groups

**Table 1** Characteristics of the investigated populations

	Survivors	Non-survivors	P-value
<b>EU-CERT-ICD</b>			
N	1654	294	
Age (years)	64 (55–71)	69 (62–75)	<0.001
Females/males	336/1318	45/249	0.046
Heart rate (b.p.m.)	68.9 (59.8–79.2)	72.9 (65.0–83.9)	<0.001
LVEF (%)	26 (21–31)	25 (20–30)	<0.001
QRS duration (ms)	128 (112–159)	147 (122–171)	<0.001
QTc (ms)	442 (419–467)	452 (428–485)	0.001
TCRT (°)	151.0 (115.5–165.1)	159.9 (142.7–167.4)	<0.001
QRS micro-fragmentation (%)	3.213 (2.386–4.548)	4.188 (3.005–5.598)	<0.001
<b>VA Washington</b>			
N	598	162	
Age (years)	62 (56–68)	65 (59–69)	<0.001
Heart rate (b.p.m.)	72 (61–85)	79 (66–91)	<0.001
QRS duration (ms)	110 (103–119)	112 (104–128)	0.010
QTc (ms)	419 (404–435)	420 (406–449)	0.029
TCRT (°)	102.7 (69.3–140.2)	120.6 (79.9–155)	0.003
QRS micro-fragmentation (%)	2.143 (1.586–3.155)	2.521 (1.736–4.104)	0.001
<b>Whitehall II<sup>a</sup></b>			
N	5023	48	
Age (years)	65 (61–70)	70 (61–74)	0.001
Females/males	1360/3663	8/40	0.140
Heart rate (b.p.m.)	67 (60–74)	72 (59–78)	0.102
QRS duration (ms)	106 (100–111)	107 (103–114)	0.068
QTc (ms)	423 (412–436)	426 (414–444)	0.126
TCRT (°)	45.3 (28.3–76.3)	74.4 (38.3–132.8)	<0.001
QRS micro-fragmentation (%)	1.944 (1.437–2.645)	2.439 (1.807–3.581)	0.001

The table shows medians and interquartile ranges and their comparison between 5-year survivors and non-survivors. TCRT = total cosine R to T.

<sup>a</sup>For the Whitehall II study, comparison is shown between those who did not and did die of cardiovascular death during a 5-year follow-up. Non-parametric Mann–Whitney *P*-values are shown for the comparison of numerical factors between survivors and non-survivors. The *P*-values of the differences between the proportions of non-survivors among females and males were obtained by Fisher exact test. *P*-values (log-rank test) of the differences of female vs. male Kaplan–Meier survival curves were 0.110 and 0.106, in the EU-CERT-ICD and Whitehall II populations, respectively. (Note that the VA Washington population included only males.)

QRS- $\mu f$  was a significant mortality predictor also in multivariable Cox regression models.

Of the 1948 patients of EU-CERT-ICD, clinical centres in Basel, Göttingen, Leuven, Oulu, and Utrecht contributed ECGs of 488, 441, 361, 32, and 626 patients, respectively (see [Supplementary material online, Table S5](#)). Stability of survival probability prediction was therefore tested in separate per-centre data of Basel, Göttingen, Leuven, and Utrecht. Kaplan–Meier probabilities of death distinguishing QRS- $\mu f > 3.5$  and  $\leq 3.5\%$  are shown in the bottom part of [Figure 3](#). In all four cases, the distinction was statistically significant. [Supplementary material online, Table S6](#) shows that in multivariable Cox regression analysis, QRS- $\mu f$  was found to be an independent predictor of survival in the data of three of the four centres.

### Outcome prediction in clinical subgroups

[Supplementary material online, Figures S4–S6](#) show that comparisons of death probabilities between QRS- $\mu f > 3.5$  and  $\leq 3.5\%$  sub-strata of different EU-CERT-ICD well-defined subgroups were all statistically significant. The same outcome differences were seen

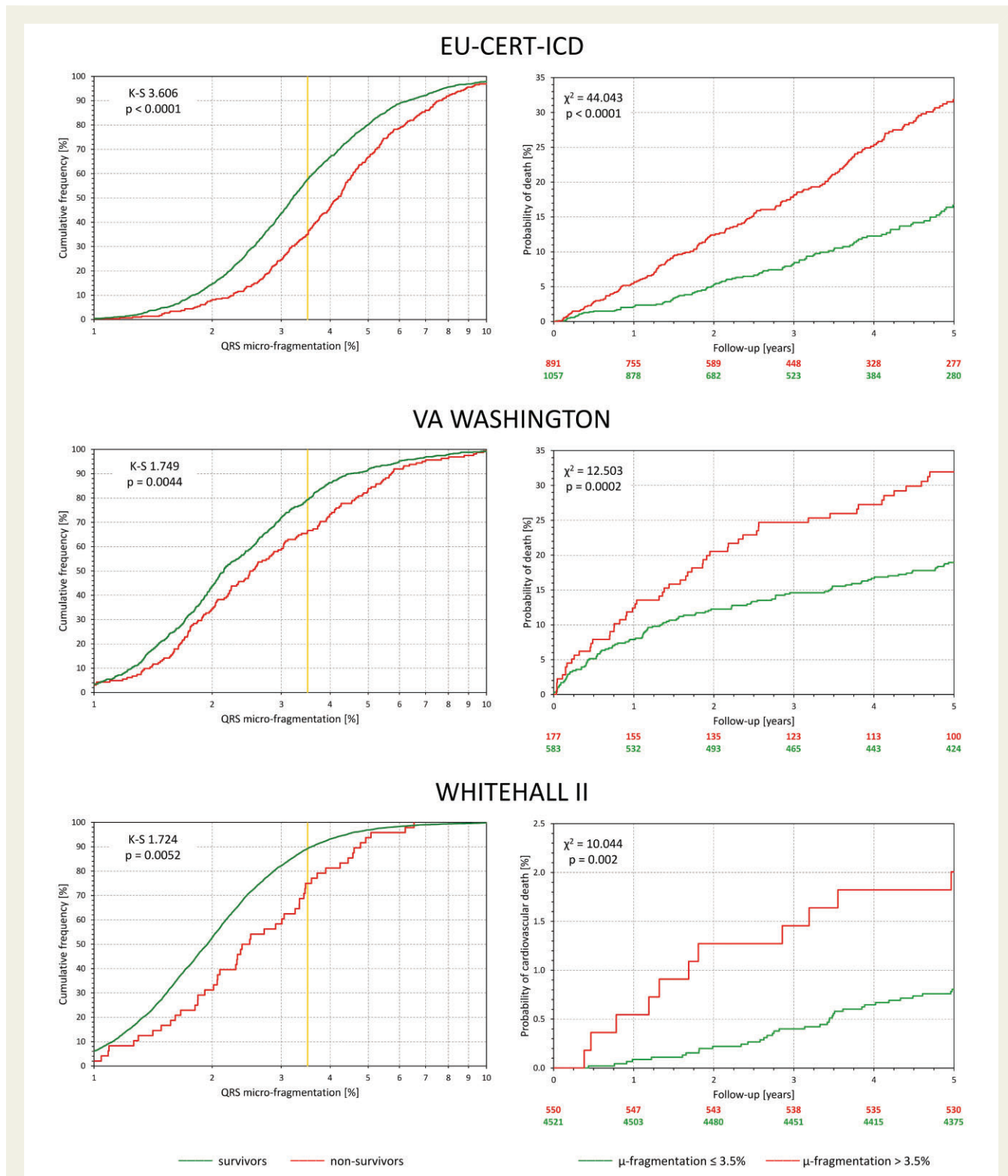
in VA Washington and Whitehall II sub-populations, although statistical significance was not always reached because of small group sizes.

[Supplementary material online, Figure S7](#) shows that comparisons of death probabilities between QRS- $\mu f > 3.5$  and  $\leq 3.5\%$  were also statistically significant in EU-CERT-ICD patients with pre-implantation creatinine levels above and below 1.35 mg/dL, as well as in patients who, for clinical reasons, had and had not a defibrillator implanted with cardiac resynchronization function.

Finally, [Supplementary material online, Figure S8](#) shows that among the EU-CERT-ICD patients, the statistical significance of death prediction by QRS- $\mu f > 3.5\%$  was not influenced by clinical decisions leading to intention to treat with beta-blockers, amiodarone, and statins.

### Outcome prediction in atrial fibrillation patients

Among the EU-CERT-ICD patients, 214 (11.0%) suffered from atrial fibrillation. The 5-year survival of these patients (76.6%) was substantially worse than that of patients with sinus rhythm



**Figure 2** For each of the investigated populations, the left panel shows the comparison between distributions of QRS micro-fragmentation values in survivors (green line) and non-survivors (red line). The distributions were compared by Kolmogorov–Smirnov test (K–S statistics values shown). The yellow vertical lines mark the 3.5% dichotomy. The right panels show the Kaplan–Meier probabilities of non-survival for subjects with QRS micro-fragmentation  $\leq$ 3.5% (green line) and  $>$ 3.5% (red line). Numbers of subjects at risk are shown below the panel in corresponding colours. The non-survival probabilities were compared by log-rank test.

**Table 2 Association between mortality<sup>a</sup> and continuous values of risk factors**

	Univariable analysis			Multivariable analysis <sup>b</sup>		
	Wald	P-value	HR (95% CI)	Wald	P-value	HR (95% CI)
<b>EU-CERT-ICD</b>						
Age (years)	48.9	<0.001	1.043 (1.031–1.055)	30.9	<0.001	1.035 (1.022–1.047)
Heart rate (b.p.m.)	30.8	<0.001	1.019 (1.012–1.026)	24.2	<0.001	1.018 (1.011–1.025)
LVEF (%)	30.1	<0.001	0.959 (0.945–0.973)	9.17	0.002	0.975 (0.958–0.991)
QRS duration (ms)	26.6	<0.001	1.009 (1.006–1.013)			
QTc (ms)	20.3	<0.001	1.006 (1.004–1.009)			
TCRT (°)	26.1	<0.001	1.010 (1.006–1.014)	7.39	0.007	1.006 (1.002–1.010)
log <sub>2</sub> (QRS micro-fragmentation)	42.9	<0.001	1.688 (1.443–1.975)	25.5	<0.001	1.540 (1.302–1.821)
<b>VA Washington</b>						
Age (years)	12.4	<0.001	1.029 (1.013–1.046)	11.4	0.001	1.029 (1.012–1.047)
Heart rate (b.p.m.)	13.6	<0.001	1.014 (1.007–1.022)	10.2	0.001	1.013 (1.005–1.021)
QRS duration (ms)	12.1	0.001	1.005 (1.002–1.008)			
QTc (ms)	7.25	0.007	1.007 (1.002–1.013)			
TCRT (°)	9.71	0.002	1.006 (1.002–1.009)	4.29	0.038	1.004 (1.000–1.007)
log <sub>2</sub> (QRS micro-fragmentation)	13.3	<0.001	1.422 (1.176–1.719)	10.1	0.002	1.367 (1.127–1.659)
<b>Whitehall II</b>						
Age (years)	11.6	0.001	1.088 (1.036–1.142)	7.79	0.005	1.072 (1.021–1.126)
Heart rate (b.p.m.)	5.41	0.020	1.026 (1.004–1.049)			
QRS duration (ms)	6.50	0.011	1.021 (1.005–1.037)			
QTc (ms)	0.52	0.472	0.997 (0.987–1.006)			
TCRT (°)	24.4	<0.001	1.016 (1.009–1.022)	15.5	<0.001	1.013 (1.006–1.019)
log <sub>2</sub> (QRS micro-fragmentation)	12.2	<0.001	1.972 (1.347–2.887)	5.12	0.024	1.555 (1.061–2.279)

CI, confidence interval; HR, hazard ratio; LVEF, left ventricular ejection fraction; TCRT, total cosine R to T.

<sup>a</sup>The outcome is all-cause mortality for the EU-CERT-ICD and VA Washington studies and cardiovascular mortality for the Whitehall II study.

<sup>b</sup>Multivariable analysis used backwards stepwise elimination. In addition to hazard ratios, Wald statistics are shown. QRS micro-fragmentation was used after logarithmic transformation with base 2—hazard ratios correspond to value increases by a factor of 2.

recordings (87.4%,  $P < 0.001$ ). *Structured Graphical Abstract* and *Supplementary material online, Figure S7* shows that QRS- $\mu f > 3.5$  and  $\leq 3.5\%$  provided significant survival separation also in atrial fibrillation patients. In a multivariable analysis, QRS- $\mu f$  was the by far strongest mortality predictor in atrial fibrillation patients (see *Supplementary material online, Table S7*). Similarly, when using Cox regression analysis of dichotomized risk values, QRS- $\mu f > 3.5\%$  was the only statistically significant risk predictor surviving the multivariable analysis in the atrial fibrillation subgroup (with a HR of 1.972, 95% CI of 1.101–3.534,  $P = 0.022$ ).

## Comparison of macro- and micro-fragmentation

The left panels of *Figure 4* show, for the separate investigated populations, the distribution of cases of positive QRS- $\mu f$  and QRS- $Mf$  (when the positive QRS- $\mu f$  was defined  $> 3.5\%$ ). The scaled Venn diagrams show that positive QRS- $\mu f$  and QRS- $Mf$  overlapped but were far from identical. The right panels of *Figure 4* show the distributions of QRS- $\mu f$  values among subjects with and without observed QRS- $Mf$ . In all three populations, the QRS- $\mu f$  values were significantly larger in subjects with QRS- $Mf$ . The left panels of *Figure 5* show the comparisons of mortality between patients with and without observed QRS- $Mf$ . In all three populations, the differences were statistically significant albeit

somewhat less strong compared with the survival differences stratified by QRS- $\mu f$  as shown in *Figure 2*. The right panels of *Figure 5* show that when subjects with observed QRS- $Mf$  are excluded, QRS- $\mu f$  dichotomized at 3.5% still significantly separated high- and low-risk subjects in all three populations.

*Supplementary material online, Figure S9* shows that when only subjects with QRS- $\mu f \leq 3.5\%$  were considered, the presence or absence of QRS- $Mf$  did not lead to statistically significant survival differences in EU-CERT-ICD or in VA Washington data. It did lead to a significant survival difference in the Whitehall II data albeit less strongly significant compared with the opposite combination of QRS- $Mf$  and QRS- $\mu f$ .

## Discussion

The study shows convincingly that the newly described ECG analysis that quantifies QRS- $\mu f$  provides a powerful mortality predictor independent of other established risk factors. We observed this in populations with different clinical characteristics and different risk profiles. Equally importantly, we observed this also in clinically well-defined sub-populations. In the EU-CERT-ICD data, this included sub-populations of patients with ischaemic and non-ischaemic heart disease as well as atrial fibrillation patients (*Structured Graphical Abstract* and *Supplementary material online,*

**Table 3 Association between mortality<sup>a</sup> and dichotomized risk factors**

	Prevalence (%)	Univariable analysis			Multivariable analysis <sup>b</sup>		
		Wald	P-value	HR (95% CI)	Wald	P-value	HR (95% CI)
<b>EU-CERT-ICD</b>							
Age > 65 years	49.6	43.1	<0.001	2.269 (1.777–2.897)	34.1	<0.001	2.097 (1.635–2.688)
Female sex	19.6	0.51	0.476	0.891 (0.648–1.224)			
Heart rate > 75 b.p.m.	35.3	19.7	<0.001	1.685 (1.338–2.121)	20.6	<0.001	1.713 (1.358–2.161)
LVEF < 25%	37.5	14.5	<0.001	1.563 (1.241–1.967)	9.68	0.002	1.444 (1.146–1.821)
QRS duration > 120 ms	62.3	24.9	<0.001	2.010 (1.528–2.643)			
QRS macro-fragmentation	32.3	9.59	0.002	1.443 (1.144–1.820)			
QTc > 450 ms	42.3	8.05	0.005	1.393 (1.108–1.752)			
TCRT > 110°	41.3	14.2	<0.001	1.554 (1.235–1.954)			
QRS micro-fragmentation >3.5%	45.7	41.8	<0.001	2.208 (1.737–2.808)	30.1	<0.001	1.987 (1.555–2.540)
<b>VA Washington</b>							
Age > 65 years	36.7	8.27	0.004	1.573 (1.156–2.142)	6.32	0.012	1.542 (1.100–2.163)
Heart rate > 75 b.p.m.	45.2	14.7	<0.001	1.846 (1.350–2.526)	8.03	0.005	1.645 (1.166–2.322)
QRS duration > 120 ms	24.1	8.81	0.003	1.644 (1.184–2.283)			
QRS macro-fragmentation	15.2	9.48	0.002	1.779 (1.233–2.568)			
QTc > 450 ms	13.8	11.7	0.001	2.011 (1.347–3.002)	6.49	0.011	1.711 (1.132–2.586)
TCRT > 110°	54.1	5.31	0.021	1.455 (1.058–2.002)	3.93	0.048	1.432 (1.004–2.044)
QRS micro-fragmentation >3.5%	23.3	12.2	<0.001	1.789 (1.290–2.480)	5.86	0.015	1.578 (1.091–2.283)
<b>Whitehall II</b>							
Age > 65 years	47.5	6.86	0.009	2.230 (1.224–4.065)	5.06	0.025	1.997 (1.093–3.647)
Female sex	27.0	2.54	0.111	0.540 (0.253–1.153)			
Heart rate > 75 b.p.m.	22.8	7.46	0.006	2.239 (1.255–3.993)	7.26	0.007	2.214 (1.241–3.949)
QRS duration > 120 ms	6.4	7.96	0.005	2.983 (1.396–6.373)			
QRS macro-fragmentation	6.4	7.83	0.005	2.955 (1.383–6.312)			
QTc > 450 ms	8.0	1.33	0.249	1.654 (0.703–3.891)			
TCRT > 110°	14.6	18.0	<0.001	3.548 (1.978–6.365)	13.8	<0.001	3.073 (1.698–5.564)
QRS micro-fragmentation >3.5%	10.8	9.23	0.002	2.753 (1.432–5.290)	5.51	0.019	2.214 (1.140–4.300)

CI, confidence interval; HR, hazard ratio; LVEF, left ventricular ejection fraction; TCRT, total cosine R to T.

<sup>a</sup>The outcome is all-cause mortality for the EU-CERT-ICD and VA Washington studies and cardiovascular mortality for the Whitehall II study.

<sup>b</sup>Multivariable analysis used backwards stepwise elimination. In addition to hazard ratios, Wald statistics are shown. Note that the VA Washington population included only males.

Figure S7 and Table S7). This is of additional importance since a number of previously proposed ECG-based risk stratifiers<sup>21,22</sup> are not applicable to atrial fibrillation recordings.

This strong risk predictor is based on a standard 10-s 12-lead ECG, i.e. on a clinical test that is routinely and repeatedly performed in the vast majority of healthcare settings. It thus might be widely applied.

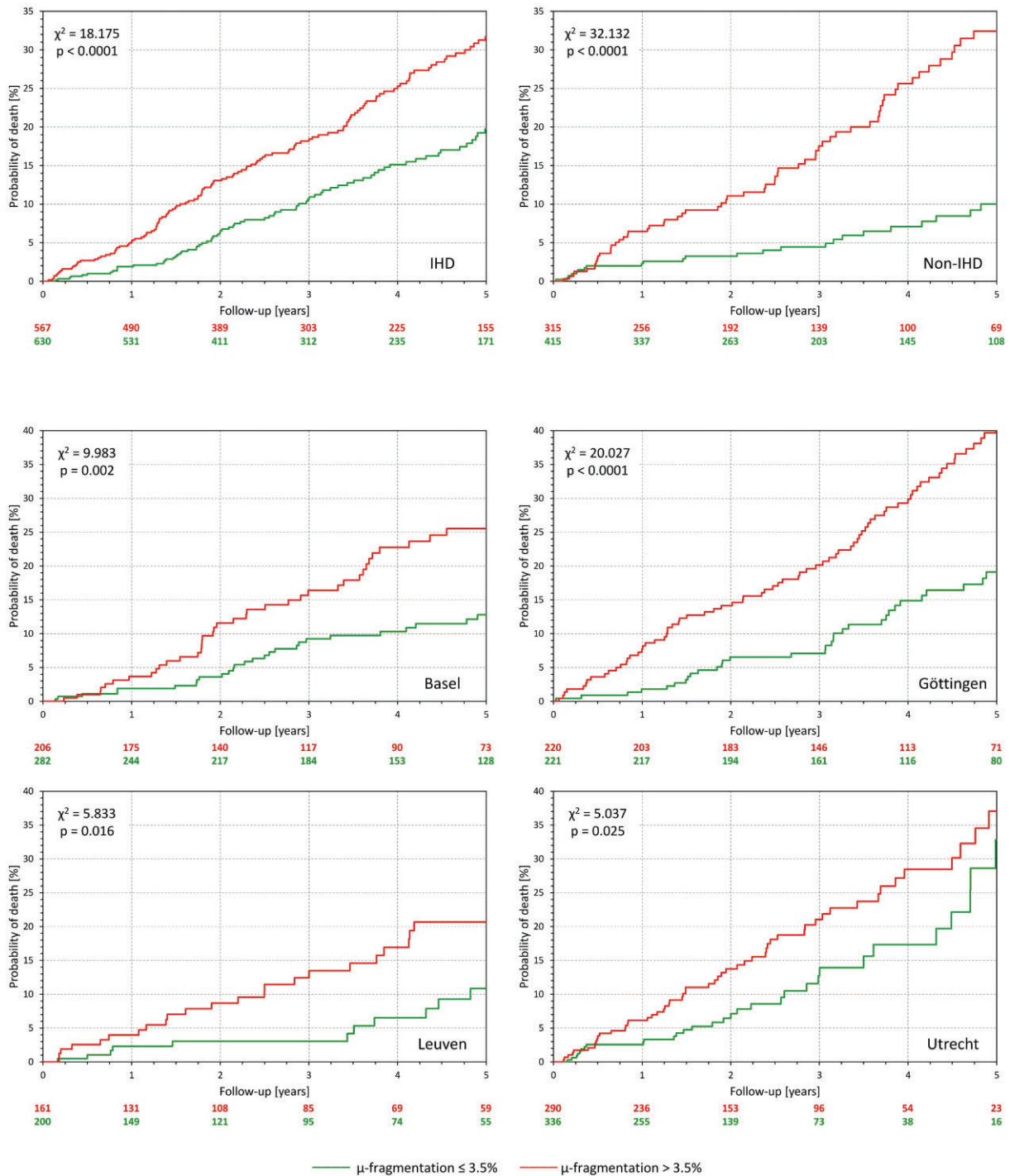
## Outcome prediction

We show the association of QRS- $\mu f$  with mortality risk compellingly. Because of the data character, QRS- $\mu f$  relates to cardiovascular mortality. In the EU-CERT-ICD and VA Washington populations of severe cardiac patients, all-cause deaths were reasonable approximations of cardiovascular mortality. Contrary to cardiovascular mortality, non-cardiovascular mortality was not significantly predicted in the Whitehall II data (details not shown).

Since the very strong distinction between low- and high-risk strata was observed among the EU-CERT-ICD patients who were all ICD protected, it seems more likely that increased QRS- $\mu f$  signifies

tendency to heart failure rather than propensity to arrhythmic complications. This also appears to agree with previous observations that linked QRS- $\mu f$  to myocardial scarring, interstitial fibrosis, and subclinical myocardial damage.<sup>23,24</sup> We hypothesize that increased QRS- $\mu f$  reflects similar abnormalities. This is further supported by our observation (details not shown) that when QRS- $\mu f$  was used to predict first appropriate ICD shock rather than death in the EU-CERT-ICD data, the univariable prediction was only borderline significant ( $P=0.044$ ,  $\log_2$ QRS- $\mu f$  HR of 1.216 with 95% CI of 1.005–1.472). Although we do not have data on anti-tachycardia pacing therapy (and might have thus missed some sustained tachycardia episodes that the ICDs terminated without using a shock), we believe that the prediction of ICD shocks would have been stronger if increased QRS- $\mu f$  were not predominantly linked to non-arrhythmic complications. Indeed, in agreement with our observation of strong QRS- $\mu f$ -based risk prediction among non-ischaeemic ICD patients, abnormalities within signal-averaged QRS complex were previously observed among hypertrophic cardiomyopathy patients who died non-suddenly (but not in those who died suddenly).<sup>25</sup>

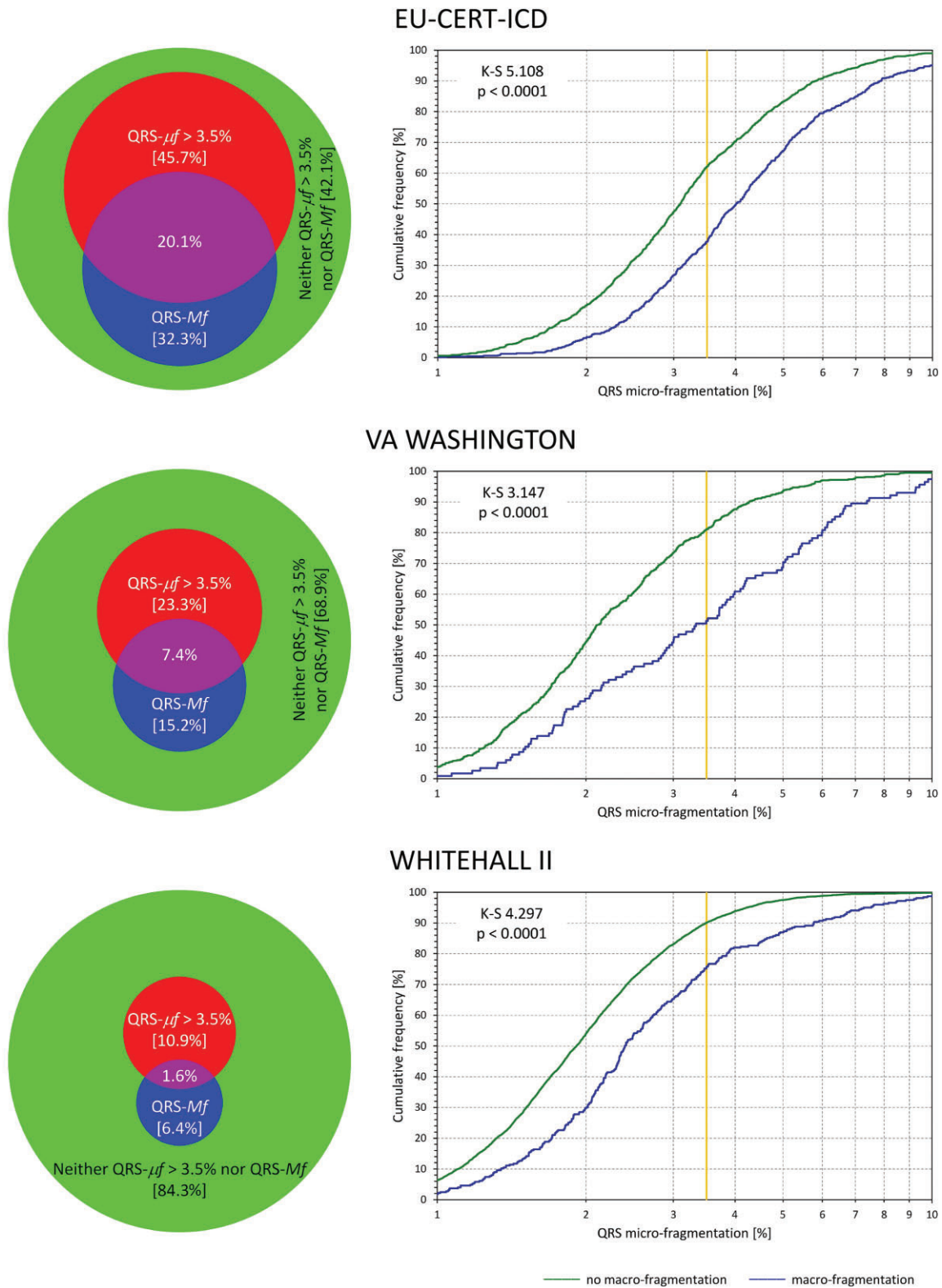
EU-CERT-ICD



**Figure 3** All panels show Kaplan–Meier probabilities of death in different subgroups of the EU-CERT-ICD population. Green and red lines correspond to patients with QRS micro-fragmentation  $\leq 3.5\%$  and  $> 3.5\%$ , respectively. The top two panels show sub-populations with ischaemic heart disease and non-ischaemic heart disease. The bottom four panels correspond to the sub-populations of four different centres that contributed more than 100 patients. Numbers of patients at risk are shown below each panel in corresponding colours. The non-survival probabilities were compared by log-rank test.

The differences between the EU-CERT-ICD and Washington VA populations deserve a more detailed explanation. While the 5-year mortality was greater in the Washington VA population

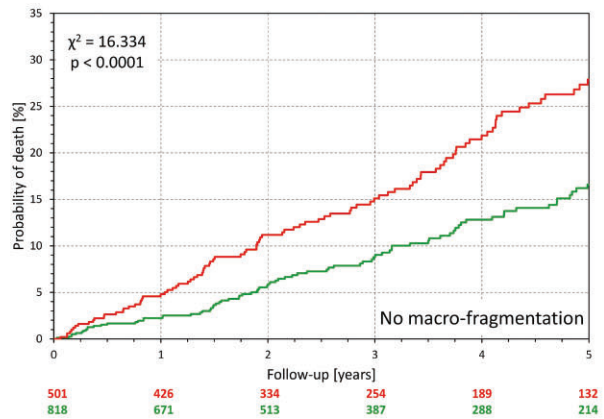
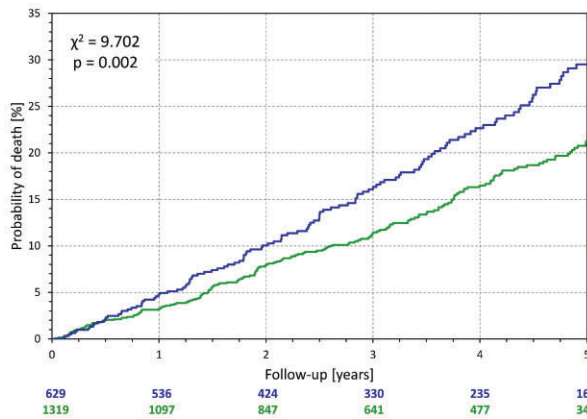
(21.3%) than in the EU-CERT-ICD population (15.1%), the QRS- $\mu f$  measurements led to larger values in the EU-CERT-ICD recordings (Table 1). This suggests that lower mortality rates in



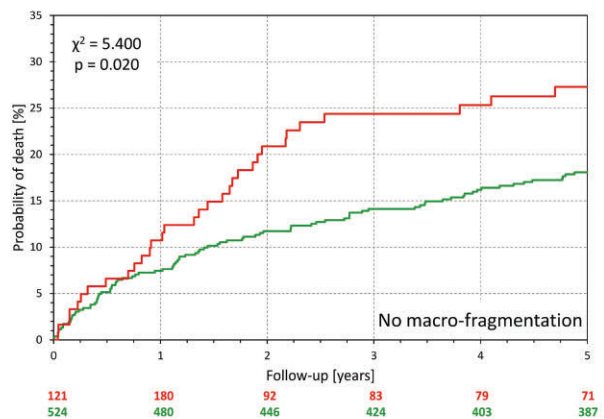
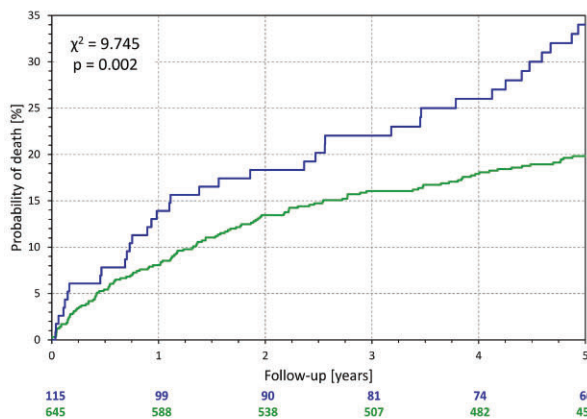
**Figure 4** For each of the investigated populations, the scaled Venn diagram on the left shows the proportions of subjects observed. Red circle: QRS micro-fragmentation  $> 3.5\%$  (QRS- $\mu f > 3.5\%$ ). Blue circle: QRS macro-fragmentation (QRS- $Mf$ ). Violet overlap between the red and blue circle: Both QRS macro-fragmentation and QRS micro-fragmentation  $> 3.5\%$ . Green reminder of the background circle: No QRS macro-fragmentation and QRS micro-fragmentation  $\leq 3.5\%$ . The sizes of the red and blue circles are in proportion of the background circle corresponding to the total population. The percentages of the categories are shown. The panels on the right show the comparisons between distributions of QRS micro-fragmentation values in subjects with (blue line) and without observed QRS macro-fragmentation (green line). The distributions were compared by Kolmogorov–Smirnov test (K–S statistics values shown). The yellow vertical lines mark the 3.5% dichotomy.



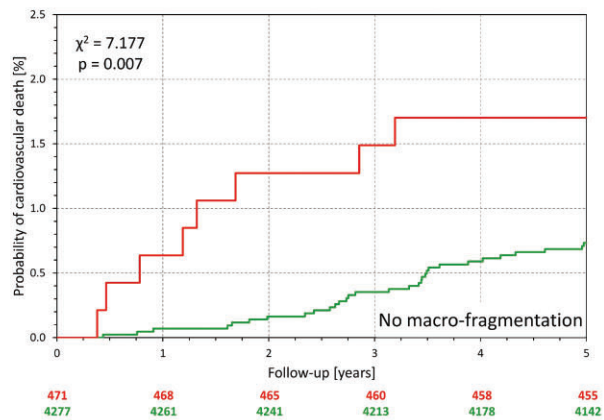
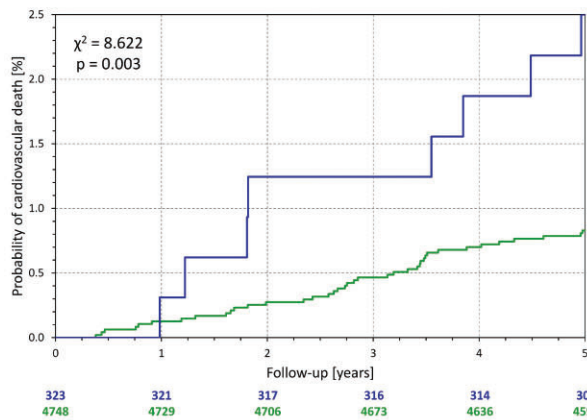
### EU-CERT-ICD



### VA WASHINGTON



### WHITEHALL II



— no macro-fragmentation — macro-fragmentation

—  $\mu$ -fragmentation  $\leq 3.5\%$  —  $\mu$ -fragmentation  $> 3.5\%$

**Figure 5** For each of the investigated populations, the panel on the left shows Kaplan–Meier probabilities of non-survival for subjects with (blue line) and without observed QRS macro-fragmentation (green line). The panels on the right show Kaplan–Meier probabilities of non-survival in subjects without QRS macro-fragmentation stratified by QRS micro-fragmentation above (red line) and below (green line) of the 3.5% dichotomy. Numbers of patients at risk are shown below each panel in corresponding colours. The non-survival probabilities were compared by log-rank test.

EU-CERT-ICD existed despite the observation of more pronounced ECG depolarization heterogeneity. This is explained not only by the defibrillator protection of the EU-CERT-ICD patients but also by the time span of some two decades between these two data collections. More recent advances of clinical care thus necessarily reduced the EU-CERT-ICD mortality.

## Micro- and macro-fragmentation

As previously explained, QRS- $\mu f$  computation considers all eight independent ECG leads together and extracts as much as possible of the multi-lead signal that could be attributed to the movement of a depolarization dipole in three orthogonal dimensions. The rest of the eight-lead signal is explained by movements in ‘algebraic’ 4th, 5th and so on dimensions always taking as much as possible of the remaining signal into the next dimension. This means that QRS- $\mu f$  (sum of the components in the 4th to 6th dimensions) represents localized heterogeneities and abnormalities of the depolarization wavefront that cannot be explained by simple three-dimensional convolution of the depolarization dipole movement (otherwise, they would fit into the first three reconstructed dimensions) but still have a common expression in more than one or two ECG leads. Only the decomposition in the 7th and 8th dimensions is, based on the previous considerations, attributed to noise and signal imperfection.<sup>12</sup>

This consideration also explains the principal difference between QRS- $Mf$  and QRS- $\mu f$ . As already stated, micro-fractionation is not the refinement of visible macro-fractionation. Abnormal three-dimensional depolarization dipole movements might easily lead to dual R or S waves or other macro-fragmentation patterns while contributing little to the ECG signal beyond the three orthogonal dimensions (see [Supplementary material online, Figure S10](#)). On the contrary, even large values of QRS- $\mu f$  might be associated with QRS complex patterns that are not visibly fragmented. Hence, QRS- $\mu f$  should not be understood as increased precision of QRS- $Mf$ . Both concepts complement but do not refine each other. In other words, QRS- $Mf$  and QRS- $\mu f$  do not need to correlate. Nevertheless, our findings indicate that when QRS- $Mf$  is found without abnormally increase values of QRS- $\mu f$ , the risk prediction is absent or substantially reduced.

In this sense, [Figures 4](#) and [5](#) must not be overinterpreted—although 3.5% dichotomy was prospectively applied, the continuous scale of QRS- $\mu f$  makes the relationship to QRS- $Mf$  more complex. Still, both QRS- $Mf$  and QRS- $\mu f$  depict abnormalities in the depolarization sequence. The Cox regression comparisons ([Table 3](#)) might suggest that the abnormalities that contribute to QRS- $\mu f$  (also present in macro-fragmented QRS complexes) might be the mechanistic link between QRS abnormalities and worsened outcome. Nevertheless, more detailed analyses of other data are needed to elucidate this concept further.

## Covariates

Although the relationship between QRS- $\mu f$  of QRS duration was rather weak (intentionally, we used Kendall’s  $\tau$  to express the similarities of selecting high-risk population subgroups), such a relationship exists and was observed not only in these data but also in the previous analysis of ECGs of healthy subjects.<sup>12</sup> The same considerations of the underlying component might therefore be also made for the risk

prediction by increased QRS duration. Importantly, QRS duration (considered as a continuous variable or dichotomized at 120 ms) and diagnosis of QRS- $Mf$  were both eliminated in the multivariable Cox regression models when QRS- $\mu f$  was included.

Previous analyses aiming at the detection of conduction abnormalities hidden in the QRS complex were based on different analyses of high-fidelity signal-averaged ECG recordings, well beyond the clinical practicality of standard short-term ECGs that we have analysed. Their prediction strength was also modest.<sup>11,26</sup> Analyses of quadrupolar ECG components were mainly applied to body surface maps and little is known on their predictive strength.<sup>27</sup> While we have presently applied this type of SVD decomposition to QRS complex signals, the same analysis might also prove valuable for the T wave analysis (to quantify repolarization abnormalities with possible arrhythmic risk implications) and perhaps also P waves (to assess atrial electrophysiology abnormalities with possible links to atrial fibrillation risk).

## Practical implications

Evaluation of QRS- $\mu f$  does not demand any advanced ECG interpretation. While the visual diagnosis of QRS- $Mf$  might be disputable in borderline cases, QRS- $\mu f$  assessment requires only defining the window between QRS onset and offset. Previous observations in healthy subjects suggest that no particular precision of this analysis window is needed<sup>12</sup> and our preliminary observations in the EU-CERT-ICD data suggest that the same might also apply to clinical recordings in cardiac patients (details not shown) although we cannot comment on recordings in different clinical settings. The algorithms to assess QRS- $\mu f$  are also not computationally demanding and could easily be linked to or implemented within the standard equipment for digital ECG acquisition. Expressing QRS- $\mu f$  on a continuous scale also avoids the problem of categorical yes/no classification needed for QRS- $Mf$  which might potentially be problematic in borderline cases.<sup>28</sup>

To demonstrate the predictive power of QRS- $\mu f$ , the Cox regression models evaluated different risk factors as if in competition for a best predictor position. In practice, however, combinations of different risk indicators need to be considered. This particularly applies to factors that might be derived from a standard 12-lead ECG recording, e.g. the spatial QRS-T angle that we found, in agreement with previous observations,<sup>18,19</sup> to be another independent risk indicator. Importantly, we found QRS- $\mu f$  unrelated to other risk factors suggesting that in future studies, it is suitable to be combined with other ECG-based predictors (elementary example in [Supplementary material online, Figure S11](#)).

## Outlook

The assessment of QRS- $\mu f$  appears ready to be implemented in ECG screening programmes and studies of patients at cardiac risk, especially if QRS- $\mu f$  assessment is used as an initial risk indicator and followed by characteristics derived from biochemistry, long-term and high-fidelity ECGs, blood pressure, stress testing, cardiac imaging, etc. The HRs associated with an increased QRS- $\mu f$  (similar to the Harrell’s C-index values and areas under the ROC curves) might be perceived as only modest although they compare favourably with other risk factors derived from the same short-term ECGs. To further utilize risk assessment based on QRS- $\mu f$ , the value

to predict different mortality modes (e.g. arrhythmic vs. heart failure) needs to be investigated. These distinctions were not available in the data that we analysed. Prospective ICD studies (including the prospective EU-CERT-ICD part<sup>29</sup>) could be helpful in that respect when sufficient follow-up data are available. If confirmed that increased QRS- $\mu f$  implies a risk of ICD-non-preventable cardiac death, applications might include the selection of ICD candidates with low QRS- $\mu f$  values (combined with other indicators<sup>21,22</sup>) to increase the device efficacy. Our observation that QRS- $\mu f$ -based risk prediction was particularly strong in non-ischaemic patients (Figure 3) might importantly help stratifying these ICD candidates in whom the therapy is presently uncertain.<sup>30</sup> Even without mechanistic details, future screening programmes and studies of haemodialysis, hypertensive, and diabetic patients would likely benefit from QRS- $\mu f$  assessment since it might, especially if combined with other ECG-based factors, differentiate between patients who do and do not require enhanced clinical attention. QRS- $\mu f$  might also be valuable in the assessment of cardiac resynchronization therapy since more synchronous myocardial activation should lead to a less convoluted three-dimensional depolarization front. Finally, since QRS- $\mu f$  is designed to quantify any departures from regular myocardial activation wavefront, we also hypothesize that it might be helpful in early diagnosis of interstitial myocardial pathologies ranging from amyloidosis, sarcoidosis, and lipomatosis to cellular transplant rejection.

## Limitations

In the categorical analyses, we have only used the QRS- $\mu f$  dichotomy at 3.5% as previously proposed based on independent data in healthy subjects.<sup>12</sup> It is possible if not likely that this QRS- $\mu f$  cut-off could be further optimized in the analysed populations. We have not attempted such optimizations since the prospective nature of the positive QRS- $\mu f$  distinction would have been lost. Intentionally, we have compared QRS- $\mu f$  mainly to risk factors that can be obtained from standard ECG recordings. In real-life situations, other risk indicators also need to be considered. These were, however, not available for the analysed populations and we thus could not have included other factors in the multivariable analyses. Similarly, future studies are needed to assess QRS- $\mu f$ -based predictions of different mortality modes. We were unable to verify the predictive value in atrial fibrillation patients in the Washington VA and Whitehall II populations since by design of these data collections, only ECG obtained in sinus rhythm were available. Finally, both QRS- $\mu f$  and QRS- $Mf$ , similar to QRS width and QT interval duration, were assessed in representative median beats of filtered ECG signals. Since we used the filtering technique available from many previous ECG studies,<sup>17</sup> optimizing ECG pre-processing and filter setting might further increase the predictive power of QRS- $\mu f$  assessment.

## Conclusion

The presented analyses confirm that QRS- $\mu f$  is a new potent risk indicator available from objective analysis of standard 12-lead ECGs. In three populations of different clinical characteristics and in a number of clinically defined sub-populations, including atrial fibrillation patients, we found this risk factor to be a predictor of

mortality independent of several other previously established risk indices. It seems plausible to speculate that the electrophysiologic abnormalities that contribute to increased QRS- $\mu f$  values are responsible for the predictive power of visible QRS fragmentation and perhaps also contributing to the predictive value of prolonged QRS complex.

## Supplementary material

Supplementary material is available at *European Heart Journal* online.

## Funding

The EU-CERT-ICD study was funded by the European Community's 7th Framework Programme (HEALTH-F2-2009-602299). The ECG analyses were supported in part by British Heart Foundation (NH/16/2/32499).

**Conflict of interest:** Dr Hnatkova reports support from European Community's Seventh Framework Programme, during the study, and from British Heart Foundation, during the study, and personal royalties from St Paul's Cardiac Electrophysiology; Dr Andršová reports personal consulting fees from St Paul's Cardiac Electrophysiology, and personal lecture honoraria from Servier Laboratories; Dr Novotný reports support from European Community's Seventh Framework Programme, during the study, and personal consulting fees from St Paul's Cardiac Electrophysiology; Dr Britton reports no conflict of interest; Dr Shipley reports no conflict of interest; Dr Vandenberg reports fellowship funding from Frans Van de Werf Fund for Clinical Cardiovascular Research; Dr Sprenkeler reports no conflict of interest; Dr Junttila reports no conflict of interest; Dr Reichlin reports institutional consultation fees from Biosense Webster, Boston Scientific, Biotronik, Farapulse, Bayer, BMS-Pfizer, and Medtronic, institutional lecture honoraria from Biosense Webster, Bayer, BMS-Pfizer, and Medtronic, and institutional meeting support from Bayer, BMS-Pfizer, and Biotronik; Dr Schlögl reports from European Community's Seventh Framework Programme, during the study, and private investor income from Johnson and Johnson, and Bayer AG; Dr Vos reports a grant from the Horizon 2020 programme; Dr Friede reports support from European Community's Seventh Framework Programme, during the study, personal consultation fees from Bayer, CSL Behring, Galapagos, Minoryx, Vifor, Novartis, and LivaNova, lecture fees from Fresenius Kabi, and personal fees for Advisory and Data Safety Monitoring boards from Bayer, Biosense Webster, Janssen, Novartis, Roche, and BSM; Dr Bauer reports grant from Medtronic Bakken Research Center, and lecture fees from Medtronic; Dr Huikuri reports no conflict of interest; Dr Willems reports support from European Community's Seventh Framework Programme, during the study, post-doctoral clinical researcher support by the Fund for Scientific Research Flanders, during the study, institutional research grants from Abbott, Biotronik, Boston Scientific, and Medtronic, institutional lecture fees from Abbott, Biotronik, Boston Scientific, Medtronic, Daichi Sankyo, and Boehringer Ingelheim, meeting support from Daichi Sankyo, and unpaid Secretary position at the Belgian Heart Rhythm Society; Dr Schmidt reports his Chair positions of the Association of Medical Ethics Committees in the Federal Republic of Germany; Dr Franz reports no conflict of interest; Dr Sticherling reports support from European Community's Seventh Framework Programme, during the study, consulting fees from Abbott, Biotronik, Boston Scientific, and Medtronic, and lecture honoraria from Abbott, Biotronik, Boston Scientific, and Medtronic; Dr Zabel reports support from European

Community's Seventh Framework Programme, during the study; Dr Malik reports support from European Community's Seventh Framework Programme, during the study, and from British Heart Foundation, during the study, personal royalties from St Paul's Cardiac Electrophysiology, personal royalties from Elsevier Academic Press, and institutional consultation fees from Sosei Heptares, BioCryst Pharmaceuticals, and Helsinn Healthcare.

## Data availability

The data underlying this article will be shared on reasonable request to the corresponding author.

## References

- Peterson PN, Greiner MA, Qualls LG, Al-Khatib SM, Curtis JP, Fonarow GC, et al. QRS duration, bundle-branch block morphology, and outcomes among older patients with heart failure receiving cardiac resynchronization therapy. *JAMA* 2013; **310**:617–626.
- Bauer A, Watanabe MA, Barthel P, Schneider R, Ulm K, Schmidt G. QRS duration and late mortality in unselected post-infarction patients of the revascularization era. *Eur Heart J* 2006; **27**:427–433.
- Das MK, Zipes DP. Fragmented QRS: a predictor of mortality and sudden cardiac death. *Heart Rhythm* 2009; **6**:S8–S14.
- Terho HK, Tikkanen JT, Junttila JM, Anttonen O, Kenttä TV, Aro AL, et al. Prevalence and prognostic significance of fragmented QRS complex in middle-aged subjects with and without clinical or electrocardiographic evidence of cardiac disease. *Am J Cardiol* 2014; **114**:141–147.
- Rosengarten JA, Scott PA, Morgan JM. Fragmented QRS for the prediction of sudden cardiac death: a meta-analysis. *Europace* 2015; **17**:969–977.
- Cetin MS, Ozcan Cetin EH, Canpolat U, Cay S, Topaloglu S, Temizhan A, et al. Usefulness of fragmented QRS complex to predict arrhythmic events and cardiovascular mortality in patients with noncompaction cardiomyopathy. *Am J Cardiol* 2016; **117**:1516–1523.
- Marume K, Noguchi T, Kamakura T, Tateishi E, Morita Y, Miura H, et al. Prognostic impact of multiple fragmented QRS on cardiac events in idiopathic dilated cardiomyopathy. *Europace* 2021; **23**:287–297.
- Bokma JP, Winter MM, Vehmeijer JT, Vliegen HW, van Dijk AP, van Melle JP, et al. QRS fragmentation is superior to QRS duration in predicting mortality in adults with tetralogy of Fallot. *Heart* 2017; **103**:666–671.
- Roudijk RW, Bosman LP, van der Heijden JF, de Bakker JMT, Hauer RNW, van Tintelen JP, et al. Quantitative approach to fragmented QRS in arrhythmogenic cardiomyopathy: from disease towards asymptomatic carriers of pathogenic variants. *J Clin Med* 2020; **9**:545.
- Kelen GJ, Henkin R, Starr AM, Caref EB, Bloomfield D, el-Sherif N. Spectral turbulence analysis of the signal-averaged electrocardiogram and its predictive accuracy for inducible sustained monomorphic ventricular tachycardia. *Am J Cardiol* 1991; **67**:965–975.
- Kulakowski P, Hnatkova K, Bashir Y, Heald SC, Staunton A, Malik M, et al. Influence of the infarct site on the identification of patients with ventricular tachycardia after myocardial infarction based on the time-domain and spectral turbulence analysis of the signal-averaged electrocardiogram. *Clin Cardiol* 1995; **18**:39–44.
- Hnatkova K, Andršová I, Toman O, Smetana P, Huster KM, Šišáková M, et al. Spatial distribution of physiologic 12-lead QRS complex. *Sci Rep* 2021; **11**:4289.
- Sticherling C, Arendacka B, Svendsen JH, Wijers S, Friede T, Stockinger J, et al. Sex differences in outcomes of primary prevention implantable cardioverter-defibrillator therapy: combined registry data from eleven European countries. *Europace* 2018; **20**:963–970.
- Zabel M, Malik M, Hnatkova K, Papademetriou V, Pittaras A, Fletcher RD, et al. Analysis of T-wave morphology from the 12-lead electrocardiogram for prediction of long-term prognosis in male US veterans. *Circulation* 2002; **105**:1066–1070.
- Marmot MG, Smith GD, Stansfeld S, Patel C, North F, Head J, et al. Health inequalities among British civil servants: the Whitehall II study. *Lancet* 1991; **337**:1387–1393.
- Jandackova VK, Britton A, Malik M, Steptoe A. Heart rate variability and depressive symptoms: a cross-lagged analysis over a 10-year period in the Whitehall II study. *Psychol Med* 2016; **46**:2121–2131.
- Malik M, Andreas JO, Hnatkova K, Hoekendorff J, Cawello W, Middle M, et al. Thorough QT/QTc study in patients with advanced Parkinson's disease: cardiac safety of rotigotine. *Clin Pharmacol Therap* 2008; **84**:595–603.
- Zabel M, Acar B, Klingenhoben T, Franz MR, Hohnloser SH, Malik M. Analysis of 12-lead T-wave morphology for risk stratification after myocardial infarction. *Circulation* 2000; **102**:1252–1257.
- Hnatkova K, Seegers J, Barthel P, Novotny T, Smetana P, Zabel M, et al. Clinical value of different QRS-T angle expressions. *Europace* 2018; **20**:1352–1361.
- Jr H F, Califf RM, Pryor DB, Lee KL, Rosati RA. Evaluating the yield of medical tests. *JAMA* 1982; **247**:2543–2546.
- Bauer A, Klemm M, Rizas KD, Hamm W, von Stülpnagel L, Dommasch M, et al. Prediction of mortality benefit based on periodic repolarisation dynamics in patients undergoing prophylactic implantation of a defibrillator: a prospective, controlled, multicentre cohort study. *Lancet* 2019; **394**:1344–1351.
- Dommasch M, Steger A, Barthel P, Huster KM, Müller A, Sinnecker D, et al. Nocturnal respiratory rate predicts ICD benefit: a prospective, controlled, multicentre cohort study. *EClinicalMedicine* 2021; **31**:100695.
- Ferrero P, Piazza I, Grosu A, Brambilla P, Sironi S, Senni M. QRS fragmentation as possible new marker of fibrosis in patients with myocarditis. Preliminary validation with cardiac magnetic resonance. *Eur J Heart Fail* 2019; **21**:1160–1161.
- Bi X, Yang C, Song Y, Yuan J, Cui J, Hu F, et al. Quantitative fragmented QRS has a good diagnostic value on myocardial fibrosis in hypertrophic obstructive cardiomyopathy based on clinical-pathological study. *BMC Cardiovasc Disord* 2020; **20**:298.
- Englund A, Hnatkova K, Kulakowski P, Elliot PM, McKenna WJ, Malik M. Wavelet decomposition analysis of the signal averaged electrocardiogram used for risk stratification of patients with hypertrophic cardiomyopathy. *Eur Heart J* 1998; **19**:1383–1390.
- Odemuyiwa O, Malik M, Poloniecki J, Farrell T, Kulakowski P, Millane T, et al. Frequency versus time domain analysis of signal-averaged electrocardiograms. III. Stratification of postinfarction patients for arrhythmic events. *J Am Coll Cardiol* 1992; **20**:144–150.
- Arthur RM, Geselowitz DB, Briller SA, Trost RF. Quadrupole components of the human surface electrocardiogram. *Am Heart J* 1972; **83**:663–677.
- Malik M. Electrocardiographic smoke signals of fragmented QRS complex. *J Cardiovasc Electrophysiol* 2013; **24**:1267–1270.
- Zabel M, Willems R, Lubinski A, Bauer A, Brugada J, Conen D, et al. Clinical effectiveness of primary prevention implantable cardioverter-defibrillators: results of the EU-CERT-ICD controlled multicentre cohort study. *Eur Heart J* 2020; **41**:3437–3447.
- Køber L, Thune JJ, Nielsen JC, Haarbø J, Videbæk L, Korup E, et al. Defibrillator implantation in patients with nonischemic systolic heart failure. *N Engl J Med* 2016; **375**:1221–1230.

## QRS micro-fragmentation as a mortality predictor

by

Katerina Hnatkova<sup>1</sup>, Irena Andršová<sup>2,3</sup>, Tomáš Novotný<sup>2,3</sup>, Annie Britton<sup>4</sup>, Martin Shipley<sup>4</sup>,  
Bert Vandenberk<sup>5</sup>, David J Sprenkeler<sup>6</sup>, Juhani Junntila<sup>7</sup>, Tobias Reichlin<sup>8</sup>, Simon Schlögl<sup>9,10</sup>,  
Marc A Vos<sup>6</sup>, Tim Friede<sup>11,10</sup>, Axel Bauer<sup>12</sup>, Heikki V Huikuri<sup>7</sup>, Rik Willems<sup>5</sup>, Georg Schmidt<sup>13,14</sup>,  
Michael R Franz<sup>15</sup>, Christian Sticherling<sup>16</sup>, Markus Zabel<sup>9,10</sup>, Marek Malik<sup>1,3</sup>

<sup>1</sup> National Heart and Lung Institute, Imperial College, London, England,

<sup>2</sup> Department of Internal Medicine and Cardiology, University Hospital Brno, Brno, Czech Republic,

<sup>3</sup> Department of Internal Medicine and Cardiology, Masaryk University, Brno, Czech Republic,

<sup>4</sup> Research Department of Epidemiology and Public Health, University College London, England,

<sup>5</sup> Department of Cardiovascular Sciences, University of Leuven, Leuven, Belgium,

<sup>6</sup> Department of Medical Physiology, University Medical Center Utrecht, Utrecht, The Netherlands,

<sup>7</sup> University Central Hospital of Oulu and University of Oulu, Finland,

<sup>8</sup> Department of Cardiology, Inselspital, Bern University Hospital, Bern, Switzerland

<sup>9</sup> Department of Cardiology and Pneumology, University Medical Center, Göttingen, Germany,

<sup>10</sup> German Center for Cardiovascular Research (DZHK), partner site Göttingen, Göttingen, Germany

<sup>11</sup> Department of Medical Statistics, University Medical Center Göttingen, Göttingen, Germany

<sup>12</sup> University Hospital for Internal Medicine III, Medical University Innsbruck, Innsbruck, Austria,

<sup>13</sup> Klinikum rechts der Isar, Technical University of Munich, Munich, Germany,

<sup>14</sup> German Center for Cardiovascular Research partner site Munich Heart Alliance, Munich, Germany,

<sup>15</sup> Veteran Affairs and Georgetown University Medical Centers, Washington, DC, USA,

<sup>16</sup> Department of Cardiology, University Hospital of Basel, Basel, Switzerland.

## Supplementary Tables and Figures

Supplementary Tables and Figures are presented in the order  
as they are referred to in the text of the article.

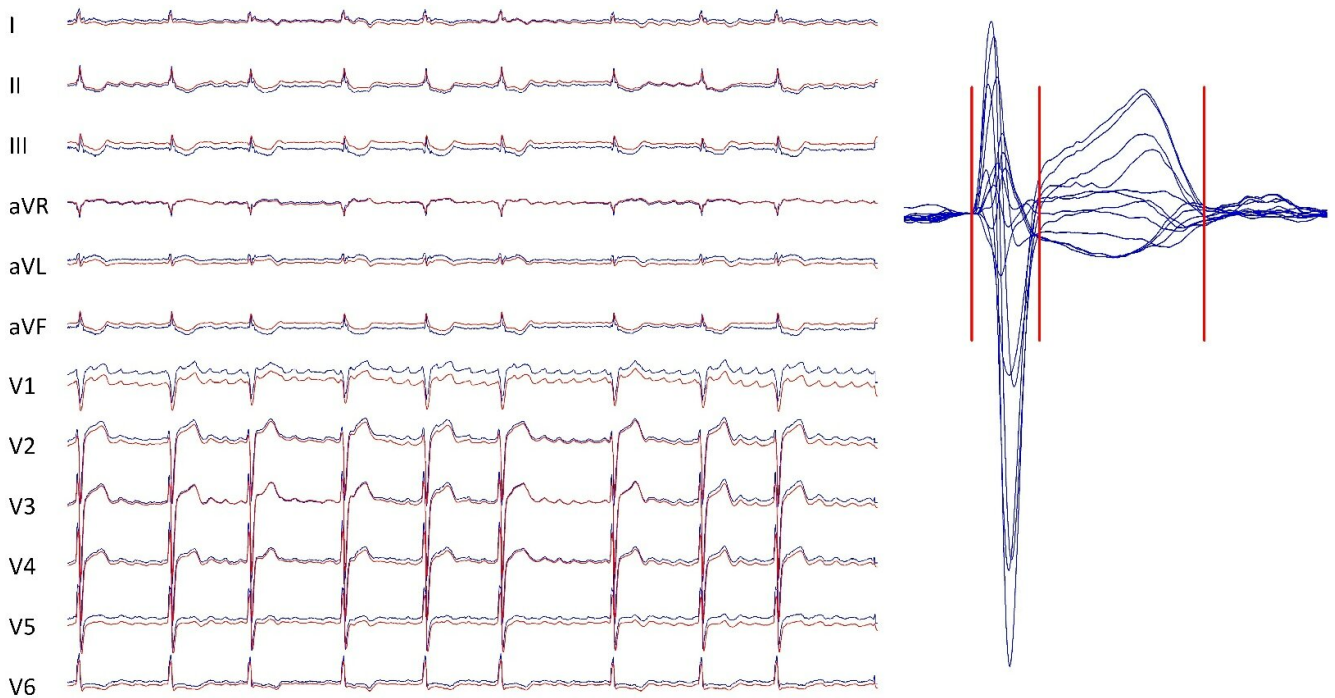
## Supplementary Table 1

### Recording characteristics of analysed short-term ECGs

Data source	Equipment model	Exported sampling frequency	Exported LSB resolution	Analysed ECG Duration
<b>EU-CERT-ICD</b>				
Basel	Schiller CS-200	500 Hz	4.0 $\mu$ V	10 s
Göttingen	Schiller CS-200	500 Hz	4.0 $\mu$ V	10 s
Leuven	GE MAC 5500	250 Hz	4.88 $\mu$ V	10 s
Oulu	Mortara ELI 380	1000 Hz	2.5 $\mu$ V	8 s
Utrecht	GE MAC 5500	500 Hz	4.88 $\mu$ V	10 s
<b>VA Washington</b>				
VA Washington	Marquette MAC/MUSE	250 Hz	4.88 $\mu$ V	10 s
<b>Whitehall II</b>				
Whitehall II	Getemed CM 3000-12 BT	1024 Hz	2.93 $\mu$ V	10 s

Standard settings of the equipment were used with removal of alternating current frequencies. Where the exported sampling frequency differed from 1000 Hz, cubic spline re-sampling to this frequency was used. Although low-pass filtering with 100 Hz cut-off was applied (see subsequent Supplementary Figure 1), the 1000 Hz frequency was used for the purposes of obtaining interval measurements (in representative beats) with 1 millisecond precision. LSB – least significant bit, s -seconds.

## Supplementary Figure 1



Example of ECG pre-processing shown in a case of an atrial fibrillation patient. The left panel shows the original ECG signal in blue superimposed by filtered signals in red. The filtering was performed in two steps: (a) A low pass infinite-impulse-response Butterworth filter with 100 Hz cut-off frequency was used to eliminate high-frequency noise (it also harmonised the frequency contents of all the study ECGs). (b) Subsequently, for each detected QRS complex (combination of maximum absolute amplitudes in the native signal and its derivative) a window of preceding 100 ms was used to identify the point with minimum standard deviation across all leads. These points identified baseline wander nodes and a cubic spline interpolation across these nodes was subtracted from the filtered signal to remove baseline wander.

The right panel shows representative beatforms derived, for each ECG lead, by obtaining sample by sample medians across all superimposed QRS complexes. These representative beatforms of all 12 leads were superimposed on the same isoelectric axis and the resulting image was used to detect the global QRS onset and offset as well as the T wave offset (red vertical lines).

## Supplementary Table 2

Kendall's  $\tau$  coefficients  
between QRS micro-fragmentation and other risk factors

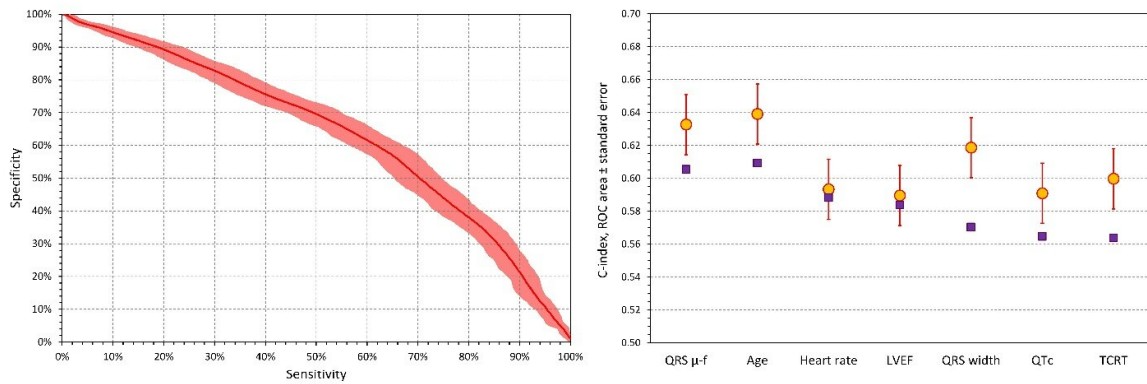
	EU-CERT-ICD		VA Washington		Whitehall	
	$\tau$	p-value	$\tau$	p-value	$\tau$	p-value
Age [years]	0.098	<0.001	0.049	0.046	0.042	<0.001
Heart rate [bpm]	-0.024	0.107	-0.011	0.658	-0.058	<0.001
LVEF [%]	-0.104	<0.001				
QRS duration [ms]	0.358	<0.001	0.338	<0.001	0.304	<0.001
QTc [ms]	0.240	<0.001	0.156	<0.001	0.071	<0.001
TCRT [deg]	0.087	<0.001	0.141	<0.001	0.060	<0.001

Bpm – beats per minute, deg – degrees, LVEF – left ventricular ejection fraction, ms – milliseconds, TCRT – total cosine R to T

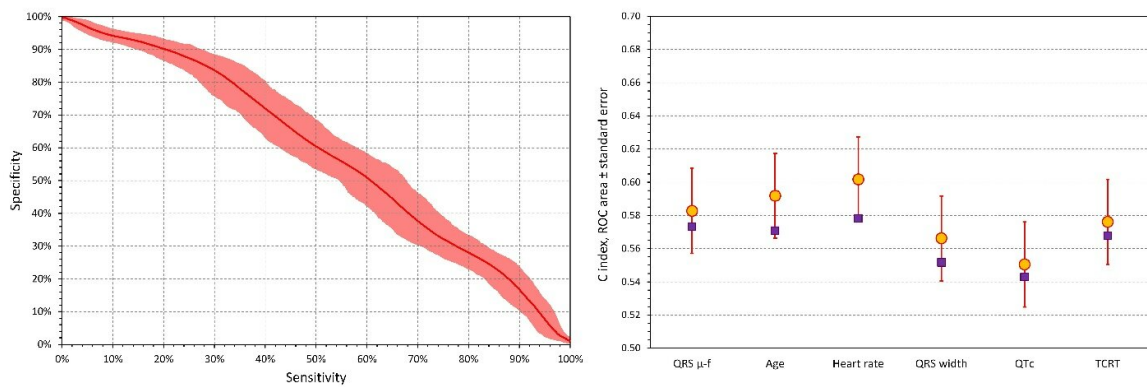


## Supplementary Figure 2

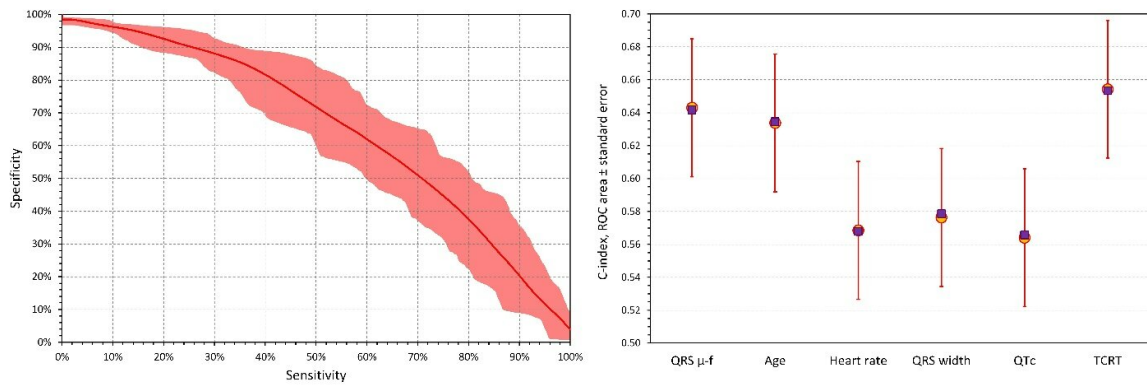
### EU-CERT-ICD



### VA WASHINGTON



### WHITEHALL II



For each of the investigated populations, the left panels show QRS micro-fragmentation receiver operator characteristic (ROC) for events during the complete follow-up, together with its 90% confidence band obtained by bootstrap with 1000 repetitions. The right panels show the areas under the ROC curve for different continuous risk predictor together with their standard errors (red marks) and the Harrell's C-index values (dark violet marks). Note the differences between the ROC areas and the C-index values due to follow-up influence.

LVEF – left ventricular ejection fraction, TCRT – total cosine R to T,  $\mu$ -f – QRS micro-fragmentation.

### Supplementary Table 3

#### Multivariable Harrell's C-index statistics

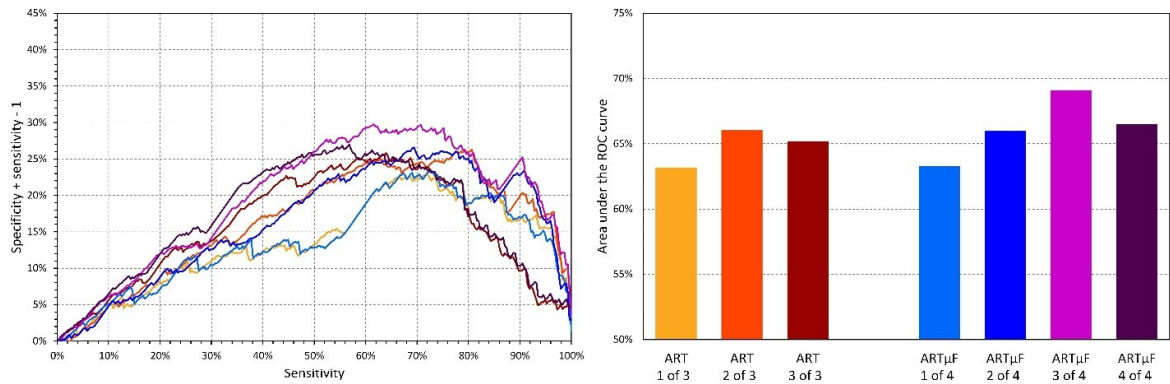
	Model of Score 1	Model of Score 2
<b>EU-CERT-ICD</b>		
Age [years]	0.036618	0.033671
Heart rate [bpm]	0.016280	0.017610
LVEF [%]	-0.028609	-0.025182
QTc [ms]	0.003667	0.001400
TCRT [deg]	0.005332	0.005427
log <sub>2</sub> (QRS μ-fragmentation)		0.407542
Cox regression $\chi^2$	104.2	138.7
Area under the ROC curve	0.698	0.715
Harrell's C-index	0.652	0.667
<b>VA Washington</b>		
Age [years]	0.031944	0.032516
Heart rate [bpm]	0.010328	0.011130
QTc [ms]	0.005928	0.004068
TCRT [deg]	0.006194	0.005320
log <sub>2</sub> (QRS μ-fragmentation)		0.260371
Cox regression $\chi^2$	35.0	41.2
Area under the ROC curve	0.648	0.657
Harrell's C-index	0.615	0.627
<b>Whitehall II</b>		
Age [years]	0.072306	0.067307
TCRT [deg]	0.013992	0.012176
log <sub>2</sub> (QRS μ-fragmentation)		0.448389
Cox regression $\chi^2$	40.4	47.5
Area under the ROC curve	0.714	0.739
Harrell's C-index	0.702	0.728

For each of the investigated population, multivariable Cox regression model involving the continuous variables as shown in Table 2 of the article was computed without (Model of Score 1) and with (Model of Score 2) QRS micro-fragmentation. The table shows the resulting beta coefficients (log hazard ratios) assigned to each of the variables that were retained during the backwards stepwise elimination for Model Score 1. The Model score 2 shows the Cox regression beta coefficients after QRS micro-fragmentation was added to the variables of Model Score 1. The beta coefficients were used as weights of the variables to obtain weighted average risk scores. The blue lines of the table show the overall  $\chi^2$  statistics of the Cox regression models that provided the beta coefficients, areas under the receiver operator characteristic of the derived risk scores (for events across the complete follow-up), and the Harrell's C-index values of the derived risk scores. Note that in all three populations, the inclusion of QRS micro-fragmentation increased the  $\chi^2$  statistics, the area under the receiver operator characteristic, and the C-index statistics.

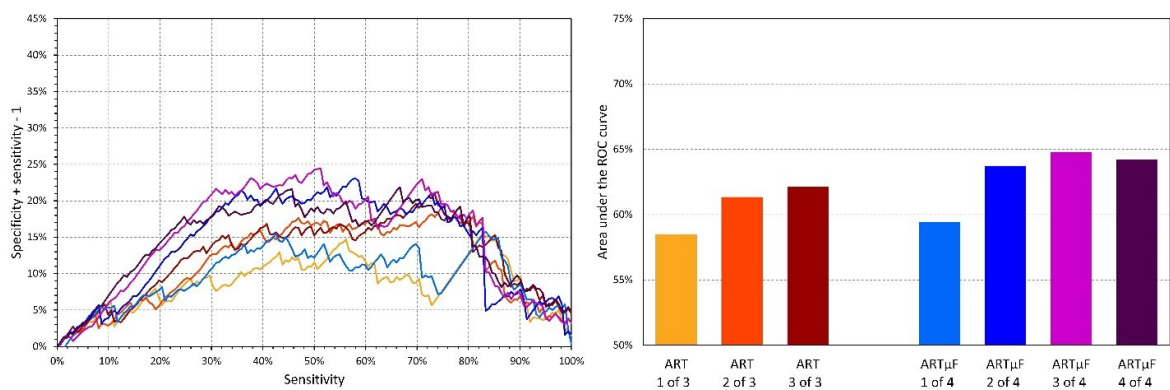
bpm – beats per minute, deg – degrees, ms – milliseconds, ROC – receiver operator characteristic, TCRT – total cosine R to T, μ-fragmentation – micro-fragmentation.

## Supplementary Figure 3

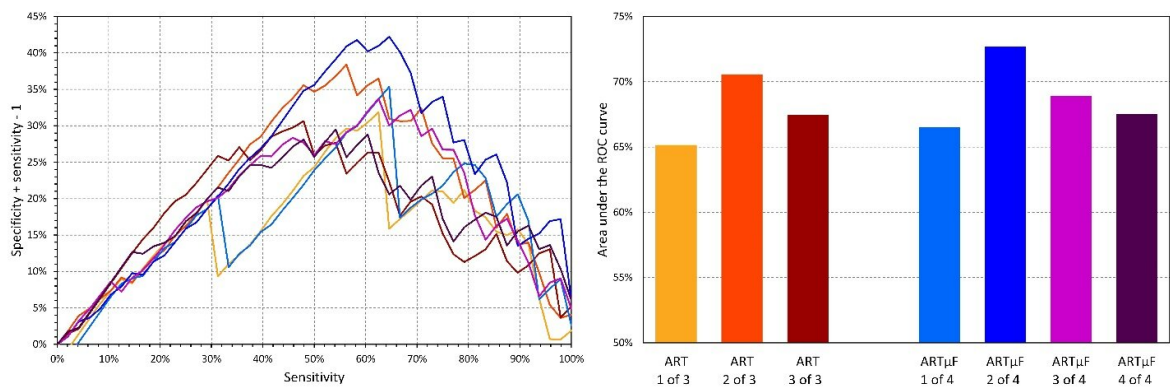
### EU-CERT-ICD



### VA WASHINGTON



### WHITEHALL II



For each of the investigated populations, the left panels show multifactorial receiver operator characteristic (ROC) for events during the complete follow-up. The right panels show the areas under these ROC curves. Two groups of ROC curves are shown: Those labelled ART combined age, heart rate, and total cosine R to T; those labelled ART $\mu$ F included also QRS micro-fragmentation. Within each group, the ROC curves differed by the definition of true/false positive/negative: as the dichotomies of the risk factors involved were varied, for each of their combinations, positive cases were defined as those subjects for whom the values of 1, 2, 3, or 4 risk factors were above the given dichotomy. To ease the comparison of the ROC curves, their values are shown above the 50% identity line, i.e., the panels on the left show the dependency of (specificity+sensitivity-1) on sensitivity. The colours of these curves correspond to the bar graphs.

### Supplementary Table 4

#### Association between mortality and continuous values of risk factors in aetiology sub-groups of EU-CERT-ICD

	Univariable analysis			Multivariable analysis		
	Wald	p-value	HR (95% CI)	Wald	p-value	HR (95% CI)
<b>Ischaemic heart disease</b>						
Age	42.3	<0.001	1.056 (1.038 - 1.073)	30.1	<0.001	1.048 (1.031 - 1.066)
Heart rate [bpm]	16.1	<0.001	1.017 (1.009 - 1.026)	11.0	0.001	1.015 (1.006 - 1.023)
LVEF [%]	18.0	<0.001	0.958 (0.940 - 0.977)	6.83	0.009	0.972 (0.952 - 0.993)
QRS duration [ms]	18.6	<0.001	1.010 (1.005 - 1.014)	5.55	0.018	0.992 (0.985 - 0.999)
QTc [ms]	16.9	<0.001	1.007 (1.004 - 1.011)	4.11	0.043	1.005 (1.000 - 1.009)
TCRT [deg]	25.2	<0.001	1.012 (1.007 - 1.017)	12.8	<0.001	1.010 (1.004 - 1.015)
log <sub>2</sub> (QRS $\mu$ -fragmentation)	21.5	<0.001	1.568 (1.297 - 1.897)	13.5	<0.001	1.533 (1.220 - 1.926)
<b>Non-ischaemic heart disease</b>						
Age	6.58	0.01	1.023 (1.005 - 1.042)	13.4	<0.001	1.025 (1.012 - 1.039)
Heart rate [bpm]	18.0	<0.001	1.027 (1.014 - 1.039)			
LVEF [%]	13.8	<0.001	0.951 (0.926 - 0.976)	6.27	0.012	0.965 (0.938 - 0.992)
QRS duration [ms]	13.2	<0.001	1.012 (1.006 - 1.019)			
QTc [ms]	8.23	0.004	1.007 (1.002 - 1.013)			
TCRT [deg]	5.90	0.015	1.010 (1.002 - 1.018)			
log <sub>2</sub> (QRS $\mu$ -fragmentation)	24.6	<0.001	2.077 (1.556 - 2.772)	21.1	<0.001	1.986 (1.482 - 2.662)

Multivariable analysis used backwards stepwise elimination. In addition to hazard ratios, Wald statistics are shown. QRS micro-fragmentation was used after logarithmic transformation with base 2 – hazard ratios correspond to value increases by a factor of 2.

CI – confidence interval, bpm- beats per minute, deg – degrees, HR – hazard ratio, LVEF – left ventricular ejection fraction, ms – milliseconds, TCRT – total cosine R to T,  $\mu$ -fragmentation – micro-fragmentation.

## Supplementary Table 5

### Characteristics of EU-CERT-ICD population per contributing centre

	Survivors	Non-survivors	p-value
<b>BASEL</b>			
N	423	65	
Age [years]	64 (54 - 70)	69 (62 - 74)	0.0001
Heart rate [bpm]	66 (58.9 - 77.4)	75 (65.1 - 83.2)	0.0050
LVEF [%]	27 (24 - 33)	25 (22 - 30)	0.0012
QRS duration [ms]	124 (109 - 156)	152 (120 - 174)	<0.0001
QTc [ms]	447 (424 - 472)	458 (432 - 494)	0.0140
TCRT [deg]	149 (102 - 165)	160 (136 - 165)	0.0278
QRS $\mu$ -fragmentation [%]	3.133 (2.289 - 4.37)	4.070 (2.748 - 6.747)	<0.0001
<b>GÖTTINGEN</b>			
N	334	107	
Age [years]	67 (57 - 74)	71 (67 - 77)	<0.0001
Heart rate [bpm]	70.7 (62.8 - 80.6)	73.5 (66.3 - 84.8)	0.0268
LVEF [%]	25 (20 - 30)	25 (20 - 30)	0.1850
QRS duration [ms]	134 (115 - 163)	147 (120 - 169)	0.0322
QTc [ms]	435 (413 - 459)	444 (421 - 471)	0.0390
TCRT [deg]	153 (118 - 166)	158 (145 - 168)	0.0029
QRS $\mu$ -fragmentation [%]	3.211 (2.451 - 4.543)	4.186 (3.186 - 5.203)	<0.0001
<b>LEUVEN</b>			
N	327	34	
Age [years]	61 (53 - 69)	65 (56 - 70)	0.1538
Heart rate [bpm]	65.6 (57.1 - 75.2)	64.3 (59.1 - 77.3)	0.5496
LVEF [%]	27 (20 - 33)	25 (20 - 30)	0.1687
QRS duration [ms]	137 (116 - 165)	146 (127 - 174)	0.1730
QTc [ms]	449 (425 - 478)	466 (425 - 495)	0.1764
TCRT [deg]	151 (120 - 165)	164 (145 - 169)	0.0050
QRS $\mu$ -fragmentation [%]	3.242 (2.467 - 4.812)	4.246 (3.015 - 5.235)	0.0717
<b>OULU</b>			
N	30	2	
Age [years]	59 (51 - 65)	69 , 71	
Heart rate [bpm]	71.7 (59.1 - 82.2)	70.6 , 74.4	
LVEF [%]	30 (26 - 35)	21 , 26	
QRS duration [ms]	142 (112 - 155)	128 , 168	
QTc [ms]	453 (428 - 471)	414 , 469	
TCRT [deg]	165 (152 - 170)	169 , 171	
QRS $\mu$ -fragmentation [%]	3.375 (2.55 - 4.932)	3.460 , 6.036	

	Survivors	Non-survivors	p-value
<b>UTRECHT</b>			
N	540	86	
Age [years]	64 (57 - 72)	68 (60 - 74)	0.0313
Heart rate [bpm]	70.5 (61.4 - 81.6)	73.5 (66.4 - 87.0)	0.0204
LVEF [%]	25 (20 - 29)	20 (18 - 26)	0.0001
QRS duration [ms]	125 (112 - 154)	144 (123 - 170)	<0.0001
QTc [ms]	437 (416 - 462)	456 (437 - 489)	<0.0001
TCRT [deg]	150 (119 - 164)	159 (139 - 167)	0.0056
QRS $\mu$ -fragmentation [%]	3.224 (2.367 - 4.49)	4.271 (2.845 - 5.708)	0.0001

For individual centres of EU-CERT-ICD population, the table shows medians and inter-quartile ranges and their comparison between 5-year survivors and non-survivors. Non-parametric Mann-Whitney p-values are shown. The comparisons were omitted for the Oulu centre since only 2 non-survivors were contributed by the centre (instead of median and inter-quartile ranges, both values are shown for Oulu centre non-survivors).

Interestingly, when non-parametric Kruskal-Wallis one-way analysis of variance was used to test that the distribution of the risk factors shown is the same across centres, the distributions of all variables with the exception of QRS micro-fragmentation were found highly significantly different between centres ( $p < 0.0001$  for age, heart rate, LVEF, QRS duration, and QTc interval;  $p = 0.0007$  for TCRT). However, no differences were found between the distributions of QRS micro-fragmentation ( $p = 0.4173$ ).

bpm – beats per minute, deg – degrees, ms – milliseconds, TCRT – total cosine R to T,  $\mu$ -fragmentation – micro-fragmentation.

## Supplementary Table 6

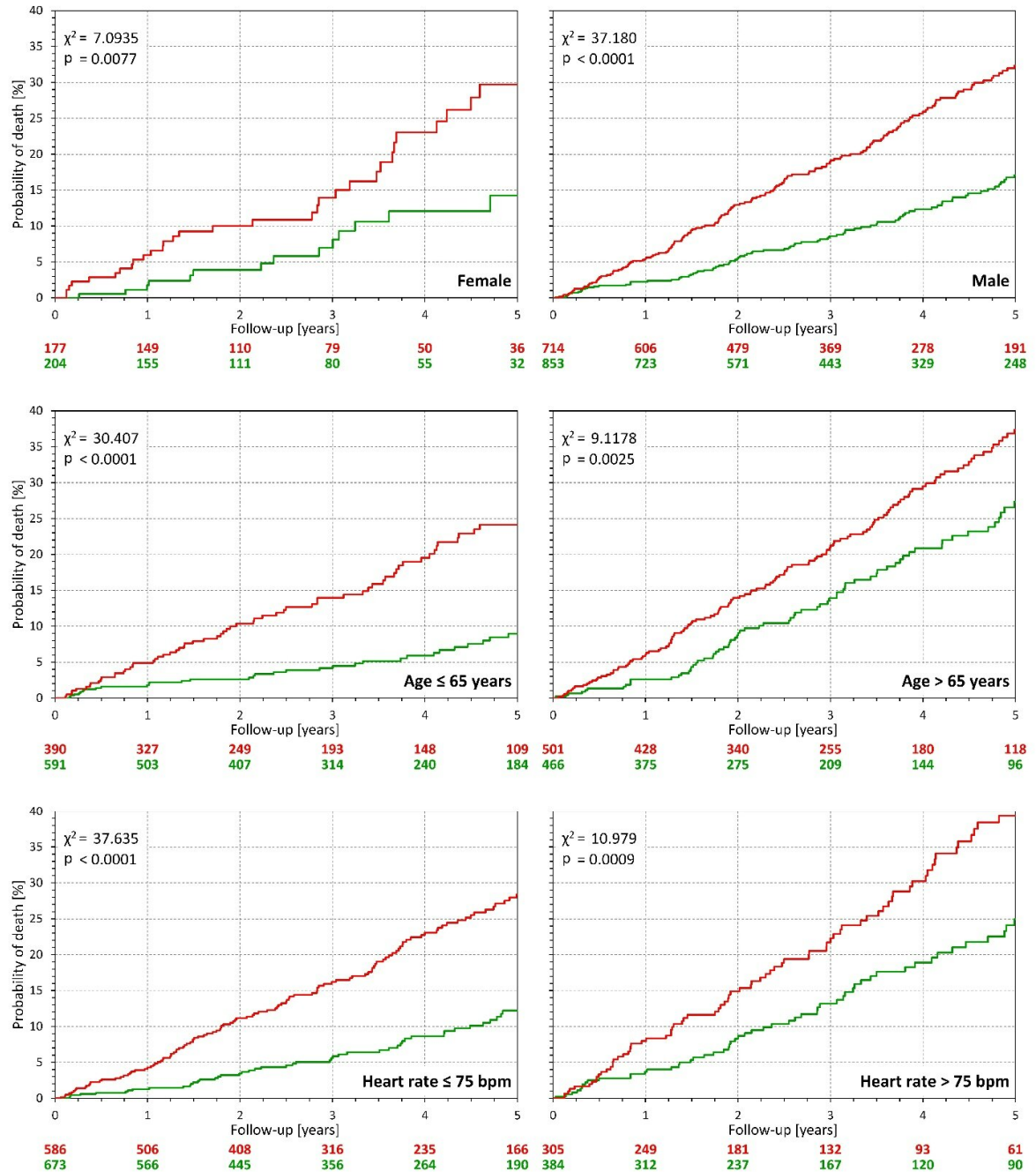
### Association between mortality and continuous values of risk factors in contributing centres of EU-CERT-ICD

	Univariable analysis			Multivariable analysis		
	Wald	p-value	HR (95% CI)	Wald	p-value	HR (95% CI)
<b>BASEL</b>						
Age [years]	17.0	<0.001	1.057 (1.030 - 1.086)	12.9	<0.001	1.052 (1.023 - 1.082)
Heart rate [bpm]	10.2	0.001	1.023 (1.009 - 1.038)	11.0	0.001	1.026 (1.011 - 1.042)
LVEF [%]	10.5	0.001	0.948 (0.918 - 0.979)	5.66	0.017	0.953 (0.916 - 0.992)
QRS duration [ms]	18.7	<0.001	1.016 (1.009 - 1.024)			
log <sub>2</sub> (QRS $\mu$ -fragmentation)	22.6	<0.001	2.113 (1.552 - 2.877)	14.2	<0.001	1.827 (1.336 - 2.499)
<b>GÖTTINGEN</b>						
Age [years]	23.5	<0.001	1.055 (1.033 - 1.079)	17.8	<0.001	1.05 (1.026 - 1.074)
Heart rate [bpm]	5.68	0.017	1.015 (1.003 - 1.027)	7.61	0.006	1.017 (1.005 - 1.030)
LVEF [%]	2.74	0.098	0.978 (0.954 - 1.004)			
QRS duration [ms]	3.02	0.082	1.005 (0.999 - 1.011)			
log <sub>2</sub> (QRS $\mu$ -fragmentation)	12.0	0.001	1.660 (1.247 - 2.211)	7.84	0.005	1.552 (1.141 - 2.111)
<b>LEUVEN</b>						
Age [years]	1.45	0.229	1.020 (0.988 - 1.054)			
Heart rate [bpm]	2.84	0.092	1.022 (0.996 - 1.048)			
LVEF [%]	2.78	0.095	0.968 (0.932 - 1.006)	2.78	0.095	0.968 (0.932 - 1.006)
QRS duration [ms]	0.94	0.332	1.005 (0.995 - 1.016)			
log <sub>2</sub> (QRS $\mu$ -fragmentation)	1.40	0.237	1.324 (0.831 - 2.109)			
<b>UTRECHT</b>						
Age [years]	2.00	0.158	1.015 (0.994 - 1.036)			
Heart rate [bpm]	4.72	0.030	1.013 (1.001 - 1.025)			
LVEF [%]	5.90	0.015	0.959 (0.927 - 0.992)	5.19	0.023	0.961 (0.929 - 0.994)
QRS duration [ms]	7.32	0.007	1.010 (1.003 - 1.017)			
log <sub>2</sub> (QRS $\mu$ -fragmentation)	7.15	0.007	1.486 (1.112 - 1.986)	6.44	0.011	1.465 (1.091 - 1.968)

Multivariable analysis used backwards stepwise elimination. In addition to hazard ratios, Wald statistics are shown. QRS micro-fragmentation was used after logarithmic transformation with base 2 – hazard ratios correspond to value increases by a factor of 2.

CI – confidence interval, bpm- beats per minute, deg – degrees, HR – hazard ratio, LVEF – left ventricular ejection fraction, ms – milliseconds,  $\mu$ -fragmentation – micro-fragmentation.

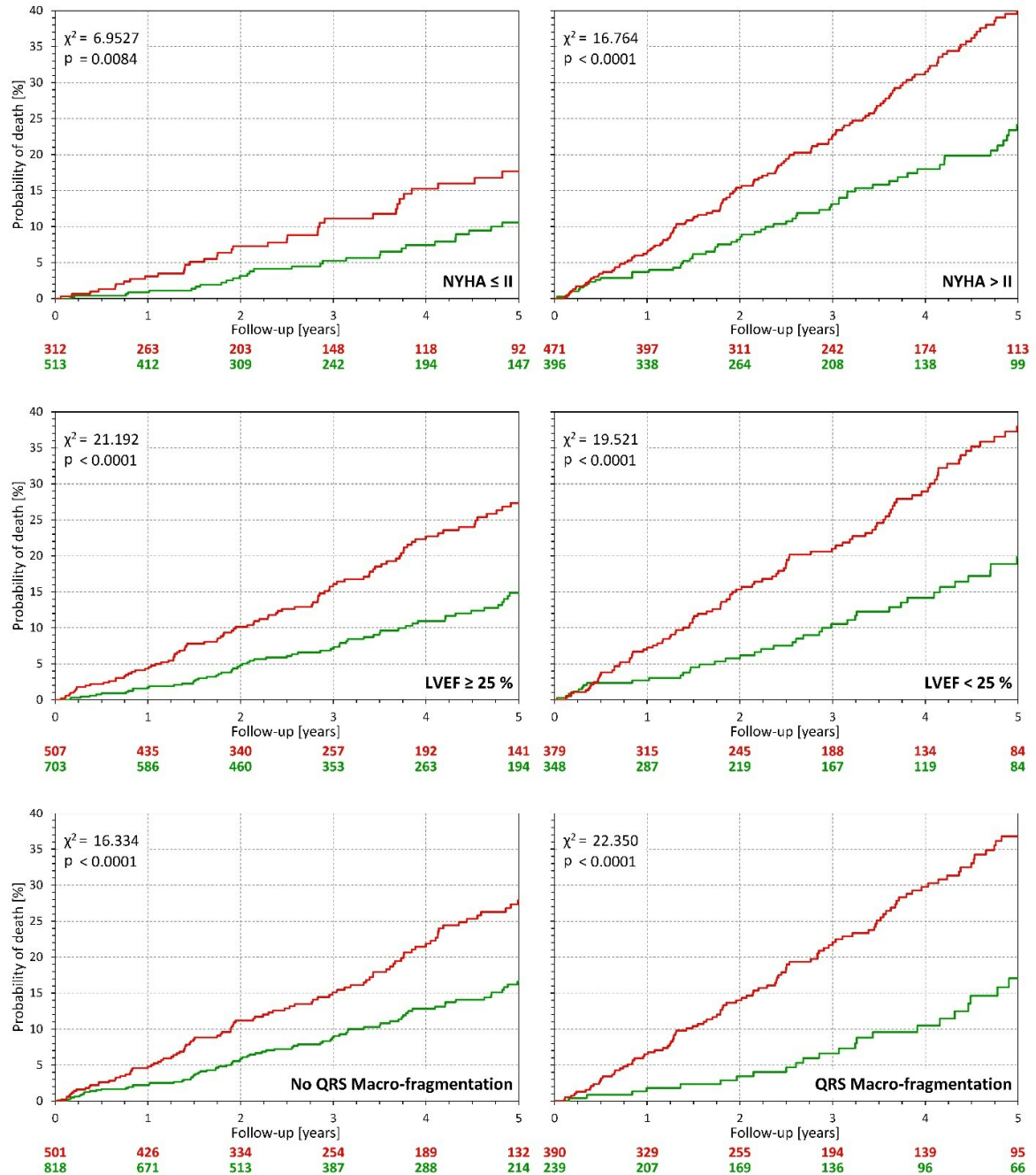
## Supplementary Figure 4



Individual panels of the figure show survival differences stratified by QRS micro-fragmentation  $\leq 3.5\%$  (green lines) and  $> 3.5\%$  (red lines) in sub-populations of the EU-CERT-ICD data defined by sex (top row); by age dichotomised at 65 years (middle row), and by heart rate dichotomised at 75 beats per minute (bottom row). In each panel, the  $\chi^2$  statistics is shown together with the corresponding p-value (log-rank test). Numbers of patients at risk in the different strata are shown below the panels in colours corresponding to the Kaplan-Meier survival curves.

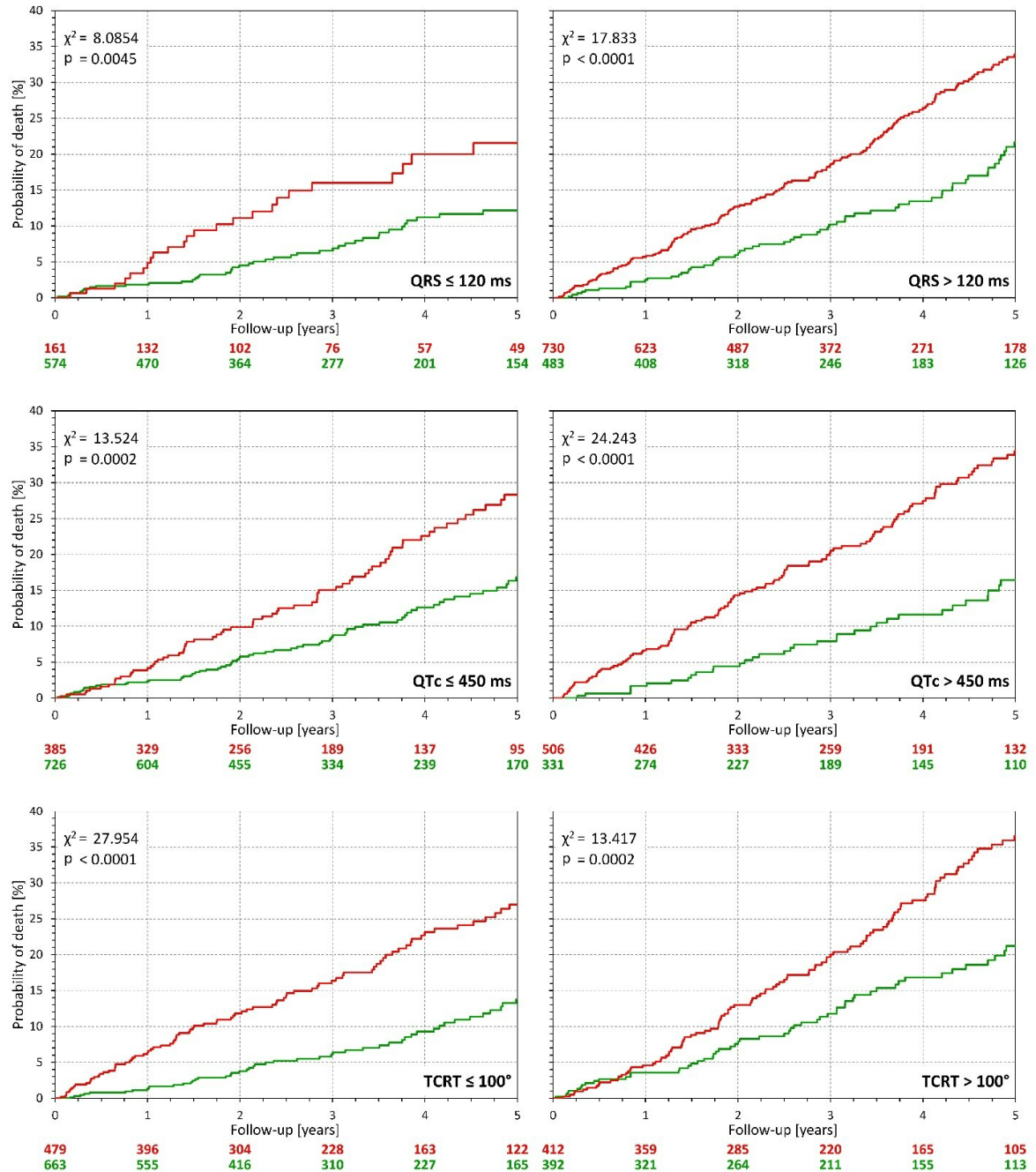


## Supplementary Figure 5



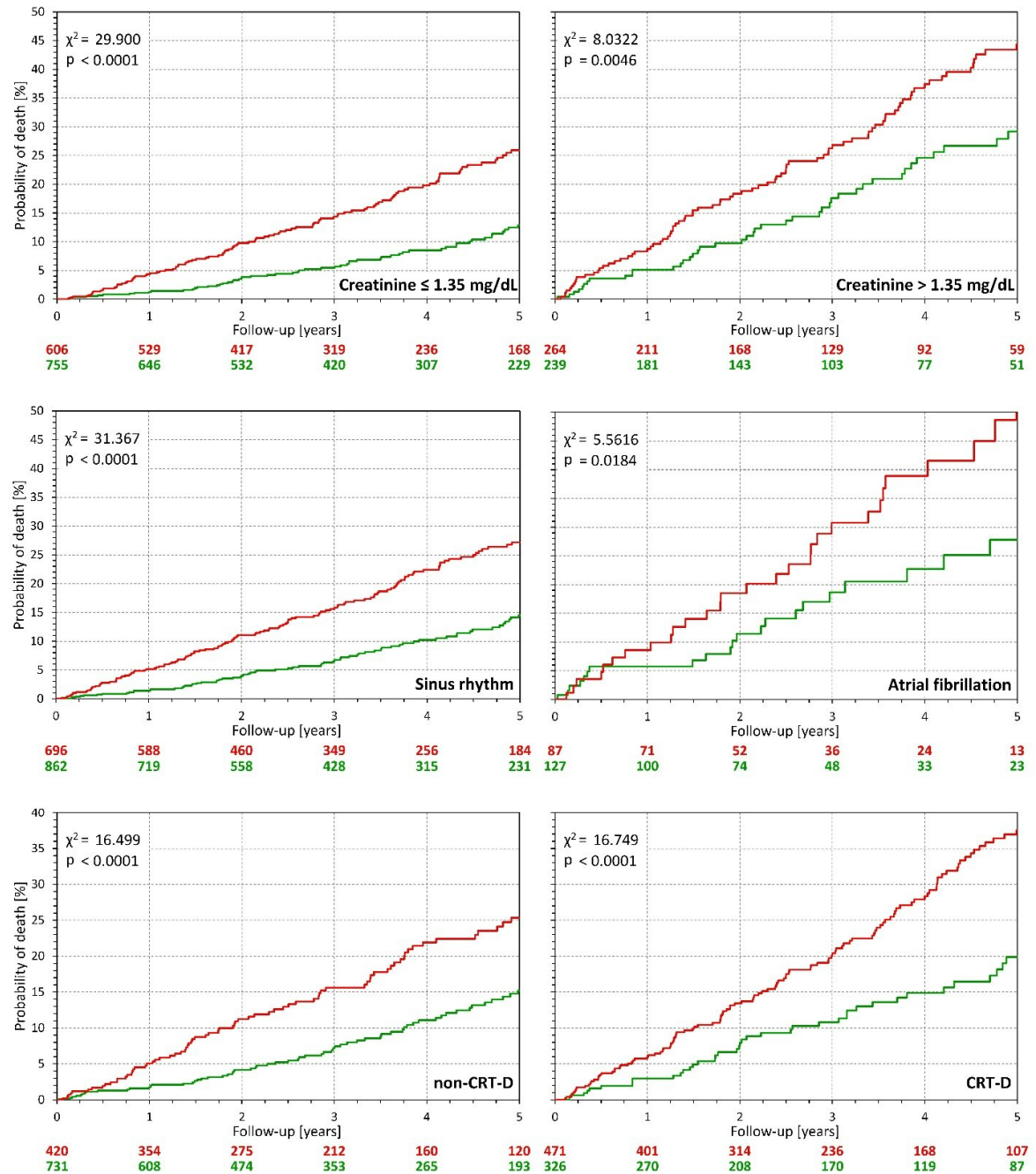
Individual panels of the figure show survival differences stratified by QRS micro-fragmentation  $\leq 3.5\%$  (green lines) and  $> 3.5\%$  (red lines) in sub-populations of the EU-CERT-ICD data defined by New York Heart Association class (NYHA) assessed at ICD implantation and divided into classes I+II and III+IV (top row); by left ventricular ejection fraction (LVEF) dichotomised at 25% (middle row); and by the presence or absence of visible QRS complex macro-fragmentation (bottom row). In each panel, the  $\chi^2$  statistics is shown together with the corresponding p-value (log-rank test). Numbers of patients at risk in the different strata are shown below the panels in colours corresponding to the Kaplan-Meier survival curves (small number of cases with missing data excluded).

## Supplementary Figure 6



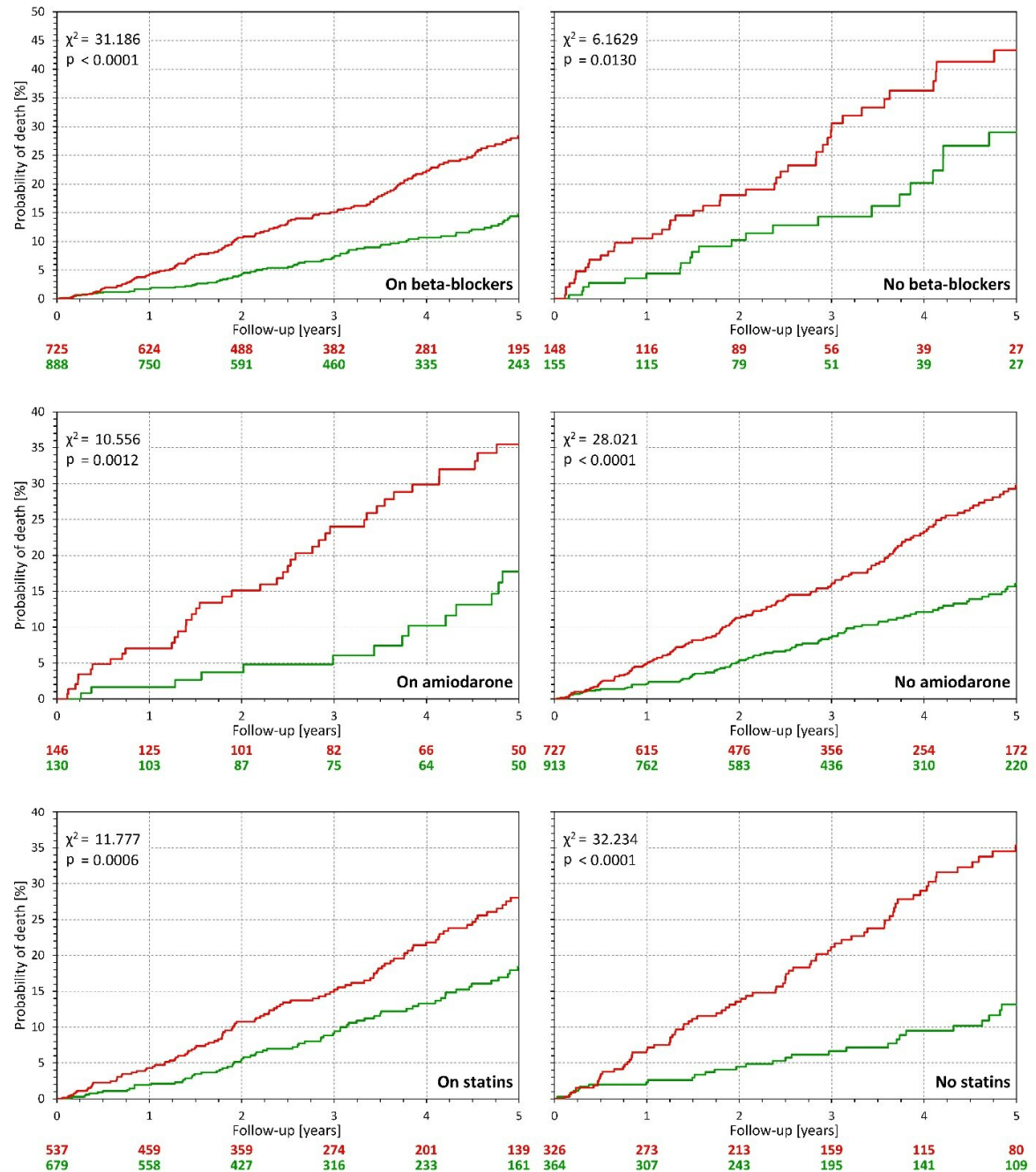
Individual panels of the figure show survival differences stratified by QRS micro-fragmentation  $\leq 3.5\%$  (green lines) and  $> 3.5\%$  (red lines) in sub-populations of the EU-CERT-ICD data defined by QRS duration dichotomised at 120 ms (top row); by QTc interval dichotomised at 450 ms (middle row), and by the total cosine R to T (TCRT) dichotomised at  $100^\circ$  (bottom row). In each panel, the  $\chi^2$  statistics is shown together with the corresponding p-value (log-rank test). Numbers of patients at risk in the different strata are shown below the panels in colours corresponding to the Kaplan-Meier survival curves (small number of cases with missing data excluded).

## Supplementary Figure 7



Individual panels of the figure show survival differences stratified by QRS micro-fragmentation  $\leq$  3.5% (green lines) and  $>$  3.5% (red lines) in sub-populations of the EU-CERT-ICD data defined by creatinine plasma levels dichotomised at 1.35 mg/dL (top row); by the rhythm of the analysed electrocardiogram (middle row – see Supplementary Table 6 for further details); and by the distinction on whether the patients were, for clinical reasons, implanted with a cardiac resynchronisation defibrillator or with a device without the resynchronisation function (bottom row). In each panel, the  $\chi^2$  statistics is shown together with the corresponding p-value (log-rank test). Numbers of patients at risk in the different strata are shown below the panels in colours corresponding to the Kaplan-Meier survival curves (small number of cases with missing data excluded).

## Supplementary Figure 8



Individual panels of the figure show survival differences stratified by QRS micro-fragmentation  $\leq 3.5\%$  (green lines) and  $> 3.5\%$  (red lines) in sub-populations of the EU-CERT-ICD data defined by intention to treat by beta-blockers (top row); amiodarone (middle row), and statins (bottom row). In each panel, the  $\chi^2$  statistics is shown together with the corresponding p-value (log-rank test). Numbers of patients at risk in the different strata are shown below the panels in colours corresponding to the Kaplan-Meier survival curves (small number of cases with missing data excluded).

## Supplementary Table 7

### Association between mortality and continuous values of risk factors in EU-CERT-ICD in sinus rhythm and in atrial fibrillation

	Univariable analysis			Multivariable analysis†		
	Wald	p-value	HR (95% CI)	Wald	p-value	HR (95% CI)
<b>Patients in sinus rhythm (n=1558)</b>						
Age [years]	28.3	<0.001	1.039 (1.024 - 1.054)	20.0	<0.001	1.033 (1.019 - 1.048)
Heart rate [bpm]	26.9	<0.001	1.022 (1.014 - 1.031)	20.7	<0.001	1.020 (1.011 - 1.029)
LVEF [%]	24.5	<0.001	0.955 (0.937 - 0.972)	8.86	0.003	0.969 (0.950 - 0.989)
QRS duration [ms]	20.7	<0.001	1.011 (1.006 - 1.015)			
QTc [ms]	11.7	0.001	1.006 (1.003 - 1.010)			
TCRT [deg]	20.2	<0.001	1.011 (1.006 - 1.015)	5.81	0.016	1.006 (1.001 - 1.011)
log <sub>2</sub> (QRS μ-fragmentation)	27.9	<0.001	1.691 (1.391 - 2.055)	15.9	<0.001	1.521 (1.237 - 1.869)
<b>Patients in atrial fibrillation (n=214)</b>						
Age [years]	1.58	0.209	1.022 (0.988 - 1.058)			
Heart rate [bpm]	0.77	0.379	1.008 (0.990 - 1.026)			
LVEF [%]	3.35	0.067	0.964 (0.928 - 1.003)			
QRS duration [ms]	2.98	0.085	1.007 (0.999 - 1.016)			
QTc [ms]	5.08	0.024	1.006 (1.001 - 1.012)			
TCRT [deg]	3.60	0.058	1.011 (1.000 - 1.022)	3.97	0.046	1.011 (1.000 - 1.022)
log <sub>2</sub> (QRS μ-fragmentation)	10.7	0.001	1.692 (1.235 - 2.318)	14.0	<0.001	1.898 (1.358 - 2.654)

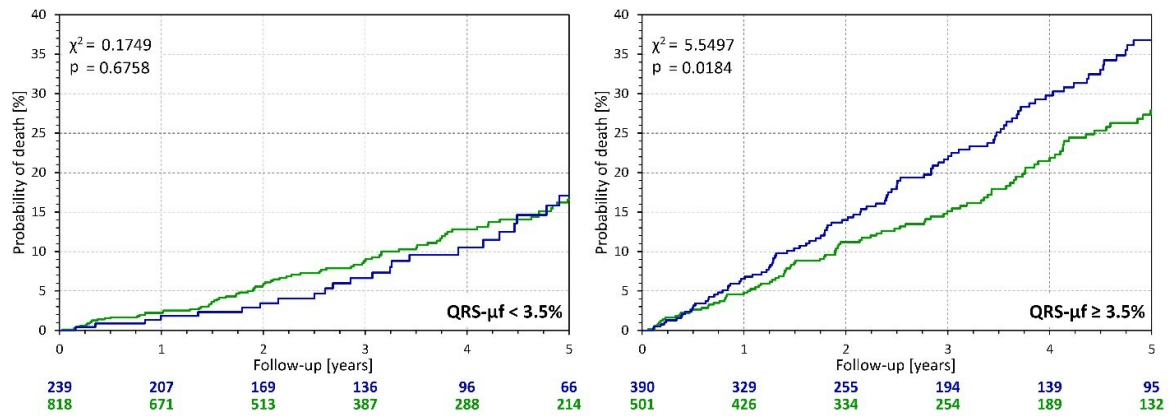
Of the 1948 patients of the EU-CERT-ICD data collection, 1558 had the ECG classified as sinus rhythm, 214 were in atrial fibrillation, 123 had the rhythm classified as “other” (trigeminy, frequent ectopic beats, atrial flutter, paced rhythm, etc.) and 53 patients had the rhythm unclassified. The analyses shown in this table show only patients with confirmed sinus rhythm and confirmed atrial fibrillation.

Multivariable analysis used backwards stepwise elimination. In addition to hazard ratios, Wald statistics are shown. QRS micro-fragmentation was used after logarithmic transformation with base 2 – hazard ratios correspond to value increases by a factor of 2.

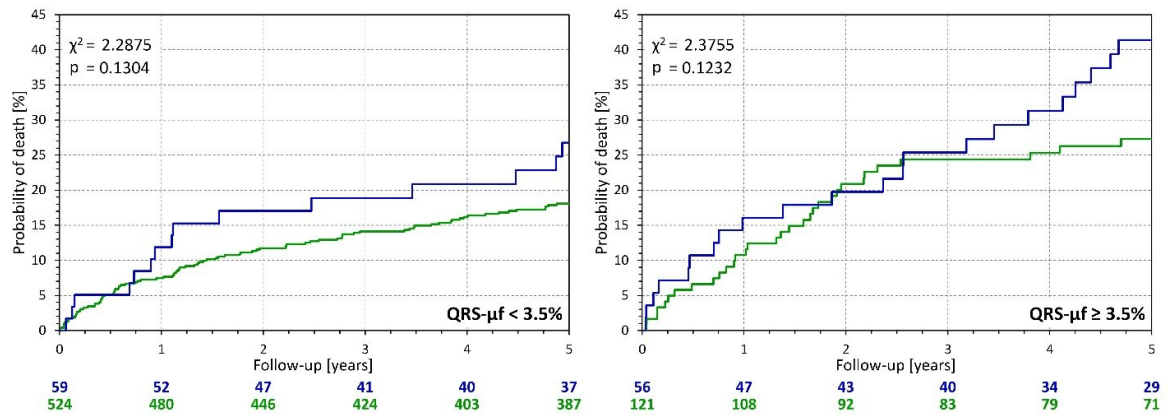
CI – confidence interval, bpm- beats per minute, deg – degrees, HR – hazard ratio, LVEF – left ventricular ejection fraction, ms – milliseconds, μ-fragmentation – micro-fragmentation.

## Supplementary Figure 9

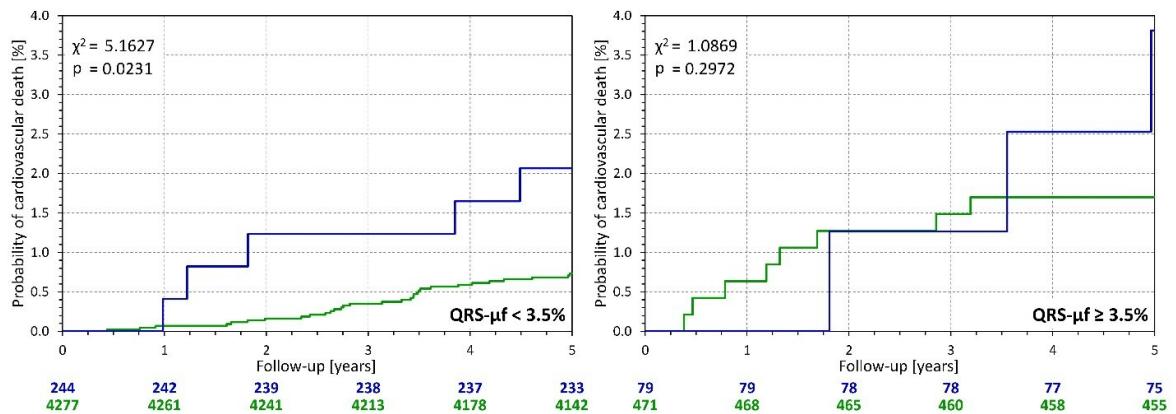
### EU-CERT-ICD



### VA WASHINGTON

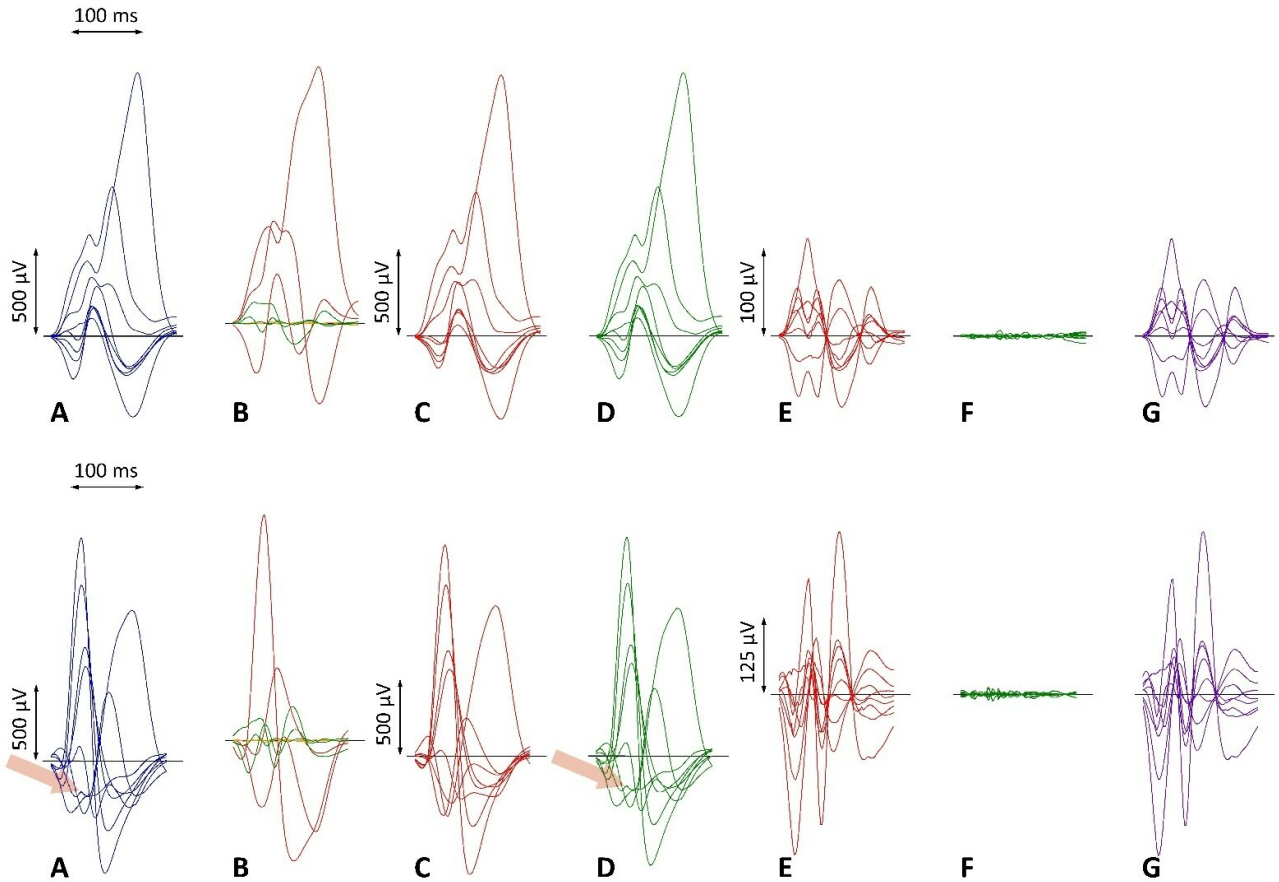


### WHITEHALL II



For each of the investigated populations, the panels show survival differences stratified by the presence (blue lines) and absence (green lines) of visible QRS macro-fragmentations in subpopulations with QRS micro-fragmentation < 3.5% (left panels) and  $\geq$  3.5% (right panels). In each panel, the  $\chi^2$  statistics is shown together with the corresponding p-value (log-rank test). Numbers of patients at risk in the different strata are shown below the panels in colours corresponding to the Kaplan-Meier survival curves.

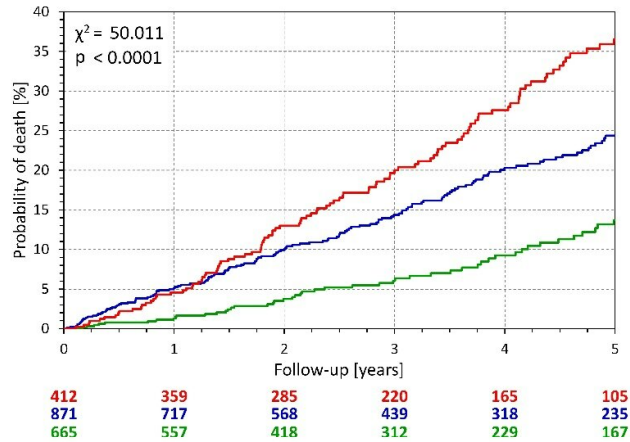
## Supplementary Figure 10



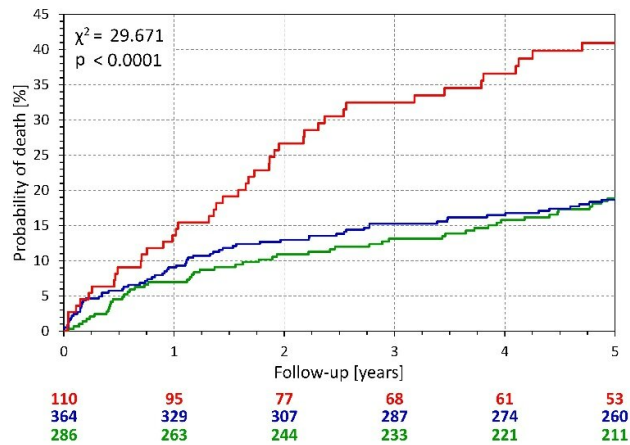
The panels of the Figure have the same meaning as the panels of Figure 1 of the main manuscript. The top and bottom rows correspond to 52-year and 67-year old male patients who died 4 years and 2 months later, respectively. Note that in the top row (QRS width of 172 ms), the clear macro-fragmentation of the QRS complex is reproduced in the reconstruction by the first 3 components (i.e., visible on panel C) and thus is present in the convolution of the 3-dimensional depolarisation vector. Other abnormalities of the ECG correspond to QRS micro-fragmentation of 9.429%. On the contrary, in the bottom row (QRS width of 158 ms) the macro-fractionation seen in lead V2 (arrow in panel A) is not reproduced in the 3-dimensional reconstruction but is present in the 6-dimensional reconstruction (arrow in panel D). This means that the abnormality of this macro-fragmentation is also present (but not clearly visible) in other leads and contributes to the QRS micro-fragmentation of 16.942%.

## Supplementary Figure 11

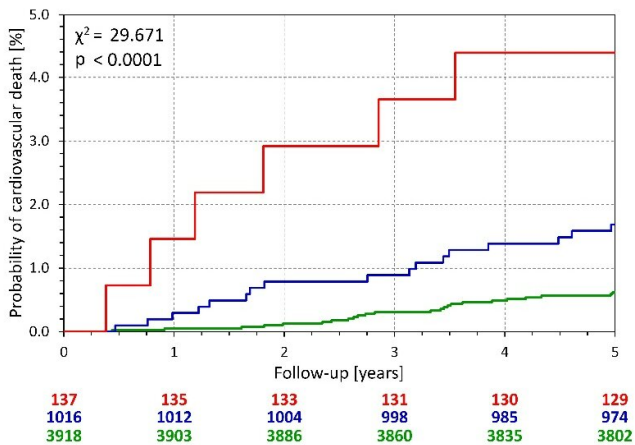
EU-CERT-ICD



VA WASHINGTON



WHITEHALL II



For each of the populations, the graphs show outcome probabilities in sub-groups stratified by a combination of QRS micro-fragmentation dichotomised at 3.5% and of total cosine R to T (TCRT) dichotomised at 100°. The green, blue, and red lines correspond to both factors normal, only one factor normal, and both factor abnormal, respectively. In each panel, the  $\chi^2$  statistics is shown together with the corresponding p-value (log-rank test). Numbers of patients at risk in the different strata are shown below the panels in colours corresponding to the Kaplan-Meier survival curves.



## 5. Závěr

NSS je jednoznačně multifaktoriální problém, který má u různých pacientů různé patologické a elektrofyziologické pozadí. Je proto nevhodné očekávat, že existuje nějaký „svatý grál“ v tom smyslu, že by pro predikci rizika NSS byla univerzálně použitelná jediná metoda hodnocení rizika nejen v různých klinických populacích, ale dokonce i u různých pacientů s podobnými klinickými charakteristikami. Spíše je potřeba použít kombinaci různých metod hodnocení rizik, aby se identifikace rizikových pacientů postupně zlepšovala. Z těchto důvodů jsme se soustředili na různé způsoby analýzy EKG, které by mohly přispět k tomuto postupnému procesu hodnocení rizika NSS.

Elektrokardiogram je komplexní biologický signál, který více než 100 let po uvedení do praxe stále přináší nové informace. Zavedení digitální elektrokardiografie umožnilo použití nových podrobnějších metod analýzy tohoto signálu a také vznik rozsáhlých databází EKG záznamů v nejrůznějších populacích zdravých i nemocných jedinců různých věkových kategorií.

Analýzy dynamických charakteristik elektrokardiogramu, které jsme provedli na dlouhodobých EKG záznamech u vzorků zdravé populace, nejenže poskytly cenné fyziologické údaje, ale také otevřely další otázky. Takovými je například vliv autonomní regulace na úhel-QRS nebo na QRS- $\mu f$ . Tyto parametry zřejmě nejsou, oproti jiným repolarizačním charakteristikám (QTV, QT a dalším), závislé na změnách SF, ale pravděpodobně přímo odráží vliv autonomní regulace myokardu na úrovni srdečních komor. Další analýza právě v populaci s myokardiálními abnormalitami může přinést poznatky v patologii srdeční autonomní regulace. Časová dynamika depolarizačních charakteristik, jako QRS- $\mu f$ , je také málo známá a může v kombinaci s dalšími parametry podstatně posunout hodnocení rizika NSS.

Uvedené dynamické EKG parametry, jejichž metodika měření byla jasně definována u zdravé dospělé populace, jsou nyní připraveny k dalšímu klinickému zkoumání. V budoucnu podrobíme těmto analýzám i náš rozsáhlý soubor dlouhodobých EKG záznamů získaných od více než 1000 dětí a adolescentů během posturálního testu. Spolupracujeme také s jinými klinickými centry a tato spolupráce nám umožní aplikovat vyvinuté technologie na rozsáhlé soubory EKG záznamů získaných od různých skupin pacientů. Velké soubory EKG signálů, získané v obecné populaci (například na pohotovostních odděleních nemocnic) nebo u příjemců ICD v rámci multicentrických studií, umožní nejen charakterizovat prediktivní sílu metod, které jsme vyvinuli a zkoumali, ale také analyzovat rozdíly mezi úmrtím z arytmiické a nearytmické příčiny. Očekáváme, že takové metodologické odlišení přispěje mimo jiné ke zlepšení výběru kandidátů v rámci primárně preventivní implantace ICD tím, že identifikuje pacienty, kteří pravděpodobně budou mít prospěch z tohoto přístroje, navzdory pouze hraničnímu splnění současných výběrových kritérií, a naopak rozpoznáním pacientů, kteří

pravděpodobně podlehnou srdečnímu selhání bez ohledu na primárně preventivní implantaci defibrilátoru.

Věříme proto, že všechny výše uvedené práce povedou k dalšímu pokroku moderní dynamické elektrokardiografie, která i přes stoletou historii stále plně nevyužívá klinický potenciál základních elektrokardiografických záznamů.

## 6. Seznam literatury doprovodného komentáře

- 1 Roberts WC. Sudden cardiac death: definitions and causes. *Am J Cardiol* 1986; 57:1410-1413.
- 2 Myerburg RJ, Kessler KM, Castellanos A. Sudden cardiac death. Structure, function, and time-dependence of risk. *Circulation* 1992; 85:12-110.
- 3 Reinier K, Stecker EC, Uy-Evanado A, Chugh HS, Binz A, Nakamura K, Sargsyan A, Jui J, Chugh SS. Sudden Cardiac Death as First Manifestation of Heart Disease in Women: The Oregon Sudden Unexpected Death Study, 2004-2016. *Circulation* 2020; 141:606-608.
- 4 Křivan L. Náhlá srdeční smrt, jak jí předcházet. *Kardiol Rev* 2006; 8:20-24.
- 5 Kozák M, Křivan L, Semrád B. Cirkadiánní a sezónní variace výskytu komorových tachyarytmií detekovaných kardiovertory-defibrilátory (ICD). *Cor Vasa* 2000; 42:36-37.
- 6 Becker L, Eisenberg M, Fahrenbruch C, Cobb L. Public locations of cardiac arrest: Implications for public access defibrillation. *Circulation* 1998; 97:2106-2109.
- 7 Myerburg RJ, Kessler KM, Castellanos A. Sudden cardiac death: Epidemiology, transient risk, and intervention assessment. *Am Intern Med* 1993; 119:1187-1197.
- 8 Svane J, Lynge TH, Hansen CJ, Risgaard B, Winkel BG, Tfelt-Hansen J. Witnessed and unwitnessed sudden cardiac death: a nationwide study of persons aged 1-35 years. *Europace*. 2021; 23:898-906.
- 9 Myerburg RJ, Interian A Jr, Mitrani RM, Kessler KM, Castellanos A. Frequency of sudden cardiac death and profiles of risk. *Am J Cardiol* 1997; 80:10F-19F.
- 10 Myerburg RJ. Sudden cardiac death: exploring the limits of our knowledge. *J Cardiovasc Electrophysiol* 2001; 12:369-381.
- 11 Huikuri HV, Castellanos A, Myerburg R. Sudden death due to cardiac arrhythmias. *N Engl J Med* 2001; 345,20:1473-1482.
- 12 Malik M, Camm AJ (eds). *Dynamic Electrocardiography, Section IV*, Futura/Blackwell Publishing, 2004, New York, ISBN 1-405-11960-8.
- 13 Wellens HJ, Schwartz PJ, Lindemans FW, Buxton AE, Goldberger JJ, Hohnloser SH, Huikuri HV, Kääh S, La Rovere MT, Malik M, Myerburg RJ, Simoons ML, Swedberg K, Tijssen J, Voors AA, Wilde AA. Risk stratification for sudden cardiac death: current status and challenges for the future. *Eur Heart J*. 2014 Jul 1; 35(25):1642-51.
- 14 Zabel M, Acar B, Klingenhoben T, Franz MR, Hohnloser SH, Malik M. Analysis of 12-lead T-wave morphology for risk stratification after myocardial infarction. *Circulation* 2000; 102:1252-1257.
- 15 Aro AL, Huikuri HV, Tikkanen JT, Junttila MJ, Rissanen HA, Reunanen A, Anttonen O. QRS-T angle as a predictor of sudden cardiac death in a middle-aged general population. *Europace* 2012; 14:872-876.
- 16 Hnatkova K, Andršová I, Novotný T, Britton A, Shipley M, Vandenberg B, Sprenkeler DJ, Junttila J, Reichlin T, Schlögl S, Vos MA, Friede T, Bauer A, Huikuri HV, Willems R, Schmidt G, Franz MR, Sticherling C, Zabel M, Malik M. QRS micro-fragmentation as a mortality predictor. *Eur Heart J* 2022; 43:4177-4191.

- 17 Bänsch D, Antz M, Boczor S, Volkmer M, Tebbenjohanns J, Seidl K, Block M, Gietzen F, Berger J, Kuck KH. Primary prevention of sudden cardiac death in idiopathic dilated cardiomyopathy. The cardiomyopathy trial (CAT). *Circulation* 2002; 105:1453-1458.
- 18 Arya A, Haghjoo M, Sadr-Ameli MA. Risk stratification for arrhythmic death after myocardial infarction: current perspective and future direction. *Int J Cardiol* 2006; 108:155-64.
- 19 Huikuri HV, Mäkikallio TH, Raatikainen MJ, Perkiömäki J, Castellanos A, Myerburg RJ. Prediction of sudden cardiac death: appraisal of the studies and methods assessing the risk of sudden arrhythmic death. *Circulation* 2003; 108:110-115.
- 20 La Rovere MT, Bigger JT Jr, Marcus FI, Mortara A, Schwartz PJ. Baroreflex sensitivity and heart-rate variability in prediction of total cardiac mortality after myocardial infarction. ATRAMI (Autonomic Tone and Reflexes After Myocardial Infarction) Investigators. *Lancet* 1998; 351:478-484.
- 21 Bauer A, Guzik P, Barthel P, Schneider R, Ulm K, Watanabe MA, Schmidt G. Reduced prognostic power of ventricular late potentials in post-infarction patients of the reperfusion era. *Eur Heart J* 2005; 26:755-761.
- 22 Exner DV, Kavanagh KM, Slawnych MP, Mitchell LB, Ramadan D, Aggarwal SG, Noullett C, Van Schaik A, Mitchell RT, Shibata MA, Gulamhussein S, McMeekin J, Tymchak W, Schnell G, Gillis AM, Sheldon RS, Fick GH, Duff HJ; REFINE Investigators. Noninvasive risk assessment early after a myocardial infarction: The REFINE study. *J Am Coll Cardiol* 2007; 50:2275-2284.
- 23 Ikeda T, Saito H, Tanno K, Shimizu H, Watanabe J, Ohnishi Y, Kasamaki Y, Ozawa Y. T-wave alternans as a predictor for sudden cardiac death after myocardial infarction. *Am J Cardiol*, 2002; 89:79-82.
- 24 Honzikova N, Fiser B, Semrad B. Critical value of baroreflex sensitivity determined by spectral analysis in risk stratification after myocardial infarction. *Pacing Clin Electrophysiol* 2000; 23:1965-1967.
- 25 Baumert M, Porta A, Vos MA, Malik M, Couderc JP, Laguna P, Piccirillo G, Smith GL, Tereshchenko LG, Volders PG. QT interval variability in body surface ECG: measurement, physiological basis, and clinical value: position statement and consensus guidance endorsed by the European Heart Rhythm Association jointly with the ESC Working Group on Cardiac Cellular Electrophysiology. *Europace* 2016; 18:925-944.
- 26 Verrier RL, Klingenhöben T, Malik M, El-Sherif N, Exner DV, Hohnloser SH, Ikeda T, Martínez JP, Narayan SM, Nieminen T, Rosenbaum DS. Microvolt T-wave alternans: physiological basis, methods of measurement, and clinical utility - consensus guideline by International Society for Holter and Noninvasive Electrocardiology. *J Am Coll Cardiol* 2011; 58:1309-1324.
- 27 Breithardt G, Cain ME, el-Sherif N, Flowers N, Hombach V, Janse M, Simson MB, Steinbeck G. Standards for analysis of ventricular late potentials using high resolution or signal-averaged electrocardiography. A statement by a Task Force Committee between the European Society of Cardiology, the American Heart Association and the American College of Cardiology. *Eur Heart J* 1991; 12:473-480.
- 28 Jouvan X, Desnos M, Guerot C, Ducimetière P. Predicting sudden death in the population: the Paris Prospective Study I. *Circulation* 1999; 99:1978-1983.

- 29 Austin MA, Psaty BM, Lemaitre RN, Arbogast P, Raghunathan TE, Cobb LA. Family history as a risk factor for primary cardiac arrest. *Circulation* 1998; 97:155-160.
- 30 Spooner PM, Albert C, Benjamin EJ, Boineau R, Elston RC, George AL Jr, Jouven X, Kuller LH, MacCluer JW, Marbán E, Muller JE, Schwartz PJ, Siscovick DS, Tracy RP, Zareba W, Zipes DP. Sudden cardiac death, genes, and arrhythmogenesis : consideration of new population and mechanistic approaches from National Heart, Lung, and Blood Institute workshop, part I. *Circulation* 2001; 103:2361-2364.
- 31 Spooner PM, Albert C, Benjamin EJ, Boineau R, Elston RC, George AL Jr, Jouven X, Kuller LH, MacCluer JW, Marbán E, Muller JE, Schwartz PJ, Siscovick DS, Tracy RP, Zareba W, Zipes DP . Sudden cardiac death, genes and arrhythmogenesis: consideration of new population and mechanistic approaches from a National Heart, Lung, and Blood Institute workshop, Part II. *Circulation* 2001; 103:2447-2452.
- 32 Stecker EC, Sono M, Wallace E, Gunson K, Jui J, Chugh SS. Allelic variants of SCN5A and risk of sudden cardiac arrest in patients with coronary artery disease. *Heart Rhythm* 2006; 3:697-700.
- 33 Albert CM, Nam EG, Rimm EB, Jin HW, Hajjar RJ, Hunter DJ, MacRae CA, Ellinor PT. Cardiac sodium channel gene variants and sudden cardiac death in women. *Circulation* 2008; 117:16-23.
- 34 Tester DJ, Spoon DB, Valdivia HH, Makielski JC, Ackerman MJ. Targeted mutational analysis of the RyR2-encoded cardiac ryanodine receptor in sudden unexplained death: a molecular autopsy of 49 medical examiner/ coroner's cases. *Mayo Clin Proc* 2004; 79:1380-1384.
- 35 Friedlander Y, Siscovick DS, Weinmann S, Austin MA, Psaty BM, Lemaitre RN, Arbogast P, Raghunathan TE, Cobb LA. Family history as a risk factor for primary cardiac arrest. *Circulation* 1998; 97:155-160.
- 36 Ashar FN, Mitchell RN, Albert CM, Newton-Cheh C, Brody JA, Müller-Nurasyid M, Moes A, Meitinger T, Mak A, Huikuri H, Juntila MJ, Goyette P, Pulit SL, Pazoki R, Tanck MW, Blom MT, Zhao X, Havulinna AS, Jabbari R, Glinge C, Tragante V, Escher SA, Chakravarti A, Ehret G, Coresh J, Li M, Prineas RJ, Franco OH, Kwok PY, Lumley T, Dumas F, McKnight B, Rotter JI, Lemaitre RN, Heckbert SR, O'Donnell CJ, Hwang SJ, Tardif JC, VanDenburgh M, Uitterlinden AG, Hofman A, Stricker BHC, de Bakker PIW, Franks PW, Jansson JH, Asselbergs FW, Halushka MK, Maleszewski JJ, Tfelt-Hansen J, Engstrøm T, Salomaa V, Virmani R, Kolodgie F, Wilde AAM, Tan HL, Bezzina CR, Eijgelsheim M, Rioux JD, Jouven X, Käåb S, Psaty BM, Siscovick DS, Arking DE, Sotoodehnia N. A comprehensive evaluation of the genetic architecture of sudden cardiac arrest. *Eur Heart J* 2018; 39:3961-3969.
- 37 Schwartz PJ, Gentilini D. Can genetics predict risk for sudden cardiac death? The relentless search for the Holy Grail. *Eur Heart J* 2018; 39:3970-3972.
- 38 Tomaselli GF, Beuckelmann DJ, Calkins HG, Berger RD, Kessler PD, Lawrence JH, Kass D, Feldman AM, Marban E. Sudden cardiac death in heart failure. The role of abnormal repolarization. *Circulation* 1994; 90:2534-2539.
- 39 Thurston E. The length of the systole of the heart, as estimated from sphygmographic tracings. *J Anat Physiol* 1876; 10:494-501.
- 40 Donders FC. On rhythm of the sounds of the heart. *Nederlandish Archief voor Genees-en Natuurkunde*. Utrecht, 1865 (translated in the *Dublin Quaterly Journal of Medical Science*. February 1868).

- 41 Garrod AH. Proc Royal Soc Lond, 1870:351.
- 42 Garrod AH. On cardiograph tracings from the human chest-wall. Journal of Anatomical Physiology 1871; 5:2-27.
- 43 Bazett HC. An analysis of time relations of electrocardiograms. Heart 1920; 7:353-370.
- 44 Fridericia LS. Die Systolendauer im Elektrokardiogramm bei normalen Menschen und bei Herzkranken. Acta Medica Scandinavica, 1920; 53:469-486.
- 45 Malik M. Problems of heart rate correction in assessment of drug-induced QT interval prolongation. J Cardiovasc Electrophysiol 2001; 12:411-420.
- 46 Ljung O. A simple formula for clinical interpretation of the QT interval data. Acta Med Scand 1949; CXXXIV:79-86.
- 47 Hodges M. Rate Correction of the QT Interval. Cardiac Electrophysiol Rev 1997; 3:360-363.
- 48 Rautaharju PM, Warren JW, Calhoun HP. Estimation of QT prolongation. A persistent, avoidable error in computer electrocardiography. J Electrocardiol 1990; 23 Suppl:111-117.
- 49 Sagie A, Larson MG, Goldberg RJ, Bengtson JR, Levy D. An improved method for adjusting the QT interval for heart rate (the Framingham study). Am J Cardiol. 1992; 70:797-801.
- 50 Hodges M, Salerno D, Erlie D. Bazett's QT correction reviewed: evidence that a linear QT correction for heart rate is better. J Am Coll Cardiol. 1983; 1: 694.
- 51 Funck-Brentano K., Jaillon P. (1993) Rate-corrected QT interval: Techniques and limitations. Am J Cardiol 1993; 72:17B-22B.
- 52 Aytemir K, Maarouf N, Gallagher MM, Yap YG, Waktare JEP, Malik M. Comparison of formulae for heart rate correction of QT interval in exercise electrocardiograms. Pacing Clin Electrophysiol 1999; 22:1397-1401.
- 53 Malik M. The Imprecision in heart rate correction may lead to artificial observations of drug-induced QT interval changes. Pacing Clin Electrophysiol 2002; 25:209-216.
- 54 Rickards AF, Norman J. Relation between QT interval and heart rate. New design of physiologically adaptive cardiac pacemaker. Br Heart J 1981; 45:56-61.
- 55 Browne KF, Prystowsky E, Heger JJ, Zipes DP. Modulation of the Q-T Interval by the Autonomic Nervous System. Pacing Clin Electrophysiol 1983; 6:1050-1056.
- 56 Cappato R, Alboni P, Pedroni P, Gilli G, Antonioli GE. Sympathetic and vagal influences on rate-dependent changes of QT interval in healthy subjects. Am J Cardiol 1991; 68:1188-1193.
- 57 Malik M. Is there a physiologic QT/RR relationship? J of Cardiovasc Electrophysiol 2002; 13:1219-1221.
- 58 Malik M, Färbom P, Batchvarov V, Hnatkova K, Camm AJ. Relation between QT and RR intervals is highly individual among healthy subjects: implications for heart rate correction of the QT interval. Heart, 2002; 87:220-228.
- 59 Batchvarov VN, Ghuran A, Smetana P, Hnatkova K, Harries M, Dilaveris P, Camm AJ, Malik M. QT-RR relationship in healthy subjects exhibits substantial intersubject variability and high intrasubject stability. Am J Physiol Heart Circ Physiol 2002; 282:H2356-H2363.
- 60 Malik M. If Dr. Bazett had had a computer... Pacing Clin Electrophysiol. 1996; 19:1635-1639.

- 61 Malik M, Hnatkova K, Kowalski D, Keirns JJ, van Gelderen EM. QT/RR curvatures in healthy subjects: sex differences and covariates. *Am J Physiol Heart Circ Physiol* 2013; 305:H1798-H1806.
- 62 Hnatkova K, Vicente J, Johannesen L, Garnett C, Stockbridge N, Malik M. Errors of fixed QT heart rate corrections used in the assessment of drug-induced QTc changes. *Front Physiol* 2019; 10:635.
- 63 Benatar A, Feenstra A. QT correction methods in infants and children: effects of age and gender. *Ann Noninvasive Electrocardiol* 2015; 20:119-125.
- 64 Lau CP, Freedman AR, Fleming S, Malik M, Camm AJ, Ward DE. Hysteresis of the ventricular paced QT interval in response to abrupt changes in pacing rate. *Cardiovasc Res* 1988; 22:67-72.
- 65 Franz MR, Swerdlow CD, Liem LB, Schaefer J. Cycle length dependence of human action potential duration in vivo: Effects of single extrastimuli, sudden sustained rate acceleration and deceleration, and different steady-state frequencies. *J Clin Invest* 1988; 82:972-979.
- 66 Pueyo E, Smetana P, Caminal P, de Luna AB, Malik M, Laguna P. Characterization of QT interval adaptation to RR interval changes and its use as a risk-stratifier of arrhythmic mortality in amiodarone-treated survivors of acute myocardial infarction. *IEEE Trans Biomed Eng* 2004; 51:1511-1520.
- 67 Malik M, Hnatkova K, Schmidt A, Smetana P. Accurately measured and properly heart-rate corrected QTc intervals show little daytime variability. *Heart Rhythm*. 2008; 5:1424-1431.
- 68 Malik M, Hnatkova K, Novotny T, Schmidt G. Subject-specific profiles of QT/RR hysteresis. *Am J Physiol Heart Circ Physiol* 2008; 295:H2356-H2363.
- 69 Malik M, Hnatkova K, Sisakova M, Schmidt G. Subject-specific heart rate dependency of electrocardiographic QT, PQ, and QRS intervals. *J Electrocardiol*. 2008; 41:491-497.
- 70 Xue Q, Reddy S. Algorithms for computerized QT analysis. *J Electrocardiol* 1997; 30:181-186.
- 71 Porthan K, Viitasalo M, Jula A, Reunanen A, Rapola J, Vaananen H, Nieminen MS, Toivonen L, Salomaa V, Oikarinen L. Predictive value of electrocardiographic QT interval and T-wave morphology parameters for all cause and cardiovascular mortality in a general population sample. *Heart Rhythm* 2009; 6:1202-1208.
- 72 Friedman HS. Determinants of the total cosine of the spatial angle between the QRS complex and the T wave (TORT): implications for distinguishing primary from secondary T-wave abnormalities. *J Electrocardiol* 2007; 40:12-17.
- 73 Wilson FN, Macleod AG, Barker PS, Johnston FD. The determination and the significance of the areas of the ventricular deflections of the electrocardiogram. *Am. Heart J* 1934; 10:46-61.
- 74 Geselowitz DB. The ventricular gradient revisited: Relation to the area under the action potential. *IEEE Trans Biomed Eng* 1983; 30:76-77.
- 75 Zabel M, Acar B, Klingenhoben T, Franz MR, Hohnloser SH, Malik M. Analysis of 12-lead T-wave morphology for risk stratification after myocardial infarction. *Circulation* 2000; 102:1252-1257.
- 76 de Torbal A, Kors JA, van Herpen G, Meij S, Nelwan S, Simoons ML, Boersma E. The electrical T-axis and the spatial QRS-T angle are independent predictors of long-term mortality in patients admitted with acute ischemic chest pain. *Cardiology* 2004; 101:199-207.
- 77 Lown MT, Munyombwe T, Harrison W, West RM, Hall CA, Morrell C, Jackson BM, Sapsford RJ, Kilcullen N, Pepper CB, Batin PD, Hall AS, Gale CP; Evaluation of methods and management of

- acute coronary events (EMMACE) investigators. Association of frontal QRS-T angle--age risk score on admission electrocardiogram with mortality in patients admitted with an acute coronary syndrome. *Am J Cardiol* 2012; 109:307-313.
- 78 Sweda R, Sabti Z, Strebel I, Kozhuharov N, Wussler D, Shrestha S, Flores D, Badertscher P, Lopez-Ayala P, Zimmermann T, Michou E, Gualandro DM, Häberlin A, Tanner H, Keller DI, Nowak A, Pfister O, Breidhardt T, Mueller C, Reichlin T. Diagnostic and prognostic values of the QRS-T angle in patients with suspected acute decompensated heart failure. *ESC Heart Fail* 2020; 7:1817-1829.
- 79 Jensen CJ, Lambers M, Zadeh B, Wambach JM, Nassenstein K, Bruder O. QRS-T angle in patients with hypertrophic cardiomyopathy – a comparison with cardiac magnetic resonance imaging. *Int. J. Med. Sci* 2021; 18:821-825.
- 80 Walsh JA 3rd, Soliman EZ, Ilkhanoff L, Ning H, Liu K, Nazarian S, Lloyd-Jones DM. Prognostic value of frontal QRS-T angle in patients without clinical evidence of cardiovascular disease (from the Multi-Ethnic Study of Atherosclerosis). *Am J Cardiol* 2013; 112:1880-1884.
- 81 Smetana P, Batchvarov VN, Hnatkova K, Camm AJ, Malik M. Sex differences in repolarization homogeneity and its circadian pattern. *Am J Physiol Heart Circ Physiol*. 2002 May; 282(5):H1889-97.
- 82 Garnett CE, Zhu H, Malik M, Fossa AA, Zhang J, Badilini F, Li J, Darpö B, Sager P, Rodriguez I. Methodologies to characterize the QT/corrected QT interval in the presence of drug-induced heart rate changes or other autonomic effects. *Am Heart J* 2012; 163:912-930.
- 83 Day CP, McComb LM, Campbell RWF. QT dispersion: an indication of arrhythmia risk in patients with long QT intervals. *Br. Heart J* 1990; 63:342-344.
- 84 Okin PM, Devereux RB, Howard BV, Fabsitz RR, Lee ET, Welty TK. Assessment of QT interval and QT dispersion for prediction of all-cause and cardiovascular mortality in American Indians. The Strong Heart Study. *Circulation* 200; 101:61-66.
- 85 Malik M, Acar B, Gang Y, Yap YG, Hnatkova K, Camm AJ. QT dispersion does not represent electrocardiographic interlead heterogeneity of ventricular repolarization. *J. Cardiovasc. Electrophysiol* 2000; 11: 835-843.
- 86 Smetana P, Schmidt A, Zabel M, Hnatkova K, Franz M, Huber K, Malik M. Assessment of repolarization heterogeneity for prediction of mortality in cardiovascular disease: peak to the end of the T wave interval and nondipolar repolarization components. *J Electrocardiol*. 2011; 44:301-308.
- 87 Tse G, Gong M, Wong WT, Georgopoulos S, Letsas KP, Vassiliou VS, Chan YS, Yan BP, Wong SH, Wu WKK, Ciobanu A, Li G, Shenthar J, Saguner AM, Ali-Hasan-Al-Saegh S, Bhardwaj A, Sawant AC, Whittaker P, Xia Y, Yan GX, Liu T. The  $T_{peak} - T_{end}$  interval as an electrocardiographic risk marker of arrhythmic and mortality outcomes: A systematic review and meta-analysis. *Heart Rhythm* 2017; 14:1131-1137.
- 88 Sicouri S, Antzelevitch C. A subpopulation of cells with unique electrophysiological properties in the deep subepicardium of the canine ventricle. The M cell. *Circ. Res* 1991; 68: 1729-1741.
- 89 Antzelevitch C, Di Diego JM. Tpeak-Tend interval as a marker of arrhythmic risk. *Heart Rhythm* 2019; 16:954-955.



- 90 O'Neal WT, Singleton MJ, Roberts JD, Tereshchenko LG, Sotoodehnia N, Chen LY, Marcus GM, Soliman EZ. Association Between QT-Interval Components and sudden cardiac death: The ARIC study (Atherosclerosis Risk in Communities). *Circ Arrhythm Electrophysiol* 2017; 10:e005485.
- 91 Seegers J, Hnatkova K, Friede T, Malik M, Zabel M. T-wave loop area from a pre-implant 12-lead ECG is associated with appropriate ICD shocks. *PLoS One* 2017; 12:e0173868.
- 92 Malik M, Huikuri H, Lombardi F, Schmidt G, Zabel M; e-Rhythm Study Group of EHRA. Conundrum of the Tpeak-Tend interval. *J Cardiovasc Electrophysiol* 2018; 29:767-770.
- 93 Huikuri HV, Verrier RL, Malik M, Lombardi F, Schmidt G, Zabel M. Our doubts about the usefulness of the Tpeak-Tend interval. *Heart Rhythm* 2019; 16:e49.
- 94 Fischer C, Seeck A, Schroeder , Goernig M, Schirdewan A, Figulla HR, Baumert M, Voss A. QT variability improves risk stratification in patients with dilated cardiomyopathy. *Physiol. Meas.* 2015; 36:699-713.
- 95 Monasterio V, Martínez JP, Laguna P, McNitt S, Polonsky S, Moss AJ, Haigney M, Zareba W, Couderc JP. Prognostic value of average T-wave alternans and QT variability for cardiac events in MADIT-II patients. *J. Electrocardiol* 2013; 46:480-486.
- 96 Viigimae M, Karai D, Pilt K, Pirn P, Huhtala H, Polo O, Meigas K, Kaik J. QT interval variability index and QT interval duration during different sleep stages in patients with obstructive sleep apnea. *Sleep Med* 2017; 37:160-167.
- 97 Baumert M, Porta A, Vos MA, Malik M, Couderc JP, Laguna P, Piccirillo G, Smith GL, Tereshchenko LG, Volders PG. QT interval variability in body surface ECG: measurement, physiological basis, and clinical value: position statement and consensus guidance endorsed by the European Heart Rhythm Association jointly with the ESC Working Group on Cardiac Cellular Electrophysiology. *Europace* 2016; 18:925-944.
- 98 Smoczyńska A, Loen V, Sprenkeler DJ, Tuinenburg AE, Ritsema van Eck HJ, Malik M, Schmidt G, Meine M, Vos MA. Short-term variability of the QT interval can be used for the prediction of imminent ventricular arrhythmias in patients with primary prophylactic implantable cardioverter defibrillators. *J Am Heart Assoc* 2020; 23:e018133.
- 99 van den Berg ME, Kors JA, van Herpen G, Bots ML, Hillege H, Swenne CA, Stricker BH, Rijnbeek PR. Normal Values of QT Variability in 10-s electrocardiograms for all ages. *Front Physiol* 2019; 10:1272.
- 100 Vrtovec B, Okrajsek R, Golicnik A, Ferjan M, Starc V, Radovancevic B. Atorvastatin therapy increases heart rate variability, decreases QTc variability, and shortens QTc interval duration in patients with advanced chronic heart failure. *J Card Fail* 2005; 11:684.
- 101 Hinterseer M, Beckmann BM, Thomsen MB, Pfeufer A, Ulbrich M, Sinner MF, Perz S, Wichmann HE, Lengyel C, Schimpf R, Maier SK, Varró A, Vos MA, Steinbeck G, Käb S. Usefulness of short-term variability of QT intervals as a predictor for electrical remodeling and proarrhythmia in patients with nonischemic heart failure. *Am J Cardiol* 2010; 106:216.
- 102 Lengyel C, Orosz A, Hegyi P, Komka Z, Udvardy A, Bosnyák E, Trájer E, Pavlik G, Tóth M, Wittmann T, Papp JG, Varró A, Baczkó I. Increased short-term variability of the QT interval in professional soccer players: possible implications for arrhythmia prediction. *PLoS One* 2011; 6:e18751.
- 103 Feeny A, Han L, Tereshchenko LG. Repolarization lability measured on 10-second ECG by spatial TT' angle: reproducibility and agreement with QT variability. *J Electrocardiol* 2014; 47:708-715.

- 104 Stein KM. Noninvasive risk stratification for sudden death: signal-averaged electrocardiography, nonsustained ventricular tachycardia, heart rate variability, baroreflex sensitivity, and QRS duration. *Prog Cardiovasc Dis* 2008; 51:106-117.
- 105 Katritsis DG, Siontis KC, Bigger JT, Kadish AH, Steinman R, Zareba W, Siontis GC, Bardy GH, Ioannidis JP. Effect of left ventricular ejection fraction and QRS duration on the survival benefit of implantable cardioverter-defibrillators: meta-analysis of primary prevention trials. *Heart Rhythm* 2013; 10:200-206.
- 106 Sipahi I, Chaudhry SP, Issa M, Ambati M, Dagdelen S, Fang JC. Impact of QRS duration on survival benefit with prophylactic implantable cardioverter-defibrillators: a meta-analysis of randomized controlled trials. *J Cardiovasc Med (Hagerstown)* 2015; 16:811-816.
- 107 Mäkikallio TH, Barthel P, Schneider R, Bauer A, Tapanainen JM, Tulppo MP, Schmidt G, Huikuri HV. Prediction of sudden cardiac death after acute myocardial infarction: role of Holter monitoring in the modern treatment era. *Eur Heart J* 2005; 26:762-769.
- 108 Huikuri HV, Tapanainen JM, Lindgren K, Raatikainen P, Mäkikallio TH, Juhani Airaksinen KE, Myerburg RJ. Prediction of sudden cardiac death aftercardial infarction in the beta-blocking era. *J Am Coll Cardiol* 2003; 42:652-658.
- 109 Josephson M, Hein J, Wellens J. Implantable defibrillators and sudden cardiac death. *Circulation* 2004; 109:2685-2691.
- 110 Rijnbeek PR, van Herpen G, Bots ML, Man S, Verweij N, Hofman A, Hillege H, Numans ME, Swenne CA, Witteman JC, Kors JA. Normal values of the electrocardiogram for ages 16-90 years. *J Electrocardiol* 2014; 47:914-921.
- 111 Macfarlane PW, McLaughlin SC, Devine B, Yang TF. Effects of age, sex, and race on ECG interval measurements. *J Electrocardiol* 1994; 27:14-19.
- 112 Hnatkova K, Smetana P, Toman O, Schmidt G, Malik M. Sex and race differences in QRS duration. *Europace*. 2016; 18:1842-1849.
- 113 Sia CH, Dalakoti M, Tan BYQ, Lee ECY, Shen X, Wang K, Lee JS, Arulanandam S, Chow W, Yeo TJ, Yeo KK, Chua TSJ, Tan RS, Lam CSP, Chong DTT. A Population-wide study of electrocardiographic (ECG) norms and the effect of demographic and anthropometric factors on selected ECG characteristics in young, Southeast Asian males-results from the Singapore Armed Forces ECG (SAFE) study. *Ann Noninvasive Electrocardiol* 20019; 24:e12634.
- 114 Vanhaebost J, Faouzi M, Mangin P, Michaud K. New reference tables and user-friendly Internet application for predicted heart weights. *Int J Legal Med* 2014; 128:615-620.
- 115 Veeraraghavan R, Gourdie RG, Poelzing S. Mechanisms of cardiac conduction: a history of revisions. *Am J Physiol Heart Circ Physiol*. 2014; 306:H619-H627. Mason JW, Badilini F, Vaglio M, Lux RL, Aysin B, Moon TE, Heinz B, Strachan I. A fundamental relationship between intraventricular conduction and heart rate. *J Electrocardiol*. 2016; 49:362-370.
- 116 Acar B, Köymen H. SVD-based on-line exercise ECG signal orthogonalization. *IEEE Trans Biomed Eng* 1999; 46:311-321.
- 117 Yana K, Shichiku H, Satoh T, Mizuta H, Ono T. An improved QT interval measurement based on singular value decomposition. *Conf Proc IEEE Eng Med Biol Soc* 2006; 2006:3990-3993.

- 118 Acar B, Yi G, Hnatkova K, Malik M. Spatial, temporal and wavefront direction characteristics of 12-lead T-wave morphology. *Med Biol Eng Comput* 1999; 37:574-584.
- 119 Terho HK, Tikkanen JT, Junttila JM, Anttonen O, Kenttä TV, Aro AL, Kerola T, Rissanen HA, Reunanen A, Huikuri HV. Prevalence and prognostic significance of fragmented QRS complex in middle-aged subjects with and without clinical or electrocardiographic evidence of cardiac disease. *Am J Cardiol* 2014; 114:141-147.
- 120 Rosengarten JA, Scott PA, Morgan JM. Fragmented QRS for the prediction of sudden cardiac death: a meta-analysis. *Europace* 2015; 17:969-977.
- 121 Marume K, Noguchi T, Kamakura T, Tateishi E, Morita Y, Miura H, Nakaoku Y, Nishimura K, Yamada N, Tsujita K, Izumi C, Kusano K, Ogawa H, Yasuda S. Prognostic impact of multiple fragmented QRS on cardiac events in idiopathic dilated cardiomyopathy. *Europace*. 2021; 23:287-297.
- 122 Morita H, Kusano KF, Miura D, Nagase S, Nakamura K, Morita ST, Ohe T, Zipes DP, Wu J. Fragmented QRS as a marker of conduction abnormality and a predictor of prognosis of Brugada syndrome. *Circulation*. 2008; 118:1697-704.
- 123 Rattanawong P, Riangwiwat T, Prasitlumkum N, Limpruttidham N, Kanjanahattakij N, Chongsathidkiet P, Vutthikraivit W, Chung EH. Baseline fragmented QRS increases the risk of major arrhythmic events in Brugada syndrome: Systematic review and meta-analysis. *Ann Noninvasive Electrocardiol*. 2018; 23:e12507.